

Mechanistic Aspects of Inorganic Reactions

Mechanistic Aspects of Inorganic Reactions

David B. Rorabacher, EDITOR

Wayne State University

John F. Endicott, EDITOR

Wayne State University

Based on the Conference
on Inorganic Reaction Mechanisms
at Wayne State University,
Detroit, Michigan,
June 10–12, 1981.

A C S S Y M P O S I U M S E R I E S **198**

AMERICAN CHEMICAL SOCIETY
WASHINGTON, D. C. 1982



Library of Congress Cataloging in Publication Data

Mechanistic aspects of inorganic reactions.
(ACS symposium series, ISSN 0097-6156; 198)

"Based on the Conference on Inorganic Reaction Mechanisms at Wayne State University, Detroit, Michigan, June 10-12, 1981."

Includes bibliographies and index.

1. Chemical reactions—Congresses. 2. Chemistry, Inorganic—Congresses.

I. Rorabacher, David, 1935- . II. Endicott, John, 1932- . III. Conference on Inorganic Reaction Mechanisms (1981: Wayne State University). IV. Series.

QD501.M43 1982 541.3'9 82-13817
ISBN 0-8412-0734-8 ACSMC8 198 1-486
1982

Copyright © 1982

American Chemical Society

All Rights Reserved. The appearance of the code at the bottom of the first page of each article in this volume indicates the copyright owner's consent that reprographic copies of the article may be made for personal or internal use or for the personal or internal use of specific clients. This consent is given on the condition, however, that the copier pay the stated per copy fee through the Copyright Clearance Center, Inc. for copying beyond that permitted by Sections 107 or 108 of the U.S. Copyright Law. This consent does not extend to copying or transmission by any means—graphic or electronic—for any other purpose, such as for general distribution, for advertising or promotional purposes, for creating new collective work, for resale, or for information storage and retrieval systems. The copying fee for each chapter is indicated in the code at the bottom of the first page of the chapter.

The citation of trade names and/or names of manufacturers in this publication is not to be construed as an endorsement or as approval by ACS of the commercial products or services referenced herein; nor should the mere reference herein to any drawing, specification, chemical process, or other data be regarded as a license or as a conveyance of any right or permission, to the holder, reader, or any other person or corporation, to manufacture, reproduce, use, or sell any patented invention or copyrighted work that may in any way be related thereto.

PRINTED IN THE UNITED STATES OF AMERICA

**American Chemical
Society Library**

1155 16th St. N. W.

In Mechanistic Aspects of Inorganic Reactions; Rorabacher, D., et al.;
ACS Symposium Series; American Chemical Society: Washington, DC, 1982.

ACS Symposium Series

M. Joan Comstock, *Series Editor*

Advisory Board

David L. Allara

Robert Baker

Donald D. Dollberg

Robert E. Feeney

Brian M. Harney

W. Jeffrey Howe

James D. Idol, Jr.

Herbert D. Kaesz

Marvin Margoshes

Robert Ory

Leon Petrakis

Theodore Provder

Charles N. Satterfield

Dennis Schuetzle

Davis L. Temple, Jr.

Gunter Zweig

FOREWORD

The ACS SYMPOSIUM SERIES was founded in 1974 to provide a medium for publishing symposia quickly in book form. The format of the Series parallels that of the continuing ADVANCES IN CHEMISTRY SERIES except that in order to save time the papers are not typeset but are reproduced as they are submitted by the authors in camera-ready form. Papers are reviewed under the supervision of the Editors with the assistance of the Series Advisory Board and are selected to maintain the integrity of the symposia; however, verbatim reproductions of previously published papers are not accepted. Both reviews and reports of research are acceptable since symposia may embrace both types of presentation.

PREFACE

MOST INORGANIC MECHANISTIC INFORMATION is obtained from kinetic studies, and, partly as a consequence of increased utilization of fast reaction techniques, major progress in this area has been made during the past 25 years.

Although experimental kinetic parameters generally reflect the most energetically favorable pathway, other reaction pathways are always available, and a change in reaction conditions (temperature, pressure, reaction matrix, structural modifications of the reactants, etc.) may alter the relative significance of competing pathways. As the theory of reaction energetics has become increasingly sophisticated, so each available reaction pathway can be considered to represent a specific cross-section of a continuous multidimensional potential energy hypersurface connecting the ground-state reactants and products. Even with the advent of large, high-speed computers, the theoretical models must be simplified in some manner if the calculations are to become manageable. The approach taken in the selection of appropriate simplifications remains an area of active controversy.

Theoretical models generally evolve from an effort to explain experimental results; however, the ultimate test of any theoretical model is its ability to predict new experimental results. This volume brings together the views of leading experimental and theoretical chemists regarding the current status of our understanding of the principles underlying the apparent mechanisms of inorganic chemical reactions.

Major emphasis is placed on the reactions of metal complexes in solution undergoing either inner-sphere ligand substitution or electron transfer to and from the metal center. Such studies relate to the important selective role of metal catalysts in many areas of enzymatic, commercial, and modern synthetic chemistry. Clearly, this field has now matured to the point where basic theoretical considerations, although incomplete, can provide a logical framework for understanding the chemical reactivity of such systems and stimulate the investigation of (1) new and unique reaction pathways, (2) modified reagents, and (3) unorthodox matrices.

Reactions involving nonmetallic species or nontraditional reactions of metal complexes (unusual oxidation states, reactions with different reaction partners, etc.) are less commonly studied but are becoming of increased interest as mechanistic inorganic chemistry has come of age. A

small sampling of such areas is included in this volume. Some of these studies have been stimulated by the emphasis on solar energy conversion, environmental contamination, nitrogen fixation, biological processes, or theoretical curiosity; but all such studies have added to our understanding of the relative energetics of competing pathways.

The articles and discussion comments contained in this volume derive from a Conference on Inorganic Reaction Mechanisms. The organization of the conference was stimulated both by an interest of the National Science Foundation in surveying the current status of this area and by a need expressed by some 100 researchers active in mechanistic investigations whose opinions were canvassed by the organizers.

The major goals of this conference were to provide a forum for the assessment of the current state of the various areas of mechanistic inorganic chemistry and to generate extensive dialogue among the participants that might facilitate the articulation of existing problem areas. To this end, nearly half the conference was devoted to open discussion. Many of the concerns of the 130 active researchers who participated in this conference were expressed in the General Discussions following the papers or in informal discussions. This volume includes revised material from these oral discussions and short oral presentations. In addition, chapter nine was pieced together by revising three of the short oral contributions and one of the poster presentations. Therefore, there is no discussion following this chapter.

In organizing this conference, the editors were generously and actively assisted by many faculty and staff at Wayne State University and by many conference participants. We are particularly grateful for the assistance rendered by the other members of the organizing committee: Ralph Wilkins, Norman Sutin, Richard Lindvedt, and Stanley Kirshner. Because so many were involved, a complete list of acknowledgments is impossible, but we wish to extend to all those who contributed so generously to the success of this conference our heartfelt thanks and appreciation. Finally, we acknowledge the financial support of the National Science Foundation, Dow Chemical Company, and Wayne State University.

DAVID B. RORABACHER
JOHN F. ENDICOTT
Wayne State University
Department of Chemistry
Detroit, Michigan

March 1982

Substitution Reactions of Chelates

DALE W. MARGERUM

Purdue University, Department of Chemistry, West Lafayette, IN 47907

The kinetics and mechanisms of substitution reactions of metal complexes are discussed with emphasis on factors affecting the reactions of chelates and multidentate ligands. Evidence for associative mechanisms is reviewed. The substitution behavior of copper(III) and nickel(III) complexes is presented. Factors affecting the formation and dissociation rates of chelates are considered along with proton-transfer and nucleophilic substitution reactions of metal peptide complexes. The rate constants for the replacement of tripeptides from copper(II) by triethylenetetramine decrease by 10^8 as methyl groups replace hydrogens in the second and third amino acid residues of the tripeptides. This is attributed to steric hindrance in the ligand-ligand displacement reactions.

In recent years there has been a tendency to assume that the mechanisms of substitution reactions of metal complexes are well understood. In fact, there are many fundamental questions about substitution reactions which remain to be answered and many aspects which have not been explored. The question of associative versus dissociative mechanisms is still unresolved and is important both for a fundamental understanding and for the predicted behavior of the reactions. The type of experiments planned can be affected by the expectation that reactions are predominantly dissociative or associative. The substitution behavior of newly characterized oxidation states such as copper(III) and nickel(III) are just beginning to be available. Acid catalysis of metal complex dissociation provides important pathways for substitution reactions. Proton-transfer reactions to coordinated groups can accelerate substitutions. The main

0097-6156/82/0198-0003\$10.00/0
© 1982 American Chemical Society

topic of this lecture concerns the mechanisms of chelate and multidentate ligand substitutions, an area replete with fascinating, important, and often unexpected results.

Dissociative versus Associative Mechanisms

The success of the Eigen-Wilkins mechanism (1-4) in correlating the characteristic metal ion water exchange rate constant with ligand substitution rate constants has been impressive. The concepts are now incorporated in many textbooks and the predictions have been very useful, but the emphasis has been on the dissociative nature of these reactions. In many cases a dissociative interchange (I_d) mechanism (5) has been assumed for metal ion substitutions, with a consequent tendency to neglect the properties of entering ligands. Yet there has long been evidence that entering ligands can have very pronounced effects on the rates of aquo metal ion substitution reactions. A comparison of rate constants for monodentate ligand substitution reactions of trivalent aquo metal ions shows a strong dependence on the nature of the entering ligand and suggests associative mechanisms (6). This is the case for Ti^{3+} , V^{3+} , Cr^{3+} , Fe^{3+} , Mo^{3+} and In^{3+} and indicates that an associative interchange (I_a) mechanism is likely. In recent years there has been a growing recognition of the importance of associative mechanisms, in part due to the studies of activation volumes.

Stranks and Swaddle (7) found a sizeable negative value ($-9.3 \text{ cm}^3 \text{ mol}^{-1}$) for the activation volume (ΔV^\ddagger) of H_2O exchange with $Cr(H_2O)_6^{3+}$. A negative activation volume is characteristic of an associative or associative interchange reaction rather than a dissociative reaction, because the volume of water in the bulk solvent is greater than the volume of a coordinated water molecule. Although the ΔV^\ddagger value is slightly positive (8) for the water exchange with $Co(NH_3)_5H_2O^{3+}$, the values are negative for the corresponding reactions of the pentaammine complexes of Cr(III) (9), Rh(III) (9), and Ir(III) (10) as shown in Table I. This suggests an associative interchange (I_a) mechanism for these reactions. On the other hand an I_d mechanism is consistent with the positive ΔV^\ddagger value of $+7.1 \text{ cm}^3 \text{ mol}^{-1}$ found for $Ni(H_2O)_6^{2+}$ (11). Recently Merbach and coworkers (12) have cited evidence for a gradual changeover of mechanism from I_a to I_d for the water exchange reactions of divalent metal ions in going

from $\text{Mn}(\text{H}_2\text{O})_6^{2+}$ to $\text{Ni}(\text{H}_2\text{O})_6^{2+}$. It appears that associative mechanisms are quite common and not restricted to trivalent metal ions. It is clear that we need to pay more attention to the effect of the entering ligand in regard to its nucleophil-

Table I
Activation Volumes for H_2O Exchange

Complex	ΔV^\ddagger , $\text{cm}^3 \text{mol}^{-1}$	Ref.
$\text{Cr}(\text{H}_2\text{O})_6^{3+}$	-9.3	(7)
$\text{Cr}(\text{NH}_3)_5\text{H}_2\text{O}^{3+}$	-5.8	(9)
$\text{Co}(\text{NH}_3)_5\text{H}_2\text{O}^{3+}$	+1.2	(8)
$\text{Rh}(\text{NH}_3)_5\text{H}_2\text{O}^{3+}$	-4.1	(9)
$\text{Ir}(\text{NH}_3)_5\text{H}_2\text{O}^{3+}$	-3.2	(10)
$\text{Mn}(\text{H}_2\text{O})_6^{2+}$	-5.4	(12)
$\text{Fe}(\text{H}_2\text{O})_6^{2+}$	+3.8	(12)
$\text{Co}(\text{H}_2\text{O})_6^{2+}$	+6.1	(12)
$\text{Ni}(\text{H}_2\text{O})_6^{2+}$	+7.2	(11)

icity, steric effects or other properties that it may have in substitution reactions.

Ten years ago Rorabacher (13) observed the substitution rate constants for aquonickel(II) ion with different amines (Table II). There is a decrease in the rate constants by a factor of 14 in going from ammonia to dimethylamine. If nickel(II) substitution reactions are dissociative, then why is the effect this large? Is this a steric effect with some associative contribution or is it an outer-sphere effect? There has been surprisingly little investigation of the nature of the entering ligand so far as its bulk or its nucleophilicity is concerned even for what have been generally considered as simple substitution reactions.

Table II
Rate Constant for the Formation
of $\text{NiL}(\text{H}_2\text{O})_5^{2+}$ from $\text{Ni}_{\text{aq}}^{2+}$ (13)

L	k, $\text{M}^{-1}\text{s}^{-1}$
NH_3	4.5×10^3
CH_3NH_2	1.3×10^3
$\text{C}_2\text{H}_5\text{NH}_2$	8.7×10^2
$(\text{CH}_3)_2\text{NH}$	3.3×10^2

Copper(III) and Nickel(III) Substitution Reactions

The sluggish substitution properties of copper(III) and nickel(III) peptide complexes have permitted the isolation of complexes with these oxidation states (14, 15). Thus, the trivalent peptide complexes pass through a cation exchange resin which readily strips copper(II) or nickel(II) from the corresponding complexes. We now have a little more information about the substitution characteristics of the trivalent metal complexes.

Figure 1 shows the reactions of the triply-deprotonated tetraglycine (H_{-3}G_4) complex of copper(III) with acid (16). Protons add rapidly to the free carboxylate group (K_{H}) and to the peptide oxygen ($\text{K}_{2\text{H}}$) to give structure III. The complex then undergoes a dissociation reaction with a first-order rate constant (k_3) of 0.3 s^{-1} , where a peptide nitrogen is displaced from copper(III). Slower redox reactions are observed subsequently and no more dissociation steps can be identified, but this places an upper limit of 10^{-3} s^{-1} for any additional dissociation rate constant. Other Cu(III)-peptide complexes also show relatively labile reactions for the fourth equatorially coordinated peptide group and sluggish reactions for the rest of the in-plane coordination positions. The copper(III) peptides are square-planar complexes with no evidence of axial ligand coordination either in solution (17) or in the crystalline state (18).

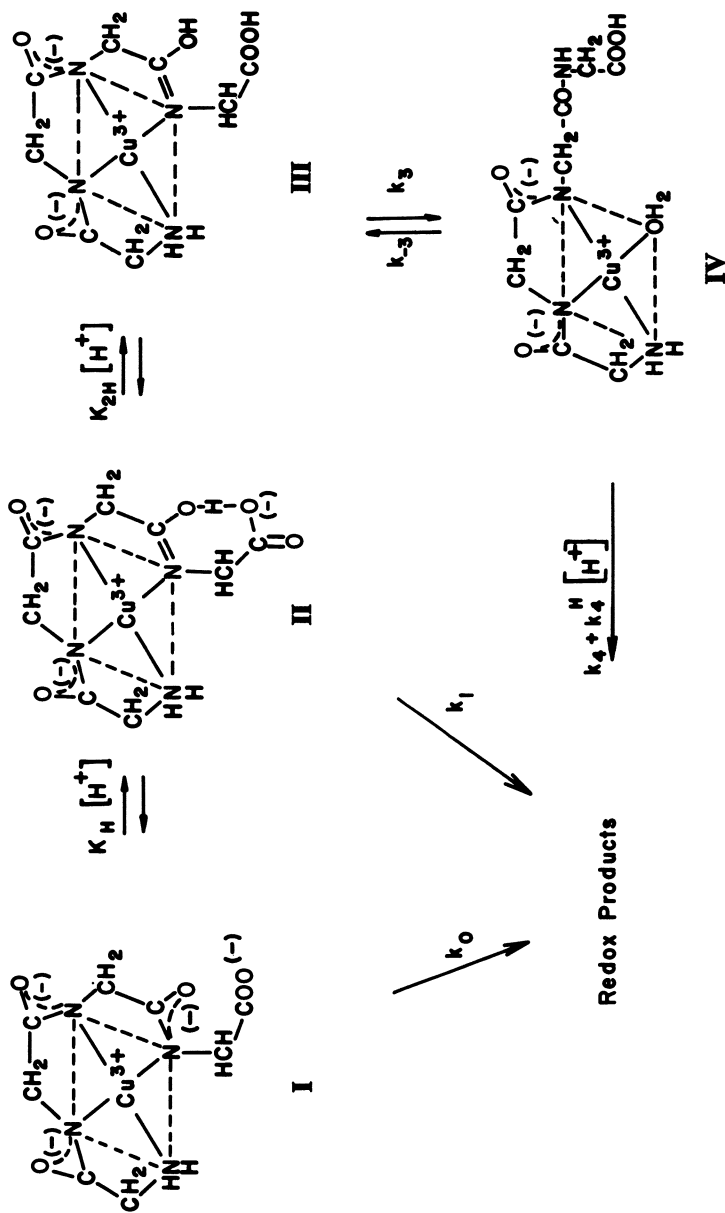


Figure 1. Mechanism for the acid decomposition of Cu(III) tetraglycine. The substitution reaction III to IV has a rate constant $k_3 = 0.3 \text{ s}^{-1}$. Other substitution steps have rate constants less than 10^{-3} s^{-1} .

Nickel(III) peptide complexes have a tetragonally-distorted octahedral geometry as shown by electron spin resonance studies (19) and by reaction entropies for the Ni(III,II) redox couple (17). Axial substitutions for Ni(III)-peptide complexes are very fast with formation rate constants for imidazole greater than $10^6 \text{ M}^{-1} \text{ s}^{-1}$ (20). On the other hand, equatorial substitution of nickel(III) is relatively slow except for the terminal peptide group. One way to observe equatorial substitution is to react the nickel(III) peptide complex with strong acid. When this is done with $\text{Ni}^{\text{III}}(\text{H}_3\text{G}_4)^-$, protons add rapidly to the carboxylate group to give $\text{Ni}^{\text{III}}(\text{H}_3\text{G}_4)\text{H}$ and to the peptide oxygen to give $\text{Ni}^{\text{III}}(\text{H}_3\text{G}_4)\text{H}_2^+$ analogous with the reaction of $\text{Cu}^{\text{III}}(\text{H}_3\text{G}_4)^-$ in Figure 1. The two protonated nickel(III) complexes then undergo substitution reactions for the terminal peptide nitrogen with rate constants of 0.94 s^{-1} and 17 s^{-1} , respectively (21). It is interesting that the corresponding nickel(II) complexes have similar but somewhat larger rate constants. Thus, $\text{Ni}^{\text{II}}(\text{H}_3\text{G}_4)\text{H}^-$ dissociates with a rate constant of 5.6 s^{-1} and, in 0.05 M HClO_4 , the dissociation rate constant for the nickel(II) complex increases to 156 s^{-1} (22). However, the subsequent acid dissociation reactions of the nickel(II)-peptides are rapid, whereas additional substitution reactions of nickel(III) peptides are sluggish. For the tetraglycinamide complex (G_4a), the rate constant for the loss of Ni(III), due to redox decomposition reactions, equals $(7.8 \times 10^{-4} + 5.8 \times 10^{-3} [\text{H}^+]) \text{ s}^{-1}$ (23). The redox decomposition prevents the observation of additional substitution reactions, but it shows that substitutions of the other three equatorial nickel(III)-peptide coordination sites are sluggish with rate constants generally less than 10^{-3} s^{-1} .

Figure 2 shows the proposed mechanism (21) for the acid dissociation of $\text{Ni}^{\text{III}}(\text{H}_3\text{G}_4\text{a})$. The reactions of nickel(III) can be followed by ESR since this d^7 electronic state has one unpaired electron. Figure 3 shows the changes in the room temperature ESR signal as the pH changes from 6.5 to 1.2 (21). Stopped-flow vidicon spectroscopy (24) provides another convenient handle (Figure 4) to observe the conversion of one nickel(III) complex to another prior to the redox reaction in which the peptide is oxidized and nickel(II) is formed (21). For the mechanism in Figure 2 the values of the constants are $k_0 < 0.02 \text{ s}^{-1}$,

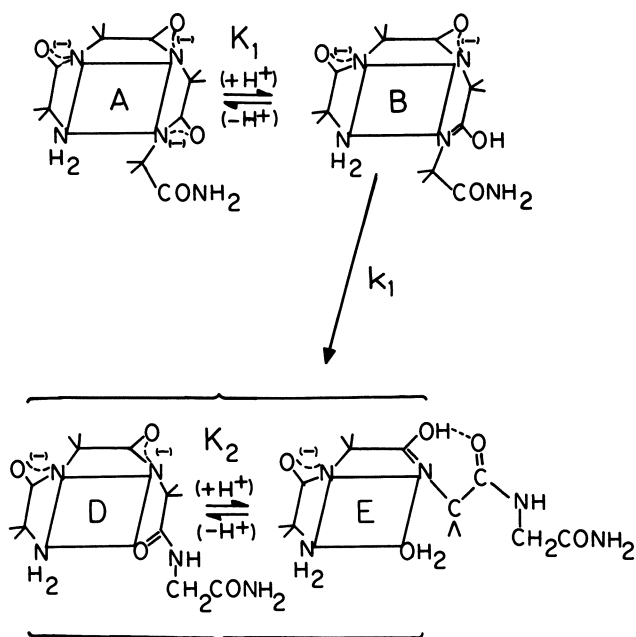


Figure 2. Proposed reactions of Ni(III)(H₃G₄a) with acid prior to redox decomposition. The substitution reaction for species B to E has a rate constant $k_1 = 15.3 \text{ s}^{-1}$. Other substitution steps have rate constants less than 10^{-3} s^{-1} .

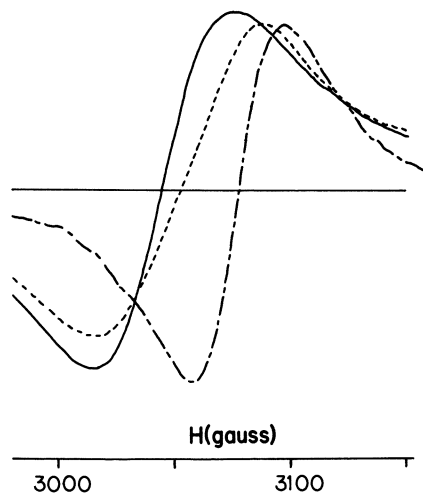


Figure 3. ESR spectral changes (25°C) for the Ni(III)-G_{1a} complex showing the effect of the coordination changes given in Figure 2. Key for pH values: —, 6.5 (A); ---, 3.0 (B); and — · —, 1.2 (D or E).

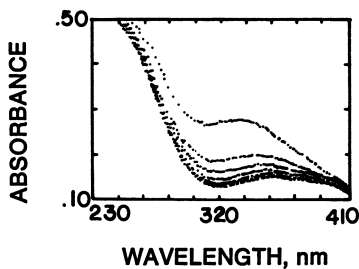


Figure 4. Vidicon rapid scan UV-visible spectral changes on the addition of acid to Ni(III)(H₃G_{1a}), corresponding to the coordination changes in Figure 2. Absorbance decreases with time for spectra recorded at 0.02, 0.09, 0.16, 0.23, 0.30, 0.37, 0.42, and 0.49 s.

$K_1 = 2.2 \text{ M}^{-1}$ and $k_1 = 15.3 \text{ s}^{-1}$. Thus, the reactivity of $\text{Ni}^{\text{III}}(\text{H}_3\text{G}_4\text{a})\text{H}^+$ is very similar to that of $\text{Ni}^{\text{III}}(\text{H}_3\text{G}_4)\text{H}_2^+$, which also has a protonated peptide oxygen. The terminal peptide coordination position (i.e., the fourth planar position of the ligand) is relatively labile in strong acid with half lives of only 40-45 milliseconds. However, nickel(III) peptide complexes can be passed through Chelex ion exchange columns as is the case with copper(III) peptides, indicating that the remaining substitution steps are slow.

Axial substitution rate constants have been determined by Haines and McAuley (25) for anions reacting with nickel(III)-cyclam and some of the constants are given in Table III. The rate constants for the replacement of an axial water molecule by a halide ion are in the vicinity of 10^2 to $10^3 \text{ M}^{-1} \text{ s}^{-1}$ which is rapid, but much slower than for axial substitution of nickel(III)-peptide complexes. The in-plane substitution is naturally slowed down by the presence of the macrocyclic ligand, but, in any case, the in-plane substitution is negligible and the axial substitution is fast.

Table III
Axial Substitution Rate Constants
for $\text{Ni}(\text{III})\text{Cyclam}(\text{H}_2\text{O})_2^{3+}$ (25)

Ligand	Stability Constant, M^{-1}	Formation Rate Constant, $\text{M}^{-1} \text{ s}^{-1}$
Cl^-	210	902
Br^-	50	210
SCN^-	2000	1160

Factors Affecting Formation Rate Constants of Chelates

Rate constants for the formation of complexes from the aquometal ion and various chelating ligands are often predicted from the expected outer-sphere association constant (K_{os}) and the characteristic water exchange rate constant ($k^{\text{M-H}_2\text{O}}$). However, as summarized in Table IV, the observed formation rate constants are often significantly smaller than the predicted k_f values and occasionally are much larger. Steric effects can cause k_f values to be smaller for chelates as well as for mono-

dentate substitution reactions. In some cases, such as the reaction of Hen^+ with $\text{Cu}^{2+}_{\text{aq}}$, the rate-determining step in the formation of Cuen^{2+} appears to be the proton transfer step from the monodentate CuenH^{3+} complex (6).

Table IV
Some Factors which Affect the Formation Rate Constant (k_f)
in Substitution Reactions

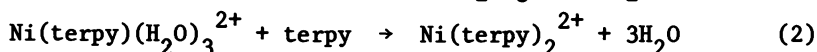
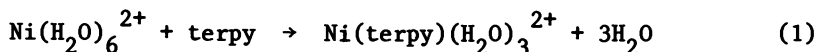
1. k_f may depend on the nucleophilicity of the reacting ligand in an associative mechanism
 2. k_f smaller than predicted from $k^{\text{M-H}_2\text{O}}$ values:
 - a. steric effects
 - b. chelation-controlled substitution
 - c. limiting proton-transfer rate
 3. k_f larger than predicted from $k^{\text{M-H}_2\text{O}}$ values
 - a. internal conjugate base mechanism (H-bonding)
 - b. stacking interactions
-

In a great many cases the first bond formation of chelates is not the rate-determining step, but rather the chelate ring formation is rate-limiting. This chelation-controlled substitution (6) is often recognized by smaller k_f values. However, chelate-controlled substitution can occur even when k_f values are not smaller than predicted. Other factors which help to increase the rate of first bond formation are often not taken into account. A critical review of the formation kinetics of aminocarboxylates suggests that most react by chelation-controlled substitution, where ring closure rather than first bond formation is the rate-determining step (6).

One of the factors which can cause larger k_f values than normally predicted is found in the internal conjugate base mechanism of Rorabacher (26). This effect is seen in the relative rate constant of nickel(II) with ethylenediamine ($3.2 \times 10^5 \text{ M}^{-1} \text{ s}^{-1}$) compared with ethylamine ($7.9 \times 10^2 \text{ M}^{-1} \text{ s}^{-1}$). The large increase in k_f for ethylenediamine can be attributed to an increased K_{os} value caused by hydrogen bonding between a coordinated water molecule and the electron pair on one amine nitrogen which permits the adjacent position on the metal ion to undergo substitution. At least two donor groups in the same ligand are needed for the ICB mechanism to permit one to hydro-

gen bond while the other donor group rotates freely to occupy an inner-sphere coordination position. With ethylenediamine first bond formation is the rate-determining step, but the rate is accelerated by a larger outer-sphere association constant.

Another factor which increases outer-sphere association and leads to an increase in formation rate is caused by stacking interactions (27). In 1966 Wilkins (28) observed that the rate constant for reaction 1 was $1.4 \times 10^3 \text{ M}^{-1} \text{ s}^{-1}$ while the rate



constant for reaction 2 was $2.2 \times 10^5 \text{ M}^{-1} \text{ s}^{-1}$. Similar increases in the rate of second terpy addition was found for the Co(II) and Fe(II) complexes. Rablen and Gordon (29) measured the water exchange rate constants for $\text{Ni}(\text{terpy})(\text{H}_2\text{O})_3^{2+}$ and found it to be $5.2 \times 10^4 \text{ s}^{-1}$, compared to a value of $3.4 \times 10^4 \text{ s}^{-1}$ for $\text{Ni}(\text{H}_2\text{O})_6^{2+}$. Hence, the water exchange rate constant cannot account for the increase in the ligand substitution rate constant by a factor of more than 100. Cayley and Margerum (27) observed that $\text{Ni}(\text{phen})(\text{H}_2\text{O})_4^{2+}$ reacting with ammonia or with a second 1,10-phenanthroline shows no enhancement, but that a rate enhancement factor of 23 is found for the reaction with bipyridyl. The explanation is that bipy associates with $\text{Ni}(\text{phen})(\text{H}_2\text{O})_4^{2+}$ by a stacking interaction as shown in Figure 5. A second phen would stack even better than bipy, but it would not be free to substitute because it is not flexible. The stacking increases the outer-sphere association and the effect increases as the number of rings which can overlap in stacking increases (Figure 6). The stacking interactions are also enhanced by methyl substituents on the aromatic rings and rate enhancements as large as 2100 have been observed. The stacking interaction is attributed to hydrophobic bonding and to polarization effects. The rates of reaction in methanol-water mixtures have much lower rate enhancements due to the loss of favorable stacking interaction as the hydrophobic bonding effect is reduced.

Acid-Catalyzed Chelate Ring Opening of $\text{Ni}(\text{en})(\text{H}_2\text{O})_4^{2+}$. The factors which determine the rate of chelate ring opening reactions and make the dissociation process so much slower than the corresponding monodentate dissociation rate are not well established. Angular expansion of bond angles in the chelate ring seems to be more important than hindered rotation of the

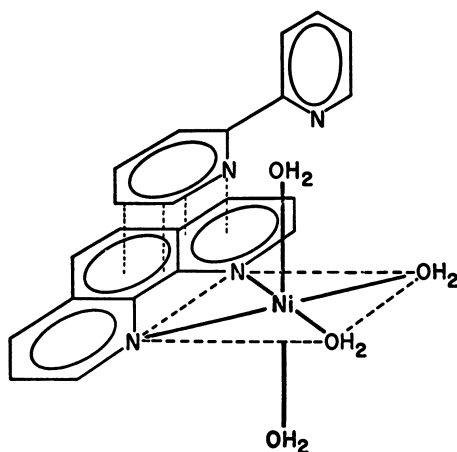


Figure 5. Stacking interaction proposed in the reaction between bipy and $Ni(phen)(H_2O)_4^{2+}$ immediately prior to the first bond coordination of bipy. (Reproduced, with permission, from Ref. 27. Copyright 1974, J. Chem. Soc., Chem. Commun.)

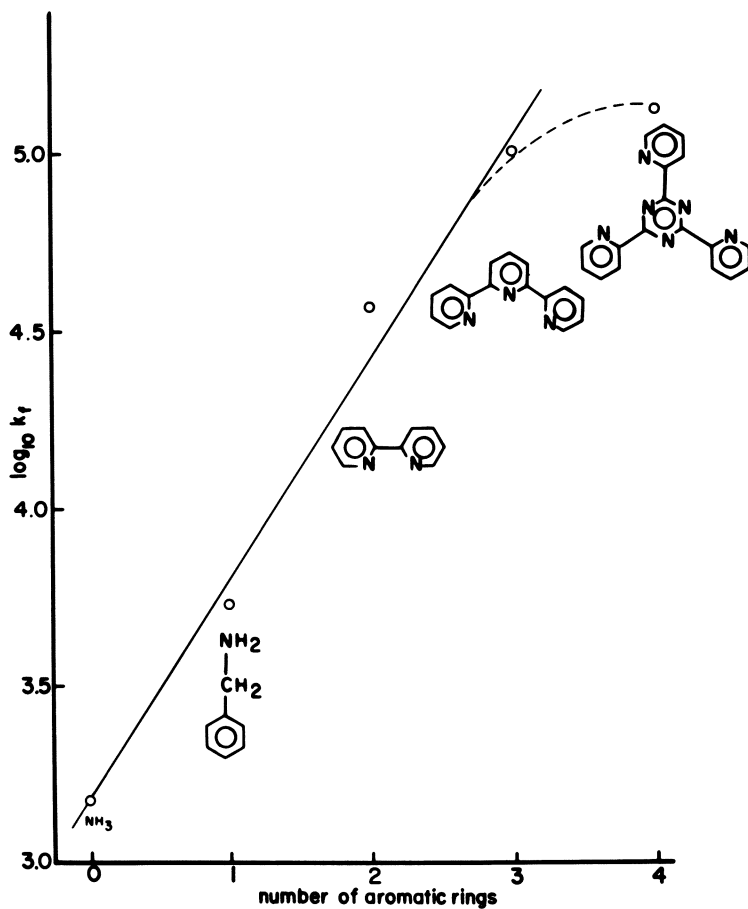


Figure 6. Formation rate constants for ligands reacting with $\text{Ni}(\text{phen})(\text{H}_2\text{O})_4^{2+}$ showing the effect of increasing stacking interaction with increasing number of aromatic rings.

chelating ligand (6). A recent study of the acid dissociation of Nien^{2+} has shown that protonation of one of the ethylenediamine nitrogens can occur while it is still within the first coordination sphere (30). That is, even when the chelate ring has not opened sufficiently to move the nitrogen donor out of the first coordination sphere, it is possible to protonate the donor atom. This protonation accelerates the dissociation reaction.

Ahmed and Wilkins (31-33) found that the dissociation rate of Nien^{2+} increases by a factor of 20 when the pH is lowered from 7 to 4 and then levels off from pH 4 to 2. The rate reaches a plateau because ring opening becomes the rate-determining step. They observed some increase in rate at higher acidity and we have explored this in much more detail (30). Figure 7 shows the effect of pH on the dissociation rate constant for Nien^{2+} . (This figure is a composite of data at 0.6 °C (32) and at 25.0 °C adjusted to one ordinate.) The additional increase in the rate constant (for the region labeled k_{2H}) below pH 1.5 was verified. The commonly accepted way in which acid assists the dechelation of a polyamine complex is by protonation of a donor after solvent separates it from the metal (34). However, this corresponds to the k_{1d} plateau in Figure 7 and does not account for the increase as the acidity is increased further. The mechanism proposed (6, 30) to explain the latter effect is the addition of a proton to the amine nitrogen before the nitrogen leaves the first coordination sphere as shown in Figure 8. The proton adds before or during the solvation of the metal ion, thereby enhancing the dissociation rate by causing the chelate ring to open more rapidly.

Table V
Rate Constants for the Solvent and Protonation Pathways
in Complex Dissociation (30)

Complex	k_{1d}, s^{-1}	$k_{2H}, \text{M}^{-1} \text{s}^{-1}$	$k_{2H}/k_{1d}, \text{M}^{-1}$
Nien^{2+}	0.108	0.056	0.52
Nien_3^{2+}	68	19	0.28
NiNH_3^{2+}	5.76	0.54	0.09

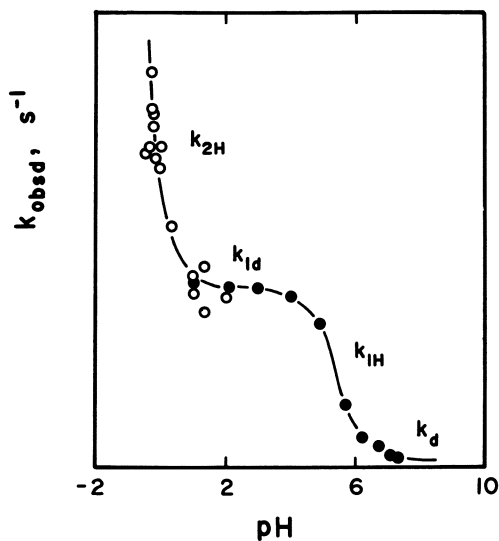


Figure 7. Observed rate constants for the dissociation of $\text{Nien}(\text{H}_2\text{O})_4^{2+}$ as a function of pH.

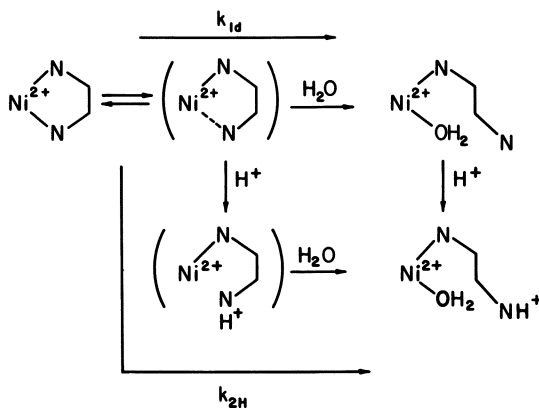


Figure 8. Proposed mechanism for the acid-catalyzed dissociation of Nien^{2+} where a proton adds to an amine N while it is still in the first coordination sphere of the Ni ion. The species in parentheses may be transition states rather than intermediates.

Table V compares the k_{1d} and k_{2H} rate constants for Nien^{2+} , Nien_3^{2+} and NiNH_3^{2+} . The k_{1d} value for Nien^{2+} is a factor of 53 smaller than k_{1d} value for NiNH_3^{2+} , showing the effect of chelate ring opening in slowing the dissociation step. However, the ratio of k_{2H}/k_{1d} for Nien^{2+} is 0.52 which is much larger than the ratio of 0.09 for NiNH_3^{2+} . The restrictions imposed by the chelate ring opening may hold the donor in the first coordination sphere making it more susceptible to protonation. The small effect seen for NiNH_3^{2+} suggests that even here the ligand may be trapped by a cage formed from solvent molecules in the second coordination sphere. The effect of the solvent cage is a less important factor than the effect of the chelate ring in determining the relative rates of the solvent-separation and protonation pathways.

The mechanism outlined for the k_{2H} path in Figure 8 suggested that general acids might catalyze the rate and we found this to be the case (30). The results in Table VI are surprising because all the carboxylic acids are more effective than H_3O^+ and the weakest acid, CH_3COOH , is the most effective as seen in the k_{2HB} values. This is the opposite of normal general acid reactions where the rate increases with acid strength. On the other hand, no acceleration is detected with pyridinium ion. It appears that the carboxylic acids are associating with Nien^{2+} either by hydrogen bonding interaction or by replacement of a water molecule (Figure 9). General acid catalysis is not detected in the dissociation of Nien_3^{2+} . The most effective acids for Nien^{2+} are those which are the best coordinating acids, where one part of the molecule coordinates (or hydrogen bonds) while the other donates the proton. Coordinating acids have also been found to assist proton-transfer reactions of metal-peptide complexes (22, 35-39).

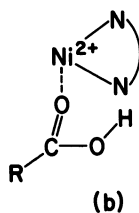
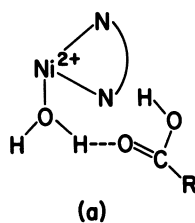
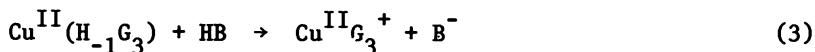


Figure 9. Possible general acid interaction with $Nien^{2+}$ by (a) hydrogen bonding to a coordinated H_2O molecule or (b) carboxylic acid oxygen coordination to Ni . In both cases the proton of the carboxylic acid is available to be transferred to an amine N as proposed in Figure 8.

Table VI
Rate Constants for the Acid Pathway
in the Dissociation of Nien^{2+} (30)

Acid	pK_a	$k_{2\text{HB}}, \text{M}^{-1} \text{s}^{-1}$
CH_3COOH	5.01	0.30
ClCH_2COOH	3.02	0.14
Cl_2CHCOOH	0.87	0.08
Cl_3CCOOH	0.66	0.10
H_3O^+	-1.73	0.056

Proton-transfer Reactions of Metal-Peptides. Two pathways found for the reactions of acids with deprotonated-peptide complexes (22, 35, 39) are depicted in Figure 10. In one path rapid protonation of the peptide oxygen is followed by metal-N(peptide) bond cleavage and solvation of the metal. The "outside protonated" species is a true intermediate and this path is not subject to general acid catalysis because the rate-determining step occurs after protonation. In the other path proton transfer occurs by direct reaction with the coordinated peptide nitrogen. This path is general-acid catalyzed. The proton transfer and metal-peptide bond breaking occur simultaneously so the species shown for the inside protonation pathway is not a true intermediate but is either the transition state or is a virtual intermediate. One of the fascinating properties of the general acid-catalyzed path is shown by the Brønsted plot in Figure 11 (40). This plot has the shape of an Eigen-type Brønsted plot (41) in which the alpha value changes from 1 to 0 as the diffusion limit is reached. However, the rate constants for the slope of zero are as small as $10^5 \text{ M}^{-1} \text{ s}^{-1}$ rather than the diffusion-limiting value of $10^{10} \text{ M}^{-1} \text{ s}^{-1}$. Figure 11 gives data for the copper complex with singly-deprotonated triglycine, as shown in eq 3, and similarly shaped Brønsted plots with $\text{Cu}^{\text{II}}(\text{H}_{-2}\text{G}_3)^-$ and with $\text{Cu}^{\text{II}}(\text{H}_{-3}\text{G}_4)^{2-}$ (40, 43).



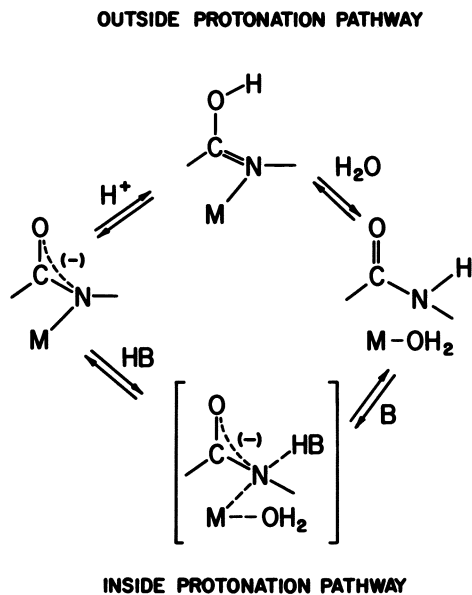


Figure 10. Proposed mechanism for the proton-transfer reactions of metal-peptide complexes.

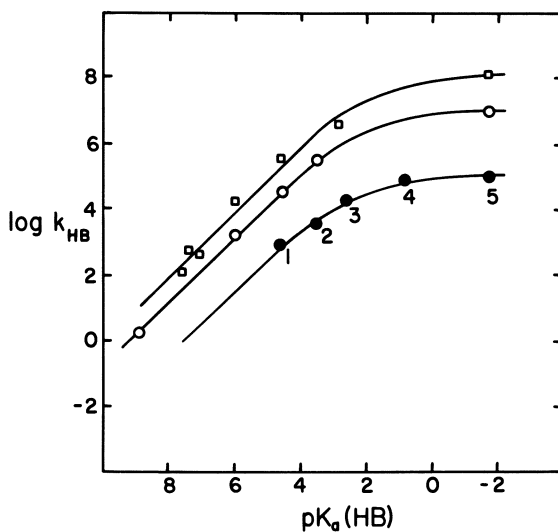


Figure 11. Brønsted plots for the proton transfer reactions of Cu-triglycine and Cu-tetraglycine complexes. Key: \square , $\text{Cu}(\text{H}_{-3}\text{G}_4)^{2-}$; \circ , $\text{Cu}(\text{H}_{-2}\text{G}_3)^{-}$; and \bullet , $\text{Cu}(\text{H}_{-1}\text{G}_2)$ (numbers refer to the acids: 1, CH_3COOH ; 2, HCOOH ; 3, ClCH_2COOH ; 4, Cl_2CHCOOH ; and 5, H_3O^+).

It is traditional to treat H_3O^+ as an exceptional acid with unusual proton-transfer rate properties which preclude it from being included in such a Brønsted plot. In this case H_3O^+ follows a trend which is typical of other strong acids (Cl_2CHCOOH and ClCH_2COOH) and need not be considered as an exception. This is also true for many other reactions (35, 44) which we have studied for a wide range of acids. If only the three left hand points had been available to compare with the H_3O^+ value, then the latter point would have appeared to fall off an extrapolated Brønsted plot and might have erroneously been assigned to an exceptional class. However, in reality the entire curve has an abrupt change in slope and can be accounted for by use of a modified Marcus theory (38, 44) of proton transfer. The modification changes the W_R value in the Marcus theory from a simple work term required to bring the reactant together to a larger energy term which includes additional factors that are independent of the acid and base strength of the reactants. In this case the larger W_R term appears to arise from the need to solvate the metal ion as shown in Figure 10 for the inside protonation pathway. The Marcus dependence is given in eq 4.

$$\begin{aligned} \Delta G^\ddagger &= W_R + \frac{\lambda}{4} \left(1 + \frac{\Delta G_{\text{HB}}^\circ - C}{\lambda}\right)^2 & |\Delta G_{\text{HB}}^\circ - C| \leq \lambda & \quad (4) \\ \Delta G^\ddagger &= W_R & (\Delta G_{\text{HB}}^\circ - C) < -\lambda & \\ \Delta G^\ddagger &= \Delta G_{\text{HB}}^\circ + W_R - C & (\Delta G_{\text{HB}}^\circ - C) > \lambda & \end{aligned}$$

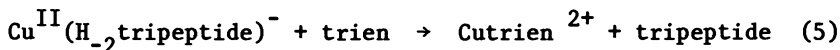
where $C = \Delta G_{\text{HS}}^\circ - W_P + W_R$

In the present case the intrinsic barrier ($\lambda/4$) is small and, therefore, the reactions have a strong dependence on the pK_a value of the reacting acids, which accounts for the abrupt change of slope for the Brønsted plots in Figure 11. However, as the W_R terms increase, the rate constants plateau at lower values. Table VII summarizes some of the $\lambda/4$ and W_R values for different metal-peptide reactions with acids. The W_R values increase with the strength of the metal-peptide bond whereas the $\lambda/4$ values are unchanged. Thus, the proton-transfer rate constants appear to be unaffected by the need to solvate the metal ion as the peptide nitrogen bond to the metal breaks. In general, proton transfer and other reactions of electrophiles with chelate complexes need further investigation.

Table VII
Modified Marcus Parameters for Proton-Transfer Reactions
with Deprotonated Metal Peptide Complexes

Complex	Energy Barrier (kcal mol ⁻¹)		
	\underline{W}_R	$\underline{\lambda}/4$	\underline{C}
Cu(H ₋₃ G ₄) ²⁻	6.0	1.8	2.1
Cu(H ₋₂ G ₃) ⁻	7.7	1.6	3.3
Cu(H ₋₁ G ₃)	10.4	1.1	3.2
Ni(H ₋₂ G ₃) ⁻	10.6	2.0	3.8

Nucleophilic substitution reactions of trien with copper-(II)-tripeptide complexes. I have long been fascinated by multidentate ligand substitution reactions, particularly by reactions in which one multidentate ligand replaces another. I now want to focus on steric effects in a reaction of this type in which triethylenetetramine (trien) displaces a doubly-deprotonated tripeptide ligand from copper(II) (eq 5) (45).



The rate is first order in each reactant (eq 6) and there are no observable concentrations of intermediate species. The coor-

$$\frac{d[\text{Cutrien}^{2+}]}{dt} = k[\text{Cu}^{\text{II}}(\text{H}_{-2}\text{tripeptide})^{-}][\text{trien}] \quad (6)$$

dination of the tripeptide complexes is shown in Figure 12. Other studies (46) with en and dien show that the substitution reactions proceed from the carboxylate end through a series of mixed tripeptide-polyamine ternary complexes. However, the rate-determining step is relatively early in the trien displacement of the tripeptide and subsequent reactions are rapid by comparison, so that intermediate ternary complexes are not seen in the trien reactions. In the observed rate the tripeptide ligand is completely displaced, but the rate of this displacement is greatly affected by the nature of the amino acid residues in rings 2 and 3. As shown in Table VIII, rate constants for the trien reactions change by eight orders of magnitude as hydrogens in triglycine (G₃ or GGG) are replaced by methyl sub-

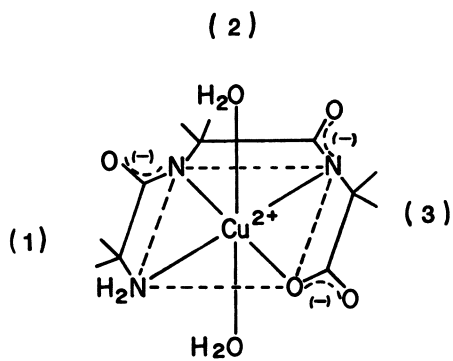


Figure 12. *Cu(II)-tripeptide complexes.*

stituents in the tripeptide of aminoisobutyric acid (Aib₃). Table IX shows that the stability constants for the tripeptide complexes involving the two extreme cases, GGG and Aib₃, differ by a factor of only 65, so that the large kinetic effect of the methyl groups cannot be attributed just to changes in copper-peptide stability. Furthermore, the proton-transfer rate constants for these complexes are little affected by methyl substituents. It is only the nucleophilic substitution reactions that are greatly affected. Methyl substituents in the first chelate ring have only a small effect on the trien substitution rate constant as seen for the results with AAA versus GAA and AGA versus GGA. Methyl substituents in the second chelate ring slow the trien substitution rate a great deal as seen for GAG vs. GGG and for GAibG vs. GGG. Methyl substituents in the third chelate ring also slow the substitution as seen for GGA vs. GGG and for GGAib vs. GGG. The effect of methyl groups in both the second and third chelate rings is cumulative so that the reaction with Aib₃ is 10⁸ times slower than the reaction with GGG.

The methyl groups sterically hinder the trien displacement reaction. There is good evidence from earlier studies with ammonia, ethylenediamine, and diethylenetriamine that the reacting amine needs a foothold in an equatorial position for the displacement to proceed as shown by the mechanisms in Figure 13. Methyl groups in the third ring simply make it sterically difficult for trien to get a foothold and this is one of the reasons why the rate constant is reduced by as much as four orders of magnitude when two methyl groups are in the third ring. The rate-determining step is proposed as the first chelate ring closure reaction of trien which coincides with the first peptide bond breaking from copper. Methyl groups in the second peptide chelate ring apparently make it difficult for this ring to open in the nucleophilic displacement reaction with trien and, of course, methyl groups in the third chelate ring may also be sterically hindering this step (k_2 in Figure 13).

The pH dependence of the trien reaction indicates that no protons are added before the rate-determining step. Hence, this step cannot come after the peptide bond breaks, because the metal-free peptide group must add a proton. Thus, the subsequent displacement reactions of the donors in the first chelate ring occur after the rate-determining step, which agrees with the lack of methyl group effects in this ring.

The results suggest that the five-membered peptide chelate ring, in which the atoms are nearly coplanar, may be more subject to steric effects than is the case for the gauche conformation of chelate rings of ethylenediamine and its C-methyl derivatives. However, the corresponding nucleophilic displacement reactions have not been studied and it is too early to draw

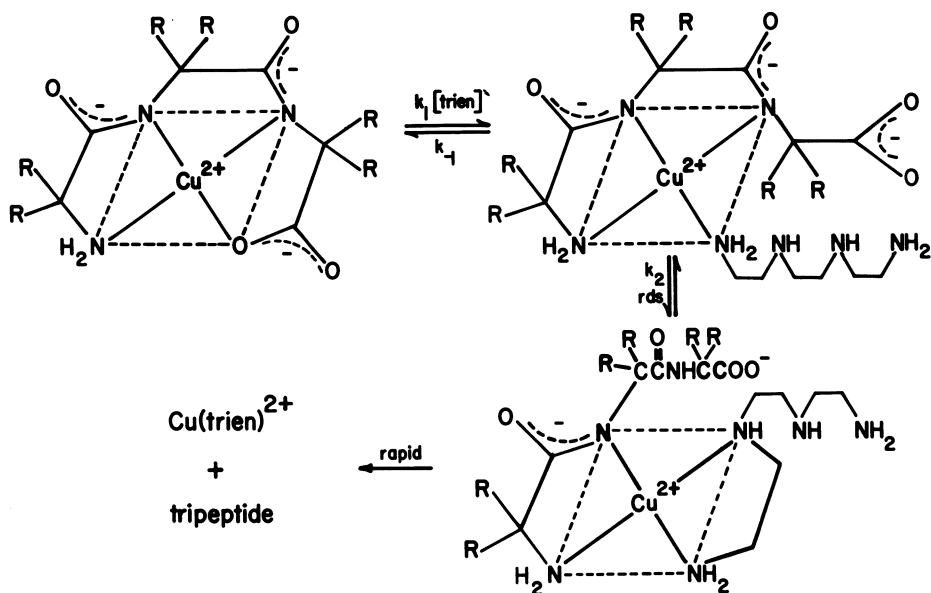


Figure 13. Proposed mechanism for the displacement of the tripeptide from $\text{Cu}(\text{II})$ by trien. The rate-determining step (k_2) is the opening of the second peptide N and its replacement by a trien N.

Table VIII
 Second-order Rate Constants (25.0°C) for the
 Reactions of Trien with $\text{Cu}^{\text{II}}(\text{H}_{-2}\text{tripeptides})^-$.

Peptide	Methyl Substituents in Chelate Ring			$k, \text{M}^{-1}\text{s}^{-1}$
	C_1	C_2	C_3	
GGG	$\frac{C_1}{0}$	$\frac{C_2}{0}$	$\frac{C_3}{0}$	1.1×10^7
GAG	0	1	0	1.3×10^5
GGA	0	0	1	1.1×10^5
AGA	1	0	1	6.0×10^4
GAA	0	1	1	2.3×10^3
AAA	1	1	1	1.7×10^3
GGAib	0	0	2	5.6×10^2
GAibG	0	2	0	7.0×10^1
Aib ₃	2	2	2	1.4×10^{-1}

Table IX.
 Stability Constants of Copper(II)
 Tripeptide Complexes (47)

Complex	$\log \beta_{1,-2,1}^a$
$\text{Cu}(\text{H}_{-2}\text{G}_3)^-$	-6.76
$\text{Cu}(\text{H}_{-2}\text{Aib}_3)^-$	-4.95

$$^a \beta_{1,-2,1} = \frac{[\text{Cu}(\text{H}_{-2}\text{L})^-][\text{H}^+]^2}{[\text{Cu}^{2+}][\text{L}^-]}$$

conclusions. The very large steric effects observed in the peptide displacement reactions certainly merit additional study.

Summary

Our knowledge and understanding of the kinetics and mechanisms of substitution reactions are limited, particularly in the area of chelate and multidentate ligand substitutions. There are electrophilic, nucleophilic and steric effects in the reactions of classical complexes which need to be investigated and the areas of organometallic chemistry and cluster complexes are even more unexplored. The lack of knowledge of substitution reactions is really quite striking and I hope my comments will encourage more investigations of these important reactions.

Acknowledgments

I wish to thank the many students and coworkers who contributed to this work and to the National Institute of General Medical Sciences (Public Health Service Grants GM-12152 and GM-19775) for its support of major portions of our research work presented here.

Literature Cited

1. Eigen, M. Z. Electrochem. 1960, 64, 115.
2. Eigen, M. Pure Appl. Chem. 1963, 6, 97.
3. Wilkins, R. G.; Eigen, M. Adv. Chem. Ser. 1965, 49, 55.
4. Wilkins, R. G. Acc. Chem. Res. 1970, 3, 408.
5. Langford, C. H.; Gray, H. B. "Ligand Substitution Processes"; W. A. Benjamin: New York, 1966.
6. Margerum, D. W.; Cayley, G. R.; Weatherburn, D. C.; Pagenkopf, G. W. "Coordination Chemistry"; Martell, A. E., Ed.; American Chemical Society: Washington, D. C., 1978; Vol. 2, pp 1-220.
7. Stranks, D. R.; Swaddle, T. W. J. Am. Chem. Soc. 1971, 93, 2783.
8. Hunt, H. R.; Taube, H. J. Am. Chem. Soc. 1958, 80, 2642.
9. Swaddle, T. W.; Stranks, D. R. J. Am. Chem. Soc. 1972, 94 8357.
10. Tong, S. B.; Swaddle, T. W. Inorg. Chem. 1974, 13, 1538.
11. Ducommun, Y.; Earl, W. L.; Merbach, A. E. Inorg. Chem. 1979, 18, 2754.
12. Ducommun, Y.; Newman, K. E.; Merbach, A. E. Inorg. Chem. 1980, 19, 3696.
13. Rorabacher, D. B.; Melendez-Cepeda, C. A. J. Am. Chem. Soc. 1971, 93, 6071.
14. Margerum, D. W.; Chellappa, K. L.; Bossu, F. P.; Burce, G. L. J. Am. Chem. Soc. 1975, 97, 6894.

15. Bossu, F. P.; Margerum, D. W. J. Am. Chem. Soc. 1976, 98, 4003.
16. Rybka, J. S.; Kurtz, J. L.; Neubecker, T. A.; Margerum, D. W. Inorg. Chem. 1980, 19, 2791.
17. Youngblood, M. P.; Margerum, D. W. Inorg. Chem. 1980, 19, 3068.
18. Diaddario, L. L.; Robinson, W. R.; Margerum, D. W., to be published.
19. Lappin, A. G.; Murray, C. K.; Margerum, D. W. Inorg. Chem. 1978, 17, 1630.
20. Murray, C. K.; Margerum, D. W., to be published.
21. Subak, E. J., Jr.; Loyola, V. M.; Margerum, D. W., to be published.
22. Paniago, E. B.; Margerum, D. W. J. Am. Chem. Soc. 1972, 94, 6704.
23. Loyola, V. M.; Subak, E. J., Jr.; Margerum, D. W., to be published.
24. Ridder, G. M.; Margerum, D. W. Anal. Chem. 1977, 49, 2098.
25. Haines, R. I.; McAuley, A. Inorg. Chem. 1980, 19, 719.
26. Rorabacher, D. B. Inorg. Chem. 1966, 5, 1891.
27. Cayley, G. R.; Margerum, D. W. J. Chem. Soc., Chem. Commun. 1974, 1002.
28. Holyer, R. H.; Hubbard, C. D.; Kettle, S. F. A.; Wilkins, R. G. Inorg. Chem. 1966, 5, 622.
29. Rablen, D.; Gordon, G. Inorg. Chem. 1969, 8, 395.
30. Read, R. A.; Margerum, D. W. Inorg. Chem. 1981, 20, 3143.
31. Ahmed, A. K. S.; Wilkins, R. G. Proc. Chem. Soc. 1959, 399.
32. Ahmed, A. K. S.; Wilkins, R. G. J. Chem. Soc. 1959, 3700.
33. Ahmed, A. K. S.; Wilkins, R. G. J. Chem. Soc. 1960, 2895.
34. Wilkins, R. G. "The Study of Kinetics and Mechanism of Reactions of Transition Metal Complexes"; Allyn and Bacon: Boston, 1974; pp 108-110, 205-206.
35. Bannister, C. E.; Margerum, D. W.; Raycheba, J. M. T.; Wong, L. F. Faraday Sym. Chem. Soc. 1975, 10, 78.
36. Wong, L. F.; Cooper, J. C.; Margerum, D. W. J. Am. Chem. Soc. 1976, 98, 7268.
37. Billo, E. J.; Margerum, D. W. J. Am. Chem. Soc. 1970, 92, 6811.
38. Bannister, C. E.; Margerum, D. W. Inorg. Chem. 1981, 20, 3149.
39. Margerum, D. W.; Dukes, G. R. "Metal Ions in Biological Systems", Sigel, H., Ed.; Marcel Dekker: New York, 1974; Vol. 1, p 157.
40. Wang, Y. H. C.; Margerum, D. W., to be published.
41. Eigen, M. Angew. Chem. Int. Ed. 1964, 3, 1.
42. Pagenkopf, G. K.; Margerum, D. W. J. Am. Chem. Soc., 1968, 90, 6963.
43. Youngblood, M. P.; Margerum, D. W. Inorg. Chem. 1980, 19, 3072.
44. Bannister, C. E.; Margerum, D. W., to be published.

45. Schwederski, B.; Raycheba, J. M. T.; Margerum, D. W., to be published.
46. Hauer, H.; Billo, E. J.; Margerum, D. W. J. Am. Chem. Soc. 1971, 93, 4173.
47. Hamburg, A. W.; Margerum, D. W., to be published.

RECEIVED April 5, 1982.

General Discussion—Substitution Reactions of Chelates

Leader: Cooper H. Langford

DR. COOPER LANGFORD (Concordia University): I would like to comment on the significance of the apparent, and I think quite real, success of the Eigen-Wilkins mechanism in organizing a great deal of data. It seems to me that the important point to be noted is that this mechanism underlines an important difference between the typical behavior of octahedral complexes and the square-planar or tetrahedral systems. The leaving ligand is a critically important one in the octahedral complex and can't be overwhelmed by other groups. If you will, in the octahedral complex, the leaving group determines the ballpark in which you play, even if the entering group may determine who wins the game. That certainly is not true for tetrahedral cases, where variations in the entering group can move you from one end of the league to the other.

Now, if we want to understand that, I suggest we begin to move into a territory which is under-explored. Something which we might call the Ingold-Hughes-Tobe-Basolo-Pearson-Eigen-Wilkins-Langford-Gray myopia has implicitly defined the reaction coordinate for substitution reactions. That implicit definition is based on the emphasis that is given to the relative role of the entering and leaving groups, with the comparative neglect of the other ligands.

One of the conclusions that one may draw from the talk which Dr. Margerum has given us here is the lesson from chelate systems, showing the very important role played by other parts of the molecule in determining what the reaction coordinate really looks like. This is something that has interested us a good deal since we tried some years ago to compare the differences in the substitution rates for the halopentaammine chromium complexes and the halopentaaquo chromium complexes.

One specific question which I would like to address to Dr. Margerum concerns the very interesting series of substitution reactions for the polypeptide complexes that are of similar stability and yet exhibit remarkably different substitution rates. What would you say about the implications of that observation for the formation processes of the copper polypeptide complexes?

DR. MARGERUM: We are now looking at those kinetics. There is a significant effect on the rates of formation and rates of dissociation of these complexes in the aquo replacement reactions, but perhaps not as great as for the polyamine substitution reactions.

DR. RALPH WILKINS (New Mexico State University): What is the rate of the reaction of trien with your copper macrocyclic tetrapeptide complex? Based on your mechanism it should be

extremely slow if you are worrying about getting a foothold for the trien.

DR. MARGERUM: Yes. I didn't show those data but we have a system in which a macrocyclic tetrapeptide is coordinated to copper and we have looked at its reaction with trien [Rybka, J. S.; Margerum, D. W. Inorg. Chem. 1980, 19, 2784]. The trien will not react until we protonate a group, even in basic solutions, and this rate constant is 10^{-3} s^{-1} . So, in order for the incoming trien ligand to obtain a foothold, a solvent molecule must first replace one of the peptide groups.

DR. WILKINS: You mean you have three groups of the macrocycle coordinated and one free?

DR. MARGERUM: Right. The macrocyclic complex first adds a proton following which trien reacts to form a mixed complex. The latter species then reacts with solvent to become further protonated before trien replaces the cyclic peptide.

DR. WILKINS: The other question is as follows: It seems quite clear that the first bond formation step is rate-determining for many metal ions reacting with terpyridine in aqueous solution. In fact, Robinson and White [J. Chem. Soc., Faraday Trans. 1978, 2625] recently looked at nickel reacting with PADA in which they used a photochemical perturbation. They managed to build up a large amount of the intermediate with one end only of PADA coordinated and actually measured intrinsically the rate constant for ring closure. Although there was a slight amount of competition, the substitution of the first donor atom into the inner-coordination sphere is rate-determining.

Now, a couple years ago Brown, Howarth, Moore, and Parr [J. Chem. Soc., Dalton Trans. 1978, 1776] looked at $\text{Al}(\text{DMSO})_6^{3+}$ reacting with terpyridine. By using a very neat NMR method, they could unambiguously show that the first nitrogen donor atom going on was quite rapid -- requiring the use of the flow NMR -- the second nitrogen substitution was much slower, and the third nitrogen substitution exhibited a half life of 20 minutes or so at much higher temperatures. I am intrigued by that, and I wonder what you feel about the mechanism where the substitution of the third donor atom is so much slower than the first one in the context of this talk.

DR. MARGERUM: I can't explain that. But it is an interesting observation.

DR. RAMESH PATEL (Clarkson College): I have a question on the comparison you showed for manganese that seems to react by

an associative mechanism. Now, manganese has been a very popular candidate for the replacement of magnesium, which very clearly does react by a dissociative mechanism. In view of the importance of replacement of magnesium by manganese in many biological processes, can you think of possibilities in which this associative factor can be used to an advantage to get additional information?

DR. MARGERUM: As Merbach points out in his paper -- and, of course, that is Merbach's work which I quoted here -- the substitution behavior is not greatly different for manganese relative to the other divalent metal ions, even though he clearly identified its mode of substitution as an associative phenomenon. From that point of view, one might not have a great deal of luck. But I can't give you examples.

DR. DAVID PENNINGTON (Baylor University): In regard to this question about the differences in reactive behavior between manganese and magnesium, it is conceivable that, within the pH range where such substitutions are measured for manganese, one is dealing with a partially hydrolyzed manganese species. I think Swaddle in his talk later will discuss the fact that there is, perhaps, a difference in the volumes of activation for the hexaquo versus the hydroxopentaaquo complexes.

DR. PATEL: I was referring to the low pH region where such hydrolyzed species should not be significant.

DR. KENNETH KUSTIN (Brandeis University): Some years ago, you studied reactions of the type $\text{MX} + \text{Y} = \text{MY} + \text{X}$ and found some interesting effects, such as chain reactions and phenomena of that sort. You also found that there was autocatalysis of such ligand substitution reactions by, I believe, triglycine. Has that turned up again? Are other tripeptides or polypeptides autocatalytic? How does that fit in with the base catalysis concept?

DR. MARGERUM: Yes, it does turn up in a number of instances. The example you are talking about was an EDTA reaction with a copper triglycine in which the released triglycine catalyzed the substitution of the EDTA. This resulted from the fact that the bis-triglycine complex is faster to undergo substitution than is the mono complex. The released triglycine formed a bis complex and the EDTA then attacked that.

This again is a consequence of a steric effect in substitution which is not very well understood, but I think is very evident. One of the slight discouragements about studying these systems is that, if one gets into a system that has general acid catalysis, one has to vary the buffer concentration at each pH to find out what is really happening. This significantly in-

creases the amount of work which one has to do to reach the correct mechanistic conclusions.

If one encounters an additional effect, such as a situation in which the ligand that is released also catalyzes the reaction, another entire series of experiments is mandated. We went to computerized flow systems a number of years ago in order to overcome some of these intrinsic problems.

DR. DAVID RORABACHER (Wayne State University): As Dr. Margerum has just pointed out, the increase in the number of experiments one needs expands dramatically as one encounters kinetic contributions from other species in the reaction mixture. We have recently encountered such a phenomenon in our laboratory which merits some comment within this context. This phenomenon involves an effect of so-called inert anions upon complex formation and dissociation kinetics which we find very disturbing. The implication of this phenomenon is that now, not only is it necessary to vary the concentration of the buffer along with the concentrations of reactants and products, but one must also vary the concentration of every other species in the system.

The systems with which we have been working involve aquo-copper(II) ion reacting with a series of cyclic and open-chain polythioether ligands, each with four or more donor atoms. We first noticed that, as one increases the concentration of "inert" anions, such as ClO_4^- , BF_4^- , and CF_3SO_3^- , the stability of the copper polythioether complexes also appears to increase [Sokol, L. S. W. L.; Ochrymowycz, L. A.; Rorabacher, D. B. *Inorg. Chem.* 1981, 20, 3189]. Kinetic studies have revealed that, as one increases the perchlorate concentration, the formation rate constants increase slightly while the dissociation rate constant exhibits a marked decrease.

Originally, we were unable to explain this type of behavior in any satisfactory manner. But, some careful equilibrium measurements in our laboratory have finally given us the clue as to what is happening. The Cu^{2+} ion first forms a complex with the polythioether ligand following which the complex forms an association with the anion. The resulting ternary complex appears to be a more stable species than the Cu(II) polythioether complex alone.

The nature of the ternary species is unclear but the addition of perchlorate to the complex causes no detectable shift in the position of the peaks in the visible spectrum. This may indicate that the anion effect involves an outer-sphere association or it may involve a weak axial inner-sphere coordination.

Whatever the nature of this interaction may be, we find that, if we interpret the observed dissociation rate constant to arise from the contribution of two complex species, one having

an associated anion and one without, we obtain a linear relationship when we plot the reciprocal of the observed dissociation rate constants against the appropriate function of the perchlorate concentration. As a result, we are able to resolve the two individual dissociation rate constants from the slope and intercept.

If this should be a general phenomenon, it is something that we all need to look for. With systems which involve charged ligands, of course, the effect will be greatly masked by ionic strength effects since it is impossible to vary the anion without altering the ionic strength. Furthermore, if the ligand being studied undergoes protonation, this anion phenomenon will be somewhat masked by the changes in the protonation constants as a function of the ionic strength and the protonation constants will have to be determined for each ionic strength studied. It is obvious that if one has several such phenomena contributing to the observed kinetics, the number of required experiments becomes rather immense.

The existence of such anion effects also implies that, if one wishes to do temperature studies, one cannot simply sit at a constant ionic strength and obtain meaningful activation parameters, because the equilibrium constant involving the association with the anion will also change, of course, as one varies the temperature. Thus, it is necessary to resolve out each rate constant at each temperature and then do the temperature dependencies on individual rate constants.

We also encountered the latter type of problem a number of years ago when we were doing solvent studies. Our studies involved the determination of the effect of solvent composition on the formation and dissociation rate constants for the reactions of solvated divalent metal ions (such as Ni(II), Co(II), or Cu(II)) with ammonia to form the 1:1 complex. In a mixed solvent system, such as methanol-water, a large number of solvated metal ion species coexist including the species with six coordinated waters, the species with five waters and one methanol, etc., as the solvent composition was varied from pure water to pure methanol. For the reactions involving solvated nickel or cobalt, we observed a maximum in the formation rate constant at a solvent composition corresponding to the insertion of a single methanol into the inner-coordination sphere. But the point at which this maximum occurs changes with temperature. So, again, one has to resolve out all of the rate constants for each of the solvated species at each temperature and then determine the temperature dependencies on these individual rate constants. To obtain such data, one must first determine the ligand protonation constants and the complex stability constants for each solvent composition at each temperature studied as well as the equilibrium constants for the various solvated species at each temperature. The amount of work required to resolve such a system properly is obviously enormous.

Both the solvent effects and the anion effects represent extensions of the under-investigated areas which Dr. Margerum was talking about. But these effects are somewhat frightening from the standpoint of the amount of data that one is going to have to collect in order to evaluate the contributions of these phenomena. If several of these effects occur at once, the problem may become so immense that it will be impossible to resolve out all the contributing parameters. But perhaps the most important point to note is that temperature studies carried out under constant conditions of buffer concentration, anion concentration, solvent composition, etc., yield activation parameters which are virtually meaningless when such competing reactions are present.

DR. JACK VRIESEN (Syracuse University): I would like to put forth the idea that mechanistic substitution chemistry has reached an impasse. And the impasse really derives from the lack of available techniques which are capable of determining specific stereochemistry on a short time scale. We have been working on one approach to circumvent this difficulty, involving the nmr of paramagnetic complexes. Thus far we have had a great deal of success in being able to observe a large number of species and look at all the different isomers and all the different isomerization rates.

As a particular example, we have been looking at Co(II) complexes where we can vary the number of coordinated pyridine molecules and look at the inner-sphere solvent exchange rates in methanol. We have observed both trans effects and cis effects on solvent exchange rates which are quite dramatic, varying by orders of magnitude. On top of that, several strange phenomena have been observed. For example, where one would expect the trans bis-complex to be more stable, the cis complex is actually more stable. In the case of tris complexes, the isomerization between cis and trans (i.e., facial and orthogonal) isomers is dominated by only certain solvent exchange sites. There are also indications that we have a wide variety of reaction intermediates, depending on which coordination site is lost.

With the advent of techniques such as this, I believe that in the next ten years our understanding of substitution kinetics is going to take a giant step forward. We are going to be able to make observations which the organic chemist is able to make now, that is, take an instantaneous snapshot of the relative arrangement of the atoms in the complex, and draw mechanistic conclusions based on stereochemistry.

DR. WILLIAM WOODRUFF (University of Texas at Austin): I'd like to make a brief comment in a similar manner which applies to both substitution and electron transfer reactions. By and large, I think mechanistic inorganic chemists lack the equipment to study reaction rates in the subnanosecond time range. Yet

there are some very important reactions that take place in that time frame: geminate recombinations, intramolecular electron transfers, etc.

We need to be aware of the instrumentation that is required to make such measurements. It is extremely expensive just as the sophisticated nmr spectrometers are. However, studies need to be made on the important fundamental processes which occur within that time domain. Therefore, it is essential that many investigators learn to employ the new technology.

DR. LANGFORD: I would like to make a small pitch for another complication in our lives, colloidal media, which, as we shall hear later on in this conference, are becoming fairly fashionable in other types of studies. The use of colloidal media is something that perhaps should also become a bit more fashionable in substitution studies. There is, in fact, a substantial group of clients for the results of such work, which, to the student of substitution mechanisms, must sound like a remarkable circumstance. This group of clients includes the environmental and geochemists, who have been making very simplified models of the nature of complex species in natural water systems. The ligands with which they work are really fearsome. The simplified models are almost certainly wrong, but I don't think that point is going to be well understood until some serious mechanistic work has been done.

As an illustration, we have collected a few rate constants for the reaction of sulfosalicylic acid with an iron complex of a simple soil organic material, fulvic acid. We find several kinetic terms when iron(III) is simply equilibrated with this material and some of the rate constants change when the samples have been filtered.

If one wants to understand why such changes occur, one can look at a few of the basic equilibrium properties of such complexes. Figure 1 illustrates the trends which occur when a sample is titrated with copper, monitoring three different parameters. The black dots indicate the relative amount of bound copper as indicated by free copper ions sensed with an ion-selective electrode (X_c of left ordinate). The triangles represent the change of the absorbance of the solution at 465 nm (right ordinate). The curve with the open circles is the relative quenching of the fulvic acid fluorescence (Q of left ordinate). We see that we are able to probe several different types of sites with different types of probes for this multidentate system.

If one really wants to understand just how nasty this system is, one can look at what has been happening to the light scattering of that same sample as one titrates it with copper. The resulting data indicate that the metal ion induces aggregation.

The study of colloidal systems may be a little frightening, but I think it also represents a very interesting area.

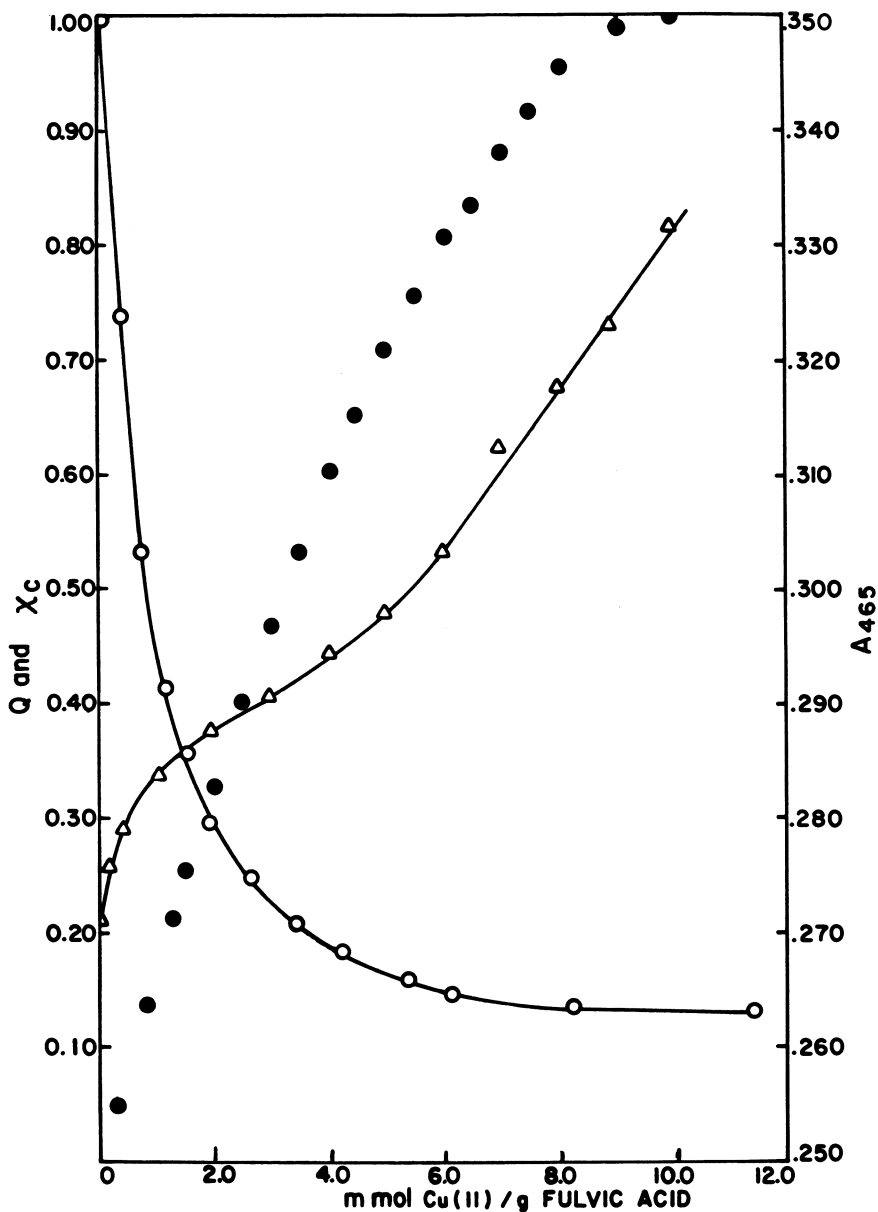


Figure 1. Trends in three experimentally observed parameters during a titration of fulvic acid with Cu(II) ion. Key: ●, relative amount of bound Cu ion (X_c of left ordinate); △, absorbance of the solution at 465 nm (right ordinate); and ○, relative quenching of the fulvic acid fluorescence (Q of left ordinate).

Pressure Effects and Substitution Mechanisms

T. W. SWADDLE

University of Calgary, Department of Chemistry, Calgary, Alberta, T2N 1N4
Canada

An attempt is made to account quantitatively for the volumes of activation, ΔV^* , of ligand substitution processes. Causes of the pressure-dependence of ΔV^* include solvational change, for which a versatile analysis is developed. The pressure-independent ΔV^* values of solvent exchange reactions are good measures of the non-solvational components of ΔV^* for related net reactions. For water exchange, one can predict $-7 \lesssim \Delta V^* < 0$ for I_a and $0 < \Delta V^* \lesssim +7$ for I_d processes, with satisfactory correlation with independent mechanistic assignments. The molal volumes of the transition states for series of water exchange reactions ($M^{2+}(aq)$, $M^{3+}(aq)$, $M(NH_3)_5-OH_2^{3+}$) are insensitive to the nature of M; the kinetic characteristics are governed mainly by initial, not transition, state properties.

It is customary to justify the study of pressure effects on reaction rates on the grounds that it can elucidate reaction mechanisms. A somewhat different and, I think, more constructive viewpoint is that pressure effects constitute important natural phenomena in themselves, and that our comprehension of reaction kinetics is incomplete if it does not enable us to understand the effects of pressure on reaction rates.

In this spirit, an attempt will be made to account for the magnitude of pressure effects on ligand substitution reaction rates. Attention will necessarily be confined to a few simple model systems; two recent reviews (1, 2) of pressure effects on reactions of transition metal complexes in solution may be consulted for more comprehensive surveys of the field.

0097-6156/82/0198-0039\$07.00/0
© 1982 American Chemical Society

Kinetics in Relation to Thermodynamics

A central theme of our work in Calgary has been to seek connections between equilibrium and kinetic properties--that is, between thermodynamic and extrathermodynamic quantities (3). An equilibrium constant K is governed by

$$(\partial \ln K/\partial P)_T = -\Delta V/RT \quad (1)$$

where the volume of reaction ΔV may be independently measured by dilatometry, or from the algebraic sum of the partial molal volumes \bar{V} of products and reactants, which can also be determined independently.

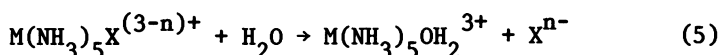
$$\Delta V = \Sigma \bar{V}(\text{products}) - \Sigma \bar{V}(\text{reactants}) \quad (2)$$

In kinetics, similar relationships apply, but the volume of activation ΔV^* can be determined only from the pressure dependence of the rate coefficient k , since the partial molal volumes \bar{V}^* of transition states are not directly measurable. Conversely, however, equation 4 can yield values of \bar{V}^* .

$$(\partial \ln k/\partial P)_T = -\Delta V^*/RT \quad (3)$$

$$\Delta V^* = \bar{V}^* - \Sigma \bar{V}^*(\text{reactants}) \quad (4)$$

Some of our first publications in this field (4 - 6) dealt with the linear correlations that exist between ΔV^* and ΔV for reactions of the type



where $M = \text{Co}$ or Cr . We have recently repeated some of that work in greater detail (7). It was confirmed that ΔV^* for reaction 5 can be markedly pressure-dependent when $n = 1$ or 2 , i.e., $\ln k$ is then not a linear function of P . However, $\ln k$ is strictly a linear function of P , within experimental uncertainty, for all single-path solvent exchange reactions studied to date (e.g., $X^{n-} = \text{H}_2\text{O}$ in eq. 5). This is illustrated in Figure 1; the exchange of N,N -dimethylformamide (DMF) solvent on chromium(III) was chosen for the comparison simply because the 400 MPa capacity of our equipment was fully exploited.

Pressure Dependence of Volumes of Activation

When, and how, does this pressure-dependence of ΔV^* arise? Empirically, we find four reaction types which give non-linear $\ln k$ vs. P plots.

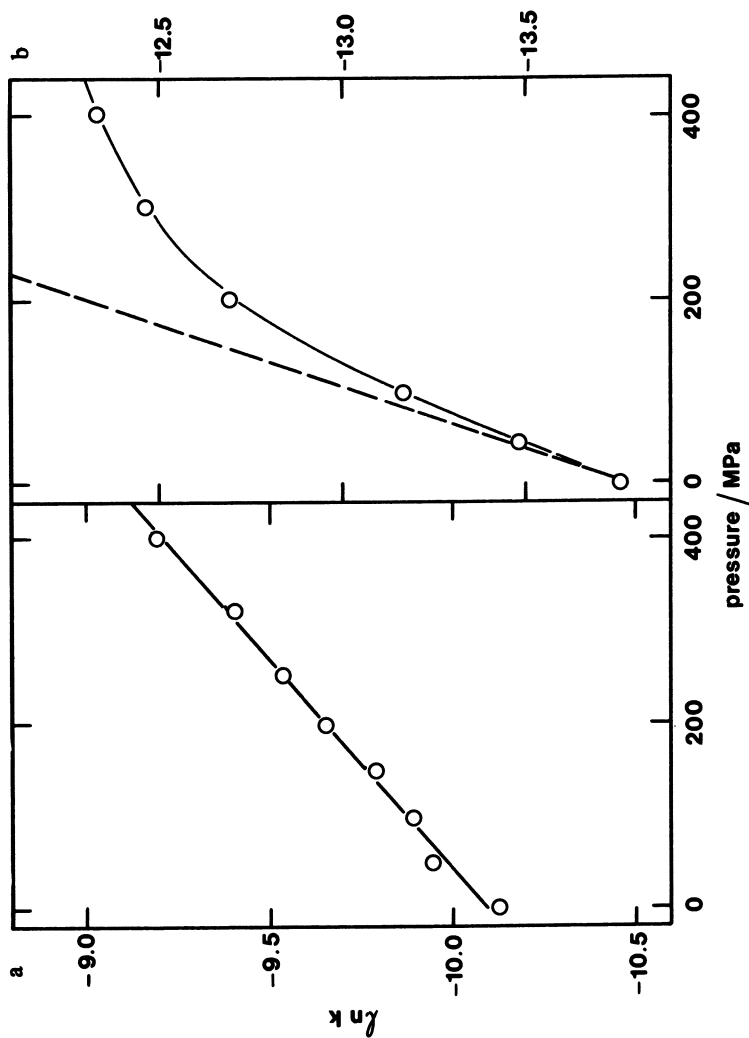
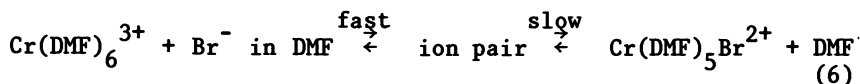


Figure 1. Constancy of ΔV^\ddagger for solvent exchange reactions where $\Delta V^\ddagger = -6.3 \text{ cm}^3/\text{mol}$ for $\text{Cr}(\text{DMF})_6^{3+}$ -DMF solvent exchange at 338 K (a); and pressure dependence of ΔV^\ddagger for reactions involving charge development and, hence, solvational change where $\Delta V^\ddagger = -18.5 \text{ cm}^3/\text{mol}$ for $\text{Co}(\text{NH}_3)_6\text{SO}_4^{2+}$ direct aquation at 298 K (b).

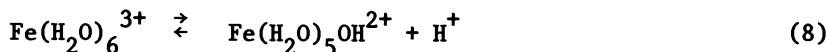
(a) Multi-step or incomplete reactions, e.g., bromide ion ligation of $\text{Cr}(\text{DMF})_6^{3+}$ in DMF, in which the ion pairing is almost complete at $\sim 0.1 \text{ mol kg}^{-1} \text{ Br}^-$ at atmospheric pressure but progressively less complete, leading to incompleteness of the overall reaction, as the pressure is raised.



(b) Reactions proceeding by parallel pathways of different ΔV^\ddagger , as in the exchange of water on iron(III) in acidic aqueous solution (8). Figure 2 shows that this is governed by a two-term rate law

$$k = k_1 + k_2[\text{H}^+]^{-1} \quad (7)$$

in which the acid-independent rate is increased, and the inversely-acid-dependent rate reduced, by applied pressure. In Figure 3, $\ln k_1$ and $\ln k_2$ are seen to be linear functions of P , giving $\Delta V_1^\ddagger = -5.4$ and $\Delta V_2^\ddagger = +7.8 \text{ cm}^3 \text{ mol}^{-1}$, respectively, but the combined rate represented by $\ln k$ is non-linear in P , and at acidities around 1.5 mol kg^{-1} $\ln k$ first falls, then rises with increasing pressure as the k_2 term is progressively "squeezed out". From optical measurements under pressure, we find $\Delta V = +0.8 \text{ cm}^3 \text{ mol}^{-1}$ for the equilibrium



so that ΔV^\ddagger for water exchange on $\text{Fe}(\text{H}_2\text{O})_6^{3+}$ and $\text{Fe}(\text{H}_2\text{O})_5\text{OH}^{2+}$ is -5.4 and $+7.0 \text{ cm}^3 \text{ mol}^{-1}$, respectively.

(c) Reactions involving stereochemical change in chelate complexes, as in the trans→cis isomerization of $\text{Co}(\text{en})_2(\text{OH}_2)_2^{3+}$ (9) which has a large, positive, pressure-dependent ΔV^\ddagger while stereoretentive water exchange on the trans-complex has a smaller, pressure-independent ΔV^\ddagger (10). This suggests a "sweeping aside" of solvating water during the reorganization of the chelate ring positions during isomerization, and might be regarded as a special case of category (d).

(d) Reactions involving significant solvational change between the initial and transition states, as in reaction 5, in which an additional x molecules of water are needed to solvate the incipient $3+$ and $n-$ ions in the transition state. One can regard

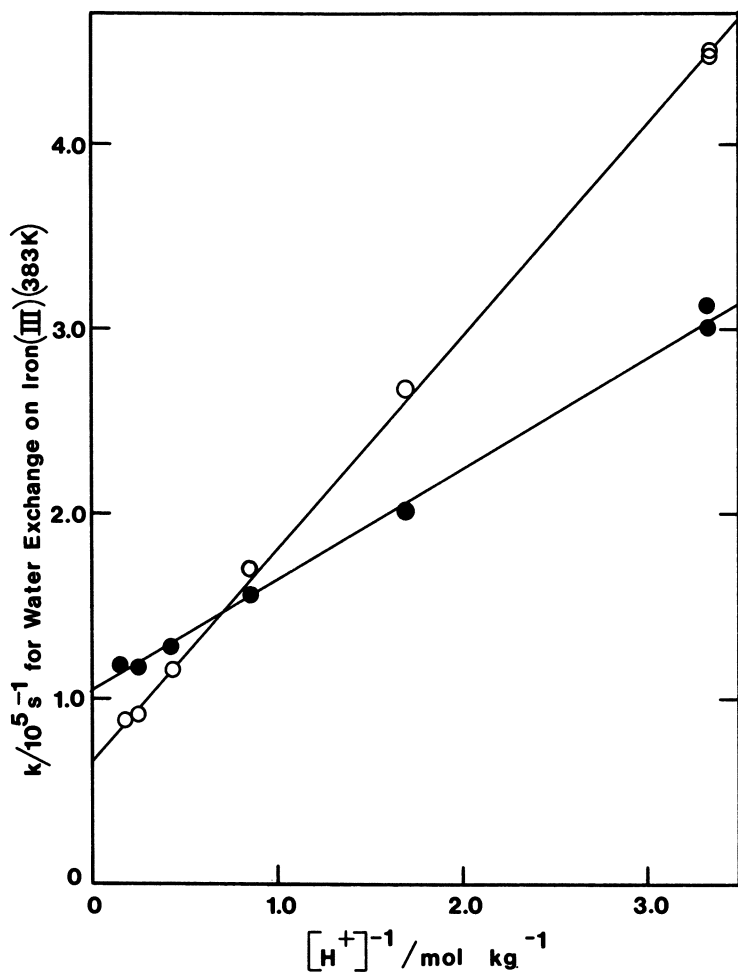


Figure 2. Hydrogen ion dependence of the rate of exchange of H_2O on $Fe(III)$ in H_2O . Conditions: 382.8 K; ionic strength, 6.0 mol/kg; and 0.1 (○) and 240 MPa (●).

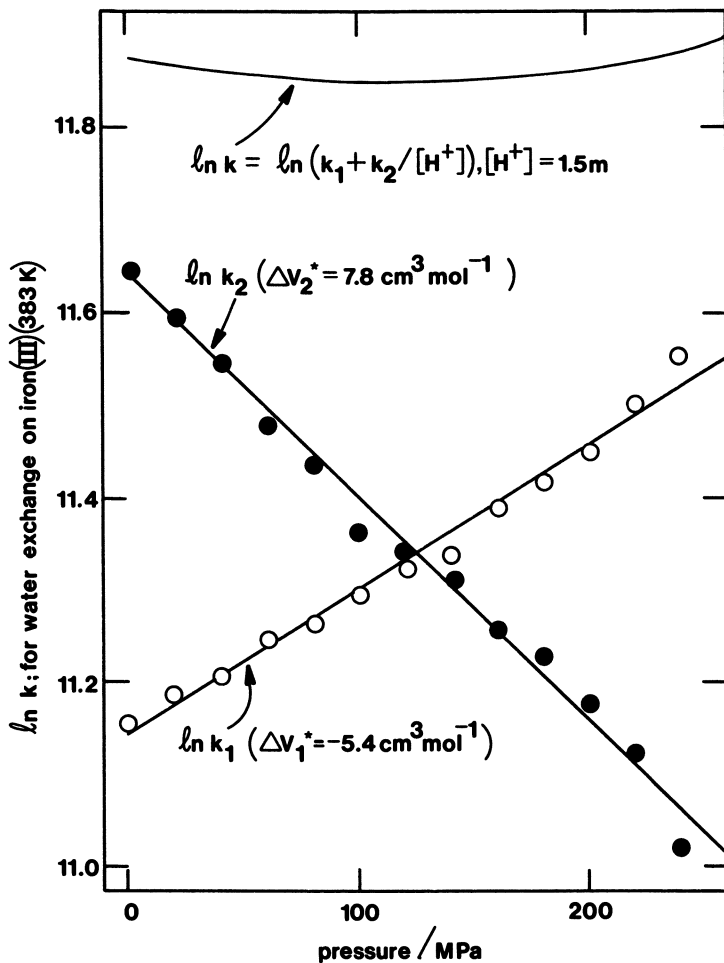


Figure 3. Pressure dependence of the acid independent (k_1) and inversely acid dependent (k_2) components of the rate coefficient for H_2O exchange on $\text{Fe}(\text{III})$ at 382.8 K, ionic strength 6.0 mol/kg.

ΔV^* as the sum of an intrinsic part, ΔV_{int}^* , which is made up of bond-making or -breaking and similar terms, and a solvational part, ΔV_{sol}^* . ΔV_{sol}^* can be so large as to swamp ΔV_{int}^* completely; this may make the extraction of information on the intimate mechanism difficult, but conversely it can provide special insights into solvational factors.

Analysis in terms of solvational change

The key assumption to be made in interpreting the pressure data in terms of solvational change is that neither the ligands in the first coordination sphere of the complex nor the solvating solvent molecules are significantly compressible relative to bulk solvent (volume V^s), the compression of which is described by the modified Tait equation

$$(V_0^s - V_p^s)/V_0^s = \rho \log_{10}(1 + P/\Pi) \quad (9)$$

in which ρ and Π are empirical constants characteristic of the solvent (they can, however, be given a theoretical basis (11)). The validity of this assumption is demonstrated by Stranks' theoretical calculations (12), but can also be supported by reference to compressibility data for ionic solids relative to those for liquids (the former being less than 10% of the latter) since the complex ion can be regarded, in crystal field fashion, as a fragment of an ionic crystal lattice. Further, the molal compressibilities of aqueous ions are negative (e.g., about $-0.07 \text{ cm}^3 \text{ mol}^{-1} \text{ MPa}^{-1}$ for typical $M^{2+}(\text{aq})$ at 298 K), because water taken into the solvational shell of the ion loses some 90% of its compressibility. It follows that ΔV_{int}^* will be virtually independent of pressure, but any solvational change will lead to a significant and pressure-dependent ΔV_{sol}^* contribution. Equations 3 and 9 then lead (5) to eq 10

$$\ln k = \ln k_0 - P\Delta V_0^*/RT - xV^s\rho\{(\Pi+P)\ln(1+P/\Pi) - P\} \quad (10)$$

in which the curvature of the $\ln k$ vs. P plot resides in the last term. This term gives the single parameter x , the gain in the number of solvating molecules, and, incidentally, is roughly proportional to P^2 at relatively low pressures, so that a simple quadratic in P often gives a good empirical fit of kinetic data (13).

Figure 4 shows that, for reaction 5 with $M = \text{Co}$ or Cr , the zero-pressure volume of activation correlates with the solvational gain x with a slope of $-2.5 \text{ cm}^3 \text{ mol}^{-1}$ for both series. The slope represents the volume change per mole of

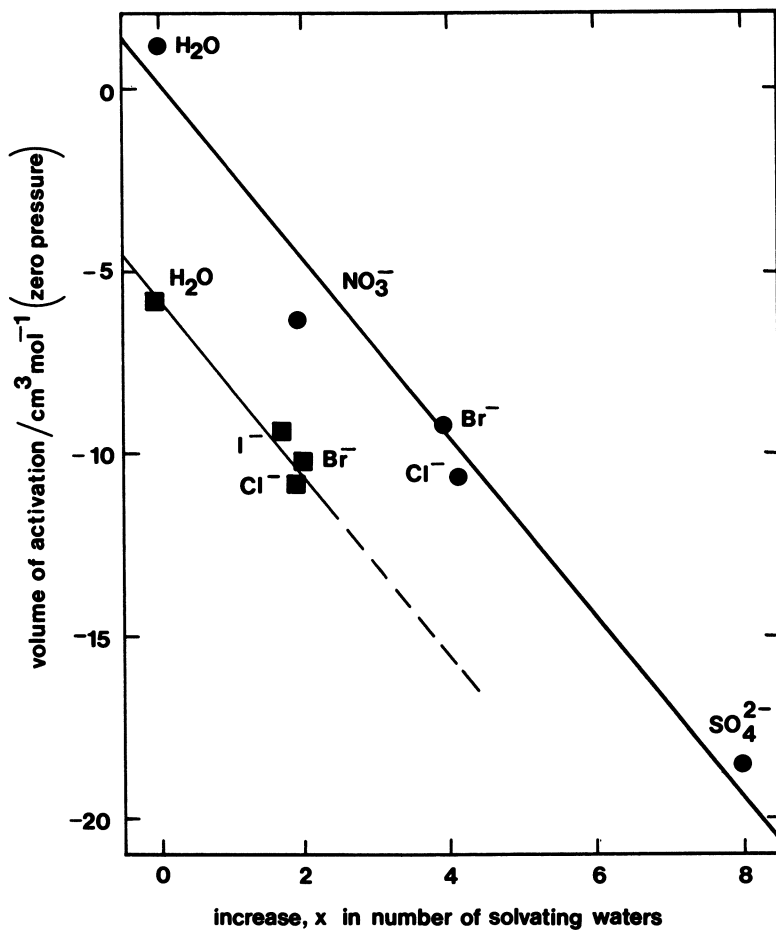


Figure 4. Correlation between ΔV_0^\ddagger and solvational change, x (Eq. 10). Key for aquation of amines: \blacksquare , $\text{Cr}(\text{NH}_3)_5\text{X}^{(3-n)+}$; and \bullet , $\text{Cr}(\text{NH}_3)_5\text{X}^{(3-n)+}$. Conditions: 25°C and slopes ~ -2.5 .

solvating water added to the outer (second, etc.) coordination sphere or solvation sheath. This compares well with the results of static methods of estimating the mean volume change per water molecule involved in hydrating M^{2+} ions in water (-3.2 (14), -3.3 (15), -2.7 (16), -2.1 (17)). Clearly, the total ΔV_{sol}^* is -2.5 x, and for the Co(III) series this almost completely overwhelms ΔV_{int}^* except in the exchange case (18). The existence of these linear correlations implies that ΔV_{int}^* is roughly the same throughout each series, being represented by the intercept at $x = 0$; thus, the pressure-independent ΔV^* values for solvent exchange give a good measure of ΔV_{int}^* for each series. The negative ΔV_{int}^* for the Cr(III) series reflects associative activation; the very slightly positive ΔV_{int}^* for the Co(III) complexes is consistent with an I_d mechanism.

As a check on the validity of this analysis based on eq. 10, one can compute the temperature dependence of ΔV_0^* on the assumption (cf., compressibility) that the thermal expansivities of coordinated or solvating molecules are small compared with that of the bulk solvent, so that $-(\partial \Delta V_0^*/\partial T)_p$ should be given by x times the molar expansivity of water. For the direct aquation of $Co(NH_3)_5SO_4^+$, pressure effects give $x = 8$, whence $(\partial \Delta V_0^*/\partial T)_p$ should be about $-0.06 \text{ cm}^3 \text{ mol}^{-1} \text{ K}^{-1}$; the measured value (7) is -0.07 ± 0.03 .

Establishment of likely limits to ΔV^* for water exchange

If we consider water molecules to be spheres of radius 138 pm, then the molar volume of water in a closest-packed array is $9 \text{ cm}^3 \text{ mol}^{-1}$, and, furthermore, the octahedral interstices would be about the size of a typical M^{3+} ion. Thus, for "hard" metal ions in the "hard" solvent water (i.e., where the volumetric effects of covalent bonding are minimal), the volume change for an extreme dissociative (D) (19) process of water replacement in an octahedral complex should be the molar volume of bulk water less $9 \text{ cm}^3 \text{ mol}^{-1}$, which is just over $9 \text{ cm}^3 \text{ mol}^{-1}$ (20).

Indeed, Palmer and Kelm (21) found $\Delta V^* = +9 \text{ cm}^3 \text{ mol}^{-1}$ for the replacement of H_2O in aqueous $Co(CN)_5OH_2^{2-}$ by each of Br^- , I^- and NCS^- , the series of reactions which provides the classic Haim-Wilmarth example of the D mechanism.

For an associative mechanism (A) (19), the continued pres-

American Chemical
Society Library

1155 16th St. N. W.

In Mechanistic Aspects of Inorganic Reactions; Rorabacher, D., et al.; ACS Symposium Series, American Chemical Society, Washington, DC, 1982.

Washington, D. C. 20036

ence of the leaving group in the transition state complicates matters, but if the dominant feature is addition of H_2O to a vacant coordination site one can expect $\Delta V^* \sim -9 \text{ cm}^3 \text{ mol}^{-1}$; ΔV^* for the aquation of $Pt(\text{dien})Cl^+$ and $Pt(\text{dien})Br^+$ is -10 and $-9.5 \text{ cm}^3 \text{ mol}^{-1}$, respectively (22).

For water exchange by an interchange mechanism (19), water is transferred between the first and outer coordination spheres in temporal isolation from bulk solvent. We have₃ seen that water in the outer sphere has a molar volume 2.5 cm^3 less than for bulk water; thus, the maximum value of $|\Delta V^*|$ for water exchange will be $(18 - 2.5) - 9$ or about $7 \text{ cm}^3 \text{ mol}^{-1}$. According to the "pressure-coordination rule" of Gutmann and Mayer (20, 23), an increase in primary coordination number is always favored by increasing the pressure, despite any increase in nearest-neighbor distances; conversely, applied pressure works to suppress any reduction in primary coordination number. Thus, we can expect:

- for associative interchange (I_a), $-7 < \Delta V^* < 0 \text{ cm}^3 \text{ mol}^{-1}$
- for dissociative interchange (I_d), $0 < \Delta V^* < +7 \text{ cm}^3 \text{ mol}^{-1}$

To test this, we list in Table I all those water-exchange reactions of metal ions for which a positive ΔV^* has been found.

Table I

Pressure-decelerated water exchange reactions and evidence for dissociative interchange in corresponding net substitution reactions

ML_5^{n+} in $ML_5OH_2^{n+}$	ΔV^* for H_2O -exchange $/\text{cm}^3 \text{ mol}^{-1}$	Dependence of ligation rate on nucleophile ^a
$Ni(H_2O)_5^{2+}$	+7.2 (25)	very slight
$Co(H_2O)_5^{2+}$	+6.1 (25)	very slight
$Fe(H_2O)_5^{2+}$	+3.8 (25)	negligible?
$Fe(H_2O)_4OH^{2+}$	+7.0 (8)	$R = 0.9$
$Co(NH_3)_5^{3+}$	+1.2 (18)	$R = 0.5$
$t\text{-Co(en)}_2OH_2^{3+}$	+5.8 (10)	

^a $R =$ relative rate of ligation, NCS^-/Cl^-

In the last column, the Langford-Gray criterion (19) for the I_d mechanism for the corresponding net substitution reactions is shown to be met in virtually all cases, although data for Fe(II) are sparse. Where applicable, Sasaki and Sykes' version (24) of the Langford-Gray criterion is used, viz., that R , the rate of attack of NCS^- relative to Cl^- , should be close to (in practice, slightly less than) unity in an I_d reaction, disregarding ion pairing. For the $Co^{III}(NH_3)_5$ case, ΔV^* for water exchange (and, indeed, ΔV_{int}^* for reaction 5 in general) is just barely positive, but for $trans-Co(en)_2(OH_2)_2^{3+}$ it is closer to the predicted limit for an I_d process.

In Table II, markedly negative ΔV^* values for water ex-

Table II

Pressure-accelerated water exchange reactions and evidence for associative interchange in corresponding net substitution reactions

ML_5^{n+} in $ML_5OH_2^{n+}$	ΔV^* for H_2O -exchange $/cm^3 mol^{-1}$	Dependence of ligation rate on nucleophile
$Cr(H_2O)_5^{3+}$	-9.3 (26)	$R = 55$
$Fe(H_2O)_5^{3+}$	-5.4 (8)	$R = 19$
$Mn(H_2O)_5^{2+}$	-5.4 (25)	?
$Cr(NH_3)_5^{3+}$	-5.8 (27)	$R = 6$
$Rh(NH_3)_5^{3+}$	-4.1 (27)	$R = 0.6$
$Ir(NH_3)_5^{3+}$	-3.2 (28)	

change correlate with Sasaki-Sykes criteria for associative interchange in net substitution reactions in at least three instances (see (29) and (30) for commentaries on the $Cr^{III}(NH_3)_5$ case). Data for the very fast reactions of Mn(II) are limited, but the sensitivity of the rates to the nature of the nucleophile may well be slight, leading to an assignment of an I_d mechanism even if, as ΔV^* suggests, activation is associative (20, 25); the problem here may lie with the operational nature of the Langford-Gray and Sasaki-Sykes criteria (30). For the Rh(III) case, various lines of evidence suggest weak associative

activation (31), and the small R value might be related to the greater stability of the S-thiocyanato linkage isomer for Rh(III), but the assignment of mechanism in reactions of Rh(III) cations is undoubtedly going to remain debatable for some time.

The results of our recent study of water exchange on iron(III) (8), summarized above, strongly indicate a change in the mode of activation from associative to dissociative on removing a proton from $\text{Fe}(\text{H}_2\text{O})_6^{3+}$. This conclusion is not vulnerable to Langford's criticism of the mechanistic interpretation of ΔV^\ddagger (32) (that changes in the non-reacting metal-ligand bond lengths may influence ΔV^\ddagger materially), since all the bonds concerned are $\text{Fe}^{\text{III}}-\text{O}$. In addition, Table III shows that ΔV^\ddagger values for water exchange and for net substitution on the conjugate base $\text{Fe}(\text{H}_2\text{O})_5\text{OH}^{2+}$ are the same within the experimental uncertainty, as expected for a mechanism involving a common intermediate, $\text{Fe}(\text{H}_2\text{O})_4\text{OH}^{2+}(\text{aq})$. The generally negative and different ΔV^\ddagger values for substitution on $\text{Fe}(\text{H}_2\text{O})_6^{3+}$ itself serve to confirm associative activation in its reactions.

Table III

$\Delta V^\ddagger / (\text{cm}^3 \text{mol}^{-1})$ for reactions of $\text{Fe}^{3+}(\text{aq})$ with X^{n-}

X^{n-}	$\text{Fe}(\text{H}_2\text{O})_6^{3+}$	$\text{Fe}(\text{H}_2\text{O})_5\text{OH}^{2+}$	Ref.
Cl^-	-4.5	+7.8	(33)
Br^-	-8		(34)
NCS^-	~0	+7.1	(35)
H_2O	-5.4	+7.0	(8)

Non-Aqueous Solvent Exchange Reactions

It is unrealistic to treat molecules of solvents such as N,N-dimethylformamide (DMF) as spheres in estimating ΔV^\ddagger for solvent exchange as for water. One can, however, anticipate that solvents which have unusually open structures because of extensive hydrogen bonding (notably water) will lose a relatively large fraction of their molar volume V^s on coordination to a metal ion, whereas for dipolar aprotic solvents this fraction will be much less, with partially H-bonded solvents

such as alcohols coming in between. Indeed, Table IV shows that $|\Delta V^*|/V^S$ for solvent exchange decreases in the order water > alcohols > dipolar aprotic solvents, at least for ΔV^* values sufficiently removed from zero.

Nevertheless, the striking feature of Table IV is that ΔV^*

$\Delta V^*(\text{cm}^3 \text{mol}^{-1})$ for solvent exchange on M^{2+} in various solvents				
Solvent:	$\text{H}_2\text{O}^{\text{a}}$	$\text{CH}_3\text{OH}^{\text{b}}$	DMF^{c}	$\text{CH}_3\text{CN}^{\text{d}}$
$M = \text{Mn}^{2+}$	-5.4	-5.0	--	-7.0
Fe^{2+}	3.8	0.4	--	3.0
Co^{2+}	6.1	8.9	6.7	6.7
Ni^{2+}	7.2	11.4	9.1	7.3
$\Delta V^*(\text{Ni}^{2+})/V^S$	0.40	0.28	0.12	0.14
a From ^{17}O NMR (25)		b From ^1H NMR (36)		
c From ^1H NMR (37)		d From ^{14}N NMR (38)		

for solvent exchange varies relatively little with the solvent, but strongly with the metal. This lends credibility to attempts (20,25) to rationalize trends in ΔV^* for solvent exchange on the basis of the d-orbital occupancy, since this is the factor most characteristic of each metal ion. Thus it is argued (20) that associative activation may be taken as "normal" in octahedral complexes, but high interaxial (i.e., t_{2g}) electron densities work against the attainment of a 7-coordinate transition state because both the incoming and outgoing groups must move into interaxial space. We can, therefore, expect associative character to become more evident as we go from $\text{Ni(II)} \rightarrow \text{Co(II)} \rightarrow \text{Fe(II)} \rightarrow \text{Mn(II)}$ (high spin); $\text{Co}(\text{NH}_3)_5\text{X}^{(3-n)+} \rightarrow \text{Cr}(\text{NH}_3)_5\text{X}^{3-n+}$; Cr(III) to Mo(III) and W(III) (because 4d and 5d orbitals are more diffuse than 3d); low spin Co(III) to Rh(III) and Ir(III) ; etc. The degree of associative activation in Cr(III) and analogous high-spin Fe(III) complexes might be expected to be similar, both having t_{2g}^3 configurations, except that the two e_g electrons of the iron (III) will labilize the departing ligand so that the associative character will be somewhat reduced rela-

tive to Cr(III). In general, these expectations are supported by observation.

An Alternative Approach to Accounting for ΔV^* Values for Solvent Exchange Reactions

Figure 5 provides a clue to a different, basically non-mechanistic, way of rationalizing known ΔV^* values for solvent exchange and predicting new ones rather precisely. There is a reasonably good inverse linear correlation of ΔV^* for water exchange on M^{2+} ions of the first transition series with the corresponding partial molal volumes \bar{V}_M^0 of the aqueous ions themselves; the slope is about -1, and it seems that this would also be true for the $M^{3+}(\text{aq})$ ions of that series. What this means is that the sum of ΔV^* and \bar{V}_M^0 is essentially constant, or at least insensitive to the nature of M^{n+} , for a given series despite a wide range in ΔV^* . This sum is $-33 \pm 2 \text{ cm}^3 \text{ mol}^{-1}$ for $M^{2+}(\text{aq})$ and -66 ± 1 for $M^{3+}(\text{aq})$, based on infinite-dilution ionic partial molal volumes \bar{V}_M^0 (14, 39); for $M(\text{NH}_3)_5\text{OH}_2^{3+}(\text{aq})$, it is $56 \pm 2 \text{ cm}^3 \text{ mol}^{-1}$ based on ionic volumes \bar{V}_M at $[M] \sim 0.01 \text{ mol L}^{-1}$ (7). It follows from eq. 4 that this sum equals \bar{V}^* (the volume of the incoming water molecule can be ignored, being common throughout the series - it is, in any event, included in \bar{V}_M^0 for an interchange process). Thus, the molal volumes of the transition states within a given series of solvent exchange reactions are effectively the same regardless of the identity of the central ion.

This statement is based on limited data at present, but, if literally true, it permits us to predict ΔV^* for solvent exchange (and hence ΔV_{int}^* for net ligand substitution) from values of \bar{V}_M , many of which are already available (39); in principle, only one ΔV^* value per series need be measured. Even if all we can legitimately say is that \bar{V}^* is much less sensitive than ΔV^* to the nature of the central metal ion within a given series (and this seems assured), we still have gained an important insight - it is the properties of the initial state, and not the transition state, that determine in large part the kinetic characteristics of ligand substitution in a transition metal complex. This is welcome news, as we can obtain factual information regarding initial states directly by numerous experimental techniques, whereas discussions of transition state properties can never be better than hypothetical.

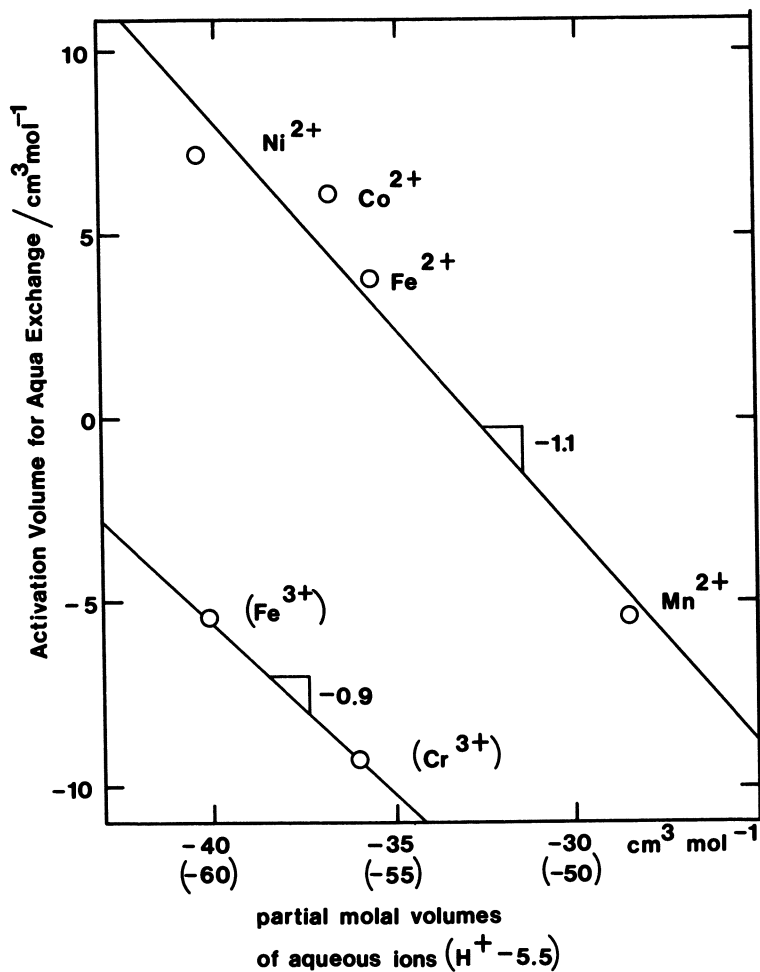


Figure 5. Correlation between ΔV^* for solvent exchange and \bar{V}° for ions of the first transition series.

These conclusions are independent of mechanistic considerations of the usual kind, and indeed provide a rationale for certain ΔV^* values near zero for solvent exchange without indecisive resort to the I_a/I_d dichotomy. One can, however, interpret the apparent constancy of \bar{V}^* to mean that the transition state of water exchange is a relatively unstructured high energy aggregate of water molecules held together by the centripetal field of an "anonymous" n^+ charge; only in the low-energy initial state do structures characteristic of the particular M^{n+} exist. Where such a structure is open (relatively positive \bar{V}_M), associative activation is possible; where it is tightly packed (low \bar{V}_M), activation tends to the dissociative limit. It may be better, however, to speak only of a collapse or expansion, respectively, of a structured ground state on going to a relatively unstructured transition state.

Acknowledgment

I thank the Natural Sciences and Engineering Research Council Canada for their continuing financial support of our work in this field.

Literature Cited

1. Palmer, D. A.; Kelm, H. Coord. Chem. Rev. 1981, 36, 89.
2. van Eldik, R.; Kelm, H. Rev. Phys. Chem. Japan 1980, 50, 185.
3. Swaddle, T. W. Coord. Chem. Rev. 1974, 17, 214.
4. Jones, W. E.; Swaddle, T. W. J. Chem. Soc. Chem. Commun. 1969, 998.
5. Jones, W. E.; Carey, L. R.; Swaddle, T. W. Can. J. Chem. 1972, 50, 2739.
6. Guastalla, G.; Swaddle, T. W. Can. J. Chem. 1973, 51, 821.
7. Sisley, M. J.; Swaddle, T. W. Inorg. Chem. 1981, 20, 2799.
8. Swaddle, T. W.; Merbach, A. E. Inorg. Chem., in press.
9. Stranks, D. R.; Vanderhoek, N. Inorg. Chem. 1976, 15, 2639.
10. Tong, S. B.; Krouse, H. R.; Swaddle, T. W. Inorg. Chem. 1976, 15, 2643.
11. Neece, G. A.; Squire, D. R. J. Phys. Chem. 1968, 72, 128.
12. Stranks, D. R. Pure Appl. Chem. 1974, 38, 303.
13. Lohmüller, R.; Macdonald, D. D.; Mackinnon, M.; Hyne, J. B. Can. J. Chem. 1978, 56, 1739.
14. LoSurdo, A.; Millero, F. J. J. Phys. Chem. 1980, 84, 710.
15. Shimizu, K. Bull. Chem. Soc. Japan 1979, 52, 2429.
16. Millero, F. J.; Ward, G. K.; Lepple, F. K.; Hoff, E. V. J. Phys. Chem. 1974, 78, 1636.

17. Padova, J. J. Chem. Phys. 1964, 40, 691.
18. Hunt, H. R.; Taube, H. J. Am. Chem. Soc. 1958, 80, 2642.
19. Langford, C. H.; Gray, H. B. "Ligand Substitution Processes"; Benjamin: New York, 1966.
20. Swaddle, T. W. Inorg. Chem. 1980, 19, 3203.
21. Palmer, D. A.; Kelm, H. Z. anorg. allgem. Chem. 1979, 450, 50.
22. Rindermann, W.; Palmer, D. A.; Kelm, H. Inorg. Chim. Acta 1980, 40, 179.
23. Gutmann, V.; Mayer, H. Struct. Bonding (Berlin) 1976, 31, 49.
24. Sasaki, Y.; Sykes, A. G. J. Chem. Soc. Dalton 1975, 1048.
25. Ducommun, Y.; Newman, K. E.; Merbach, A. E. Inorg. Chem. 1980, 19, 3696.
26. Stranks, D. R.; Swaddle, T. W. J. Am. Chem. Soc. 1971, 93, 2783.
27. Swaddle, T. W.; Stranks, D. R. J. Am. Chem. Soc. 1972, 94, 8357.
28. Tong, S. B.; Swaddle, T. W. Inorg. Chem. 1974, 13, 1538.
29. Ferrer, M.; Sykes, A. G. Inorg. Chem. 1976, 18, 3345.
30. Swaddle, T. W. Rev. Phys. Chem. Japan 1980, 50, 230.
31. Swaddle, T. W. Can. J. Chem. 1977, 55, 3166.
32. Langford, C. H. Inorg. Chem. 1979, 18, 3288.
33. Hasinoff, B. B. Can. J. Chem. 1976, 54, 1820.
34. Hasinoff, B. B. Can. J. Chem. 1979, 57, 77.
35. Jost, A. Ber. Bunsenges. phys. Chem. 1976, 80, 316.
36. Meyer, F. K.; Newman, K. E.; Merbach, A. E. J. Am. Chem. Soc. 1979, 101, 5588.
37. Meyer, F. K.; Newman, K. E.; Merbach, A. E. Inorg. Chem. 1979, 18, 2142.
38. Yano, Y.; Fairhurst, M. T.; Swaddle, T. W. Inorg. Chem. 1980, 19, 3267; and unpublished work with M. J. Sisley.
39. Millero, F. J. In "Water and Aqueous Solutions"; Horne, R. A., Ed.; Wiley-Interscience, New York, 1972; p.519.

RECEIVED April 5, 1982.

General Discussion—Pressure Effects and Substitution Mechanisms

Leader: Ramesh Patel

DR. KENNETH KUSTIN (Brandeis University): When a table or a chart contains only activation parameters, one loses sight of what is actually going on in the system. When you recall that the solvent exchange rate constant for Mn(II) is very large, I wonder if it is possible that the negative volume of activation might have nothing to do with the substitution process. It might simply reflect the fact that the substitution is so rapid that it overlaps with the formation rate of the ion pair, and you really couldn't distinguish the two steps in that case. So what you might be seeing is really some squeezing down on the ion pair formation, rather than the substitution itself, for a metal ion which is substituting at almost the diffusion controlled limit.

DR. SWADDLE: We are measuring the volume of activation for solvent exchange in a region where it is in the NMR time frame; in other words, where the NMR line broadening is exchange controlled, i.e., $k \approx 10^5 \text{ s}^{-1}$.

If one goes to still lower temperatures, one usually sees evidence for outer-sphere effects, which is what you are referring to. In the cases which I have discussed here, either one does not see any evidence for outer-sphere effects or else one can choose to operate in a region where the outer-sphere effects are known to be unimportant.

DR. RAMESH PATEL (Clarkson College): Couldn't one pick certain systems in which the ion pairing effect would be very large? One would then be able to make some comments about the influence of volume changes on ion pair formation for rapidly exchanging systems.

DR. SWADDLE: In the future, undoubtedly, we will move into this area. We have to do the easy things first. In the systems I have discussed, we have essentially a noncomplexing counterion, namely perchlorate, and see no evidence of ion pairing. Perhaps this was not made clear.

DR. DAVID RORABACHER (Wayne State University): A point which is frequently overlooked is that the calculations generally applied for determining the extent of ion-pair (or outer-sphere complex) formation in substitution reactions may be overly simplistic. There are many types of interactions which tend to perturb the extent of outer-sphere complex formation relative to the purely statistical calculation commonly made which takes into account only the reactant radii and electrostatic factors.

In particular, there are a number of specific interactions between outer-sphere species and the coordinated inner-sphere groups which can significantly enhance the extent of outer-sphere complex formation. Dr. Margerum has elucidated the stacking interactions which can occur between the aromatic rings of coordinated and outer-sphere ligands. Similarly, the internal conjugate base (ICB) mechanism, which we formulated a number of years ago, involves the formation of hydrogen bonds between outer-sphere nitrogen donor atoms and inner-sphere water molecules. Both of these phenomena increase the extent of outer-sphere association and thereby promote complex formation of multidentate ligands. However, as Jack Vriesenga has shown in a poster presentation at this Conference, such outer-sphere hydrogen bond formation may retard complex formation when unidentate ligands are involved by making the lone donor atom unavailable for inner-sphere insertion as long as it remains tied up in a hydrogen bond. The increase in outer-sphere complex formation combined with a decrease in inner-sphere insertion might provide conditions of the type Dr. Patel suggests.

In studies on solvent effects involving variation in the composition of two component mixtures, similar types of outer-sphere interactions yield preferential solvation wherein the solvent composition of the outer-sphere may differ markedly from the bulk solvent composition. Supporting electrolyte species and buffer components may also participate in outer-sphere interactions thereby changing the apparent nature (charge, bulk, lability) of the reacting solvated metal ion or metal complex as perceived by a reacting ligand in the bulk solvent.

DR. ALBERT HAIM: (State University of New York at Stony Brook): I guess you know as well as I do, and as most people do, how difficult it is to find evidence for a mechanism, whether it is dissociative or associative or falls in between. You have measured volumes of activation, and have obtained information from them. You seem to be very certain as to the conclusions that you can draw from the various numbers which you obtained. Suppose that one were a little skeptical about the value of these numbers and wanted to ask how they compared with other parameters that one can measure in the same systems, such as entropies of activation, or energies of activation. From the point of view of volumes of activation, is a picture obtained which is consistent with what one may derive from other measurements?

DR. SWADDLE: The problem with entropies of activation is that they are obtained in conjunction with the enthalpies. Those of us who have worked in NMR line broadening can relate numerous stories about entropies of activation which range all over the place, depending on exactly how one analyzes the data [See, e.g., Newman, K. E.; Meyer, F. K.; Merbach, A. E. J. Am. Chem.

Soc. 1979, 101, 1470]. Perhaps the NMR case is a particularly extreme example, but the point is that one has two compensating parameters in temperature effects.

In the pressure effect, it is true that one also has two parameters, the log k at zero pressure (but that is something one can measure) and the slope. The slope of that line gives the volume of activation. So, even with rather poor data, one can measure the volume of activation quite accurately, within fractions of a cubic centimeter per mole.

Thus, from the point of view of the numerical integrity of these results, I stand by them. Of course, the interpretation is, as always in mechanistic studies, open to debate.

DR. PATEL: In the early stages of some of this work, due to calculations on crystal field stabilization energies, it was thought that vanadium(III) and titanium(III) could be very good candidates for an associative mechanism. Now, there has been some work done on these systems, having to do with enthalpies of activation, which seems to substantiate an associative mechanism.

What would you think about measuring volumes of activation for such systems and then trying to compare them with such calculations?

DR. SWADDLE: I would guess that the volume of activation for aquo-exchange on vanadium(III) or titanium(III) would be on the order of about -7 cc per mole.

DR. JACK VRIESEN (Syracuse University): You pointed out the dangers involved in extracting entropies and enthalpies from NMR data, not only as a result of the cross-correlation between the two, but also their correlation to other NMR parameters. I thought it might be useful for you to comment on the effect of pressure on the other NMR parameters, besides the kinetic control? For example, you commented about the role played by the outer-sphere relaxation in the interpretation of NMR relaxation data. How would this be affected by pressure?

DR. SWADDLE: Yes, that is correct. As I stated, we have been careful to work in areas where at least 90 percent of the line broadening is controlled by solvent exchange. I think John Hunt is the person to comment on what happens to the other NMR parameters under pressure. I believe he has found some pressure-dependence of T_{2m} .

DR. JOHN HUNT (Washington State University): With regard to determining activation parameters from NMR data, it is mostly a matter of doing a good job of it. If one does a proper fit of the data, using the complete Swift-Connick equations and signal averages over a long enough period of time, one can get quite

reliable enthalpies. The entropies are then no worse than usual.

With regard to the pressure effects, we have, as usual, been interested in systems that are not simple. One system we have been looking at involves water-soluble porphyrins. Actually, the only reactions we have studied thus far involve the iron(III) and manganese(III) tetra(4-N-methylpyridyl)porphyrin complexes. These complexes are in the form of tosylate salts, which causes some problems. The rate constants are on the order of 10^6 s^{-1} for axial water exchange. The volumes of activation are $+2 \text{ cc mol}^{-1}$ for Fe(III) and -2 cc mol^{-1} for Mn(III). We believe that there is one water per metal ion in these complexes, but I couldn't defend that position very strongly.

These systems do involve some interpretation of the effect of pressure on T_{2m} , but we think that our resolved volumes of activation are valid. The signs are correct, and they are probably good to 1 or 2 cc mol^{-1} , which still allows one to keep the signs. I am not going to attempt to interpret these values. I thought Dr. Swaddle might understand why one gets a difference in sign between the iron(III) and the manganese(III) systems. These are high-spin complexes and don't show any pressure-dependence on the volume of activation, nor a temperature-dependence. The actual numbers will change a little bit.

I promised Dr. Swaddle that we would look at nickel and ammonia. We have made such a study in 15-molar aqueous ammonia which is a mixed solvent system. It is really only necessary to obtain solvent interchange between the inner-sphere and the outer-sphere in a case like this because outer-sphere formation is diffusion controlled. In this system we obtain a positive ΔV^\ddagger in the range of 4 to 6 cc mol^{-1} , a region of some uncertainty because the blank data are not as good as we would like to have.

Incidentally, one of the problems that always bothers me somewhat is that I think one really ought to use blanks, with a diamagnetic ion, that resemble the solution one is trying to interpret, rather than simply using water itself. Even though the effects are relatively small, one might learn something interesting about diamagnetic systems that way.

DR. JAMES ESPENSON (Iowa State University): I should like to raise a slightly different aspect of substitution reactions, an aspect which relates to a different kind of mechanism. This involves a change from the conventional heterolytic process of metal ligand bond cleavage to one dealing with homolytic bond cleavage.

I have raised the question with regards to the iodochromium(III) ion as to whether the substitution reaction can occur

by a homolytic pathway instead of, or as well as, by a heterolytic pathway (Scheme I). The heterolytic pathway in this particular case is quite a favorable reaction, with a sizeable equilibrium constant, although it occurs slowly. We can calculate the value for the equilibrium constant for homolytic dissociation because the reduction potentials are known. In this case the equilibrium constant has quite a small value. It is 10^{-27}

As a consequence, even if the reverse reaction occurred at the diffusion controlled rate ($k_{-1} \leq 10^{10} \text{ M}^{-1} \text{ s}^{-1}$), the rate of homolytic dissociation should be immeasurably small ($k_1 \leq 10^{-17} \text{ s}^{-1}$); the unimportance of homolysis was confirmed some years ago [Schmidt, A. R.; Swaddle, T. W. *J. Chem. Soc., Dalton Trans.* 1970, 1927].

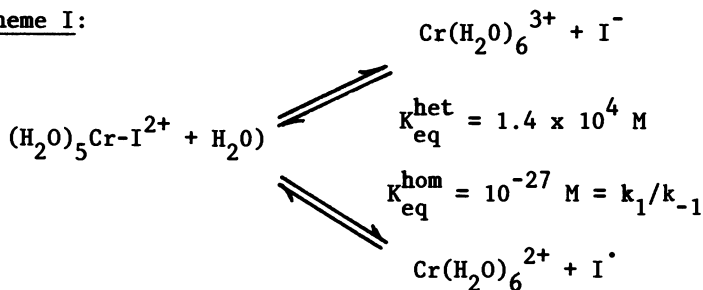
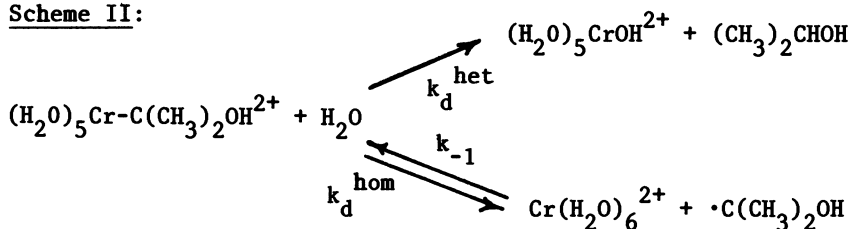
However, consider the corresponding situation for a closely related complex in which, instead of an iodide ion bound to pentaquo chromium, there is an aliphatic fragment such as an alkyl group. As one example, we may consider the hydroxyisopropyl chromium cation. Here the possibility for both homolytic and heterolytic substitution exists (Scheme II). With proper experiments, one can evaluate separately the rate constant values for cleavage by each of these pathways.

The pathway corresponding to heterolytic metal ligand cleavage can be evaluated by suppressing the homolysis reaction by addition of an excess of Cr^{2+} , providing a measurement of the heterolytic chromium-carbon bond cleavage reaction.

On the other hand, the homolysis reaction, an unfavorable equilibrium, can be drawn to the right by adding scavenging reagents for Cr^{2+} or carbon-centered radicals. In that case we can measure the rate constant for homolytic dissociation, which in this particular instance is 0.127 s^{-1} , accompanied by a large positive entropy of activation and a large enthalpy of activation.

Since Meyerstein has measured the reverse reaction rate constant, i.e., the combination rate constant between Cr^{2+} and the hydroxyisopropyl radical, the ratio of those values affords the equilibrium constant for homolytic dissociation, $2.5 \times 10^{-9} \text{ M}$ in the case of this particular complex.

By studying a series of complexes in which the various substituents on the alpha-carbon atom are varied, we can look at the change in the magnitude of the rate constant for homolytic dissociation as a function of these substituents. The values range from $3.5 \times 10^{-5} \text{ s}^{-1}$ for $\text{CrCH}_2\text{OH}^{2+}$ to $\sim 3 \times 10^2 \text{ s}^{-1}$ for $\text{Cr}(\text{CH}_3)(\text{CMe}_3)\text{OH}^{2+}$ or lifetimes from 7.5 hours to $\sim 3 \text{ ms}$.

Scheme I:Scheme II:

At 25.0°C: $k_{\text{d}}^{\text{het}} = 3.3 \times 10^{-3} + 4.7 \times 10^{-3} [\text{H}^+] \text{ s}^{-1}$

$$k_{\text{d}}^{\text{hom}} = 0.127 \text{ s}^{-1} \text{ (homolysis)}^{\text{a}}$$

$$\Delta H^{\ddagger} = 27.4 \text{ kcal/mol}$$

$$\Delta S^{\ddagger} = 29.4 \text{ cal mol}^{-1} \text{ K}^{-1}$$

$$k_{-1} = 5.1 \times 10^7 \text{ M}^{-1} \text{ s}^{-1} \text{ (pulse radiolysis)}^{\text{b}}$$

$$K_{\text{eq},298} = 2.5 \times 10^{-9} \text{ M}$$

$$\Delta G_{298}^0 = 12 \text{ kcal/mol}$$

$$\Delta H^0 \cong 27 \text{ kcal/mol}$$

^aBakac, A.; Kirker, G. W.; Espenson, J. H., unpublished results

^bCohen, H.; Meyerstein, D. *Inorg. Chem.* 1974, **13**, 2434

In a qualitative sense, the rate constants correlate with the change in degree of steric hindrance provided by the increasing bulk of the substituents. We can relate those changes, which span a factor of 10^7 in the homolytic dissociation rate constant, to the free energy of activation for the homolytic cleavage of correspondingly substituted ethanes. There is a substantial correlation for every system except the benzyl complex (Figure 1). The slope of the line is 0.3. If the correlation were exact, one would have expected a value of 0.5, there being a square root relationship in the rate constants, or a factor of 2 in the free energies, because in the ethanes we substitute symmetrically on both sides and in the chromium complexes on one side only.

These observations suggest that bond dissociation reactions, occurring in a homolytic fashion for this family of complexes, are controlled largely, if not entirely, by steric factors, provided that one stays within a family of complexes in which special electronic effects, such as might be found in the benzyl chromium ion, do not play an important role.

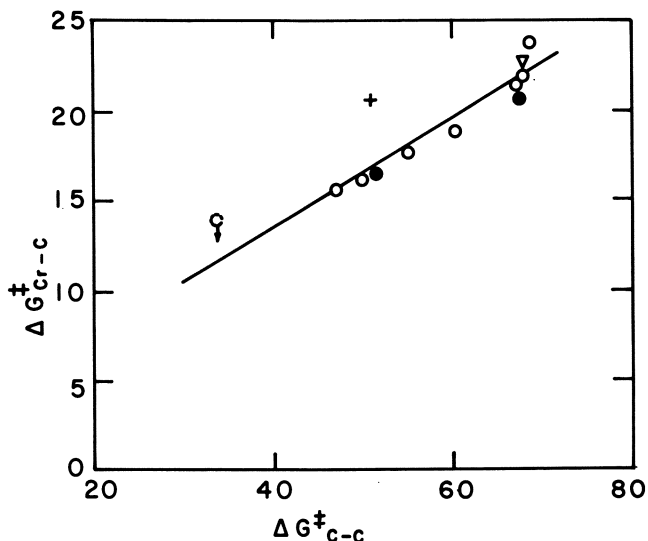


Figure 1. Plot of ΔG_{98}^{\ddagger} for the homolysis of organochromium cations vs. ΔG^{\ddagger} for the homolysis of the correspondingly substituted ethanes (with OH replaced by CH_3). Key for organochromium ions: ○, $\text{CrC}(\text{R},\text{R}')\text{OH}^{2+}$; ●, $\text{CrC}(\text{R},\text{R}')\text{OR}''^{2+}$; ▽, $\text{CrCH}(\text{CH}_3)_2^{2+}$; and +, $\text{CrCH}_2\text{Ph}^{2+}$.

Proton-Transfer Reaction Rates and Mechanisms

EDWARD M. EYRING, DAVID B. MARSHALL, FRANK STROHBUSCH

University of Utah, Department of Chemistry, Salt Lake City, UT 84112

R. SÜTTINGER

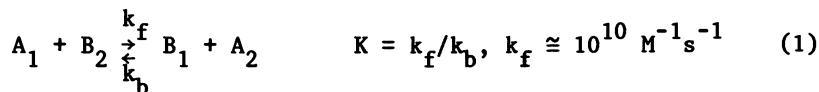
Institut für Physikalische Chemie der Universität Freiburg, D-78 Freiburg,
Federal Republic of Germany

Eight generalizations are given arising from world-wide studies of proton transfer reactions in aqueous media carried out over the past twenty-five years. Future directions of research on proton transfer kinetics are predicted, and recent kinetic studies by the authors on proton transfer in nonaqueous media (methanol, acetonitrile, and benzonitrile) are reviewed.

Inorganic solution chemistry often involves proton transfers to and from solvated metal ions as well as to and from the acids and bases that complex metal ions. Eight generalizations are presented below that attempt to summarize the insights regarding proton transfer reactions that have emerged in the past quarter century. The masterful reviews by Eigen (1) and Bell (2) provide much more extensive analysis of most of these points.

Eight Generalizations

1. For thermodynamically favorable reactions ($K \gg 1$) of the type

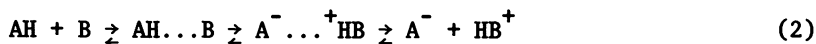


involving oxygen or nitrogen acids with H_2O , H_3O^+ , or OH^- in aqueous solution at room temperature, $k_f \sim 10^{10} \text{ M}^{-1} \text{ s}^{-1}$ and the rate constant is smaller by a factor of $10^{\Delta pK}$ in the reverse (unfavorable) direction (1,2).

2. Eigen's mechanism for proton transfer reactions between acids (AH) and bases (B) proceeds through a neutral hydro-

0097-6156/82/0198-0063\$06.00/0
© 1982 American Chemical Society

gen bonded complex (AH...B) and an ion pair ($A^- \dots {}^+HB$)



with these intermediates undetectable in aqueous solution but observable in polar organic solvents under suitable conditions (3).

3. Rate constants for the diffusion-controlled reaction between a proton and a species A in water decrease (4) by a factor of 0.3 to 0.5 for each positive charge added to the reactant A. Thus the rate constant for the reaction of a hydrolyzed metal ion such as $AlOH^{2+}(aq)$ with a solvent proton will decline with the increasing positive electrostatic charge of the hydrolyzed metal ion species.

4. Intramolecular hydrogen bonding, steric hindrance, and location of the mobile proton on a carbon atom ("carbon acids") can all act to decrease somewhat the reaction rates (5).

5. Removal of the proton from an intramolecular hydrogen bond by a base occurs in a two-step mechanism (a rapid equilibrium between H-bonded and non-H-bonded forms followed by base catalyzed proton removal from the non-H-bonded form) rather than by direct attack of the base on the intramolecularly hydrogen bonded species (6).

6. Nuclear reorganization or the rehybridization of the carbon is a main factor in the retardation of proton transfer involving carbon acids, and solvation changes have much less impact (7).

7. Proton transfer between electronegative atoms is faster the greater the electronegativity of the atoms between which the proton is moving. Thus proton transfer between nitrogen atoms is slower and rate limiting over a wider range of ΔpK than for proton transfer between oxygen atoms (8).

8. Proton exchange rates in aqueous solutions are enhanced by small amounts (0.5% V/V) of hydrophobic substances (e.g., methanol, dioxane) because of a consequent increase in H-bonded water structure in the hydration shells through which the proton transfer is mediated (9).

Amplification of Generalized Conclusions

In the following amplification of these generalizations, some attention will be given to controversial aspects of these statements. It is interesting that an area of scientific study such as proton transfer kinetics could be an active one for over 25 years, particularly because of relaxation techniques, and still be one for which it is difficult to make many generalizations that workers in the field can endorse without major reservations.

The first generalization simply asserts that there are many

reactions involving acids, such as hydrofluoric acid and water, for which the rates are diffusion controlled with rate constants of the order of $10^{10} \text{ M}^{-1} \text{ s}^{-1}$ in aqueous solution for the combination of the ions. In fact, it is generally found that when the reacting partners in reaction 1 have $\Delta pK > 0$ (i.e., $K \gg 1$), the value of k_f is independent of ΔpK (diffusion controlled) as indicated by Bronsted plots of $\log k_f$ vs. ΔpK having zero slope in this region. Conversely, when $\Delta pK < 0$ (i.e., $K \ll 1$), a plot of $\log k_f$ vs. ΔpK will have unit slope. Such Bronsted plots are discussed extensively by Eigen (1) and are also considered by Margerum (10).

The second statement has to do with the notion that in the Eigen mechanism for proton transfer there must be intermediate ion pairs. The reference to the unpublished work of Kreevoy and Liang (3) reflects the impact of their studies on some of our own recent work surveyed below. In fact, there is an extensive published literature concerning phenol-amine complexes in which the existence of the intermediates in equation 2 has been established in different organic solvents. One of the oldest such papers is that of Bell and Barrow (11) going back to 1959. Others include Hudson and co-workers (12) in 1972, and Baba and co-workers (13) in 1969.

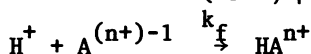
The next generalization, number 3 above, has to do with the notion that two simple cations will react with one another less rapidly than a cation and an anion of corresponding size would. Table I presents examples from the literature, where, in every case, a proton reacts with species of different charge types, and there is a steady decrease in the rate of reaction as one proceeds from top to bottom in that table.

Table II summarizes a temperature jump study (14) of the reaction of hydroxide ion with various intramolecularly hydrogen bonded malonic acid monoanions and points up the fact that, as the steric hindrance increases, a considerable strengthening in the hydrogen bond occurs with a concomitant slowing down of the rate at which the reaction proceeds (generalization number 4). At the time the authors did not foresee that it would be possible to distinguish between whether the hydrogen bond was broken directly by the attacking base or whether, in fact, there first had to be a collapse of the hydrogen bond into an open form of the anion that would subsequently react with the base. Thus, they simply postulated the former mechanism (direct attack).

Generalization number 5 reflects the work of Hibbert and Awwal (6) who have concluded that it is the latter kind of mechanism (involving the open form of the anion) that prevails in intramolecular hydrogen bond breaking reactions. This is a point, however, on which there is still room for equivocation.

Table I

Experimental Rate Constants for Base Protonation Illustrating the Influence of Ionic Charge on Protonation Reactions in Aqueous Solution (25 C, $\mu = 0$ M)



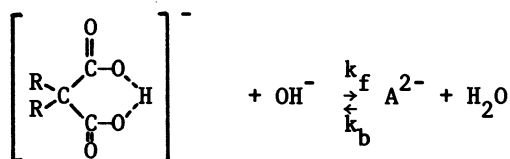
Reactants	$k_f, \text{M}^{-1}\text{s}^{-1}$	Method
$\text{H}^+ + \text{HS}^-$	7.5×10^{10}	E-disp
$\text{H}^+ + \text{N}(\text{CH}_3)_3$	2.5×10^{10}	NMR
$\text{H}^+ + \text{CuOH}^{\ddagger}$	$\sim 1 \times 10^{10}$	Sound
$\text{H}^+ + (\text{NH}_3)_5\text{CoOH}^{2+}$	1.4×10^9	T-jump
$\text{H}^+ + \text{Pt}(\text{en})_2(\text{en}^*)^{3+}$	2.6×10^8	T-jump

Ref: Eigen, M.; Kruse, W.; Maass, G.; DeMaeyer, L. Progr. React. Kin. 1964, 2, 287.

Note that the rate constant for diffusion controlled reactions between a proton and a base decreases by a factor of 0.3 to 0.5 for each positive charge added to the base.

Table II

Experimental Rate Constant Data Illustrating the Role of Steric Effects in Strengthening the Intramolecular Hydrogen Bond in the Monoanion of 2,2-Disubstituted Malonic Acids in Aqueous Solution (25 C, 0.1 M NaClO₄)



Substituents on Malonic Acid	$k_f, \text{M}^{-1} \text{s}^{-1}$	E_a^a	$\Delta G_f^\ddagger^a$	$\Delta H_f^\ddagger^a$	$\Delta S_f^\ddagger^b$	$\Delta S_b^\ddagger^b$
Diethyl	28×10^7	5	6	4.5	-5	+3
Ethyl-n-butyl	16×10^7	6	6.5	5.5	-3	+6
Ethylisoamyl	16×10^7	6	6.5	5.5	-3	+6
Ethylphenyl	14×10^7	6	6.5	5	-4	+2
Di-n-butyl	14×10^7	6	6.5	5	-4	+6
Di-n-heptyl	14×10^7	6	6.5	5	-4	+6
Di-n-propyl	13×10^7	6.5	6.5	6	-1	+6
Ethylisopropyl	15.5×10^7	7.5	7	7	0	+12
Diisopropyl	4.5×10^7	8	7	7.5	+2	+16

^a
^b Units: kcal/mol
Units: e.u.

Ref: Miles, M. H.; Eyring, E. M.; Epstein, W. W.; Ostlund, R. E. *J. Phys. Chem.* 1965, **69**, 467.

Note that the primary effect of the alkyl substituents is steric, rather than electronic, with only branching on the carbon attached to the parent malonic acid effective in closing the jaws to strengthen the intramolecular hydrogen bond. Taking the "melting" of one water molecule from the dianion to contribute 5 e.u. to ΔS_b^\ddagger , one may estimate the number of solvent molecules that must be removed in the reverse reaction to form the activated complex.

Perlmutter-Hayman and Shinar (15, 16) have studied by temperature-jump the reactions of bases with different acid-base indicators having intramolecular hydrogen bonds. With Tropaeolin O, direct attack of the base on the hydrogen bridge predominates according to their interpretation, whereas, for Alizarin Yellow G, the observed relaxation is ascribed chiefly to diffusion controlled reaction between the base and that part of the indicator present in the open form. Thus, data exist that lead one to doubt the generality of statement number 5.

Statement number 6 has to do with carbon acids and is supported by reference (7). There are, in fact, other references that suggest solvent plays a much more direct role in the kinetics of protonating carbanions than statement number 6 would imply. For example, there is evidence that nuclear reorganization and rehybridization of the carbon atom are too rapid to have much kinetic importance when compared with solvent reorientation. The strong dependence of carbanion protonation rates on the solvent supports this view. These rates are typically much faster in organic solvents, such as DMSO, than in water. A particular reaction that was studied in different solvents (17) is



In cyclohexanol and in isobutanol the rates are diffusion controlled and 10^5 times faster than they are in water, even though in all solvents the same rehybridization occurs. A recent comparison (18) of rates of protonation and methyl mercuriation of delocalized carbanions in aqueous solution by Raycheba and Geier also addresses generalization number 6. Only the methylmercuriations are diffusion controlled and three to four orders of magnitude faster than the protonation. Thus, the wrong hydrogen bond structure around the carbanion in water strongly inhibits proton transfer, whereas attack of the methyl mercury ion is not influenced because this ion does not interact significantly with the hydrogen bonded network.

In reference to statement number 7, Kresge's kinetic studies (8) indicate that a proton transfer from one oxygen to another would be faster than that from a nitrogen to another nitrogen. Some of Kresge's recent unpublished work (19) suggests that the transfer of a proton from phosphorus to oxygen is somewhat slower than the corresponding transfer between nitrogen and oxygen. While there is nothing particularly the matter with statement number 7 as written, it is one that clearly is going to undergo more elaboration.

The last of these eight statements has to do with the idea that, if a very small amount of an organic solvent such as methanol is introduced into an aqueous solution, the rate of reaction (involving proton transfer) may speed up because of the increased hydrogen-bonded water structure.

Future Trends

Table III suggests some of the proton transfer kinetic studies one is likely to hear most about in the near future. The very first entry, colloidal suspensions, is one that Professor Langford mentioned earlier in these proceedings. In the relaxation field, one of the comparatively new developments has been the measurement of kinetics of ion transfer to and from colloidal suspensions. Yasunaga at Hiroshima University is a pioneer in this type of study (20, 21, 22). His students take materials such as iron oxides that form colloidal suspensions that do not precipitate rapidly and measure the kinetics of proton transfer to the colloidal particles using relaxation techniques such as the pressure-jump method.

Such studies engender interest in quarters that one would not anticipate. For example, a civil engineer at Stanford University recently sought information about the electric field jump (E-jump) relaxation technique. It is quite surprising that this least widely used of the relaxation methods would appeal to engineers as a means of measuring the kinetics of transfer of heavy metals to and from colloidal suspensions as is done in clearing water. This, of course, is a very practical problem for which engineers can deduce interesting features from this type of fundamental kinetic measurement.

As for studies of ice, a search of the recent proton transfer literature discloses that ice is one of the substances that still generates interest (23, 24) particularly as it relates to membrane proton-transfer problems. Solid battery electrolytes can also involve (25, 26, 27) proton transfers, although these are obviously very slow compared to the kinds of rates that we are used to considering in aqueous inorganic solutions.

Picosecond time regime kinetic studies of proton transfer are coming into vogue (28, 29, 30), particularly for intramolecular processes that can be very fast. Bound to play an increasingly important role in the elucidation of proton transfers are the gas phase ion-solvent cluster techniques that reveal dramatically the role played by solvent molecules in these reactions (31, 32).

Dr. Swaddle's discussion of volume measurements (33) is an interesting one from our point of view, because we lately have built an electric-field-jump cell that would work at fairly high pressures. Our reason for doing so may be amusing. We thought that perhaps it would be possible to solvate ions, or at least ion pairs, using xenon as a solvent. This possibility had been suggested to us by the work of Peter Rentzepis (34). We discovered, to our chagrin, that while one can indeed dissolve rather large molecules, such as lysozyme, in liquid xenon, none of the ion pairs that we tried, including some very large ions in which the charge was spread over a fairly large sized

Table III**Eight Areas for Future Research in the Study
of Proton Transfer Kinetics**

1. Colloidal suspensions
 2. Ice
 3. Solid battery electrodes
 4. Picosecond time regime
 5. Gas phase ion-solvent interactions
 6. Volumes of activation
 7. Solvent effects
 8. Laser induced solvent ionization
-

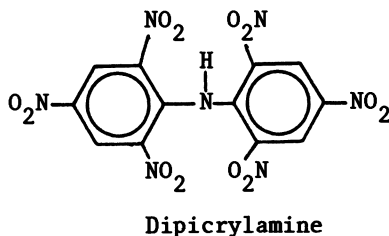
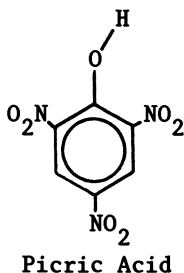
molecule, actually dissolve in the liquid xenon (35). So we are apparently never going to be doing E-jump studies at comparatively high pressures in liquid xenon. But there is no reason, in principle, why one could not perform electric field jump kinetic studies over an extended range of pressures on many of the aqueous systems studied previously only at atmospheric pressure and thus deduce volumes of activation for proton transfer and other rapid reactions involving charge neutralization.

Before treating the last two topics in Table III let us consider a rhetorical question: If indeed many of the problems relating to proton transfer are reasonably well solved from the point of view of someone who, like Dale Margerum, goes ahead and measures kinetics of ligand exchange, are the kinetics of proton transfers in homogeneous aqueous and non-aqueous solutions still going to be studied for other reasons? The obvious answer is "Yes" since one will use proton transfer kinetics studies as a tool for investigating other properties of chemical systems.

In particular, we have been very much interested in using proton transfer kinetics as a means of measuring how ion solvation changes as a solute equilibrium is transferred from one organic solvent to some other organic solvent. The tool that we have used in most of these studies has been the electric-field-jump technique. The square, high voltage wave instrumentation with spectrophotometric detection (36,37) is very different from the dispersive E-jump apparatus with a Wheatstone bridge detector (38) that Ken Kustin taught me how to use in Eigen's laboratory over 20 years ago. In the present day instrument the exponential decay in the photomultiplier voltage, after the high voltage has been taken off the sample cell, yields the chemical relaxation (or relaxations) of the chemical equilibrium (or equilibria). The time constant of the last exponential decay is the chemical information of interest in such proton transfer kinetic studies.

Proton Transfers in Methanol, Acetonitrile, and Benzonitrile

Methanol is one of the easy solvents to work with using the electric-field-jump technique. The preparation of the solvent is not nearly as arduous as is that of some other solvents such as acetonitrile. In methanol we observed that picric acid anion protonates at the diffusion controlled rate whereas dipicrylamine sterically hinders the proton from recombining with it. (39).

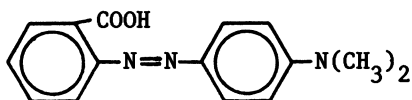


In another study (40) we found that protonation of pyridine is diffusion-controlled with a one-to-one solute-methanol complex as the reactive species. Thus, while methanol plays essentially no role in the proton transfer to dipicrylamine in the first study, it is indeed intimately involved in the proton transfer to pyridine.

Now let us consider the results of an E-jump study (14) of proton transfer between picric acid (A) and methyl red (B)

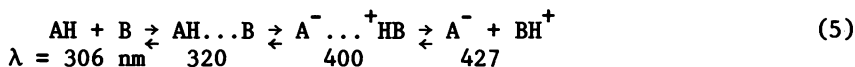


in acetonitrile. The formula for methyl red is



Rates are found to be a factor of ten slower than diffusion control suggesting a requirement for solvent reorganization around the strongly solvated cations.

Another proton transfer studied by the E-jump technique in acetonitrile (42) is that between *p*-nitrophenol (AH) and triethylamine (B). The extinction coefficients for each of the species in the following equilibrium have been measured by Kreevoy and Liang (3):



One can be excited about a spectrophotometric E-jump study of this system because, in principle, it should be possible to measure the relaxation times associated with each of the successive equilibria. The intermediates are stable, but the relaxation data are consistent with the single equilibrium



regardless of the monitoring wavelength. The ion recombination rate constant, $\sim 9 \times 10^9 \text{ M}^{-1} \text{ s}^{-1}$, is 5 times slower than a diffusion controlled rate. A requirement for solvent reorganization around the cation is again postulated. Thus, in both cases involving acetonitrile, solvent movement is intimately involved in proton transfer.

Whereas in acetonitrile the rate limiting step is an opening of the solvent shell of a reactant, in benzonitrile the back reaction of (5) between the protonated acridine orange cation (BH^+) and the 3-methyl-4-nitrophenolate ion (A^-) to form the ion pair is diffusion controlled (although the overall reaction to the neutral molecules is an endothermic process). Because of its lower dielectric constant than acetonitrile, the electrostatic interactions between reactants in benzonitrile outweigh specific solvent effects. In other words, in benzonitrile a rate limiting coupling of proton transfer to the reorientation of solvent dipoles does not occur and the measured rates are very fast. The ion recombination $(\text{I}) + (\text{II}) \rightarrow$ in benzonitrile has a diffusion controlled specific rate (theoretical) $k = (4.3 - 5.6) \times 10^9 \text{ M}^{-1} \text{ s}^{-1}$ and a measured (T-jump) specific rate $k = (3.5 \pm 0.8) \times 10^9 \text{ M}^{-1} \text{ s}^{-1}$ at 0.1 M ionic strength.

Table IV is an attempt to summarize the results of these proton transfer studies in nonaqueous solvents. There is no systematic trend in what seems to be the rate limiting step in contrast to the attractive Eigen-Wilkins generalization for the mechanism of metal ion complexation. Obviously, many more proton transfer kinetic studies in nonaqueous solutions are needed for beautiful generalizations to emerge. Whether investigators will have the patience to carry them out or not is the only uncertainty.

Proton Transfer in IR Laser Excited Solvents

Another situation in which an already well-studied proton transfer reaction serves as a probe of a physical phenomenon has been suggested by Knight, Goodall and Greenhow (43, 44). They ionized water with single photons of Nd:glass laser infrared radiation and measured an ion recombination rate constant for the reaction



in excellent agreement with that reported by Eigen and De Maeyer (45). One might at first wonder why, more than two decades after the classic Eigen-De Maeyer experiments, someone would remeasure the kinetics of ion recombination in water. The

Table IV

Summary of the Relationships between Nonaqueous Solvent Properties and Rate Limiting Steps for Proton Transfer

Solvent Type	Solvents	Rate Limiting Step
Polar, Protic	Water, Methanol	Diffusion together of reactants
Polar, Aprotic	Acetonitrile	Solvent reorganization
Moderately Polar, Aprotic	Benzonitrile	Diffusion together of reactants
Low Polar, Aprotic	Chlorobenzene	Rotation of encounter complex

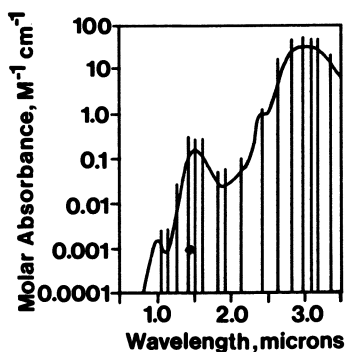


Figure 1. The near IR absorption spectrum of anhydrous liquid hydrofluoric acid with a few of the many possible IR wavelengths obtainable from a neodymium-doped glass laser superimposed.

intriguing aspect of such an experiment in any neat solvent is that the ion-creating mechanism competes successfully in time with the thermalization of the near infrared laser energy deposited in the solvent vibrations. Clearly, one ought to study other ultrapure, autoionizing solvents to see whether there is something intrinsically peculiar about water, such as its hydrogen bonded structure, that makes possible a long lifetime for the delocalization of the thermal energy deposited by the laser. As Figure 1 suggests, it is now easy to generate infrared pulses from a laser at a variety of wavelengths and thus excite a particular solvent at many different infrared wavelengths to see what impact that variable has on this process of creating ions in the pure solvent. Hydrogen fluoride is the most obvious of several autoionizing solvents that an inorganic chemist could probe in this fashion.

Acknowledgments

We thank Professors M. M. Kreevoy and A. J. Kresge for enlightening comments and the donors of the Petroleum Research Fund, administered by the American Chemical Society, for partial support of this research.

Literature Cited

1. Eigen, M. Angew. Chem., Int. Ed., Engl. 1964, 3, 1.
2. Bell, R. P. "The Proton in Chemistry;" Chapman and Hall, London, 1973, pp.130, 194.
3. Kreevoy, M. M.; Liang, T. M., unpublished work.
4. De Maeyer, L.; Kustin, K. Ann. Rev. Phys. Chem. 1963, 14, 5.
5. Bell, R. P. op. cit., pp. 130, 131.
6. Hibbert, F.; Awwal, A. J. Chem. Soc., Perkin II 1978, 939.
7. Okuyama, T.; Ikenouchi, Y.; Fueno, T. J. Am. Chem. Soc. 1978, 100, 6162.
8. Kresge, A. J. Pure Appl. Chem. 1981, 53, 189.
9. Nicola, C. U.; Labhardt, A.; Schwarz, G. Ber. Bunsenges. Phys. Chem. 1979, 83, 43; for an alternative view see Symons, M. C. R. Acc. Chem. Res. 1981, 14, 179.
10. Margerum, D. W. This Volume, American Chemical Society: Washington, D. C., 1982.
11. Bell, C. L.; Barrow, G. M. J. Chem. Phys. 1959, 31 1158.
12. Hudson, R. A.; Scott, R. M.; Vinogradov, S. N. J. Phys. Chem. 1972, 76, 1989.
13. Baba, H.; Matsuyama, A.; Kokubun, H. Spectrochim. Acta 1969, 25A, 1709.
14. Miles, M. H.; Eyring, E. M.; Epstein, W. W.; Ostlund, R. E. J. Phys. Chem. 1965, 69, 467.
15. Perlmutter-Hayman, B.; Shinar, R. Int. J. Chem. Kinet. 1977, 9, 1.

16. Perlmutter-Hayman, B.; Shinar, R. Int. J. Chem. Kinet. 1978, 10, 407.
17. Chaudri, S. A.; Asmus, K.-D. J. Chem. Soc., Faraday I 1972, 68, 385.
18. Raycheba, J. M. T.; Geier, G. Inorg. Chem. 1979, 18, 2486.
19. Kresge, A. J. Private communication.
20. Ashida, M.; Sasaki, M.; Kan, H.; Yasunaga, T.; Hachiya, K.; Inoue, T. J. Colloid Interface Sci. 1978, 67, 219.
21. Hachiya, K.; Ashida, M.; Sasaki, M.; Kan, H.; Inoue, T.; Yasunaga, T. J. Phys. Chem. 1979, 83, 1866.
22. Astumian, R. D.; Sasaki, M.; Yasunaga, T.; Schelly, Z. A. J. Phys. Chem., in press.
23. Knapp, E. W.; Schulten, K.; Schulten, Z. Chem. Phys. 1980, 46 215.
24. Kunst, M.; Warman, J. M. Nature 1980, 288, 465.
25. Farrington, G. C.; Briant, J. L. Mat. Res. Bull. 1978, 13, 763.
26. Farrington, G. C.; Briant, J. L. Science 1979, 204, 1371.
27. Roth, W. L.; Anne, M.; Tranqui, D. Revue de Chimie Minerale 1980, 17, 379.
28. Smith, K. K.; Kaufmann, K. J.; Huppert, D.; Gutman, M. Chem. Phys. Lett. 1979, 64, 522.
29. Hetherington, W. M., III; Miukeels, R. H.; Eisenthal, K. B. Chem. Phys. Lett. 1979, 66, 230.
30. Barbara, P. F.; Brus, L. E.; Rentzepis, P. M. J. Am. Chem. Soc. 1980, 102, 5631.
31. Farneth, W. E.; Brauman, J. I. J. Am. Chem. Soc. 1976, 98, 7891.
32. McDonald, R. N.; Chowdhury, A. K.; Setser, D. W. J. Am. Chem. Soc. 1980, 102, 4836.
33. Swaddle, T. W. This Volume, American Chemical Society: Washington, D. C., 1982.
34. Rentzepis, P. M.; Douglass, D. C. Biophys. J. 1981, 33, 271a.
35. Marshall, D. B.; Strobusch, F.; Eyring, E. M. J. Chem. Eng. Data 1981, 26, 333.
36. Olsen, S. L.; Silver, R. L.; Holmes, L. P.; Auburn, J. J.; Warrick, P., Jr.; Eyring, E. M. Rev. Sci. Instrum. 1971, 42, 1247.
37. Olsen, S. L.; Holmes, L. P.; Eyring, E. M. Rev. Sci. Instrum. 1971, 45, 859.
38. Eigen, M.; De Maeyer, L. "Investigation of Rates and Mechanisms of Reactions," Technique of Organic Chemistry, Vol. 8, Part 2, Friess, S. L.; Lewis, E. S.; Weissberger, A. Eds.; Interscience Publishers: New York, 1963; p. 988.
39. Strobusch, F.; Marshall, D. B.; Vazquez, F. A.; Cummings, A. L.; Eyring, E. M. J. Chem. Soc., Faraday I 1979, 75, 2137.

40. Marshall, D. B.; Eyring, E. M.; Strohbusch, F.; White, R. D. J. Am. Chem. Soc. 1980, 102, 7065.
41. Strohbusch, F.; Marshall, D. B.; Eyring, E. M. J. Phys. Chem. 1978, 82, 2447.
42. Marshall, D. B.; Strohbusch, F.; Eyring, E. M. J. Phys. Chem. 1981, 85, 2270.
43. Goodall, D. M.; Greenhow, R. C. Chem. Phys. Lett. 1971, 9, 583.
44. Knight, B.; Goodall, D. M.; Greenhow, R. C. J. Chem. Soc., Faraday II 1979, 75, 841.
45. Eigen, M.; De Maeyer, L. Z. Elektrochem. 1955, 59, 986.

RECEIVED April 5, 1982.

General Discussion—Proton-Transfer Reaction Rates and Mechanisms

Leader: Ramesh Patel

DR. RAMESH PATEL (Clarkson College): It appears that studies on colloidal systems may represent an extremely important area for the future. We have also been doing some colloidal work, particularly dealing with the solution chemistry that precedes the formation of very highly monodispersed colloidal particles. One such system with iron phosphate has been included in the poster presentation.

Yasunaga has studied colloidal systems involving titanium dioxide. What I find very curious is that he reports that the recombination rate of hydroxyl ions reacting with the titanium is orders of magnitude smaller than what one finds in other systems, including ice, of course, and other solutions. I was wondering whether you have any comment.

DR. EYRING: I have no explanation for it either, but in fact, what you say is true.

DR. PATEL: One reason for much of the interest which prevails in this area right now, especially with iron(II), has to do with the corrosion of steel in industry and also in nuclear reactors. Normally one thinks of forming precipitates or particles by adding base to a solution and cooling it down. If iron(III) solutions are made more acidic and if you raise the temperature, these conditions lead to the formation of very, very well-defined particles. A very important event in this is the proton transfer kinetics that lead to the formation of the hydrolysis of many of these trivalent ions.

DR. THOMAS MEYER (University of North Carolina): First, do you have any comments to make about chemical reactions in which proton transfer accompanies electron transfer? Second, do you have any comments to make on situations where proton transfer takes place between interfaces, e.g., from one solvent to another or perhaps from a solvent into a membrane?

DR. EYRING: Certainly the latter of the two subjects you are talking about is one that is of particular interest to us. We have invested a great deal of our recent effort on a technique called photoacoustic spectroscopy, which we initially thought we could use for looking at reactions occurring at a surface. Up to this point, however, we have been disappointed because, in fact, the signal-to-noise ratio is so bad that it would take a very long time to obtain satisfactory data. Thus, the reaction would have to be extremely slow before we would be able to say anything about it from photoacoustic spectroscopic measurements.

DR. EPHRAIM BUHKS (University of Delaware): I would like to ask your opinion about a possible interpretation of proton transfer in terms of nuclear tunneling effects. Might it be possible that as the energy of the vibrational modes becomes very large, the classical rate theory might not work?

DR. EYRING: Well, I think we are all conscious of the fact that Bell writes extensively on the subject of tunneling in connection with proton transfer. In fact, there is a recent book that was published within the last year that is on that particular topic [Bell, R. P. "The Tunnel Effect in Chemistry"; Chapman and Hall: London, 1980].

DR. NORTON (Colorado State University): As a novice in this field, something that is starting to worry me about metallic systems is the difficulty of distinguishing between an orthodox proton transfer as opposed to an electron transfer followed by hydrogen atom transfer in the reverse direction. Is this ever a problem in the kinds of more classical systems you have been describing?

DR. EYRING: If it is, I am not aware of it. One of the attractive features about the early fast reaction studies of proton transfer systems is that they were comparatively simple. Some of the problems which have been mentioned today, such as perchlorate ions causing complications, are not present in extra pure water to which Dr. Ken Kustin has added just a trace of HF. If you take a membrane or some other kind of a surface, the proton transfer is certainly a great deal more complex.

My research group has not tried to do it. We have gone off on a tangent, where we went looking for a probe that would be useful for looking at surfaces kinetically, and discovered, to our chagrin, that photoacoustic spectroscopy is much more suitable for investigating the infrared spectrum of polyacetylene. That happens to be an exciting topic, and there are indeed publications arising from our work on photoacoustic spectroscopy. But I must confess, it is a little frustrating to have become involved in a field like that, fully intending to use it as a kinetic tool, and then discovering that it just isn't very suitable. It may be suitable for making kinetic studies at electrode surfaces. Bard at Texas has done some interesting experiments which suggest that if one is looking at a small difference between two big features, as may be the case at the surface of an electrode, perhaps photoacoustic spectroscopy may be used for kinetic measurements. But for the kinds of systems that we thought would be interesting, such as proton transfer to and from a membrane, this technique does not appear to be a promising kinetic tool.

DR. J. KERRY THOMAS (University of Notre Dame): Is there anything wrong with putting a fluorescent probe that is pH

dependent in these systems? Fluorescence is a very sensitive method. It is used in many membrane studies where monitoring of a specific process is required. One could locate such a probe in a selected position and essentially use this as a method for checking diffusion in that region. We do this in micelle systems, and it is a relatively easy method.

DR. EYRING: That is distinctly possible.

Nucleophilic Substitution

MARK J. PELLERITE and JOHN I. BRAUMAN

Stanford University, Department of Chemistry, Stanford, CA 94305

A variety of studies on nucleophilic displacement reactions have been carried out in the gas phase, utilizing pulsed ion cyclotron resonance (ICR) spectroscopy. Many of these reactions occur with conveniently measurable efficiencies ($k_{\text{observed}}/k_{\text{collision}}$) of 10^{-1} - 10^{-3} . Using the measured reaction efficiencies, and making estimates regarding the structure of the transition state, a microcanonical version of unimolecular reaction rate theory, such as RRKM or QET, can be used to derive a value for the energy of the transition state relative to the energy of the reactants. Thus, if the energies of the reactants are known, an absolute value can be obtained for the energy of the gas-phase transition state, and direct information about solvent free barrier heights. Finally, Marcus theory has been applied to some of these gas phase ionic reactions. The results provide interesting insights into "intrinsic" reactivity in ionic reactions. Presumably, this information can be contrasted to the behavior of similar reactions occurring in the solution phase to provide information on solvent effects.

Nucleophilic substitution reactions are among the most widely studied reactions in chemistry (1). This is due, in part, to their synthetic utility, to the wide range of substrates and reactants, and to their relatively clean kinetic behavior. In contrast to thermodynamically based studies of structure and reactivity (e.g., Hammett correlations of acidity), a satisfactory understanding of kinetic reactivity in S_N2 reactions has yet to be achieved, albeit not for lack of talent or effort expended.

0097-6156/82/0198-0081\$06.50/0
© 1982 American Chemical Society

At least a portion of the problem lies in our inability to separate solvent-free from solvent-dependent quantities. Even in attempting to apply theories such as that of Marcus (2, 3), there remains considerable uncertainty when the analysis is complete.

Thus, we are left with a set of important, challenging questions:

1. Can we learn something from studying such reactions?
2. Are there good descriptions which have reasonable generality and predictive power?
3. What do we mean by the statement: X is a good nucleophile?
4. Why is X a good nucleophile?

Our approach to these problems has been to study S_N2 reactions in the gas phase. Ion-molecule studies have proven very effective in understanding equilibrium behavior of ions in solution (4), and we think there is great potential in the dynamic areas. As it happens, we find that Marcus' theory may be especially applicable, in that the process of interest is a unimolecular one and obviates dealing with encounters, work terms, etc. Thus, we can readily extract solvent free quantities of interest.

Methodology

In order to answer the questions we have posed, we need to accomplish a number of things. First, we need to measure a reaction rate in the gas phase. Second, we need a framework for interpreting the rate constant and relating the measurement to a potential surface. Third, we need to acquire sufficient information to allow us to extract the value of a barrier height. Then, we can apply theories for interpreting these barrier heights in terms of chemical structure.

Rate Measurement. We have used pulsed ion cyclotron resonance (ICR) spectroscopy to study these gas-phase, ion-molecule reactions. The method has been described elsewhere in considerable detail (5). Basically, ions are generated by pulsed electron impact and held in a magnetic-electric field trap for times up to about 1 sec, during which they can react with a selected neutral gas maintained at a pressure of about 10^{-6} Torr. After a certain time has elapsed following ion formation, the number of ions present at the m/e of interest is detected (reactant or product), and, finally, the ions are ejected from the cell. The process is repeated, and the time

to detection is varied. Thus, the process can be thought of as a sequence of one-point kinetic determinations (concentration of ions vs. time) at a fixed pressure. The pressure can be selected to give measurable rate constants and can be varied to provide a range of data. Because the concentration of ions is so low ($\sim 10^5 \text{ cm}^{-3}$) the kinetics are pseudo first-order. The bimolecular rate constant is calculated by dividing the pseudo first-order rate constant by the neutral reactant pressure.

Because the collisions between ions and molecules in the gas phase are governed by physical (ion-dipole, ion-induced dipole) rather than chemical forces, it is possible to calculate rather accurately the collision rate constant (6, 7). We then express the efficiency of the reaction as the fraction of collisions which lead to products.

Potential Energy Surface. The forces between ions and neutral molecules are attractive at long ($\sim 10 \text{ \AA}$) distances, so that the (rotationless) potential surface always has downward curvature. If the surface has only a single minimum as shown in Figure 1 and if the energy is statistically distributed in all available modes, we expect that exothermic reactions will be essentially unit efficient, and thermoneutral reactions will have efficiencies of one-half (8).

In order to interpret the observation of reactions which have low efficiencies, we have suggested a double well potential surface model (8) illustrated in Figure 2. This is the simplest model which is consistent with available data. At the low pressures typically used in ICR, long collision times ensure that the system contains its initial total energy throughout the reaction. The efficiency for an exothermic reaction is given by $k_2/(k_{-1} + k_2)$. Passage over the central barrier (k_2) is slow even though energetically favorable, because the entropy associated with this transition state is relatively low due to its tightness. The reverse decomposition transition state (k_{-1}) is entropically more favorable because the particles are separated to about 6 \AA and have more rotational entropy.

Using unimolecular rate theory, the branching ratio k_2/k_{-1} for decomposition of the chemically activated encounter complex can be computed for any energy if the geometry and vibrational frequencies for the transition states leading to the two channels are known (8, 9, 10). These can be estimated fairly easily, since both transition states are well characterized. The calculation is simplified by the cancellation of all properties of the encounter complex, since we are calculating only a ratio of rate constants.

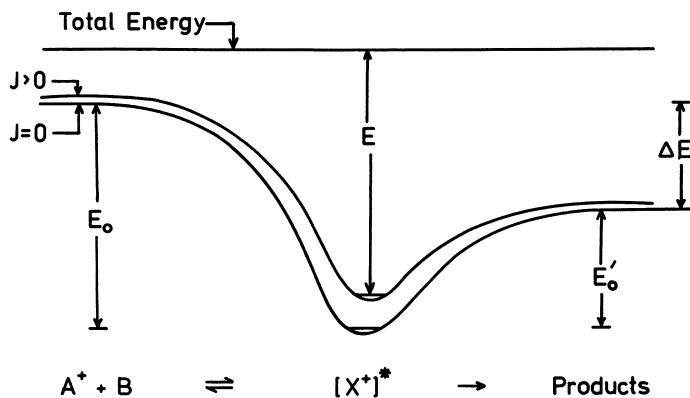


Figure 1. Hypothetical single-minimum potential surface for ion-molecule reactions.

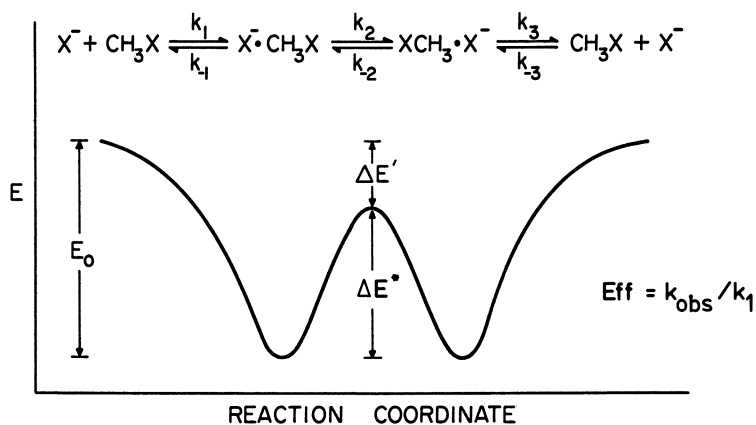
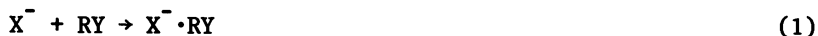


Figure 2. Proposed double-minimum potential surface for gas-phase nucleophilic displacement reactions.

The density of states for a transition state depends upon the non-fixed energy minus the critical energy. Taking the critical energy for the central transition state as an adjustable parameter, we can calculate efficiencies until we find a match with experiment. We have already demonstrated that our calculations for the decomposition transition state (k_{-1}), using no adjustable parameters, are accurate (11). Thus, we determine in this way the energy at the top of the central barrier relative to that of the transition state for back dissociation to reactants. Note that we do not need to know the well depth to calculate the efficiencies and determine the difference in energy between the two transition states. Deeper wells would give smaller rate constants (k_{-1}, k_2) but their ratio would remain unchanged.

We do need to determine the well depth, however, in order to evaluate the absolute barrier height. The well depth corresponds to ΔH^0 for the reaction



In some cases (e.g., $Cl^- + CH_3Cl$; $Br^- + CH_3Br$) these values are known experimentally (9-10 kcal/mol) (12, 13, 14). In others we can estimate the value in a straightforward manner since the binding is governed primarily by the polarizability and dipole moment of the neutral molecule rather than the structure of the ion. Thus, we assume ΔH^0 in reaction 1 to be dependent only on the structure of RY, and not on that of X^- .

Intrinsic Barriers

The activation energy for a reaction is affected by the exothermicity. As suggested long ago by Bell, Evans, and Polanyi (15, 16), the transition state properties should reflect, in part, the properties of reactants and products, and some of the thermodynamic stabilization of products will appear in the transition state. This general suggestion is given quantitative expression in the equations developed by Marcus (2). Murdoch (17) has shown that the Marcus equations follow from the Leffler and Grunwald (18) suggestion that the transition state stabilization is linearly related to changes in reactant and product energies.

The Marcus equations (2, 17) are

$$\Delta E^* = [(\Delta E)^2 / 16\Delta E_0^*] + \Delta E_0^* + 1/2 \Delta E \quad (2)$$

$$\alpha = [\Delta E / 8\Delta E_0^*] + 1/2 \quad (3)$$

where ΔE^* is the barrier at overall free energy change ΔE , and

ΔE_0^* is the intrinsic barrier at $\Delta E = 0$ (see Figure 3). Since eqs 2 and 3 are applicable only to elementary reactions, we apply them to that portion of the potential surface representing passage from the reactant complex $X^- \cdot CH_3Y$ to the product complex $Y^- \cdot CH_3X$. Thus, ΔE is the energy difference between the two complexes. When the reactant and product neutrals have similar polarizabilities and dipole moments, this difference will be very close to the overall reaction exothermicity. When it is not, we can easily make appropriate corrections.

It should be noted that application of the Marcus theory to these reactions is much more straightforward than application to reactions in solution. Since we are dealing with a single unimolecular step, namely, rearrangement of the reactant complex to the product complex, we need not be concerned with the work terms (2) which must be included in treatments of solution-phase reactions. These terms represent the work required to bring reactants or products to their mean separations in the activated complex, and include Coulombic and desolvation effects.

The intrinsic barrier, ΔE_0^* , is the barrier the reaction would have if it were thermoneutral. Thus, use of this equation allows us to separate quantitatively the kinetic (intrinsic) and thermodynamic contributions to a reaction's energy barrier. Following Marcus (2), we can regard the intrinsic barrier for a "cross" reaction as the mean of the barriers for the component "exchange" reactions. Thus, for the cross reaction $RX + Y^- \rightarrow RY + X^-$, $\Delta E_0^*(RX + Y^-)$ is assumed to be the geometric mean of the identity reactions:

$$\Delta E_0^*(RX + Y^-) = \frac{1}{2}[\Delta E_0^*(RX + X^-) + \Delta E_0^*(RY + Y^-)].$$

We can measure some of these reactions (and ΔE_0^*) directly, for example (8) $Cl^- + CH_3Cl$, using the procedure outlined above. For others, such as $CH_3O^- + CH_3Cl$, we know the overall exothermicity and can estimate the exothermicity of complex to complex reaction. Using the geometric mean assumption and the central barrier height determined from RRKM analysis of the experimental reaction efficiency, we can then evaluate ΔE_0^* for a degenerate exchange reaction which proceeds too slowly for us to measure. For the reactions described here we find $\Delta E_0^*(Cl^- + CH_3Cl) = 10.2$ kcal/mol, $\Delta E_0^*(CH_3O^- + CH_3Cl) = 18.4$ kcal/mol ($\Delta H^\circ = -42$ kcal/mol), and $\Delta E_0^*(CH_3O^- + CH_3OCH_3) = 26.6$ kcal/mol. We have applied this procedure to all of the reactions shown in Table I.

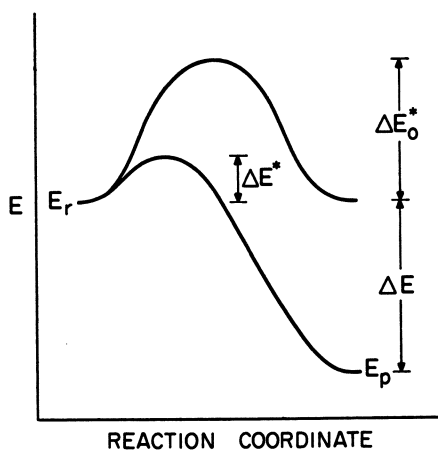


Figure 3. Relationship between the Marcus equation quantities ΔE^* , ΔE_o^* and ΔE .

Table I
Rate Constants and Efficiencies

Reaction	k^a	k_{coll}	Efficiency	ΔH° , kcal/mole
$\text{CH}_3\text{O}^- + \text{CH}_3\text{Cl} \rightarrow \text{Cl}^- + \text{CH}_3\text{OCH}_3$	6.0 ± 0.6	19.9	0.30 ± 0.03	-42
$t\text{-BuO}^- + \text{CH}_3\text{Cl} \rightarrow \text{Cl}^- + t\text{-BuOCH}_3$	1.6 ± 0.2	15.9	0.10 ± 0.01	-35
$\text{CH}_3\text{O}^- + \text{CH}_3\text{Cl} \rightarrow \text{Br}^- + \text{CH}_3\text{OCH}_3$	7.3 ± 0.2	18.0	0.40 ± 0.01	-49
$t\text{-BuO}^- + \text{CH}_3\text{Br} \rightarrow \text{Br}^- + t\text{-BuOCH}_3$	4.1 ± 0.5	13.5	0.30 ± 0.04	-43
$\text{F}^- + \text{CH}_3\text{Cl} \rightarrow \text{Cl}^- + \text{CH}_3\text{F}$	5.8 ± 0.3	23.4	0.25 ± 0.01	-28
$\text{HCC}^- + \text{CH}_3\text{Cl} \rightarrow \text{Cl}^- + \text{CH}_3\text{CCH}$	0.52 ± 0.07	21.4	0.024 ± 0.003	-51
$\text{HCC}^- + \text{CH}_3\text{Br} \rightarrow \text{Br}^- + \text{CH}_3\text{CCH}$	3.1 ± 0.30	19.6	0.16 ± 0.02	-59
$\text{CH}_3\text{CO}_2^- + \text{CH}_3\text{Br} \rightarrow \text{Br}^- + \text{CH}_3\text{CO}_2\text{CH}_3$	0.20 ± 0.04	14.4	0.014 ± 0.003	-17

^aUnits of $10^{-10} \text{ cm}^3 \text{ mol}^{-1} \text{ s}^{-1}$.

The height of the central barrier to the exchange reaction $X^- + CH_3X \rightarrow XCH_3 + X^-$ we define as the intrinsic nucleophilicity of the species X^- toward a methyl center. This definition of intrinsic nucleophilicity provides a useful way of describing reactivity in S_N2 reactions. For instance, within this framework nucleophilicity and leaving group ability become equivalent. Also, we expect good nucleophiles to have low barriers to reaction, and poor nucleophiles to have large barriers. We now explore some of the implications of this model.

Results and Discussion

The rate constants, efficiencies, and thermodynamic data used to extract intrinsic barriers via the analysis outlined above appear in Table I. Sample input parameters for RRKM calculations have been published elsewhere. Table II and Figure 4 contain the intrinsic barriers for the systems we have examined.

Table II
Selected Intrinsic Nucleophilicities

X^-	$\Delta E_0^*(X^- + CH_3X)$ (kcal/mol)
Cl^-	10.2
Br^-	11.2
F^-	26.2
CH_3O^-	26.6
$t-BuO^-$	28.8
$CH_3CO_2^-$	18.4
HCC^-	37.4
H^-	$\sim 65.0^a$

^aTheoretical (ref. 23).

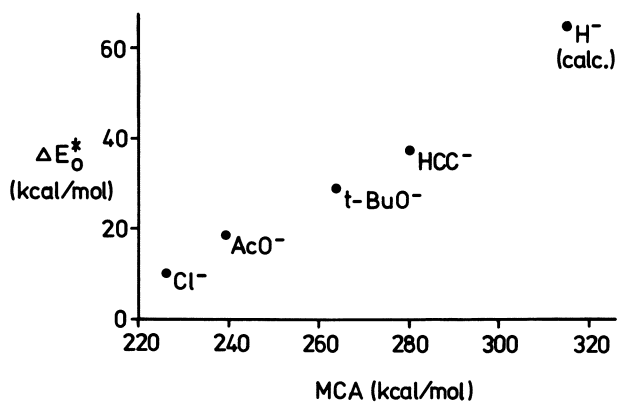
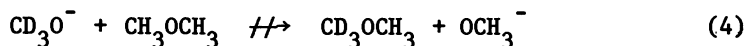


Figure 4. Plot of intrinsic barrier to degenerate exchange (intrinsic barrier for $X^- + \text{CH}_3X$) vs. methyl cation affinity for selected nucleophiles.

As pointed out previously (19), the intrinsic barriers are sensitive to changes in the RRKM input parameters. This sensitivity is largest for the small polyatomic nucleophiles (HCC^- and CH_3O^-) in reactions with efficiencies larger than ~ 0.1 , for which the computed intrinsic barriers to exchange were found to vary over a range of up to $\pm \sim 7$ kcal/mol for the different RRKM models used. Barriers for t-BuO^- and F^- exchange are much less sensitive to the model. In view of these results, the absolute values of the barriers cannot be known with certainty. However, qualitative trends are clear, and these trends are the principal object of subsequent discussion.

Comparison of Exchange Barriers. Among the most interesting results we have obtained are the intrinsic barriers for halide and alkoxide exchanges, shown in Table II. Note that the exchange barriers for $\text{Cl}^- + \text{CH}_3\text{Cl}$ and $\text{Br}^- + \text{CH}_3\text{Br}$ are much lower than those for F^- or alkoxide exchange. This means experimentally that the Cl^- exchange reaction proceeds with a measurable rate in our apparatus while the analogous exchanges $\text{F}^- + \text{CH}_3\text{F}$ and $\text{RO}^- + \text{CH}_3\text{OR}$ are predicted to have intrinsic barriers so large as to make them immeasurably slow. This prediction has been verified experimentally for the case of the methoxide exchange reaction in eq 4. No evidence for occurrence



of this reaction to any detectable extent in our ICR was found (8), implying an upper limit to the reaction efficiency of $\sim 10^{-4}$. In fact, there is some evidence to suggest that even when methoxide displacement from dimethyl ether is made significantly exothermic by choosing OH^- and NH_2^- as nucleophiles, the reaction still does not proceed to any measurable extent (20).

Comparison with Solution Behavior. This behavior is similar to that observed in solution. Although $\text{Cl}^- + \text{CH}_3\text{Cl}$ exchange proceeds readily in both polar and nonpolar solvents, alkoxides do not react measurably with alkyl ethers. In the past, this large difference in reactivity has been attributed to differential solvation effects, in which the transition state for $\text{S}_{\text{N}}2$ exchange is assumed to be much less well solvated than the reactants. Since alkoxides are better solvated than

Cl^- , the differential solvation effect is more pronounced for these cases and, hence, the barrier to exchange is large. However, our work predicts and demonstrates qualitatively identical behavior in the gas phase as well, and thus provides the first evidence that the low reactivity of alkoxides toward others is at least, in part, an intrinsic property of the reaction system and not due exclusively to differential solvation.

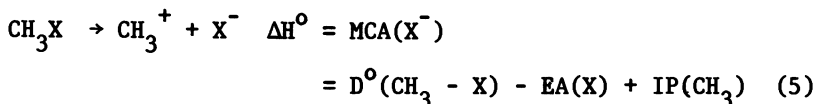
The concept of intrinsic barriers provides insight into the poor leaving group ability of alkoxides in other $\text{S}_{\text{N}}2$ reactions as well. For instance, the methoxide exchange component of the intrinsic barrier to the reaction $\text{X}^- + \text{CH}_3\text{OCH}_3 \rightarrow \text{XCH}_3 + \text{OCH}_3^-$ is so large that, regardless of the nature of X^- , the reaction is predicted to be slow unless it is also extremely exothermic. Cl^- , on the other hand, does not have this problem since the intrinsic barrier to its reaction with CH_3Cl appears to be much smaller; thus, Cl^- functions as a good leaving group while CH_3O^- does not.

Intrinsic Nucleophilicity vs. Leaving Group Ability. As pointed out earlier, our definition of intrinsic nucleophilicity in terms of barriers to degenerate exchange reactions necessarily implies that nucleophilicity and leaving group ability are equivalent. This can be seen in either of two ways. First, in the degenerate reaction $\text{X}^- + \text{CH}_3\text{X} \rightarrow \text{XCH}_3 + \text{X}^-$, the species X^- functions both as a nucleophile and as a leaving group: hence, there is no distinction between these "modes" of reactivity. Alternatively, note that the intrinsic barrier for the reaction $\text{X}^- + \text{CH}_3\text{Y} \rightarrow \text{Y}^- + \text{CH}_3\text{X}$ is the same in the forward and reverse directions, since by considering the intrinsic barrier we have effectively made the reaction thermoneutral. Thus, any species which is a good nucleophile in the Marcus sense is also a good leaving group, and poor nucleophiles are also poor leaving groups. This is consistent with the classical picture of Cl^- as both a good nucleophile and good leaving group, but not with that of methoxide which is generally considered a good nucleophile and poor leaving group.

The resolution of this latter discrepancy lies in the distinction between kinetic and thermodynamic nucleophilicity. Although a reaction such as $\text{CH}_3\text{O}^- + \text{CH}_3\text{Cl} \rightarrow \text{Cl}^- + \text{CH}_3\text{OCH}_3$ has a very large intrinsic barrier, overall the reaction is also strongly exothermic. This large thermodynamic effect lowers the barrier to the point where the reaction proceeds readily,

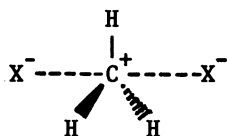
both in the gas phase and in solution. Thus, kinetically methoxide is a poor nucleophile, but strongly favorable thermodynamics make it relatively reactive with substrates such as CH_3Cl .

Correlation with Methyl Cation Affinity. Intrinsic barrier data for some of the other systems we have examined are shown in Table II and Figure 4. Note that the barriers vary widely with structure. Some insight into the mechanism of this variation is obtained by noting that the only thermodynamic parameter which correlates well with the purely kinetic intrinsic barriers is the methyl cation affinity (MCA) of the nucleophile X^- . This quantity is defined in eq 5 and is essentially the heterolytic bond dissociation enthalpy of the $\text{X}-\text{CH}_3$ bond.



A plot of intrinsic barrier vs. methyl cation affinity for several systems examined appears in Figure 4. In contrast to the excellent correlation shown in this figure, correlations between intrinsic barrier and $\text{EA}(\text{X})$, $\text{D}^\circ(\text{CH}_3 - \text{X})$, or gas phase proton affinity of X^- , are very poor.

Note that the intrinsic barrier increases with methyl cation affinity. Such a correlation between purely kinetic and purely thermodynamic properties is not surprising in view of theoretical studies (21, 22) which have shown there to be significant contributions to the $\text{S}_{\text{N}}2$ transition state from resonance structures such as the following:



Thus, formation of the transition state in the $\text{S}_{\text{N}}2$ exchange is formally analogous to the process represented by the methyl cation affinity; we believe this factor to be the origin of the observed correlation. The slope of the least-squares line through the points is about 0.5, which is consistent with partial charge development in the transition state. However, at this point we have no model which suggests that the relationship must be rigorously linear.

Summary

We propose that potential surfaces for gas-phase S_N2 reactions may be correlated using Marcus rate-equilibrium theory. The result is a model for intrinsic nucleophilicity in displacements at methyl centers, which, as demonstrated above, can be useful in descriptions of intrinsic reactivity in these systems. We are currently attempting to apply this model to other systems, in hopes of elucidating effects of structural features such as charge delocalization on reactivity. Finally, in view of recent work along these lines on reactions in solution (3), our model may be of potential use in bridging the gap between gas-phase and solution behavior.

Acknowledgments

We are grateful to the National Science Foundation and to the Donors of the Petroleum Research Fund, administered by the American Chemical Society, for support of this research. We thank the National Science Foundation for Fellowship support for M. J. P.

Literature Cited

1. See, for instance, Hartshorn, S. R. "Aliphatic Nucleophilic Substitution"; Cambridge University Press: London, 1973; Streitwieser, A., Jr., *Chem. Rev.* 1956, 56, 571.
2. Marcus, R. A. *J. Phys. Chem.* 1968, 72, 891.
3. Albery, W. J.; Kreevoy, M. M. *Adv. Phys. Org. Chem.* 1978, 16, 87.
4. Pellerite, M. J.; Brauman, J. I. "Gas-Phase Carbanion Chemistry"; part A, E. Bunzell and T. Durst, Eds., Elsevier: Amsterdam, 1980; Chap. 2, and references cited therein.
5. McIver, R. T., Jr. *Rev. Sci. Instr.* 1978, 49, 111.
6. Su, T.; Bowers, M. T. *J. Chem. Phys.* 1973, 58, 3027.
7. Su, T.; Bowers, M. T. *Int. J. Mass Spec. Ion Phys.* 1973, 12, 347.
8. Olmstead, W. N.; Brauman, J. I. *J. Am. Chem. Soc.* 1977, 99, 4219.
9. Forst, W. "Theory of Unimolecular Reactions"; Academic Press: New York, 1973.
10. Robinson, P. J.; Holbrook, K. A. "Unimolecular Reactions"; Wiley-Interscience: New York, 1972.
11. Jasinski, J. M.; Rosenfeld, R. N.; Golden, D. M.; Brauman, J. I. *J. Am. Chem. Soc.* 1979, 101, 2259.
12. Dougherty, R. C.; Dalton, J.; Roberts, J. D. *Org. Mass Spectrom.* 1974, 8, 77.
13. Dougherty, R. C.; Roberts, J. D. *ibid*, 1974, 8, 81.
14. Dougherty, R. C. *ibid*, 1974, 8, 85.
15. Bell, R. P. *Proc. Royal Soc.* 1936, A154, 414.

16. Evans, M. G.; Polanyi, M. Trans. Faraday Soc. 1938, 34, 11; and references cited therein.
17. Murdoch, J. R. J. Am. Chem. Soc. 1972, 94, 4410.
18. Leffler, J. E.; Grunwald, E. "Rates and Equilibria of Organic Reactions"; Wiley: New York, 1963; p.157.
19. Pellerite, M. J.; Brauman, J. I. J. Am. Chem. Soc. 1980, 102, 5993.
20. Bierbaum, V. M., personal communication.
21. Dedieu, A.; Veillard, A. J. Am. Chem. Soc. 1972, 94, 6730.
22. Bader, R. F. W.; Duke, A. J.; Messer, R. R. J. Am. Chem. Soc. 1973, 95, 7715.
23. Leforestier, C. J. Chem. Phys. 1977, 68, 4406.

RECEIVED April 21, 1982.

General Discussion—Nucleophilic Substitution

Leader: H. Bernhard Schlegel

DR. DAVID MITCHELL (Queen's University): For some time, we have been interested in theoretical approaches to S_N2 potential energy surfaces. We have been particularly influenced by Professor Brauman. I would like to report some work that I have done, along with Professors H. Bernhard Schlegel of Wayne State University and Saul Wolf of Queen's University in Kingston, on this problem, particularly in relation to the application of Marcus theory.

Figure 1 reiterates the double-well potential and provides definitions of quantities which Dr. Brauman has already mentioned. In our case, his $\Delta E'$ becomes ΔE^b the energy difference between the transition state and the reactants. ΔE^w is the well depth. We now see two different ΔE quantities, ΔE which is the cluster-to-cluster or complex-to-complex energy change and ΔE° , which is the energy difference between the separated reactants and the separated products.

Our actual approach has been to calculate *ab initio* the structures and energies of these wells and the transition states. All the calculations that I will report here are at the 4-31G single determinant level, with complete geometry optimization of all parameters.

Our task, then, is to test whether or not the Marcus relation will work, having obtained all of the potential energy quantities that we need from this figure. So I have rewritten the Marcus relation (eq 1) in a slightly different form than Dr. Brauman did, including here the definition of the intrinsic barrier for the cross-reaction as being the mean of the two degenerate exchange reactions.

$$\Delta E_{x,y}^\ddagger = \frac{1}{2}(\Delta E_{x,x}^\ddagger + \Delta E_{y,y}^\ddagger) + \frac{1}{2}\Delta E + \frac{\Delta E^2}{8(\Delta E_{x,x}^\ddagger + \Delta E_{y,y}^\ddagger)} \quad (1)$$

We must first obtain the intrinsic barriers. This we have done by calculating the ion-molecule clusters and transition states for a large number of degenerate exchange reactions. Some of the barriers, particularly, are somewhat different from what Professor Brauman has reported. This may well be a function of the relatively small basis set that has been used, and addition of polarization functions, for example, could significantly affect their absolute magnitudes. Still, the observed trend is undoubtedly correct. Species such as hydride (57.3), acetylide (50.4), and cyanide (43.8) have very high intrinsic barriers; a set of three oxygen nucleophiles, lower barriers; fluorine (11.7) and chlorine (5.5), the lowest of all.

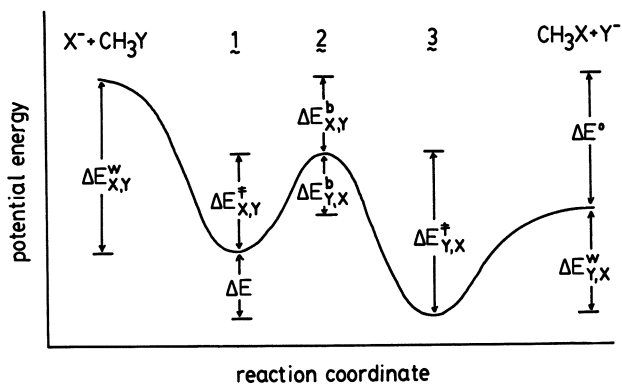


Figure 1. Reaction coordinate for the gas-phase displacement reaction $X^- + CH_3Y \rightarrow XCH_3 + Y^-$ and definitions of the quantities in Eqs. 1-3.

Once we have obtained these barriers, we are now able to go back, insert these values into the cross-relation, and test the predicted $\Delta E_{x,y}^\ddagger$ against that actually obtained from the ab initio calculations. A plot of the Marcus relationship for ten different cross-reactions gives an extremely good correlation with the theoretical unit slope and a mean deviation of less than a kilocalorie [Wolfe, S.; Mitchell, D. J.; Schlegel, H. B. *J. Am. Chem. Soc.* 1981, **103**, 7694].

We were also curious to extend the Marcus relation a bit further to see if we could somehow eliminate the need to calculate two very expensive ion-molecule clusters for each cross-reaction required to obtain ΔE . As Professor Brauman pointed out, the energy difference between the transition state and the separated reactants can be used as a measure of the overall efficiency of the reaction for structurally similar reactions.

If we could develop an expression for $\Delta E_{x,y}^b$ alone, potentially we could eliminate having to calculate the cluster energies.

An observation on our part is that the sum of the well depths for the two different sides of the cross-reaction turn out to be very similar to the sum of the well depths for the two intrinsic complexes as expressed in eq 2.

$$\Delta E_{x,y}^w + \Delta E_{y,x}^w \cong \Delta E_{x,x}^w + \Delta E_{y,y}^w \quad (2)$$

Again, there is not much scatter in that data, with agreement within a kilocalorie or slightly more. Whether this would pan out experimentally, I am not sure, but I think it is probably worth a look.

As a result of this behavior we can substitute back into the Marcus equation and find this relationship now in terms of the ΔE^b , which is the energy difference between the transition state and the reactants. As a second approximation, the overall energy change, ΔE° , is substituted for ΔE (the cluster-to-cluster energy difference) in eq 1. This leads to the modified Marcus relation shown in eq 3.

$$\Delta E_{x,y}^b = \frac{1}{2}(\Delta E_{x,x}^b + \Delta E_{y,y}^b) + \frac{1}{2}\Delta E^\circ + \frac{\Delta E^{\circ 2}}{8(\Delta E_{x,x}^\ddagger + \Delta E_{y,y}^\ddagger)} \quad (3)$$

This relationship also turns out to give very good agreement with experimental data. There is slightly more scatter, with a mean deviation, I think, of about 1.4 kilocalories [Wolfe, S., et al., *op. cit.*].

These results suggest that the Marcus equations can be applied quite successfully to gas phase displacement reactions, as suggested by Professor Brauman. We are currently generating more cross reactions and intend to test other rate-equilibrium relationships using our data.

DR. COOPER LANGFORD (Concordia University): I have some very short notes here, which are, in fact, a cautionary final note on the use of Marcus theory with respect to the transfer of very large groups. Quite frankly, our studies were stimulated by reading the outrageous remarks at the beginning of John Albery's paper in the last volume of the Annual Review of Physical Chemistry [Albery, W. J. *Ann. Rev. Phys. Chem.* 1980, 31, 227]. When people say outrageous things, it is more enjoyable to try to find out if there might be some way to show them wrong.

Analysis of rate constants, rate laws, and their parametric dependence on variables such as pressure and temperature yield only information on the difference between the ground state and the transition state, according to transition state theory. However, I wish to argue that the correlation of rate constants with equilibria, linear free energy relationships (LFER), allows the development of information on the shape of the potential functions and the number of degrees of freedom involved in the reaction coordinate. According to Marcus theory (see Albery's review), the LFER slope, α , has the following properties. If the slope is near 1, the reaction is endothermic, if α is near 0, the reaction is exothermic, and if ΔG^0 is near 0, then α is near 0.5.

However, students of substitution reactions of octahedral complexes know that reactions with ΔG^0 near 0 can have α approximately equal to 1. This is evident, for example, in Albert Haim's collection of data for the halopentaamines of cobalt(III) [Haim, A. *Inorg. Chem.* 1970, 9, 426].

How does this happen? The answer is easily envisioned if the assumption in Marcus treatments, that the relevant potential surfaces cross only and always in the harmonic parabolic region, is dropped. When the crossing of potential surfaces for reactant and product occurs in the highly anharmonic region near the dissociation limit, then ΔG^0 is about equal to 0, but α is closer to 1. Despite clever remarks in Albery's review, this limit on the utility of Marcus parabolic potentials was recognized in 1974 by Professor Swaddle. Swaddle considered reactant and product surface crossing in the nearly linear anharmonic region, which he suspected might approximate associative ligand substitution. The α values prove to be near 0.5 for small ΔG^0 in the linear region, according to Swaddle's analysis.

One might ask how the Marcus case of crossing in the harmonic region can arise. In a sense, that is the surprising situation. How can significant reaction occur without reaching the anharmonic part of the potential? To think of this, it is probably wise to remember that Marcus theory was first applied to electron transfer of the outer-sphere variety. Albery answers by pointing out that a reaction coordinate which is constructed from the intersection of parabolic surfaces for several

degrees of freedom is still parabolic. A Marcusian reaction, (if I may use that terminology) is constructed, perhaps, from relatively small displacements along a number of nuclear degrees of freedom. Non-Marcusian reactions, which are common in ligand substitution processes, involve large displacements in a small number of normal coordinates.

Non-Marcusian linear free energy relationships (if I may again be permitted that barbarism) provide direct evidence for this type of potential surface in octahedral ligand substitution reactions. Both dissociative (e.g., the chloropentaamine of cobalt(III)) and associative systems (e.g., chloropentaaquo chromium(III)) may have values of slopes for the linear free energy relationships indicating non-Marcusian behavior.

Thus we conclude that the potential surfaces involve large displacements in specific normal coordinates of the molecule, not small displacements on many coordinates.

DR. WILLIAM TROGLER (Northwestern University): I have a question about the status of sulfur nucleophiles. The calculations suggested that hydrosulfide ion was a very poor nucleophile. It has always puzzled me, at least in organic chemistry, that sulfur is such a great nucleophile. Have you done any experiments?

DR. BRAUMAN: I am glad you asked that question. Mercaptide ions are frequently pictured in organic chemistry as being incredibly reactive and having unusual properties. However, our experimental results indicate that they fit exactly on the plot which I showed. Thus, in the gas phase, their behavior appears normal.

It is mysterious to me why thiolates look so good in organic chemistry in solution. I think that is something we have to understand better, but it appears not to be an intrinsic property of thiolate ions. Thiolates will not displace each other, they are not good leaving groups, and so on, in the gas phase. Their reactivity is exactly what one would predict.

May I make some additional comments? There were three things I wanted to stress that I am not sure came across as well as I would have liked. One is that I don't have an absolute position on whether Marcus theory is applicable to these reactions. But it is obviously the correct way to start. What is particularly attractive about what we are doing and what this theory is doing is that we are dealing with a unimolecular process in which one simply goes well-to-well through a transition state and doesn't have, for example, work terms and solvent reorganization contributions which are of great importance in solution but very difficult to evaluate.

The second point is that, at least for my experiments and the theoretical approach which we take, we have not said anything about what the structure of the complex is. In fact, I

have no supporting information from any experiment that I do. Although the theoretical calculation will tell us a structure, there are probably many structures of fairly similar energy that exist. One should keep that in mind in looking at these things. For example, one should not decide arbitrarily that a nucleophile is nestled in on the back side. That doesn't have to be true.

The final comment I want to make is that if there is any system which is exceptionally difficult to calculate, it is a system which has too many electrons such as a negative ion. That is one of the reasons why I like to do these experiments.

If there is a little bit of disagreement between the calculation and the experiment, that is perfectly fine. Especially because of electron correlations, these are very difficult calculations to do. It is hard to imagine anything much more difficult given the current state of art. And the "experimental results" have substantial uncertainties as well in some of these cases.

DR. THOMAS MEYER (University of North Carolina): I find this conversation about the use of the Marcus theory remarkable. I almost understand its application to electron transfer. I would point out to you that there it is very carefully couched in terms of free energies. Also, there is a big difference between electron transfer reactions, where there is weak electronic coupling, and reactions involving bond breaking. If you go to quantum-mechanical treatments to do electron transfer calculations, where weak electronic coupling is assumed, the Marcus type of algebraic relationship can be derived in a very simple fashion. But then to find that the same relationships survive in these cases where there is strong vibrationally-dependent electronic coupling must be pure luck.

DR. BRAUMAN: First of all, the difference between whether one uses ΔG or ΔE depends on whether one is using a gas phase potential surface or not. Marcus specifically points out that one should use E and not G for this type of reaction. In fact, in this case it doesn't really matter which one uses. Using free energy will yield the same result because the entropies basically don't change. So that wouldn't make any difference.

Second, Marcus goes through a number of derivations of how one might get such a relationship, and Murdoch has shown that, if one simply makes some assumptions about linear stabilization, these equations will result. You are absolutely right, it doesn't have to be true. That is why I say I view this as a postulate. The calculations, I think, are helpful in that regard, because they suggest that the postulate might be right. But to have believed it without investigating it would be silly.

DR. MEYER: In electron transfer one can describe the problems in terms of well defined theoretical models. In the type of reactions which you are treating, you have found this nice empirical way to put things together but there is no fundamental basis for it. It is just a way to keep track of experimental facts.

DR. H. BERNHARD SCHLEGEL (Wayne State University): I would like to comment on that. I have a suspicion that what is at the root of the Marcus relation, especially considering Murdoch's derivation, is something akin to differential geometry. It has nothing to do with chemistry; it has to do with the geometry of surfaces and connecting these surfaces through transition states. So I think there is something quite fundamental there. And perhaps there is a little bit of luck involved in the fact that with parabolas, or with intersecting Morse curves, we can come up with something that behaves similar to the Marcus relation.

DR. ALBERT HAIM (State University of New York at Stony Brook): The examples that you gave us on the nucleophilic reactions have to do with systems which one knows in solution would be of the typical S_N2 type. What happens if you go into the gas phase with systems which we know from solution would be typically S_N1 ? What observations do you make in systems such as tertiary butyl, if you can do that type of work?

DR. BRAUMAN: Well, there is good news and bad news. If you take tertiary butyl, you get elimination. We have explored the stereochemistry in other reactions, so we know that these are really backside reactions. If we take something like 2,2,2-bicyclooctyl or adamantyl halides (i.e., bridge-head compounds), they don't react.

But something like neopentyl will react, and it does seem to show some indication of steric incumbrance. Unfortunately, we haven't been able to explore, say, a range of primary-secondary-tertiaries to see how the rates would depend. That is a very interesting problem, and I just don't know the answer. But you can't really see S_N1 reactions.

Electron Transfer in Weakly Interacting Systems

NORMAN SUTIN and BRUCE S. BRUNSCHWIG

Brookhaven National Laboratory, Department of Chemistry, Upton, NY 11973

A recently proposed semiclassical model, in which an electronic transmission coefficient and a nuclear tunneling factor are introduced as corrections to the classical activated-complex expression, is described. The nuclear tunneling corrections are shown to be important only at low temperatures or when the electron transfer is very exothermic. By contrast, corrections for nonadiabaticity may be significant for most outer-sphere reactions of metal complexes. The rate constants for the $\text{Fe}(\text{H}_2\text{O})_6^{2+}$ - $\text{Fe}(\text{H}_2\text{O})_6^{3+}$, $\text{Ru}(\text{NH}_3)_6^{2+}$ - $\text{Ru}(\text{NH}_3)_6^{3+}$ and $\text{Ru}(\text{bpy})_3^{2+}$ - $\text{Ru}(\text{bpy})_3^{3+}$ electron exchange reactions predicted by the semiclassical model are in very good agreement with the observed values. The implications of the model for optically-induced electron transfer in mixed-valence systems are noted.

The study of electron transfer reactions in solution is characterized by a strong interplay of theory and experiment. Theory has suggested systems for study, and experiments have suggested modifications to the theory. Although a number of theories have been proposed (1-13), there is general agreement that the crux of the electron transfer problem is the fact that the equilibrium nuclear configuration of a species changes when it gains or loses an electron. In the case of a metal complex, this configuration change involves changes in the metal-ligand and intraligand bond lengths and angles as well as changes in the vibrations and orientations of the surrounding solvent dipoles. In view of these configuration changes, the rate constants for electron transfer reactions are determined by nuclear as well as electronic factors. The first factor depends on the difference in the nuclear configurations of the reactants and products; the smaller this difference, the more rapid the reaction. The second

0097-6156/82/0198-0105\$08.75/0
© 1982 American Chemical Society

factor is a function of the electronic interaction of the two reactants; the larger this interaction, the more rapid the electron transfer.

Since the electronic interaction of the two reactants becomes more favorable with decreasing separation, the most favorable configuration for electron transfer is generally one in which the two reactants are in close proximity. Opposing this is the coulombic work required to bring similarly-charged reactants together, and ultimately the electron-electron repulsions. Consequently, in bimolecular reactions the electron transfer occurs over a range of separation distances, each with its own transfer probability, and it is necessary to integrate with respect to the separation distance in order to obtain the rate constant for the reaction:

$$k = \int_0^{\infty} \frac{4\pi N r^2}{1000} g(r) k_{el}(r) dr \quad (1)$$

In this equation $g(r)$ is the equilibrium radial distribution function for a pair of reactants (14), $g(r)4\pi r^2 dr$ is the probability that the centers of the pair of reactants are separated by a distance between r and $r + dr$, and $k_{el}(r)$ is the (first-order) rate constant for electron transfer at the separation distance r . Intramolecular electron transfer reactions involving "floppy" bridging groups can, of course, also occur over a range of separation distances; in this case a different normalizing factor is used.

In the conventional Debye-Hückel treatment the equilibrium radial distribution function for a pair of reactants $g(r)$ is simply equal to $\exp(-w/RT)$ with w given by (15)

$$w = \frac{z_2 z_3 e^2}{2D_s r} \left(\frac{\exp(\beta \sigma_2 \sqrt{\mu})}{1 + \beta \sigma_2 \sqrt{\mu}} + \frac{\exp(\beta \sigma_3 \sqrt{\mu})}{1 + \beta \sigma_3 \sqrt{\mu}} \right) \exp(-\beta r \sqrt{\mu}) \quad (2)$$

where z_2 and z_3 are the charges on the two reactants, D_s is the static dielectric constant of the medium, $\sigma_2(\sigma_3)$ is the sum of the radii of reactant 2(3) and the main ion of opposite charge in its ion atmosphere (the latter radius was assumed to be zero in (15)), and β is given by

$$\beta = \left(\frac{8\pi N e^2}{1000 D_s kT} \right)^{1/2} \quad (3)$$

Although more complex pair-correlation functions are available, the Debye-Hückel expression is adequate for our present purpose. It is valid when the work required to bring the reactants

together is predominantly coulombic and the ionic strength is low.

Classical Formalism

In the classical formalism it is assumed that bimolecular electron transfer occurs in a precursor complex in which the inner-coordination shells of the reactants are in contact, that is, $r = \sigma = (a_2 + a_3)$, where a_2 and a_3 are the hard-sphere radii of the reactants (16). Under these conditions the activation-controlled rate constant is given by the product of K_A , the equilibrium constant for the formation of the precursor complex, and $k_{el}(\sigma)$, the first-order rate constant for electron transfer within the precursor complex:

$$k = K_A k_{el}(\sigma) \quad (4a)$$

$$K_A = \frac{4\pi N\sigma^3}{3000} \exp\left(-\frac{w(\sigma)}{RT}\right) \quad (4b)$$

$$w(\sigma) = \frac{z_2 z_3 e^2}{D_s \sigma (1 + \beta \sigma \sqrt{\mu})} \quad (5)$$

The above expression for K_A has been derived from free volume considerations (17) as well as from the forward and reverse rates of diffusion-controlled reactions (18); the expression for w is valid when the radii of all the ions are equal. The relation between the above formulation and eq 1 may be seen from the following considerations. If most of the contribution to the observed rate comes from electron transfer over a small range of r values then

$$k \sim \frac{4\pi N \bar{r}^2}{1000} \delta r g(\bar{r}) k_{el}(\bar{r}) \quad (6)$$

where \bar{r} is the value of r corresponding to the maximum value of the integrand and δr is the range of r values over which the rate is appreciable (19). For typical outer-sphere reactions $\sigma \sim \bar{r} = 6-8 \text{ \AA}$ and, provided that the reaction does not border on the nonadiabatic, $\delta r \sim 2 \text{ \AA}$. Under these conditions the rate constants calculated from eq 4 and 1 will not differ significantly.

We next consider the expression for k_{el} in the classical formalism. According to the Franck-Condon principle, internuclear distances and nuclear velocities do not change during the actual electron transfer. This requirement is incorporated into the classical electron-transfer theories by postulating that the electron transfer occurs at the intersection of two potential energy surfaces, one for the reactants

(precursor complex) and the other for the products (successor complex). This is illustrated in Figure 1. The Franck-Condon principle is obeyed since the nuclear configurations and energies of the reactants and products are the same at the intersection. It is further assumed that the electron transfer occurs with unit probability in the intersection region, that is, the reaction is assumed to be adiabatic. In terms of the surfaces in Figure 1, H_{AB} , the electronic coupling of the initial and final states, is assumed to be large enough so that the system remains on the lower potential energy surface on passing through the intersection region, but small enough so that it may be neglected in calculating the height of the potential barrier ($H_{AB} \ll E_{th}$). Under these conditions the rate constant for the conversion of the precursor to the successor complex is independent of the magnitude of the electronic coupling and depends only on the nuclear factor

$$k_{e1} = \nu_n \exp(-(\Delta G_{in}^* + \Delta G_{out}^*)/RT) \quad (7)$$

where ν_n is the effective (nuclear) frequency with which the system crosses the barrier and ΔG_{in}^* and ΔG_{out}^* are the contributions of the inner-shell and outer-shell (solvent) reorganizations to the free energy barrier. The effective frequency (8) and the reorganization energies (1,2) for an exchange reaction are given by

$$\nu_n = \left(\frac{\nu_{in}^2 \Delta G_{in}^* + \nu_{out}^2 \Delta G_{out}^*}{\Delta G_{in}^* + \Delta G_{out}^*} \right)^{1/2} \quad (8)$$

$$\Delta G_{in}^* = \frac{1}{2} \sum f_i (\Delta d_i^0/2)^2 \quad (9)$$

$$\Delta G_{out}^* = \frac{(\Delta e)^2}{4} \left(\frac{1}{2a_2} + \frac{1}{2a_3} - \frac{1}{r} \right) \left(\frac{1}{D_{op}} - \frac{1}{D_s} \right) \quad (10)$$

In the above expressions ν_{in} is the average metal-ligand stretching frequency (300-500 cm^{-1}), ν_{out} is an average solvent orientation frequency (the vibrational spectrum of water exhibits a number of bands with a major band at $\sim 1 \text{ cm}^{-1}$ and with additional bands at higher frequency; 30 cm^{-1} is used as an average frequency (13)), f_i is a reduced force constant equal to $2f_i^A f_i^B / (f_i^A + f_i^B)$ where f_i^A and f_i^B are the force constants for the i^{th} vibration in the one reactant in its initial and final states (i.e., in its oxidized and reduced forms, and vice versa for the other reactant), $\Delta d_i^0 = |d_i^A - d_i^B|$ where d_i^A and d_i^B are the corresponding equilibrium bond distances (the sum is over all the vibrations of the reactants), D_{op} is the optical dielectric constant of the medium (equal to the square of the refractive index), and, as before, $r = \sigma = (a_2 + a_3)$, where a_2 and a_3 are the radii of the reactants.

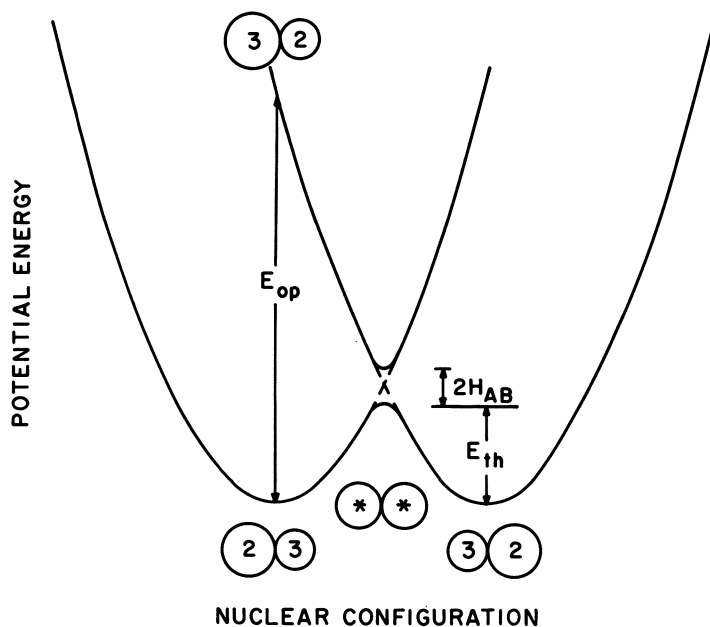


Figure 1. Potential energy plot of the reactants (precursor complex) and products (successor complex) as a function of nuclear configuration: E_{th} is the barrier for the thermal electron transfer, E_{op} is the energy for the light-induced electron transfer, and $2H_{AB}$ is equal to the splitting at the intersection of the surfaces, where H_{AB} is the electronic coupling matrix element. Note that $H_{AB} \ll E_{th}$ in the classical model. The circles indicate the relative nuclear configurations of the two reactants of charges +2 and +3 in the precursor complex, optically excited precursor complex, activated complex, and successor complex.

The inner-shell and outer-shell distortions of the reactants leading to the activated complex are illustrated in Figure 2. The ellipses depict equipotential sections through the potential energy surfaces for the precursor and successor complexes. The initial distortion of the precursor complex is predominantly along the low-frequency solvent coordinate. When the solvent configuration appropriate to the activated complex has been reached, the system continues to ascend to the top of the barrier by distorting primarily along the inner-sphere coordinate (defined by the steepest descent pathway). The electron transfer occurs at the top of the barrier and the system passes over the barrier with an effective frequency ν_n to form the successor complex.

Comparison of Observed and Calculated Exchange Rate Constants. The rate constants for the $\text{Fe}(\text{H}_2\text{O})_6^{2+} - \text{Fe}(\text{H}_2\text{O})_6^{3+}$, $\text{Ru}(\text{NH}_3)_6^{2+} - \text{Ru}(\text{NH}_3)_6^{3+}$ and $\text{Ru}(\text{bpy})_3^{2+} - \text{Ru}(\text{bpy})_3^{3+}$ exchange reactions calculated from eq 4,5 and 7-10 are compared with the observed values in Table I. The agreement of the calculated and observed rate constants is very good for the $\text{Fe}(\text{H}_2\text{O})_6^{2+} - \text{Fe}(\text{H}_2\text{O})_6^{3+}$ exchange but is less satisfactory for the $\text{Ru}(\text{NH}_3)_6^{2+} - \text{Ru}(\text{NH}_3)_6^{3+}$, and $\text{Ru}(\text{bpy})_3^{2+} - \text{Ru}(\text{bpy})_3^{3+}$ exchanges. The slow rate of the $\text{Fe}(\text{H}_2\text{O})_6^{2+} - \text{Fe}(\text{H}_2\text{O})_6^{3+}$ exchange is a consequence of large inner-shell and solvent reorganization barriers. By contrast, the $\text{Ru}(\text{bpy})_3^{2+} - \text{Ru}(\text{bpy})_3^{3+}$ exchange is very rapid because of its negligible inner-shell and small solvent reorganization barrier. The $\text{Ru}(\text{NH}_3)_6^{2+} - \text{Ru}(\text{NH}_3)_6^{3+}$ exchange is intermediate in character, but with the bulk of the barrier arising from ΔG_{out}^* .

Semiclassical Formalism

In the classical activated-complex formalism nuclear tunneling effects are neglected. In addition, the electron transfer is assumed to be adiabatic. These assumptions are relaxed in the semiclassical model.

The frequencies relevant to the electron transfer process are shown in Table II.

The difference in the time-scales for electronic and nuclear motions is, of course, the basis of the Born-Oppenheimer approximation (and the Franck-Condon principle). This approximation allows for the separation of nuclear and electronic coordinates in the wave equation and is implicit in the calculation of the potential energy surfaces illustrated in Figures 1 and 2. Such surfaces describe the electronic energy of the system as a function of the nuclear coordinates. Classically, the rate of electron transfer is determined by the rate of passage of the system over the barrier defined by the surfaces. In the semiclassical model (13) a nuclear tunneling factor that measures the increase in rate arising from

Table I. Comparison of Observed and Calculated Rate Constants for Exchange Reactions at 25 °C.

	$\text{Fe}(\text{H}_2\text{O})_6^{2+/3+}$	$\text{Ru}(\text{NH}_3)_6^{2+/3+}$	$\text{Ru}(\text{bpy})_3^{2+/3+}$	Reference
Δd^0 , Å	0.14	0.04	~ 0	20-23
$(a_2 + a_3)$, Å	6.5	6.7	~ 14	20-23
ΔG_{in}^* , kcal mol ⁻¹	8.34	0.76	~ 0	
ΔG_{out}^* , kcal mol ⁻¹	6.92	6.72	3.21	
μ , M	0.55	0.10	0.10	
k_{calcd} , M ⁻¹ s ⁻¹	0.96	2.8×10^5	8.0×10^9 ^a	
k_{obsd} , M ⁻¹ s ⁻¹	4.2	4.3×10^3	4.2×10^8	24-26

^a Not corrected for diffusion.

Table II. Characteristic frequencies for electron transfer

electronic (delocalized orbital)	$10^{15} - 10^{16} \text{ s}^{-1}$
vibrational (M-L, C-H, O-H)	$10^{13} - 10^{14} \text{ s}^{-1}$ $300 - 3000 \text{ cm}^{-1}$
orientational (solvent dipoles)	$10^{11} - 10^{12} \text{ s}^{-1}$ $3 - 30 \text{ cm}^{-1}$

quantum-mechanical tunneling through the barrier is included. In addition, the possibility that the electron transfer may not occur even when the nuclear configurations of the reactants are appropriate (for example, when the reactants are far apart or the electron transfer is spin forbidden) is allowed for by introducing an electronic transmission coefficient (13). The rate constant for electron transfer within the semiclassical formalism is thus given by

$$k = \int_{\sigma}^{\infty} \frac{4\pi N r^2}{1000} \exp\left[-\frac{w(r)}{RT}\right] \kappa(r) \Gamma_n v_n(r) \exp\left[-\frac{(\Delta G_{in}^* + \Delta G_{out}^*(r))}{RT}\right] dr \quad (11)$$

where Γ_n is the nuclear tunneling factor and κ is the electronic transmission factor. These factors are considered in turn.

Nuclear tunneling. Nuclear tunneling is important for a particular mode when $h\nu > kT$. Since $v_{in} > v_{out}$ nuclear tunneling will be more important for the inner-sphere than for the solvent modes. For the purposes of the present discussion we will assume that nuclear tunneling of the solvent modes may be neglected, that is, we assume that it is necessary for the solvent to acquire the nuclear configuration appropriate to the top of the barrier (activated complex) as a prerequisite for electron transfer. This assumption is probably valid above 50 K. Because of nuclear tunneling it is not necessary for the inner-sphere to achieve the configuration of the activated complex; rather electron transfer may occur at any inner-sphere configuration. This is illustrated in Figure 3.

According to a recent model (13) nuclear tunneling factors for the inner-sphere modes can be defined by

$$\ln \Gamma_n = (\Delta G_{in}^* - \Delta G_{in}^*(T))/RT$$

where $\Delta G_{in}^*(T)$ is a temperature-dependent inner-shell reorganization energy that approaches the classical value ΔG_{in}^* at high temperature. A particularly useful expression for $\Delta G_{in}^*(T)$ is obtained using Holstein's saddle-point method (13,27). Use of this expression leads to the following expression for the

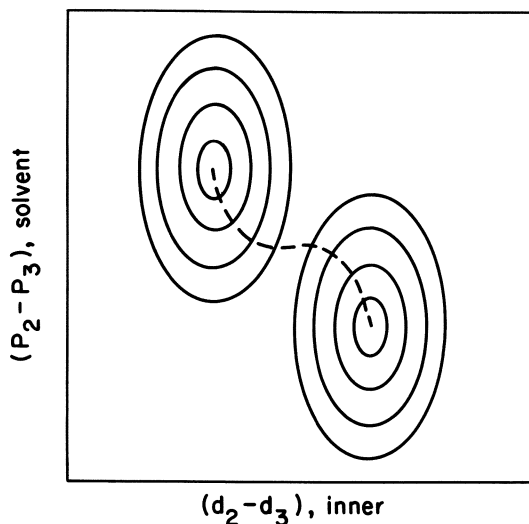


Figure 2. Equipotential sections through the potential energy surface for an exchange reaction. The sections define ellipses if the surfaces are parabolic: the top left set refer to the initial state (precursor complex) and the bottom right set refer to the final state (successor complex). The dashed line indicates the reaction coordinate. Parameters P_2 and P_3 reflect the state of polarization of the solvent, and coordinates d_2 and d_3 reflect the inner-shell configurations of the two reactants (products).

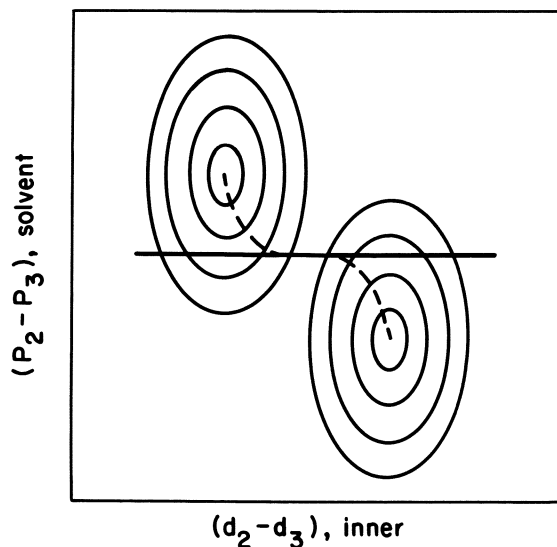


Figure 3. Equipotential sections through the potential energy surface for an exchange reaction, as in Figure 2. The heavy horizontal line indicates the solvent configuration appropriate to the activated complex and is the solvent configuration at which inner-sphere tunneling takes place.

first-order rate constant for an exchange reaction

$$k_{el} = \kappa \nu_n \exp \left(- \frac{E_{in}}{Nh\nu_{in}} \tanh \left(\frac{Nh\nu_{in}}{4RT} \right) - \frac{E_{out}}{4RT} \right) \quad (12)$$

where $E_{in} \sim 4\Delta G_{in}^*$ and $E_{out} \sim 4\Delta G_{out}^*$. An equivalent approach (13) leads to the following expression for Γ_n

$$\Gamma_n = A \sum_m \exp \left[- \frac{\epsilon_m}{RT} \right] S_{m,m}^2 \quad (13)$$

where A is a normalization factor, $S_{m,m}^2$ is the square of the overlap (the Franck-Condon factor) of the m^{th} vibrational state of the reactants with the m^{th} vibrational state of the products, and ϵ_m is the energy of the m^{th} vibrational level. (See Figure 4; note that this formalism is very similar to one proposed in an early paper (28) on the basis of a perceived analogy between electron transfer reactions and ordinary electronic transitions.)

The value of $\log \Gamma_n$ for the $\text{Fe}(\text{H}_2\text{O})_6^{2+} - \text{Fe}(\text{H}_2\text{O})_6^{3+}$ exchange (which features a relatively large inner-sphere barrier) is plotted as a function of $1/T$ in Figure 5. The nuclear tunneling factors are close to unity at room temperature but become very large at low temperatures. As a consequence of nuclear tunneling, the electron transfer rates at low temperatures will be much faster than those calculated from the classical model.

The value of $\log \Gamma_n$ at 300 K for a (hypothetical) reaction having the same inner-sphere parameters as the $\text{Fe}(\text{H}_2\text{O})_6^{2+} - \text{Fe}(\text{H}_2\text{O})_6^{3+}$ couple is plotted as a function of ΔG^0 in Figure 6. The nuclear tunneling factors at first decrease and then become very large at high driving force. The dramatic increase in Γ_n corresponds to the onset of the inverted free-energy region of the classical formalism (1). Although nuclear tunneling will reduce the rate decreases predicted for the inverted region, substantial decreases are still expected. There is only meager experimental support for the predicted rate decreases (29,30) and this area is currently receiving much attention (31-35).

The Effective Nuclear Frequency. When nuclear tunneling is important we suggest that the individual frequencies should be weighted by their effective barriers, that is, instead of eq 8 it may be more appropriate to use eq 14

$$\nu_n = \left(\frac{\frac{3}{2kT} \frac{h\nu_{in}}{2kT} E_{in} \operatorname{csch} 2\nu'_{in} + \nu_{out}^2 E_{out}}{\frac{h\nu_{in}}{2kT} E_{in} \operatorname{csch} 2\nu'_{in} + E_{out}} \right)^{1/2} \quad (14)$$

in which E_{in} has been replaced by its quantum-mechanical analogue

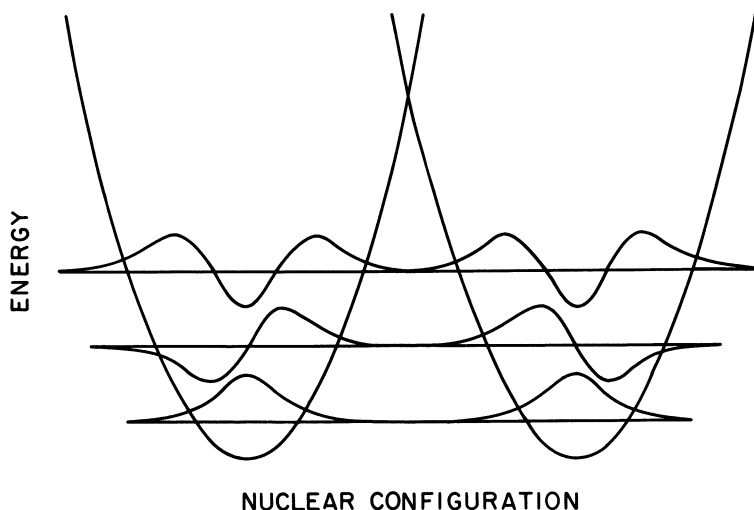


Figure 4. Illustration of inner-sphere tunneling in an exchange reaction. The reactants and products are assumed to have the same reduced force constant, and only the energy levels and wave functions for the lowest vibrational states of the reactants and products are shown.

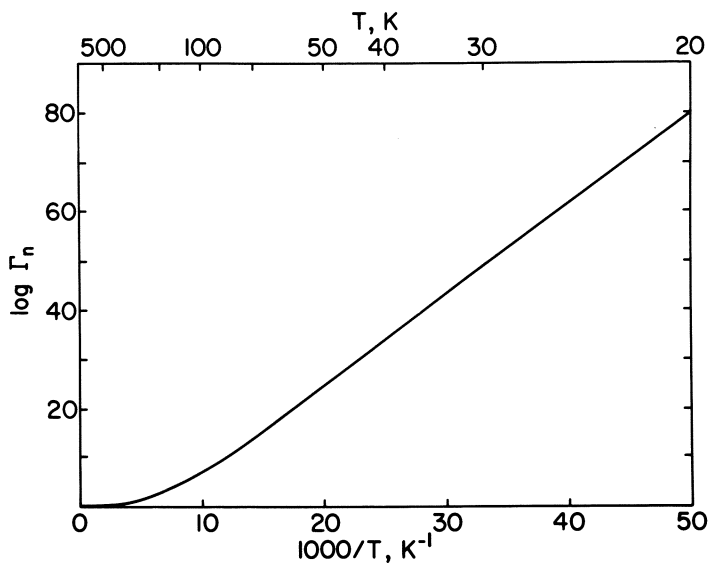


Figure 5. Plot of the logarithm of the nuclear tunneling factor vs. $1/T$ for the $\text{Fe}(\text{H}_2\text{O})_6^{2+} - \text{Fe}(\text{H}_2\text{O})_6^{3+}$ exchange reaction. The slope of the linear portion below 150 K is equal to $E_{in}/4R$ (13).

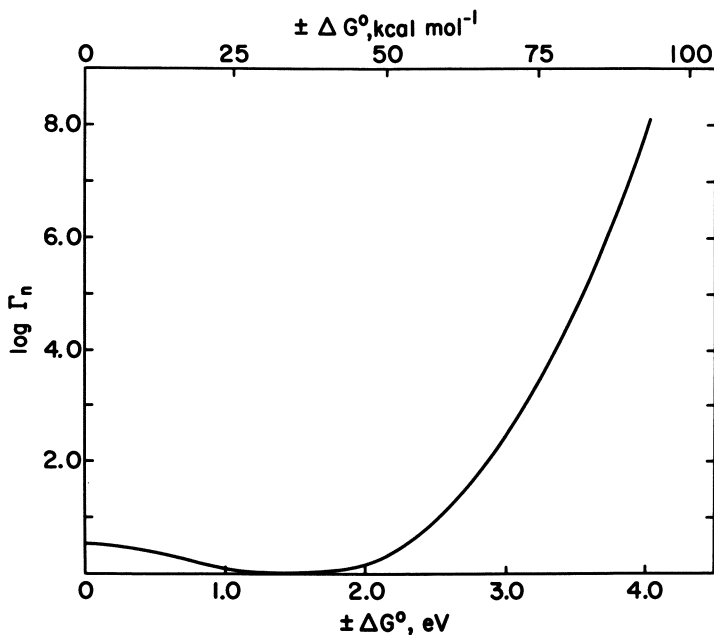


Figure 6. Plot of the logarithm of the nuclear tunneling factor vs. ΔG° for an electron transfer reaction accompanied by a net chemical change. The following parameters were used to calculate $\log \Gamma_n$: ν_{in} , 432 cm^{-1} ; ΔG_{in}^* , 8.34 kcal/mol; and ΔG_{out}^* , 0 at 300 K. The nuclear tunneling factors were calculated by modifying the expression for electron hopping in solids derived by Holstein (12). In general, substitution of an average frequency for the inner-sphere and solvent modes into the modified expression yields $\Delta G^*(T)$ values that are in excellent agreement with those given by the full quantum-mechanical expressions with $\Delta G_{out}^* > 0$ and $G^\circ \leq 0$. A detailed description of these calculations will be presented elsewhere.

$2\nu_{in}'E_{in} \operatorname{csch} 2\nu_{in}'$ where $\nu_{in}' = Nh\nu_{in}/4RT = h\nu_{in}/4kT$. It should be noted that the effective nuclear frequency tends towards the solvent frequency when nuclear tunneling by the inner-sphere modes becomes very important. However, in most cases at room temperature ν_n approaches ν_{in} .

Electronic Transmission Coefficient. The probability that the electron transfer will occur in the intersection region (in other words, the probability that the system will remain on the lower adiabatic surface on passing through the intersection region) is given by (36)

$$\kappa = \frac{2(1 - \exp(-\nu_{el}/2\nu_n))}{2 - \exp(-\nu_{el}/2\nu_n)} \quad (15)$$

where ν_{el} , the frequency of electron transfer within the activated complex, is given by

$$\nu_{el} = \frac{2H_{AB}^2}{h} \left(\frac{\pi^3}{(E_{in} + E_{out})RT} \right)^{1/2} \quad (16)$$

(The ν_{el} defined here should not be confused with the electronic frequency ν_{el}^0 in Table II which is the frequency for a fully delocalized electron. When the interaction between the potential energy surfaces is very large then $\nu_{el} \rightarrow \nu_{el}^0$. Also, when nuclear tunneling is important E_{in} in the denominator should be replaced by $2\nu_{in}'E_{in} \operatorname{csch} 2\nu_{in}'$.) It is evident from eq 15 that $\kappa = 1$ (the electron transfer is adiabatic) when $\nu_{el} \gg 2\nu_n$ and that $\kappa = \nu_{el}/\nu_n$ (the electron transfer is nonadiabatic) when $\nu_{el} \ll 2\nu_n$. In the nonadiabatic limit the frequency factor is an electronic (ν_{el}) rather than a nuclear (ν_n) frequency, that is, the rate constant for a nonadiabatic reaction is

$$k = \int_{\sigma}^{\infty} \frac{4\pi Nr^2}{1000} \exp\left[-\frac{w(r)}{RT}\right] \nu_{el}(r) \Gamma_n \exp\left[-\frac{(\Delta G_{in}^* + \Delta G_{out}^*(r))}{RT}\right] dr \quad (17)$$

The reason for the absence of the nuclear frequency from eq 17 is that the slowest process in a nonadiabatic reaction is, by definition, the electron transfer; that is, $\nu_{el} \ll \nu_n$ for a nonadiabatic reaction.

The magnitude of the electronic interaction between the reactants is exceedingly important. If H_{AB} is very small then the coupling of the initial and final states of the system will be very weak, the electron transfer will be slow, and the reaction will be nonadiabatic. The procedures used for estimating H_{AB} or κ include the following:

- (a) Ab initio calculations (4,37).
- (b) Approximate theoretical models (38,39).

(c) Intensities of charge-transfer bands: H_{AB} may be estimated from the intensity of the intervalence charge-transfer band in mixed-valence systems using the Hush relation (40)

$$H_{AB} = \frac{2.06}{r} \left(\epsilon_{\max} \bar{\nu}_{\max} \Delta \bar{\nu}_{1/2} \right)^{1/2} \text{ cm}^{-1} \quad (18)$$

where ϵ_{\max} is the molar absorptivity at the absorbance maximum $\bar{\nu}_{\max}$, and $\Delta \bar{\nu}_{1/2}$ is the full width of the band at half maximum.


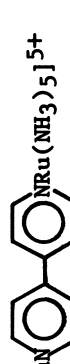

(d) Temperature dependence of the rate: κ can be estimated from the entropy of activation for the electron-transfer reaction. However this procedure must be used with caution since nuclear tunneling contributions and the temperature dependence of the electrostatic work terms will also tend to make the entropy of activation more negative.

(e) The limiting rate constant at high driving force: normally $k \rightarrow k_d$, the diffusion-controlled rate constant, as ΔG° becomes more negative. However if κ is small then $k \rightarrow K_A \kappa \nu_n$ as ΔG° becomes more negative ($\Delta G^\ddagger \rightarrow 0$). Thus κ can be obtained if rate saturation below the diffusion limit is observed. (Care must be exercised in this case, too, since rate saturation below the diffusion limit may be observed for other reasons, including a preequilibrium change on one of the reactants (41,42), substitution control (43), etc.)

Values of H_{AB} and κ obtained using the first three procedures are presented in Table III. On the basis of Newton's calculations (37), the $\text{Fe}(\text{H}_2\text{O})_6^{2+} - \text{Fe}(\text{H}_2\text{O})_6^{3+}$ exchange at $r = 6.4 \text{ \AA}$ is nonadiabatic. On the other hand, calculations for the $\text{Cr}(\text{H}_2\text{O})_6^{2+} - \text{Cr}(\text{H}_2\text{O})_6^{3+}$ exchange performed by Hush (4) indicate that this exchange is adiabatic. In contrast to the $\text{Fe}(\text{H}_2\text{O})_6^{2+} - \text{Fe}(\text{H}_2\text{O})_6^{3+}$ exchange in which the two oxidation states differ by an electron in a t_{2g} orbital, in the $\text{Cr}(\text{H}_2\text{O})_6^{2+} - \text{Cr}(\text{H}_2\text{O})_6^{3+}$ exchange the two oxidation states differ by an e_g electron. Evidently the electronic coupling in the latter exchange, but not the former, is considerably enhanced by mixing in the orbitals of the intervening water molecules. Based on direct 4d - 4d overlap (37), the $\text{Ru}(\text{NH}_3)_6^{2+} - \text{Ru}(\text{NH}_3)_6^{3+}$ exchange is barely adiabatic (43,44) while the $\text{Ru}(\text{bpy})_3^{2+} - \text{Ru}(\text{bpy})_3^{3+}$ exchange is highly nonadiabatic! Presumably it is the delocalization of the metal t_{2g} electron density onto the π^* orbitals of the bipyridine ligands that makes the $\text{Ru}(\text{bpy})_3^{2+} - \text{Ru}(\text{bpy})_3^{3+}$ exchange so rapid. Estimates of the magnitude of the electronic coupling provided by the $\pi^* - \pi^*$ interaction of the two reactants are consistent with this interpretation (43).

Table III also includes values of H_{AB} and κ estimated from the properties of the intervalence band observed for mixed-valence diruthenium complexes. Coupling by the pyrazine in these complexes is very strong and is particularly striking when compared with the coupling provided by the through-space interaction of two ruthenium centers at comparable r as

Table III. Estimates of Electronic Coupling Matrix Elements and Adiabaticity Factors^a

	τ	$-H_{AB}$	κ	Reference
	\AA	cm^{-1}		
$\text{Fe}(\text{H}_2\text{O})_6^{2+} \text{Fe}(\text{H}_2\text{O})_6^{3+}$	6.4	31	$\sim 10^{-2}$	<u>37</u>
$\text{Cr}(\text{H}_2\text{O})_6^{2+} \text{Cr}(\text{H}_2\text{O})_6^{3+}$	~ 6.5	~ 180	~ 1	<u>4</u>
$\text{Ru}(\text{NH}_3)_6^{2+} \text{Ru}(\text{NH}_3)_6^{3+}$	6.4	67 ^b	0.2 ^b	<u>36, 37</u>
$\text{Ru}(\text{bpy})_3^{2+} \text{Ru}(\text{bpy})_3^{3+}$	14	$\sim 0^c$	$< 10^{-6}^c$	<u>43</u>
	12.3	87	$\sim 1^d$	<u>43</u>
	10.8	400	1.0	<u>36, 46, 47</u>
	6.9	~ 3000	---	<u>36, 48, 49</u>

^a Further details of some of the calculations are given in (36).

^b Most of the electronic interaction is through the H atoms of the ligands (44).

^c Estimated assuming electron transfer by direct 4d-4d overlap.

^d Estimated assuming electron transfer through the π^* orbitals of the bipyridine ring system.

manifested in the $\text{Ru}(\text{NH}_3)_6^{2+} - \text{Ru}(\text{NH}_3)_6^{3+}$ exchange. Coupling of the ruthenium centers by the 4,4'-bipyridine group is strong enough for the intramolecular electron exchange to be adiabatic. Introduction of a $-\text{CH}_2-$ group between the two pyridine rings reduces the coupling so that the electron transfer becomes nonadiabatic.

For many purposes H_{AB} may be approximated by (38,39)

$$H_{AB} = H_{AB}^0 \exp(-\beta'(r-\sigma)) \quad (19)$$

where H_{AB}^0 is the value of H_{AB} at $r = \sigma$. The values of β' are $\sim 1.7 \text{ \AA}^{-1}$ for the $\text{Fe}(\text{H}_2\text{O})_6^{2+} - \text{Fe}(\text{H}_2\text{O})_6^{3+}$ exchange at $r \sim \sigma$ (37), $\sim 2.5 \text{ \AA}^{-1}$ for the $\text{Cr}(\text{H}_2\text{O})_6^{2+} - \text{Cr}(\text{H}_2\text{O})_6^{3+}$ exchange at $r \sim \sigma$ (4), and $\sim 1.0 \text{ \AA}^{-1}$ for two parallel aromatic rings such as anthracene and its radical anion (39).

An important conclusion that can be drawn from the above discussion is that most outer-sphere electron transfer reactions of metal complexes are, at best, marginally adiabatic and that the reaction will rapidly become nonadiabatic with increasing separation of the reactants. In view of these considerations, eq 11 can be integrated to give (50)

$$k = \frac{4\pi N\sigma^2}{2000\beta'} \exp\left[-\frac{w(\sigma)}{RT}\right] \kappa(\sigma) \Gamma_{\text{N}} \nu_{\text{N}}(\sigma) \exp\left[-\frac{(\Delta G_{\text{in}}^* + \Delta G_{\text{out}}^*(\sigma))}{RT}\right] \quad (20)$$

which is valid provided that $\sigma \gg 1/\beta'$. Inspection of eq 20 shows that the effective δr for a nonadiabatic reaction is $1/2\beta'$. Thus for $\beta' = 1.7 \text{ \AA}^{-1}$, δr for a nonadiabatic reaction is $\sim 1/5$ that for an adiabatic reaction at comparable σ .

We next reconsider the systems in Table I in the light of eq 20. The results of the calculations are presented in Table IV which includes the classical and experimental results. The rate constants for the $\text{Ru}(\text{NH}_3)_6^{2+} - \text{Ru}(\text{NH}_3)_6^{3+}$ and $\text{Ru}(\text{bpy})_3^{2+} - \text{Ru}(\text{bpy})_3^{3+}$ exchanges calculated from the semiclassical expressions are in much better agreement with the observed values than are the rate constants given by the classical expressions. On the other hand, the agreement with the observed value of the $\text{Fe}(\text{H}_2\text{O})_6^{2+} - \text{Fe}(\text{H}_2\text{O})_6^{3+}$ exchange is much poorer for the semiclassical calculation. However, good agreement can be obtained for this system, too, if the EXAFS value of Δd^0 (0.11 \AA (51)) rather than the crystallographic value (0.14 \AA (20)) is used. (Use of the smaller Δd^0 value lowers the inner-shell reorganization barrier leaving more room for nonadiabaticity; use of the crystallographic value of Δd^0 leads to a calculated rate constant that is much lower than the observed value if $\kappa \sim 10^{-2}$.) Unfortunately the smaller value of Δd^0 cannot be used with confidence at this time since recent EXAFS measurements yield a Δd^0 value closer to the crystallographic value (52). Clearly the

Table IV. Comparison of Semiclassical and Classical Calculations of Rate Constants for Exchange Reactions at 25 °C

	$\text{Fe}(\text{H}_2\text{O})_6^{2+/3+}$	$\text{Ru}(\text{NH}_3)_6^{2+/3+}$	$\text{Ru}(\text{bpy})_3^{2+/3+}$
k_{sc}^{a} , $\text{M}^{-1} \text{s}^{-1}$	1.3×10^{-3}	7.4×10^3	8.6×10^8
k_{c}^{b} , $\text{M}^{-1} \text{s}^{-1}$	0.96 ^c	2.8×10^5	8.0×10^9
k_{obsd} , $\text{M}^{-1} \text{s}^{-1}$	4.2	4.3×10^3	4.2×10^8

^a Semiclassical calculation using eq 20 together with eq 5, 9, 10 and 13-16.

^b Classical calculation using eq 4, 5 and 7-10.

last word on the $\text{Fe}(\text{H}_2\text{O})_6^{2+} - \text{Fe}(\text{H}_2\text{O})_6^{3+}$ exchange has not yet been written.

Conclusions

The above discussion shows that very good agreement of observed and calculated exchange rate constants can be obtained using the semiclassical formalism. In the bimolecular reactions discussed in this paper the reactants were treated as hard spheres and an outer-sphere mechanism was assumed. If the electronic interaction of the reactants is very weak, then the coupling may be increased through interpenetration of the inner-coordination shells of the reactants (36,43,44); in the limit this may give rise to an inner-sphere mechanism. Under either of these conditions the observed rates can be larger than those calculated from the outer-sphere model.

The semiclassical formalism reduces to the classical formalism when the electron transfer is adiabatic and nuclear tunneling effects are neglected. When these conditions are not satisfied, the semiclassical formalism gives results for exchange reactions that are identical over the entire temperature range with those given by the full quantum-mechanical treatment (13). The semiclassical formalism allows for the different time-scales characterizing the electron transfer process (Table II) in a natural manner. The fastest motion, that of the electrons (ν_{el}^0), defines the potential energy surfaces for the reaction. The slower nuclear processes (in this discussion, the solvent motion) take place on the surface and define a classical barrier for the reaction ΔG_{out}^* . By contrast, the faster nuclear processes (here, the inner-sphere motion) are not required to remain on the surface; rather they can tunnel through the barrier $\Delta G_{\text{in}}^*(T)$. Finally, the slower of the electron hopping (ν_{el}) and the average nuclear (ν_n) frequencies becomes a prefactor in the rate expression.

Nonequilibrium effects. In applying the various formalisms, a Boltzmann distribution over the vibrational energy levels of the initial state is assumed. The rate constant calculated on the basis of the equilibrium distribution, k_{eq} , is the maximum possible value of k_{el} . If the electron transfer is very rapid then the assumption of an equilibrium distribution over the energy levels is not valid, and it is more appropriate to treat the nuclear fluctuations in terms of a steady-state rather than an equilibrium formalism. Although a rigorous treatment of this problem has not yet appeared, intuitively it seems that since the slowest nuclear fluctuation will generally be a solvent orientational motion, k_{el} will equal k_{eq} when $\nu_{\text{out}} \gg k_{\text{eq}}$ and k_{el} will tend to ν_{out} when $\nu_{\text{out}} \ll k_{\text{eq}}$ (a simple treatment gives $1/k_{el} = 1/\nu_{\text{out}} + 1/k_{\text{eq}}$). These considerations are

unlikely to be important for most bimolecular reactions since the reactions will become diffusion controlled before they become subject to solvent reorientation control. However, the above considerations will be important in calculating the activation-controlled rate constants for reactions that are close to or at the diffusion-controlled limit and in calculating the rates of very rapid "intramolecular" electron transfer reactions.

A nonequilibrium distribution of nuclear configurations can, of course, be deliberately produced by optical excitation of the system. In this case the state immediately formed possesses the inner-sphere and the solvent configuration of the initial state but the electronic configuration of the final state (Figure 1). Relaxation to the nuclear configuration appropriate to the final state requires both inner-sphere and solvent reorganization. The former will occur rapidly, the latter only relatively slowly. Consequently, the initially formed state will first relax to an intermediate state having the inner-sphere configuration appropriate to the final electronic configuration, but with a solvent configuration which is still appropriate to the initial electronic configuration. At this stage solvent relaxation to the final state competes with back electron-transfer to the initial state. The quantum yield for the formation of the final state will be approximately equal to $v_{out}/(\kappa v_{in} + v_{out})$ which is $\ll 1$ when $\kappa \sim 1$. This type of explanation can account for the low yields ($< 10\%$) of the electronic isomer formed after optical excitation in the intervalence band of certain mixed-valence systems (53). Although formation of the final state will be favored if the electronic coupling is very weak ($\kappa \ll 1$), the intensity of the intervalence transition will also be very weak under these conditions.

To summarize, in this article we have discussed some aspects of a semiclassical electron-transfer model (13) in which quantum-mechanical effects associated with the inner-sphere are allowed for through a nuclear tunneling factor, and electronic factors are incorporated through an electronic transmission coefficient or adiabaticity factor. We focussed on the various time scales that characterize the electron transfer process and we presented one example to indicate how considerations of the time scales can be used in understanding nonequilibrium phenomena.

Acknowledgments. The authors wish to acknowledge very helpful discussions with Drs. C. Creutz and R. A. Marcus. This research was supported by the Office of Basic Energy Sciences of the U. S. Department of Energy.

Literature Cited

1. Marcus, R. A. Annu. Rev. Phys. Chem. 1964, 15, 155.
2. Marcus, R. A. J. Chem. Phys. 1965, 43, 679.
3. Hush, N. S. Trans. Faraday Soc. 1961, 57, 557.
4. Hush, N. S. Electrochim. Acta 1968, 13, 1005.
5. Kestner, R. N.; Logan, J.; Jortner, J. J. Phys. Chem. 1974, 78, 2148.
6. Dogonadze, R. R.; Kuznetsov, A. M.; Levich, V. G. Electrochim. Acta 1968, 13, 1025.
7. German, E. D.; Dvali, V. G., Dogonadze, R. R.; Kuznetsov, A. M. Elektrokimiya 1976, 12, 639.
8. Dogonadze, R. R. In "Reactions of Molecules at Electrodes", Hush, N. S., Ed.; Wiley-Interscience: New York, 1971; Chapter 3, p 135.
9. Van Duyne, R. P.; Fischer, S. F. Chem. Phys. 1974, 5, 183.
10. Ulstrup, J.; Jortner, J. J. Chem. Phys. 1975, 63, 4358.
11. Efrima, S.; Bixon, M. Chem. Phys. 1976, 13, 447.
12. Chance, B., DeVault, D. C., Frauenfelder, H., Marcus, R. A., Schrieffer, J. B., Sutin, N. Eds. "Tunneling in Biological Systems"; Academic Press: New York, 1979.
13. Brunschwig, B. S.; Logan, J.; Newton, M. D.; Sutin, N. J. Am. Chem. Soc. 1980, 102, 5798.
14. Friedman, H. L. Pure. Appl. Chem. 1981, 53, 1277-1290.
15. Debye, P. Trans. Electrochem. Soc. 1942, 82, 265.
16. Brown, G. M.; Sutin, N. J. Am. Chem. Soc. 1979, 101, 883.
17. Fuoss, R. M. J. Am. Chem. Soc. 1958, 80, 5059.
18. Eigen, M. Z. Phys. Chem. (Frankfurt am Main) 1954, 1, 176.
19. Reynolds, W. L.; Lumry, R. W. "Mechanisms of Electron Transfer"; Ronald Press: New York, 1966.
20. Hair, N. J.; Beattie, J. K. Inorg. Chem. 1977, 16, 245.
21. Stynes, H. C.; Ibers, J. A. Inorg. Chem. 1971, 10, 2304.
22. Zalkin, A.; Templeton, D. H.; Ueki, T. Inorg. Chem. 1973, 12, 1641.
23. Baker, J.; Engelhardt, L. M.; Figgis, B. N.; White, A. H. J. Chem. Soc., Dalton Trans. 1975, 530.
24. Silverman, J.; Dodson, R. W. J. Phys. Chem. 1952, 56, 846.
25. Meyer, T. J.; Taube, H. Inorg. Chem. 1968, 7, 2369.
26. Young, R. C.; Keene, F. R.; Meyer, T. J. J. Am. Chem. Soc. 1977, 99, 2468.
27. Holstein, T. Philos. Mag. 1978, 37, 49.
28. Sutin, N. Annu. Rev. Nucl. Sci. 1962, 12, 285.
29. Creutz, C.; Sutin, N. J. Am. Chem. Soc. 1977, 99, 241.
30. Beitz, J. V.; Miller, J. R. J. Chem. Phys. 1979, 71, 4579.
31. Ballardini, R.; Varani, G.; Indelli, M. T.; Scandola, F.; Balzani, V. J. Am. Chem. Soc. 1978, 100, 7219.
32. Brunschwig, B.; Sutin, N. J. Am. Chem. Soc. 1978, 100, 7568.

33. Bock, C. R.; Connor, J. A.; Guitierrez, A. R.; Meyer, T. J.; Whitten, D. G.; Sullivan, B. P.; Nagle, J. K. Chem. Phys. Lett. 1979, 61, 522.
34. Nagle, J. K.; Dressick, W. J.; Meyer, T. J. J. Am. Chem. Soc. 1979, 101, 3993.
35. Bock, C. R.; Connor, J. A.; Gutierrez, A. R.; Meyer, T. J.; Whitten, D. G.; Sullivan, B. P.; Nagle, J. K. J. Am. Chem. Soc. 1979, 101, 4815.
36. Sutin, N. In "Inorganic Reactions and Methods", Zuckerman, J. J. Ed.; Springer-Verlag: West Berlin, in press.
37. Newton, M. D. Int. J. Quant. Chem., Symp. 1980, 14, 363.
38. Hopfield, J. J. Proc. Natl. Acad. Sci. U.S.A. 1974, 71, 3640.
39. Buhks, E.; Jortner, J. FEBS Lett. 1980, 109, 117.
40. Hush, N. S. Prog. Inorg. Chem. 1967, 8, 391.
41. Marcus, R. A.; Sutin, N. Inorg. Chem. 1975, 14, 213.
42. Hoselton, M. A.; Drago, R. S.; Wilson, L. J.; Sutin, N. J. Am. Chem. Soc. 1976, 98, 6967.
43. Creutz, C.; Sutin, N. In "Inorganic Reactions and Methods", Zuckerman, J. J., Ed.; Springer-Verlag: West Berlin, in press.
44. Newton, M. D. this volume.
45. Rieder, K.; Taube, H.; J. Am. Chem. Soc. 1977, 99, 7891.
46. Tom, G. M.; Creutz, C.; Taube, H. J. Am. Chem. Soc. 1974, 96, 7827.
47. Creutz, C.; Inorg. Chem. 1978, 17, 3723.
48. Creutz, C.; Taube, H. J. Am. Chem. Soc. 1973, 94, 1086.
49. Piepho, S. B.; Krausz, E. R.; Schatz, P. N. J. Am. Chem. Soc. 1978, 100, 2996.
50. Marcus, R. A. Int. J. Chem. Kin. 1981, 13, in press.
51. Sham, T. K.; Hastings, J. M.; Perlman, M. L. J. Am. Chem. Soc. 1980, 102, 5904.
52. Sham, T. K. personal communication.
53. Creutz, C.; Kroger, P.; Matsubara, T.; Netzel, T. L.; Sutin, N. J. Am. Chem. Soc. 1979, 101, 5442.

RECEIVED April 21, 1982.

General Discussion—Electron Transfer in Weakly Interacting Systems

Leader: Robert Balahura

DR. DAVID McMILLIN (Purdue University): In view of all of this, would you comment on the differences between the self-exchange rate constants for the cobalt hexaammine, trisethylenediamine, and sepulchrate complexes (i.e., $\text{Co}(\text{NH}_3)_6^{3+,2+}$, $\text{Co}(\text{en})_3^{3+,2+}$, and $\text{Co}(\text{sep})^{3+,2+}$)? If tunneling can be fairly effective, what do you feel is responsible for dramatically changing the self-exchange rate constant of cobalt in these three closely related amine complexes?

DR. SUTIN: The cobalt systems that you mention differ from the iron and ruthenium systems I discussed in that the electron transfer is also accompanied by a spin change: the cobalt(III) complexes are low-spin and the cobalt(II) complexes are high-spin. Thus, the electron transfer is spin forbidden and should not occur since $H_{AB} = 0$. It becomes allowed through spin-orbit coupling which mixes the excited-state and ground-state wave functions of the complexes. The extent of mixing of the wave functions is very important for it determines the degree of adiabaticity of the reaction. Recent calculations show the adiabaticity factor for the cobalt hexaammine exchange to be very small [Buhks, E.; Bixon, M.; Jortner, J.; Navon, G. *Inorg.Chem.* 1979, 18, 2014].

Another factor in the cobalt systems is that the electron transfer involves the e_g^* antibonding orbitals. As a consequence, the nuclear configurations of the inner-spheres of the cobalt(II) and cobalt(III) complexes will be very different. In the hexaamines the cobalt(II)-nitrogen and the cobalt(III)-nitrogen distances differ by 0.18-0.20 Å. This may be compared with the ferrous/ferric couple, for which $\Delta d = 0.14$ Å, or the hexaammine ruthenium couple, for which Δd is only 0.04 Å.

In the cobalt system one thus has large inner-sphere barriers and small adiabaticity factors. In some systems the electron transfer may proceed via the excited states of cobalt(II) or cobalt(III) present in thermal equilibrium with the ground states. Although such excited-state reactions would be more adiabatic, the preequilibrium constants for forming the excited states are generally not very favorable. I think that each cobalt system is unique in regard to the mix of excited states, inner-sphere barriers, and adiabaticity. Variations in these factors could give rise to rather dramatic rate changes.

DR. HENRY TAUBE (Stanford University): These cobalt systems now appear to be less interesting than we had originally believed. Much of the literature data upon which our interest

in these systems was based now appear to be wrong. Firstly, the published self-exchange rate constant for $\text{Co}(\text{NH}_3)_6^{3+,2+}$ is, I am quite certain, incorrect. If you examine Stranks' paper critically, there is no basis for dismissing the observed rate as being due to a term which has a simple first-order dependence on $\text{Co}(\text{NH}_3)_6^{3+}$ [Biradar, N. S.; Stranks, D. R.; Vaidya, M. S. Trans. Faraday Soc. 1962, 58, 2421]. We have now returned to a measurement of this system.

Secondly, the literature value for the cobalt(II)-nitrogen distance in $\text{Co}(\text{NH}_3)_6^{3+,2+}$ is incorrect. The difference between the $\text{Co}(\text{NH}_3)_6^{3+,2+}$ and $\text{Co}(\text{en})_3^{3+,2+}$ self-exchange rate constants can almost be accounted for simply by the Franck-Condon factor.

As for the difference observed for the sepulchrate complex, that may have to do with strain in the ligand. A student of mine has done some calculations considering the fact that the ligand itself may change the preferred distance and change the frequencies. This could account for a large part of the difference between the self-exchange rate constants for the sepulchrate and trisethylenediamine complexes.

DR. RICHARD PIZER (Brooklyn College): In Alan Sargeson's laboratory, molecular-mechanics calculations have been done, principally by Dr. Rodney Geue, on the electron transfer self-exchange rate constants of $\text{Co}(\text{sep})_3^{3+,2+}$, $\text{Co}(\text{en})_3^{3+,2+}$, and $\text{Co}(\text{NH}_3)_6^{3+,2+}$. We see no difference between the behavior of the latter two complexes, supporting Dr. Taube's viewpoint. These calculations also support the notion that the fast electron transfer in the sepulchrate couple is due to release of internal ligand strain in the transition state.

DR. SUTIN: Various values for the cobalt-nitrogen distances in the hexaammines have been reported. Part of this variation is almost certainly due to lattice (counter-ion) effects. Recent literature values for the Co-N distances in $\text{Co}(\text{NH}_3)_6^{3+}$ are fairly close, ranging only from 1.96 Å [Herlinger, A. W.; Brown, J. N.; Dwyer, M. A.; Pavkovic, S. F. Inorg. Chem., 1981, 20, 2366] to 1.98 Å [Iwata, M. Acta Cryst. 1977, B33, 59]. I understand that Freeman has very recently obtained a value of 2.16 Å for the Co-N distance in $\text{Co}(\text{NH}_3)_6^{2+}$. The difference between the Co-N distances in $\text{Co}(\text{NH}_3)_6^{2+}$ and $\text{Co}(\text{NH}_3)_6^{3+}$ thus appears to be about 0.18-0.20 Å, which is very similar to the value reported by Stynes and Ibers [Stynes, H.C.;

Ibers, J. A. Inorg. Chem. 1971, 10, 2304] and to the Δ_d value for the sepulchrates reported by Sargeson [Sargeson, A. M. Chem. Brit. 1979, 15, 23].

DR. EPHRAIM BUHKS (University of Delaware): There is a difference of three orders of magnitude between the self-exchange rate constants of $\text{Fe}(\text{H}_2\text{O})_6^{3+,2+}$ and $\text{Ru}(\text{NH}_3)_6^{3+,2+}$ while the ratio of their Franck-Condon factors is 10^8 . The corresponding rate constant for $\text{Mn}(\text{H}_2\text{O})_6^{3+,2+}$ is close to that for $\text{Fe}(\text{H}_2\text{O})_6^{3+,2+}$ despite the fact that the difference between their Franck-Condon factors is 10^5 (these estimates being based on the difference in metal-ligand distances). One cannot fit the 12-fold difference in the $\text{Co}(\text{H}_2\text{O})_6^{3+,2+}$ and $\text{Co}(\text{NH}_3)_6^{3+,2+}$ self-exchange rate constants to the ratio of the Franck-Condon factors which is 10^3 . I would like to suggest that there may be many aquo compounds of the transition metal ions in which the self-exchange rate constants which have been reported do not represent outer-sphere processes.

DR. SUTIN: I think that this is always a problem with exchange reactions involving aquometal ions. The manganese system bears out what Dr. Taube said: we have to be sure of the numbers which we are attempting to interpret. In this regard, I believe that the manganese self-exchange rate constant which you referred to was not measured directly.

There are only a few reactions involving aquometal ions that can be confidently characterized as outer-sphere. One example in the $\text{Fe}^{3+}/\text{V}^{2+}$ redox reaction, in which the electron transfer is faster than the loss of water molecules from the metal centers. This is the type of criterion for an outer-sphere reaction with which one feels comfortable.

The mechanism of the $\text{Fe}^{3+,2+}$ exchange is certainly open to question; however, the similarities of the $\text{Fe}^{3+,2+}$ and $\text{Fe}^{3+}/\text{V}^{2+}$ reactions (both of which exhibit $\Delta S^\ddagger \cong -25$ eu) suggest that there is no dramatic mechanistic difference for electron transfer in these two systems. Although such comparisons must be made with caution, I know of no strong evidence requiring the $\text{Fe}^{3+,2+}$ exchange to be inner-sphere.

DR. NOEL HUSH (University of Sydney): It is very pleasing to think that we now have a general description of outer-sphere electron transfer which we may believe to be generally correct. It is also very satisfying that a large body of experimental

information is thereby systematized and its general features understood.

I think it is unique in chemistry that such complicated reactions can be understood semiquantitatively in quite simple physical terms. And I believe it is a great achievement that this very accurate experimental information has been acquired and that it is possible to make such direct successful comparison with theory.

It is at this stage that we should now begin to look into the details and ask just the sorts of questions that Dr. Sutin is raising -- e.g., the importance of nuclear tunneling or of electronic nonadiabaticity. These are, as we might say, the fine structure of the problem.

First, in considering the question of whether or not in a particular case we do have an outer-sphere process, we need to know accurately such quantities as bond distances. I have brought some data (shortly to be published) from Dr. J. K. Beattie's laboratory in Sydney, which show that in the $\text{Co}(\text{OH}_2)_6^{3+,2+}$ complex ions the difference between the lengths of the cobalt(II)- and cobalt(III)- H_2O bonds is very large. This rules out, I would think completely, a dominant outer-sphere mechanism for that system, because the observed rate is just too fast to be compatible with this. The self-exchange reaction must almost certainly proceed most favourably via an inner-sphere mechanism. More data of this kind are evidently needed.

As for the $\text{Co}(\text{NH}_3)_6^{3+,2+}$, exchange, which has been thought to be a problem for many years, I think Professor Taube's point is correct. It now appears that the rate is not as slow as it has previously been thought to be. Thus, it may well prove to be explicable in terms of the usual theory.

On the question of obtaining estimates of the electronic nonadiabaticity factor, you hinted at, but I don't think explicitly mentioned, one approximate approach. That is the method used by Dogonadze and German [German, E. D.; Dogonadze, R. R. *Izv. Akad. Nauk SSSR, Ser. Khim.* 1973, 2155; *Chem. Abstr.* 1974, 80, 30998a], who compared the entropies of activation of a number of self-exchanges of different charge types, 1-2, 2-3, 3-4 and so on. The largest contribution to the entropy of activation, apart from some small terms, comes from the work terms, which depend on the product of the charges, $Z_1 Z_2$, times a dielectric factor. If one plots activation entropies for homogeneous transfer in water, one obtains roughly a straight line. The slope corresponds to an average inter-ion distance of ca 7 Å, which is close to that usually assumed. Although this is not conclusive, it does strongly suggest that departures from electronic adiabaticity are fairly small in outer-

sphere reactions. That is, one does indeed generally have reactions which are essentially electronically adiabatic. Of course, further work is necessary to get accurate estimates of small nonadiabatic effects.

One final point should be noted. Theoretical discussions of electron transfer processes have focused almost entirely on outer-sphere processes. When we have an inner-sphere mechanism, or sufficient electronic interaction in a dynamically trapped mixed-valence complex to produce a large separation between upper and lower potential surfaces, the usual weak-interaction approach has to be abandoned. Thus a detailed knowledge of a potential surface which is not describable as an intersection surface of perturbed harmonic surfaces, for example, is required. For this purpose, detailed calculations will be required. The theory of these processes will be linked more closely to those of atom transfers, where the motion is normally essentially confined to a lower potential surface. Recent theoretical work in my laboratory has been concerned with the latter [Cribb, P. H.; Nordholm, S.; Hush, N. S. Chem.Phys. 1978, 29, 31; ibid., 43; ibid. 1979, 44, 315].

Reverting to outer-sphere processes, one should bear in mind that the observed spread of reaction rates for these is very large indeed--in fact, it is on the order of magnitude of the age of the universe in seconds! So I think that Dr. Sutin is doing very well in explaining it.

DR. SUTIN: When you say that I explain it, I have, of course, drawn heavily on aspects of the models which you have contributed.

DR. ARTHUR WAHL (Washington University in St. Louis): I would like to make a few comments concerning the experimental evidence for electrolyte and solvent effects on electron transfer reactions. I might start by reminding you of some old work which was published in 1967 showing the effects of various cations on the rate of the $\text{Fe}(\text{CN})_6^{3-,4-}$ self-exchange reaction [Campion, R. J.; Deck, C. F.; King, P., Jr.; Wahl, A. C. Inorg. Chem. 1967, 6, 672]. The cation effect was tremendous--spanning two or three orders of magnitude--and occurred at low concentration levels.

Many electron transfer reactions are, of course, studied at quite high electrolyte concentrations, and effects of this type, even with what are usually inert electrolytes, can be important. We think this effect is due mainly to ion association, so that ion pairs, triplets, etc., are involved as reactants.

Similar effects occur for electron transfer between cations, the reactions being catalyzed by anions. We have investigated the oxidation of tris(4,7-dimethylbipyridyl)-

osmium(II) by the corresponding ferric complex in acetonitrile [Stalnaker, N. D.; Solenberger, J. C.; Wahl, A. C. *J. Phys. Chem.* 1977, **81**, 601]. Here the effects of perchlorate and hexafluorophosphate ions are different. Both catalyze the reaction much more than one calculates from activity-coefficient effects. We postulate again that the effects are due to ion association. An ion pair, having a smaller charge (+2) than the +3 reactant would react more rapidly with the +2 reactant. This investigation has been extended by Tom Braga, who measured the temperature effect of the kinetics and made conductivity measurements to determine the equilibrium constants for ion association, K_A , at a number of temperatures [Braga, T., Ph.D. Dissertation; Washington University: St. Louis, 1979]. From data for the analogous cobalt(III) complex with perchlorate and hexafluorophosphate as anions, he found association constants of about 900 and 300, with distances of closest approach of 5 or 6 Å, respectively. These values seem reasonable. For the iron(II) compound with the hexafluorophosphate or perchlorate, the ion association constants were too small to measure ($\leq \sim 50$).

Kinetic measurements for the same osmium(II)-iron(III) reaction were made at a number of temperatures. At 25 C the intercept at zero electrolyte concentration is about $5 \times 10^5 \text{ M}^{-1} \text{ s}^{-1}$ ($= k_1$). The slopes of the curves in ClO_4^- and PF_6^- are different. The products of the rate constant and the equilibrium constant, $k_2 K_A$, are 1.0×10^{10} and 2.5×10^9 , respectively. Division of these values by the measured equilibrium constants gives the rate constants for reactions involving ion pairs. The two k_2 values are essentially the same, about $1 \times 10^7 \text{ M}^{-1} \text{ s}^{-1}$, 20 times larger than k_1 for the reaction between the 2+ and 3+ ions.

The simple, classical Marcus model gives predictions that are one to two orders of magnitude too large for both k_1 and k_2 . The temperature dependence is quite small: $\Delta H^\ddagger \sim 0$, $\Delta S_1^\ddagger = -27 \pm 10 \text{ eu}$, $\Delta S_2^\ddagger = -18 \pm 10 \text{ eu}$. These values seem reasonable.

Further evidence for the ion-pair formation has come from ^{19}F -NMR studies of the association of PF_6^- with the $\text{Cr}(\text{phen})_3^{3+}$ complex [Triegaardt, D. M.; Wahl, A. C., work in progress]. An increase in the line width and a shift in the line position with increasing $[\text{Cr}(\text{phen})_3^{3+}]$, has been observed. The system is in the fast-exchange limit, and the measured values depend on the degree of ion association and on the line width of the

fluorine in the ion pair. If the same parameters determined from the conductivity measurements are used, the data at the lower concentrations can be represented quite well, but the calculated curve falls well below the data for the higher concentrations. To represent these data, different activity coefficient corrections need to be made and the resulting equilibrium constant values, although not uniquely determined, are roughly a few hundred, in agreement with the conductivity results.

We have investigated the ferrocene/ferrocenium ion exchange to determine the effects of different solvents on electron-transfer rates. There is probably only a very small work term and very little internal rearrangement in this system. Thus the rates should reflect mostly the solvent reorganization about the reactants, the outer-sphere effect. We measured the exchange rates in a number of different solvents and did not find the dependence on the macroscopic dielectric constants predicted by the simple model [Yang, E. S.; Chan, M.-S.; Wahl, A. C. *J. Phys. Chem.* 1980, **84**, 3094]. Very little difference was found for different solvents, indicating either that the formalism is incorrect or that the microscopic values of the dielectric constants are not the same as the macroscopic ones.

In more recent work, we have investigated another exchange system, $\text{Ru}(\text{hfac})_3^{0,-}$ [Chan, M. -S.; Wahl, A. C. *J. Phys. Chem.*, submitted for publication]. For this reaction, we found the expected dependence on the macroscopic values of the dielectric constants. An exception occurs for chloroform in which ion association may be unusually large. Li and Brubaker have investigated the chromium(0,I) biphenyl exchange and have found a similar relationship [Li, T. T.-T.; Brubaker, C. H., Jr. *Organomet. Chem.*, in press]. Thus, the predicted dependence does hold in some cases, but it does not hold in others.

DR. RICHARD DODSON (Brookhaven National Laboratory): For many years there has been discussion of whether the Tl^{3+} , Tl^+ electron exchange occurs in a single, two-equivalent step or in two successive one-equivalent steps involving Tl^{2+} as an intermediate. In informal discussions accompanying this Conference, interest has been expressed concerning this type of system. I would like to summarize some experimental evidence which seems to provide a compelling answer.

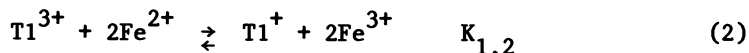
The question is: Does the electron exchange mechanism involve the reproporationation-disproportionation reaction represented as in reaction 1? The apparent answer is that it



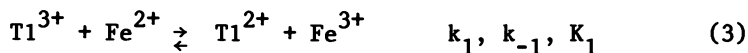
does not. The observed exchange reaction is many orders of

magnitude too fast to be accounted for by this reaction in view of what has been learned about the properties of Tl^{2+} . There are three pieces of work which speak rather decisively to this question. I'll outline one of them and mention the other two.

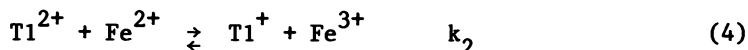
An important reaction in our approach to the problem is the reduction of thallic ion by ferrous ion, as shown in reaction (2),



which was studied very beautifully in the early 1950's by Ashurst and Higginson [Ashurst, K. G.; Higginson, W. C. E. *J. Chem. Soc.* 1953, 3044]. They found that the progress of the reaction is diminished as products accumulate and, specifically, that iron(III) retards the reaction. And the conclusion was very persuasive that the reaction occurs in two steps involving Tl^{2+} as an intermediate. Thus, the first step is represented in reaction (3). The second, and very rapid, step is given



in reaction (4).



The rate parameters that can be extracted from the thermal kinetics, k_1 and the ratio k_{-1}/k_2 , are not quite enough for present purposes. Nevertheless, the first reaction of the Ashurst-Higginson mechanism can serve as the key to the problem.

What we wanted eventually to obtain--and we used this work to do so--were the specific forward and reverse rate constants for the reportionation reaction, k_{rep} and k_{dis} . We know k_1 experimentally. The value of k_{-1} would then define the equilibrium properties of Tl^{2+} through the equilibrium constant, $K_1 = k_1/k_{-1}$. We know the ratio k_{-1}/k_2 so, if we can measure k_2 , we can evaluate k_{-1} . The question then becomes: How can we obtain k_2 ? One approach is to generate Tl^{2+} by pulse radiolysis, react it with Fe^{2+} , confirm the kinetics, and measure the rate constant. (For experimental reasons, we preferred this approach to a direct measurement of Tl^{2+} with Fe^{3+}). And this we did [Schwarz, H. A.; Constock, D.; Yandell, J. K.; Dodson, R. W. *J. Phys. Chem.* 1974, 78, 488]. The result was $k_2 = 6.7 \times 10^6$

$M^{-1} s^{-1}$. Together with the experimental value of k_{-1}/k_2 this gives $k_{-1} = 3.4 \times 10^5 M^{-1} s^{-1}$. From the measured value of k_1 we now have $K_1 = 4.1 \times 10^{-8}$. Together with published oxidation potentials, we calculate $K_{1,2} = 4 \times 10^{17}$. The equilibrium constant of the reproporationation reaction is then $K_{rep} = K_1^2/K_{1,2} = 4 \times 10^{-33}$.

The disproportionation reaction rate constant of Tl^{2+} under our experimental conditions (1 M $HClO_4$, 23 C) was measured by pulse radiolysis as $k_{dis} = 1.9 \times 10^8 M^{-1} s^{-1}$. The reproporationation rate constant is now $k_{rep} = k_{dis} K_{rep} = 7.6 \times 10^{-25} M^{-1} s^{-1}$, which is too slow to account for anything. A comparable value of the exchange rate constant is $1.2 \times 10^{-4} M^{-1} s^{-1}$. In view of the twenty orders of magnitude discrepancy, one concludes that reaction 1 cannot contribute significantly to the observed rate of exchange.

The finding of Stranks and Yandell [Stranks, D. R.; Yandell, J. K. *J. Phys. Chem.* 1969, **73**, 840] that Tl^{2+} rapidly exchanges with Tl^+ and Tl^{3+} must now be taken into account. From their rate constants one calculates that in an assumed Tl^+ , Tl^{3+} , Tl^{2+} equilibrium mixture, the rate contributed by these additional exchange reaction pathways is still too slow by eight orders of magnitude, which seems sufficient for the argument.

At about the same time that our study was being conducted, a similar study, pursuing a slightly different route, was made by Falcinella, Felgate, and Laurence [Falcinella, B.; Felgate, P. D.; Laurence, G. S. *J. Chem. Soc., Dalton Trans.* 1974, 1367; *ibid.* 1975, 1]. They used flash photolysis to generate Tl^{2+} and studied its reactions with both Fe^{3+} (to produce Tl^{3+} and Fe^{2+}) and Co^{2+} (to produce Tl^+ and Co^{3+}). From their results, they drew the same conclusions regarding the mechanism of the Tl^+ , Tl^{3+} exchange.

Finally, I should mention that the Ashurst-Higginson mechanism, together with the results of Stranks and Yandell, implies that the addition of ferrous ion should accelerate the Tl^+ , Tl^{3+} exchange. We actually tried this experiment, in work which preceded the pulse radiolysis and flash photolysis studies, and found that such is the case [Warnqvist, B.; Dodson, R. W. *Inorg. Chem.* 1971, **10**, 2624]. The results again agree [Dodson, R. W. *J. Radioanal. Chem.* 1976, **30**, 245].

There is much else which could be said about the properties of thallium(II) in aqueous solution, but there is not time to cover those here. Perhaps an interesting point to mention, however, is that it is a powerful oxidizing agent. In 1 M HClO_4 , the formal potential, $E^{\circ'}$, for the $\text{Tl}^{2+}, +$ couple is 2.22 V.

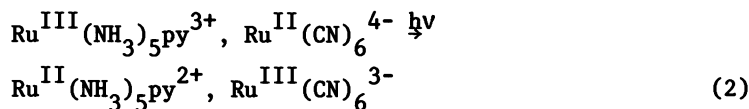
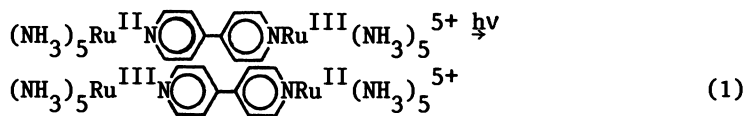
Optical Charge-Transfer Transitions

THOMAS J. MEYER

University of North Carolina, Department of Chemistry, Chapel Hill, NC 27514

A theoretical formalism is available for understanding optical charge transfer processes in a variety of chemical systems (mixed-valence ions, donor-acceptor complexes, metal-ligand charge transfer chromophores, etc) where the extent of charge transfer is large and where electronic coupling between the electron donor and acceptor sites is relatively small.

Optical charge transfer (CT) is commonly observed in unsymmetrical molecules or molecular complexes in which there are sites of distinctly different ionization energies and electron affinities. The origin and properties of optical charge transfer transitions provide the basis for this account. A convenient place to begin chemically is with mixed-valence compounds and two examples are shown below (1-3). In the first (eq 1), the sites of different oxidation states are held in close



proximity by a bridging ligand which can also serve to encourage electronic interactions by orbital mixing with metal orbitals. In the second (eq 2), the electron donor and acceptor sites are held together by electrostatic attraction. In systems like these or in closely related mixed-metal systems, low energy absorption bands are frequently observed.

0097-6156/82/0198-0137\$06.00/0
 © 1982 American Chemical Society

Mixed-valence chemistry was reviewed in the late 1960's both by Robin and Day (4) and by Hush (5). Their work provided the beginnings of a theoretical background for understanding the properties of mixed-valence compounds including the low energy absorption bands which have been termed Intervalence Transfer (IT) or Metal-Metal Charge Transfer (MMCT) bands.

Most of the mixed-valence systems mentioned by Robin and Day and by Hush were in the solid state. The problem of creating discrete chemical systems for which experiments could be carried out either in solution or in the solid state was first attacked experimentally by Creutz and Taube (6). Their approach was to link together the two metal sites through a ligand bridge, which led to dimers and oligomers.


For convenience, many of the examples cited here will come from our own work. In our work we have taken advantage of the synthetic flexibility offered by the system shown below which is based on the ligand 2,2'-bipyridine (bpy). Synthetic studies



have shown that the bridging group can be any of a variety of bipyridine or diphosphine type ligands.

"Localized" and "Delocalized" Systems

In any mixed-valence compound, the first problem to be addressed is one of description. Is the compound "localized" or "delocalized"? In a localized description the stationary state quantum mechanical solution for the odd electron is oscillatory in nature and has the electron transferring back and forth between the metal ion sites. Spectroscopic data are available for

the bpy dimer, where L = pyrazine ()₂, which show that it

is localized (7). On the other hand, making what appears to be a slight chemical modification, exchanging an oxo for a pyrazine bridging ligand, leads to a different conclusion. For the mixed-valence oxo-dimer, $(\text{bpy})_2\text{ClRuORuCl}(\text{bpy})_2^{3+}$, the electronic distribution of the odd electron appears to be delocalized in the same sense as the π electrons in an aromatic molecule like benzene, and molecular orbital theory provides an appropriate basis for dealing with electronic structure.

In the present treatment, attention will be focused on localized systems. It is convenient to break the localized classification down even further, where the basis for the distinction lies in experimental observations. In the bpy dimer, where the bridging ligand is pyrazine, the rate of electron oscillation between Ru(II) and Ru(III) sites is slower than the vibrational timescale, at least for those vibrational levels

which are significantly populated at the background thermal energy (kT). It is these levels which are of importance in defining the energy and shapes of CT absorption bands. Because the electronic transition is slow on the vibrational timescale, it is possible to take advantage of the Born-Oppenheimer approximation in defining potential surfaces and in treating transition rates. This situation corresponds to the so-called "non-adiabatic" limit. However, if the rate of electron oscillation is sufficiently rapid that it approaches the vibrational timescale, which appears to be the situation for the Creutz and Taube dimer (below) (6), the problem is much more difficult (see the discussion by Schatz (8,9) which appears in this same volume).



For the 2,2'-bipyridine and related dimers, IT bands appear as broad structureless features in the near infrared (~ 7000 - $10,000 \text{ cm}^{-1}$). The origins of the transitions leading to the bands are in optically-induced electron transfer from one side of the molecule to the other (eqs 1,2). Hush has pointed out that a close relationship should exist between optical charge transfer and thermal charge transfer. In the thermal process, the electron is trapped and only those systems which acquire sufficient thermal energy to penetrate or cross the barrier can undergo electron transfer.

The origin of the barrier to electron transfer is vibrational in nature. The electron becomes trapped at one site as a consequence of changes in molecular and medium structure and/or vibrations with changes in the electron position. As an example, addition of an electron to $\text{Fe}(\text{H}_2\text{O})_6^{3+}$ leads to a significant lengthening of the Fe-O bond ($\Delta r = 0.12 \text{ \AA}$) in the resulting ion, $\text{Fe}(\text{H}_2\text{O})_6^{2+}$ (10). By the same token, in the medium surrounding the reacting ions, significant changes can also occur; the estimated enthalpy of hydration for the gas phase ion, $\text{Fe}(\text{H}_2\text{O})_6^{3+}(\text{g})$, is more exothermic by $\sim 13 \text{ eV}$ than for the +2 ion.

Relationship to Potential Energy Surface Diagrams

The effect of vibrational trapping is shown in the energy diagram in Fig. 1. The coordinate in the diagram is an anti-symmetric combination of the coordinates for appropriate normal modes at the electron donor and acceptor sites. The result is the familiar double well energy surface. When summed over all of the contributing normal mode combinations, the intersection between potential energy surfaces gives the classical energy of activation, at least in the limit of weak electronic coupling

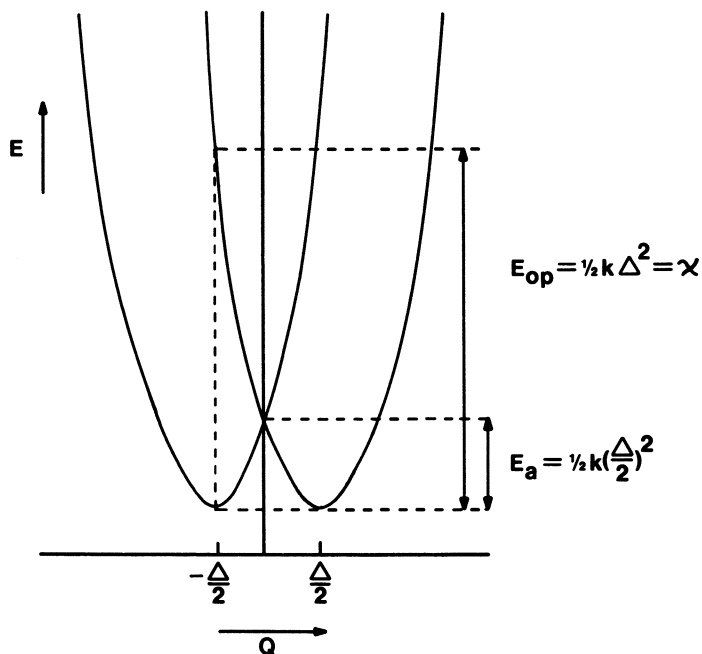


Figure 1. Potential energy vs. normal mode coordinate for symmetrical electron transfer, $\Delta E = 0$. As shown, the diagram is in the classical (high temperature) limit where $h\omega \ll k_B T$; $E_{op} = \frac{1}{2} k \Delta^2 = \chi$; and $E_a = \frac{1}{2} k (\Delta/2)^2$.

between the electron donor and acceptor sites. The picture that emerges here is straightforward. Rates of electron transfer will be determined by the statistical population of a collection of vibrational levels at the right energies. The right energies are those which correspond to the intersections between energy surfaces in Fig. 1. Of course, we have yet to put into the problem the actual electron transfer step which leads to barrier crossing and introduces the necessary time dependence. This can be done exactly in the limit of weak electronic coupling, the non-adiabatic limit, using time-dependent perturbation theory and applying the Born-Oppenheimer separation of nuclear and electronic motion (11,14).

Fig. 1 also leads to some relatively straightforward conclusions about the relationships between optical and thermal electron transfer. For a chemically symmetrical system (e.g., eq 1), the energy of the optical transition should be related to the classical vibrational barrier ($\chi/4$) as in eq 3. Eq 3 includes the separation of the vibrational barrier into intra-

$$E_{\text{op}} = \chi = 4E_{\text{a}} = \chi_{\text{o}} + \chi_{\text{i}} \quad (3)$$

molecular (χ_{i}) and medium components (χ_{o}). For an unsymmetrical case (e.g., eq 2), the situation is more complicated. Now the internal energy difference between the ground and mixed-valence excited states (ΔE) must be included giving eq 4.

$$E_{\text{op}} = \chi + \Delta E = \chi_{\text{i}} + \chi_{\text{o}} + \Delta E \quad (4)$$

The energy of activation is then given by eq 5.

$$E_{\text{a}} = \frac{\chi}{4} \left(1 + \frac{\Delta E}{\chi} \right)^2 = \frac{E_{\text{op}}^2}{4(E_{\text{op}} - \Delta E)} \quad (5)$$

Theoretical Limitations

Eqs 3-5 provide a relatively simple theoretical basis for understanding optical charge transfer and the relationship between optical and thermal electron transfer. One implication is that if E_{op} and ΔE are known, it should be possible to calculate the energy of activation for the thermal process. It is possible to measure or to estimate ΔE by temperature dependent redox potential measurements on the two component redox couples which are involved in the CT step. However, there are three complications which limit the validity of such equations:

- (1) The equations rely on the assumption of harmonic oscillators and equal force constants in both the reactant and product states. Deviations from

these assumptions in real systems can lead to deviations from calculated band widths based on harmonic oscillator models and to the loss of the contributions from entropic factors in rate equations.

(2) The assumption of weak electronic coupling may not be valid for vibrational levels near the region where the reactant and product surfaces intersect. If the extent of electronic coupling is sufficient (tens of cm^{-1}), the timescale for electron transfer for vibrational levels near the intersectional region will approach the vibrational timescale, electronic and nuclear motions are coupled, and the Born-Oppenheimer approximation is no longer valid. Such timescale problems are of less importance for the optical transition since it involves vibrational levels well away from the intersection region for both the ground and excited states.

(3) Inherent in point (2) above is the fact that, at the microscopic scale at which chemical reactions occur, processes are quantum mechanical in nature and deviations from classical predictions frequently occur. In order to deal with the problem of barrier crossing or penetration, it is necessary to determine potential energy surfaces, to solve the Schrödinger equation in order to obtain vibrational energy levels and wave functions, and to calculate population distributions, and then to calculate vibrational wave function overlaps which give transition probabilities from reactant vibrational levels to isoenergetic product vibrational levels (11-15). For an IT or MMCT absorption band, there should be vibrational structure as is often observed for electronic transitions in organic compounds and metal complexes. Vibrational structure is not usually observed for IT bands, apparently because the most important vibrations are usually skeletal in nature, occur at low energies, and are difficult to resolve experimentally.

With the limitations above noted, let us return to the application of eqs 3-5 to IT transitions and to optical charge transfer (CT) in general. These equations, in fact, prove to be remarkably successful in providing a basis for understanding optical CT processes in a number of chemical systems. It was suggested above that the vibrational term, χ , has both intramolecular and medium contributions. From dielectric loss and related measurements, the collective vibrations of the medium occur at low frequencies for most solvents, the energy spacings between levels are small, and equations based on the classical

approximation should be valid. The frequencies of intramolecular vibrations of importance could vary widely ($\sim 200\text{--}4000\text{ cm}^{-1}$). In all cases, they are sufficiently near kT (200 cm^{-1} at 25C) that their contribution should be treated quantum mechanically. However, for relatively low frequency vibrations near room temperature, the quantum mechanical and classical results may not differ significantly as shown for $\text{Fe}(\text{H}_2\text{O})_6^{2+/3+}$ self-exchange (15). This result arises, in part, because vibrational wave function overlap increases markedly as the intersection region between surfaces is approached. At lower temperatures the situation is quite different and electron transfer is dominated by vibrational tunneling through levels below the intersection region.

Returning to χ_0 , eq 6 is available from dielectric continuum theory. In eq 6, D_{op} and D_{s} are the optical and static dielectric constants of the medium, E_{f} and E_{i} are the electric

$$\chi_0 = \frac{1}{2} \left(\frac{1}{D_{\text{op}}} - \frac{1}{D_{\text{s}}} \right) \int (\vec{E}_{\text{f}} - \vec{E}_{\text{i}})^2 dV \quad (6)$$

field vectors associated with the final and initial charge distributions in the absence of the medium, and the integration is over the volume element, dV . Integration of eq 6 for the case where the electron donor and acceptor sites are non-overlapping spheres and neglecting the volumes of the sites, gives eq 7 where a_1 and a_2 are the molecular radii and d is the inter-nuclear separation.

$$\chi_0 = (\Delta e)^2 \left(\frac{1}{2a_1} + \frac{1}{2a_2} - \frac{1}{d} \right) \left(\frac{1}{D_{\text{op}}} - \frac{1}{D_{\text{s}}} \right) \quad (7)$$

Eq 7 calculates the energy difference arising from the medium between the thermally equilibrated mixed-valence ground state and a vibrationally nonequilibrium, mixed-valence excited state. The value of Δe depends on the nonequilibrium state: 1) For optical charge transfer, $\Delta e = e$, the unit electron charge. 2) For thermal electron transfer between chemically symmetrical sites, $\Delta e = e/4$. 3) For a chemically unsymmetrical electron transfer (16), $\Delta e = \frac{e}{2} \left(1 + \frac{\Delta E}{\chi} \right)$.

Approaches for Experimental Verification

We are now in a position to search for experimental tests of the theoretical treatment as it has been developed so far. By combining eqs 3, 6, and 7 for a symmetrical dimer, E_{op} should vary directly with $(1/D_{\text{op}} - 1/D_{\text{s}})$ as shown in eq 8

($a_1 \sim a_2$). That such relationships exist has been shown for

$$E_{op} = \chi_i + \frac{1}{2} \left(\frac{1}{D_{op}} - \frac{1}{D_s} \right) \int (\vec{E}_f - \vec{E}_i)^2 dV \cong \chi_i + e^2 \left(\frac{1}{a} - \frac{1}{d} \right) \left(\frac{1}{D_{op}} - \frac{1}{D_s} \right) \quad (8)$$

several dimeric systems including $(NH_3)_5RuN \langle \text{C}_6\text{H}_4 \rangle \langle \text{C}_6\text{H}_4 \rangle NRu(NH_3)_5^{5+}$ (1,2), $(C_5H_5)Fe(C_5H_4-C_5H_4)Fe(C_5H_5)^+$ (17), and $(bpy)_2ClRu(L)RuCl(bpy)_2^{3+}$ where L is a bridging diazine or phosphine ligand (18).

Even here, specific solvent effects which are not considered in the continuum theory begin to appear, most notably for hydroxylic solvents. However, recent work of our own suggests that it may be possible to make straightforward empirical corrections to the dielectric continuum model for such cases.

A second test involves the role of internuclear separation between the electron donor and acceptor sites. Rearrangement of eq 8 leads to the prediction of a $-1/d$ dependence for E_{op} . In this case, the experiment becomes an exercise in synthetic chemistry. One approach has been to vary d by using a series of related dimers, $(bpy)_2ClRu(L)RuCl(bpy)_2^{3+}$, where L is varied systematically (18,19) from $N \langle \text{C}_6\text{H}_4 \rangle N$ to $trans-N \langle \text{C}_6\text{H}_4 \rangle CH=CH \langle \text{C}_6\text{H}_4 \rangle N$,

(18,19); another has been to use a series of biferrocenium ions (17). In both cases the expected $-1/d$ dependence was observed. However, for the Ru dimers, the assumption of non-overlapping spheres is inappropriate and the slope and intercept calculated for a plot of E_{op} vs $1/d$ using eq 8 deviate from experiment. For these systems a more appropriate model is probably the dipole in a sphere model developed by Cannon (20).

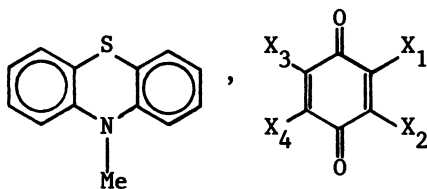
Unsymmetrical Systems

Turning to chemically unsymmetrical systems, recall that the situation is complicated by the appearance in the equations of the internal energy difference between the ground and excited state, oxidation state isomers, (eq 9).

$$E_{op} = \chi_i = \chi_o + \Delta E = \chi_i + \frac{1}{2} \left(\frac{1}{D_{op}} - \frac{1}{D_s} \right) \int (\vec{E}_f - \vec{E}_i)^2 dV + \Delta E \quad (9)$$

Eq 9 can be tested several ways, again based on using a closely

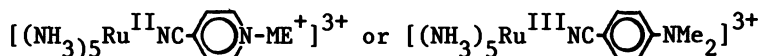
related series of chemical systems. One approach is to measure E_{op} for a series of structurally related compounds in which case a linear correlation should exist between E_{op} and ΔE . Such experiments have been successfully carried out for the ion-pairs, $M^{II}(CN)_6^{4-}$, $Ru^{III}(NH_3)_5L^{3+}$ ($M = Fe, Ru, Os$; $L =$ pyridine or substituted pyridine), and for a series of donor-acceptor complexes (21):



In these experiments, ΔE was obtained from temperature dependent redox potential measurements for the isolated, monomeric couples based on a thermochemical cycle.

Another way of testing eq 9 is by using the same chemical system in a series of solvents. Clearly the situation is more complicated since there are two solvent dependences in the experimental measurement, one arising from χ_o and one from ΔE . The latter can be approximated from redox potential measurements in the series of solvents of interest and linear plots of $E_{op} - \Delta E$ vs. $(1/D_{op} - 1/D_s)$ have been observed for mixed-valence ions (21,23), donor-acceptor complexes (21,22), and MLCT or LMCT transitions based on polypyridyl complexes of Ru and Os (22,24). In these systems additional complications arise, for example, from using $\Delta E_{1/2}$, which is a free energy change, for ΔE ; but it is beyond the purposes of the present discussion to consider such problems in detail.

In turning to cases where strong, specific interactions with the solvent are expected, the picture can change considerably and it is no longer obvious that dielectric continuum theory provides a reasonable basis for calculating χ_o . It is apparent that dielectric continuum theory can not be used to account for solvent induced variations in ΔE but, as mentioned earlier, there is hope that a combination of dielectric continuum theory and the use of empirically determined solvent parameters can provide a framework for understanding solvent effects. The importance of specific solvent effects shows up dramatically for MLCT or LMCT transitions in complexes such as shown below (21):



Concluding Remarks

In closing, there are at least three important thoughts to keep in mind concerning the work that I have described here. The first is that the close relationships between optical and thermal electron transfer, at least under certain limiting conditions, is striking and useful. It shows a satisfying generality for two seemingly disparate types of processes. It also allows for the calculation of electron transfer rate constants from spectral measurements (25-26), which is striking since it suggests that information about chemical reactivity is directly obtainable from spectral measurements on a system at equilibrium. The second point is one of generality. From our work it appears that there exists a straightforward theoretical basis for understanding charge transfer processes in a general way: in mixed-valence ions, in donor-acceptor complexes, in charge transfer transitions. It should be possible, for example, to take empirical solvent scales, based on the Kosower Z parameter or the E_T parameter, and show the origin of their success and of their limitations based on a realistic theoretical model. The third point may be the most important. Provided with a theoretical basis, it should be possible to acquire data on the solvent dependence of CT transitions which could lead to a real advance in our understanding of solvation and the effects of solvation.

Acknowledgment

I would like to acknowledge support by the Army Research Office-Durham for much of the work described in this account.

Literature Cited

1. Creutz, C. Inorg. Chem. 1978, 17, 3723.
2. Tom, G. M.; Creutz, C.; Taube, H. J. Am. Chem. Soc. 1974, 96, 7827.
3. Curtis, J. C.; Meyer, T. J. J. Am. Chem. Soc. 1978, 100, 6284.
4. Robin, M. B.; Day, P. Adv. Inorg. Chem. Radiochem. 1967, 10, 247.
5. Hush, N. S. Progr. Inorg. Chem. 1967, 8, 391.
6. Creutz, C.; Taube, H. J. Am. Chem. Soc. 1973, 95, 1086.
7. Callahan, R. W.; Meyer, T. J. Chem. Phys. Lett. 1976, 39, 82.
8. Piepho, S. B.; Krausz, E. R.; Schatz, P. N. J. Am. Chem. Soc. 1978, 100, 2996.
9. Piepho, S. B.; Krausz, E. R.; Schatz, P. N. Chem. Phys. Lett. 1976, 55, 1539.
10. Hair, N. J.; Beattie, J. K. Inorg. Chem. 1977, 16, 245.

11. Kestner, N. R.; Logan, J.; Jortner, J. J. Phys. Chem. 1974, **78**, 2148.
12. Jortner, J. J. Chem. Phys. 1976, **64**, 4860.
13. "Tunneling in Biological Systems", Chance, B.; et.al., Eds.; Academic Press: New York, 1979.
14. Soules, T. F.; Duke, C. B. Phys. Rev. 19, **B3**, 262.
15. Brunswig, B. S.; Logan, J.; Newton, M. D.; Sutin, N. J. Am. Chem. Soc. 1980, **102**, 5798.
16. Meyer, T. J., in "Mixed-Valence Compounds," Brown, D., Ed.; D. Reidel Publ. Co.: Dordrecht, Netherlands, 1980; pp 75-113.
17. Powers, M. J.; Meyer, T. J. J. Am. Chem. Soc. 1978, **100**, 4393.
18. Powers, M. J.; Meyer, T. J. J. Am. Chem. Soc. 1980, **102**, 1289.
19. Meyer, T. J. Accts. Chem. Res. 1978, **11**, 94.
20. Cannon, R. D. Adv. Inorg. Chem. Radiochem. 1978, **21**, 179.
21. Curtis, J. D.; Sullivan, B. P., to be submitted for publication.
22. Sullivan, B. P.; Curtis, J. C.; Kober, E. M.; Meyer, T. J. Nouv. J. Chim. 1980, **4**, 643.
23. Powers, M. J.; Salmon, D. J.; Callahan, R. W.; Meyer, T. J. Inorg. Chem. 1976, **15**, 1457.
24. Kober, E. M., work in progress.
25. Meyer, T. J. Chem. Phys. Lett. 1979, **64**, 417.
26. Curtis, J. C.; Sullivan, B. P.; Meyer, T. J. Inorg. Chem. 1980, **19**, 3833.

RECEIVED April 21, 1982.

General Discussion—Optical Charge-Transfer Transitions

Leader: John Malin

DR. JOHN MALIN (National Science Foundation): I have been ruminating on a couple of points related to substitutional and electron transfer chemistry. I have been struck by the tremendous difference in the level of sophistication between theoretical treatments of electron transfer and what people know and can say about substitution. I think Professor Swaddle brought out some hopeful thoughts. It's going to be interesting to see what the theoreticians can do for us in understanding substitution processes.

I would like to pose a question for Dr. Meyer dealing with specific solvation, the problem being that very often when one is dealing with medium effects one has a mixed solvent. One doesn't know on a local scale which of the two components (or three or n components) of the solvent is really interacting with the ion pair or with the binuclear complex or whatever. I'm wondering if there is a way that one can get some kind of diagnostic information about specific solvation in a mixed solvent using intervalence transfer.

American Chemical
Society Library
1155 16th St. N. W.

DR. MEYER: That is a very interesting point and it's one that obviously is suggested by the strong solvent dependencies of these optical transitions. In fact, Jeff Curtis' thesis includes a lovely experiment in which he looked at metal-ligand charge transfer in mixed solvents, whose static dielectric constants are about the same, but whose optical dielectric constants are quite different so that the spectra were quite different in the pure solvents. In mixtures of DMF and DMSO there was a large shift in the absorption maximum over the range 0 to 10% DMSO in DMF. Beyond that point the changes were small. These observations certainly suggest that selective solvation is occurring and that it is possible to probe the microenvironment in this way.

DR. JACK NORTON (Colorado State University): This discussion reminds me of the related case of infrared band widths, which is a subject that has perhaps been too much explored over the years. Historically, for the line width to fail to depend on mole fraction in a linear way is taken as evidence of a specific solvent interaction.

DR. DAVID McMILLIN (Purdue University): Can you detect the hydrogen bonding interactions of an amine, for example, in contrast to a polypyridyl?

DR. MEYER: I suspect the answer is yes, but the experiment has not been carried out.

DR. PAUL SCHATZ (University of Virginia): I think I know what Dr. Meyer meant in his talk, but all mixed-valence systems have stationary states. For example, consider the ammonia molecule. It tunnels back and forth between two umbrella forms, perhaps 10^9 or 10^{10} times per second. Nevertheless, the ammonia molecule has stationary states.

DR. MEYER: Yes, I misspoke in my comment about stationary states and their time dependence.

DR. GLENN CROSBY (Washington State University): It's really a question of how long you care to wait. In ammonia, as Dr. Schatz said, it's 10 picoseconds. So if you care to wait a long time compared to that, ammonia is a D_{3h} molecule. If you are on a sub-picosecond timescale, ammonia is a C_{3v} molecule. It is simply a matter of the timescale.

DR. MEYER: With regard to the question of time dependence, a point that I was trying to make relates to the normalization of the timescale. Consider benzene as being delocalized. Now consider the rate of electron oscillation: in a mixed-

valence ion, if it is slow on the vibrational timescale, we are at the nonadiabatic limit and the Fermi Golden Rule applies. If the rate of electron oscillation is allowed to increase, it is no longer possible to use the Born-Oppenheimer approximation and the problem is difficult to solve. Finally, at the limit of rapid electron oscillation we reach the benzene-like case where molecular orbital theory can be applied to the electronic structure. In a system in which electron transfer is relatively slow, the electron distribution is inherently time dependent.

DR. SCHATZ: All mixed valence systems have stationary states. In any such state the probability distribution is time independent. Hence, it is incorrect to say that a mixed valence state is inherently time dependent.

DR. ALBERT HAIM (State University of New York at Stony Brook): Dr. Meyer considered plots of optical transition energy versus $1/D(\text{optical})$ minus $1/D(\text{static})$ for various types of systems, some of which were binuclear and clearly delocalized. If instead, one considers a ruthenium(II) pentaamine bound to N-methyl-4,4'-bipyridinium, is this in any way different from the bridging situation? In some instances there was a similar dependence for both the mononuclear systems and the binuclear systems. But some of these mononuclear systems did not seem to behave similarly. Is there any connection between whether that simple linear relationship works or not and whether the system is localized or delocalized?

DR. MEYER: In the metal-ligand charge transfer transitions, the initial wave function is largely ruthenium in character, perhaps 90 or 95 percent, with some ligand mixing. The excited state is largely ligand π^* in character, with some ruthenium character. We are looking at the optical charge transfer process which connects these two states. The evidence suggests that the metal-ligand case cited here is clearly not a delocalized system in the same sense as a mixed-valence compound might be. But still, the sites are mainly of one orbital character or the other and in different places in the molecule. The charge transfer process does respond to the solvent in a systematic way consistent with the ideas we have used on the mixed-valence compounds. Presumably, in other metal-ligand cases, where the extent of electronic mixing is greater, the same difficulties will arise as arise for mixed-valence compounds.

DR. MEYER: Dr. Schatz has led me to believe in certain things, and I want to ask him a question. It occurs to me that the Landau-Zener equation cannot work except in the nonadiabatic limit. Do you have any comments on that?

DR. SCHATZ: No.

DR. MARSHALL NEWTON: (Brookhaven National Laboratory): The Landau-Zener theory in the weak-coupling regime may be derived by perturbation theory, as Dr. Sutin mentioned earlier. The complete derivation is much more general than the perturbation theory, and allows one to include an arbitrary degree of coupling. Thus, one can go continuously from nonadiabatic to the adiabatic limits.

DR. JOHN BRAUMAN (Stanford University): I have a question about the empirical correlations for quantities like charge transfer band energies versus parameters such as the Kosower Z-value. There is a very large literature of that type and there are many, many good correlations for a variety of parameters. You obtain straight lines with your simple dielectric continuum model. It seems to me, however, that one ought to be able to derive these types of relationships directly from the model. And it doesn't seem to be very helpful to say that these relationships are simply empirical and, therefore, not worth the attention. What you want to do is derive the equations and see whether they, in fact, all reduce to the same terms.

DR. MEYER: I am very sensitive to the points you are making and I should not have demeaned them in the sense that I did. They are clearly very useful parameters. The basic problem is that the Kosower parameters are useful for some correlations while a different parameter works better for other correlations. There appears to be no fundamental understanding of the factors which distinguish between the different types of cases.

DR. BRAUMAN: They all correlate with each other.

DR. MEYER: The critical point to recognize is the factoring. The energy expressions contain a ΔE term which has its own solvent dependence, and the electron transfer part has its own solvent dependence. When you start breaking the problem down into its component parts, instead of attempting to derive a single parameter fit, it may be possible to treat the problem in a general way.

A difficulty which arises in some of the correlations is that there are specific solvent effects which must be brought into the problem empirically since there is no available theory for dealing with them.

Observations on Atom-Transfer Reactions

HENRY TAUBE

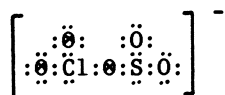
Stanford University, Department of Chemistry, Stanford, CA 94305

Some of the issues involved in trying to understand atom transfer processes are illustrated by a discussion of the observations on the reduction of perchlorate ion. No examples are known of oxygen removal from ClO_4^- under mild conditions by orthodox nucleophilic agents, and all the reactions which have been studied in any detail involve metal ions. The stability of the bond to oxygen, formed in the oxidized product, appears to be very important in affecting rates. In all of the cases in which reaction takes place at room temperature at a reasonable rate, the formation of an "yl" product--vanadyl, for example, when $\text{V}^{2+}(\text{aq})$ is the reducing agent--is possible. A rationalization is offered of the unsymmetrical coordination which is characteristic of "yl" ions.

The title indicates a return on my part to active research in a class of redox reactions to which I devoted considerable attention quite early in my career. Tracer experiments by Halperin (1) in 1950 showed that when ClO_3^- and ClO_2^- in acidic aqueous solution react with S(IV) , respectively 2.4 and 1.4 of the oxygen atoms carried by the oxidants appear in the product sulfate. We concluded from these and additional results that the redox changes involve intimate contact of the reagents, and that oxygen transfer in the steps $\text{ClO}_3^- \rightarrow \text{ClO}_2^-$ and $\text{ClO}_2^- \rightarrow \text{ClO}^-$ is essentially quantitative, the defect from complete transfer occurring in the HOCl stage. The first step can be understood then on the basis that SO_2 adds to an oxygen of ClO_3^- (S(IV) in acidic solution is present largely as SO_2);

0097-6156/82/0198-0151\$08.25/0
© 1982 American Chemical Society

substitution on ClO_3^- , even in acid, is slow (vide infra) to produce



which then can decompose to $\text{ClO}_2^- + \text{OSO}_2$, or by involvement of H_2O , directly to $\text{ClO}_2^- + \text{OSO}_3^{2-} + 2\text{H}^+$. These conclusions about mechanism though satisfying and in accord with the observations, fail to engage the basic issue of how the reaction rate can be predicted from properties of the reactants.

Before proceeding further, the sense in which "atom transfer" will be used in this paper should be defined. The term implies that an atom originating in the oxidizing agent is transferred to the reducing agent so that in the activated complex both centers are bound to the atom being transferred. In using the term in this way, no position is taken on the question of whether the entity transferred is in an atomic state, or whether the reaction can be better understood as involving electron flow from reducing agent to the oxidizing agent concomitant with the motion of the ligand ion from the oxidant to the reductant. This distinction is meaningful only if one point of view, as a first approximation, more readily correlates a set of observations. The term "atom" is used only to distinguish the reactions being considered from the class in which large bridging ligands are transferred by remote attack (2). Many of the latter involve only weak electronic interactions in the activated complexes and, for this reason, are set apart from the cases where oxidizing and reducing centers are separated by single atoms, so that electronic coupling in the activated complexes can be very large. In some of the examples which will be considered, it appears to be very large indeed.

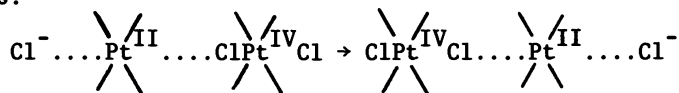
Atom transfer reactions, as defined, are widely recognized as being extremely important, both in the sense that they pose basic significant questions, and, particularly where carbon compounds are involved, as being extremely useful in a practical sense. Nevertheless, much more attention has been devoted to the class of redox reactions loosely described as involving "electron transfer." The reasons for this are quite understandable. It is difficult to estimate electron delocalization energies from first principles, at least when the interactions are large. For many outer-sphere electron transfer reactions, the electronic coupling is weak enough so that the energy of the activated complex is little affected by electron delocalization, but strong enough to ensure that the reactions are adiabatic. This simplification does not seem to apply to most of the reactions which we will consider.

The focus of this paper in terms of descriptive material is

on oxygen atom transfer, specifically in the reduction of ClO_4^- . This choice was made for several reasons. Perchlorate ion is a strong reducing agent and there are many reactions which are favorable in terms of ΔG° , but which, nevertheless, can be very slow. The rates of reactions differ enormously, ranging from those that are "too slow to measure" to some which proceed readily under mild conditions. Those that have been measured show no obvious correlation with driving force. It seems likely that ideas of general import will emerge from a study of the reactions. Such study is in progress in my laboratories, though I must hasten to add that this has not advanced far enough to be featured significantly here. But before dealing with the specific chemistry, it seems appropriate to make a few general observations by way of preparation.

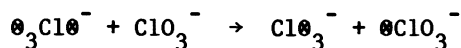
Atom Transfer in $2e^-$ Changes

An important distinction in redox reactions devolves on the question of whether reaction occurs by a $1e^-$ or $2e^-$ change. One-electron changes can take place by inner-sphere or outer-sphere mechanisms, but most $2e^-$ changes seem to involve atom transfer. When the ligands themselves are not easily oxidized or reduced, as is the case for most ordinary saturated ones, $2e^-$ changes call for drastic reorganization of the first coordination spheres of the reacting partners--e.g., $\text{Cl(VII)} - \text{Cl(V)} - \text{Cl(III)} - \text{Cl(I)} - \text{Cl(-I)}$; $\text{Sn(IV)} - \text{Sn(II)}$; $\text{Pt(IV)} - \text{Pt(II)}$; $\text{V(IV)} - \text{V(II)}$; $\text{CO}_2 - \text{H}_2\text{CO}_2 - \text{H}_2\text{CO} - \text{CH}_3\text{OH} - \text{CH}_4$. When the changes in the coordination spheres of the reaction partners are complementary, atom transfer is an economical way for reaction to be consummated, economical in the sense that the critical events involving the changes in the coordination spheres at the two centers are correlated. The results described by Basolo and Pearson, et al. (3, 5), and by Martin, et al. (4), on the oxidation of Pt(II) by Pt(IV) provides an elegant illustration of this point. The reaction between $\text{Pt}(\text{NH}_3)_4^{2+}$ and $\text{trans-Pt}(\text{NH}_3)_4\text{Cl}_2^{2+}$ involves also Cl^- and can be represented as follows:

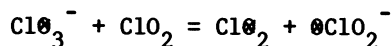


The simple motion of a bridging chloride from Pt(IV) to Pt(II) concomitant with motions of the exterior chloride ions effects the reversal of the oxidation states of the metal. Satisfactory though the insight implied by the above may be, it does not cover the important question of what the activation barrier to

the reaction is, and how this will change from one system to a related one. Reciprocity of the changes at the reacting center by no means guarantees a facile reaction. The process



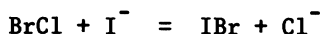
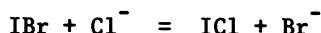
is extremely slow (though just how slow is not known). The barrier is undoubtedly only partly electrostatic; even in the absence of such a barrier, as for example in



reaction can be extremely slow (6).

Nucleophilic Substitution in Relation to Redox Changes

Certain redox changes involving atom transfer can usefully be dealt with applying the ideas which have been developed for nucleophilic substitution. There is, in fact, no sharp distinction between a $2e^-$ redox change involving atom transfer and an orthodox nucleophilic substitution. This point is illustrated by the two reactions



where the second only is a redox process as ordinarily defined. Orthodox nucleophilic substitution implies that the nucleophile acts on a center which is more electropositive than the nucleophile; when the center is more electronegative (Br more electronegative than I) the reaction is classified, following accepted conventions, as a redox change.

This point was recognized quite early by Edwards (7) in correlating the rates at which H_2O_2 reacts with a series of nucleophiles. The Edwards equation⁷

$$\log \frac{k}{k_0} = \alpha E_n + \beta H$$

where E_n and H are properties of the nucleophile and α and β of the substrate, successfully correlates orthodox substitution by nucleophiles at carbon and at H_2O_2 (most of the latter are classified as involving redox changes). According to the analysis, the difference between C and O as substrates resides in α and β being larger in magnitude for the latter. Typical values for the former are 2.0 and 0.07; for H_2O_2 , α and β are 6.31 and -0.394. The specific rates for the reactions of I^- and

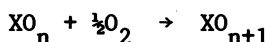
Br^- with H_2O_2 are, respectively, 0.7 and $2.3 \times 10^{-5} \text{ M}^{-1}\text{s}^{-1}$, the rate ratio being 3×10^4 . For substitution at C, typical ratios are 10 to 100. In Edwards' analysis, no allowance for the contribution to the rate by differences in driving force is made. The value of $-\Delta G^\circ$ for the reaction of I^- with H_2O_2 is greater than that of Br^- , the hypohalous acid and hydroxide ion being taken to be the products, by $15.8 \text{ kcal mol}^{-1}$; for substitution in CH_3OH , the difference is about zero (8). If it were possible to factor out effects arising from differences in driving force, the rate pattern for nucleophilic substitution at oxygen in peroxides might prove to be little different from that at carbon.

A particularly important reaction of H_2O_2 is oxygen exchange between H_2O_2 and H_2O , a reaction which has for many years been known to be slow enough to make feasible definitive oxygen tracer studies on reactions of H_2O_2 in aqueous solution. Edwards' correlation yields 10^{-10} s^{-1} as the specific rate for this exchange. It is interesting to note that Anbar and Guttmann (9) measured this rate as $0.5 \times 10^{-9} \text{ s}^{-1}$ at 60° . If the activation energy is assumed to be 30 kcal, a reasonable estimate in view of the slowness of the exchange, the specific rate at 25°C becomes 10^{-11} s^{-1} , in remarkably good agreement with Edwards' estimate.

Reduction of ClO_4^- - General

Unfortunately, the ideas on nucleophilic substitution are not particularly useful in trying to understand the existing data on the reduction of ClO_4^- . The reductions which have been studied involve metal ions. The mode of action of several such potential reductants-- Sn(II) and low spin Co(I) , for example--can profitably be viewed in the light of ideas developed for nucleophilic substitution, but this is not obviously the case for many others-- Ti(III) or Cr(II) , for example.

Before introducing a discussion of the observations on the reduction of ClO_4^- , some properties of this and related species which are germane to the central issue will be considered. Of paramount importance are data on the stability of the species: how does the strength of the bond between halogen and oxygen vary with oxidation state? The existing data are summarized in Table I. The entries pertain to the reaction:



values of ΔG° rather than of ΔH° being chosen because the former are more complete.

One trend in the data seems reasonable enough: the increasing strength of the XO^- bond in the series ClO^- , BrO^- , IO^- , the difference in electronegativity increasing in the same order. Less easy to rationalize are the data on successive additions of $\frac{1}{2}\text{O}_2$ to the same halogen. The increase in bond strength in the series ClO^- , ClO_2^- and ClO_3^- might at first sight seem anomalous because it can reasonably be argued that an increasing content of the electronegative oxygen will contract the lone pair orbitals on halogen and, thus, successively weaken the Cl-O bond. By way of qualitative rationalization, compensating countervailing effects can be found. Two such which have gained some currency in discussions of this kind are these: (i) lone pair repulsions will decrease as the number of lone pairs on chlorine are decreased; (ii) the 3d orbitals become increasingly stable as the oxidation number of the central atom increases. As to the latter point, bond distances are in line with the idea that the Cl-O bond in ClO_4^- has a great deal of double bond character. These arguments do not suffice to explain the fact that the O bond in ClO_4^- is weaker than in ClO_3^- , a fact that is especially significant in view of the facility with which ClO_3^- is reduced relative to ClO_4^- . Finally, we draw attention to the fact that there is no ready simple explanation of the data shown in the last row of Table I.

Table I
Values of $\Delta G^\circ(25\text{C})$ for Reaction with O_2^a

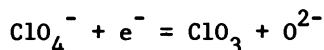
	Cl	Br	I
$\text{X}^- \rightarrow \text{XO}^-$	22.5	16.6	3.8
$\text{XO}^- \rightarrow \text{XO}_2^-$	11.6	--	--
$\text{XO}_2^- \rightarrow \text{XO}_3^-$	-3.7	--	--
$(\text{XO}^- \rightarrow \text{XO}_3^-)$	7.9	12.5	-23.8)
$\text{XO}_3^- \rightarrow \text{XO}_4^-$	0.1	24.6	19.1
^a	Ref. 8, except for entries in bottom row, which are taken from ref. 10.		

This discussion of the energetics of the halogenate ions is in no way a digression. In the first place, when the reaction coordinate within a series is the same, a connection between driving force and rate can be expected. In the second place, it is important to realize that, if we are unable to understand the equilibrium stability in a basic way, we are hardly in position to deal effectively with the stabilities of the activated complexes. Increased concern with the stabilities of this important family of molecules, both at the experimental and theoretical levels, is justified.

Also important for understanding the redox chemistry of the oxyanions is their substitution lability. This can be inferred from the rate of exchange of oxygen between the oxyanions and water, and for the more highly oxidized members of the family this is virtually the only substitution reaction which lends itself to direct study. As to perchlorate ion: substitution takes place extremely slowly, so slowly that the rate of this reaction has never been determined. Hoering, et al. (11), report that there is no exchange in 63 days at 100C in 9.5 M HClO_4 , and the specific rate can safely be set as $< 10^{-8} \text{ s}^{-1}$. As is the case with other oxyanions, the rate is expected to decrease sharply with acidity, and thus the rate of exchange in 1 M HClO_4 would be very slow indeed. It is remarkable that oxygen exchange for BrO_4^- , which reacts with reducing agents much more rapidly than does ClO_4^- , is also extremely slow. Appelman, et al. (12), report less than 1% exchange between BrO_4^- and H_2O in 0.06 M HNO_3 after 19 days at 94C. The substitution lability of ClO_3^- (11) is much greater than that of ClO_4^- , suggesting that the activation process for the two systems is different. A possibility for ClO_3^- , which is much less likely for ClO_4^- , is attack by the incoming nucleophile, here H_2O , on chlorine, in an $\text{S}_{\text{N}}2$ process. Hoering, et al. (11), have shown that, on this basis, a successful correlation of the rate of oxygen exchange with the rates of reduction by the halide ions is achieved. In Table II, their results are summarized. Since oxygen exchange must involve substitution at chlorine, the success of the correlation implies that the halides, in being oxidized, also attack at chlorine. In the absence of evidence to the contrary, the redox reactions could also reasonably be taken as proceeding by attack at oxygen.

Before considering the few systems in which the rate of reduction of ClO_4^- has been measured, some general comments on its reducibility are in order. Perchlorate ion is resistant

to attack by electrons in liquid ammonia and in water. This is not altogether surprising. On the one hand, the intact molecule has no low-lying orbitals to accommodate the electron; on the other, the process



cannot be expected unless some group is available to stabilize O^{2-} . Protons would, of course, stabilize O^{2-} but are incompatible with e^-_{am} or e^-_{aq} . Perchlorate resists attack by orthodox nucleophilic reagents, at least under mild conditions. Especially important among the nucleophilic reactions is the process

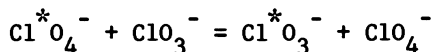


Table II
Nucleophilic Attack on ClO_3^- ^a

Nucl.	Rate Law: $k[\text{Nucl}][\text{H}^+][\text{ClO}_3^-]$	
	$k_{\text{obs}}, \text{M}^{-1} \text{s}^{-1}$	$k_{\text{calc}}^{\text{b}}, \text{M}^{-1} \text{s}^{-1}$
H_2O	1.6×10^{-9}	--
$\text{Cl}^- \text{ } ^{\text{c}}$	4.5×10^{-5}	4.7×10^{-5}
$\text{Br}^- \text{ } ^{\text{c}}$	9.3×10^{-5}	7.1×10^{-5}
$\text{I}^- \text{ } ^{\text{c}}$	2.0×10^{-3}	1.8×10^{-3}

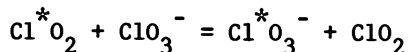
^a At 25C

^b Using $\log k/k_0 = \alpha E_n + \beta H$ and values of E_n and H as tabulated by Edwards.

^c Ref. 13.

which is the analog in atom transfer to the "self exchange" reactions for electron transfer. Conceivably, an elaboration of the Marcus type of correlation also underlies atom transfer processes, though it may be difficult to formulate if, as seems likely, many of these reactions do not conform to the weak overlap limit. For this reason alone, it is important to have meas-

urements of rates such as these, slow though the reactions are. (It is interesting to note in passing that the oxochlorine system of species also provides access to an example of the $1e^-$ atom transfer process



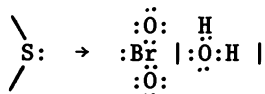
General experience, using perchlorate media for redox reactions of other reagents, teaches that the reduction of ClO_4^- by SO_3^{2-} , P(OR)_3 , Sb(III) , or Sn(II) is also extremely slow, so slow that complications attributable to the reaction of ClO_4^- with these reagents has not been reported. Slow though these reactions are, they must occur at a finite rate, and it would be both interesting and useful if the rates were known. Much can undoubtedly be surmised about the rates of reaction of ClO_4^- with "nucleophilic" reducing agents from the results which have been obtained with BrO_4^- as oxidizing agent (12), several of these reactions being rapid enough for convenient study. In the two cases among those studied in which definitive oxygen tracer experiments are possible, namely with S(IV) and As(III) as reductants, it was found that one atom of oxygen is transferred to the reducing agent when it is oxidized by BrO_4^- . The specific rate, k , in the rate law

$$\frac{d[\text{BrO}_3^-]}{dt} = k[\text{SO}_3^{2-}] [\text{BrO}_4^-]$$

is $5.8 \times 10^{-3} \text{ M}^{-1} \text{ s}^{-1}$ at 25C, which seems remarkably rapid considering the charge types of the reagents. The reaction of S(IV) with BrO_4^- is 24.5 kcal mol⁻¹ more exothermic than that with ClO_4^- . It is reasonable to suppose that the reaction coordinates for the two reactions are similar. If it is assumed then that half of the difference in driving force is reflected in the rate, the specific rate for the reaction of SO_3^{2-} with ClO_4^- would be $10^{-11} \text{ M}^{-1} \text{ s}^{-1}$ which corresponds to a half-life for ClO_4^- in 1 M $\text{SO}_3^{2-}(\text{aq})$ of 2×10^3 yr. The reaction is probably more rapid than this and the rate may well be measureable if a judicious choice of conditions is made.

The reaction of ClO_3^- with a number of the nucleophilic

reagents mentioned and with Cl^- , Br^- , and I^- all proceed at rates which are rather conveniently measurable. In all the cases which have been studied, only the paths involving also protons in the activated complex have been uncovered. This comment takes on significance in the light of the observations (12) made on the oxidation by BrO_4^- or BrO_3^- of S(IV). In acidic solution, the latter reacts more rapidly than the former, but in alkaline solution the reverse is true. These observations are consistent with the idea that reduction of BrO_4^- involves substitution on oxygen, while reduction of BrO_3^- involves attack on Br. There is no particular reason for protons to assist in the former case; in the latter, protons would be useful in weakening the $\text{Br(V)}-\text{O}^{2-}$ bond



Since the relative reactivities of ClO_3^- and ClO_4^- do not reflect the relative strengths of the Cl-O bonds in the two molecules, it is reasonable to suppose that a difference in mechanism similar to that proposed for BrO_4^- vs. BrO_3^- holds for the ClO_4^- - ClO_3^- case.

Reduction of ClO_4^- by Metal Ions

We turn now to the reduction of ClO_4^- by transition metal ions, several of which are known to react under quite mild conditions. A listing of a number of transition metal ion redox couples appears in Table III. These are classified into the categories: lanthanides and actinides, first row transition series, second row transition series.

A survey of the rate data for the reducing agents which are featured in Table III follows, but the rate data for the ruthenium couples are reserved for later discussion because they feature some points of special interest. In discussing the remaining couples, we will deal first with those systems in which data on the rate of reduction of ClO_4^- have been recorded. As an exception to the behavior of several much stronger reducing agents listed in Table III, we have Ti^{3+} , which reduces ClO_4^- rapidly enough so that an analytical procedure for the determination of ClO_4^- is based on this process. For reaction at 25C, $\mu = 1.0$, the rate law:

Table III
A Roster of Redox Couples

	E° or E_f^a	Conditions	Ref.
$e^- + Yb^{3+} = Yb^{2+}$	-1.15		14
$e^- + Eu^{3+} = Eu^{2+}$	-0.43		8
$e^- + U^{4+} = U^{3+}$	-0.63	1 M HClO ₄	15
$2e^- + 4H^+ + UO_2^+ = U^{3+} + 2H_2O$	-0.13	1 M HClO ₄	16
$e^- + Ti(IV) = Ti^{3+}$	~0.1		8
$e^- + V^{3+} = V^{2+}$	-0.25		8
$2e^- + 2H^+ + VO^{2+} = V^{2+} + H_2O$	0.05		8
$e^- + 2H^+ + VO^{2+} = V^{3+} + H_2O$	0.36		8
$2e^- + 4H^+ + VO_2^+ = V^{3+} + 2H_2O$	0.68		8
$e^- + Cr^{3+} = Cr^{2+}$	-0.41		8
$2e^- + Cr(IV) = Cr^{2+}$	>0.9 ^b		

Continued on next page.

Table III (cont.)
A Roster of Redox Couples

	E° or E_f^a	Conditions	Ref.
$e^- + Ru(NH_3)_6^{3+} = Ru(NH_3)_6^{2+}$	0.051	0.1 M NaBF ₄	18
$e^- + Ru(NH_3)_5H_2O^{3+} = Ru(NH_3)_5H_2O^{2+}$	0.066	$\mu = 0.2$	18
$e^- + Ru(H_2O)_6^{3+} = Ru(H_2O)_6^{2+}$	0.23		20
$e^- + Ru(bpy)_2pyOH_2^{3+} = Ru(bpy)_2pyOH_2^{2+}$	0.78	$\mu = 0.10$	21
$2e^- + 2H^+ + Ru(bpy)_2pyO^{2+} = Ru(bpy)_2pyOH_2^{2+}$	0.89	$\mu = 0.10$	21

(a) E° understood unless conditions given.

(b) Estimated on the basis of the observation (17) that Cr³⁺ in acidic solution is much less efficient in scavenging atomic chlorine than is Co²⁺, Ce³⁺ or even Pr³⁺.

(c) The electrochemical results cited in Ref. 14 are in good agreement with those reported by Matsubara and Ford (18).

$$-\frac{d[\text{Ti}^{3+}]}{dt} = [\text{Ti}^{3+}][\text{ClO}_4^-](1.89 \times 10^{-4} + 1.25 \times 10^{-4}[\text{H}^+])$$

has been reported (22), and these data, at least insofar as the first term is concerned, are consistent with earlier ones obtained at 40C (23). The chemistry of V^{2+} is often studied in ClO_4^- medium, but the reduction of ClO_4^- is rapid enough so that, in experiments over an extended period, allowance for it must be made. At 25C and $\mu = 2.0$, in the rate law ($\text{V(II)} \rightarrow \text{V(III)}$)

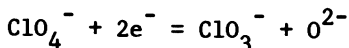
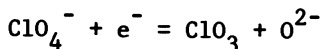
$$-\frac{d[\text{V}^{2+}]}{dt} = k[\text{V}^{2+}][\text{ClO}_4^-]$$

k (hereinafter used to represent the coefficient for the rate term $[\text{Reductant}][\text{ClO}_4^-]$, the rate being defined by $-\frac{d[\text{reductant}]}{dt}$; except for certain of the ruthenium systems, Cl^- is the reduction product) is reported (24) as $5.3 \times 10^{-7} \text{ M}^{-1} \text{ s}^{-1}$, and is independent of $[\text{H}^+]$ over a limited range. Deutsch (25) has recorded for k at 25C and $\mu = 1.0$ a value of $7.6 \times 10^{-7} \text{ M}^{-1} \text{ s}^{-1}$, which is in satisfactory agreement with that of Adin and Sykes. These data are consistent with those obtained by King and Garner (26) at 50C. The latter authors report for k the value $2.8 \times 10^{-6} \text{ M}^{-1} \text{ s}^{-1}$, and for the reaction of V(III) with ClO_4^- , the value $3.0 \times 10^{-6} \text{ M}^{-1} \text{ s}^{-1}$. In both cases a weak dependency of k on $[\text{H}^+]$ is mentioned, but in view of the fact that the ionic strength was not kept constant, it is by no means certain that a proton dependent term is present. In fact, the proton dependent term in the reaction of ClO_4^- with Ti^{3+} also may not be real. Ionic strength was maintained (22) using NaClO_4 to replace HClO_4 and spurious rate terms can arise simply because the activity coefficients of the reactants do not remain constant in such mixtures as the ratio of Na^+/H^+ is changed. It is likely that U^{3+} also reduces ClO_4^- at room temperature. Uranium(III) is known to disappear more rapidly in a solution of HClO_4 than in one of HCl . The observations by Sato (27) on this point are consistent with the rate measurements of Peretrukhin, et al. (28), for the reaction at 22C which yielded, for the disappearance of U^{3+} in 0.5 M HClO_4 , the value of $1.8 \times 10^{-5} \text{ s}^{-1}$. However, since in neither case are products

specified, it is, of course, possible that the oxidation of U^{3+} by H^+ was being followed in perchloric acid media.

Despite Eu^{2+} being a stronger reducing agent than V^{2+} , V^{3+} or Ti^{3+} , it reacts with ClO_4^- much less rapidly than does any member of the latter group. From Adin and Sykes' (24) observations, k for the reaction of ClO_4^- with Eu^{2+} at 25C is less than $3 \times 10^{-8} M^{-1} s^{-1}$. Even $Yb^{2+}(aq)$, which is a very strong reducing agent indeed, reacts with ClO_4^- slowly enough so that Yb^{2+} can be prepared and studied in ClO_4^- media without interference from the reaction of the reducing agent with ClO_4^- (29). General experience with solutions of Cr^{2+} in aqueous perchlorate suggests that k for the reduction of ClO_4^- is less than $10^{-8} M^{-1} s^{-1}$ at 25C.

A significant feature of the reaction kinetics outlined is that, for each reducing agent for which the reaction rate was measured, the activated complex for the dominant path contains only the reducing agent, perchlorate ion, and no protons. In the absence of protons to stabilize the oxide ion which is released, whether the reduction is by a $1e^-$ or $2e^-$ change:



an important requirement must be that the oxidized metal product makes a strong bond to the oxide being released. Unusually strong metal to oxygen bonds are found in the "yl" ions. A remarkable feature of the chemistry of metal ions in the aquo or ammono system is the abrupt change in acidity which can occur at a critical stage in the stepwise increase in oxidation state.

Two examples will suffice for illustration. When $V(H_2O)_6^{2+}$ is oxidized to $V(H_2O)_6^{3+}$, nothing particularly remarkable happens, and the increase in acidity of the aquo ion is perhaps a factor of 10^5 , the dissociation constant of $V(H_2O)_6^{3+}$ being about 10^{-3} (30). But on increasing the oxidation number by one more unit, the enhancement in acidity is very great indeed, there being complete dissociation of two protons to yield VO^{2+} (i.e., $VO(H_2O)_4^{2+}$). The behavior of the aquo uranium system is even more striking. Here the change in oxidation state from 4+ to 5+

changes the acidity even more drastically. The dissociation constant for $U^{4+}(\text{aq})$ is about 10^{-2} (30). Increasing the oxidation state by one more unit, in the absence of special effects, would lead to the expectation that perhaps one to two protons would be released. Instead, the oxidation leads to the complete release of four protons, UO_2^+ being the product. The sharp increase in acidity is a consequence of the fact that the metal ion exerts a selective polarization of the surrounding waters. Thus V(IV) selects one water molecule from the environment and interacts with it particularly strongly, leading to complete proton dissociation for that water, rather than gathering electron density evenly from the surrounding molecules.

The basic driving force for the formation of "yl" ions can be understood by taking polarization effects into account. Thus consider the two states for the species $M^{z+}O_2H_2$:



To produce state B from state A will cost

$$RT \ln \frac{K_{\text{OH}}^a}{K_{\text{OH}_2}^a}$$

where the K^a 's are the association constants for H^+ on coordinated O^{2-} and on coordinated OH^- . However, the polarizability of the combination $O^{2-} + H_2O$ is greater than that of $2OH^-$ (the polarizability of O^{2-} decreases enormously with the addition of the first proton, much less with the addition of the second), and state B is stabilized relative to A by a term

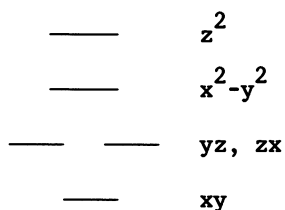
$$- \frac{z^2}{r^4} \Delta P$$

where ΔP is the polarizability of B less that of A. The increase in the second term relative to the first as z increases can be very sharp. Not only does the polarization term increase with z^2 , but, as z increases, the radius r decreases and, furthermore, the factor

$$\frac{K_{\text{OH}}^a}{K_{\text{OH}_2}^a}$$

becomes smaller. Thus, the abrupt appearance of the "yl" form in general terms can be understood in terms of polarization effects, the polarization leading to non-equivalence or disproportionation of the ligands in the first coordination sphere. It is not unreasonable to suppose that the polarization term on changing the oxidation number by one unit increases enough not only to account for the stabilization of B with respect to A, but also with respect to $M^{Z+}(\text{OH})$, which might be the dominant form in the absence of selective interactions.

In applying these ideas, polarizing power and polarizability must be interpreted in terms of the electronic structures of the central metal and the ligands. Polarizing power is not simply a function of z/r [thus note that the ionizing potential of Ag is 7.58 V (radius of Ag^+ 1.13Å) while that of Na is 5.38V (radius 0.98Å)], nor is the polarizability of the ligand, in the sense in which it is important here, simply a function of charge and size (the yl ions are stabilized by multiple bond formation and π bonds for oxygen tend to be stronger than for sulfur). To understand the chemistry of the yl ions, the electronic structure of the central ion must be taken into account. In producing the multiple bonded unit $M^{Z+}\text{O}$ or linear OM^{Z+}O , the d_{yz} and d_{zx} orbitals are promoted in energy, the resulting hierarchy of d-orbital energies being



The observations which have been made on the reduction of ClO_4^- by metal ion reducing agents conform to the idea that those which react relatively rapidly can produce an "yl" oxidized product. This is true of Ti(IV), V(II) (if attack is by a $2e^-$ change), V(III) (if attack is by a $1e^-$ or $2e^-$ change), and U(III) (if attack is by a $2e^-$ change). For Eu^{2+} and Yb^{2+} , the only accessible higher oxidation state is the 3+, and the 3+ ion does not lend itself to the formation of the "yl" bond. Chromium(II) as reducing agent calls for special mention. On the basis of the ideas introduced, the change $\text{Cr}^{2+} \rightarrow \text{Cr}^{3+}$ is not expected to lead to rapid reduction of ClO_4^- : the ratio z/r for Cr(III) is not high enough to produce the "yl" bond

and, furthermore, there is a barrier arising from electronic destabilization. The formation of an η^1 bond would call for the promotion of two electrons, or if the d_{yz} , d_{zx} against d_{xy} splitting is great enough, for destabilization by electron pairing. Chromium(IV) can presumably form an η^1 ion, but, in forming it, a penalty in electron destabilization is exacted, and this may be a factor in accounting for the fact that the Cr(II)-Cr(IV) couple is so weakly reducing. No such penalty is exacted in the case of Ti(IV) or V(IV).

The observations on the reactions of ruthenium(II) complexes with ClO_4^- are in accord with the idea that the formation of an η^1 ion in the product is an important factor. The pronounced acidity of an ammineruthenium(IV) species was demonstrated by Rudd, et al. (31), and the characterization of Ru(IV) bearing an oxygen as an η^1 species has been convincingly completed by Meyer and coworkers (21, 32, 33). Quite early in the rather recent resurgence of interest in the chemistry of ruthenium in the lower oxidation states, it was noted that both $\text{Ru}(\text{NH}_3)_6^{2+}$ and $\text{Ru}(\text{NH}_3)_5\text{H}_2\text{O}^{2+}$ are incompatible with ClO_4^- . The specific rate, k , for the reaction of the latter ion with ClO_4^- was reported (34, 35) as $2.6 \times 10^{-2} \text{ M}^{-1}\text{s}^{-1}$. At the time this work was done, it was assumed that, once the first stage of reduction had been achieved, the subsequent reduction of ClO_3^- would be rapid. But, in view of the fact that substitution in $\text{Ru}(\text{NH}_3)_5\text{H}_2\text{O}^{2+}$ is by no means instantaneous, ClO_3^- may actually accumulate. At any rate, $2.6 \times 10^{-2} \text{ M}^{-1}\text{s}^{-1}$ is an upper limit for the rate at which the first reaction stage occurs. If the net product is ClO_2^- , the specific rate for the rate determining step is $1.6 \times 10^{-2} \text{ M}^{-1}\text{s}^{-1}$, and, if it is Cl^- , the specific rate becomes $3.3 \times 10^{-3} \text{ M}^{-1}\text{s}^{-1}$. In any event, this rate is slower than expected for substitution on $\text{Ru}(\text{NH}_3)_5\text{H}_2\text{O}^{2+}$ where a specific rate in the range 1 to 10 is expected for a mononegative entering group (18). This point takes on interest in the context of the results which have been reported for $\text{Ru}(\text{H}_2\text{O})_6^{2+}$ as the reducing agent. Kallen and Earley (36) have compared the specific rate of the first step in the reaction of $\text{Ru}(\text{H}_2\text{O})_6^{2+}$ with ClO_4^- (37) with the rate of substitution into the aquo ion by Cl^- , Br^- , I^- . These rates are all similar, ranging from $3.2 \times 10^{-3} \text{ M}^{-1}\text{s}^{-1}$ for ClO_4^- to $9.7 \times 10^{-3} \text{ M}^{-1}\text{s}^{-1}$ for Br^- , and the ac-

tivation parameters ΔS^\ddagger and ΔH^\ddagger are very much alike for the series. In this case it appears that substitution is rate determining for the reduction of ClO_4^- .

Reduction of ClO_4^- by Ru(II) is not limited to the rather strongly reducing complexes but is reported also for $\text{Ru}(\text{bpy})_2\text{pyH}_2\text{O}^{2+}$ (38). Nor is the activity limited to Ru(II). In fact, in an early study of catalysis by ruthenium salts of the reduction of ClO_4^- by HBr_{aq} (98C), the conclusion was reached (39) that a Ru(III) species is responsible for attack on ClO_4^- . Broomhead, et al. (40), report that $\text{Ru}(\text{NH}_3)_5\text{Cl}^{2+}$ is converted by 0.10 M HClO_4 to $[\text{Ru}(\text{NH}_3)_4(\text{OH})\text{NO}]^{2+}$ in a matter of hours on a steam bath. The corresponding reaction with $\text{Ru}(\text{NH}_3)_6^{3+}$ is much slower, suggesting that ClO_4^- occupies a normal coordination site on being reduced by ruthenium. Osmium salts are also known (41) to be catalysts for the reduction of perchlorate, and experience with the chemistry of the osmium in lower oxidation states shows that ClO_4^- can be involved as an oxidant. Osmium also makes very strong bonds to oxygen in the higher oxidation states, and an "yl" oxygen species may well react for Os(IV) as an intermediate.

It has been reported (35) that $\text{Ru}(\text{NH}_3)_6^{2+}$ also reduces ClO_4^- , the implication being that the open normal coordination site is not necessary for facile reaction. Though an attack by a transfer of an atom of oxygen to a face of the octahedron, O being converted to O^{2-} , would confer some stability on the immediate product of the reaction, it is difficult to see how a strong Ru(IV)- O^{2-} bond could be formed in this situation. The system is being reinvestigated, acetonitrile being added to the reaction solution so as to scavenge $\text{Ru}(\text{NH}_3)_5\text{H}_2\text{O}^{2+}$ which may be present initially, or which will be formed by slow loss of NH_3 from $\text{Ru}(\text{NH}_3)_6^{2+}$. We (42) now find that the direct reaction of $\text{Ru}(\text{NH}_3)_6^{2+}$ is at least a factor of 20 slower than our earlier results indicated. A contamination of 1% of $\text{Ru}(\text{NH}_3)_5\text{H}_2\text{O}^{2+}$ in the hexaammine used in our earlier work would account for the published rates.

The observations cited do seem to support the point of view that, for facile reduction, it is important that an especially

stable bond to O^{2-} be formed by the oxidized product. This conclusion, even if accepted, is by no means tantamount to understanding the reduction of perchlorate and, at best, represents the beginning of an understanding. The electronic structures and how they affect the energy of activation must be understood much more completely if we are to provide satisfactory answers to questions such as these. Why does V^{3+} , which is a much weaker reducing agent than V^{2+} , react as rapidly as does V^{2+} ? Why is Ti^{3+} so much more reactive than either? Titanium(III) is restricted to a $1e^-$ change and in reducing ClO_4^- must leave chlorine in the very unstable state, ClO_3 . Why are the Ru(II) species, though by far not the strongest reductants, so remarkably reactive in reducing ClO_4^- ? In converting Ru(II) to a ruthenyl(IV) species, there is a spin change. The stability gained by unpairing electrons may compensate for the promotion of the d_{yz} , d_{zx} orbitals accompanying multiple bond formation, but there is the possibility that the spin change itself can affect the reaction rate adversely.

The foregoing discussion by no means covers the entire roster of metal ion species which are known to reduce ClO_4^- readily. Considerable attention has been devoted to the interaction of ClO_4^- with a very reactive molybdenum species, but there is disagreement about its identity (43-47). A difficulty is that the Mo(IV) and Mo(V) species ordinarily studied are bi- or polynuclear, while the reactive species may actually be mononuclear. A priori, mononuclear Mo(IV) would appear to be a better prospect than Mo(V) for facile reaction with ClO_4^- . In the former case, replacement by ClO_4^- only of a coordinated water would be required, but, in the latter, of a coordinated OH^- or O^{2-} if a normal coordination site is to be used for reduction. There are numerous examples of the reduction of ClO_4^- in heterogeneous systems. The likelihood of understanding these on the short term is very small, considering the difficulties we face even in cases where the compositions of the activated complexes are known.

Though the reduction of ClO_4^- is only one of many atom transfer processes that might be considered and is far from the most important one, the foregoing discussion serves to show the need for a systematic experimental approach and does, perhaps,

illustrate the point that such a study can lead to ideas which can be useful in a much wider context.

Literature Cited

1. Halperin, J.; Taube, H. J. Am. Chem. Soc. 1950, 72, 3319; ibid., 1952, 74, 375.
2. Taube, H.; Gould, E. S. Acc. Chem. Res. 1969, 2, 321.
3. Basolo, F.; Willis, P. H.; Pearson, R. G.; Wilkins, R. G. J. Inorg. Nucl. Chem. 1958, 6, 161.
4. Cox, L. T.; Collins, S. B.; Martin, D. S. J. Inorg. Nucl. Chem. 1961, 17, 383.
5. Basolo, F.; Morris, M. L.; Pearson, R. G. Discuss. Faraday Soc. 1960, 29, 80.
6. Taube, H.; Dodgen, H. J. Am. Chem. Soc. 1949, 71, 3330.
7. Edwards, J. O. J. Am. Chem. Soc. 1954, 76, 1540.
8. Latimer, W. M. "Oxidation Potentials"; 2nd ed., Prentice-Hall: Englewood Cliffs, N.J., 1952.
9. Anbar, M.; Guttmann, S. J. Am. Chem. Soc. 1961, 83, 2035.
10. Johnson, G. K.; Smith, P. N.; Appelman, E. H.; Hubbard, W. N. Inorg. Chem. 1970, 9, 119.
11. Hoering, T. C.; Ishimori, F. T.; McDonald, H. O. J. Am. Chem. Soc. 1958, 80, 3876.
12. Appelman, E. H.; Klänning, U. K.; Thompson, R. C. J. Am. Chem. Soc. 1979, 101, 929.
13. Skrabal, A.; Schreiner, H. Monatsh. Chem. 1935, 65, 213.
14. Laitinen, H. A. J. Am. Chem. Soc. 1942, 64, 1133.
15. Kritchevsky, E. S.; Hindman, J. D. J. Am. Chem. Soc. 1949, 71, 2096.
16. Newton, T. W. "The Kinetics of Actinide Oxidation Reduction Reactions" of Erda Critical Review Series TID - 26506, 1975.
17. Taube, H. J. Am. Chem. Soc. 1943, 65, 1880.
18. Lim, H. S.; Barclay, D. J.; Anson, F. C. Inorg. Chem. 1972, 11, 1460.
19. Matsubara, T.; Ford, P. C. Inorg. Chem. 1976, 15, 1107.
20. Buckley, R. R.; Mercer, E. E. J. Phys. Chem. 1966, 70, 3103.
21. Moyers, B. A.; Meyer, T. J. J. Am. Chem. Soc. 1978, 100, 3601.
22. Cope, V. W.; Miller, R. G.; Fraser, R. T. M. J. Chem. Soc. A 1967, 301.
23. Duke, F. R.; Quinney, P. D. J. Am. Chem. Soc. 1954, 76, 3800.
24. Adin, A.; Sykes, A. G. J. Chem. Soc. A 1966, 1230.
25. Deutsch, E. A., Ph.D. Dissertation, Stanford University, 1967.
26. King, W. R., Jr.; Garner, C. S. J. Phys. Chem. 1954, 58, 29.

27. Sato, A. Bull. Chem. Soc. Japan, 1967, 40, 2107.
28. Peretrukhin, V. F.; Krot, N. N.; Gelman, A. D. Sov. Radiochem. (Engl. Transl.) 1970, 12, 85.
29. Christensen, R. J.; Espenson, J. H.; Butcher, A. B. Inorg. Chem. 1973, 12, 574.
30. "Stability Constants of Metal Ion Complexes." Special Pub. 17 & 25, The Chemical Society: London (1964, 1971).
31. Rudd, DeF. P.; Taube, H. Inorg. Chem. 1971, 10, 1543.
32. Moyer, B. A.; Meyer, T. J. J. Am. Chem. Soc. 1979, 101, 1326.
33. Moyer, B. A.; Thompson, M. S.; Meyer, T. J. J. Am. Chem. Soc. 1980, 102, 2310.
34. Endicott, J. F.; Taube, H. J. Am. Chem. Soc. 1962, 84, 4984.
35. Endicott, J. F.; Taube, H. Inorg. Chem. 1965, 4, 437.
36. Kallen, T. W.; Earley, J. E. Inorg. Chem. 1971, 10, 1149.
37. Seewald, D.; Sutin, N.; Watkins, K. O. J. Am. Chem. Soc. 1969, 91, 7307.
38. Referred to in Moyer, B. A.; Sipe, B. K.; Meyer, T. J., submitted for publication.
39. Crowell, W. R.; Yost, D. M.; Carter, J. M. J. Am. Chem. Soc. 1929, 51, 986.
40. Broomhead, J. A.; Taube, H. J. Am. Chem. Soc. 1969, 91, 1261.
41. Crowell, W. R.; Yost, D. M.; Roberts, J. D. J. Am. Chem. Soc. 1940, 62, 2176.
42. Louis, P., work in progress, Stanford University.
43. Bredig, G.; Michel, J. Z. Phys. Chem. 1922, 100, 124.
44. Haight, G. P., Jr.; Sager, W. F. J. Am. Chem. Soc. 1952, 74, 6056.
45. Haight, G. P., Jr. Acta Chem. Scand. 1961, 15, 2012.
46. Rechnitz, G. A.; Laitinen, H. A. Anal. Chem. 1961, 33, 1473.
47. Kolthoff, M.; Hodara, I. J. Electroanal. Chem. 1963, 5, 2.

RECEIVED April 21, 1982.

General Discussion—Observations on Atom-Transfer Reactions

Leader: John Malin

DR. JOHN MALIN (National Science Foundation): I wanted to ask Dr. Taube whether he thought that, in the case of the reaction of vanadium(II) with perchlorate, the reaction might also be facilitated by an attack at the t_{2g} orbital. Of course, the driving force is provided by the formation of vanadium(IV) oxo ion.

DR. TAUBE: The number of d electrons in the reducing agents does seem to be an important factor, and since above a certain number both σ and π orbitals are populated, in that sense at least orbital symmetry plays a role. Perhaps the most instructive example is Ti^{3+} which has a single πd electron and reduces ClO_4^- with considerable ease. This is to be contrasted with orthodox electrophilic donors, none of which appear to be very effective. As pointed out in the paper, $Ti(IV)$ can make a stable "yl" ion because it has low-lying πd orbitals to accommodate the π bonds between the metal ion and O^{2-} . When the number of d electrons increases, anti-bonding effects limit the stability of the "yl" ion. An interesting example to study would be $Co(I)$ which is known to be a good electrophile, but because of the number of d electrons which would be left even on $2e^-$ oxidation is not expected to form a stable "yl" ion.

DR. JOSEPH EARLEY (Georgetown University): Would you care to comment on the use of tin(II) as a reducing agent for perchlorate?

DR. TAUBE: I don't think that $Sn(II)$ will reduce ClO_4^- at all rapidly. In saying this, I'm relying on the experience with other reducing agents which are orthodox nucleophiles. Because only outer d orbitals are available for π bonding, $Sn(IV)$ isn't expected to have the tendency that $Ti(IV)$ has to make an "yl" ion--that is a product in which one oxide is very tightly bound, even at the expense of loosening the binding to the metal of other ligands.

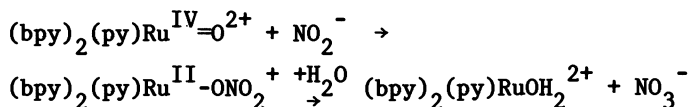
DR. GILBERT HAIGHT (University of Illinois): Some of you may recall that I reduced perchlorate with tin(II), but in the presence of molybdates. And we came to the conclusion that molybdenum(IV) was produced but it was not the reducing agent for perchlorate; it was catalytic. Recently we've been able to make a tin(II)-molybdenum(IV) complex and add it to perchloric acid. The tin is oxidized extremely rapidly and the molybdenum is not. So the molybdenum is serving as a pathway for electrons to get through an oxygen bridge, and then it holds the oxygen.

DR. TAUBE: A problem with the molybdenum catalysis is that the species which reacts readily with ClO_4^- may be an unstable, possibly mononuclear, species rather than one of the condensed forms which we ordinarily encounter. Paffett and Anson [Paffett, M. T.; Anson, F. C. *Inorg. Chem.* 1981 **20**, 3967] have shown that mononuclear Mo(V) reacts moderately rapidly with ClO_4^- . My guess is that mononuclear Mo(IV) would be even more reactive. Mononuclear Mo(IV) is probably a typical "yl" ion, that is, it has both H_2O and O^{2-} coordinated to it. Mo(V) on the other hand will have OH^- and O^{2-} as ligands. Replacement of H_2O by ClO_4^- is easier than replacement of OH^- .

DR. HAIGHT: We are now about to tackle the problem of distinguishing between the reactivities of mononuclear and polynuclear molybdenum species. We added mononuclear molybdenum-tin(II) complexes to water and to perchlorate and our evidence right now is that it becomes a cluster very fast when you do this.

DR. EARLEY: We had expected to find ruthenium(III) dimers as products of the reaction of Ru(II) with perchlorate ion but we found none. We had expected ruthenium(II) to go to ruthenium(IV) and the Ru(IV) to react with a second Ru(II) to form a dimer, but this did not occur.

DR. THOMAS MEYER (University of North Carolina): Wagner de Giovanni, in my lab, is studying the reaction between an oxo ruthenium compound and NO_2^- :



When you carry out the reaction in this direction you can actually see the nitrate complex build up in the solution. The rate constant for its formation is about $10^2 \text{ M}^{-1} \text{ s}^{-1}$. The next step involves an aquation and the rate constant is about 0.1 s^{-1} . It is a stoichiometrically clean reaction yielding nitrate. The reaction provides a reinforcement of Dr. Earley's point. However, one other appealing aspect of this reaction is that the free energy change is close to zero. The critical step in the forward direction is attack of the coordinated oxo ligand on nitrite. The specific rate constant for that step is actually pretty large. Applying microscopic reversibility takes us back to Dr. Earley's point that, for the reverse reaction, the slow step is the substitution and not the redox step.

DR. JAMES ESPENSON (Iowa State University): Murmann's data [Murmann, R. K. Inorg. Chim. Acta 1977, 25 L43] on the exchange of the oxo oxygen of vanadium(IV) would certainly suggest that it would be possible to prove whether or not the oxygen was really transferred from perchlorate during its reaction with vanadium(II). Has that experiment actually been done?

DR. RICHARD THOMPSON (University of Missouri): I do not believe that experiment will work. In addition to the presumably slow reduction of the perchlorate ion by vanadium(II), the V(II)-V(IV) reaction would be rapid enough to preclude the generation of much VO^{2+} [Newton, T. W.; Baker, F. B. Inorg. Chem. 1964, 3, 569].

Another point to remember is that some of the precipitations for ^{18}O analysis can be very troublesome, and vanadium(IV) is no exception. However, the work of Murmann, which you have cited, has opened the possibility of testing for oxygen atom transfer to vanadium(II), provided the redox reaction is rapid.

DR. TAUBE: Murmann's published exchange studies on V(V) are limited to condensed species and the results are not applicable to an immediate product of oxidation, which presumably is a mononuclear species. He has some still unpublished results (K. Rahmoeller, as coworker) on VO_2^+ and finds oxygen exchange to be quite rapid with $k \sim 0.03 \text{ s}^{-1}$ at 0° . The specific rate for exchange between VO^{2+} and water at 0° is $2.9 \times 10^{-5} \text{ s}^{-1}$ [Murmann, R. K.; op.cit.]. Both rates are so rapid compared to the reactions of V^{3+} or V^{2+} with ClO_4^- as to invalidate the oxygen tracer approach to determining the mechanism.

DR. ESPENSON: Carboxylate radical anion from radiation chemistry ought to be well set up in the formation of carbonate ion to meet just this requirement. Yet I'm under the impression that the carboxylate radical anion doesn't react with perchlorate.

DR. TAUBE: With unstable intermediates, there is the problem of competing rates. My guess is that, if you could keep the carboxylate anion long enough, it would reduce ClO_4^- . The specific rate is certainly not $10^9 \text{ M}^{-1} \text{ s}^{-1}$, but it might be as large as for some of the other reagents for which measurements have been made.

DR. ROBERT BALAHURA (University of Guelph): When you make chromium(II) solutions by the Taube method, you usually find a

lot of chloride ion in the solution. What do you envisage as the releasing agent: chromium(I) or some combination of chromium(I) and hydrogen?

DR. TAUBE: There are numerous examples of reduction of ClO_4^- at the surfaces of solids, including one from work in my own laboratories done by Zabin [Zabin, B. A.; Taube, H. *Inorg. Chem.* 1964, 3, 963]. When Cr^{2+} reduces MnO_2 in the presence of ClO_4^- , there is copious production of Cl^- . The heterogeneous reductions are even less well understood than the homogeneous, and for this reason I have omitted them from my account. In the systems you refer to, there is always a solid phase present.

What is your experience on the durability of a chromium(II) solution after the reaction becomes homogeneous?

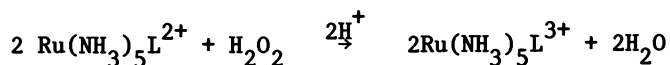
DR. BALAHURA: We have analyzed chromium(II) solutions two or three times a week and they seem to be stable for about two weeks with the concentrations we're using (0.2-0.4 M). But we also have lithium perchlorate present to suppress some of those reactions.

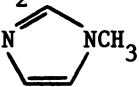
DR. KENNETH KUSTIN (Brandeis University): You mentioned that perchlorate is resistant to attack by the hydrated electron. I think that is even more remarkable when you realize that a similarly usually inert anion, nitrate, is rapidly attacked by the hydrated electron. Even though the hydrated electron has no place in which to go, it adds on, forming NO_3^{2-} which hangs around long enough for the radiation chemists to monitor its decay mode. And that doesn't happen at all with perchlorate, which I do not understand.

DR. REX SHEPHERD (University of Pittsburgh): About a year ago, we started to look at the reaction of hydrogen peroxide with $(\text{NH}_3)_5\text{Ru}^{\text{II}}\text{L}$ complexes where L could be ammonia, water and other nitrogen bases.

Actually, Dr. Taube had tried previously to measure the rate of oxidation of $\text{Ru}(\text{NH}_3)_6^{2+}$ by H_2O_2 . As a secondary reaction after the initial oxidation of hexaammine by molecular oxygen and under his conditions in acid solution, he obtained zero-order kinetics. We employed a phosphate buffer, and were able to see the intrinsic reaction for peroxide and these ruthenium(II) complexes. There are two interesting results. The first is that the rate saturates in $[\text{H}_2\text{O}_2]$. The second is that we found ΔH^\ddagger to be nearly independent of L and ΔS^\ddagger to be very negative (work in collaboration with Mr. C.R. Johnson). The values obtained are shown in Table I.

Table I
Kinetic Activation Parameters for the Oxidation of
Ruthenium(II) Complexes by Hydrogen Peroxide



<u>L</u>	ΔH^\ddagger (kcal/mole)	ΔS^\ddagger (eu)
NH ₃	5.87 ± 1.27	-41.9 ± 4.3
H ₂ O	5.32 ± 0.36	-36.8 ± 1.2
	5.46 ± 0.48	-50.6 ± 1.6

Ref: Kristine, F. J.; Johnson, C. R.; O'Donnell, S.; Shepherd, R. E. Inorg. Chem. 1980, 19, 2280.

We hypothesized that $\Delta S^\ddagger \ll 0$ could result if $\text{Ru}(\text{NH}_3)_6^{2+}$ were undergoing some type of distribution process which allowed for seven coordination with peroxide attacking on a face to produce a chemical intermediate (Scheme I). This species could suffer a number of possible fates: (A) the formation of the ruthenium(IV)-oxyl ligand plus water; (B) the formation of coordinated hydroxide with expulsion of hydroxyl; or (C) the formation of coordinated hydroxyl with free hydroxide. The latter two pathways ultimately yield the hydroxyl radical.

The completion of the mechanism is the reduction of either hydroxyl or ruthenium(IV) by a second mole of $\text{Ru}(\text{NH}_3)_6^{2+}$ going on to product. We wanted to see if we could find anything that would tell us whether we had the case for ruthenium(IV) as opposed to the hydroxyl radical pathways. To accomplish this we employed the organic radical-trapping reagents, PBN and DMPO.

The radical addition products are nitroxyl radicals which are readily characterized by means of their EPR spectra. We used both radical trapping agents to carry out some of the studies. The PBN system is less diagnostic because it is not as sensitive to trapping all the radical species as DMPO. The data in Table II are for the DMPO trap. We also generated hydroxyl by means of two other reagents, $\text{Fe}(\text{EDTA})^{2-}$ and $\text{Ti}(\text{EDTA})(\text{H}_2\text{O})^-$, which are alleged to make hydroxyl in their reactions with H_2O_2 .

If there's nothing in the solution except the reactants, the trapping agent and the solvent, we find that we trap a species which is the same for all three reagents (the two controls and $\text{Ru}(\text{NH}_3)_6^{2+}$ with H_2O_2) which is similar to that of the hydroxyl radical adduct of DMPO. In the presence of alcohols or in an acetone solvent we found evidence only for trapped hydroxyl or for a kinetically determined distribution of hydroxyl and the radical formed by hydrogen atom abstraction from the solvent.

Finally, we have also investigated the $\text{Ru}(\text{NH}_3)_6^{2+}/\text{ClO}_4^-$ reaction reported by Endicott and Taube, and thought to involve O-atom transfer [Endicott, J. F.; Taube, H. *Inorg. Chem.* 1965, 4, 437; Taube, H., "Electron Transfer Reactions of Complex Ions in Solution," Academic Press: New York, 1970]. In this experiment we were unable to trap any radical. So, presumably, the radical pathway is blocked and only the Ru(IV) pathway is involved (Scheme II).

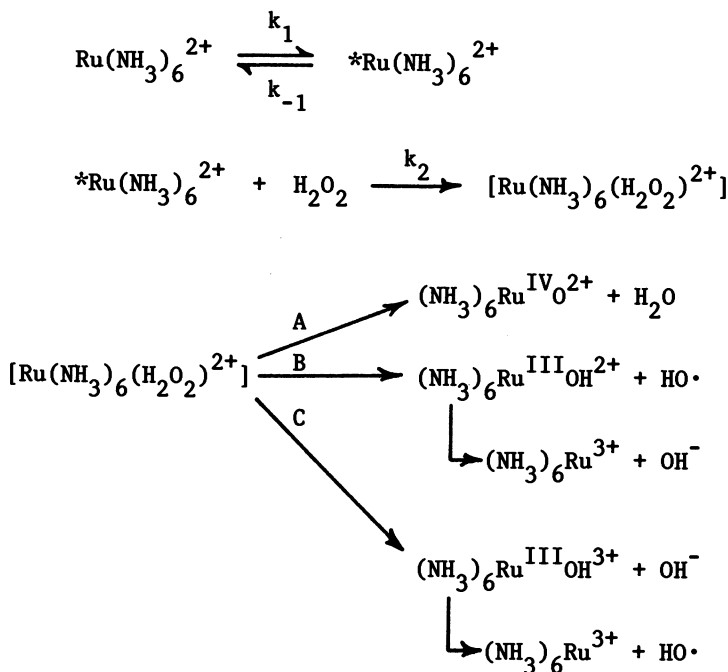
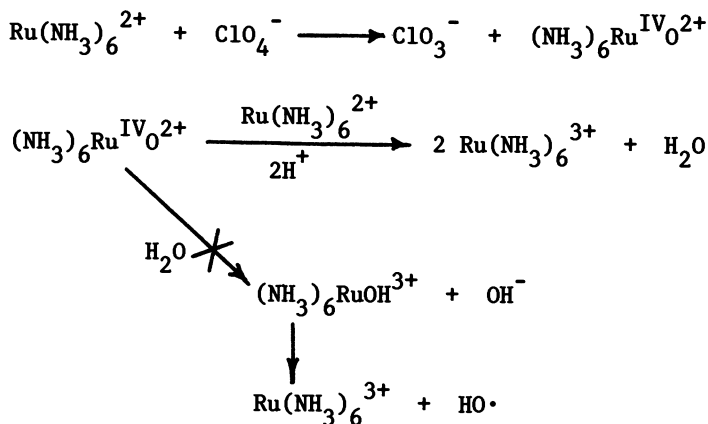
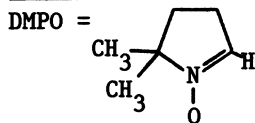
Scheme IScheme II

Table II
Results of Radical Trapping Studies

Substrate	H ₂ O ₂ ⁺ Reagent	A _N (Gauss)	A _H (Gauss)	DMPO Radical Trapped
H ₂ O	Fe	15.07	15.07	HO·
	Ti	15.1	15.1	(15.3, 15.3)*
	Ru	15.05	15.05	
CH ₃ OH	Fe	16.0	22.7	HOCH ₂ ·
	Ti	16.4	22.6	(14.7, 20.7)*
	Ru	16.2	23.2	
CH ₃ CH ₂ OH	Fe	16.0	22.8	CH ₃ ĊHOH
	Ti	16.2	23.1	(15.0, 22.5)*
	Ru	16.5	23.9	
(CH ₃) ₃ COH	Fe	16.5 [15.0]	24.1 [15.0] ‡	·CH ₂ C(CH ₃) ₂ OH HO· ²
(CH ₃) ₂ CO	Fe	15.0	15.0	HO·
	Ti	15.0 [16.1]	15.0 [23.8]	HO· ·CH ₂ CO(CH ₃)
	Ru	15.0 [16.5]	15.0 [23.8]	HO· ·CH ₂ CO(CH ₃)
	O ₂ +Ru	15.0	15.0	HO·



‡ [] - Denotes minor species,

* Janzen, E.; Liu, F. *J. Mag. Res.*, 1973, **9**, 510 (Values in benzene)

Some Comparisons Between the Energetics of Electrochemical and Homogeneous Electron-Transfer Reactions

MICHAEL J. WEAVER and JOSEPH T. HUPP

Michigan State University, Department of Chemistry, East Lansing, MI 48824

Some conceptual relationships between the kinetics of corresponding electrochemical and homogeneous redox processes are discussed and applied to experimental data for suitable outer-sphere reactions in order to illustrate the utility of electrochemical kinetics for gaining some fundamental insights into the energetics of electron-transfer processes. It is pointed out that electrochemical kinetic and thermodynamic measurements, as a function of temperature and electrode potential, yield direct information on the shapes of the potential-energy surfaces and free energy barriers for individual redox couples. Comparisons between kinetic parameters for corresponding electrochemical and homogeneous exchange reactions show reasonable agreement with the predictions of the conventional "weak overlap" model for several aquo redox couples, but exhibit substantial disagreement for couples containing amines and related ligands. These latter discrepancies may arise from the closer approach of the amine reactants to the electrode surface compared with the strongly solvated aquo complexes. A comparison is also made between the effects of varying the thermodynamic driving force upon the kinetics of related electrochemical and homogeneous reactions. It is shown that the apparent discrepancies seen between the predictions of the harmonic oscillator model and experimental data for some highly exoergic homogeneous reactions may be related to the anomalously small dependence of the rate constant upon overpotential observed for the electrooxidation of aquo complexes. This behavior seems most likely to be due

0097-6156/82/0198-0181\$09.00/0
© 1982 American Chemical Society

to a marked asymmetry of the reactant and product free energy barriers for these half reactions.

The kinetics of inorganic electrode reactions have long been the subject of experimental study. The advances in methodology, both in the precise treatment of mass transfer effects and the evolution of electrochemical relaxation techniques, have allowed the kinetics of a wide variety of electrode reactions to be studied. In addition, double-layer structural data are becoming available for a wide range of metal-electrolyte interfaces, which is enabling the kinetics of electrode reactions to be explored quantitatively in a variety of interfacial environments. However, electrode kinetics is a relatively underdeveloped area in comparison with homogeneous redox kinetics, not only in terms of the availability of accurate kinetic data but also in the degree of molecular interpretation.

Nevertheless, simple electrochemical processes of the type



where both Ox and Red are solution species, form a valuable class of reactions with which to study some fundamental features of electron transfer in condensed media. Such processes involve the activation of only a single redox center, and the free energy driving force can be continuously varied at a given temperature simply by altering the metal-solution potential difference, ϕ_m , by means of an external potential source. In addition, electrode surfaces may exert only a weak electrostatic influence upon the energy state of the reacting species, so that in some cases they could provide a good approximation to the "outer-sphere, weak overlap" limit described by conventional electron-transfer theory. The study of electrochemical kinetics, therefore, provides a unique opportunity to examine separately the reaction energetics of individual redox couples ("half-reactions") which can only be studied in tandem in homogeneous solution. In this paper, some relationships between the kinetics of heterogeneous and homogeneous redox processes are explored in order to illustrate the utility of electrochemical kinetics and thermodynamics for gaining fundamental insights into the energetics of outer-sphere electron transfer.

Electrochemical Rate Formulations

Similar to homogeneous electron-transfer processes, one can consider the observed electrochemical rate constant, k_{ob} , to be related to the electrochemical free energy of reorganization for the elementary electron-transfer step, ΔG^\ddagger , by

$$k_{ob} = A \exp(-w_p) \exp(-\Delta G^*/RT) \quad (2)$$

where A is a frequency factor, and w_p is the work required to transport the reactant from the bulk solution to a site sufficiently close to the electrode surface ("precursor" or "pre-electrode" state) so that thermal reorganization of the appropriate nuclear coordinates can result in electron transfer. Also, for one-electron electroreduction reactions [eq 1] ΔG^* can usefully be separated into "intrinsic" and "thermodynamic" contributions according to (1-3)

$$\Delta G^* = \Delta G_{ie}^* + \alpha [F(E - E^\circ) + w_s - w_p] \quad (3)$$

where E is the electrode potential at which k_{ob} is measured, E° is the standard (or formal) potential for the redox couple concerned, w_s is the work required to transport the product from the bulk solution to the "successor" state which is formed immediately following electron transfer, α is the (work-corrected) electrochemical transfer coefficient, and ΔG_{ie}^* is the "intrinsic" free energy of activation for electrochemical exchange (3). This last term equals ΔG^* for the particular case when the precursor and successor states have equal energies, i.e., when the free energy driving force for the elementary reaction $[F(E - E^\circ) + w_s - w_p]$ equals zero. The electrochemical transfer coefficient, α , reflects the extent to which ΔG^* is altered when this driving force is nonzero; α therefore provides valuable information on the symmetry properties of the elementary electron-transfer barrier (4).

It is conventional (and useful) to define a "work-corrected" rate constant k_{corr} that is related to k_{ob} at a given electrode potential by

$$k_{corr} = k_{ob} \exp \{ [w_p + \alpha(w_s - w_p)]/RT \} \quad (4)$$

This represents the value of k_{ob} that (hypothetically) would be obtained at the same electrode potential if the work terms w_p and w_s both equalled zero. For outer-sphere reactions, the work terms can be calculated approximately from a knowledge of the average potential on the reaction plane ϕ_{rp} , since $w_p = ZF\phi_{rp}$ and $w_s = (Z - 1)F\phi_{rp}$, where Z is the reactant's charge number. Eq 4 can then be written as

$$k_{corr} = k_{ob} \exp \{ [(Z - \alpha)F\phi_{rp}]/RT \} \quad (5)$$

Usually ϕ_{rp} is identified with the average potential across the diffuse layer ϕ_d^{GC} as calculated from Gouy-Chapman theory using the diffuse-layer charge density obtained from thermodynamic data. In view of the usefulness of k_{corr} , it is also convenient to define a "work-corrected" free energy of activation ΔG_e^* at a given electrode potential, which is related to k_{corr} by [cf. eq 2]:

$$k_{corr} = A \exp(-\Delta G_e^*/RT) \quad (6)$$

so that eq 3 can be written simply as

$$\Delta G_e^* = \Delta G_{ie}^* + \alpha F(E - E^0) \quad (7)$$

Therefore the value of k_{corr} measured at E^0 , i.e., the "standard" rate constant, k_{corr}^S , is directly related to the intrinsic barrier ΔG_{ie}^* .

In addition, temperature derivatives of k_{corr} can be measured which allows the enthalpic and entropic components of ΔG_e^* to be obtained. Here an apparent difficulty arises in that a multitude of different Arrhenius plots may be obtained for an electrochemical reaction at a given electrode potential (inevitably measured with respect to some reference electrode), depending upon the manner in which the electrical variable is controlled as the temperature is varied. However, two types of electrochemical activation parameters provide particularly useful information (5-8). The first type, which have been labelled "real" activation parameters (ΔH_r^* , ΔS_r^*) (5, 6), are extracted from an Arrhenius plot of k_{corr}^S as a function of temperature. The significance of these quantities is analogous to that for the activation parameters for homogeneous self-exchange reactions. Thus, ΔH_r^* equals the activation enthalpy for conditions where the enthalpic driving force, ΔH_{rc}^0 , for the electrochemical reaction 1 equals zero. Similarly, ΔS_r^* equals the activation entropy for the (albeit hypothetical) circumstance where the entropic driving force ΔS_{rc}^0 (the "reaction entropy" (9)) is zero (6). The quantities ΔH_r^* and ΔS_r^* are, therefore, equal to the "intrinsic" enthalpic and entropic barriers, ΔH_{ie}^* and ΔS_{ie}^* , respectively, which together constitute the intrinsic free energy barrier, ΔG_{ie}^* . However, although the activation free energy ΔG_e^* , determined at E^0 , will equal ΔG_{ie}^* [eq 7], the enthal-

pic and entropic barriers at E° , ΔH_e^* and ΔS_e^* , will differ from ΔH_{ie}^* and ΔS_{ie}^* . This is because, at E° , generally $\Delta S_{rc}^\circ \neq 0$ (9), and since $\Delta H_{rc}^\circ = T\Delta S_{rc}^\circ$, then also $\Delta H_{rc}^\circ \neq 0$.

Reasonable estimates of ΔH_e^* and ΔS_e^* at a given electrode potential can be obtained from an Arrhenius plot measured at the required electrode potential held constant at all temperatures using a "nonisothermal cell" arrangement with the reference electrode compartment maintained at a fixed temperature (8). These quantities, which have been termed "ideal" activation parameters ΔH_i^* and ΔS_i^* , can be identified with ΔH_e^* and ΔS_e^* since the use of such a nonisothermal cell maintains the Galvani metal-solution potential difference, ϕ_m , and, hence, the energy of the reacting electron, essentially constant as the temperature is varied (8, 9).

Similarly, the reaction entropy, ΔS_{rc}° , for a given redox couple can be determined from the temperature derivative of the standard potential, E_{ni}° , measured using a nonisothermal cell, i.e., $\Delta S_{rc}^\circ = F(dE_{ni}^\circ/dT)$, since (dE_{ni}°/dT) should approximately equal the desired temperature dependence of the standard Galvani potential, $(d\phi_m^\circ/dT)$ (9). The reaction entropy provides a useful measure of the changes in the extent of solvent polarization for a single redox couple brought about by electron transfer (9). Since $\Delta G_{rc}^\circ = F(E - E^\circ)$, the corresponding enthalpic driving force, ΔH_{rc}° , for the electrode reaction can be found from $\Delta H_{rc}^\circ = F(E - E^\circ) + T\Delta S_{rc}^\circ$. It is simple to show that the corresponding values of ΔH_i^* and ΔH_r^* , and ΔS_i^* and ΔS_r^* at a given electrode potential are related by (6)

$$\Delta H_i^* = \Delta H_r^* + \alpha T\Delta S_{rc}^\circ \quad (8)$$

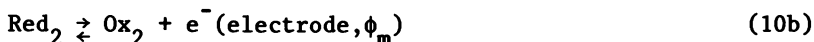
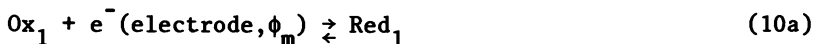
and

$$\Delta S_i^* = \Delta S_r^* + \alpha \Delta S_{rc}^\circ \quad (9)$$

Consequently, a wealth of information on the energetics of electron transfer for individual redox couples ("half-reactions") can be extracted from measurements of reversible cell potentials and electrochemical rate constant-overpotential relationships, both studied as a function of temperature. Such electrochemical measurements can, therefore, provide information on the contributions of each redox couple to the energetics of the bimolecular homogeneous reactions which is unobtainable from ordinary chemical thermodynamic and kinetic measurements.

Relationship Between Electrochemical and Homogeneous Reaction Energetics

Consider the following pair of electrochemical reduction and oxidation reactions



and the corresponding homogeneous cross reaction



Providing that the interactions between the reactant and the electrode in the electrochemical transition state, and between the two reactants in the homogeneous transition state, are negligible ("weak overlap" limit), the activation barriers for reactions 10 and 11 will be closely related.

At a given value of ϕ_m (and, hence, electrode potential E), the thermodynamics of reactions 10 and 11 are identical since the energy required to transport the electron across the metal-solution interface in the half reactions 10a and 10b will then cancel. The overall activation free energy, $\Delta G_{h,12}^*$, for reaction 11 can be considered to consist of separate contributions, $\Delta G_{h,1}^*$ and $\Delta G_{h,2}^*$, arising from the activation of Ox and Red, respectively. Although a multitude of different transition-state structures may be formed, corresponding to different individual values of $\Delta G_{h,1}^*$ and $\Delta G_{h,2}^*$, the predominant reaction channel will be that corresponding to a minimum in the activation free energy, $(\Delta G_{h,1}^* + \Delta G_{h,2}^*)_{\min}$ (10). In the "weak overlap" limit, each pair of values of $\Delta G_{h,1}^*$ and $\Delta G_{h,2}^*$ satisfying the thermodynamic constraints of reaction 11 will be identical to the corresponding pair of electrochemical free energies of activation, $\Delta G_{e,1}^*$ and $\Delta G_{e,2}^*$, for reactions 10a and 10b, respectively, having the same transition-state structures. Therefore the energetics of reactions 10 and 11 are related in the "weak overlap" limit by

$$(\Delta G_{e,1}^* + \Delta G_{e,2}^*)_{\min}^E = (\Delta G_{h,1}^* + \Delta G_{h,2}^*)_{\min} = \Delta G_{h,12}^* \quad (12)$$

where $(\Delta G_{e,1}^* + \Delta G_{e,2}^*)_{\min}^E$ refers to the particular electrode potential where the sum of $\Delta G_{e,1}^*$ and $\Delta G_{e,2}^*$ is a minimum. Only the sum $(\Delta G_{h,1}^* + \Delta G_{h,2}^*)_{\min}$ can be determined experimentally for a given homogeneous reaction. In contrast, the values of

$\Delta G_{e,1}^*$ and $\Delta G_{e,2}^*$ may be examined individually as a function of the free energy driving forces, ΔG_1^0 and ΔG_2^0 , for these two half reactions, 10a and 10b, which equal $F(E - E_1^0)$ and $F(E - E_2^0)$, respectively, where E_1^0 and E_2^0 are the corresponding standard electrode potentials.

This relationship is illustrated schematically in Figure 1. Curves 11' and 22' represent plots of ΔG_e^* against the reaction free energy $F(E - E^0)$ for a pair of cathodic and anodic half reactions on a common scale of electrode potential FE ; such curves are generally expected to be curved in the manner shown (vide infra) so that a shallow minimum in the plot of $(\Delta G_{e,1}^* + \Delta G_{e,2}^*)$ versus FE will be obtained. In practice, unless ΔG_e^* is small ($\lesssim 3-4$ kcal mol⁻¹), the slopes of these plots, i.e., the cathodic and anodic transfer coefficients, are often to be found to be equal and close to 0.5 so that to a good approximation (11,12)

$$2\Delta G_{e,12}^* = \Delta G_{h,12}^* \quad (13)$$

where $\Delta G_{e,12}^*$ is the value of ΔG_e^* at the intersection of the $(\Delta G_{e,1}^* - E)$ and $(\Delta G_{e,2}^* - E)$ plots. [A previous claim (11) that eq 13 is applicable in the "weak overlap" limit when $\Delta G_{e,1}^*$ and $\Delta G_{e,2}^*$ exhibit a quadratic dependence upon $(E - E^0)$ (1) is not entirely correct. The energy minimization condition $\{\partial(\Delta G_{e,1}^* + \Delta G_{e,2}^*)/\partial\beta = 0\}$ employed in the appendix of ref. 11 leads to eq 12, eq 13 only being obtained as a special case when the slopes of the $(\Delta G_{e,1}^* - E)$ and $(\Delta G_{e,2}^* - E)$ plots are equal but of opposite sign at the intersection point].

For the special case where the cathodic and anodic half-reactions are identical, since the two plots of $\Delta G_e^* - E$ must intersect at E^0 for the redox couple, then eq 13 can be written in terms of the electrochemical and homogeneous intrinsic barriers:

$$2\Delta G_{ie}^* = \Delta G_{ih}^* \quad (14)$$

Relationships having the same form as eq 14 can also be written for the enthalpic and entropic contributions to the intrinsic free energy barriers (10). Provided that the reactions are adiabatic and the conventional collision model applies, eq 14 can be written in the familiar form relating the rate constants of electrochemical exchange and homogeneous self-exchange reactions (13):

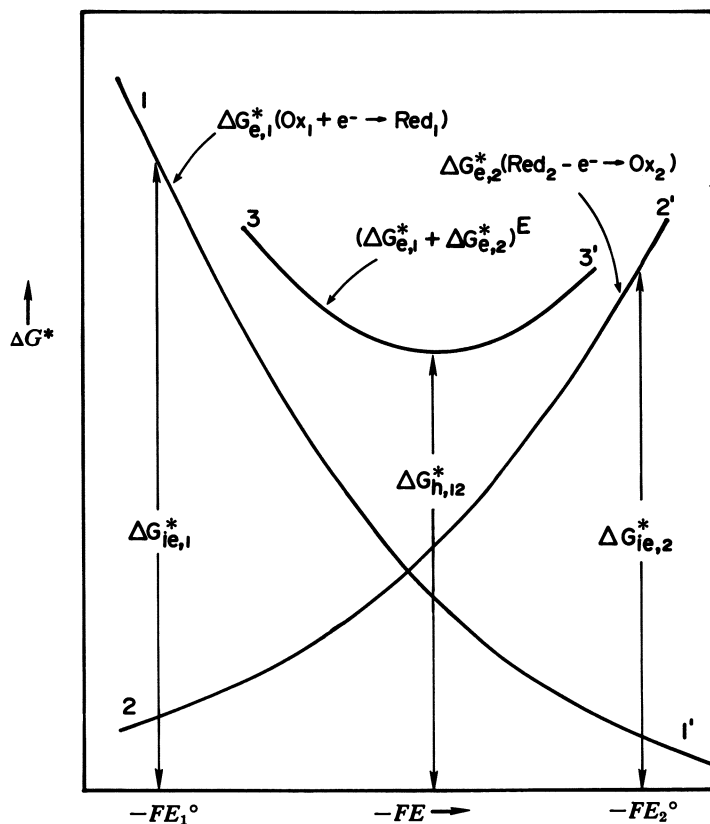


Figure 1. Schematic illustration of the general relationship between electrochemical and homogeneous redox reaction energetics. Curve 1-1' is a plot of activation free energy, ΔG_e^* , vs. thermodynamic driving force, $-FE$, for an electroreduction [$\Delta G_{e,1}(Ox_1 + e^- \rightarrow Red_1)$] reaction; and Curve 2-2' is a plot of ΔG_e^* vs. $-FE$ for an electrooxidation [$\Delta G_{e,2}(Red_2 - e^- \rightarrow Ox_2)$] reaction (Reactions 10a and 10b, respectively). E_1° and E_2° are the standard electrode potentials for these two redox couples. Curve 3-3' is formed by the sum $(\Delta G_{e,1}^* + \Delta G_{e,2}^*)^E$. The corresponding homogeneous activation barrier, $\Delta G_{h,12}^*$, is, in the "weak over-lap" limit, given by the minimum in this curve (Eq. 12).

$$\frac{(k_{\text{corr}}^{\text{s}})^2}{(Z_{\text{e}})^2} = \frac{k_{\text{corr}}^{\text{h,ex}}}{Z_{\text{h}}} \quad (15)$$

where $k_{\text{corr}}^{\text{h,ex}}$ is the (work-corrected) rate constant for homogeneous self exchange, and Z_{e} and Z_{h} are the electrochemical and homogeneous collision frequencies, respectively.

In the following sections, we shall explore the applicability of such relationships to experimental data for some simple outer-sphere reactions involving transition-metal complexes. In keeping with the distinction between intrinsic and thermodynamic barriers [eq 7], exchange reactions will be considered first, followed by a comparison of driving force effects for related electrochemical and homogeneous reactions.

Electron Exchange

Tables I and II contain electrochemical kinetic and related thermodynamic parameters for several transition-metal redox couples gathered at the mercury-aqueous interface. These systems were selected since the kinetics can be measured accurately under experimental conditions where the diffuse-layer potentials, ϕ_{d} , are small and/or could be estimated with confidence, yielding trustworthy estimates of $k_{\text{corr}}^{\text{s}}$ from the observed values, k_{ob}^{s} [eq 5]. (Details are given in refs 11 and 14.)

Also, the observed rates probably refer to outer-sphere pathways, and the rate constants for the corresponding homogeneous self-exchange reactions are available or can be estimated from rate data for closely related cross reactions (15). These latter values, $k_{\text{corr}}^{\text{h,ex}}$, which are also corrected for electrostatic work terms (15), are given alongside in Table I for comparison. Also included are estimates of $k_{\text{corr}}^{\text{h,ex}}$, $k_{\text{corr}}^{\text{h,ex}}(\text{calc})$, that were obtained from the corresponding values of $k_{\text{corr}}^{\text{s}}$ using eq 15.

[Values of $5 \times 10^3 \text{ cm s}^{-1}$ and $2 \times 10^{11} \text{ M}^{-1} \text{ s}^{-1}$ were employed for Z_{e} and Z_{h} , respectively, appropriate for a "typical" reactant mass of 200 and radius 3.5\AA . The estimate of Z_{h} given in refs 11 and 15 ($6 \times 10^{10} \text{ M}^{-1} \text{ s}^{-1}$) is incorrect due to calculational error.]

It is seen that the values of $k_{\text{corr}}^{\text{h,ex}}$ for the five aquo couples in Table I are uniformly larger than the corresponding

Table I
 Rate Constants and Thermodynamic Parameters for Selected Electrochemical Exchange
 and Homogeneous Self-Exchange Reactions at 25°C.

Redox Couple	E^f ^a mV vs. s.c.e.	ΔS_{rc}° ^b cal deg ⁻¹ mol ⁻¹	k_{corr}^s ^c cm s ⁻¹	$k_{corr}^{h,ex}$ ^d M ⁻¹ s ⁻¹	$k_{corr}^{h,ex}$ ^e (calc) M ⁻¹ s ⁻¹
Ru(OH ₂) ₆ ^{3+/2+}	-15 (0.3)	36	2 x 10 ⁻²	200	3
V(OH ₂) ₆ ^{3+/2+}	-475 (0.2)	37	1 x 10 ⁻³	3 x 10 ⁻²	8 x 10 ⁻³
Fe(OH ₂) ₆ ^{3+/2+}	500 (0.2)	43	~1 x 10 ⁻⁴	15	8 x 10 ⁻⁵
Eu(OH ₂) ₆ ^{3+/2+}	-625 (0.2)	48	8 x 10 ⁻⁵	4 x 10 ⁻⁴	5 x 10 ⁻⁵
Cr(OH) ₆ ^{3+/2+}	-660 (1)	49	2 x 10 ⁻⁶	2 x 10 ⁻⁶	3 x 10 ⁻⁸
Ru(NH ₃) ₆ ^{3+/2+}	-180 (0.2)	18	>10	5 x 10 ⁴	>8 x 10 ⁵
Co(en) ₃ ^{3+/2+} ^j	-460 (1)	37	5 x 10 ⁻² ^f	2.5 x 10 ⁻⁴	20
Co(bpy) ₃ ^{3+/2+} ^k	70 (0.05)	22	~5 x 10 ⁻⁴ ^f	~80	2 x 10 ⁻³
Co(EDTA) ^{-/2-}	135 (0.5) ⁱ	-8	~5 x 10 ⁻² ^g	~1 x 10 ⁻⁶ ^h	20

Notes to Table I

- ^a Formal potential of redox couple, determined at ionic strength noted in parentheses. Data from ref. 9 unless otherwise indicated.
- ^b Reaction entropy of redox couple, determined at same ionic strength as E^f . Data from ref. 9 unless otherwise indicated.
- ^c Standard rate constant for redox couple measured in 0.1-0.4 M KPF_6 and/or $NaClO_4$ supporting electrolytes, corrected for electrostatic double-layer effect using eq. 5 assuming that $\phi_{rp} = \phi_d^{GC}$. Kinetic data from ref. 11 unless otherwise stated.
- ^d Rate constant for homogeneous self exchange, corrected for electrostatic work terms using Debye-Hückel-Bronsted model. Data taken from sources quoted in ref. 15 unless otherwise stated.
- ^e Rate constant for homogeneous self exchange, calculated from corresponding value of k_{corr}^s using eq. 14, assuming that $Z_e = 5 \times 10^3 \text{ cm s}^{-1}$, and $Z_h = 2 \times 10^{11} \text{ M}^{-1} \text{ s}^{-1}$ (see text).
- ^f Sahami, S.; Farmer, J.; Weaver, M. J., unpublished results.
- ^g Tanaka, N.; Yamada, A. *Electrochim. Acta*, 1969, 14, 491.
- ^h Quoted in R. G. Wilkins, R. E. Yelin, *Inorg. Chem.*, 1968, 7, 2667.
- ⁱ Yee, E. L.; Weaver, M. J., unpublished results.
- ^j en = ethylenediamine.
- ^k bpy = 2,2'-bipyridine.

Table II
Comparison between Experimental Reorganization Parameters
for some Electrochemical and Homogeneous Exchange Reactions

Redox Couple	<u>a</u> $2\Delta G_{ie}^*$ kcal mol ⁻¹	<u>b</u> $2\Delta H_{ie}^*$ kcal mol ⁻¹	<u>c</u> $2\Delta S_{ie}^*$ cal deg ⁻¹ mol ⁻¹	<u>d</u> ΔG_{ih} kcal mol ⁻¹	<u>e</u> ΔH_{ih}^* kcal mol ⁻¹	<u>f</u> ΔS_{ih}^* cal deg ⁻¹ mol ⁻¹
$V(OH_2)_6^{3+/2+}$	18.2	16.5	-5.5	17.5	13.0	-15
$Eu(OH_2)_6^{3+/2+}$	21.2	17.2	-9	20.0	~15.5	(-15)
$Cr(OH_2)_6^{3+/2+}$	25.6	23.4	-7.5	23.2	~18.5	(-15)
$Co(en)_3^{3+/2+}$	13.6	~0 g	-45	20.3	13.8	-22

a Twice the intrinsic electrochemical free energy of activation, obtained from value of k_{corr}^s at mercury-aqueous interface given in Table I using $\Delta G_{ie}^* = -RT \ln(k_{corr}^s/Z_e)$, where $Z_e = 5 \times 10^3 \text{ cm s}^{-1}$.

b Twice the intrinsic ("real") electrochemical enthalpy of activation, obtained from $H_{ie}^* = -R[d(\ln k_{corr}^s - \ln T^{1/2})/d(1/T)]$ (see text). See refs. 8 and 11 for original data, except where indicated.

c Twice the intrinsic ("real") electrochemical entropy of activation, obtained from $2T\Delta S_{ie}^* = 2\Delta H_{ie}^* - 2\Delta G_{ie}^*$.

d Intrinsic free energy of activation for homogeneous self-exchange, obtained from values of $k_{corr}^{h,ex}$ given in Table I using $\Delta G_{ih}^{h,ex} = -RT \ln(k_{corr}^{h,ex}/Z_h)$, where $Z_h = 2 \times 10^{11} \text{ M}^{-1} \text{ s}^{-1}$.

Notes to Table II Continued.

- e** Intrinsic enthalpy of activation for homogeneous self-exchange. Values for $V_{aq}^{3+/2+}$ and $Co(en)_3^{3+/2+}$ obtained experimentally (see ref. 15 for sources and calculational details). Values for $Eu_{aq}^{3+/2+}$ and $Cr^{3+/2+}$ obtained from ΔG_{ih}^* assuming that $\Delta S_{ih}^* = -15$ e.u.
- f** Intrinsic entropy of activation for homogeneous self-exchange. Values for $V_{aq}^{3+/2+}$ and $Co(en)_3^{3+/2+}$ obtained from $T\Delta S_{ih}^* = \Delta H_{ih}^* - \Delta G_{ih}^*$. Values in parentheses are estimates, based on the observation that $\Delta S_{ih}^* \sim -15$ e.u. for several related aquo redox couples (15).
- g** Farmer, J.; Weaver, M. J., unpublished results.

values of $k_{\text{corr}}^{\text{h,ex}}(\text{calc})$ by typically 1-2 orders of magnitude, although the value of $k_{\text{corr}}^{\text{h,ex}}$ for $\text{Fe}_{\text{aq}}^{3+/2+}$ (where "aq" denotes aquo ligands) is over 10^5 -fold larger than $k_{\text{corr}}^{\text{h,ex}}(\text{calc})$. Such discrepancies have been discussed previously (11). The most general derivation of eq 14 [and hence eq 15] involves the assumption that the stabilization of the electrochemical transition state resulting from the proximity of the reactant to the electrode surface will equal one half of the corresponding stabilization of the homogeneous transition state arising from the approach of the two reactants (13). In terms of the conventional model, this will occur when the distance R^{h} between the homogeneous reactants equals the distance R^{e} between the heterogeneous reactant and its electrostatic image in the electrode (13). The observation that $k_{12}^{\text{h,ex}} > k_{12}^{\text{h,ex}}(\text{calc})$, and, hence, $2\Delta G_{\text{ie}}^* > \Delta G_{\text{ih}}^*$, is expected for electrochemical outer-sphere reactions on this basis since the reactant plus coordinated ligands will be separated from the electrode surface by the "inner layer" of solvent molecules (i.e., the electrode's "coordination layer") so that generally $R^{\text{e}} > R^{\text{h}}$. From the rate responses for $\text{Cr}_{\text{aq}}^{3+}$ and $\text{Eu}_{\text{aq}}^{3+}$ reduction at the mercury-aqueous interface to systematic variations in the double-layer structure, it has been concluded that at least two, and possibly three, water molecules lie between the electrode surface and the metal cations in the transition state (16).

Additional insight can be obtained by comparing the electrochemical and homogeneous activation parameters. Table II contains values of $2\Delta G_{\text{ie}}^*$, $2\Delta H_{\text{ie}}^*$, and $2\Delta S_{\text{ie}}^*$ for three aquo couples [$\text{V}_{\text{aq}}^{3+/2+}$, $\text{Eu}_{\text{aq}}^{3+/2+}$, and $\text{Cr}_{\text{aq}}^{3+/2+}$] for which work term corrections can be reliably made as a function of temperature (8). The values of ΔG_{ie}^* were obtained from the corresponding values of $k_{\text{corr}}^{\text{S}}$ using eq 6, assuming that the frequency factor A equals Z_{e} ($5 \times 10^3 \text{ cm s}^{-1}$). The intrinsic enthalpies of activation ΔH_{ie}^* were obtained from the slope of a plot of $-\text{R}(\ln k_{\text{corr}}^{\text{S}} - \ln T^{3/2})$ versus $1/T$ (8) and the corresponding intrinsic entropies of activation ΔS_{ie}^* from $\Delta S_{\text{ie}}^* = (\Delta H_{\text{ie}}^* - \Delta G_{\text{ie}}^*)/T$. Table II also contains the intrinsic free energies (ΔG_{ih}^*), enthalpies (ΔH_{ih}^*), and entropies of activation (ΔS_{ih}^*) for the corresponding homogeneous self-exchange reactions. These were similarly obtained from the work-corrected homogeneous rate constants. (See ref 15 for calculational details and data sources.)

Comparison of the corresponding electrochemical and homogeneous reorganization parameters reveal that $2\Delta G_{ie}^* > \Delta G_{ih}^*$, which follows from the observation that $k_{corr}^{h,ex} > k_{corr}^{h,ex}(calc)$ [eq 14]. This inequality in free energies is paralleled by greater differences between $2\Delta H_{ie}^*$ and ΔH_{ih}^* , these being partially compensated by values of $2\Delta S_{ie}^*$ that are significantly less negative than ΔS_{ih}^* . The classical model of outer-sphere electron transfer predicts that both ΔS_{ie}^* and ΔS_{ih}^* should be close to zero (within ca. 1 eu) (11,17). Part, but probably not all, of the observed negative values of ΔS_{ie}^* can be ascribed to the influence of nuclear tunneling and nonadiabaticity (17); these factors may account entirely for the observed small negative values of ΔS_{ie}^* . The larger negative values of ΔS_{ih}^* may arise partly from the solvent ordering that probably attends the formation of the highly charged precursor complex from the separated cationic reactants (15). Nevertheless, by and large the relative values of the electrochemical and homogeneous reorganization parameters are reasonably close to the expectations of the weak overlap model (13). The observed differences are consistent with the anticipated smaller extent of the reactant-electrode interactions as compared with the homogeneous reactant-reactant interactions in the transition states for electron transfer.

The remaining four redox couples in Table I, containing amine and related ligands, exhibit values of $k_{corr}^{h,ex}$ that are very different from the corresponding electrochemical estimates $k_{corr}^{h,ex}(calc)$. Similar discrepancies between the experimental results and the predictions of eq 15 have been observed previously (18-20), although corrections for work terms have seldom been made. A puzzling feature of these data is the relatively small variation in k_{corr}^s and hence $k_{corr}^{h,ex}(calc)$ for the three Co(III)/(II) couples compared with $k_{corr}^{h,ex}$. These discrepancies may arise from differences in electronic transmission coefficients at the electrode surface and in the bulk solution (18), from additional contributions to the work terms not considered in the Debye-Hückel and/or Gouy-Chapman models, or from unexpected differences in the outer-shell reorganization energies in the surface and bulk environments (11).

Electrochemical and homogeneous reorganization parameters for $Co(en)_3^{3+/2+}$ are also given in Table II. The large disparity between the electrochemical and homogenous parameters is high-

lighted by a value of ΔH_{ie}^* that is close to zero. Since the inner-shell contribution to ΔH_{ie}^* is undoubtedly large (≈ 5 kcal mol⁻¹), this result indicates that the electrode is markedly influencing the transition-state structure. We have also obtained comparable electrochemical reorganization parameters for the $\text{Co}(\text{NH}_3)_6^{3+/2+}$ couple. Since there is strong evidence that ammine complexes can approach the electrode surface more closely than the more strongly solvated aquo complexes (16), it seems likely that this unexpected electrochemical behavior of $\text{Co}(\text{en})_3^{3+/2+}$ arises from a specific influence of the interfacial environment.

Influence of the Thermodynamic Driving Force

Given that the reorganization parameters for electrochemical exchange of various aquo redox couples are in acceptable agreement with the corresponding homogeneous rate parameters on the basis of the weak overlap model, it is of interest to compare the manner in which the energetics of these two types of redox processes respond to the application of a net thermodynamic driving force.

For one-electron electrochemical reactions, the harmonic oscillator ("Marcus") model (21) yields the following predicted dependence of ΔG_e^* upon the electrode potential:

$$\Delta G_e^* = \Delta G_{ie}^* \pm 0.5 F(E - E^\circ) + \frac{F(E - E^\circ)^2}{16\Delta G_{ie}^*} \quad (16)$$

where the plus/minus sign refers to reduction and oxidation reactions, respectively. The transfer coefficient α [eq 7] is, therefore, predicted to decrease linearly from 0.5 with increasing electrochemical driving force $\pm F(E - E^\circ)$. The derivation of eq 16 involves the assumption that the reactant and product free energy barriers are parabolic and have identical shapes, and that the reactions are adiabatic yet involve only a small "resonance splitting" of the free energy curves in the intersection region (21).

A number of experimental tests of eq 16 have been made for inorganic reactants (14, 22). Generally speaking, it has been found that, $\alpha \sim 0.5$ at small to moderate overpotentials, in agreement with eq 16. Tests of this relationship over sufficiently large ranges of overpotential, where the quadratic term becomes significant, are not numerous. A practical difficulty with multicharged redox couples is that the extent of the work term corrections is frequently sufficiently large to make the extraction of k_{corr} , and, hence, ΔG_e^* and α , from the observed

rate-potential behavior, fraught with uncertainty. However, we have recently obtained kinetic data for $\text{Cr}_{\text{aq}}^{2+}$, $\text{Eu}_{\text{aq}}^{2+}$ and $\text{V}_{\text{aq}}^{2+}$ electro-oxidation over wide ranges of anodic overpotential (up to 900 mv) under conditions where the electrostatic work terms are small (14). The anodic transfer coefficients, α_a , for all those reactions were found to decrease with increasing anodic overpotential, but to a greater extent than predicted by eq 16. This behavior contrasts that found for cathodic overpotentials, where the cathodic transfer coefficients α_c remain essentially constant at 0.5, even over regions of overpotential where detectable decreases in α_c are predicted by eq 16 (14, 23). These aquo redox couples, therefore, exhibit a markedly different overpotential dependence of the anodic and cathodic rate constants; this contrasts with the symmetrical dependence predicted by eq 16. An example of this behavior is shown in Figure 2 which is a plot of ΔG_e^* versus $(E - E^0)$ for $\text{Cr}_{\text{aq}}^{3+/2+}$ at the mercury-aqueous interface at both anodic and cathodic overpotentials. The solid curves are obtained from the experimental data and the dashed lines show the overpotential dependence of ΔG_e^* predicted from eq 16.

The prediction corresponding to eq 16 for driving force effects upon homogenous kinetics is (21)

$$\Delta G_{h,12}^* = \Delta G_{ih,12}^* + 0.5 \Delta G_{12}^0 + \frac{(\Delta G_{12}^0)^2}{16\Delta G_{ih,12}^*} \quad (17)$$

where $\Delta G_{ih,12}^*$ is the mean of the intrinsic barriers for the parent self-exchange reactions, $[0.5(\Delta G_{ih,1}^* + \Delta G_{ih,2}^*)]$, and ΔG_{12}^0 is the free energy driving force for the cross reaction. Equation 17 has been found to be in satisfactory agreement with experimental data for a number of outer-sphere cross reactions having small or moderate driving forces. However, there appear to be significant discrepancies for some reactions having large driving forces (where the last term in eq 17 becomes important) in that the rate constants do not increase with increasing driving force to the extent predicted by eq 17; i.e., the values of $\Delta G_{h,12}^*$ are larger than those calculated from the corresponding values of $\Delta G_{ih,12}^*$ and ΔG_{12}^0 using eq 17 (15, 24-26).

It has been suggested that these apparent discrepancies could be due to the values of $\Delta G_{h,12}^*$ and $\Delta G_{ih,12}^*$ that are obtained from the experimental work-corrected rate constants being incorrectly large due to nonadiabatic pathways (24-26), or to the presence of additional unfavorable work terms arising from

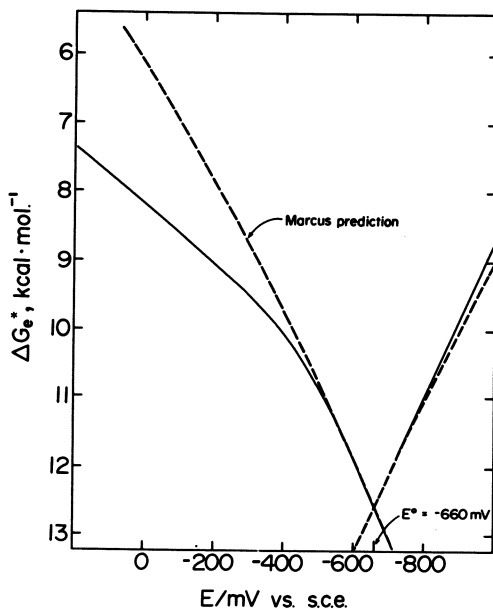


Figure 2. The electrochemical free energy of activation, ΔG_e^\ddagger , for $\text{Cr}(\text{OH})_2^{3+/2+}$ at the mercury–aqueous interface, plotted against the electrode potential for both anodic and cathodic overpotentials. Solid lines are obtained from the experimental rate constant–overpotential plot in Ref. 14, using Eq. 6 (assuming $A = 5 \times 10^8 \text{ cm} \cdot \text{s}^{-1}$). Dashed lines are the predictions from Eq. 16.

the solvent orientation required to form the highly charged precursor complex (15). An alternative, or additional, explanation is that the free energy barriers are anharmonic so that the quadratic driving force dependence of eq 17 is inappropriate. It is interesting to note that the form of the discrepancies between the kinetic data for the electrooxidation of aquo cations and eq 16, and between the homogeneous rate data and eq 17, is at least qualitatively similar in that both involve unexpectedly small dependencies of the rate constants upon the thermodynamic driving force. Moreover, the large majority of homogeneous reactions for which such discrepancies have been observed involve the oxidation of aquo cations (15, 24). However, nonadiabaticity effects cannot explain the asymmetry between the $(\Delta G_e^* - E)$ plots at anodic and cathodic overpotentials (Figure 2). Also, any specific work term effects should be different (and probably smaller) at the mercury-aqueous interface compared with homogeneous reactions between multicharged cations (11); yet any anharmonicity of the free energy barriers should be similar, at least on the basis of the weak overlap model. A quantitative comparison of the driving force dependence of the kinetics of related electrochemical and homogeneous reactions should, therefore, shed light on the causes of the observed discrepancies for the latter, more complicated processes.

One can generally express the free energy barriers, ΔG_e^* , for the pair of cathodic and anodic electrochemical reactions 10a and 10b as [cf., eqs 7 and 16]:

$$\Delta G_{e,1}^* = \Delta G_{ie,1}^* + \alpha_1 \Delta G_1^{\circ} \quad (18a)$$

and

$$\Delta G_{e,2}^* = \Delta G_{ie,2}^* + \alpha_2 \Delta G_2^{\circ} \quad (18b)$$

where α_1 and α_2 are the transfer coefficients for these two reactions at a given electrode potential. A similar relationship may be written for the free energy barrier, $\Delta G_{h,12}^*$, of the corresponding homogeneous cross reaction (11) [cf., eq 17]:

$$\Delta G_{h,12}^* = \Delta G_{ih,12}^* + \alpha_{12} \Delta G_{12}^{\circ} \quad (19)$$

where α_{12} is a "chemical" transfer coefficient. Although α_1 and α_2 are determined only by the shapes of the free energy barriers for the individual redox couples at a given driving force, α_{12} is a composite quantity which is determined not only by both α_1

and α_{12} but also by the relative magnitudes of $\Delta G_{ih,1}^*$, $\Delta G_{ih,2}^*$ and $\Delta G_{h,12}^*$.

Nevertheless, comparison of values of $\Delta G_{h,12}^*$ for a series of related cross reactions having systematically varying driving forces can yield useful information. Figure 3 is a plot of $\Delta G_{h,12}^*/\Delta G_{ih,12}^*$ versus $\Delta G_{12}^{\circ}/\Delta G_{ih,12}^*$ for a series of cross reactions involving the oxidation of various aquo complexes. (The values of ΔG_{12}^* and $\Delta G_{ih,12}^*$ were obtained from the measured homogeneous rate constants in the same way as the homogeneous free energies of activation given in Tables I and II. Details are given in ref. 15.) The graphical presentation in Figure 3 has the virtue that the values of $\Delta G_{h,12}^*$ for different cross reactions are normalized for variations in the intrinsic barriers $\Delta G_{ih,12}^*$; the driving force dependence of $\Delta G_{h,12}^*$ predicted by the Marcus model all fall on a common curve (shown as a solid line in Figure 3) when presented in this manner (27). [Omitted from Figure 3 are reactions involving $\text{Co}_{aq}^{3+/2+}$ since there is evidence that the measured self-exchange rate constant does not correspond to an outer-sphere pathway (28).] It is seen that the experimental points deviate systematically from the Marcus predictions in that the apparent values of α_{12} [eq 19] are significantly smaller than predicted from eq 17 at moderate to high driving forces. Figure 4 consists of the same plot as Figure 3 but for a number of outer-sphere cross reactions involving reductants other than aquo complexes (27). In contrast to Figure 3, reasonable agreement with the Marcus prediction is obtained (cf., ref. 27). The data in Figure 3 are also shown in Figure 5 as a plot of $[\Delta G_{12}^* - \Delta G_{i,12}^*]$ versus $-[0.5\Delta G_{12}^{\circ} + (\Delta G_{12}^{\circ})^2/16\Delta G_{i,12}^*]$. Since this plot is an expression of eq 17, the Marcus model predicts a slope of unity (the solid line in Figure 5). However, the experimental points (closed symbols) are almost uniformly clustered beneath this predicted line, and increasingly so as $-\Delta G_{12}^{\circ}$ increases, again indicating that α_{12} tends to be smaller than predicted.

It therefore seems feasible that these anomalously small values of α_{12} , noted from Figures 3 and 5, have their primary origin in the oxidation half-reactions which uniformly involve aquo complexes. This possibility was explored by converting the electrooxidation data into a form suitable for direct comparison with the homogeneous data in Figure 5 in the following manner. As noted above, the free energy barrier $\Delta G_{h,12}^*$ for each outer-sphere cross reaction will consist of contributions $\Delta G_{h,1}^*$ and

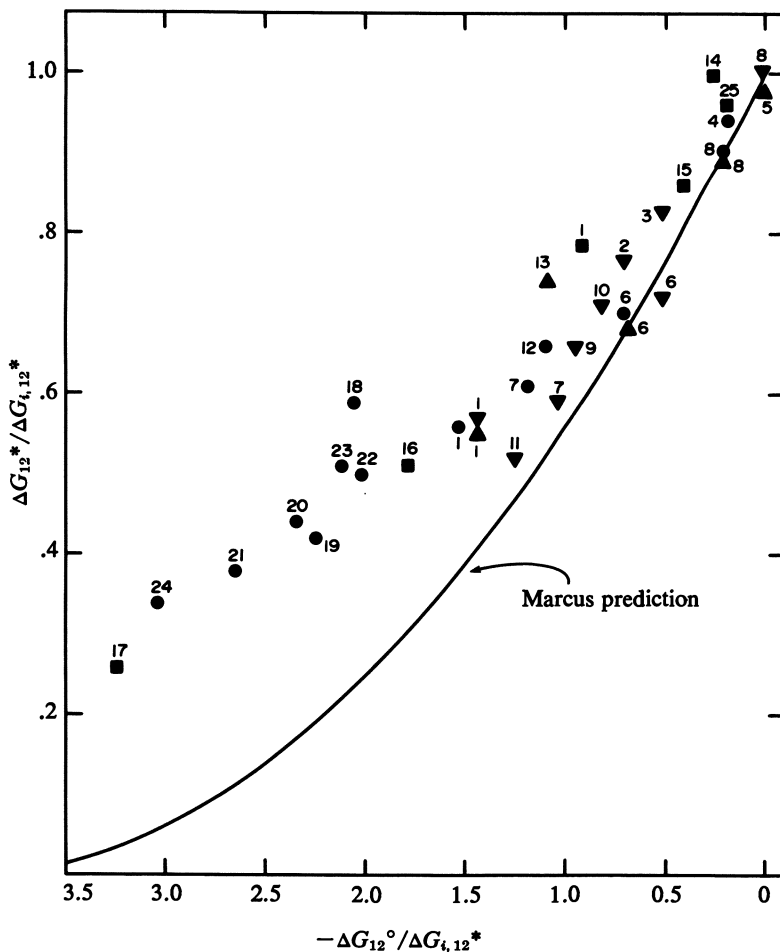


Figure 3. Plot of $\Delta G_{12}^*/\Delta G_{1,12}^*$ against $-\Delta G_{12}^\circ/\Delta G_{1,12}^*$ for homogeneous cross reactions involving oxidation of aquo cations. Reductants: ●, $\text{Eu}_{\text{aq}}^{2+}$; ▲, $\text{Cr}_{\text{aq}}^{2+}$; ▼, $\text{V}_{\text{aq}}^{2+}$; and ■, $\text{Ru}_{\text{aq}}^{2+}$. Key to oxidants and data sources: 1, $\text{Fe}_{\text{aq}}^{3+}$; 2, $\text{Ru}_{\text{aq}}^{3+}$; 3, $\text{Np}_{\text{aq}}^{4+}$; 4, $\text{V}_{\text{aq}}^{3+}$; 5, $\text{Eu}_{\text{aq}}^{3+}$; 6, $\text{Ru}(\text{NH}_3)_6^{3+}$; 7, $\text{Ru}(\text{NH}_3)_5\text{py}^{3+}$; 8, $\text{Co}(\text{en})_3^{3+}$; 9, $\text{Co}(\text{phen})_3^{3+}$; 10, $\text{Co}(\text{bpy})_3^{3+}$ (1–10 are from Ref. 15); 11, $\text{Ru}(\text{NH}_3)_5\text{isn}^{3+}$ (Ref. 25); 12, $\text{Co}(\text{phen})_3^{3+}$ (Ref. 24); 13, $\text{Co}(\text{phen})_3^{3+}$ (Ref. 32); 14 to 17 and 25 are from Ref. 33; 14, $\text{Co}(\text{phen})_3^{3+}$; 15, $\text{Ru}(\text{NH}_3)_5\text{isn}^{3+}$; 16, $\text{Os}(\text{bpy})_3^{3+}$; 17, $\text{Ru}(\text{bpy})_3^{3+}$; 18 to 22 are from Ref. 34; 18, $^*\text{Ru}[4,4'(\text{CH}_3)_2\text{bpy}]_3^{2+}$; 19, $^*\text{Ru}(\text{phen})_3^{2+}$; 20, $^*\text{Ru}(\text{bpy})_3^{2+}$; 21, $^*\text{Ru}(5\text{-Cl phen})_3^{2+}$; 22, $^*\text{Ru}[4,7\text{-}(\text{CH}_3)_2\text{phen}]_3^{2+}$; 23, $^*\text{Os}(5\text{-Cl phen})_3^{2+}$ (Ref. 35); 24, $\text{Ru}[4,7\text{-}(\text{CH}_3)_2\text{phen}]_3^{3+}$ (Ref. 36); 25, $\text{Ru}(\text{NH}_3)_5\text{py}^{3+}$. An asterisk (*) indicates the oxidant is a photoexcited state reactant.

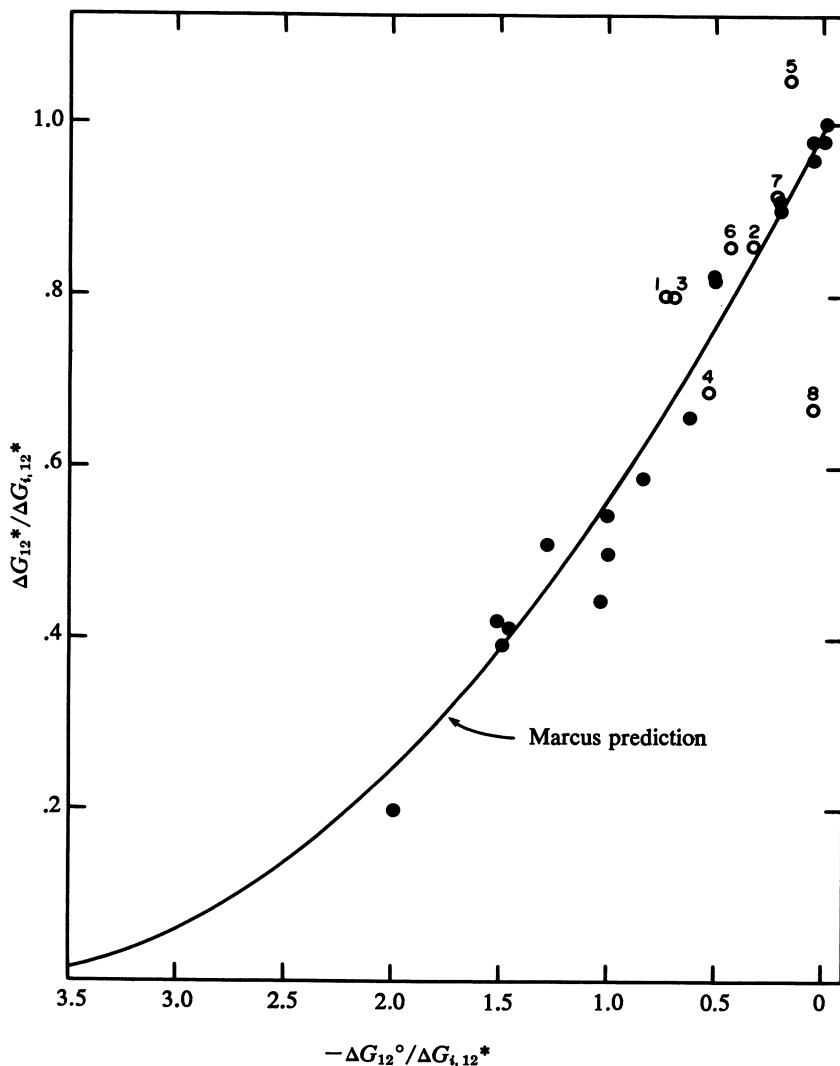


Figure 4. Plot as for Figure 3, but involving reductants other than aquo complexes. Key to reactions and data sources: ●, Co(III)/(II) macrocycle oxidants (data are given in Figures 2, 5, 6, and Ref. 27); ○, other nonaquo oxidants; 1, $\text{Ru}(\text{NH}_3)_5\text{py}^{3+} + \text{Ru}(\text{NH}_3)_6^{2+}$; 2, $\text{Ru}_{\text{aq}}^{3+} + \text{Ru}(\text{NH}_3)_6^{2+}$; 3, $\text{Co}(\text{phen})_3^{3+} + \text{Ru}(\text{NH}_3)_6^{2+}$; 4, $\text{Co}(\text{bpy})_3^{3+} + \text{Ru}(\text{NH}_3)_6^{2+}$; 5, $\text{Co}(\text{phen})_3^{3+} + \text{Ru}(\text{NH}_3)_5\text{py}^{2+}$ (1-N from Ref. 15); 6, horse heart ferricytochrome c + $\text{Ru}(\text{NH}_3)_6^{2+}$ (Ref. 37); 7, $\text{Co}(\text{phen})_3^{3+}$ + horse heart ferrocycytochrome c (Ref. 38); 8, $\text{Ru}(\text{NH}_3)_5\text{bpy}^{3+} + \text{Ru}(\text{NH}_3)_5\text{py}^{2+}$ (Ref. 24).

$\Delta G_{h,2}^*$ from the oxidant and reductant, respectively. In the "weak overlap" limit, $\Delta G_{h,1}^*$ and $\Delta G_{h,2}^*$ will equal the free energy barriers $\Delta G_{e,1}^*$ and $\Delta G_{e,2}^*$ for the corresponding electrochemical reactions at an electrode potential where the sum ($\Delta G_{e,1}^* + \Delta G_{e,2}^*$) is a minimum [eq 12 and Figure 1]. Estimates of $\Delta G_{h,2}^*$ for $\text{Eu}_{\text{aq}}^{2+}$, $\text{Cr}_{\text{aq}}^{2+}$, and $\text{V}_{\text{aq}}^{2+}$ oxidation as a function of the half-reaction driving force $\Delta G_2^\circ [= -F(E - E_2^\circ)]$ were obtained from the corresponding ($\Delta G_e^* - E$) plots (see Figure 2 and ref. 14) by assuming that they have the same shape but replacing the value of ΔG_e^* at $\Delta G_2^\circ = 0$ (i.e., ΔG_{ie}^*) by $0.5 \Delta G_{ih}^*$. [This procedure corrects for any differences between ΔG_{ie}^* and $0.5\Delta G_{ih}^*$ (Table II) resulting from the limitations of the weak overlap model (eq 14)]. The accompanying plots of $\Delta G_{h,1}^*$ versus ΔG_1° for the reduction half reactions involved in Figure 5 were constructed using the experimental value of $\Delta G_{ih,12}^*$ by assuming that the harmonic oscillator model applies, i.e., by utilizing eq 16 written for homogeneous half reactions:

$$\Delta G_{h,1}^* = 0.5 \Delta G_{ih,12}^* + 0.5 \Delta G_1^\circ + (\Delta G_1^\circ)^2 / 8 \Delta G_{ih,12}^* \quad (20)$$

These pairs of ($\Delta G_{h,1}^* - \Delta G_1^\circ$) and ($\Delta G_{h,2}^* - \Delta G_2^\circ$) curves were plotted on a common driving force (i.e., electrode potential) axis such that $(\Delta G_1^\circ - \Delta G_2^\circ) = \Delta G_{12}^\circ$, and the required estimates of $\Delta G_{h,12}^*$ for each cross reaction were then obtained from the sum ($\Delta G_{h,1}^\circ + \Delta G_{h,2}^\circ$) at the value of ΔG° where the quantity has a minimum value [eq 12]. These estimates of $\Delta G_{h,12}^*$ are plotted as open symbols in Figure 5 for the reactions having moderate to large driving forces ($-\Delta G_{12}^\circ > 8 \text{ kcal mol}^{-1}$), alongside the corresponding experimental values of $\Delta G_{h,12}^*$ (closed symbols). It is seen that the "electrochemical" estimates of values of $\Delta G_{h,12}^*$ diverge from the straight line predicted from the harmonic oscillator model to a similar, albeit slightly smaller, extent than the experimental values. Admittedly, there is no particular justification for assuming that the reduction half reactions obey the harmonic oscillator model. However, it turns out that the estimates of $\Delta G_{h,12}^*$ are relatively insensitive to alterations in the shapes of the ($\Delta G_{h,1}^* - \Delta G_1^\circ$) plots.

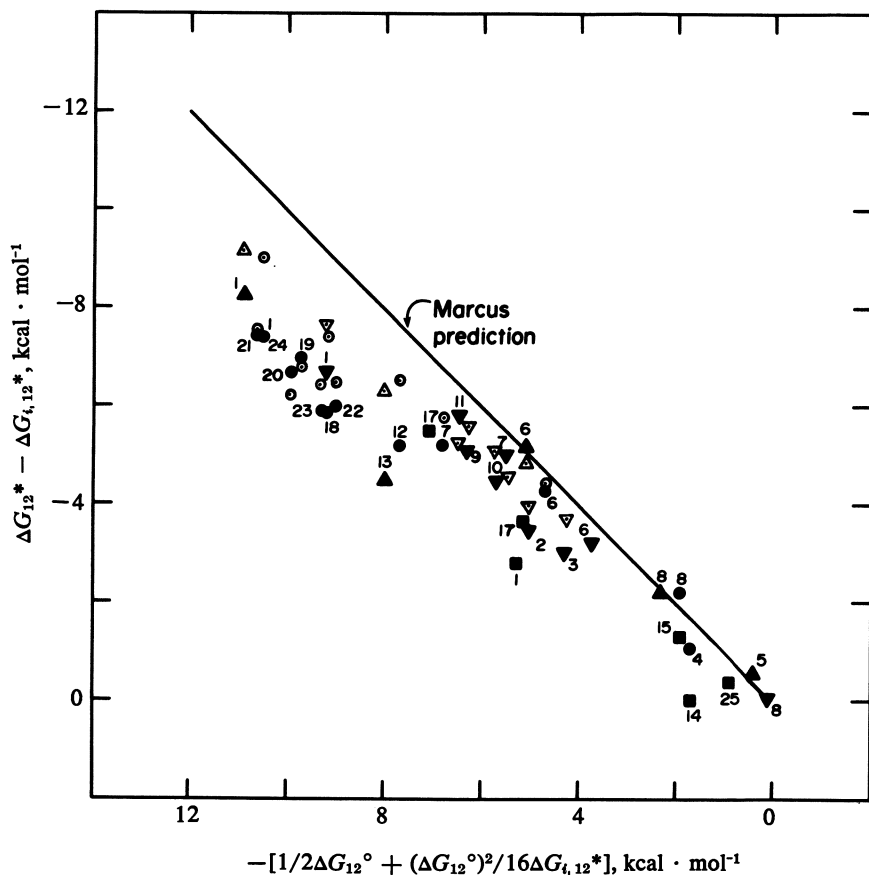


Figure 5. Plot of $(\Delta G_{12}^* - \Delta G_{1,12}^*)$ for homogeneous cross-reactions involving oxidation of aquo complexes given in Figure 3, against the thermodynamic driving force function $-[0.5\Delta G_{12}^\circ + (\Delta G_{12}^\circ)^2/16\Delta G_{1,12}^*]$. Closed symbols are obtained from homogeneous data; key to points as in Figure 3. Open symbols are corresponding points obtained from electrochemical kinetic data for oxidation of aquo cations. Reductants: ○ and ●, $\text{Eu}_{\text{aq}}^{2+}$; △ and ▲, $\text{Cr}_{\text{aq}}^{2+}$; ▽ and ▼, $\text{V}_{\text{aq}}^{2+}$; and ■, $\text{Ru}_{\text{aq}}^{2+}$.

It therefore seems reasonable that the deviations of the activation free energies for highly exoergic electrochemical and homogeneous reactions, illustrated in Figures 2 and 5, may arise partly from the same source, i.e., from values of α_2 for the oxidation half reactions that are unexpectedly small.² That is not to say that other factors are not responsible, at least in part, for these discrepancies. Nonadiabaticity, work terms, specific solvation, and other environmental effects may all play important roles depending on the reactants. For example, there is evidence to suggest that the true rate constant for outer-sphere $\text{Fe}_{\text{aq}}^{3+/2+}$ self-exchange is significantly smaller than the directly measured value (29); this can account for a good part of the unexpectedly slow rates of cross reactions involving this couple.

It remains to consider possible reasons for these apparent deficiencies of the harmonic oscillator model for the oxidation of aquo cations. Some discussion of the electrochemical results has been given previously (14). It was concluded that the most likely explanation for the observed disparities between the experimental results and the predictions of eq 16 (Figure 2) is that the reactant and product free energy barriers for the aquo redox couples have markedly different shapes. Such an asymmetry of the free energy barriers is unlikely to arise from inner-shell (metal-ligand vibrational) contributions, at least within the confines of a classical model. Thus, choosing even unreasonably large differences in vibrational force constants for the oxidized and reduced forms generates much smaller differences in the shapes of the resulting anodic and cathodic Tafel plots than are observed experimentally (Figure 2; also see 14). Indeed, such calculations performed for homogeneous reactions led to an earlier assertion that anharmonicity effects were unlikely to account for the extent of the observed breakdowns in the applicability of the Marcus cross relationship [eq 17] as exemplified in Figures 3 and 5 (24). A plausible, albeit somewhat inaccessible, source of asymmetry in the free energy barriers could lie in major differences in short-range solvent structure between the reduced and oxidized aquo complexes. There is strong evidence that tripositive aquo complexes induce extensive solvent ordering via field-assisted hydrogen bonding with the aquo ligands, which is partly dissipated upon reduction to the dipositive species (9, 30). This short-range reorientation of water molecules may well contribute unequally to the individual free energy curves for the oxidized and reduced species, thereby generating the required nonsymmetry. A related point is that the reactant and product potential-energy barriers will be highly nonsymmetrical even when the free-energy driving force, $\Delta G_{\text{rc}}^{\circ}$, is zero (i.e., at E°), as a result of the especially large positive values of $\Delta S_{\text{rc}}^{\circ}$ for the aquo redox couples (Table I). Thus,

the electrooxidation reactions will be highly exothermic ($-\Delta H_{rc}^{\circ} \approx 15 \text{ kcal mol}^{-1}$) even when $\Delta G_{rc}^{\circ} = 0$, and increasingly so at anodic overpotentials. In contrast, the electroreduction reactions are endothermic ($\Delta H_{rc}^{\circ} > 0$) within the entire overpotential range that is accessible to experiment.

Conclusions

It seems clear that kinetic as well as thermodynamic data gathered for simple electrode reactions can contribute significantly towards the development of our fundamental understanding of electron transfer in condensed media. In particular, detailed studies of electrochemical kinetics, with due regard for work term corrections, can yield information on the shapes of free energy barriers, and also their enthalpic and entropic components, that are largely inaccessible from studies of homogeneous redox kinetics. The former can provide a direct means of detecting deficiencies in the applicability of the harmonic oscillator model which forms the kernel of most contemporary treatments of electron transfer.

Experimental comparisons between the kinetics of related electrochemical and homogeneous reactions in suitable cases can also yield insights into the differences, as well as similarities, between these two major types of redox processes (3, 11, 31). Unfortunately, there is still a paucity of electrochemical kinetic data on substrates other than mercury. However, recent advances in the methods for preparing and characterizing clean metal surfaces, particularly for single crystals, should allow the acquisition of quantitative data for a much wider range of reactions and surface environments than hitherto available. It is hoped that a greater comparison of results for heterogeneous and homogeneous processes will occur in the future; this should be to the benefit of both areas.

Acknowledgements

We are grateful to Prof. John Endicott for sending us a copy of ref. 28 prior to publication. This work is supported in part by the Air Force Office of Scientific Research and the Office of Naval Research.

Literature Cited

1. Marcus, R. A. *J. Phys. Chem.* 1968, 72, 891.
2. Sutin, N. *Acct. Chem. Res.* 1968, 1, 225.
3. Weaver, M. J. *Inorg. Chem.* 1979, 18, 402.
4. Parsons, R. *Croat. Chim. Acta* 1970, 42, 281.
5. Temkin, M. *Zh. Fiz. Khim.* 1948, 22, 1081.

6. Weaver, M. J. J. Phys. Chem. 1976, 80, 2645.
7. Weaver, M. J. Israel J. Chem. 1979, 18, 35.
8. Weaver, M. J. J. Phys. Chem. 1979, 83, 1748.
9. Yee, E. L.; Cave, R. J.; Guyer, K. L.; Tyma, P. D.; Weaver, M. J. J. Am. Chem. Soc. 1979, 101, 1131.
10. Newton, T. W. J. Chem. Educ. 1968, 45, 571.
11. Weaver, M. J. J. Phys. Chem. 1980, 84, 568.
12. Weaver, M. J. Inorg. Chem. 1976, 15, 1733.
13. Marcus, R. A. J. Phys. Chem. 1963, 67, 853.
14. Tyma, P. D.; Weaver, M. J. J. Electroanal. Chem. 1980, 111, 195.
15. Weaver, M. J.; Yee, E. L. Inorg. Chem. 1980, 19, 1936.
16. Weaver, M. J.; Satterberg, T. L. J. Phys. Chem. 1977, 81, 1772.
17. Brunschwig, B. S.; Logan, J.; Newton, M. D.; Sutin, N. J. Am. Chem. Soc. 1980, 102, 5798.
18. Endicott, J. F.; Schroeder, R. R.; Chidester, D. H.; Ferrer, D. R. J. Phys. Chem. 1973, 77, 2579.
19. Saji, T.; Yamada, T.; Aoyagui, S. J. Electroanal. Chem. 1975, 61, 147.
20. Saji, T.; Mariyama, Y.; Aoyagui, S. J. Electroanal. Chem. 1978, 86, 219.
21. Marcus, R. A. J. Chem. Phys. 1965, 43, 679.
22. See ref. 14 for references to earlier work.
23. Weaver, M. J.; Anson, F. C. J. Phys. Chem. 1976, 80, 1861.
24. Chou, M.; Creutz, C.; Sutin, N. J. Am. Chem. Soc. 1977, 99, 5615.
25. Brown, G. M.; Krentzien, H. J.; Abe, M.; Taube, H. Inorg. Chem. 1979, 18, 3374.
26. Balzani, V.; Scandola, F.; Orlandi, G.; Sabbatini, N.; Indelli, M. T. J. Am. Chem. Soc. 1981, 103, 3370.
27. Endicott, J. F.; Durham, B.; Glick, M. D.; Anderson, T. J.; Kuszaj, J. M.; Schmonsees, W. G.; Balakrishnan, K. P. J. Am. Chem. Soc. 1981, 103, 1431.
28. Endicott, J. F.; Durham, B.; Kumar, K. Inorg. Chem. in press.
29. Hupp, J. T.; Weaver, M. J., to be submitted for publication.
30. Weaver, M. J.; Nettles, S. M. Inorg. Chem. 1980, 19, 1641.
31. For example, see Guyer, K. L.; Barr, S. W.; Cave, R. J.; Weaver, M. J., in "Proc. 3rd Symp. on Electrode Processes", Bruckenstein, S.; McIntyre, J. D. E.; Miller, B.; Yeager, E., Eds., Electrochemical Society: Princeton, NJ, 1980; p. 390.

32. Przystas, T.J.; Sutin, N. J. Am. Chem. Soc. 1973, 95, 5545.
33. Böttcher, W; Brown, G.M.; Sutin, N. Inorg. Chem. 1979, 18, 1447
34. Creutz, C. Inorg. Chem. 1978, 17, 1056.
35. Creutz, C.; Chow, M.; Netzel, T.L.; Okumura, M.; Sutin, N. J. Am. Chem. Soc. 1980, 102, 1309.
36. Lin, C.-T.; Böttcher, W.; Brown, G.M.; Creutz, C.; Sutin, N. J. Am. Chem. Soc. 1976, 98, 6536
37. Ewall, R.X.; Bennett, L.E. J. Am. Chem. Soc. 1974, 96, 940.
38. McArdle, J.V.; Gray, H.B.; Creutz, C.; Sutin, N. J. Am. Chem. Soc. 1974, 96, 5737.

RECEIVED April 21, 1982.

General Discussion—Some Comparisons Between the Energetics of Electrochemical and Homogeneous Electron-Transfer Reactions

Leader: Stephen Isied

DR. NOEL HUSH (University of Sydney): On the question of the correlation between the free energy of activation for the homogeneous and the heterogeneous processes (e.g., $\text{Fe}^{3+,2+}$), some years ago I suggested that there is probably an important difference between these processes [Hush, N. S. *Electrochim. Acta* 1968, **13**, 1004]. If one uses the model in which there is an outer-sphere contribution arising from the interaction with the dielectric and an inner-shell contribution due to vibrational modes, then it is reasonable to suppose that the inner-shell contribution for the homogeneous process will be twice that for the corresponding heterogeneous reaction. However, such a relationship need not necessarily hold for the remaining terms. When we bring two ions together to separation R in the homogeneous case, we have a term proportional to $-1/R$ in the free energy of activation, which reduces the dielectric interaction energy. But in the case of reaction at a metallic electrode, an analogous term will be present only if there is an appreciable image effect.

My conclusion (based on double-layer theory) was that, under the usual experimental conditions, the image term is almost entirely screened off. When this is so, the dielectric contribution to the activation free energy is essentially the same for the homogeneous and the heterogeneous process.

A number of years ago, John Hale made calculations of the free energies of activation for transfers at metallic electrodes using that assumption, and obtained quite reasonable agreement with experiment [Hale, J. M., in "Reactions of Molecules at Electrodes," Hush, N. S., Ed.; Wiley-Interscience: New York, N.Y., 1971; Chapter 4]. So if that is the case, one would not expect to get a 1:2 heterogeneous:homogeneous ratio when the dielectric term was particularly small. This may arise for certain classes of molecules in which the dominant terms are the inner-shell ones. But for the small aquo ions, for example, one might well expect the ratio of reorganizational energy parameters to differ from 1:2. Of course, a detailed calculation may suggest some small contribution from image effects under the usual experimental conditions of reasonably high ionic strength, but I do not think that this has yet been demonstrated.

DR. WEAVER: As I have shown in Tables I and II of my contribution, the activation free energies, and especially the activation enthalpies, for electrochemical exchange of aquo cations are significantly greater than one-half the corresponding activation energies of the homogeneous self-exchange reactions. This is qualitatively in accord with the model you cited which asserts that there is no imaging in the electrochemical case.

Nevertheless, I think imaging remains significant because there is no way that the image in a transition state can be entirely screened by surrounding ions. One is, in a sense, getting two transition states because of the Franck-Condon barrier, and there is no way that the surrounding ions can entirely screen both the reactant and product transition states at the same time. Also, as I have pointed out in my presentation and in reference 11, the activation energy for the outer-sphere electrochemical exchange is generally expected to be greater than one-half of the homogeneous activation energy even on the basis of the imaging model since the presence of the inner layer of solvent molecules will make the distance between the reacting ion and its image in the electrode greater than the contact distance between the reacting ions in homogeneous solution.

DR. HUSH: There is thought to be a mystery as to why the $\text{Eu}^{3+,2+}$ self-exchange is so slow in aqueous solution. I believe the reason is very simple. The coordination number and symmetry of the water molecules in the first shell around the two aquo ions is completely different so the electron-exchange reaction is inhibited by the slow rate of dissociating a water molecule and reorganizing the inner-coordination sphere. It is quite unnecessary, I believe, to invoke possible electronic nonadiabaticity to account for the observed slow kinetics.

In the electrochemical case, this ought to be reflected both in slow exchange kinetics and also in a value of the transfer coefficient significantly different from one-half. Dr. Vlcek originally attributed the observed slow electrochemical rate to transfer via excited electronic states. I do not think that is correct. I believe that slow kinetics of ligand exchange in the first solvation shells are generally responsible for the unusual features of the $\text{Eu}^{3+,2+}$ exchange rates.

We carried out some measurements some years ago in order to measure the transfer coefficient in DMF for this couple at a mercury electrode [Hush, N. S.; Dyke, J. M. J. Electroanal. Interfac. Electrochem. 1974, 53, 253]. The deviation from one-half for the value so obtained was consistent with reasonable values for the free energy of activation of ligand exchange in the inner-coordination spheres.

Thus, in my opinion, nonadiabaticity does not have to be invoked to explain the slow homogeneous and heterogeneous $\text{Eu}^{3+,2+}$ exchange rates.

DR. WEAVER: I agree that the difference in coordination numbers between Eu^{3+} and Eu^{2+} could contribute importantly to the observed slow rates of electron transfer. However, it is true to say, from our data, anyway, that the way in which the

alpha for the $\text{Eu}^{3+,2+}$ couple depends upon the overpotential in aqueous media is very similar to the behavior of the $\text{Cr}^{3+,2+}$ and the $\text{V}^{3+,2+}$ couples as well.

DR. HUSH: The work of Anson showed that Parsons' and Passeron's experiments [Parsons, R.; Passeron, E. J. *Electroanal. Chem.* 1966, 12, 524] on the dependence of alpha for $\text{Cr}^{3+,2+}$ upon potential were incorrect [Anson, F. C.; Rathjen, N.; Frisbee, R. D. *J. Electrochem. Soc.* 1970, 117, 477].

DR. WEAVER: Anson only looked at the cathodic side which yields very little change in alpha with overpotential. The anodic side, as I showed, exhibits a very marked dependence of alpha on overpotential.

DR. HENRY TAUBE (Stanford University): Though I agree that present evidence points to the conclusion that the slow rate for the aquo $\text{Eu}^{3+,2+}$ exchange is attributable to differences in solvation between the two oxidation states, I still find it very puzzling that these differences are greater for this system than for aquo $\text{Fe}^{3+,2+}$ where the radii are much smaller. When an ion gets large enough, specific solvation must lose its meaning. For Cs^+ , I imagine there are many solvent configurations about the metal ion which have approximately the same energy.

DR. WEAVER: With regard to the assignment of the very slow exchange rate for aquo $\text{Eu}^{3+,2+}$ to nonadiabaticity or to solvational rearrangement, we find that encapsulation of europium inside a 2.2.1- or 2.2.2-cryptand, forming a macrobicyclic ligand shell around the ion, results in homogeneous self-exchange rates approaching $10 \text{ M}^{-1} \text{ s}^{-1}$ in contrast to $\sim 10^{-5} \text{ M}^{-1} \text{ s}^{-1}$ for aquo $\text{Eu}^{3+,2+}$ [Yee, E. L.; Weaver, M. J., unpublished results]. We don't believe that those results can be easily explained by electron tunneling since the f-orbital overlap is likely to be smaller for the europium cryptate couple.

DR. DAVID RORABACHER (Wayne State University): We have recently obtained very similar results for the $\text{Cu}^{2+,+}$ couple. This is one of the classic redox couples involving a large change in coordination number, Cu(II) preferring a tetragonal geometry while Cu(I) is predominantly tetrahedral. For aquo $\text{Cu}^{2+,+}$, we have recently estimated that the self-exchange rate constant at 25 C is $\sim 2 \times 10^{-6} \text{ M}^{-1} \text{ s}^{-1}$. When complexed with macrocyclic tetrathiaether (S_4) ligands, however, the self-ex-

change rate constant increases by about eight orders of magnitude to $\sim 10^2 \text{ M}^{-1} \text{ s}^{-1}$ [Martin, M. J.; Koenigbauer, M. J.; Endicott, J. F.; Rorabacher, D. B., unpublished results]. When a macrocyclic pentathiaether (S_5) ligand is used, the self-exchange rate constant increases further to $\sim 10^4 \text{ M}^{-1} \text{ s}^{-1}$.

We believe that these large changes in rate constant are primarily attributable to restrictions imposed upon the inner-coordination sphere by the macrocyclic ligands. Presumably, the use of a suitable macrobicyclic ligand, such as you have used with europium, would induce even larger changes in the Cu^{2+} self-exchange rate constant. We are planning to pursue such studies in the near future.

DR. EPHRAIM BUHKS (University of Delaware): Is there any experimental evidence indicating the possibility of electron transfer from the electrode into the excited electronic state of a transition metal ion?

DR. WEAVER: Such a process is possible but I don't know of any data which would provide direct evidence. At metal surfaces, at least, excited electronic states of nearby reacting ions might be expected to be quenched rapidly. Semiconductor surfaces would provide more systems with which to search for such an effect.

DR. ALBERT HAIM (State University of New York at Stony Brook): When you vary the free energy of reactions and go to very exoergic reactions, you enter into a region which is sometimes called the inverted region or the abnormal region. Has anything similar been observed in very highly exoergic reactions in electrochemical reductions or oxidations?

DR. WEAVER: The major problem seems to be that when we talk about a fast reaction in electrode kinetics, with rate constants in the range $0.1 - 10 \text{ cm s}^{-1}$, we are referring to a process which has an activation energy equivalent to a homogeneous reaction having a rate constant about $10^5 \text{ M}^{-1} \text{ s}^{-1}$. We are not able to explore such a large range of rate constants and, hence, driving force in electrochemical processes because diffusion becomes the overall rate-limiting step at much smaller rates than occurs in homogeneous solution, two-dimensional diffusion being much less efficient than three-dimensional diffusion. Therefore, it is extremely difficult to measure rate constants that correspond to a sufficiently small activation barrier to investigate the predicted onset of inversion.

Four Aspects of the Distance Dependence of Electron-Transfer Rates

EPHRAIM BUHKS—University of Delaware, Physics Department, Newark, DE 19711

RALPH G. WILKINS—New Mexico State University, Department of Chemistry, Las Cruces, NM 88003

STEPHAN S. ISIED—Rutgers University, The State University of New Jersey, Department of Chemistry, New Brunswick, NJ 08903

JOHN F. ENDICOTT—Wayne State University, Department of Chemistry, Detroit, MI 48202

In many biological systems, the electron transport chains involve some key steps in which electrons appear to move readily over large distances between prosthetic groups located at relatively fixed sites in membranes or in proteins. Such long range electron transfer processes are difficult to investigate in detail using simple, well-defined substances. Approaches to the problem of the distance dependence of electron transfer processes must include delineation of the theoretical concepts pertinent to such processes, identification of the important features of the processes manifested in well-defined biological moieties, and the modelling of selected aspects of these processes in "simple" coordination complexes. We have solicited four short essays from four different investigators to represent the approaches and concerns involved in dealing with long range electron transfer. In Part A, Buhks demonstrates how the temperature dependence of the electron transfer rate constant can be used to determine (i) the range of vibrational modes participating in electron transfer, (ii) the electron-phonon coupling, and (iii) the spatial separation between donor and acceptor centers. In Part B, Wilkins reports on the slow ($k = 2.7 \times$

0097-6156/82/0198-0213\$06.25/0
© 1982 American Chemical Society

10^{-3} s^{-1}) intramolecular disproportionation rate of a metastable (semi-met)₀ form of octameric hemerythrin. In the (semi-met)₀ form, each protein subunit contains a mixed valence [Fe(II)-Fe(III)] binuclear iron site which, upon electron rearrangement within the octamer, leads to [Fe(II)]₂ or [Fe(III)]₂ at each binuclear iron site. The square antiprismatic packing arrangement, inferred for the octamers and the subunit structures, leads to an estimated 2.8-3.0 nm separation between adjacent binuclear iron sites. In Part C, Isied describes electron transfer between Ru(II) and Co(III) centers separated by polypeptide chains differing in length and rigidity. The observed electron transfer rate tends to decrease with an increase in the number of amino acid residues in the polypeptide linkage, and temperature dependencies are observed to vary considerably with the nature of the amino acids. In Part D, Endicott describes some studies of the intermolecular quenching of electronic excited states. The quenching rates may be useful as sensitive probes for the electronic coupling between d-orbital donors and acceptors. The inferred electronic matrix elements exhibit a distance dependence ($k_q \propto V_o^2 \exp[-11R]$; R in nm) similar to that predicted theoretically, but the rapid decrease of the rate constant with increasing donor-acceptor separation can be modified by enhanced electronic interactions formulated as charge transfer forces involving coordinated ligands.

Part A. Quantum-Mechanical Theory of Diffusion Independent Electron Transfer in Biological Systems
by Ephraim Buhks (University of Delaware)

A number of publications in recent years have demonstrated an active interest in the theoretical aspects of electron transfer (ET) processes in biological systems (1-9). This interest was stimulated by the extensive experimental information regarding the temperature dependence of ET rates measured over a broad range of temperatures (10-16). The unimolecular rate of cytochrome-c oxidation in Chromatium (10-12), for example, exhibits the Arrhenius type dependence and changes by three orders of

magnitude over the temperature range 100-300K, while below 100K the mean lifetime ($\sim 10^{-6}$ s) is temperature independent. On the other hand, one of the steps of charge separation in bacterium photosynthesis, a step involving ET from bacteriopheophytin to quinone, depends weakly on temperature (13). Its mean lifetime ($\sim 10^{-10}$ s) decreases by a factor of 2 when the temperature is decreased from 300K to 83K (14). This type of behavior, characteristic of activationless processes, was also observed for the back ET reaction from quinone to chlorophyll, for which the mean lifetime ($\sim 10^{-2}$ s) increases by a factor of 3-4 as the temperature is increased from 150 to 300K, but is temperature independent below 150K (15, 16).

The transition probability for multiphonon, nonadiabatic ET can be formulated in terms of first-order perturbation theory, i.e., by means of the Fermi golden rule, as (2)

$$W = (2\pi/\hbar) |V|^2 G(\Delta\varepsilon) \quad (1)$$

In this expression, V is the one electron-two center interaction matrix element, and decreases exponentially with the distance R between donor and acceptor centers (1, 2, 6-9),

$$V = V_0 e^{-\alpha R} \quad (2)$$

As estimated for molecular crystals (8), $V_0 = 10^5 \text{ cm}^{-1}$ and $\alpha = 10 \text{ nm}^{-1}$.

The function G in eq 1 is the Franck-Condon factor which accounts for the contribution of nuclear degrees of freedom and represents the thermal average of the overlap integrals between nuclear wavefunctions with respect to conservation of energy, and is given by (2, 3, 8, 9)

$$G(\Delta\varepsilon) = (2\pi\hbar)^{-1} e^{-\phi(0)} \int_{-\infty}^{\infty} e^{i\Delta\varepsilon t/\hbar} e^{\phi(t)} dt \quad (3)$$

where

$$\phi(t) = \int \rho(\omega) \frac{\Delta_s^2}{2}(\omega) [(v(\omega) + 1)e^{i\omega t} + v(\omega)e^{-i\omega t}] d\omega \quad (4)$$

$$\rho(\omega) = \rho_s(\omega) + \sum_k \delta(\omega - \omega_k) \quad (5)$$

Eq 3 takes into account the contributions of: (i) continuum of normal vibrational modes of a solvent characterized by a density of states $\rho_s(\omega)$ with reduced equilibrium displacement $\Delta_s(\omega)$; and (ii) local vibrational modes with corresponding frequencies $\{\omega_k\}$ and reduced displacements $\{\Delta_k\}$; $\Delta\varepsilon$ is the energy gap between the final and initial electronic states for ET processes and $v(\omega) = [\exp(\hbar\omega/k_B T) - 1]^{-1}$ is the equilibrium phonon occupation number.

The temperature dependence of ET rates between cytochrome-c and the reaction center in Chromatium (Figure 1), fitted to eqs 3-5 (8), demonstrated that, unlike many redox reactions in inorganic chemistry, ET in biological systems is characterized by large configurational changes of the high frequency mode ($\hbar\omega_k \sim 500 \text{ cm}^{-1}$) and modest configurational changes due to coupling with the polar medium ($\hbar\omega_s \sim 100\text{-}300 \text{ cm}^{-1}$ for ice).

In an (average) single mode approximation, the Franck-Condon factor, eqs 3-5, can be simplified and it takes the well known form (2, 4, 7-9)

$$G = (\hbar\omega)^{-1} \exp(-S \coth x - px) I_p(S/\sinh x) \quad (6)$$

where

$$x = \hbar\omega/2k_B T, \quad S = (\Delta)^2/2, \quad p = \Delta\varepsilon/\hbar\omega,$$

and I_p is the modified Bessel functions of order p .

At high temperatures ($\hbar\omega \ll 2k_B T$), eq 6 reduces so that the rate becomes,

$$W_{HT} = (2\pi/\hbar) (4\pi E_s k_B T)^{-\frac{1}{2}} |V|^2 \exp(-E_a/k_B T) \quad (7)$$

where the activation energy is

$$E_a = (p - S)^2 \hbar\omega/4S \quad (8)$$

and $E_s = S\hbar\omega$ is the reorganization energy. At low temperatures ($\hbar\omega \gg 2k_B T$), eq 6 yields the temperature-independent Poisson distribution, resulting in the following expression for the rate,

$$W_{LT} = (2\pi/\hbar) |V|^2 e^{-S} S^p / (p!) \hbar\omega \quad (9)$$

At sufficiently large p this may be recast in the form of an energy gap law,

$$W_{LT} = (2\pi/\hbar) |V|^2 (2\pi p)^{-\frac{1}{2}} \exp(-S - \gamma p) \quad (10)$$

where $\gamma = \ln(p/s) - 1$.

A transition temperature, T_o , between the Arrhenius and temperature-independent rate forms may be defined by the equation $W_{HT}(T_o) = W_{LT}$, and is on the order of $k_B T_o \cong \hbar\omega/4$ for the strong coupling ($S \gg 1$) case (7). For the special, activationless case, for which $p = S$, $k_B T_o \cong \hbar\omega/2$ (6).

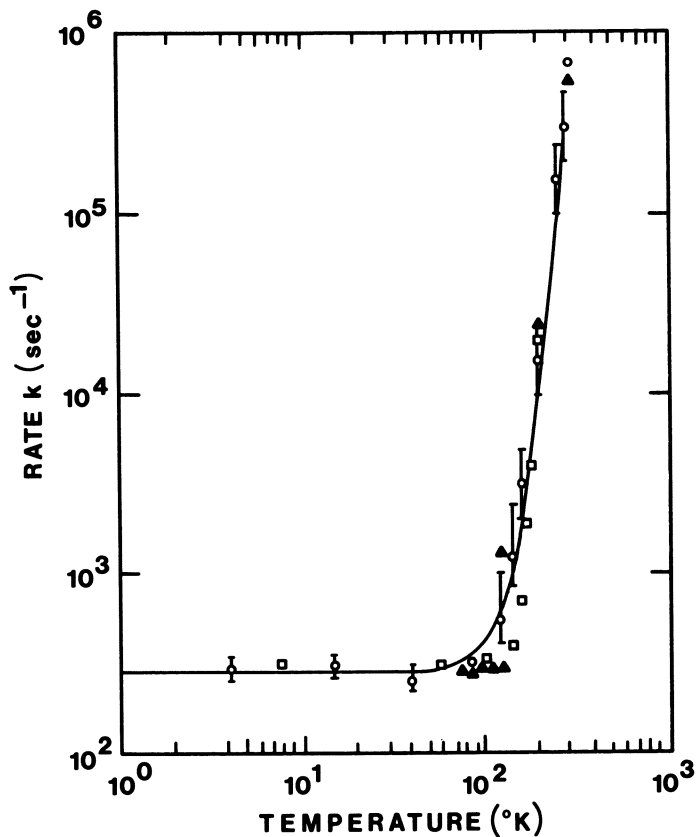


Figure 1. Theoretical fit of the temperature dependence of the rate of cytochrome oxidation in Chromatium. Experimental data are taken from Ref. 10. The details for the calculations are given in Ref. 8. Conditions: E_s , 2000 cm^{-1} ; $\hbar\omega_0$, 200 cm^{-1} ; $\hbar\Delta\omega$, 200 cm^{-1} ; E_c , 18500 cm^{-1} ; $\hbar\omega_c$, 500 cm^{-1} ; and V , 90 cm^{-1} .

Activationless ET processes (1, 4, 6, 9) are described by two diabatic potential energy surfaces crossing at the minimum of the initial surface. This limit is characterized by a rate which decreases with increasing temperature at high T (negative apparent activation energy)

$$W_{HT} = (2\pi/\hbar)|V|^2(4\pi E_S k_B T)^{-\frac{1}{2}} \quad (11)$$

At low temperature, the activationless ET processes become temperature independent (see Figure 2),

$$W_{LT} = (2\pi/\hbar)|V|^2 (2\pi\rho)^{-\frac{1}{2}} \quad (12)$$

Eqs 2 and 12 can be applied to the data for activationless ET processes to give a rough estimate of the electron exchange interaction and the spatial separation of donor and acceptor centers in biological systems (1, 2, 6-9): $V \cong 4 \text{ cm}^{-1}$ and $R \cong 1.0 \text{ nm}$ for pheophytin-quinone electron exchange; and $V \cong 10^{-4} \text{ cm}^{-1}$ and $R \cong 1.9 \text{ nm}$ for ET in the quinone-chlorophyll system. These estimates of donor-acceptor separation are in good agreement with the results of magnetic measurements (17).

Part B. Intramolecular Electron Transfer Reactions in the Respiratory Protein, Hemerythrin
by Ralph G. Wilkins (New Mexico State University)

Hemerythrin is a respiratory protein isolated from sipunculids (marine worms). All sipunculids examined have, in the coelomic fluid, erythrocytes loaded with the protein which in most species so far examined is octameric, but sometimes trimeric (18, 19) and in one instance dimeric and tetrameric (20, 21). From the retractor muscle of Themiste zostericola, the protein has been characterized as a monomer (22). The monomer (23) and the subunits of the trimer (24) and octamer (25) are remarkably similar in tertiary structure, having a M.W. of about 13,500 daltons. Each subunit contains one binuclear iron site. There is no porphyrin ring and the irons are coordinated only to amino acids, some of which, as well as probably an oxy group, form the binding atoms (26).

We have been investigating the oxidation-reduction reactions of the binuclear iron site in the protein matrix (27-32). The methemerythrin form contains both irons in the +3 oxidation state and can be reduced in two steps (by dithionite ion (27, 31), reduced methylviologen, and photochemically using a riboflavin/EDTA mixture (28)) to the deoxy form in which both irons are in the +2 oxidation state. The intermediate (semi-met)_R, in which one iron is +3 and the other iron +2, has been

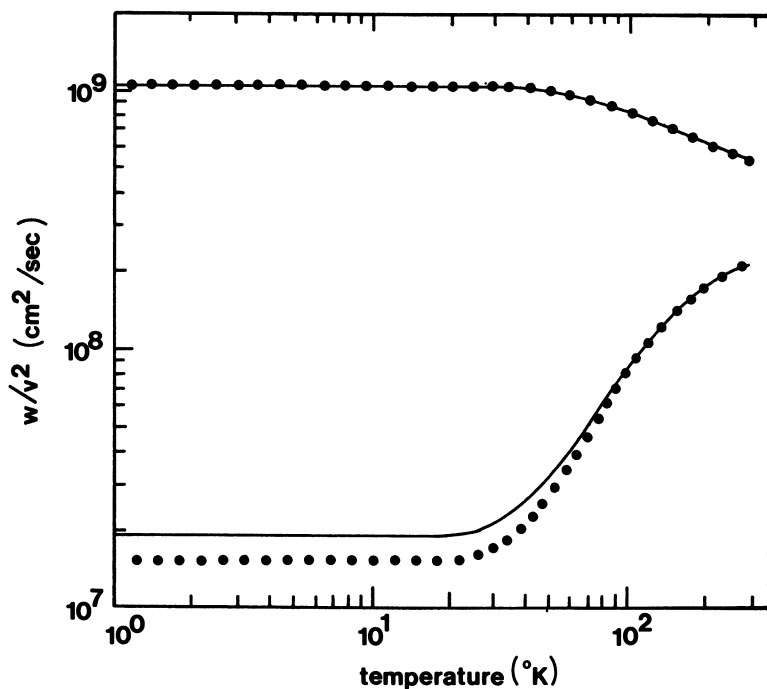
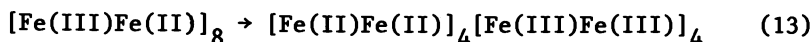


Figure 2. Theoretical prediction for the temperature dependence of the electron transfer rate for activated and for activationless processes. Solid lines are calculated for a continuum of vibrational modes; dotted lines represent the single-mode approximation (6, 8). Upper curve: ΔE , -2000 cm^{-1} ; P, 20; and S, 20. Lower curves: ΔE , -800 cm^{-1} ; P, 8; and S, 20.

thoroughly characterized (31) including EPR spectra at liquid helium temperatures (30, 32). Another distinct semi-met form is obtained by one-electron oxidation of the deoxy form by $\text{Fe}(\text{CN})_6^{3-}$ (29). This, the (semi-met)₀ form, has spectral and chemical behavioral differences from those of (semi-met)_R (28, 30, 31). The two forms, with protein from Themiste zostericola, undergo spontaneous spectral changes (28, 31) and complete loss of EPR signal (30) by a first-order rate process, with a rate constant independent of protein concentration. This change is ascribed to a remarkable intramolecular disproportionation process within the octamer:

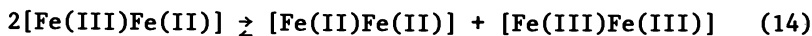


The structures are known for the octamer from Phascolopsis gouldii and Themiste dyscritum (33, 34). The eight identical subunits are packed as a "square donut" with four subunits in each of two layers. The binuclear iron units are at corners of an almost regular square antiprism with distances of 2.8-3.0 nm between adjacent binuclear iron centers. The disproportionation rate constant for reaction 13 is $2.7 \times 10^{-3} \text{ s}^{-1}$ at 25C and pH 8.2. This value can, therefore, be assigned to electron transfer over the 2.8-3.0 nm distances, making the reasonable assumption that the structure of octameric protein from Themiste zostericola is similar to those from the other proteins. A number of redox reactions of the semi-met forms are controlled by this disproportionation (29, 31). Semi-met forms of hemerythrin from Phascolopsis gouldii and Themiste dyscritum also disproportionate and at rates comparable to those for semi-met from Themiste zostericola (31).

There is currently much interest in electron transfer processes in metal complexes and biological material (1-16, 35). Experimental data for electron transfer rates over long distances in proteins are scarce, however, and the semi-methemerythrin disproportionation system appears to be a rare authentic example of slow electron transfer over distances of about 2.8 nm. Iron site and conformational changes may also attend this process and the tunneling distances from iron-coordinated histidine edges to similar positions in the adjacent irons may be reduced from the 3.0 nm value. The first-order rate constant is some 5-8 orders of magnitude smaller than those for electron transfer involving some heme proteins for which reaction distances of 1.5-2.0 nm appear established (35).

Although semi-met forms of myohemerythrin (the monomeric protein from Themiste zostericola muscle) can be obtained in a similar manner to the octamer (32), the intramolecular disproportionation path is obviously now unavailable to them. In

agreement with this, it is observed that (semi-metmyo)_O changes to (semi-metmyo)_R and the latter disproportionates by second-order reversible kinetics:



The forward and reverse second-order rate constants for reaction 14 are $0.89 \text{ M}^{-1} \text{ s}^{-1}$ and $9.4 \text{ M}^{-1} \text{ s}^{-1}$, respectively, at 25C and pH 8.2, where most of these experiments were carried out. Full details of these experiments (32) and discussion of all the results above are contained in refs (27-32). Since the protein can be found in a number of oligomeric forms (18-22), it is possible to study the effect of tertiary structure on the intramolecular electron transfer process. It is also apparent that the protein matrix confers unique behavior on the iron binuclear site, missing from simpler iron complexes.

Part C. Dynamics of Electron Transfer Across Polypeptides by Stephan S. Isied (Rutgers University)

Electron transport in many biological systems takes place with the aid of protein molecules ($\text{MW} \geq 5,000$) having prosthetic groups that are only a few percent by weight of the protein. These prosthetic groups are usually one or more metal ions (e.g., Fe, Cu), a metalloporphyrin, a flavin, or a quinone. These observations have led to many questions concerning the role of the protein and the different polypeptides surrounding the prosthetic group in the electron transfer process. Furthermore, the location of these prosthetic groups within the protein (i.e., how buried or exposed the prosthetic groups are within the protein) have also raised questions concerning the participation of neighboring peptide side chains in the electron transfer pathway (36, 37).

In order to probe these effects, a number of studies on the kinetics of electron transfer between small molecule redox reagents and proteins, as well as protein-protein electron transfer reactions, have been carried out (38-41). The studies on reactions of small molecules with electron transfer proteins have pointed to some specificity in the electron transfer process as a function of the nature of the ligands around the small molecule redox reagents, especially the hydrophobicity of these ligands. Thus, for example, $[\text{Co(phen)}_3]^{3+}$ and related redox reagents are thought to penetrate the hydrophobic surface of the protein much better than $[\text{Fe(EDTA)}]^{2-}$ reagents, and, therefore, to have access to different electron transfer mechanisms (42).

Although the above studies have been important in probing some of the features of these protein electron transfer reac-

tions, they generally suffer from the disadvantages associated with intermolecular electron transfer in small molecule redox centers. These disadvantages include the multiple elementary steps (eqs 15-17) involved, which can mask the details of the electron transfer step (eq 16):

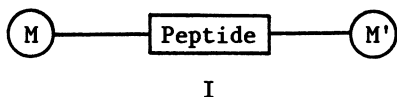


In these reactions, K is the equilibrium quotient for the formation of the precursor complex, k_{et} is the rate for electron transfer within the precursor complex, and k_3 is the rate of dissociation of the successor complex.

Intermolecular reactions involving proteins are further complicated since one is dealing with large proteins containing neutral, acidic, basic, hydrophobic, and hydrophilic side chains. The multiplicity of mechanisms possible in such large molecules makes detailed mechanistic studies very difficult. It has long been acknowledged (44-47) that, if one could isolate and study the intramolecular electron transfer step (eq 16), many ambiguities in the electron transfer reaction could be circumvented, and one could, therefore, study the factors that affect the rate of electron transfer directly, uncomplicated by substitution and other processes.

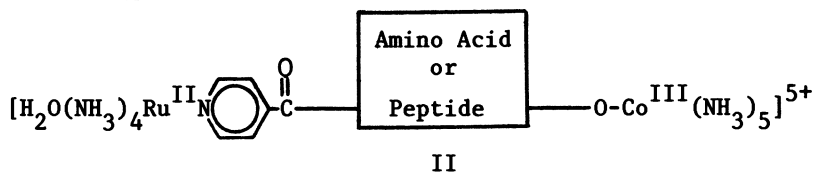
In applying this principle to proteins, one would ideally like to modify a protein at one specific site with a number of related, substitution-inert, inorganic redox reagents, and then study the intramolecular electron transfer step as a function of a wide variety of variables (e.g., the redox potential and hydrophobicity of the redox reagent). Such a study is extremely difficult to carry out with large proteins, and none has been reported thus far. We have, however, found out that horseheart cytochrome *c* is amenable to modification at a single site by the $[(NH_3)_5Ru^{II}]$ group and such a detailed study is currently underway in our laboratory (43).

Electron-Transfer in Simple Binuclear Complexes. In trying to understand the electron transfer mediation effects of peptide bonds and amino acid side chains on rates of electron transfer in simple systems that are amenable to detailed investigation, we have designed and synthesized a series of complexes which contain within a single molecule two different oxidizing agents --both of which are inert to substitution. The series of complexes we have synthesized is represented schematically by the general structure I.



A variety of amino acid and peptide moieties have been inserted in between these two oxidizing agents, M and M'. The selective reduction of one of the two metal centers allows us to form precursor complexes which contain within a single molecule an oxidizing agent and a reducing agent--both inert to substitution. Rates of electron transfer in these precursor complexes can then be measured unaffected by substitution or isomerization reactions not directly pertinent to the electron transfer step. If one maintains the same environment around the metal ion center, no change in the driving force and inner and outer sphere reorganization energies around the donor and acceptor metal ions is expected. This allows us to focus on the detailed differences between the different amino acid and peptide bridging ligands.

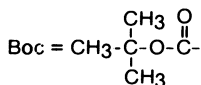
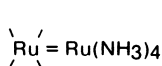
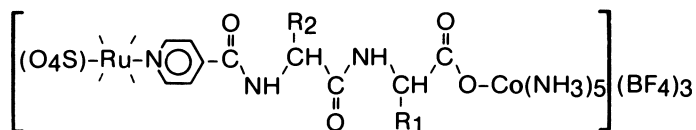
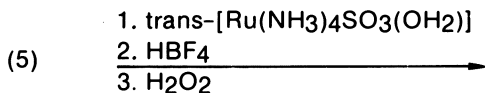
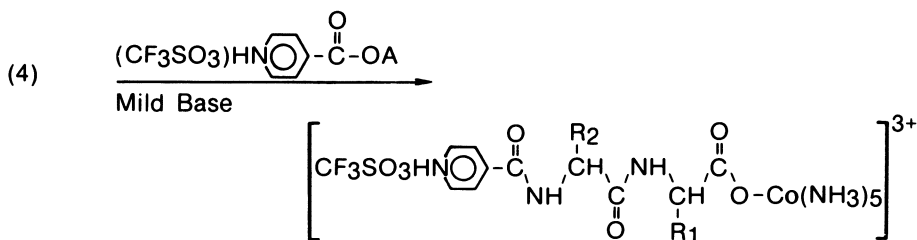
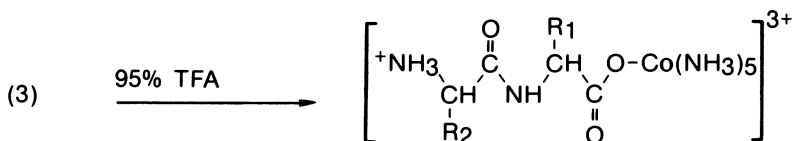
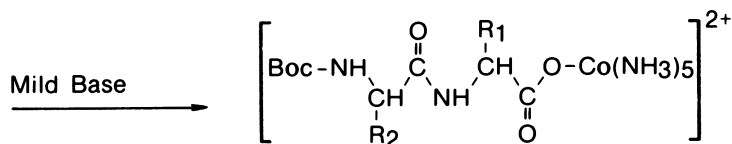
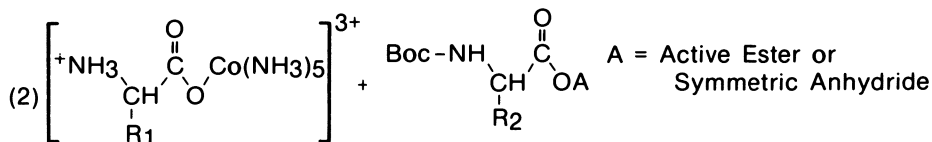
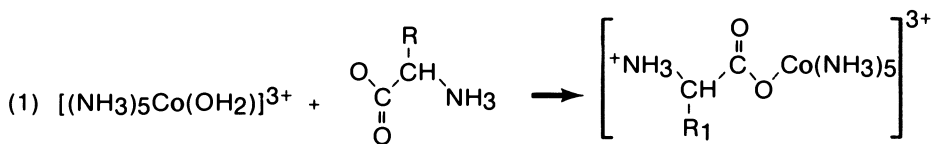
The set of metal donor and acceptor ions that has so far proved useful for peptide synthesis is the $[(\text{NH}_3)_5\text{Co}^{\text{III}}-]$ and the $[(\text{OH}_2)(\text{NH}_3)_4\text{Ru}^{\text{II}}-]$ group as acceptor and donor, respectively. This same set of metal ions has previously been used to study electron transfer in a number of related organic bridging ligands (44-47) and is represented by structure II:



The Co(III)-Ru(III) complexes were synthesized as shown in Scheme I (48, 49). These complexes were purified by chromatography and characterized by HPLC, elemental analysis, UV-Vis spectra, and electrochemical properties.

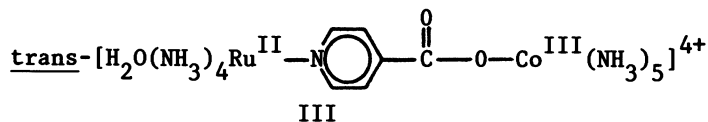
Intramolecular Electron-Transfer Rates. Experiments were carried out under inert atmosphere by reducing a known concentration of the complexes with $[\text{Ru}(\text{NH}_3)_6]^{2+}$ or Eu^{2+} . The variation of rate constants with temperature was studied over a range of twenty degrees at four different temperatures. The activation parameters ΔH^\ddagger and ΔS^\ddagger were obtained using eq 18:

$$k = \frac{k_B T}{h} e^{-\Delta H^\ddagger/RT} e^{\Delta S^\ddagger/R} \quad (18)$$



Scheme I

The rate constants and activation parameters for a series of Co(III)-Ru(II) complexes separated by Gly, Phe, Pro, and GlyGly, GlyPhe, ProPro are shown in Table I. This series of rate constants is compared to the rate constant and activation parameters for the parent compound (III) with an isonicotinate bridging ligand. In the parent compound III, the ligands around



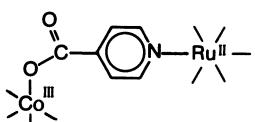
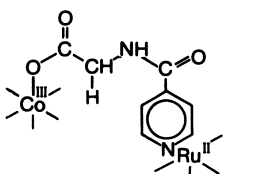
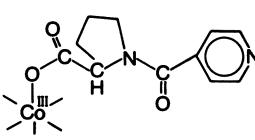
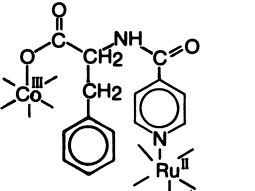
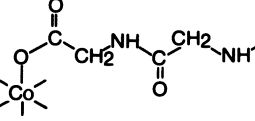
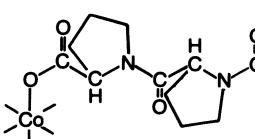
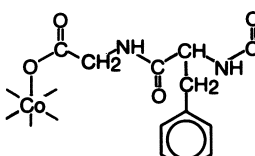
the metal ions are identical to those in the rest of the series, except with no amino acid or peptide separating the donor and acceptor metal ions.

Influence of the Amino Acid Linkages on Intramolecular Electron-Transfer Rates. There is a significant drop in the rate ($>10^2$) when one amino acid is intervening between the Co(III) and Ru(II) centers. The nature of the amino acid (i.e., rigid, flexible, hydrophobic, hydrophilic) does not affect the rate constant or activation parameters significantly (Table I). A small increase in the rate constant, however, between the two flexible amino acids (Gly and Phe) and the rigid amino acid Pro, is observed.

Inserting the second amino acid between the cobalt and ruthenium centers further decreases the rate constant for intramolecular electron transfer slightly. All the dipeptides studied so far have lower rates of electron transfer than the amino acid complexes. The rate constant for electron transfer in the flexible dipeptides GlyGly and GlyPhe decrease by a factor of 3-4 from that for the corresponding amino acid, while the rate constant for the rigid dipeptide ProPro decreases by a factor of sixteen from the corresponding proline amino acid. The results in Table I suggest that the nature of the peptide material (i.e., the amino acid side chains) may not be of great significance in determining the rate of electron transfer. Large differences, however, are observed in the temperature dependence of the rate of electron transfer (i.e., in the activation parameters). The flexible dipeptide GlyGly has a much smaller temperature dependence than the other two dipeptides studied.

It is too early to draw any conclusions about the insensitivity of the rate constants to the nature of the dipeptide. Differences among the peptides seem to be revealed more in the temperature dependencies of the rate constants for intramolecular electron transfer than in the magnitude of the rate constant itself. Work is in progress on the synthesis of other di-, tri-, and tetra-peptides separating Co(III) and Ru(II) in order to examine the temperature dependence of the intramolecular rate

Table I. Intramolecular Electron Transfer Rates and Activation Parameters*

Complex	Bridge	$\frac{k}{\text{SEC}^{-1}}$	$\frac{\Delta H^\ddagger}{\text{KCAL/MOL}}$	$\frac{\Delta S^\ddagger}{\text{E.U.}}$
	Iso	1.24×10^{-2}	19.7	-1.0
	Gly-Iso	3.8×10^{-5}	19.9	-11.9
	Pro-Iso	9.9×10^{-5}	18.7	-14.1
	Phe-Iso	3.9×10^{-5}	18.6	-14.1
	GlyGly-Iso	9.9×10^{-6}	14.0	-34.6
	ProPro-Iso	6.4×10^{-6}	18.6	-19.7
	GlyPhe-Iso	8.6×10^{-6}	20.7	-12.2

* Medium 1 M HTFA

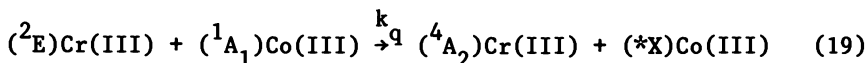
constant as a function of the structure and conformation of the peptide chain. A systematic study of the above rates and their temperature dependencies should allow systematic understanding of the effects of the amino side chains on potential electron transfer pathways.

Part D. Experimental Probes of the Electronic Component of Donor-Acceptor Interactions in Bimolecular Reactions
by John F. Endicott (Wayne State University)

One expects the impact of the electronic matrix element, eqs 1 and 2, on electron-transfer reactions to be manifested in a variation in the reaction rate constant with: (1) donor-acceptor separation; (2) changes in spin multiplicity between reactants and products; (3) differences in donor and acceptor orbital symmetry; etc. However, simple electron-transfer reactions tend to be dominated by Franck-Condon factors over most of the normally accessible temperature range. Even for outer-sphere reactions of the $\text{Co}(\text{NH}_3)_6^{3+,2+}$ and $\text{Co}(\text{OH}_2)_6^{3+,2+}$ couples, reactions in which each of the cobalt couples involves a ($^1A_{1g} \leftrightarrow ^4T_{1g}$) change in spin multiplicity, Franck-Condon factors account for ~80% of the observed activation barriers (50). Despite this dominance of Franck-Condon factors, electronic terms appear to make contributions of several orders of magnitude to the observed rates of many simple electron transfer reactions (50-54). The preceding essays have noted, explicitly or implicitly, the increasing importance of electronic factors when donor and acceptor are held at relatively large separations. It is clearly important to obtain a better understanding of the nature of the long range electronic coupling between donor and acceptor, but the details of electronic interactions in electron transfer reactions are usually masked by Franck-Condon effects; and purely theoretical estimates of V for reactions as simple as the $\text{Co}(\text{NH}_3)_6^{3+,2+}$ self-exchange (55) may be a few orders of magnitude too small (50). In seeking a class of reactions more sensitive to the nature of the electronic matrix element, we have been examining electronic energy transfer (or excited state quenching) reactions of transition metal complexes (56, 57, 58). Among these, the most promising reactions appear to involve quenching of (2E)Cr(III) excited states with transition metal complexes.

Electronic Energy Transfer: Co(III) Quenching of *Cr(III)

Most of our work has centered on the (2E)Cr(PP) $_3^{3+}/(^1A_1)$ -Co(III) reactions:



[where PP represents polypyridyl, i.e., bipyridyl, phenanthroline, etc.]. A spin conservative quenching process could yield either a triplet or quintet (e.g., $*X = {}^3T_{1g}$ or ${}^5T_{2g}$) excited state of cobalt(III).

The quenching rate constants do not follow the expected electron transfer patterns and no oxidized or reduced species have been detected. Furthermore, k_q does not appear to be sensitive to the donor-acceptor energy gap and the intrinsic reorganizational factors are small (56), indicating that Franck-Condon factors do not dictate the observed reaction patterns. This is equivalent to taking the density of states function $\rho \sim 1$ and may be a consequence of the very narrow band 2E emission, the very broad band Co(III) absorptions, and large number of low energy Co(III) states. Thus, k_q varies from $4 \times 10^6 \text{ M}^{-1}\text{s}^{-1}$ to $0.7 \times 10^6 \text{ M}^{-1}\text{s}^{-1}$ through a series of CoL_6^{3+} quenchers ($L = NH_3, H_2O, en/2, sephulchrate/6, PP/2$), with the variation being systematic in size,

$$k_q = K_o v \exp(-2\alpha R) \quad (20)$$

where K_o is the ion pair association constant as in eq 15, v is an intrinsic frequency factor and $\alpha = 5 \pm 1 \text{ nm}^{-1}$ (reactions at 25C, 1M ionic strength). For the $({}^2E)Cr(III)/Co(NH_3)_6^{3+}$ reaction, $v \sim 3 \times 10^{12} \text{ s}^{-1}$.

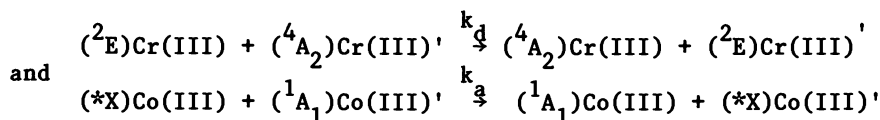
Since the quenching reaction 20 involves a forbidden transition in the donor and the acceptor, a long-range, dipole-allowed quenching mechanism is forbidden; thus, the effective distance for Förster quenching (59) is $\leq \sim 0.1 \text{ nm}$. Short range factors which would contribute to the electronic matrix element include the electron exchange interaction (60) and any other component of a very weak donor-acceptor quasi-bonding interaction (53). In an exchange-allowed quenching mechanism, the Franck-Condon component is usually formulated as the donor-acceptor spectral overlap integral (60). That this does not seem to contribute significantly to the reactions 19 we have investigated is yet another demonstration that Franck-Condon factors do not make significant contributions to these reactions.

The reciprocal of α can be viewed as a mean orbital locus for the particular donor and acceptor. Thus, one might predict $\alpha \sim 12-14 \text{ nm}^{-1}$ for low spin Co^{3+} or Cr^{3+} , and values of $\alpha =$

10^{-11} nm^{-1} have been estimated for a variety of electron transfer reactions (8, 53). Our experimental value of $\alpha \cong 5 \pm 1 \text{ nm}^{-1}$ appears to be appreciably smaller than these estimates. However, our estimate of α is based on the collisions of spheres of van der Waals radii, and Newton (53) has pointed out that the strong distance dependence of V may require some interpenetration of coordinated ligands. Allowing for such interpenetration would probably increase the numerical value of α . On the other hand, the values of α determined from experimental measurements of k_q are somewhat buffered against this element of arbitrariness in choice of R by the strong, but opposing, dependence of K_o on R (noting that α is based on variations in k_q/K_o).

Taken at face value, $\alpha \sim 5 \text{ nm}^{-1}$ implies some "expansion" of the effective d -orbital radius of donor and/or acceptor. Nephelauxetic (61) effects have been previously proposed to be important in energy transfer reactions of Cr(III) complexes (62, 63) and some increase in the effective radius of the d - π electrons of Cr(III) might be plausible. (Assuming α^{-1} to be a simple average of $R(\text{Cr})$ and $R(\text{Co})$, the implication is a quadrupling of the Cr^{3+} gaseous ion radius). However, the information now available does not allow us to separate the contributions of donor and acceptor.

Actually, the separation of donor and acceptor contributions to the electronic matrix element is not likely to be simple. One might define the resonance exchange reactions,



However, there is no reason to expect for the Franck-Condon independent terms that $V_q = (V_d V_a)^{\frac{1}{2}}$. For example,

$$\text{for } v \sim \frac{V_o^2}{h} \left[\frac{\pi^3}{[(E_{in}^* + E_S^*) RT]} \right]^{\frac{1}{2}}$$

(53) (where E_{in}^* and E_S^* are the coordination sphere and solvent reorganizational energies), we would estimate $v_a/(v_o')^2 \sim 2 \times 10^{12} \text{ s}^{-1} (\text{kJ mol}^{-1})^{-2}$ for $\text{Co}(\text{NH}_3)_6^{3+}$ while $v_d \sim 9 \times 10^{13} \text{ s}^{-1}$ for the vibronically allowed (64) resonance transfer of energy be-

tween 2E and 4A_2 Cr(III) (this leads to $k_d \sim 10^7 M^{-1}s^{-1}$ if $\alpha_d = 5.5 \text{ nm}^{-1}$ and $k_d \sim 5 \times 10^9 M^{-1}s^{-1}$ if $\alpha_d = 3.4 \text{ nm}^{-1}$, assuming $R_d = 1.34 \text{ nm}^{-1}$). For the quenching reaction, we would estimate $v_q/v_o^2 \sim 3.5 \times 10^{12} s^{-1} (\text{kJ mol}^{-1})^{-2}$, and $v_q = (v_a v_d)^{\frac{1}{2}}$ only if $v_o'/v_o \sim 0.25$.

In general, $v_q \neq (w_a w_b)^{\frac{1}{2}}$ and $\alpha_q R \neq \frac{1}{2}[\alpha_d R_d + \alpha_a R_a]$. Consequently, the often proposed factoring of "non-adiabatic" components of electron transfer reactions (51, 65) cannot be generally valid.

The Possibility of An Enhancement of the Probability of Long Range Electron Transfer

It is important to determine whether some specific donor-acceptor interactions can result in a reasonably large numerical value of V even for large donor-acceptor separations. A tentative answer seems to be provided in studies of the $\text{Co}(\text{NH}_3)_5\text{X}^{2+}$ quenching of $({}^2E)\text{Cr}(\text{PP})_3^{3+}$ (57, 58). Thus, $k_q \sim 3\text{-}5 \times 10^6 M^{-1}s^{-1}$ for $\text{X} = \text{F}, \text{CN}$ and for $\text{Co}(\text{NH}_3)_6^{3+}$, but the quenching rate constant increases with the heavier halides and pseudo-halides: $k_q = 6 \times 10^7, 1 \times 10^8, 1.6 \times 10^8, \text{ and } 2 \times 10^8 M^{-1}s^{-1}$ for $\text{X} = \text{Cl}, \text{Br}, \text{N}_3, \text{ and } \text{NCS}$, respectively. Furthermore, k_q is about 5 times larger for cis- than for trans- $\text{Co}(\text{N}_4)\text{X}_2^+$ complexes. These enhanced reactivities parallel the oxidizability of X^- and are consistent with a donor-acceptor charge transfer contribution to the interaction Hamiltonian. This Mulliken-type of interaction (66) would formally correct the ground state wave function by introducing a small contribution from a charge transfer excited state (here the excited state would be the ion pair, $\{\text{Cr}(\text{PP})_3^{2+}, \text{Co}(\text{NH}_3)_5(\cdot\text{X})^{3+}\}$). Viewed in this manner, the enhanced quenching rates of the $\text{Co}(\text{NH}_3)_5\text{X}^{2+}$ complexes are attributed to a charge-transfer component in the quasi-bonding donor-acceptor interaction. Experimentally, this leads to additional components on the order of $1\text{-}4 \text{ kJ mol}^{-1}$ in V_o .

In electron transfer reactions, the most frequently encountered, and most direct, analog of this kind of charge transfer interaction would involve a C-T excited state with an electron transferred from the reducing agent to a ligand coordinated

to the oxidant. This could be an important factor in reactions of iron or ruthenium complexes involving polypyridyl, porphyrin, etc.

Summary

Our studies of electronic energy transfer reactions are consistent with a strong decrease in the electronic interaction matrix element in accordance with eq 2. However, these studies also indicate that at least two potentially distinguishable effects can result in constants larger than one might naively predict using eq 2:

1. Nephelauxetic or other coordinated ligand effects which delocalize electron density may lead to a numerically smaller value of α than found for the free ions.
2. Specific donor-acceptor charge transfer interactions can lead to a relatively large numerical value of the electronic matrix element, possibly attributable to an increase in V_0 , and, thus, to larger rate constants than those predicted by distance variations alone.

Acknowledgements

The efforts of several co-workers are noted in the citations. This work was partly supported by the National Science Foundation.

Literature Cited

1. Hopfield, J. J. Proc. Natl. Acad. Sci. USA 1974, 71, 3640.
2. Jortner, J. J. Chem. Phys. 1976, 64, 4860.
3. Kuznetsov, A. M.; S ndergard, N. C.; Ulstrup, J. Chem. Phys. 1978, 29, 383.
4. Sarai, A. Chem. Phys. Lett. 1979, 63, 360.
5. Christov, S. G. J. Electroanal. Chem. 1979, 100, 513.
6. Buhks, E.; Jortner, J. FEBS Lett. 1980, 109, 117.
7. Buhks, E.; Jortner, J. J. Phys. Chem. 1980, 84, 3370.
8. Buhks, E.; Bixon, M.; Jortner, J. Chem. Phys. 1981, 55, 41.
9. Jortner, J. J. Am. Chem. Soc. 1980, 102, 6676.
10. DeVault, D.; Chance, B. Biophys. J. 1966, 6, 825.
11. Dutton, P. L.; Kihara, T.; McCray, J. A.; Thornber, J.P. Biochim. Biophys. Acta 1976, 226, 81.
12. Hales, B. J. Biophys. J. 1976, 16, 471.
13. Peters, K.; Avouris, Ph.; Rentzepis, P. M. Biophys. J. 1978, 23, 207.
14. Parson, W. W.; Schenk, C. C.; Blankenship, R. E.; Holten, D.; Windsor, M. W.; Shank, C. V., in "Frontiers of Biologi-

- cal Energetics," Vol. 1; Academic Press: New York, N. Y., 1978; p. 37.
15. Parson, J. W. Ann. Rev. Microbiol. 1974, 28, 41.
 16. Hoff, A. J. Phys. Reports 1975, 54, 75.
 17. Dutton, P. L.; Leigh, J. S.; Prince, R. C.; Tiede, D. M. "Tunneling in Biological Systems"; Chance, B.; DeVault, D. C.; Frauenfelder, H.; Marcus, R. A.; Schrieffer, J. R.; Sutin, N., Eds.; Academic Press: New York, 1979; p 319.
 18. Liberatore, F. A.; Truby, M. F.; Klippenstein, G. L. Arch. Biochem. Biophys. 1974, 160, 228.
 19. Addison, A. W.; Bruce, R. E. Arch. Biochem. Biophys. 1977, 183, 328.
 20. Manwell, C. Comp. Biochem. Physiol. 1977, 58B, 331.
 21. Sieker, L. C.; Bolles, L.; Stenkamp, R. E.; Jensen, L. H.; Appleby, C. A. J. Mol. Biol. 1981, 148, 493.
 22. Klippenstein, G. L.; Van Riper, D. A.; Oosterom, E. A. J. Biol. Chem. 1972, 247, 5959.
 23. Hendrickson, W. A. Naval Res. Rev. 1978, 31, 1
 24. Hendrickson, W. A.; Smith, J. L., private communication.
 25. Stenkamp, R. E.; Jensen, L. H. Adv. Inorg. Biochem. 1979, 1, 219.
 26. Stenkamp, R. E.; Sieker, L. C.; Jensen, L. H.; Sanders-Loehr, J. Nature 1981, 291, 263.
 27. Harrington, P. C.; DeWaal, D. J. A.; Wilkins, R. G. Arch. Biochem. Biophys. 1978, 191, 444.
 28. Babcock, L. M.; Bradic, Z.; Harrington, P. C.; Wilkins, R. G.; Yoneda, G. S. J. Am. Chem. Soc. 1980, 102, 2849.
 29. Bradic, Z.; Harrington, P. C.; Wilkins, R. G.; Yoneda, G. Biochemistry 1980, 19, 4149.
 30. Muhoberac, B. B.; Wharton, D. C.; Babcock, L. M.; Harrington, P. C.; Wilkins, R. G. Biochim. Biophys. Acta. 1980, 626, 337.
 31. Harrington, P. C.; Wilkins, R. G. J. Am. Chem. Soc. 1981, 103, 1550.
 32. Harrington, P. C.; Muhoberac, B. B.; Wharton, D. C.; Wilkins, R. G. Biochemistry 1981, 20, 6134.
 33. Ward, K. B.; Hendrickson, W. A.; Klippenstein, G. L. Nature, 1975, 257, 818; and unpublished results.
 34. Stenkamp, R. E.; Sieker, L. C.; Jensen, L. H.; Loehr, J. S. J. Mol. Biol 1976, 100, 23.
 35. "Tunneling in Biological Systems", Chance, B.; DeVault, D. C.; Frauenfelder, H.; Marcus, R. A.; Schrieffer, J. R.; Sutin, N., Eds.; Academic Press: New York, 1979; p 595.
 36. Moore, G. R.; Williams, R. J. P. Coord. Chem. Rev. 1976, 18, 125.
 37. Adman, E. T. Biochim. Biophys. Acta 1979, 549, 107.
 38. Wherland, S.; Gray, H. B. "Biological Aspects of Inorganic Chemistry"; Addison, A.; Cullin, W.; Dolphin, D.; James, B., Eds.; Wiley: New York, 1977; p 289.

39. Sutin, N. Adv. Chem. Ser. 1977, No. 162, 156.
40. Lappin, A.; Segal, M.; Weatherborn, D.; Sykes, A. J. Am. Chem. Soc. 1979, 101, 2297.
41. Wherland, S.; Pecht, I. Biochemistry 1978, 17, 2585.
42. Mauk, A. G.; Scott, R. A.; Gray, H. B. J. Am. Chem. Soc. 1980, 102, 4360.
43. Isied, S.; Worosila, G., Abstracts, New York ACS Meeting, September 1981.
44. Isied, S., Ph.D. Dissertation: Stanford Univ., 1973.
45. Isied, S.; Taube, H. J. Am. Chem. Soc. 1973, 95, 8198.
46. Fisher, H.; Tom, G.; Taube, H. J. Am. Chem. Soc. 1976, 98, 5512.
47. Rieder, K.; Taube, H. J. Am. Chem. Soc. 1977, 99, 7391.
48. Isied, S.; Vassilian, A.; Lyon, J. J. Am. Chem. Soc., submitted for publication.
49. Isied, S.; Kuehn, C. J. Am. Chem. Soc. 1978, 100, 6752.
50. Endicott, J. F.; Durham, B.; Kumar, K. Inorg. Chem. 1982, 21, in press.
51. Chou, M.; Creutz, C.; Sutin, N. J. Am. Chem. Soc. 1977, 101, 847.
52. Brunshwig, B. S.; Logan, J.; Newton, M. D.; Sutin, N. J. Am. Chem. Soc. 1980, 102, 5798.
53. Newton, M. D. Int. J. Quantum Chem., Quantum Chem. Symp. 1980, No. 14, 364.
54. Endicott, J. F.; Durham, B.; Glick, M. D.; Anderson, T. J.; Kuszaj, J. M.; Schmonsees, W. G.; Balakrishnan, K. P. J. Am. Chem. Soc. 1981, 103, 1431.
55. Buhks, E.; Bixon, M.; Jortner, J.; Navon, G. Inorg. Chem. 1979, 18, 2014.
56. Endicott, J. F.; Heeg, M. J.; Goswick, D. C.; Pyke, S. C. J. Phys. Chem. 1981, 85, 1777.
57. Endicott, J. F.; Gaswick, D. C.; Heeg, M. J.; Pyke, S. C. J. Am. Chem. Soc., submitted for publication.
58. Endicott, J. F.; Heeg, M. J.; Gaswick, D. C.; Brubaker, G. R.; Pyke, S. C., work in progress.
59. Förster, Th. Ann. Physik 1948, 2, 55.
60. Dexter, D. L. J. Chem. Phys. 1953, 21, 836.
61. Jørgensen, C. K.; "Orbitals in Atoms and Molecules"; Academic Press: New York, 1962.
62. Balzani, V.; Boletta, F.; Scandola, F. J. Am. Chem. Soc. 1980, 102, 2152.
63. Balzani, V.; Indelli, M. T.; Maestri, M.; Sandrini, D.; Scandola, F. J. Phys. Chem. 1980, 84, 852.
64. Sutin, N. "Inorganic Biochemistry"; Eichhorn, G. L., Ed.; Elsevier: New York, 1973; p 611.
65. Wilson, R. B.; Solomon, E. I. Inorg. Chem. 1978, 17, 1729.
66. Mulliken, R. S.; Person, W. B. "Molecular Complexes"; Wiley-Interscience: New York, 1969.

RECEIVED April 21, 1982.

Further Developments in Electron Transfer

R. A. MARCUS and PAUL SIDERS

California Institute of Technology, Arthur Amos Noyes Laboratory of Chemical Physics, Pasadena, CA 91125

The inverted region in electron transfer reactions is studied for the reaction of electronically-excited ruthenium(II) tris-bipyridyl ions with various metal(III) tris-bipyridyl complexes. Numerical calculations for the diffusion-reaction equation are summarized for the case where electron transfer occurs over a range of distances. Comparison is made with the experimental data and with a simple approximation. The analysis reveals some of the factors which can cause a flattening of the $\ln k_{\text{obs}}$ versus ΔG° curve in the inverted region. Ways of improving the chance of observing the effect are discussed.

Some time ago it was predicted (1, 2) that, in a series of weak-overlap electron transfer reactions, the rate would first increase when ΔG° was made more negative, and then, when ΔG° became very negative, eventually decrease. Evidence for such an 'inverted effect' has been given in a number of papers (3-11), but in many other studies the reaction rate reaches a limiting value, rather than a decreasing value, when $-\Delta G^{\circ}$ becomes large (e.g., (12-18)). Possible explanations for the latter result have been suggested: (a) alternate pathways for the reaction when ΔG° is very negative [such as H-atom transfer (19, 20), electronically-excited product states (11, 20), or, when the reaction was observed via quenching of fluorescence, exciplex formation (21, 22)], (b) quantum mechanical nuclear tunneling (20, 23-27), (c) masking by diffusion, and (d) reduction of the inverted effect [by electron transfer over a distance (19)].

Quantum mechanical tunneling reduces the magnitude of the predicted effect but does not eliminate it in weak-overlap sys-

0097-6156/82/0198-0235\$06.00/0
© 1982 American Chemical Society

tems, as one sees, for example, in some recent calculations for an actual experimental system (20). Moreover, there is a 1:1 correspondence between the quantum mechanically calculated charge transfer spectrum (emission or absorption $\text{vs } h\nu$) for a weak overlap redox system and the plot (eq 8 and 9 given later) of k_{act} versus the energy of reaction, ΔE (25), and hence in a series of reactions of given ΔS° , versus $-\Delta G^\circ$. Here, k_{act} is the activation-controlled quantum mechanically calculated rate constant. Thus, the well-known existence of a maximum in the charge transfer vs wavelength spectrum implies that there will be a maximum in the $\ln k_{\text{act}} \text{ vs } -\Delta G^\circ$ plot when the electron transfer is a weak-overlap reaction. This correspondence removes any question that nuclear tunneling would eliminate the inversion, since that tunneling occurs to the same extent in both the charge transfer spectrum and the $k_{\text{act}} \text{ vs } -\Delta G^\circ$ plots, and the former has a well-known maximum. It also removes any argument that large anharmonicities in practice eliminate the effect: the correspondence applies regardless of whether the vibrations are harmonic or anharmonic, as long as the electron transfer is a weak-overlap one. (The effects of having a very strong-overlap electron transfer remain to be investigated.)

In a recent paper, an approximate calculation was made of effects (b) to (d) above (19), using an approximate analytical solution for the diffusion problem, for the case where the reaction occurs readily over a short range of separation distances of the reactants. In the present report, we summarize the results of our recent calculations on a numerical solution of the same problem. A more complete description is given elsewhere (28). One additional modification made here to (19) is to ensure that the current available rate constant data at $\Delta G^\circ = 0$ (Appendix) are satisfied.

Theory

The diffusion-reaction equation for the pair distribution function $g(r,t)$ of the reactants, which react with a rate constant which at any r is $k(r)$, is given by (29-32)

$$\frac{\partial g(r,t)}{\partial t} = \frac{1}{r^2} \frac{\partial(r^2 J_r)}{\partial r} - k(r)g(r,t) \quad (1)$$

where J_r is the inward radial flux density (per unit concentration) due to diffusion and to any forced motion arising from an interaction potential energy, $U(r)$, assumed to depend only on

the separation distance r . The magnitude of J_r is given by

$$\begin{aligned} J_r &= D \frac{\partial g}{\partial r} + \frac{Dg}{k_B T} \frac{dU}{dr} \\ &\equiv De^{-U/k_B T} \frac{\partial}{\partial r} (g e^{U/k_B T}) \end{aligned} \quad (2)$$

where D is the sum of the diffusion constants of the two reactants.

The observed rate constant, k_{obs} , at time t is then given by (31, 33)

$$k_{\text{obs}} = \int_0^{\infty} k(r)g(r,t)4\pi r^2 dr \quad (3)$$

The steady-state solution to eq 1 satisfies $\partial g/\partial t = 0$, i.e., it satisfies

$$(1/r^2)d(r^2 J_r)/dr = k(r)g(r) \quad (4)$$

For the experimental conditions investigated thus far, the steady-state solution is an excellent approximation to the solution of eq 1 and we consider this case. However, in proposing some experiments in the picosecond regime to enhance the chance of observing the inverted effect, we consider the time-dependent equation 1.

The rate constant $k(r)$ is typically assumed to depend exponentially on r , varying as $\exp(-\alpha r)$. Theoretical estimates have been made for α of 1.44 \AA^{-1} when there is intervening material between the reactants (34), and 2.6 \AA^{-1} when there is not (35). A recent calculation for the hexaquoiron self-exchange reaction yielded $\alpha = 1.8 \text{ \AA}^{-1}$ (36). Experimentally, the value inferred indirectly for an electron transfer between aromatic systems in rigid media is about 1.1 \AA^{-1} (37).

These values of α are sufficiently large that $k(r)$ falls off rapidly with r . When this "reaction distance" is small relative to the distance over which the function $h(r) = g \exp(U/k_B T)$ changes significantly, i.e., over which $(h(r) - h(\sigma))/(h(\infty) - h(\sigma))$ becomes appreciable, one can introduce an approximate analytic solution to eq 4 (28, 38, 39):

$$\frac{1}{k_{\text{obs}}} = \frac{1}{k_{\text{act}}} + \frac{1}{k_{\text{diff}}} \quad (5)$$

where, in the present case, we have (from eq 3 with $g(r) \equiv 0$ for $r < \sigma$)

$$k_{\text{act}} = \int_{\sigma}^{\infty} k(r) e^{-U/k_B T} 4\pi r^2 dr \quad (6)$$

and where (40)

$$k_{\text{diff}} = 4\pi D / \int_{\sigma}^{\infty} \frac{e^{U/k_B T}}{r^2} dr \quad (7)$$

Equation 5 was actually derived for the case where reaction occurs at some contact distance $r = \sigma$. A derivation of eq 5 for the present case of a volume distributed rate constant $k(r)$ is approximate and is given elsewhere (28).

For $k(r)$ we shall assume at first, as in (19), that the reaction is adiabatic at the distance of closest approach, $r = \sigma$, and that it is joined there to the nonadiabatic solution which varies as $\exp(-\alpha r)$. The adiabatic and nonadiabatic solutions can be joined smoothly. For example, one could try to generalize to the present multi-dimensional potential energy surfaces, a Landau-Zener type treatment (41). For simplicity, however, we will join the adiabatic and nonadiabatic expressions at $r = \sigma$. We subsequently consider another approximation in which the reaction is treated as being nonadiabatic even at $r = \sigma$.

The well-known perturbation theory expression for the non-adiabatic rate constant is given by (25, 42-45)

$$k(r) \cong \frac{2\pi}{\hbar} |V(r)|^2 (\text{F.C.}) \quad (8)$$

where (F.C.) is the Franck-Condon factor and $V(r)$ is the electronic matrix element for the electron transfer. (F.C.) is given by

$$(\text{F.C.}) = \frac{1}{Q} \sum_{i,f} e^{-E_i/k_B T} |\langle i|f \rangle|^2 \delta(E_f - E_i + \Delta E) \quad (9)$$

where i and f denote initial and final (reactants' and products') nuclear configuration states, including those of the solvent; ΔE is the energy of reaction; and Q is $\sum_i \exp(-E_i/k_B T)$. The solvent will be treated classically (1) to avoid the quantum harmonic oscillator treatment of the polar solvent which is sometimes used. (The latter yields a large error for ΔS° when ΔS° is large (46)). The contribution of the polar solvent to the Franck-Condon factor is (42, cf. 1)

$$(\text{F.C.})_{\text{solvent}} = (4\pi\lambda_{\text{out}} k_B T)^{-\frac{1}{2}} \exp[-(\Delta G^{0''} + \lambda_{\text{out}})^2 / 4\lambda_{\text{out}} k_B T] \quad (10)$$

where $\Delta G^{0''} = \Delta G^{\circ} + E_f^{\text{v}} - E_i^{\text{v}}$ and the superscript v denotes (inner shell) vibrational energy.

The matching of the adiabatic and nonadiabatic expressions for $k(r)$ at $r = \sigma$ yields a value for $V(\sigma)$ given by (28)

$$\frac{2\pi}{\hbar} |V(\sigma)|^2 (4\pi\lambda k_B T)^{-\frac{1}{2}} \sim 10^{13} \text{ s}^{-1} \quad (11)$$

and, for a reorganization parameter λ of about 70 kJ/mol, yields $|V(\sigma)| \sim 0.023$ eV. This value and

$$|V(r)|^2 = |V(\sigma)|^2 \exp[-\alpha(r - \sigma)] \quad (12)$$

were introduced into eq 8 as our first approximation to $V(r)$.

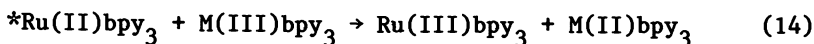
The series of electron transfer reactions (14) for which we calculated rate constants involve quenching of the lowest excited electronic state of $\text{Ru}(\text{bpy})_3^{2+}$. This $^* \text{Ru}(\text{II})$ state is a metal-to-ligand charge-transfer state (47, 48) in which an excess electron appears to be localized on one of the bipyridyl ligands (49), and this electron may be transferred to a metal-centered orbital on the oxidant, at least when an unexcited oxidant is formed. A calculation of the distance dependence of $V(r)$ for this particular transfer would be desirable, but lacking that the simple exponential form indicated in eq 12 has been used instead.

The actual numerical integration of eqs 2 and 4 was performed by converting eq 4 to a pair of ordinary differential equations, then using a standard integration routine (50) for integrating the latter, integrating outward from $r = \sigma$ to large r until $g(r)$ had its correct functional value at large r , $g(r) \sim 1 - c/r$ where c is a constant. (This functional form is the solution of eqs 2 and 4 at r large enough that $k(r) = U(r) = 0$ and for U vanishing more rapidly than $1/r$.) Because $g(\sigma)$ was unknown to a multiplicative constant initially, we actually performed the integration for a function $G(r) = g(r)c_1$, with c_1 unknown and with a preassigned value for $G(r)$ at $r = \sigma$. The terms c_1 and c could be determined from the numerical values of G at large r , and then $g(r) = G(r)/c_1$. The value of k_{obs} was calculated from the total flux at $r = \infty$:

$$k_{\text{obs}} = 4\pi D \lim_{r \rightarrow \infty} \left(r^2 \frac{dg}{dr} \right) = 4\pi D c \quad (13)$$

Results

Calculations were performed for the system studied by Creutz and Sutin (9)



where the bpy's are various bipyridyls, M is one of several metals, and the asterisk denotes an electronically-excited molecule. The question we address is how, for a model which has the "experimental" rate constant at $\Delta G^0 = 0$ ($k_{obs} \sim 4 \times 10^8 \text{ M}^{-1} \text{ s}^{-1}$) (Appendix) and the observed diffusion-limited rate constant ($k_{diff} \sim 3.5 \times 10^9 \text{ M}^{-1} \text{ s}^{-1}$) (9), do the values predicted for k_{obs} at quite negative ΔG^0 's compare with those calculated from eq 5 and with the experimental results? Is the effect of electron transfer over a range of distances sufficiently large to explain the observed results (i.e., very little fall-off of rate constant with increasing $-\Delta G^0$'s)?

We use a λ_{in} of 15.5 kJ/mol associated with a frequency of 1300 cm^{-1} (20), and λ_{out} of 54 kJ/mol at $r = \sigma$ (51). All calculations were performed with $T = 298\text{K}$. The dependence of λ_{out} on r (2) is incorporated in the calculation. An equilibrium Debye-Hückel expression for the ion-atmosphere-shielded Coulombic repulsion of the reactants is assumed (52, 53), given by

$$U(r) = \frac{z_1 z_2 e_0^2}{\epsilon r} \frac{e^{-\kappa a}}{(1 + \kappa a)} e^{-\kappa r} \quad (15)$$

for the case where the two reactants have the same radius. Here, κ is the reciprocal of the Debye-Hückel screening length, ϵ is the static dielectric constant, the $z_i e_0$ values are the ionic charges of the reactants, and a is the distance of closest approach of the ions in the ion atmosphere to a reactant ion. The distance a is $r_i + r_a$, where r_i is the radius of a reactant ion and r_a is the radius of the principal ion of opposite sign in the ionic atmosphere. When $r_i \geq r_a$, a lies between $2r_i$ and r_i , being $2r_i$ when $r_i = r_a$ and being r_i when $r_a = 0$. Using the current approximate radii we shall, for concreteness, take $a = 3\sigma/4$. (In eq 15 the reactants are assumed to have the same radius. A more general expression than eq 15 is cited in ref. 28). At the prevailing ionic strength of about 0.52 M, κ^{-1} is about 4.2 \AA . Because of this large ionic strength, $U(r)$ is quite small, even at $r = \sigma$.

Using $\alpha = 1.5 \text{ \AA}^{-1}$ and, at first, $V(\sigma) = 0.023 \text{ eV}$, k_{act} at $\Delta G^0 = 0$ is found to be $1.2 \times 10^{10} \text{ M}^{-1} \text{ s}^{-1}$ which is substantially

higher than the current experimental value (Appendix) of $\text{ca } 4 \times 10^8 \text{ M}^{-1} \text{ s}^{-1}$. Assuming the validity of the latter, either $V(\sigma)$ is less than 0.023 eV, i.e., the reaction is not adiabatic at the contact distance $r = \sigma$, or λ is higher than estimated, or eq 15 underestimates $U(r)$. We consider first using a different $V(\sigma)$, namely, 0.0045 eV, which yields the current "experimental" rate constant at $\Delta G^\circ = 0$. (The same final results for the $\ln k_{\text{obs}}$ vs ΔG° plot would be obtained, essentially, if one used instead a different $U(\sigma)$, as long as there is agreement of k_{act} at $\Delta G^\circ = 0$.)

The numerical solution of eq 4 and the rate constant data of Figure 1 agree at the data's maximum ($\sim 3.5 \times 10^9 \text{ M}^{-1} \text{ s}^{-1}$) when one chooses $3.0 \times 10^{-6} \text{ cm}^2 \text{ s}^{-1}$ for the sum of the D 's of the two reactants. This D is somewhat near those estimated rather indirectly (electrochemically) for the individual D 's of ferric and ferrous phenanthroline complexes ($\sim 1.9 \times 10^{-6}$ and $3.7 \times 10^{-6} \text{ cm}^2 \text{ s}^{-1}$, respectively) (54).

Since reaction may also yield electronically-excited products when ΔG° is sufficiently negative, we include this reaction, as we did in (20). The mean excitation energy used for the formation of the electronically-excited Ru(III) product is 1.76 eV (20). As has been explained elsewhere (20, 28), the formation of the other possible electronically excited products is, in most cases at least, less probable. The same $V(r)$ was used for formation of electronically excited $\text{Ru}(\text{bpy})_3^{3+}$ as for formation of other products because the detailed information necessary to make a distinct estimate for $V(r)$ was lacking.

We first compare the present numerical results for the solution of the steady-state eqs 3 and 4 with the approximate solution given by eqs 5, 6 and the experimental value for k_{diff} . The results agreed to about three percent when ΔG° was varied from +0.6 to -3.0 eV. The experimental value for k_{diff} and eq 7 imply a value of $D = 3.5 \times 10^{-6} \text{ cm}^2 \text{ s}^{-1}$, compared with the $3.0 \times 10^{-6} \text{ cm}^2 \text{ s}^{-1}$ found when eqs 3 and 4 were solved. Had the same D been used for both the exact (eqs 3, 4) and the approximate (eq 5) solutions, their agreement for the rate constants would have been about 10% instead of 3%, which is still very close.

The results of solving eqs 3 and 4 are next compared with the experimental data in Figure 1 (9), using $V(\sigma) = 0.0045 \text{ eV}$. The solid line refers to the formation of ground state products, and the dotted line to the formation of an electronically-excited Ru(III) product. For further comparison with the solid

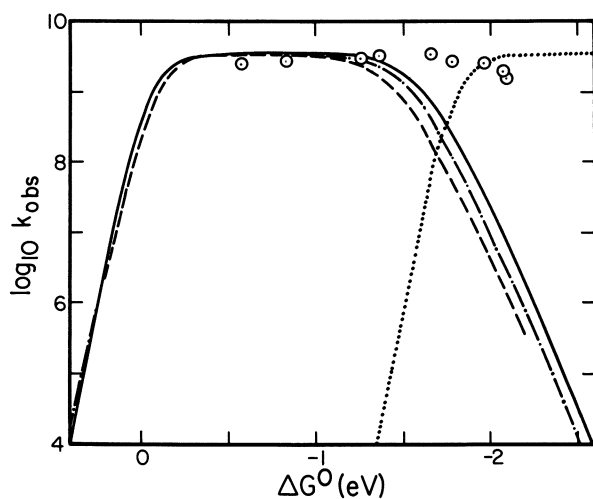


Figure 1. Calculated and experimental rate constants for Reaction 14 vs. ΔG° . Key: —, r -dependent λ_{out} ; — · —, fixed λ_{out} ; ---, from Ref. 1 in which reaction occurred only at $r = \sigma$; and · · ·, current result (r -dependent λ_{out}) for formation of an electronically excited product.

line, a calculation was made with λ_{out} held fixed (54 kJ/mol, the value at $r = \sigma$) and is given by the dash-dot line. In order to obtain agreement with the solid line at $\Delta G^{\circ} = 0$, $V(\sigma)$ was reduced to 0.0039 eV in calculating the dash-dot line. The dashed line is the result of a calculation (20) in which reaction was treated as occurring adiabatically, but only at some contact distance σ , and in which eq 5 was used, together with the experimental value for k_{diff} . The λ_{out} value used for this last curve was again 54 kJ/mol, the present $\lambda_{\text{out}}(\sigma)$.

In Figure 2 we give a comparison of the solid line of Figure 1 with that obtained using $V(\sigma) = 0.023$ eV and a larger $\lambda_{\text{out}}(\sigma) = 83$ kJ/mol). A slightly smaller D ($2.7 \times 10^{-6} \text{ cm}^2 \text{ s}^{-1}$) was required to make the latter calculation yield the experimental value of the maximum observed rate constant, $3.5 \times 10^9 \text{ M}^{-1} \text{ s}^{-1}$. Both curves have the same k_{obs} at $\Delta G^{\circ} = 0$.

Discussion

The results comparing the exact eqs 3 and 4 with the approximate eqs 5 and 6 show that the latter provide a good approximation for the present conditions, at least. The results in Figure 1 show that, to account for the experimental results at very negative ΔG° 's using the present value of λ_{out} (54 kJ/mol), it is necessary to postulate the formation of electronically-excited products. This was also the case in an earlier result (20). The sum of the two rate constants in Figure 1 yields agreement with the data in Figure 1 to a factor of about 2. If, as for the dashed line in Figure 2, the value of λ were actually appreciably larger, the formation of ground state products alone would suffice to obtain agreement. (Classically, the maximum in the k_{act} versus ΔG° curve occurs at $\Delta G^{\circ} = -\lambda$ and so is shifted to more negative ΔG° 's when λ_{out} is increased.)

Returning to Figure 1, one sees that holding λ_{out} fixed at its value at $r = \sigma$ (dash-dot line) does not cause a large deviation from the more correct result (r -dependent λ_{out} , solid line) in the inverted region. A similar approximation was used, of course, for the dashed line, where a $k(\sigma)$ was used instead of a $k(r)$.

We also have explored the solution of the time-dependent eq 1 to study the plot corresponding to Figure 1 when the observation of fluorescence quenching in reaction 14 is made at short times. In these short-time calculations we have assumed, for

simplicity, that reaction occurs only at $r = \sigma$. (Calculations are planned for the case in which electron transfer occurs over a range of distance.) Results for $k_{\text{obs}}(t)$ are given for several times in Figure 3, and curves are also given for the formation of electronically-excited products. The value of $k_{\text{obs}}(t)$ is obtained as the slope at time t of a plot of $[M(\text{III})\text{bpy}_3^{+2}]^{-1} \ln[*\text{Ru}(\text{II})\text{bpy}_3]$ vs t . The results show the enhancement of the predicted inversion effect at small times, and an experimental study of this or related systems at such times would be desirable, and may, in fact, distinguish between the possibilities cited earlier that $V(\sigma) < 0.023$ eV or that $\lambda > (15.5 + 54)$ kJ/mol; at short times there would be a double maximum in the total rate constant versus ΔG° plot in the first case and a single maximum in the second.

The details of these short-time calculations, made for the case that $U(r) \cong 0$, are given elsewhere (28). Searching for the inverted effect in unimolecular systems (reactants linked to each other) would also be very desirable since their rates would not be diffusion limited.

Appendix. 'Experimental' Rate Constant at $\Delta G^\circ = 0$

The self-exchange rate constant for reaction 14, when M is Ru and when an excited Ru(II) product is formed, has been estimated (55) to be about $10^8 \text{ M}^{-1} \text{ s}^{-1}$. The self-exchange rate constant for reaction 14, when M is Ru and when the products and reactants are in their ground electronic states, has been estimated (56) to be $1.2 \times 10^9 \text{ M}^{-1} \text{ s}^{-1}$, which is the observed rate constant for the oxidation of $\text{Ru}(\text{bpy})_3^{2+}$ by $\text{Ru}(\text{phen})_3^{3+}$, for which $\Delta G^\circ \sim 0.01$ eV. Corrected for diffusion (eq 5), the k_{act} for the latter is $2 \times 10^9 \text{ M}^{-1} \text{ s}^{-1}$. Sutin (57) has noted that the cross-relation (1, 2) should be applicable to a nonadiabatic electron transfer if the electronic matrix element, $V(r)$, for the cross-reaction is equal to the geometric mean of the matrix elements for the self-exchange reactions. Assuming that that condition is approximately satisfied, the exchange rate constant for reaction 14 when $\Delta G^\circ = 0$ is estimated to be the geometric mean, $(20 \times 1)^{\frac{1}{2}} \times 10^8 \text{ M}^{-1} \text{ s}^{-1}$, i.e., $4.5 \times 10^8 \text{ M}^{-1} \text{ s}^{-1}$. Corrected for diffusion using eq 5, this becomes $4 \times 10^8 \text{ M}^{-1} \text{ s}^{-1}$, the value given in the text.

Interestingly enough, the rate constant at $\Delta G^\circ = 0$ for reaction 14 when $*\text{Ru}(\text{II})$ and $M(\text{III})$ are replaced by $*\text{Cr}(\text{III})$ and $\text{Ru}(\text{II})$, respectively, is $\sim 2 \times 10^8 \text{ M}^{-1} \text{ s}^{-1}$ in 1 M H_2SO_4 (10).

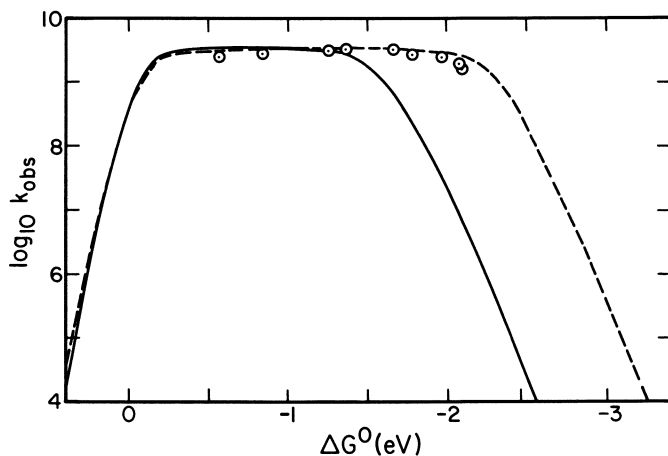


Figure 2. Calculated rate constants for Reaction 14 vs. ΔG° . Key: —, taken from solid line in Figure 1, $V(\sigma) = 0.0045$ eV, $\lambda_{out}(\sigma) = 54$ kJ/mol; and ---, $V(\sigma) = 0.023$ eV and $\lambda_{out}(\sigma) = 83$ kJ/mol.

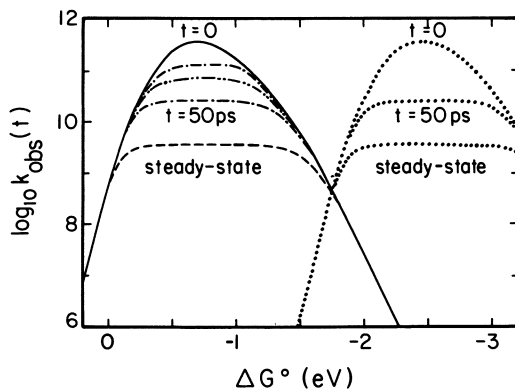


Figure 3. Time-dependent calculations of $k_{obs}(t)$ vs. ΔG° for various observation times. Key: ---, 1 ps; - · - ·, 5 ps; and · · ·, $k_{obs}(t)$ for formation of an excited-state Ru(III).

Acknowledgment

It is a pleasure to acknowledge support of this research by a grant from the National Science Foundation. Contribution No. 6494 from the California Institute of Technology.

Literature Cited

1. Marcus, R. A. Discuss. Faraday Soc. 1960, 29, 21.
2. Marcus, R. A. J. Chem. Phys. 1965, 43, 2654.
3. Allen, A. O.; Gangwer, T. E.; Holroyd, R. A. J. Phys. Chem. 1975, 79, 25.
4. Henglein, A. Can. J. Chem. 1977, 55, 2112.
5. Lipsky, S. J. Chem. Ed. 1981, 58, 93.
6. Frank, A. J.; Grätzel, M.; Henglein, A.; Janata, E. Ber. Bunsenges. Phys. Chem. 1976, 80, 294.
7. Frank, A. J.; Grätzel, M.; Henglein, A.; Janata, E. Ber. Bunsenges. Phys. Chem. 1976, 80, 547.
8. Ulstrup, J. "Charge Transfer Processes in Condensed Media, Lecture Notes in Chemistry, No. 10"; Springer-Verlag: New York, 1979; pp. 163-4.
9. Creutz, C.; Sutin, N. J. Am. Chem. Soc. 1977, 99, 241.
10. Brunshwig, B.; Sutin, N. J. Am. Chem. Soc. 1978, 100, 7568.
11. Beitz, J. V.; Miller, J. R. J. Chem. Phys. 1979, 71, 4579.
12. Rehm, D.; Weller, A. Israel J. Chem. 1970, 8, 259.
13. Romashov, L. V.; Kiryukhin, Yu. I.; Bagdasar'yan, Kh. S. Doklady Phys. Chem. (Engl. Transl.) 1976, 230, 961.
14. Scheerer, R.; Grätzel, M. J. Am. Chem. Soc. 1977, 99, 865.
15. Ballardini, R.; Varani, G.; Indelli, M. T.; Scandola, F.; Balzani, V. J. Am. Chem. Soc. 1978, 100, 7219.
16. Balzani, V.; Bolletta, F.; Gandolfi, M. T.; Maestri, M. Top. Curr. Chem. 1978, 75, 1.
17. Eriksen, J.; Foote, C. S. J. Phys. Chem. 1978, 82, 2659.
18. Vogelmann, E.; Schreiner, S.; Rauscher, W.; Kramer, H. E. A. Z. Phys. Chem. N. F. 1976, 101, 321.
19. Marcus, R. A. Int. J. Chem. Kin. 1981, 13, 865.
20. Siders, P.; Marcus, R. A. J. Am. Chem. Soc. 1981, 103, 748.
21. Weller, A.; Zachariasse, K. Chem. Phys. Lett. 1971, 10, 590.
22. Jousset-Dubien, J.; Albrecht, A. C.; Gerischer, H.; Knox, R. S.; Marcus, R. A.; Schott, M.; Weller, A.; Willig, F. Life Sci. Res. Rep. 1979, 12, 129.
23. Efrima, S.; Bixon, M. Chem. Phys. Lett. 1974, 25, 34; Chem. Phys. 1976, 13, 447.
24. Van Duyne, R. P.; Fischer, S. F. Chem. Phys. 1974, 5, 183.
25. Ulstrup, J.; Jortner, J. J. J. Chem. Phys. 1975, 63, 4358.

26. Marcus, R. A.; Sutin, N. Inorg. Chem. 1975, 14, 213.
27. Schmickler, W. J. Chem. Soc., Faraday Trans. 2 1976, 72, 307.
28. Marcus, R. A.; Siders, P. J. Phys. Chem. 1982, 86, 622.
29. Waite, T. R. J. Chem. Phys. 1958, 28, 103.
30. Pilling, M. J.; Rice, S. A. J. Chem. Soc., Faraday Trans. 2 1975, 71, 1563.
31. Butler, P. R.; Pilling, M. J.; Rice, S. A.; Stone, T. J. Can. J. Chem. 1977, 55, 2124.
32. Wilemski, G.; Fixman, M. J. Chem. Phys. 1973, 58, 4009.
33. Keizer, J. J. J. Phys. Chem. 1981, 85, 940.
34. Hopfield, J. J. Proc. Nat. Acad. Sci., USA 1974, 71, 3640.
35. Jortner, J. J. Chem. Phys. 1976, 64, 4860.
36. Newton, M. D. Int. J. Quant. Chem.: Quant. Chem. Symp. 1980, 14, 363.
37. Alexandrov, I. V.; Khairutdinov, R. F.; Zamaraev, K. I. J. Chem. Phys. 1978, 32, 123.
38. Noyes, R. M. Progr. Reaction Kinetics 1961, 1, 129.
39. Marcus, R. A. Discuss. Faraday Soc. 1960, 29, 129.
40. Debye, P. Trans. Electrochem. Soc. 1942, 82, 265.
41. Brunschwig, B. S.; Logan, J.; Newton, M. D.; Sutin, N. J. Am. Chem. Soc. 1980, 102, 5798.
42. Kestner, N.; Logan, J.; Jortner, J. J. Phys. Chem. 1974, 78, 2148.
43. Levich, V. G.; Dogonadze, R. R. Collect. Czech. Chem. Commun. 1961, 26, 193.
44. Levich, V. G. "Physical Chemistry: An Advanced Treatise"; Eyring, H.; Henderson, D.; Jost, W., Editors; Academic Press: New York, 1970; Vol. 9B.
45. Dogonadze, R. R.; Kuznetsov, A. M.; Vorotyntsev, M. A. Phys. Status Solidi B 1972, 54, 125, 425.
46. Siders, P.; Marcus, R. A. J. Am. Chem. Soc. 1981, 103, 741.
47. Palmer, R. A.; Piper, T. S. Inorg. Chem. 1966, 5, 864.
48. Lytle, F. E.; Hercules, D. M. J. Am. Chem. Soc. 1969, 91, 253.
49. Sutin, N.; Creutz, C. Adv. Chem. Ser. 1978, No. 168, 1.
50. Gordon, M. K. Sandia Laboratories Report, SAND75-0211. For a discussion of the algorithm, see Shampine, L. F.; Gordon, M. K. "Computer Solution of Ordinary Differential Equations"; Freeman: San Francisco, 1975.
51. Sutin, N. in "Tunneling in Biological Systems"; Chance, B.; DeVault, D. C.; Frauenfelder, H.; Schrieffer, J. R.; Sutin, N.; Eds., Academic Press: New York, 1979; p. 201.
52. Debye, P.; Hückel, E. Physikal Z. 1923, 24, 185.
53. Moore, W. J. "Physical Chemistry"; 4th ed.; Prentice-Hall: Englewood Cliffs, N. J., 1972; eq 10.58.
54. Ruff, I.; Zimonyi, M. Electrochimica Acta 1973, 18, 515.

American Chemical
Society Library

1155 16th St. N.W.

In Mechanistic Aspects of Inorganic Reactions; Korabacher, D., et al.; ACS Symposium Series 143; American Chemical Society: Washington, DC, 1982.

Washington, D.C. 20036

55. Lin, C-T.; Bottcher, W.; Chou, M.; Creutz, C.; Sutin, N. J. Am. Chem. Soc. 1976, 98, 6536.
56. Young, R. C.; Keene, F. R.; Meyer, T. J. J. Am. Chem. Soc. 1977, 99, 2468.
57. Sutin, N. Acc. Chem. Res. 1968, 1, 225.

RECEIVED April 21, 1982.

General Discussion—Further Developments in Electron Transfer

Leader: P. P. Schmidt

DR. THOMAS MEYER (University of North Carolina): One experimentally valid approach to this problem of the inverted region begins with a systematic study of a series of related metal bipyridine charge transfer excited states. In these excited states there are ruthenium(III) or osmium(III) cores bound, if you will, to a ligand radical anion. By making variations in the other four ligands of these six-coordinate complexes it is possible to vary systematically the energy gap (i.e., the spacing between the upper level surfaces) and to measure radiationless decay rates from lifetime and quantum yield measurements. The results show that good linear correlations exist between $\ln k_{nr}$ and ΔE in agreement with the weak vibrational coupling limit expression derived by Englman and Jortner [Englman, R.; Jortner, J. Molec. Phys. 1970, 18, 145; cf., Curtis, J. C.; Bernstein, J. S.; Schmehl, R. H.; Meyer, T. J. Chem. Phys. Lett. 1981, 81, 48].

DR. LESLIE DUTTON (University of Pennsylvania): I am intrigued by the fact that people have not taken Beitz and Miller's data more seriously [Beitz, J. V.; Miller, J. R. J. Chem. Phys. 1979, 71, 4579]. Miller showed that it is possible to find a data set for similar chemicals going two or three orders of magnitude over the hump. Why are those data being ignored?

DR. SIDERS: The data of Beitz and Miller are very interesting but I feel uncertain about their correct interpretation because the measurements were for transfer of an electron from a solvent trap rather than from a molecule. Also, there's lot of scatter in the data, although they do seem to show inversion. Finally, the data were obtained in a 2-methyl-tetrahydrofuran glass at 77°K, which may differ significantly from water at room temperature.

DR. MARSHALL NEWTON (Brookhaven National Laboratory): I'd like to ask a question about Hopfield's numbers. The alpha parameter from his 1974 paper [Hopfield, J. J. Proc. Natl. Acad. Sci., USA 1974, 71, 3640] was based not on the direct metal-metal interaction but rather was based on carbon-carbon overlap because it was two carbons which were closest together in his electron transport system. In contrast, Dr. Sutin gave some different numbers based on metal orbitals. Depending on whether one is interested in carbon-carbon overlap between two organic rings, or in direct metal-metal overlap, one might or might not opt for the Hopfield parameters. However, at the level of fuzziness which we have, it may not make any difference, I realize.

DR. SIDERS: The edge atoms on the rings of the tris-bipyridyl complexes that we considered are a long way out from the central metal ions. For that reason we thought that an estimate such as Hopfield's, based on a carbon-carbon overlap, would be more appropriate than one based on a metal-metal overlap.

DR. EPHRAIM BUHKS (University of Delaware): I would like to mention briefly some recent work which demonstrates that quantum-mechanical calculations really can provide a basis for understanding the mechanism of slow electron exchange in systems such as $\text{Co}(\text{NH}_3)_6^{3+,2+}$ [Buhks, E.; Bixon, M.; Jortner, J.; Navon, G. *Inorg. Chem.* 1979, **18**, 2014].

The electron transfer rate can be represented in terms of a product of the electron exchange matrix element and Franck-Condon factors; the latter takes into account the contributions of solvent polarization and intramolecular-vibrational modes both of the acceptor and donor ions. These factors, in general, incorporate the contribution of the frequency change. The detailed calculation, considering 30 vibrational modes, demonstrates that the frequency change is not very important for this electron-exchange reaction. It rather provides some small factor of 10^{-1} or so. The most important term, which includes the exponential of the square of the change in metal-ligand bond distances, is responsible for the eight orders of magnitude ratio between Franck-Condon factors for the $\text{Ru}(\text{NH}_3)_6^{3+,2+}$ and $\text{Co}(\text{NH}_3)_6^{3+,2+}$ exchange. The other contribution which should be taken into account is the electron exchange matrix element. Electron exchange between the ground states of $\text{Co}(\text{NH}_3)_6^{3+}$ and $\text{Co}(\text{NH}_3)_6^{2+}$ is spin forbidden. For this reason, the true electronic states should take into account a combination of the ground state with excited electronic states for both $\text{Co}(\text{II})$ and $\text{Co}(\text{III})$.

Thus, in the calculation of the electron exchange matrix element, an additional factor of 10^{-4} appears due to the mixing of the ground states with excited states and their cross terms. Altogether, theoretically, one can account for the 12 orders of magnitude difference in the reactivity of the ruthenium and cobalt couples.

An additional concern arises in regard to any differences which may exist between the classical theory and the quantum-mechanical approach in the calculation of the Franck-Condon factors for symmetrical exchange reactions. In fact, the difference is not very large. For a frequency of 400 cm^{-1} for metal-ligand totally symmetric vibrational modes, one can expect

only one order of magnitude difference between rate constants calculated using classical and quantum-mechanical models for systems exhibiting such large changes in metal-ligand distance as exhibited by the $\text{Co}(\text{NH}_3)_6^{3+,2+}$ couple [Buhks, E.; Bixon, M.; Jortner, J.; Navon, G. *J. Phys. Chem.* 1981, **85**, 3759]. On the other hand, if one considers the variation of activation energy with electronic energy gap, one finds a very large discrepancy between the quantum-mechanical and classical approaches for very exothermic reactions at room temperature (see Figure 1).

A further exploration of the nuclear tunneling phenomena was presented in the study of deuterium isotope effects on electron-exchange reactions [Buhks, E.; Bixon, M.; Jortner, J. *J. Phys. Chem.* 1981, **85**, 3763]. The main cause of the isotope effect on the rate of electron exchange originates from the changes in the metal-ligand vibrational frequencies which are induced by a change of the mass of the ligand. The effect also depends on the changes in the metal-ligand equilibrium configurations accompanying electron transfer and on temperature. For a system characterized by a substantial change in the metal-ligand distance, such as $\text{Co}(\text{NH}_3)_6^{3+,2+}$, $k_{\text{H}}/k_{\text{D}}$ changes from ~ 1.3 at room temperature to ~ 30 at fairly low temperatures, while it is unity in the high temperature classical limit. In the temperature range $0^\circ\text{-}70^\circ\text{C}$ it is expected that $\ln(k_{\text{H}}/k_{\text{D}})$ should decrease as T^{-3} . The deuterium isotope effect, $k_{\text{H}}/k_{\text{D}}$, exhibits a maximum for the symmetric electron exchange reactions, and decreases for activationless and barrierless reactions (see Figure 2).

These predictions can provide an experimental test of the mechanism for quantum-mechanical tunneling effects on electron transfer processes in solution and in glasses over a wide temperature range.

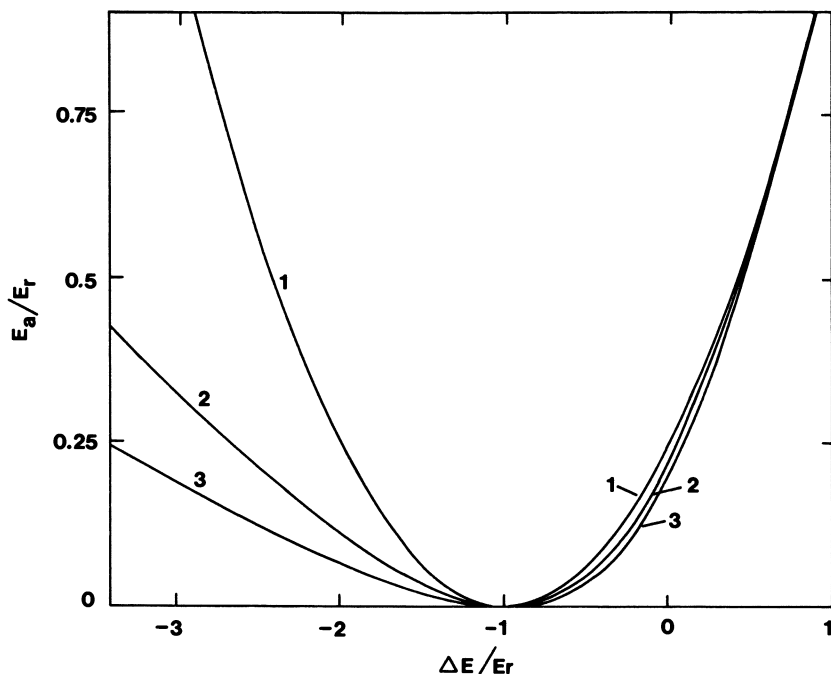


Figure 1. Activation energy of electron-transfer process as a function of electronic energy gap of a reaction. $E_r = E_a + E_c$ is the total reorganization energy where E_a is the classical solvent reorganization energy and E_c is the reorganization energy of an intramolecular mode, $\hbar\omega_c = 2k_B T$, at room temperature. Curve 1 ($E_c = 0$) represents a classical case; curve 3 ($E_a = 0$) represents quantum effects at room temperature; and curve 2 ($E_a = E_c = E_r/2$) represents the interference of the two previous cases.

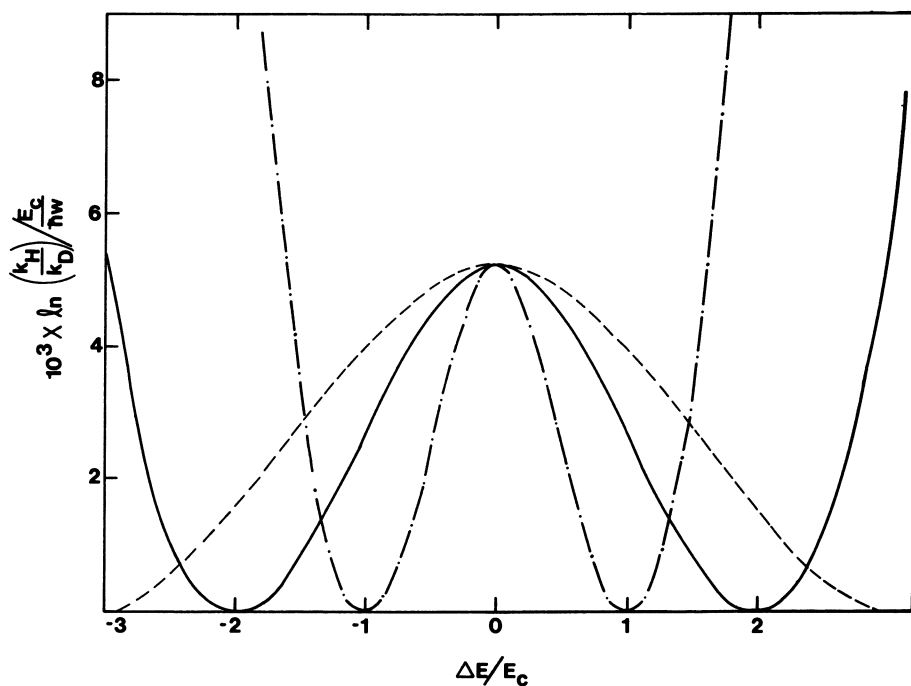


Figure 2. Deuterium isotope effect for electron transfer between ammine complexes as a function of the reduced electronic energy gap $\Delta E/E_c$ where E_r is the total reorganization energy $E_r = E_s + E_c$. Key for parameters: $-\cdot-$, $h\nu_H/k_B T = 2.0$ and $E_s/E_c = 0$; $—$, $E_s/E_c = 1$; and $- - -$, $E_s/E_c = 2$.

Mechanistic Studies of Electron Exchange Kinetics Using Ab Initio Electronic Structure Techniques

MARSHALL D. NEWTON

Brookhaven National Laboratory, Department of Chemistry, Upton, NY 11973

The rate constant for the aqueous Fe^{2+} - Fe^{3+} electron exchange reaction is calculated as $k_{\text{ex}} = \int 4\pi r^2 g(r) k_{\text{el}}(r) dr$, where k_{el} is the first-order rate constant for outer-sphere exchange when the Fe complexes are separated by r and $g(r)$ is the pair distribution function for the reacting inner-sphere complexes. A simple primitive model is employed for $g(r)$ and the effective contact distance (r_{min}) is taken as 5.5 \AA , the value at which the staggered face-to-face configuration of the "octahedral" complexes achieves van der Waals contact (via the water hydrogen atoms). The electronic contributions to $k_{\text{el}}(r)$ are obtained from large scale ab initio molecular orbital calculations carried out for the diabatic states of the reactive ion pair. The calculated rate constant, k_{ex} , and associated activation parameters are in good agreement with experimental data extrapolated to zero ionic strength and correspond to a mechanism dominated by direct Fe-Fe overlap and characterized by a modest degree of nuclear tunnelling and non-adiabatic behavior.

The theoretical aspects of electron transfer mechanisms in aqueous solution have received considerable attention in the last two decades. The early successes of Marcus (1, 2), Hush (3, 4), and Levich (5) have stimulated the development of a wide variety of more detailed models, including those based on simple transition state theory, as well as more elaborate semi-classical and quantum mechanical models (6-12).

0097-6156/82/0198-0255\$07.25/0
© 1982 American Chemical Society

Although many of these theories take formal cognizance of the central role played by atomic and molecular orbitals in the primary act of electron hopping, to date very few attempts have been made to evaluate quantitatively the off-diagonal electronic matrix elements, H'_{AB} , which arise from these orbitals. For the general case of non-orthogonal functions ($S_{AB} \neq 0$), the particular form of the matrix element required is

$$H'_{AB} = (H_{AB} - S_{AB}H_{AA}) / (1 - S_{AB}^2) \quad (1)$$

where $H'_{AB} = \int \psi_A H_{el} \psi_B d\tau$, $S_{AB} = \int \psi_A \psi_B d\tau$, H_{el} is the electronic Hamiltonian for the whole system, and the wavefunctions ψ_A and ψ_B characterize the reactant and product states, respectively (11). A quantitative determination of such matrix elements (to be elaborated below) is of crucial importance because it not only allows an absolute evaluation of the desired rate constants but also helps to reveal the qualitative aspects of the mechanism. In particular, questions regarding the magnitude of electronic transmission factors and the relative importance of ligands and metal ions in facilitating electron exchange between transition metal complexes can be assessed from a knowledge of H'_{AB} .

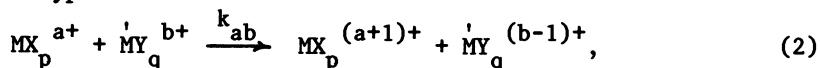
In this paper we demonstrate the feasibility of applying the techniques of ab initio molecular quantum mechanics in a determination of matrix elements and other electronic properties which give insight into the mechanism of electron exchange reactions. In addition, general kinetic formalisms are adopted which permit the overall rate constant to be calculated for bimolecular electron exchange reactions in polar solvents. Initial accounts of some of this work are given in refs (11) and (13).

The general approach is illustrated in detail for the case of aqueous ferrous and ferric ions, and the calculated rate constant and activation parameters are found to be in good agreement with the available experimental data. The formalisms we have employed in studying such complicated condensed phase processes necessarily rely on numerous approximations. Furthermore, some empirical data have been used in characterizing the solvated ions. We emphasize, nevertheless, that (1) none of the parameters were obtained from kinetic data, and (2) this is, as far as we are aware, the first such theoretical determination to be based on fully ab initio electronic matrix elements, obtained from large scale molecular orbital (MO) calculations. A molecular orbital study of the analogous hexaquo chromium system has been carried out by Hush, but the calculations were of an approximate, semi-empirical nature, based in part on experi-

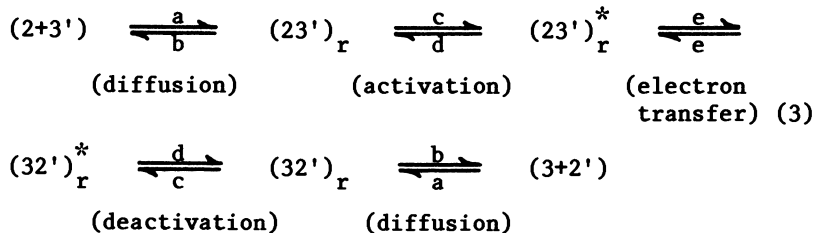
mental ESR data (4). A previous study of the MnO_4^{1-} - MnO_4^{2-} system attempted to exploit the results of earlier ab initio MO results (14). However, the calculation of the necessary matrix elements apparently involved some drastic numerical approximations.

General Considerations

Our basic goal is to understand the kinetics of reactions of the type



occurring in polar solvents between transition metal complexes, MX_p^{a+} and MY_q^{b+} . The overall process summarized in eq 2 is of course a composite of many individual steps. Since our primary focus in the remainder of this paper is the Fe^{2+} - Fe^{3+} electron exchange in aqueous solution, we illustrate the various steps for the case $a=2$, $b=3$ in eq 3, using the following shorthand: $(2+3')$ \equiv separated reactants; $(23')_r$ \equiv the reactive pair characterized by ion-ion separations between r and $r+dr$; the asterisk denotes activation or reorganization of solvent and/or inner-sphere modes associated with the reactive ion pair; and reactants $(2+3')$ and products $(3+2')$ are assumed to be distinguishable by an isotopic label (denoted by the prime).



In order to make things a bit more concrete at this point we display in Figure 1 a sterically favorable configuration for a reactive ion pair (11). Only the 3d atomic orbitals most directly involved in the electron exchange are shown. The theoretical model developed here is based on a so-called "outer-sphere" mechanism, in which the inner-sphere reactants preserve their integrity in the course of the exchange reaction (aside from bond distortions associated with the activation step). The difference in equilibrium FeO distances in the Fe^{2+} and Fe^{3+} complexes is $\sim 0.14 \text{ \AA}$ (based either on crystallographic data (15) or ab initio calculations (13)) and leads to an appreciable inner-sphere contribution to the activation energy.

In general, the effective overall rate constant associated with loss of reactants can be expressed in terms of the individual rate constants a - e in eq 3 by use of the steady state approximation. Simpler expressions can be obtained if the species related by diffusion (a, b) and activation (c, d) processes are assumed to be in thermal equilibrium. In such a case one finds straightforwardly that the effective first order rate constant, $k_{e1}(r)$, for electron transfer at separation r can be written as

$$k_{e1}(r) = \{c(r)/d(r)\}e(r) \quad (4)$$

and the overall bimolecular rate constant, k_{ex} , can be written as

$$k_{ex} = \int_{r_{\min}}^{\infty} 4\pi r^2 g(r) k_{e1}(r) dr \quad (5)$$

where

$$4\pi r^2 g(r) = a(r)/b(r) \quad (6)$$

and $g(r)$ is the radial pair distribution function for the reactive species (the rate constant for formation of ion pairs with separations in the range r to $r + dr$ is $a(r)dr$); $g(r)$ can be expressed as

$$g(r) = \exp(-\bar{u}(r)/k_B T) \quad (7)$$

where $\bar{u}(r)$ is the potential of mean force between reactants (12). The expression for the overall rate constant, k_{ex} , clearly implies some sort of spherical averaging of the reacting ions (11, 12). This point is considered in more detail in the next section where the definition of r_{\min} is also discussed.

The assumptions of equilibrium implicit in eqs 4-7 are justifiable in the case of the aqueous Fe^{2+} - Fe^{3+} reaction because the rate constant for electron transfer between activated species (e) is small by comparison with the relaxation rate associated with the activation processes (11, 12), and because the first-order rate constant $k_{e1}(r)$ is small by comparison with the diffusion rate constant b . Clearly, neither of these assumptions need be valid in cases of more rapid electron transfer (12).

Eq 5 reveals at a glance the two major components of the desired rate constant: the primary electron-hopping rate constant, $k_{e1}(r)$, which involves quantum and statistical mechanics associated with both heavy atom and electronic motion; on

the one hand, and the distribution of reactive species as governed by $g(r)$, which at some level involves all the statistical mechanical aspects of aqueous solutions, on the other. Although our major interest lies in the quantum chemical aspects of $k_{el}(r)$, a detailed consideration of both $g(r)$ and $k_{el}(r)$ is clearly necessary for any meaningful determination of k_{ex} . Accordingly, we discuss some aspects of the radial distribution of reactants in the next section before turning to a detailed formulation of $k_{el}(r)$.

Radial Distribution of Reactants

We confine our attention to the limit of zero ionic strength (i.e., an extremely dilute solution of reactants) and make comparison with experimental data extrapolated to zero ionic strength (10, 11). Furthermore, a very simple primitive model is employed in which $\bar{u}(r)$ in eq 7 is expressed as

$$\bar{u}(r) = (2)(3)/(D_s r) \quad (8)$$

where D_s is the static dielectric constant of bulk water. Such a model for $\bar{u}(r)$ can certainly be improved, but eq 8 is felt to be useful for the initial assessment of the Fe^{2+} - Fe^{3+} exchange kinetics presented here and in ref (11). (In a recent study, Tembe, Friedman and Newton (12) have investigated the use of much more elaborate models for $\bar{u}(r)$, which can be extended to solutions of moderate ionic strength).

Most previous studies have not employed the integral form of the rate constant, eq 5, because detailed information regarding the radial dependence of $k_{el}(r)$ was lacking. Instead, various non-integral forms were postulated, eq 9, which require the identification of some optimal reactant separation, \bar{r} :

$$k_{ex} = v(\bar{r})g(\bar{r})k_{el}(\bar{r}) \quad (9)$$

where $v(\bar{r})$ is the effective volume of the reactive ion pair (16). In view of the radial symmetry assumed in eq 5, one may further specify $v(\bar{r})$ in terms of an effective width, Δr ,

$$v(\bar{r}) = 4\pi\bar{r}^2\Delta r \quad (10)$$

The most probable r value is determined by the competition between $r^2g(r)$, which generally increases with r , and $k_{el}(r)$ which

is dominated by the exponentially decaying matrix element, H_{AB}' (11). In lieu of other specific information, \bar{r} is generally considered to be the "contact" separation of the reactants (1-8).

An effective spherical model is sometimes adopted (11, 17, 18) in which

$$v(\bar{r}) = (4/3)\pi\bar{r}^3 \quad (11)$$

In terms of eq 10, eq 11 implies $\Delta r = \bar{r}/3$, which in many actual situations leads to an exaggerated rate constant if \bar{r} is constrained to be the value of r which maximizes the integrand of eq 5 (12). Conversely, if \bar{r} is determined by requiring eq 9 in conjunction with eq 11 to yield the same value for k_{ex} as that given by the correct expression, eq 5, the resulting \bar{r} value will be somewhat too large in the sense that one will tend to underestimate the value of the "effective" electronic matrix element, $H_{AB}'(\bar{r})$.

Interpenetration of Reactants. A detailed structural examination (Figure 1) reveals the inherent difficulties in attempting to define a "contact" separation for reactants of the type considered here. In spite of the deceptively high symmetry (e.g., the T_h point group assumed in Figure 1 and (13)), the hexahydrate ions are seen to be far from spherical. Thus, adopting van der Waals contact between the protons of the two reacting complexes as the criterion for contact (11) (i.e., $r_{H \cdots H} = 2.4 \text{ \AA}$ (19)), we find that apex-to-apex contact leads to a value of $r \sim 7.4 \text{ \AA}$, somewhat longer than the traditional value of 6.9 \AA , whereas a staggered face-to-face approach, as in Figure 1, yields contact at $\sim 5.5 \text{ \AA}$ (11). Further structural analysis has suggested 4.5 \AA as being a lower limit for the closest possible contact of two hexa-hydrate complexes (12). Analysis of NMR relaxation of alkali ions caused by transition metal ions with $S > 1/2$ has also indicated that closest contact distances of aqueous ions are substantially smaller than those inferred from contact of the envelopes of the inner hydration shells (20).

The occurrence of significant interpenetration of solvent shells has several kinetic implications: clearly all r -dependent contributions will be affected, especially the exponentially varying matrix elements (H_{AB}'). Another consequence of the non-spherical nature of the reactant species is the need to consider a kinetic steric factor which takes account of the reduced statistical significance of interpenetrating structures as rotational degrees of freedom become increasingly restricted

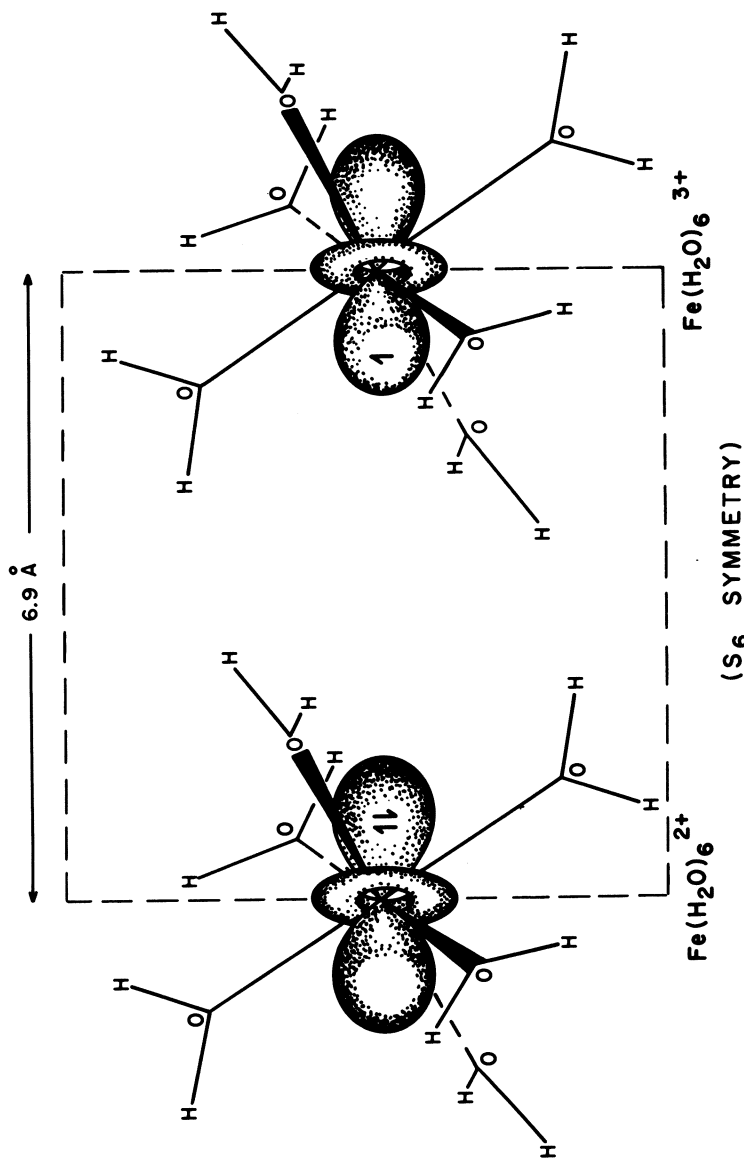


Figure 1. An $\text{Fe}(\text{H}_2\text{O})_6^{2+}$ - $\text{Fe}(\text{H}_2\text{O})_6^{3+}$ complex at the traditional inner-sphere "contact" distance with the inner-sphere complexes (T_h symmetry) oriented to give overall S_6 symmetry. This geometry is favorable for transfer of an electron between t_{2g} - $3d$ atomic orbitals (AO's, which have σ symmetry with respect to the Fe-Fe axis (defined as the z-axis). These $3d_z^2$ AO's are schematically drawn so as to enclose roughly 99% of their total electron densities. The water ligands in closest contact are enclosed by the dashed lines (Reproduced with permission, from Ref. 13. Copyright 1980, Israel Journal of Chemistry.)

with decreasing r . Proper inclusion of very short r values (e.g., as short as 4.5 \AA) would certainly require extensive modification of the expression for $\bar{u}(r)$ employed in the present study (eq 8). One simple approach is to incorporate a steric factor through the use of a switching function which varies from unity to zero as r approaches the minimum possible value (12). For present purposes we have chosen instead to keep eq 8 and to adopt 5.5 \AA as an effective lower limit for r in eq 5, based on the van der Waals contact criterion defined above (11). This cutoff value of r is seen to be roughly halfway between the closest contact estimate ($>4.5 \text{ \AA}$) and the traditional "spherical contact" distance ($\sim 7 \text{ \AA}$), and is to be interpreted as a compromise between the extremes of total rotational freedom and total suppression of rotational freedom, thus allowing an initial estimate of the effects of interpenetration of reactants. Many of the features of the calculations based on this model (11) and reported below are found to be consistent with those obtained in the more detailed studies (12).

Models for $k_{el}(r)$

Since various models for $k_{el}(r)$ based on transition state theory (TST), semiclassical theory (SCT), and quantum mechanical theory (QMT) have been thoroughly discussed in the previous literature (6-12), we will discuss them here only briefly, with emphasis on the manner in which the ab initio matrix elements are calculated and incorporated into the overall formalisms.

Coordinates and Potential Energy Surfaces. In any of the above formalisms one must identify the nuclear coordinates which contribute to the activation of the reactants. In the present case we confine our attention to two "active" modes -- the solvent polarization mode (q_{solv}) and the antisymmetric combination of inner-sphere breathing modes (q_{in}), as in Figure 2. It is formally possible to treat both q_{solv} and q_{in} in terms of a harmonic oscillator model (5). For a thermoneutral exchange reaction such as $\text{Fe}^{2+} - \text{Fe}^{3+}$, the reactant and product potential energy surfaces can be represented as two ellipsoids which are identical except for a horizontal displacement arising from shifts in the equilibrium values of q_{solv} and q_{in} in going from reactants to products (Figure 2). These two surfaces intersect in a line whose lowest-energy point defines the activation energy, E^* , as indicated by the intersection of the energy profiles in Figure 3. By resorting to dielectric continuum theory, one may express the solvent contribution to E^* as

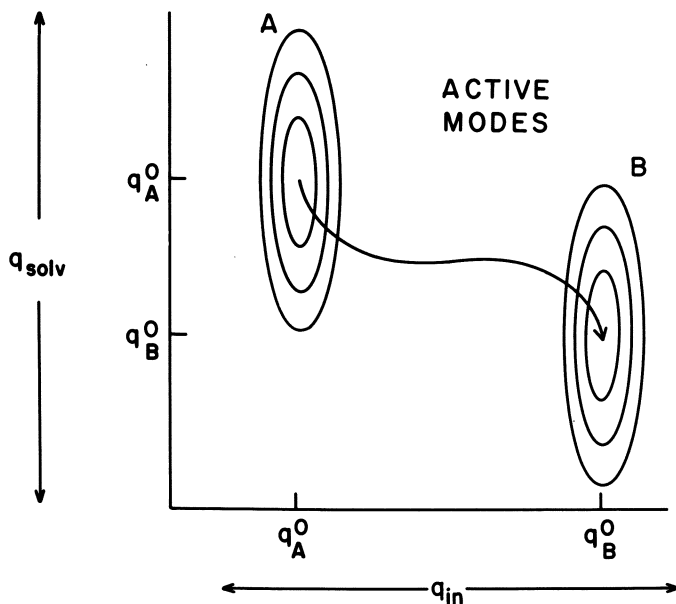


Figure 2. Initial (ψ_A) and final (ψ_B) state potential-energy contours for the complete (two-mode) active space; the abscissa refers to the inner-sphere mode and the ordinate governs the low-frequency active solvent mode. The difference in frequencies leads to a curved reaction path. Equilibrium coordinate values for the reactant (ψ_A) and product (ψ_B) states are labeled q_A^0 and q_B^0 , respectively. For the case of q_{in} , $q_B^0 - q_A^0 = \Delta q_{in}^0$, as given by Eq. 16.

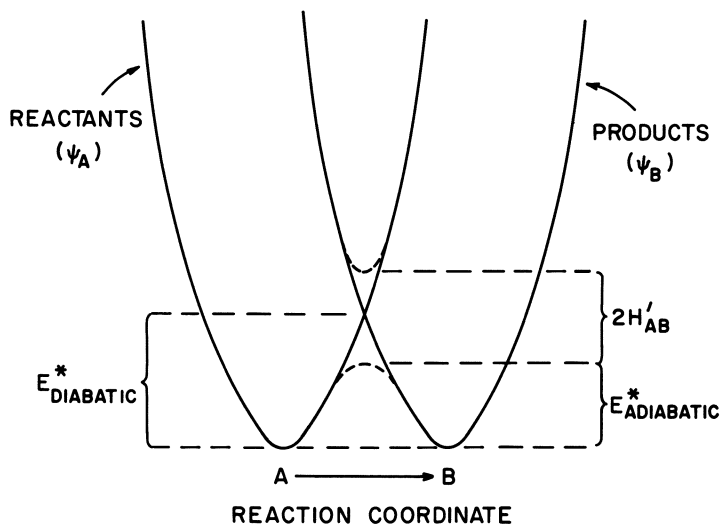


Figure 3. Parabolic energy profiles of two diabatic states (ψ_A , reactants; ψ_B , products) along the reaction path, displaying the crossing energy, $E^*_{adiabatic}$, and the splitting of the adiabatic states ($\pm H'_{AB}$ at the crossing point).

$$E_{\text{solv}}^* = (1/32\pi)(1/D_{\text{op}} - 1/D_{\text{s}}) \int (\vec{D}_{\text{reactants}} - \vec{D}_{\text{products}})^2 dt \quad (12)$$

where D_{op} and D_{s} are the optical and static dielectric constants, respectively, of bulk water, and $\vec{D}_{\text{reactants}}$ and $\vec{D}_{\text{products}}$ are the electric displacement vectors which would be created if the undistorted reactant and product charge distributions, respectively, were placed in a vacuum (1, 3, 5). For a model based on point charges in two spherical cavities, one can write

$$E_{\text{solv}}^*(r) = (1/4)(1/D_{\text{op}} - 1/D_{\text{s}})(1/r^* - 1/r) \quad (13)$$

where r^* is the common effective cavity radius of the two reacting complexes separated by r in the activated ion-pair complex (Figure 1).

The inner sphere contribution to E^* is given by

$$E_{\text{in}}^* = (1/8)\bar{F}_{\text{in}}(\Delta q_{\text{in}}^0)^2 \quad (14)$$

where \bar{F}_{in} is the average breathing force constant for the two charge states (10)

$$\bar{F}_{\text{in}} = 2 F_{\text{in}}^{2+} F_{\text{in}}^{3+} / (F_{\text{in}}^{2+} + F_{\text{in}}^{3+}) \quad (15)$$

and
$$\Delta q_{\text{in}}^0 = \sqrt{2} (r_{\text{ML}}^{2+} - r_{\text{ML}}^{3+}) \quad (16)$$

In view of the emphasis on interpenetration of reactants in the previous section, one may well wonder about the validity of using eq 13 for E_{solv}^* , since it is based on a model of non-overlapping spheres. Accordingly, in the spirit of previous work by Cannon (21) it is of interest to implement eq 12 for an ellipsoid model of the reactive ion pair in which the ellipsoid is defined to have a volume equal to that of the space enclosed by the two overlapping spheres (12). The other parameter of the ellipsoid can be defined by optimal matching to the shape of the overlapping spheres (12). The results reveal that the 2-sphere model is rather similar to the ellipsoidal model, with E_{solv}^* from the latter being $\lesssim 1$ kcal/mole greater than that from the 2-sphere model over the whole range of relevant r values (12). Presumably, the ellipsoidal results are more reliable at very short r values while the 2-sphere model should become more reliable with increasing r . All results obtained below were based on the 2-sphere model.

Transition State and Semi-Classical Models. The activation energy, E^* , defined above in terms of potential energy surfaces is to be compared with the kinetic definition

$$E_{\text{kin}}^* = -k_B d(\ln k_{\text{el}}(r))/d(1/T) \quad (17)$$

In the simple TST harmonic oscillator model, the two expressions for E^* are essentially identical with $k_{\text{el}}(r)$ given by

$$k_{\text{el}}(r) = v_{\text{eff}} \exp(-E^*/RT) \quad (18)$$

where v_{eff} is the effective frequency associated with the reaction coordinate in the activated complex (i.e., at the crossing of the diabatic surfaces in Figure 3) as discussed in (10) and (11).

In the simple semi-classical generalization of TST, electronic and nuclear quantum mechanical effects are included via an electron transmission factor, \bar{k}_{el} , and a nuclear tunnelling factor, Γ_n . Since both \bar{k}_{el} and Γ_n involve thermal averaging, E_{kin}^* (eq 17) now becomes temperature-dependent and can differ appreciably from E^* based on potential energy surfaces. In practice it has been found useful to evaluate \bar{k}_{el} using the Landau-Zener model (22, 23), leading to the expression (11, 12)

$$k_{\text{el}} = 2P_{12}^0 / (1 + P_{12}^0) \quad (19)$$

where $P_{12}^0 = 1 - \exp(-\gamma)$ (20)

and $\gamma = (H_{\text{AB}}^2 / h\nu_{\text{eff}}) (\pi^3 / k_B T (E_{\text{solv}}^* + E_{\text{in}}^*))^{1/2}$ (21)

It is apparent that for sufficiently weak electronic coupling (i.e., small H_{AB}^2) \bar{k}_{el} (and, hence, the overall rate constant) becomes directly proportional to H_{AB}^2 .

The nuclear tunnelling factor can be accurately estimated from a 1-mode model based on the high frequency inner-sphere breathing mode (10, 11)

$$\Gamma_n = (\sinh(\gamma/2)/(\gamma/2))^{1/2} \exp\{-4E_{\text{in}}^* / h\nu_{\text{in}} (\tanh(\gamma/4) - \gamma/4)\} \quad (22)$$

where $y = hv_{in}/k_B T$ and v_{in} is the average inner-sphere breathing frequency (based on \bar{F}_{in} in eq 15).

Wavefunctions and Non-Adiabatic Character. To the extent that simple TST provides a viable model, one can often avoid detailed consideration of wavefunctions for the reactant and product species (ψ_A and ψ_B), and the corresponding matrix element, H'_{AB} (eq 1). Strictly speaking, even TST requires a knowledge of H'_{AB} since the height of the zeroth order crossing (E^* diabatic in Figure 3) is reduced by $|H'_{AB}|$ when adiabatic surfaces (i.e., eigenvalues of the electronic Schrödinger equation) are considered (dashed lines in Figure 3). However, if $H'_{AB} < k_B T$, its effect on E^* can often be ignored. In the semi-classical theory (SCT, eqs 19-22) and the quantum mechanical theory (QMT) to be described below, H'_{AB} and the wavefunctions which determine it play a more fundamental role and require careful attention.

As defined above, the diabatic states ψ_A and ψ_B correspond to the valence bond structures associated, respectively, with reactants or products (i.e., $\psi_A \equiv 2+, 3+$; $\psi_B \equiv 3+, 2+$). When the reactants or products are interacting, ψ_{HA} and ψ_B can mix because $H'_{AB} \neq 0$, and in the case of the symmetric activated complex where a mirror plane bisects the M-M vector, the adiabatic states (which diagonalize the electronic Hamiltonian) are given by

$$\psi_{\pm} = (\psi_A \pm \psi_B) / (2(1 \pm S_{AB}))^{1/2} \quad (23)$$

It turns out in the present case to be most convenient to formulate the electron transfer process in terms of ψ_A and ψ_B rather than ψ_+ and ψ_- . Aside from the simple valence-structure definition of ψ_A and ψ_B (see above), these "diabatic" functions have the advantage of varying smoothly and slowly with q_{solv} and q_{in} . Hence "non-adiabatic" effects due to the action of the nuclear momentum operators on ψ_A and ψ_B can be neglected (11). Of course, the degree of "non-adiabatic character" in the electron-exchange process is an intrinsic property, independent of the wavefunction representation used to describe it. For example, in terms of ψ_+ and ψ_- , an electronically adiabatic process is one which can be analyzed in terms of a single adiabatic

potential energy surface: i.e., the adiabatic surfaces in our 2-state model must be sufficiently separated so that they exert no interference effects on each other. The splitting of the adiabatic surfaces at the diabatic crossing point (Figure 3) is given by

$$\Delta E = 2H'_{AB} \quad (24)$$

where H'_{AB} is defined in eq 1. Hence, it follows that a large H'_{AB} suppresses the influence of the upper state on ground state processes, leading to the adiabatic limit.

On the other hand, in the limit of small H'_{AB} one is dealing with an intrinsically 2-state process in which most events are non-reactive or "non-adiabatic": i.e., the system upon entering the crossing region (Figure 3) most likely remains on the same "diabatic" (reactant or product) surface (or, equivalently, jumps from one adiabatic surface to the other) and only occasionally passes from one diabatic surface to the other (i.e., reacts). In the SCT model defined above, the tendency toward non-adiabatic character is reflected in the departure of \bar{k}_{el} from unity as H'_{AB} is reduced in magnitude (eqs 19-21).

Quantum Mechanical Theory (QMT)

The Perturbation Theory Formalism. The quantum mechanical model employed here is the conventional time-dependent perturbation theory, valid for sufficiently small H'_{AB} , which leads to the familiar Golden rule expression when the final state manifold is sufficiently dense (ensured here by the presence of the solvent continuum) (6-11). Assuming a Boltzmann average over all initial states (i.e., vibrational states associated with ψ_A) and a classical solvent continuum (i.e., there is no tunneling associated with q_{solv}), one obtains

$$k_{el}(r) = H'_{AB}{}^2 / hZ_A (\pi^3 / E_{\text{solv}}^* k_B T)^{1/2} (\sum_{v_A, w_B} k_{v_A w_B}) \quad (25)$$

where

$$k_{v_A w_A} = |S_{v_A w_B}|^2 \exp[-E_{v_A}^0 / k_B T] \\ - (E_{\text{solv}}^* + \Delta E_{v_A w_B}^0 / 4)^2 / E_{\text{solv}}^* k_B T]$$

and where ν_A and w_B refer to inner-sphere vibrational levels in the initial (A) and final (B) states, ($E_{\nu_A}^0 = \nu_A h\nu_A$, $E_{w_B}^0 = w_B h\nu_B$, $\nu_A = \nu_B = \nu_{in}$), Z_A is the inner-sphere partition function, and $\Delta E_{\nu_A w_B}^0 \equiv E_{w_B}^0 - E_{\nu_A}^0$ is the vibrational energy exchange between the "active" inner-sphere and solvent modes in the $\nu_A \rightarrow w_B$ component of the total rate constant. The electronic matrix element, H'_{AB} , which is evaluated at an appropriate value of q_{in} as described below, and the Franck-Condon factors, $|S_{\nu_A w_B}|^2$, arise from a Condon factorization of the full vibronic matrix elements

$$H'_{\nu_A w_B} = \int H'_{AB} \chi_{\nu_A}^0 \chi_{w_B}^0 dq \quad (26)$$

where the χ 's are the vibrational wavefunctions and the integration in general is over all active modes (q_{solv} and q_{in}). We do not attempt a derivation of eq 25 here (see, e.g., ref (8)), but rather display just enough detail to make clear how the matrix elements actually calculated (see below) are related to the formalism. We note that eq 26 includes both electronic and nuclear quantum mechanical effects, as reflected in the Hamiltonian (H'_{AB}) and Franck-Condon ($|S_{\nu_A w_B}|^2$) matrix elements. The relationship between eq 26 and the simple SCT expressions, (eqs 19-22), has been discussed in detail in previous work (10, 11).

In constructing the formalism which leads to eq 25 and reveals the role of H'_{AB} , we must first define the effective Hamiltonian, H . Although the polarized solvent makes important contributions to the activation energy, we find it useful as a first approximation to include only the inner-sphere complexes in constructing a Hamiltonian for the purpose of calculating H'_{AB} (the neglect of long-range solvent effects on H'_{AB} is partially justified by examining the solvent contribution to the electric field in the important region between the two reactants (see Figure 3), using the same ellipsoidal model discussed above in connection with E_{solv}^*). Our Hamiltonian, H , is then simply the time-independent Schrödinger Hamiltonian and includes the important valence electrons of the reactive ion pair. The time

dependence in the problem arises from the boundary conditions to be imposed. Letting $H = T_n + H_{el}$, where T_n is the nuclear kinetic energy operator and H_{el} is the electronic Schrödinger Hamiltonian (in the Born-Oppenheimer sense), we employ the time-dependent equation, $H\psi = ih \partial\psi/\partial t$, where the vibronic wave function, ψ , is represented in our 2-state model as,

$$\psi = \psi_A(e, q)\chi_A(q, t) + \psi_B(e, q)\chi_B(q, t) \quad (27)$$

Appropriate manipulations and integration over electronic coordinates (\underline{e}), neglecting the action of T_n on ψ_A and ψ_B and omitting terms second or higher order in off-diagonal matrix elements, leads to the following equation for the vibrational wave functions, χ :

$$(T_n + H_{AA})\chi_A - ih(\partial\chi_A/\partial t) = -H'_{AB}\chi_B \quad (28)$$

A zeroth-order solution of eq 28 appropriate for the case of weak interactions (i.e., small H'_{AB}) is obtained simply by setting the right-hand side of eq 28 to zero. Since $T_n + H_{AA}$ is time independent, this procedure then defines zeroth order stationary states, χ_A^0 (i.e., $(T_n + H_{AA})\chi_A^0 = E_{vA}^0 \chi_A^0$), which, as is customary, may be approximated by harmonic oscillator wavefunctions. We may now imagine that, in effect, the right hand side of eq 28 is "turned on" at some time t (say $t = 0$). Eq 28 is now solved using time-dependent perturbation theory, where the χ 's in eq 27 are expanded in the usual manner, e.g.,

$$\chi_A = \sum_{vA} C_{vA}(t)\chi_{vA}^0 \exp(-itE_{vA}^0/h) \quad (29)$$

and the Fermi Golden rule expression for the rate constant (eq 25) is ultimately obtained (8). Thus, the "electron transfer" probability is mapped onto the composite probability of evolving from some state χ_{vA}^0 of the ψ_A manifold to some state χ_{wB}^0 of the ψ_B manifold due to the weak coupling between the initial and final states, subject, of course, to conservation of energy.

Determination of ψ_A and ψ_B . One of the main points of this brief exposition is to pinpoint the terms which determine the

electronic wave functions ψ_A and ψ_B in the present approximate treatment. In particular, H_{AA} in eq 28, which serves as the effective potential energy for nuclear motion when the system is in electronic state ψ_A , is the expectation value of the electronic Schrödinger Hamiltonian. We obtain ψ_A by assuming a single configuration molecular orbital wavefunction and minimizing the value of H_{AA} using standard self-consistent field (SCF) techniques (11). In a similar fashion, ψ_B is determined variationally by minimizing H_{BB} . Once SCF solutions for the diabatic states ψ_A and ψ_B are available, H'_{AB} is straightforwardly calculated using the same system Hamiltonian. Note that in the present perturbation formalism H'_{AB} involves the full Hamiltonian and not simply some effective 1-electron electrostatic operator, as is often assumed (6-8). The present formulation includes all valence electrons of the reactants on an equal footing and makes no specific assumption about how much of the transferring electron belongs to the metal ion and how much to the first shell ligands.

Charge Localized vs. Delocalized Wavefunctions. In the spirit of the Condon approximation discussed above, we do not include the full dependence of the purely electronic matrix elements on q_{in} , but rather evaluate them where the diabatic curves cross (Figure 3). We have already noted that, for a symmetric exchange reaction, the crossing region is characterized by a reflection plane which interconnects ψ_A and ψ_B . While such a symmetric activated configuration leads to a simple expression for the charge-delocalized adiabatic states (ψ_{\pm} , eq 23), it is interesting to note that the SCF procedure defined above still leads to the desired symmetry-broken charge-localized (i.e., 2,3 or 3,2) diabatic states, rather than ψ_+ or ψ_- (constraining the wavefunction to have the form of ψ_+ or ψ_- increases the state energies by ~ 1 eV (11)). This static result arises from the fact that overlap between ψ_A and ψ_B is weak (11) and is related to an interesting and analogous dynamical effect: when the charge-localized system in ψ_A is "suddenly" brought into the symmetric crossing region by a suitable fluctuation in q_{solv} or q_{in} , the system would be expected to oscillate between ψ_A and ψ_B and, given enough time, would eventually sweep out a "symmetric" probability distribution. However, for weak overlap of

ψ_A and ψ_B , continued motion in the q-coordinates would quickly destroy the symmetry before the above symmetrizing oscillations got started (i.e., the dynamical system spends most of its time in ψ_A or ψ_B). Hence, in the case of weak overlap, the diabatic states ψ_A and ψ_B are more useful in spite of the occurrence of temporary symmetric configurations.

Reciprocity. Finally, we note that the evaluation of H'_{AB} at the crossing (Figure 3) always guarantees that $H'_{AB} = H'_{BA}$ even for non-thermoneutral reactions (since H_{AB} and S_{AB} are Hermitian and $H_{AA} = H_{BB}$ by construction). This ensures the proper reciprocal relationship between forward and reverse processes.

Activation Parameters

When quantum effects are included via SCT (eqs 19-22) or QMT formalisms, the activation parameters become more complicated than for the simple TST case (eq 18). It is convenient to preserve the form of eq 18, but now E^* must be replaced by a temperature-dependent activation energy, $E^*(T)$, which, accordingly, can be identified as an effective activation free energy (10, 11)

$$k_{el}(r) = v_{eff} \exp(-\Delta G^*/k_B T) \quad (30)$$

The corresponding entropy and enthalpy of activation can be defined as

$$\Delta S^* = -\partial \Delta G^* / \partial T \quad (31)$$

$$\Delta H^* = \Delta G^* - T \Delta S^* \quad (32)$$

When this approach is extended to the overall rate constant, k_{ex} , expressed either in integral (eq 5) or non-integral form (eq 9), additional contributions to the activation parameters arising from the work done in bringing the reactants together must, of course, be included, and the overall activation parameters are distinguished from the above quantities by the use of a dagger (ΔG^\ddagger , etc.).

Computational Details

The SCF molecular orbital calculations were based on the structural model given in Figure 1. Detailed discussions of the calculations are given in references (11) and (24). We sum-

marize here some of the salient features: (1) metal valence electrons were represented by a large Gaussian-type-orbital (GTO) basis set, including 3d- and 4s-type atomic orbitals; the normal valence basis set was supplemented with several additional diffuse orbitals so as to ensure an adequate sampling of the inter-reactant region which is important for the necessary overlap; (2) the metal nucleus and core electrons (1s-3p) were represented by an ab initio effective core potential (25); (3) the first-shell water molecules were represented either by a) an appropriate crystal field potential for all twelve inner-shell waters, based on point charges (11), or b) by explicit inclusion of all valence electrons on the six water molecules most intimately associated with the electron transfer (contained in the dashed box in Figure 1), with ab initio effective potentials being used for the oxygen 1s electrons (26); by representing the ligands at these different levels, we made possible a test of the relative importance of ligand-ligand (L-L) coupling vs direct metal-metal coupling (MM) in the rate constant, $k_{e1}(r)$.

The matrix elements H'_{AB} were evaluated between $r = 5.0 \text{ \AA}$ and $r = 8.0 \text{ \AA}$, with $r_{FeO}^* = 2.06 \text{ \AA}$ (11) or 2.03 \AA (24). As noted above, a van der Waals contact value of 5.5 \AA was adopted for r_{min} in eq 5. The E_{in}^* value was based on $\nu_{in} = 432 \text{ cm}^{-1}$, $r_{FeO} = 2.13 \text{ \AA}$ (Fe^{2+}) and $r_{FeO} = 1.99 \text{ \AA}$ (Fe^{3+}).

Results and Discussion

Matrix Elements (H'_{AB}). The calculated results are displayed in Figure 4 as a function of $r_{Fe \dots Fe}$ and, as expected, fall off in a manner which is roughly exponential. More specifically, we note that the numerical H'_{AB} values can be fitted to within an accuracy of better than 1% or 2 cm^{-1} over the range displayed in Figure 4 (using the "crystal field" data) by the product of a fifth order polynomial and an exponential, $\exp(-\alpha r)$, with $\alpha \sim 0.9 \text{ \AA}^{-1}$. We note that this value of α is somewhat larger than the value ($\sim 0.72 \text{ \AA}^{-1}$) inferred semi-empirically by Hopfield for the case of electron transfer between two carbon atom pi orbitals (27). Calculations at 6.4 \AA for the $Ru^{2+/3+}$ hexaammine system (11), analogous to those reported here for hexaquo $Fe^{2+/3+}$, yield an H'_{AB} value of 67 cm^{-1} to be compared with the corresponding value of 31 cm^{-1} for the iron-water complex.

A particularly interesting feature of Figure 4 is the simi-

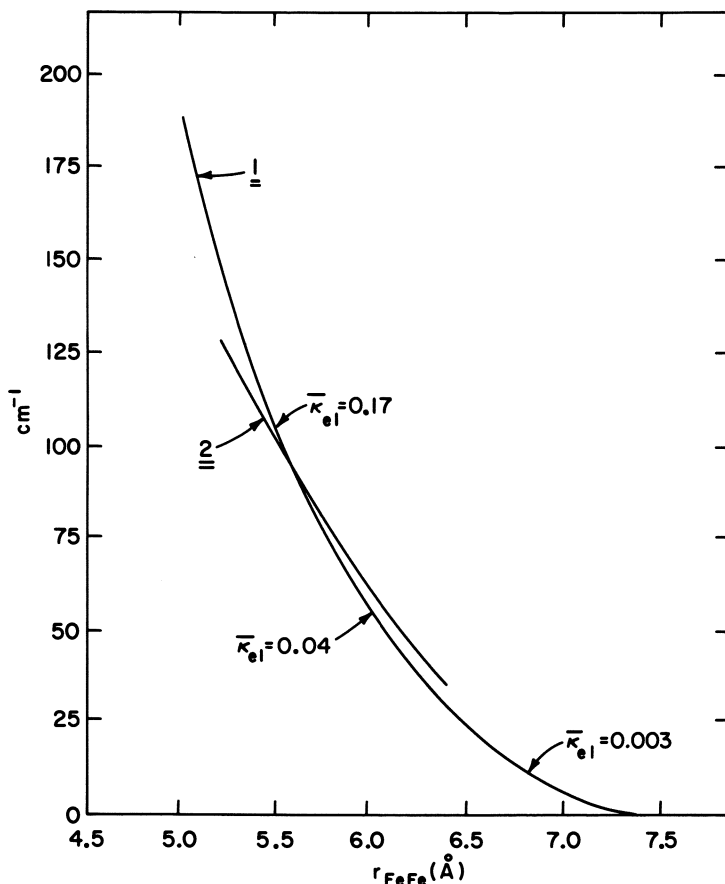


Figure 4. Calculated H_{AB}' values as a function of $Fe^{2+}-Fe^{3+}$ separation, based on the structural model given in Figure 1 and the diabatic wavefunctions ψ_A and ψ_B . Curves 1 and 2 are based on separate models in which the inner-shell ligands are represented, respectively, by a point charge crystal field model [$Fe(H_2O)_6^{2+}-Fe(H_2O)_6^{3+}$] and by explicit quantum mechanical inclusion of their valence electrons [$Fe(H_2O)_5^{2+}-Fe(H_2O)_5^{3+}$] (as defined by the dashed rectangle in Figure 1). The corresponding values of K_{el} , the electronic transmission factor, are displayed for various Fe-Fe separations of interest.

larity of the H'_{AB} magnitudes whether or not the ligand electrons are explicitly included. This supports the hypothesis (11) that the mechanism of electron exchange between aqueous Fe^{2+} and Fe^{3+} ions is dominated by direct metal-metal overlap, as opposed to electron coupling via the ligands. This model is consistent with the results of population analysis carried out on *ab initio* wavefunctions for the individual inner-shell complexes, which indicate that most of the "extra" electron in the Fe^{2+} complex resides on the metal (13, 28). Table I suggests that the mechanism for exchange in the case of $Ru^{2+/3+}$ hexaammine may be significantly different since the ligands appear to be much more involved in the exchange process as a result of the greater importance of ligand-to-metal charge transfer. We emphasize, however, that these results should only be considered as rough, qualitative indicators, since the Mulliken population analysis is a rather *ad hoc* procedure not strictly relatable to observable properties (29).

Table I
Percentage of "Exchanged Electron"
Residing in Metal (M) and Ligand (L) Orbitals^a

reactants	%M	%L
$Fe^{2+/3+}(H_2O)_6$ ^b	71	29
$Ru^{2+/3+}(H_2O)_6$ ^c	56	44
$Ru^{2+/3+}(NH_3)_6$ ^c	42	58

^a Based on Mulliken population analysis of *ab initio* molecular orbital wavefunctions for inner-sphere complexes (28).

^b High spin.

^c Low spin.

Returning to Figure 4, we note the two similar results obtained at 5.0 Å which indicate that the determination of H'_{AB} from SCF molecular orbital wavefunctions is about the same

whether one uses diabatic (charge-localized) wavefunctions ψ_A and ψ_B in conjunction with eq 1 or, alternatively, adiabatic wavefunction (ψ_{\pm} , eq 23), inferring H'_{AB} from one-half of the calculated energy splitting (eq 24) at the crossing point (see Figure 3).

At points of interest in the range 5.0 - 7.0 Å, some values of $\bar{\kappa}_{el}$ are also included in Figure 4, based on eqs 19-21. At the "spherical contact" distance of ~ 6.9 Å, one is in the strongly non-adiabatic regime (i.e., $\bar{\kappa}_{el} \ll 1$) whereas at the van der Waals cutoff distance of 5.5 Å, which corresponds to the maximum of the integral in the present implementation of eq 5, $\bar{\kappa}_{el}$ still departs appreciably from unity, but by a factor of only $\sim 1/6$. It is clear that the ability of the reactive inner-sphere complexes to interpenetrate can have a dramatic effect in reducing the degree of non-adiabatic character in the reaction.

Calculated Rate Constants and Activation Parameters. Calculated results based on the three different models (TST, SCT, and QMT) are displayed in Table II and compared with experimental results (30) extrapolated to zero ionic strength (11).

For convenience in subsequent analysis of the activation parameters (see Table III) the SCT results are based on the non-integral expression for k_{ex} (eq 9). In the case of the spherical $v(\bar{r})$, eq 11, \bar{r} was determined such that the SCT and QMT results for k_{ex} were identical. This led to a value of 6.08 Å for \bar{r} (11). A more realistic procedure is to adopt eq 10 for $v(\bar{r})$, setting \bar{r} equal to 5.5 Å (since the maximum of the integrand in eq 8 occurs at this "contact" value) and determining Δr once again by matching the SCT and QMT results. This procedure yielded a value of 0.33 Å for Δr . Sharply peaked integrands were also found in the more detailed study reported in ref (12). The \bar{r} and Δr values determined for the SCT model were employed as well in the TST calculations. The temperature dependence of \bar{r} and Δr as defined here is very small and was neglected in the calculation of activation parameters.

The main inferences to be drawn from Table II are as follows. The accord between the QMT and experimental data is seen to be very good. In general, all three models give rather good agreement with experiment, although the TST model, not surprisingly, gives a larger ΔH^{\ddagger} value and a less negative ΔS^{\ddagger} value than the other models due to omission of nuclear tunneling and non-adiabatic effects. Comparison of the SCT and TST results with the full quantum results indicates, as expected,

that the spherical model for $v(\bar{r})$ is less satisfactory than the alternative based on the van der Waals "contact" value for \bar{r} (5.5 Å) and the inferred value of 0.33 Å for Δr .

Table II
Calculated and Experimental Values of k_{ex} and Activation
Parameters at 25C for the Aqueous $Fe^{2+}-Fe^{3+}$ Reaction

Source	k_{ex} (L/mole/sec)	ΔG^\ddagger ^a (kcal/mole)	ΔH^\ddagger ^a (kcal/mole)	ΔS^\ddagger ^a (cal/mole/deg)	
Theory					
QMT ^b	0.04	19.7	9.8	-33.0	
SCT ^c	{ eq 11 ^d	0.04	19.7	10.4	-31.1
	{ eq 10 ^e	0.04	19.7	9.4	-34.4
TST ^f	{ eq 11 ^d	0.2	18.8	13.3	-18.6
	{ eq 10 ^e	0.05	19.6	12.2	-24.7
Experiment^g	~0.1	~19	≥10	≥-30	

^a The dagger refers to the overall rate constant, k_{ex} , in contrast to the analogous starred quantities which were based on $k_{el}(r)$ and defined by eqs 30-32.

^b Quantum Mechanical results (based on eq 25 and eq 5).

^c Semi-classical results (based on eqs 19-22).

^d $\bar{r} = 6.08$ Å.

^e $\bar{r} = 5.50$ Å, $\Delta r = 0.33$ Å.

^f Transition State Theory results (based on eq 18).

^g Based on original data of ref (30); see also refs (10) and (11) where uncertainties in extrapolated values are discussed, and ref (12) where calculated dependence on ionic strength is presented.

More insight into the reaction mechanism is given by the breakdowns in Table III. The negative entropy has important contributions from bimolecular work, non-adiabatic effects and nuclear tunnelling. Nuclear tunnelling ($\Gamma_n = 3.5$ (10, 11)) also reduces the effective barrier by ~ 2.0 kcal/mole (cf., 6.4 kcal/mole with the value of 8.37 kcal/mole for E_{in}^* (eq 14)).

If the model for $v(\bar{r})$ based on eq 10 is adopted as being the more suitable one, then the effective value of $\bar{\kappa}_{el}(r)$ is seen from Figure 4 to be ~ 0.17 , as noted above. This value implies that the electronic coupling is weak enough to justify the use of perturbation theory in defining the QMT model, eq 25. Similarly, the expanded form of the exponential SCT formula for κ_{el} (eq 20) is accurate to within 5%.

Table III
Decomposition of Activation Parameters
based on the SCT Rate Constant, k_{ex}

Contribution	ΔG^\ddagger (kcal/mole)		ΔH^\ddagger (kcal/mole)		ΔS^\ddagger (cal/mole/deg)	
	eq 11	eq 10	eq 11	eq 10	eq 11	eq 10
Bimolecular terms ^a	4.5	6.1	-1.5	-1.7	-20.3	-26.3
$\bar{\kappa}_{el}$ ^b	1.9	1.1	-0.3	-0.3	-7.4	-4.5
Reorganization inner-sphere ^c	7.6	7.6	6.3	6.3	-4.3	-4.3
solvent ^d	5.6	4.8	5.8	5.0	0.6	0.5
Total	19.7	19.7	10.4	9.4	-31.0	-34.3

^a Based on the $4\pi r^2(\Delta r)g(\bar{r})$ factor in eq 9.

^b Based on eqs 19-21.

^c Based on eqs 14 and 22.

^d Based on eq 13.

Conclusion

We have demonstrated the feasibility of accounting for the electronic coupling in the aqueous $\text{Fe}^{2+}\text{-Fe}^{3+}$ system in terms of information obtainable from large-scale ab initio molecular orbital calculations carried out for suitably chosen model complexes. This electronic information has been incorporated into a comprehensive kinetic formalism which allows quantitative determination of the $\text{Fe}^{2+}\text{-Fe}^{3+}$ kinetic parameters. The formalism makes use of some empirical parameters based on structural and dielectric properties of the reacting system, but no kinetic information.

The upshot of the results presented above is that a suitable QMT or SCT model which allows for interpenetration of reactants, albeit still within the realm of "outer-sphere" exchange, yields quite satisfactory detailed agreement with experiment and leads to a mechanism characterized by a modest, but nevertheless significant, degree of quantum behavior in both the electronic and nuclear aspects of the process, compactly represented by $k_{el} \sim 0.17$ and $\Gamma_n = 3.5$. The rather small value of Γ_n masks some larger quantum effects seen in the separate ΔH^\ddagger and ΔS^\ddagger terms (10, 11). The effective width of encounter distances (Δr) is found to be appreciably smaller than that implied by the spherical model for $v(\bar{r})$.

While a direct metal-metal interaction appears to account adequately for the aqueous $\text{Fe}^{2+/3+}$ data, we have seen from Table I that the role of ligands may well be much more important for other related reactants such as the $\text{Ru}^{2+/3+}$ hexaamines.

Acknowledgement

This work was carried out at Brookhaven National Laboratory under contract with the U. S. Department of Energy and supported by its Office of Basic Energy Sciences. We wish to acknowledge many valuable discussions with Prof. H. L. Friedman and Dr. B. L. Tembe and thank them for permission to refer to results of our collaborative study (12) prior to publication. We also wish to thank Dr. J. Logan for permission to use Figure 4, Dr. S. Ehrenson for supplying a computer program which was used in the ellipsoidal dielectric calculations, and Prof. N. R. Kestner for several helpful comments.

Literature Cited

1. Marcus, R. A. J. Chem. Phys. 1956, 24, 979.
2. Marcus, R. A. J. Chem. Phys. 1965, 43, 679.
3. Hush, N. S. Trans. Faraday Soc. 1961, 57, 155.
4. Hush, N. S. Electrochimica Acta 1958, 13, 1005.
5. Levich, V. G. Adv. Electrochem. Electrochem. Eng. 1966, 4, 249.
6. Efrima, S.; Bixon, M. Chem. Phys. Lett. 1974, 25, 34; Chem. Phys. 1976, 13, 447.
7. Van Duyne, R. P.; Fischer, S. F. Chem. Phys. 1974, 5, 183.
8. Kestner, N. R.; Logan, J.; Jortner, J. J. Phys. Chem. 1974, 78, 2148.
9. Chance, B.; DeVault, D. C.; Frauenfelder, H.; Marcus, R. A.; Schrieffer, J. R.; Sutin, N., Eds. "Tunnelling in Biological Systems"; Academic: New York, 1979.
10. Brunschwig, B. S.; Logan, J.; Newton, M. D.; Sutin, N. J. Am. Chem. Soc. 1980, 102, 5798.
11. Newton, M. D. Int. J. Quantum Chem.: Quantum Chemistry Symposium 1980, 14, 363-391.
12. Tembe, B. L.; Friedman, H. L.; Newton, M. D., to be published.
13. Jafri, J. A.; Logan, J.; Newton, M. D. Isr. J. Chem. 1980, 19, 340.
14. Dolin, S. P.; German, E. D.; Dogonadze, R. R. J. Chem. Soc., Faraday Trans. 1977, 273, 648.
15. Hair, N. J.; Beattie, J. K. Inorg. Chem. 1977, 16, 245.
16. Eigen, M. Z. Phys. Chem. N. F. 1954, 1, 176.
17. Fuoss, R. M. J. Am. Chem. Soc. 1958, 80, 5059.
18. Sutin, N. "Tunnelling in Biological Systems"; Academic: New York, 1979; p 201.
19. Pauling, L. "The Nature of the Chemical Bond"; Cornell Univ. Press: Ithaca, N. Y., 1960; p 260.
20. Hirata, F.; Friedman, H. L.; Holz, M.; Herz, H. G. J. Chem. Phys., in press.
21. Cannon, R. D. Chem. Phys. Lett. 1977, 49, 299.
22. Landau, L. Phys. Z. Sowjet 1932, 2, 46.
23. Zener, C. Proc. Royal Soc. London, Ser. A 1932, 137, 696; 1933, 140, 660.
24. Logan, J.; Newton, M. D., to be published.
25. Olafson, B. D.; Goddard, W. A., III Chem. Phys. Lett. 1974, 28, 457.
26. Topiol, S.; Moskowitz, J. J. Chem. Phys. 1979, 70, 3008.
27. Hopfield, J. Proc. Natl. Acad. Sci. USA 1974, 71, 3640.
28. Logan, J.; Noel, J. O.; Newton, M. D., unpublished work.
29. Mulliken, R. S. J. Chem. Phys. 1955, 23, 1833.
30. Silverman, J.; Dodson, R. W. J. Phys. Chem. 1952, 56, 846.

RECEIVED May 12, 1982.

Inclusion of Solvent Effects in a Vibronic Coupling Model for Mixed-Valence Compounds

K. Y. WONG and P. N. SCHATZ

University of Virginia, Department of Chemistry, Charlottesville, VA 22901

Solvent effects are included in a previous vibronic coupling model (PKS) of mixed-valence systems by including a second totally symmetric subunit normal coordinate. The antisymmetric combination is identified as a low frequency effective solvent mode. It is still possible to obtain the ground vibronic manifold of the system by direct diagonalization. Application is made to the Creutz and Taube ion. It proves possible to account for the observed intervalence band contour, the change in bond length between oxidation states, and weak, diffuse low energy tunneling transitions. It is also shown that in the harmonic approximation no totally symmetric vibration of the Creutz and Taube ion is expected to contribute significantly to the intervalence band width unless there is a large change in force constant between oxidation states. This contradicts other analyses in the literature. The shift of intervalence band position with solvent is discussed in general using both direct diagonalizations and analytical formulas.

A vibronic coupling model for mixed-valence systems has been developed over the last few years (1-5). The model, which is exactly soluble, has been used to calculate intervalence band contours (1, 3, 4, 5), electron transfer rates (4, 5, 6) and Raman spectra (5, 7, 8), and the relation of the model to earlier theoretical work has been discussed in detail (3-5). As formulated to date, the model is "one dimensional" (or one-mode). That is, effectively only a single vibrational coordinate is used in discussing the complete ground vibronic manifold of the system. This is a severe limitation which, among other things, prevents an explicit treatment of solvent effects which are

0097-6156/82/0198-0281\$06.00/0
© 1982 American Chemical Society

known to be of great importance. It is the purpose of this article to outline a method for including the solvent and to illustrate some of the consequences of such a treatment.

Solution of the Static Problem

We follow closely previous expositions of the theory (4, 5) and include only the particular features needed for our present discussion. Let us imagine a mixed-valence system composed of two subunits, A and B, which are associated with formal oxidation states M and N, respectively. We designate the corresponding electronic Hamiltonian operators H_{el}^A and H_{el}^B , and if the corresponding wave functions are ψ_M^A and ψ_N^B :

$$\begin{aligned} H_{el}^A \psi_M^A &= W_M^A \psi_M^A \\ H_{el}^B \psi_N^B &= W_N^B \psi_N^B \end{aligned} \quad (1)$$

Initially we hold all nuclei fixed so that the nuclear kinetic energy operator (T_n) is zero. If there is no interaction (coupling) between subunits A and B, the Schrödinger equation for the composite system, $(H_{el}^A + H_{el}^B)$, is:

$$\begin{aligned} (H_{el}^A + H_{el}^B) \psi_M^A \psi_N^B &\equiv (H_{el}^A + H_{el}^B) \psi_a \\ &= (W_M^A + W_N^B) \psi_a \equiv W_a \psi_a \end{aligned} \quad (2)$$

For simplicity, let us confine ourselves to the symmetrical case, $A = B$. Thus, we assume that centers A and B are equivalent so that another degenerate state, ψ_b , exists for which:

$$(H_{el}^A + H_{el}^B) \psi_b = (W_N^A + W_M^B) \psi_b \equiv W_b \psi_b \quad (3)$$

where $\psi_b \equiv \psi_N^A \psi_M^B$ and $W_b = W_a$.

We now allow nuclear motion and seek vibrational wave functions corresponding to states ψ_a and ψ_b . We assume throughout that the subunits have the same point group symmetry in both oxidation states (M and N), and then it is only necessary to consider explicitly totally symmetric normal coordinates of the two subunits (4, 5). Let us assume that there are two on each subunit, designated Q_A^C , Q_A^S and Q_B^C , Q_B^S . We subsequently identify Q_A^C and Q_B^C as the effective intramolecular (c = core) and Q_A^S and Q_B^S as the effective solvent (s = solvent) totally symmetric

normal coordinates. (If Q_A^S and Q_B^S are dropped, we revert to the previous (1-8) "one dimensional" (or one-mode) treatment with $Q_A^C \equiv Q_A$, $Q_B^C \equiv Q_B$ and $v_c \equiv v_-$.)

The vibrational potential energy of subunit A in oxidation state M can be written

$$W_M^A = W_M^0 + \ell_M^C Q_A^C + \frac{1}{2} k_M^C Q_A^C{}^2 + \ell_M^S Q_A^S + \frac{1}{2} k_M^S Q_A^S{}^2 \quad (4)$$

with analogous expressions for W_N^A , W_M^B and W_N^B . We define the zero of energy by $W_M^0 + W_N^0 = 0$, and arbitrarily assume that oxidation state N is lower in energy. We choose coordinate origins by setting Q_A^C, Q_A^S and Q_B^C, Q_B^S to zero at the minima of W_N^A and W_N^B , respectively, so that $\ell_N^C = \ell_N^S = 0$. With $\ell_M^C \equiv \ell^C$, $\ell_M^S \equiv \ell^S$, and introducing the new coordinates,

$$\begin{aligned} Q_{\pm}^C &\equiv (1/\sqrt{2})(Q_A^C \pm Q_B^C) \\ Q_{\pm}^S &\equiv (1/\sqrt{2})(Q_A^S \pm Q_B^S) \end{aligned} \quad (5)$$

we obtain

$$\begin{aligned} W_a = & (1/\sqrt{2})\ell^C(Q_-^C + Q_+^C) + \frac{1}{2}(k_N^C + k_M^C)(Q_-^C{}^2 + Q_+^C{}^2) \\ & + (1/\sqrt{2})\ell^S(Q_-^S + Q_+^S) + \frac{1}{2}(k_N^S + k_M^S)(Q_-^S{}^2 + Q_+^S{}^2) \\ & + \frac{1}{2}(k_M^C - k_N^C)Q_+^C Q_-^C + \frac{1}{2}(k_M^S - k_N^S)Q_+^S Q_-^S \end{aligned} \quad (6)$$

The corresponding expression for W_b is obtained if Q_-^C and Q_-^S are everywhere in eq 6 replaced by $(-Q_-^C)$ and $(-Q_-^S)$, respectively. We now make the approximations, $k_M^C = k_N^C \equiv k^C$, $k_M^S = k_N^S \equiv k^S$. In this case, the Q_+Q_- cross terms vanish and the problem is separable with respect to Q_+ and Q_- modes. In particular, the potential surfaces W_a and W_b are identical in the Q_+ modes.

This has the very important consequence, as we show in more detail later, that no totally symmetric mode of a mixed-valence compound can contribute to the intervalence bandwidth (in the approximation of equal force constants in both oxidation states). For the moment we therefore drop the terms in Q_+ and define the dimensionless variables

$$q_\alpha \equiv 2\pi(v_\alpha/h)^{1/2} Q_-^\alpha$$

$$\lambda_\alpha \equiv (8\pi^2 h v_\alpha^3)^{-1/2} \rho^\alpha \quad (7)$$

where $\alpha = c$ or s , and $v_\alpha = (2\pi)^{-1} \sqrt{k^\alpha}$. Defining $\tau \equiv v_s/v_c$, the potential surfaces in q_α space become:

$$W_a/hv_c = \frac{1}{2}(q_c^2 + \tau q_s^2) + (\lambda_c q_c + \tau \lambda_s q_s)$$

$$W_b/hv_c = \frac{1}{2}(q_c^2 + \tau q_s^2) - (\lambda_c q_c + \tau \lambda_s q_s) \quad (8)$$

The corresponding vibronic wave functions are:

$$\phi_a = \psi_a \chi_m^c \chi_{n_a}^s ; \quad \phi_b = \psi_b \chi_m^c \chi_{n_b}^s \quad (9)$$

where χ_m^c , $\chi_{n_a}^s$ and χ_m^c , $\chi_{n_b}^s$ are harmonic oscillator functions

centered, respectively, at the minima of W_a and W_b , and the corresponding vibronic energies are:

$$E_a = -\frac{1}{2}(\lambda_c^2 + \tau \lambda_s^2) h v_c + (m_a + \frac{1}{2}) h v_c + (n_a + \frac{1}{2}) h v_s$$

$$(m_a, n_a = 0, 1, 2, \dots) \quad (10)$$

with an analogous expression for E_b .

Let us now imagine that interaction symbolized by V^{AB} occurs between subunits A and B. We regard this interaction as a purely electronic coupling and write:

$$V_{ij} \equiv \langle \psi_i | V^{AB} | \psi_j \rangle \approx \langle \psi_i | V^{AB} | \psi_j \rangle^0 \equiv V_{ij}^0$$

$$(i, j = a, b) \quad (11)$$

where superscript zero indicates that the matrix element is evaluated holding the nuclei fixed. Defining a new energy zero by $V_{aa}^0 = V_{bb}^0 = 0$ and letting $\varepsilon \equiv V_{ab}^0/hv_c$, the potential surfaces become:

$$W_{1,2}/hv_c = \frac{1}{2}(q_c^2 + \tau q_s^2) \mp [\varepsilon^2 + (\lambda_c q_c + \tau \lambda_s q_s)^2]^{1/2} \quad (12)$$

Solution of the Dynamic Problem

A complete set of vibronic energies (E_k) and eigenfunctions (Φ_k), the ground vibronic manifold, are associated with the potential surfaces of eq 12. These are obtained as solutions

of the vibronic Schrödinger equation:

$$(H_{el} + T_n)\phi_k = E_k \phi_k \quad (13)$$

where $H_{el} = H_{el}^A + H_{el}^B + V^{AB}$, and T_n is the kinetic energy operator in coordinates q_c and q_s . The solution of eq 13 in the one-dimensional case (i.e., when $q_s \equiv 0$) has been discussed in detail previously (1, 4, 5), and we do not repeat that discussion. We simply note that the same method of solution may be used in the present two dimensional (or two-mode) case. Specifically, the eigenfunctions ϕ_k are written:

$$\phi_k = \psi_+ \chi_{+,k}(q_c, q_s) + \psi_- \chi_{-,k}(q_c, q_s) \quad (14)$$

where

$$\psi_{\pm} \equiv (1/\sqrt{2})(\psi_a \pm \psi_b) \quad (15)$$

and $\chi_{+,k}$ and $\chi_{-,k}$ are vibrational functions determined by a pair of coupled differential equations. The χ_{\pm} are expanded in the complete sets of harmonic oscillator functions, $\chi_n^c(q_c)$ and $\chi_m^s(q_s)$ ($n, m = 0, 1, 2, \dots, \infty$) so that:

$$\chi_{\pm, k} = \sum_{n=0}^{\infty} \sum_{m=0}^{\infty} c_{k,n,m}^{\pm} \chi_n^c(q_c) \chi_m^s(q_s) \quad (16)$$

Eq 16 is substituted into eq 14 which in turn is substituted into eq 13. The latter is multiplied in turn by ψ_+ and ψ_- and an integration over electronic coordinates is performed. The result is an infinite set of secular equations whose explicit form will be given elsewhere (9). An approximate solution is obtained by computer diagonalization using a strongly truncated basis; that is, the sums over n and m are terminated at relatively small values. In the one dimensional case (1-8), the use of d quanta ($n = 0$ to $d-1$) in the basis produces a secular determinant of dimension $2d$. In the present case, use of d quanta in each of the two modes ($n = 0$ to $d-1$, $m = 0$ to $d-1$) produces a secular determinant of dimension $d(d+1)$. Thus, the demands on computer capacity increase sharply. In the work we report here, $d = 11$, so the matrix diagonalized is 132×132 , which gives tolerable accuracy for the parameters (ϵ , λ , v_c , v_s) we use.

Application to the Intervalence Band of the Creutz and Taube (C & T) Ion

To illustrate some of the characteristics of the two-mode model, we calculate the intervalence band of the Creutz and Taube (C & T) ion $[(\text{NH}_3)_5\text{Ru-pyr-Ru}(\text{NH}_3)_5]^{5+}$ (pyr = pyrazine)(10). Previously, we did this with the one-mode model using two different sets of parameters. First (1), with $\nu_c \equiv \nu_- = 500 \text{ cm}^{-1}$, we simply found those values of the parameters ϵ and λ which gave a best fit of the band, namely, $\epsilon = -6.0$, $\lambda = 2.7$. The comparison of this calculation (solid curve) with experiment (dashed curve) is shown in Figure 1. This calculation predicts intense, low energy features which we refer to as tunneling transitions (2, 4, 5). A subsequent search of the far infrared spectrum revealed no transitions with anything like the predicted intensity (11). Furthermore, λ can be explicitly related to the difference in Ru-N bond lengths (Δr) in the two different oxidation states, namely (5),

$$\Delta r = (\lambda/2\pi)(h/3\nu_- m_L)^{\frac{1}{2}} \quad (17)$$

where m_L is the mass of the ligand (NH_3 in the case of the C & T ion). With $\lambda = 2.7$, $\Delta r \sim 0.1 \text{ \AA}$ whereas an estimate based on a comparison of the Ru^{2+} and Ru^{3+} hexaammines (12) suggests $\Delta r = 0.04 \text{ \AA}$ and hence $\lambda = 1.1$. Using this value of λ and $\epsilon = -6.35$ (to get the correct position for the band maximum), we obtain the dotted curve in Figure 1. The predicted tunneling transitions have decreased in intensity by more than an order of magnitude consistent with the absence of strong transitions in the far infrared. On the other hand, the pronounced asymmetry on the high energy side of the observed intervalence band (Fig. 1) is no longer accounted for. It was suggested (5) that this feature might arise from a second, weaker intervalence transition due to the combined effects of spin-orbit coupling and low symmetry perturbations (and this possibility is not precluded by our subsequent analysis).

We now show that the two-mode model can account for the observed intervalence band asymmetry of the C & T ion, the weak tunneling transitions and a Δr value of 0.04 \AA . We fix the values $\epsilon = -6.0$, $\lambda_c = 1.1$ ($\Delta r = 0.04 \text{ \AA}$), $\nu_c = 500 \text{ cm}^{-1}$. As a rough guide in choosing values of λ_s and ν_s , we hold the total reorganization energy (E_t) constant. This energy is the vertical distance (Franck-Condon transition energy) from the minimum of one potential surface to the intersection with the other sur-

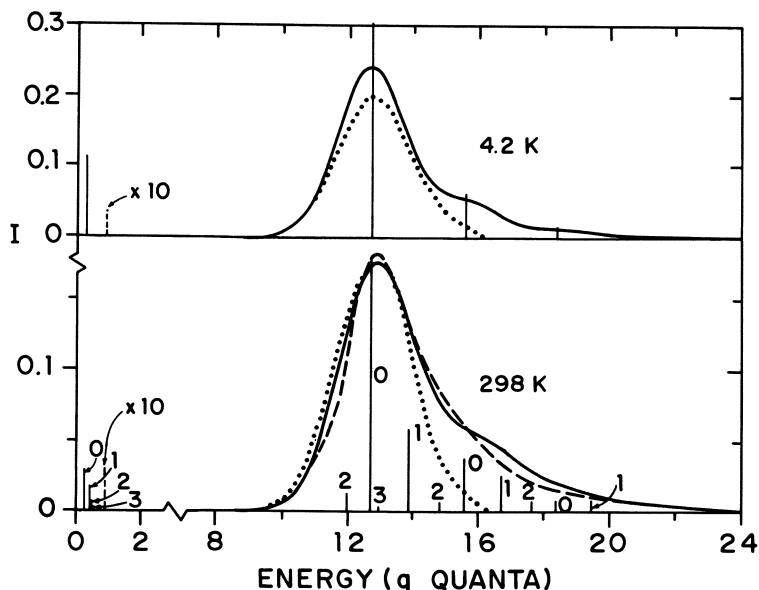


Figure 1. Intervalence band (dashed curve) of the Creutz and Taube ion at room temperature (10) scaled in intensity to the "best fit" of the model (stick spectrum and solid curve), which uses $\epsilon = -6$, $\lambda = 2.7$, $\nu \equiv \nu_c = 500 \text{ cm}^{-1}$. The corresponding model spectrum at 4.2 K is shown directly above on a vertical scale compressed by a factor of 2. The solid curves are synthesized from Gaussians taking all widths at half-height to be 2.4ν . The labels 0–3 designate transitions from the ground and first three hot vibronic levels, respectively. These three hot vibronic levels are calculated to lie respectively 131, 362, and 613 cm^{-1} above the ground vibronic level. The stick spectra shown between 0 and 2ν show the location and intensity of the calculated tunneling transitions relative to the stick spectra of the intervalence band. The dotted curve shows a fit using the parameters $\epsilon = -6.35$, $\lambda = 1.1$, $\nu = 500 \text{ cm}^{-1}$, which has been scaled to the peak height of the dashed curve. The corresponding stick spectrum is not shown. Gaussian lines were used with all widths at half-height of 2.6ν . Only a single tunneling transition is predicted, near ν , which is shown by the dashed sticks whose heights have been magnified by a factor of 10. (Reproduced, with permission, from Ref. 5. Copyright 1981, John Wiley & Sons, Inc.).

face, in the strongly localized limit ($\epsilon = 0$). From eq 8,

$$E_t = E_c + E_s = 2\lambda_c^2 h\nu_c + 2\lambda_s^2 h\nu_s \quad (18)$$

where E_c and E_s are, respectively, the intramolecular and solvent reorganization energies. In the one-mode case, the best fit is obtained (Fig. 1) for $\epsilon = -6.0$, $\lambda_c = 2.7$ and so $E_t = E_c = 7290 \text{ cm}^{-1}$. Holding E_t fixed at this value and going to $\epsilon = -6$, $\lambda_c = 1.1$ gives $2\lambda_s^2 h\nu_s = 6080 \text{ cm}^{-1}$. Figures 2-4 show three calculations based on this criterion. A quite good fit is obtained (Fig. 4) for $\lambda_s = 3.9$, $\nu_s = 200 \text{ cm}^{-1}$. Furthermore, the tunneling transitions are quite weak. We stress that our criterion of constant E_t is rather arbitrary and hence the exact values of the parameters are not significant. For example, if we increased λ_s somewhat in Figure 2, the fit could be made excellent and the lower value of ν_s (100 cm^{-1} vs 200 cm^{-1} in Fig. 4) is physically more reasonable. As a practical matter, as λ is increased, the calculation becomes increasingly unreliable because of the severely truncated basis set. The important point is that inclusion of a low frequency effective solvent mode can nicely rationalize the observed characteristics of the C & T ion. Similar improvements may be anticipated in analyzing intervalence bands in other systems.

Totally Symmetric Modes do NOT Contribute Significantly to the Intervalence Bandwidth

It has recently been suggested by Hush (13) that the asymmetry on the high energy side of the C & T ion intervalence band can be easily rationalized by including contributions from totally symmetric modes of the ion. Day (20) has interpreted the Hush treatment as suggesting the Q_+^C mode of eq 5 for this role. We now demonstrate that, to a good approximation, no totally symmetric mode of the ion can contribute to the intervalence bandwidth. Noting the discussion below eq 6, we reiterate that the potential surfaces W_a and W_b are identical in the Q_+ modes. If we explicitly carry these terms through to eq 12, they will appear in identical form on the right hand side for both W_1 and W_2 . This observation alone establishes our proposition. Regardless of the details of the dynamic coupling in the Q_- modes (eq 14), in all other modes the transition is between identical potential surfaces, and vibrational orthogonality

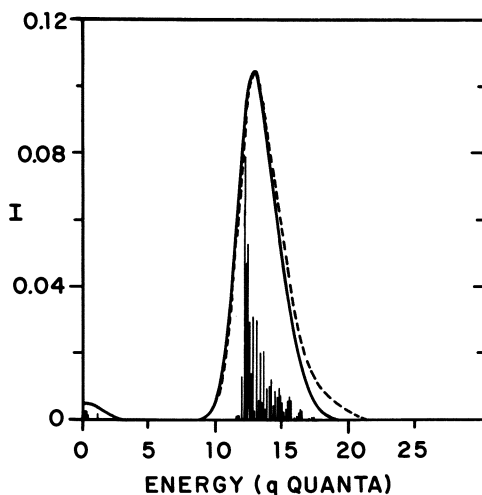


Figure 2. Experimental intervalence band (10) and calculated contour for the Creutz and Taube ion. The parameters used in the calculation are ϵ_s , -6.0 ; λ_c , 1.1 ; λ_s , 5.51 ; ν_c , 500 cm^{-1} ; and ν_s , 100 cm^{-1} at 300 K . The sticks show the relative calculated intensities, and the contour is obtained by replacing each stick by a Gaussian of $\text{FWHM} = 1.4 \nu_c$. (Some of the vertical bars—in Figure 2 only—have been omitted for clarity.) The experimental peak height is normalized to the calculated value, which is arbitrary. The calculated relative intensities among Figures 2–4 are meaningful.

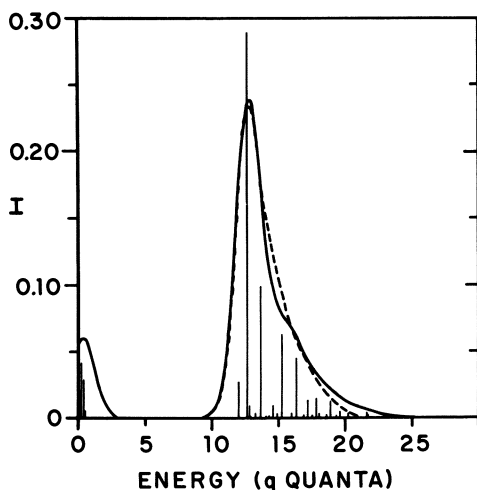


Figure 3. Experimental intervalence band (10) and calculated contour for the Creutz and Taube ion. The parameters used in the calculations are ϵ_s , -6.0 ; λ_c , 1.1 ; λ_s , 2.6 ; ν_c , 500 cm^{-1} ; and ν_s , 450 cm^{-1} at 300 K . Notation and symbols as in Figure 2 except $\text{FWHM} = 1.2 \nu_c$.

applies in the Franck-Condon overlap factors which multiply the electronic transition moment integral. Thus, no change in vibrational quantum number can occur for a Q_+ mode when transition between W_1 and W_2 occurs. Hush (13), on the other hand, maintains that totally symmetric modes contribute because bond length changes accompany such transitions. But note that, in fact, changes in bond length have been explicitly included via the λ parameters. Nonetheless, W_1 and W_2 are identical in Q_+ .

Finally, the question becomes: can some totally symmetric mode other than Q_+^C contribute to the bandwidth--the contention of Hush (13). The answer again is no. The reason is that all the vibrations of the C & T ion can be classified as Q_+ or Q_- . In our treatment, we identified Q_+^S as effective solvent modes. But these can equally well be identified as internal modes. More to the point, the generalization of eqs 4-8 to include all the molecular modes is obvious. Every Q_+ set behaves in an identical manner independent of all other sets. Thus, our previous argument holds for any totally symmetric mode of the mixed-valence system.

The only mechanism by which Q_+ can contribute to the intervalence bandwidth is by a change in force constant between the two oxidation states. We then see from eq 6 that terms containing Q_+Q_- contribute. This case has been discussed previously (1). Our calculations (9) show that this is a significant source of broadening only if the force constant difference is unreasonably large $[(k_M - k_N)/(k_M + k_N) \gtrsim 0.3]$. It is clear that this is not the mechanism proposed by Hush, and we, therefore, believe that his treatment (13) is incorrect. In summary, in the harmonic approximation, assuming purely electronic coupling between subunits, no totally symmetric mode can contribute to the intervalence bandwidth unless there is a large change in force constant between oxidation states. Finally, we reiterate that, nevertheless, many intramolecular modes can, in principle, contribute to the intervalence bandwidth. Such modes must have symmetry Q_- . Our present two-mode treatment is an explicit example if Q_-^S is identified as an intramolecular mode. It must not be thought, however, that the two-mode treatment is simply a superposition of two one-mode cases. Coordinates q_C and q_S (though not Q_+^C and Q_+^S !) are clearly coupled by the second term on the right hand side of eq 12.

Effect of Solvent on Intervalence Band Position

The position of the intervalence band is measured by the mean band energy \bar{E} :

$$\bar{E} = \int \alpha(E) E dE / \int \alpha(E) dE \quad (19)$$

where $\alpha(E)$ is the band contour as a function of photon energy, $E = h\nu$. In Figure 5 we show a plot of \bar{E} vs total reorganization energy for various values of the electronic coupling. The dashed line is simply $\bar{E} = E_t$ (eq 18) which applies when $\epsilon = 0$. The solid lines are calculated from an analytical expression (9) which is valid in both the localized and delocalized limits, i.e., when $2|\epsilon|h\nu_c/E_t \ll 1$ or $\gg 1$, respectively. These curves are not accurate in the intermediate range. They all approach a straight line parallel to the dashed line if the system is strongly delocalized ($2|\epsilon|h\nu_c/E_t \ll 1$). (This asymptote actually lies below the dashed line by $\sim 4kT$ for reasons discussed elsewhere (9).) As delocalization increases, the curves are seen to diverge sharply, leveling off to limiting values, $\bar{E} \approx 2|\epsilon|h\nu_c$. Thus, great care must be exercised in drawing conclusions from the extrapolation of E_s to zero. For example, it is customary to obtain E_c by plotting \bar{E} vs E_s using different solvents, then reading E_c off the extrapolated straight line intercept with the y-axis. It is clear from Figure 5 that a serious error can result if ϵ is appreciable.

The solid dots in Figure 5 are obtained from our two-mode model by diagonalizing a 132×132 matrix as discussed earlier and, hence, should be reasonably accurate over the entire range. In this calculation, the parameters λ_c and ϵ have been held fixed at 1.1 and -6, respectively, the C & T ion values. The results agree with the analytical calculation in the delocalized limit but diverge strongly in the intermediate region. The calculation predicts an essentially solvent independent band position for the C & T ion, as is indeed observed.

Electron Transfer Rates

Electron transfer theories in mixed-valence and related systems have been summarized elsewhere ((5) and references therein). Conventionally, the electron transfer rate is calculated perturbationally using the Fermi golden rule assuming that the electronic perturbation (ϵ) is small. The most detailed

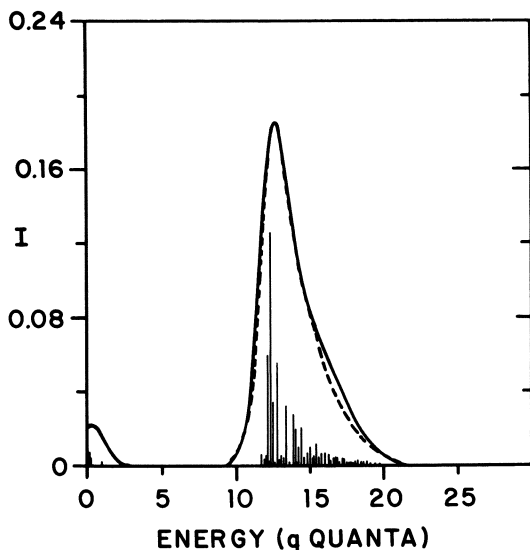


Figure 4. Experimental intervalence band (10) and calculated contour for the Creutz and Taube ion. The parameters used in the calculation are ϵ , -6.0 ; λ_e , 1.1 ; λ_s , 3.9 ; ν_e , 500 cm^{-1} ; and ν_s , 200 cm^{-1} at 300 K . Notation and symbols as in Figure 2 except $\text{FWHM} = 1.2 \nu_e$.

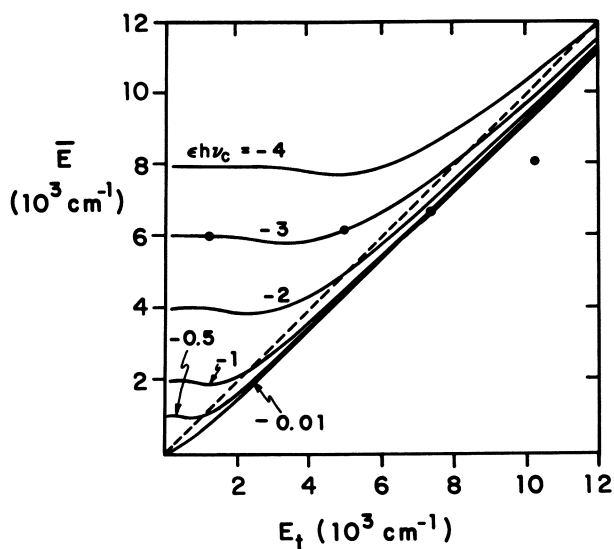


Figure 5. Mean band energy (\bar{E}) vs. total reorganization energy [Eq. (18)]. The dashed curve is the equation, $\bar{E} = E_t$. The solid curves are calculated from an analytical expression (9). The solid dots are calculated from a diagonalization of the two-mode model secular determinant with $\epsilon = -6.0$, $\lambda_e = 1.1$, and $\nu_e = 500 \text{ cm}^{-1}$.

treatments are those of Jortner (14) and Buhks (15). Before application of the perturbation (ε), the surfaces intersect--the so-called nonadiabatic or diabatic case. The problem then basically reduces to a calculation of vibrational overlap integrals between oscillator functions in the two potential wells (see (5) §IV.C.2 for a simplified example). As $|\varepsilon|$ increases from zero, the two potential surfaces separate, and a potential barrier appears in the lower (adiabatic) potential surface. As $|\varepsilon|$ grows larger, the conventional (perturbational) approaches fail. It is this situation--the so-called adiabatic case--that we briefly discuss here.

If we start with the two-mode model, the problem can be formulated as follows. If the system starts in one of the minima of the lower potential surface (W_1 of eq 12), what is the transfer rate to the other minimum? If ε is sufficiently large that the perturbational (Fermi golden rule) approach is inapplicable, it does not at present seem possible to solve this problem. Consequently, we return to the one-mode model. In this case, a solution of the problem is possible (6) using a method due to Weiner (16, 17). The details have been discussed elsewhere (4, 5, 6), and we simply summarize the results in Figure 6. The Fermi golden rule and Weiner methods agree for small $|\varepsilon|$ but diverge increasingly as $|\varepsilon|$ increases, the most pronounced difference occurring at low temperature. As an example, the parameters $\varepsilon = -3$, $\lambda = 3$ correspond roughly to the ion, $[(bpy)_2ClRu-pyr-RuCl(bpy)_2]^{3+}$ (pyr = pyrazine), prepared by Meyer and coworkers (18). In this case, we see from Figure 6 that the Weiner method predicts faster rates than the perturbation approach, the difference being about a factor of 5 at room temperature and more than an order of magnitude at low temperature. As might be expected, the two methods continue to diverge as $|\varepsilon|$ increases. If $|\varepsilon|$ gets so large that the transfer rate becomes comparable to v_c , the Landau-Zener correction ((5), eq 155) may be applied.

In the one-mode model, it seems reasonable to regard λ as an effective vibronic coupling parameter which describes both the solvent and intramolecular reorganization. Thus, using a single value of λ to fit an intervalence band should be a reasonable first approximation. And one might similarly hope that the use of this λ value in the Weiner method, when the electronic coupling is strong, is also reasonable. On the other hand, identification of such an effective λ with a molecular bond length, as for example via eq 17, seems quite unjustified. Eq 17 is much more reasonable in the two-mode model when λ is identified as λ_c .

It would clearly be of great interest to have experimental transfer rates in mixed-valence systems. We note the recent use

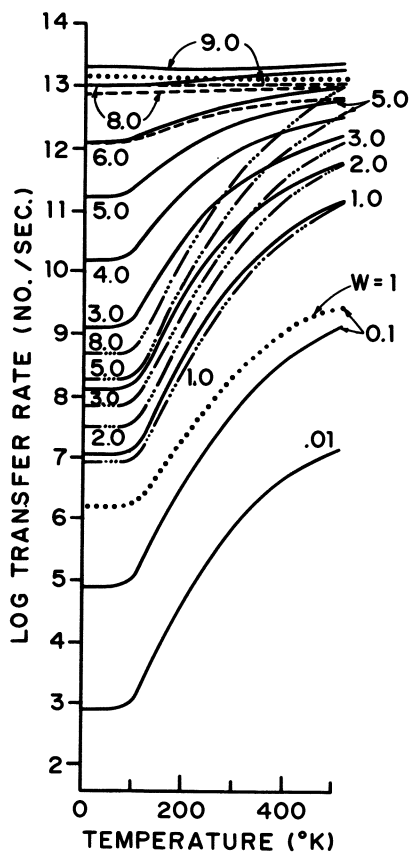


Figure 6. Log of the transfer rate vs. absolute temperature as a function of the electronic coupling (ϵ) for $\lambda = 3$, $\nu_e \equiv \nu_c = 450 \text{ cm}^{-1}$. The values of $-\epsilon$ are appended to the curves. The present calculations (—) are based on the Weiner method and an exact diagonalization of the model; the perturbational results ($\cdots\text{---}\cdots$) apply for small $|\epsilon|$. The Landau-Zener correction (---) is discussed elsewhere (4-6). The dotted horizontal line at the top is the limiting transfer rate for a single harmonic potential well with classical frequency $\nu_e = 450 \text{ cm}^{-1}$. All results are for $W = 0$ except the dotted line, $\epsilon = -0.1$, $W = 1$, which was calculated using the Jortner treatment (14). (Reproduced, with permission, from Ref. 5. Copyright 1981, John Wiley & Sons, Inc.).

of a dielectric relaxation method to measure such rates directly (19).

Concluding Remarks

We believe that our present extension of the vibronic coupling model (PKS) to include an effective solvent mode is a significant improvement. It should now be possible to take account of solvent effects explicitly and realistically. Furthermore, an analytical treatment is possible in both the localized and delocalized limits (9, 15). We note that these treatments can also be applied to unsymmetrical mixed valence systems (i.e., $A \neq B$ or $W \neq 0$). It is clearly possible to formally extend our two-mode model to any number of solvent and/or intramolecular modes. However, direct numerical diagonalization, even in the three-mode case, seems impractical in view of the enormous basis set requirements. But it is possible, in a straightforward manner, to extend the analytical treatments in both limits to any number of modes--indeed, to the continuum case. These important matters have been elegantly discussed by Buhks (15). In a subsequent paper (9), we shall present further details of the two-mode model and will discuss analytical treatments in limiting cases following the general methods of Buhks (15).

Acknowledgements

We wish to acknowledge a number of very illuminating discussions with Dr. Ephraim Buhks and have benefitted greatly from a copy of his Ph. D. Dissertation (15). We thank Dr. Peter Day for several preprints of his recent work. This work was supported by the National Science Foundation under Grant CHE8025608.

Literature Cited

1. Piepho, S. B.; Krausz, E. R.; Schatz, P. N. J. Am. Chem. Soc. 1978, 100, 2996.
2. Schatz, P. N.; Piepho, S. B.; Krausz, E. R. Chem. Phys. Lett. 1978, 55, 539.
3. Wong, K. Y.; Schatz, P. N.; Piepho, S. B. J. Am. Chem. Soc. 1979, 101, 2793.
4. Schatz, P. N. Proceedings of the NATO-ASI on Mixed Valence Compounds in Chemistry, Physics and Biology, Brown, D. B., Ed., Reidel: Dordrecht, Netherlands, 1980; p 115.
5. Wong, K. Y.; Schatz, P. N. Prog. Inorg. Chem. 1981, 28, 369.
6. Wong, K. Y.; Schatz, P. N. Chem. Phys. Lett. 1980, 71, 152.
7. Wong, K. Y.; Schatz, P. N. Chem. Phys. Lett. 1980, 73, 456.

8. Wong, K. Y.; Schatz, P. N. Chem. Phys. Lett. 1981, 80, 172.
9. Wong, K. Y.; Schatz, P. N., to be published.
10. Creutz, C.; Taube, H. J. Am. Chem. Soc. 1969, 91, 3988; 1973, 95, 1086.
11. Krausz, E. R.; Burton, C.; Broomhead, J. Inorg. Chem. 1981, 20, 434.
12. Stynes, H. C.; Ibers, J. A. Inorg. Chem. 1971, 10, 2304.
13. Hush, N. S. Proceedings of the NATO-ASI on Mixed-Valence Compounds in Chemistry, Physics and Biology, Brown, D. B., Ed., Reidel: Dordrecht, Netherlands, 1980 p 171, et seq.
14. Jortner, J. J. J. Chem. Phys. 1976, 64, 4860.
15. Buhks, E.; "Electron Transfer Processes"; Ph. D. Dissertation, Tel Aviv University: Israel, 1980.
16. Weiner, J. H. J. Chem. Phys. 1978, 69, 4743.
17. Weiner, J. H. J. Chem. Phys. 1978, 68, 2492.
18. Callahan, R. W.; Keene, F. R.; Meyer, T. J.; Salmon, D. J. J. Am. Chem. Soc. 1977, 99, 1064.
19. Bunker, B. C.; Kroeger, M. K.; Richman, R. M; Drago, R. S. J. Am. Chem. Soc. 1981, 103, 4254.
20. Day, P. International Reviews in Physical Chemistry 1981, 1, 149.

RECEIVED April 27, 1982.

General Discussion—Inclusion of Solvent Effects in a Vibronic Model for Mixed-Valence Compounds

Leader: Ephraim Buhks

DR. THOMAS MEYER (University of North Carolina): Dr. Schatz' treatment, which involved putting the solvent into the problem and watching the shoulder appear at high energies, was very nice. However, we have some experiments with osmium compounds that exhibit electronic structure in the IT region involving different, well-resolved spin orbit states. For ruthenium, spin-orbit coupling is much smaller but is still present and could be the origin for some of the structure in the IT region.

DR. SCHATZ: Are you referring to the spin-orbit coupling low-symmetry splitting? Yes. Presumably both effects could be operative.

DR. JOHN BRAUMAN (Stanford University): I have a general theoretical question. I get uncomfortable when people perform calculations on very complicated large systems without knowing what really happens on small ones. There's a wealth of interesting electron transfer literature, if you like, which has to do with atoms colliding with other atoms and small molecules colliding with atoms and things like that. These show cross sections which are highly variable, translationally-energy dependent, and so on. What is the status of calculations in that business?

DR. SCHATZ: I think those systems are not simpler. Since the intervalence band is at an order of magnitude lower energy than the intra-unit electronic transitions, one can use first-order perturbation theory in treating the former, but not the latter. I am assuming that other electronic states do not mix in significantly: i.e., it is just 2,3 and 3,2 as the electronic basis in the Creutz-Taube complex, for example. If other electronic states mix in, the model is dead.

DR. BRAUMAN: I guess what I'm saying is that, if you cannot treat something as simple as CO_2 , I find it difficult to believe that you can treat anything.

DR. P. P. SCHMIDT, (Oakland University): I'm working on lithium. That's a pretty simple system, especially without its single 2s electron. And yet it's still complicated. There are several problems. One is how to model the effect of the solvent and whether, in fact, you want to throw away the modeling that has been used, namely the continuum approximation. I think the answer to that is no, you don't want to throw it away completely. But one of the notions which has been developing, and is now being tested in the thermodynamics of solvation and other problems, is what is called the semi-continuum model. In

this approach you make the cavity bigger and bigger and put in as much solvent as necessary to carry out the calculations as accurately as possible.

Several approaches have been taken recently by a number of investigators, including Sheraga's and Warshall's groups, in developing potential energy functions for the interaction between various species. So with modern computational techniques, the answer to your question is yes, it will be possible to look at some fairly simple representative systems and to put in all of those dynamics as well as we can put them in. At the moment, agreement with theory is much better with simple-minded models which just take one step past the simple Born approximation. The results with the fancy calculations don't quite measure up, yet. However, I would say that if the spirit of Scheraga's work on proteins, with his model potentials, can be duplicated, it may be possible to do some really fantastic calculations.

DR. MARSHALL NEWTON (Brookhaven National Laboratory): I have one comment in response to Dr. Brauman. You asked an obvious question. One of the obvious answers is that there may be nothing rational about the way theories or experimental systems are chosen.

But there is a possibility of a direct answer to your question. The ideal gas phase prototype for activated charge transfer does not involve atoms, where you don't have a counterpart for reorganizational degrees of freedom. But molecular hydrogen interacting with molecular hydrogen ions is a beautiful case where, in fact, some of the experimental work has been done here at Wayne State University [Lees, A. B.; Rol, P. K. J. Chem. Phys. 1974, 61, 4444]. There have also been a number of dynamical, theoretical studies [e.g., Stine, J. R.; Muckerman, J. T. J. Chem. Phys. 1978, 68, 185] and ab initio calculations of the potential energy surfaces. I don't know if it has yet been put all together, but that is the kind of test case which is quite relevant.

It is also assumed that, when people do this in a gas phase, they're often more interested in determining how one resolves energy states than in obtaining specific information. It is the big change in the bond distance in going from H_2 to its ion, H_2^+ , which provides the analogue to the activated electron transfer problem in solution. Of course, this analogy is incomplete, since this simple gas-phase system lacks a continuum heat bath.

DR. GLENN CROSBY (Washington State University): I really think that Dr. Schatz' answer was correct: the reason why you get away with this kind of calculation is precisely that higher electronic states are removed far enough that you can ignore

them. In contrast, the Brauman systems are much more complicated, because they will require the use of a really extended basis set to mix in excited states. There would be systems, of course -- and this may be the case for the osmium systems -- where this would not apply because then the spin-orbit coupling would be big enough that these states would get involved and then it wouldn't be clear what you could do.

I have a question in two parts: one is about magnitude and the second one is concerning intensity. First, are these low-lying, tunnel-type transitions on the order of about 100 wave numbers or so?

DR. SCHATZ: Depending on the values of epsilon and lambda, they can have essentially any frequency or a vast range of intensities. So you can't make any simple general statement. For the Creutz-Taube ion, they are on the order of 50-100 wave numbers.

DR. CROSBY: It seems to me it would be possible to observe these if they're optically difficult, through electron tunneling spectroscopy.

Now the second question is, what is it in the calculation that changes the intensity so magnificently?

DR. SCHATZ: The intensities vary for two reasons. First of all, if the splitting is small, both sub-levels have appreciable population and so induced emission partially cancels the intensity. As the splitting gets larger, first-order perturbation theory no longer works and things get all mixed together. Finally, as you let the splitting get larger and larger, you reach what I call the delocalized case. At that point the tunneling transition turns back into just the ordinary infrared breathing vibration, which, in fact, is infrared forbidden, and so the intensity goes back to zero. So there is a complete correlation from one extreme to the other.

Parameters of Electron-Transfer Kinetics

NOEL S. HUSH

University of Sydney, Department of Theoretical Chemistry, Sydney, N.S.W. 2006, Australia

Over the last two decades, there has been a considerable increase in experimental information about the rates of electron transfer processes, particularly in solution in ionizing solvents. The main features (enthalpies, free energies and entropies of activation) of a large class of these reactions have been broadly understood for about the same length of time. It is interesting to note that the results of very early calculations of outer-sphere reaction rates and their temperature dependence frequently agree with recent more detailed estimates. In order to assess the applicability of different approaches, and thus to discriminate between them, it is desirable to have as much detailed information as possible about the relevant basic parameters. These include, for example, electron coupling or overlap energies, electron-phonon coupling strengths, vibrational frequencies, and spin coupling data. A brief survey is given of the types of experiment which may provide this information. With such data, discussions on matters such as the applicability of Golden Rule perturbation approaches, electronic adiabaticity, the role of nuclear tunnelling, etc., can be put on firmer ground, and some of the outstanding theoretical issues awaiting resolution are outlined.

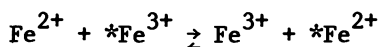
The theory of homogeneous electron transfer processes, as well as of the closely-related electron exchanges with metallic electrodes, has been the subject of considerable study. The proposal by Hush and by Marcus that these processes are, for simple systems, either usually electronically adiabatic or

0097-6156/82/0198-0301\$09.00/0
© 1982 American Chemical Society

nearly so, rather than being strongly dominated by electron tunnelling probabilities, is now generally accepted. For homogeneous transfers in ionizing solvents at ordinary temperatures, the application of absolute reaction rate theory to exchanges proceeding via an outer-sphere mechanism leads to fairly simple but general expressions for the free energy, enthalpy and entropy of activation (1-10).

Overview of Progress in Calculation of Electron-Transfer Rates

After more than two decades of investigation, it is pertinent to ask to what extent the predictions of this type of theory, and its agreement with experiment, have changed. The system which has received most study is the aquo ferrous-ferric outer-sphere symmetrical exchange:



In Table I are listed the first calculations (1961:8) of the enthalpy, entropy and free energy of activation at 298K. These are to be compared with the very recent (1980) calculations of Newton (11).

Table I
Kinetic Parameters for $\text{Fe}^{3+}/\text{Fe}^{2+}$ Self-Exchange in Water at 298K.

[Units: kcal mole⁻¹ or cal deg⁻¹ mole⁻¹].
(First values listed from Hush (8);
values in parentheses from Newton (11)).

	ΔG^*	ΔH^*	ΔS^*
contribution from intramolecular modes	5.0 (7.7)	5.0 (6.4)	0 (-4.1)
contribution from medium modes	7.3 (5.6)	7.3 (5.8)	0 (0.6)
total	20.3 (19.7)	10.8 (10.4)	-32 (-31.3)
Experiment (11)	~19	~10	> -30

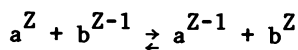
An interesting feature of this comparison is that the

variation in the contribution of 'inner' and 'outer' terms to the total values is not large, and the total values are very close indeed and also in reasonable agreement with experiment.

Now there are quite a number of differences in detail between these calculations. The more recent values from Newton, unlike the first, include *inter alia* allowance for departures from electronic and nuclear adiabaticity. There are also significant conceptual differences between the assumed models. At first sight, the overall agreement of calculations two decades apart might be taken to indicate that the models used in such calculations are too approximate for it to be possible to distinguish between them. I do not, however, believe that this is so. I think that we can be reasonably confident that the general approach is correct, but the challenge now is, indeed, to find reliable means of testing the detailed assumptions.

Contrasts in the Predicted Free Energy Dependence of Reaction Rates

A very similar situation exists with respect to cross-reactions. We have known for a long time (3, 5, 8) that the absolute reaction rate approach leads to the prediction that the free energy of activation of the process



is approximately the linear average of the aa and bb self-exchanges, plus half the overall free energy, provided that this is not too large. In Table II, the results for the first actual such calculation (5, 8) of the energetics of activation for a cross-reaction is shown. This is the plutonyl/plutonium exchange:

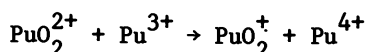


Table II
Kinetic Parameters for $\text{PuO}_2^{2+} + \text{Pu}^{3+} \rightarrow \text{PuO}_2^+ + \text{Pu}^{4+}$ Cross-exchange
Calculated from Theoretical Values for Constituent Self-exchange
in Aqueous Solution (5, 8)

		ΔH^*	ΔS^*	ΔG^*	(298K)
cal.:	(for I = 0):	4.3	-45	17.7	
exp.:	(for I = 1):	4.8	-40.4 ± 0.6	16.9	

The agreement with experiment is remarkably good and was gratifying at the time. However, we would now naturally feel impelled to examine the basic assumptions more closely before claiming too much for this. It may be asked why such a relatively complex system was chosen: the answer is that, at that time, it was the only well-characterized system for which data were available. This highlights the very great advances that have been made in measurement of electron transfer rates since that time. We now have (due, in large part, to the excellent work of Taube (12), Meyer (13), Sutin (14, 15) and their collaborators) a great deal of information about both self- and cross-exchange reactions on which to draw for comparison with theory. The existence of this body of data makes the further development of theory imperative and worthwhile. In what follows I shall consider what I think are the major points to be resolved.

At the 'classical' level [that is, one in which the frequencies of active vibrations can be assumed small relative to $k_B T$] it is usually stated [e.g., (16)] that the approaches of Hush and Marcus yield essentially identical results. This is true for self-exchanges. However, it is only true within a certain range of ΔG_0 , the overall free energy, for cross-exchanges. The energy of a chemical system is a functional of the first-order electron density [cf., (17, 18)]. The original Hush approach employs a simple one-electron density functional to calculate the difference of free energy between the activated complex and the 'precursor' complex. Assuming Born-Oppenheimer separability, the electronic wavefunction $\psi^+(\underline{r}_1, \underline{r}_2, \underline{R})$ of the transferring electron is:

$$\psi^+(\underline{r}_1, \underline{r}_2, \underline{R}) = C_1(\underline{r}_1, \underline{r}_2, \underline{R})\phi_1 + C_2(\underline{r}_1, \underline{r}_2, \underline{R})\phi_2$$

where $\underline{r}_1, \underline{r}_2$ are electron coordinates for centers 1 and 2 and \underline{R} is the internuclear separation. The electronic functions are centered on centers 1 and 2 and ϕ_1 and ϕ_2 , respectively. The amplitudes C_1 and C_2 in each state of the reaction path are as follows:

state	C_1	C_2
initial	0	1
precursor collision complex	C_{1p}	C_{2p}
activated complex	C_1^*	C_2^*
successor collision complex	C_{1s}	C_{2s}
final	1	0

The probability density for the transferring electron associated with the acceptor center 1 in state i is then:

$$|C_{1i}|^2 = \lambda_i \quad (1)$$

If we write the change of environmental energy (i.e., inner-sphere plus medium contributions) accompanying a vertical transition from precursor complex to the upper potential surface with electronic wavefunction

$$\psi^- = C_2(\underline{r}_1, \underline{r}_2, \underline{R})\phi_1 - C_1(\underline{r}_1, \underline{r}_2, \underline{R})\phi_2 \quad (2)$$

as χ (the "reorganization energy"), the formal transition-state electron densities, λ^* , and activation energies, $\Delta G^{*'}$, are as follows, where $\Delta G_0'$ is the overall free energy in the range $p \rightarrow s$:

$\Delta G_0'/\chi$	λ^*	$\Delta G^{*}'/\chi$
>1	1	$\Delta G_0'$
$\geq -1, \leq 1$	$\frac{1}{2}(1 + \frac{\Delta G_0'}{\chi})$	$\frac{(\chi + \Delta G_0')^2}{4\chi}$
$\geq -1,$	0	0

This type of approach does not explicitly involve specific energy-nuclear configuration relationships [e.g., intersecting

harmonic hypersurfaces]. However, in the range in which the ratio of the overall free energy, $\Delta G'_0$ (corrected for energies of precursor and successor state formation), to the reorganization energy, χ , is within the limits ± 1 , the above predictions are essentially the same for weak-interaction systems as those reached by the formally non-adiabatic approach of finding the intersection point of two harmonic energy hypersurfaces (the classical limit of the saddle point method). This is illustrated in Figure 1, where a quadratic dependence on overall free energy, within these limits, is seen to be predicted by either approach. Thus, in the range $1 \geq \Delta G'_0/\chi \geq -1$, it is correct to say that the Hush and Marcus approaches yield essentially the same predictions for energetics of activation of exchange. This rests ultimately, as shown in (10), on the formally identical roles of the electron density parameter λ^* and the Lagrange factor $|m|$ in the respective approaches.

Outside these limits, however, the two approaches result in different predicted kinetic behavior of both exoenergetic and endoenergetic exchanges. If the reaction is assumed to proceed classically with an energy barrier corresponding to the height of the reactant/product hypersurface intersection point, the quadratic dependence of ΔG^* on $\Delta G'_0$ is predicted to persist both for highly endoenergetic and exoenergetic reactions. The density functional approach, however, predicts activation free energies of zero and $\Delta G'_0$ for $\Delta G'/\chi < -1$, > 1 , respectively [cf., Figure 1].

The reason for this difference is very simple. It is that the density functional approach calculates the rate for the adiabatic channel. For $\Delta G'_0 \geq \chi$, this will proceed via an activated complex with successor-state formal electron density parameter $\lambda^* = 1$; for $\Delta G'_0 < -\chi$, it will proceed via an activated complex with $\lambda^* = 0$. By contrast, the rate predicted in the classical limit of the saddle point method for either a highly exoenergetic or endoenergetic process assumes (explicitly or implicitly) electron tunnelling between upper and lower surfaces, i.e., an electronically non-adiabatic pathway. Thus, insofar as the system does, in fact, remain on a potential surface associated with the electronic wavefunction ψ^+ , an adiabatic channel will dominate the exchange rate and the rates of strongly exoenergetic electron transfers of similar types will be predicted to approach a constant limiting value. In particular, no "inverse" rate/free energy relationship would be expected. This appears to be more in agreement with experiment than the prediction of an "inverse" region. In the adiabatic channel, the successor (s) complex in a strongly exoenergetic exchange will be formed in an excited vibrational state, with excess energy

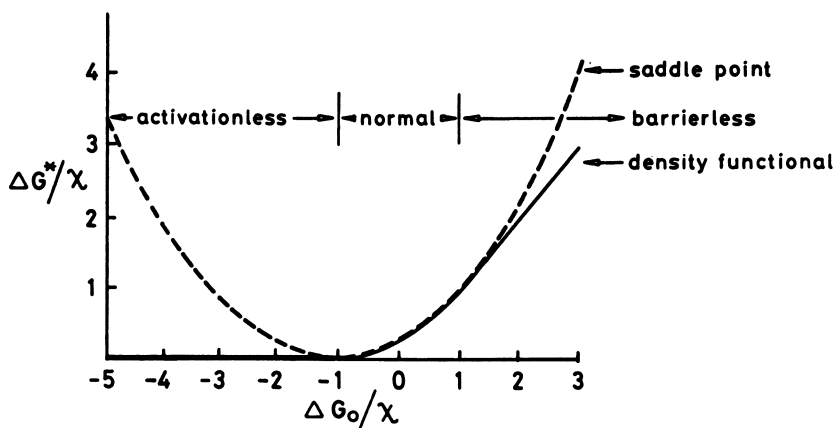


Figure 1. Relationship between activation free energy and overall free energy (values in units of electron-vibrational coupling energy χ) in high-temperature limit. Key: —, adiabatic density functional approach; and ---, nonadiabatic perturbational approach. (Work of forming precursor and successor states omitted.)

$E_{\text{vib}(s)}$ given by:

$$E_{\text{vib}(s)} \cong \Delta E'_0 - \chi \quad (3)$$

which deactivates to the final state at a rate assumed fast compared with electron exchanges in the adiabatic channel. The extent to which either limiting assumption is applicable in the exoenergetic region cannot, however, be decided definitely until more experimental and theoretical information about energy transfer rates in solution is available.

Intervalence Transfer

Where thermal electron transfer can occur, there is also always a corresponding optical transfer, which I have termed intervalence transfer (19-21). The principle is illustrated in a single coordinate representation in Figure 2. Clearly, it will be possible to relate thermal to optical transfer probabilities, and, hence, to predict the rate of one process from parameters obtained for the others. The connection is, in fact, a very close one, as indicated schematically in Figure 3.

The intervalence transfer extinction coefficient, ϵ , is proportional to a frequency-dependent conductivity, σ_ω , with a maximum at ω_0 , approximately the intervalence band maximum. If we extrapolate to zero frequency, the zero-frequency limit σ_0 of the frequency-dependent conductivity is the thermal rate. This fact is particularly important when we consider such matters as nuclear tunnelling.

Until quite recently there have not been many systems for which experimental information for both optical and thermal processes were available. One such is the Eu(II)/Eu(III) exchange in the wurtzite-type mixed-valence Eu_3S_4 lattice, with equal coordination numbers around each metal ion. Mössbauer (22) and electrical conductivity (23) data indicate that χ for this approximately symmetrical exchange is ca. 0.22 eV, so that an intervalence transfer band is predicted to exist with a maximum frequency of ca. 0.9 eV. This was, in fact, observed (at 300K) in earlier work in our laboratory; more recently, we have measured the spectral characteristics down to 10K. This enables an estimate of the frequency of the effective phonon coupling mode to be made.

Thus, as far as the overall electron-phonon coupling energy is concerned, we have reasonably good correlation here between optical and thermal processes. Recently, owing particularly to the work of Taube and of Meyer, there is beginning to be an increasing body of data of correlations of this type, which are of great importance.

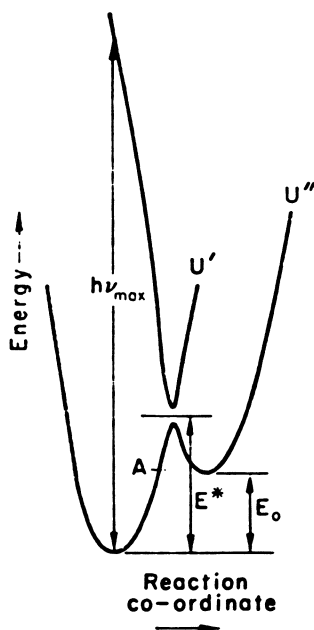


Figure 2. Intervalence band maximum ($h\nu_{max}$), thermal activation energy E^* , and overall energy E_0 for weak-interaction electron transfer.

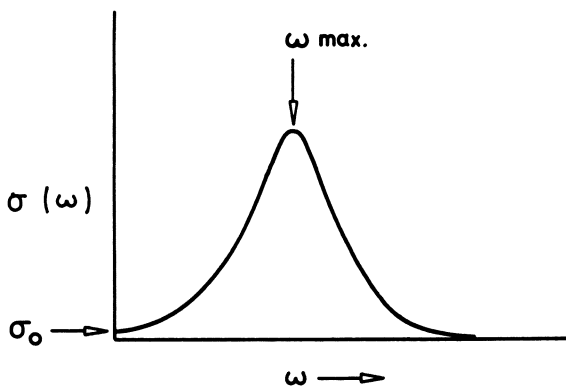


Figure 3. Frequency-dependent conductivity [$\sigma(\omega)$] for electron-transfer process.

The Electronic Interaction Term. A question raised earlier was: is the magnitude of J sufficiently small to justify the weak-interaction assumption? This is a question which can be answered, at least for mixed-valence complexes, by interpretation of the oscillator strength of the intervalence band. In Table III, some data (24, 25) for the intervalence band of the complex ion $[\text{Fe(II)Fe(III)(CN)}_{11}]^{6-}$, described initially by Ludi, et al. (26), are shown:

Table III
Parameters for Intervalence Transfer Band
of $[(\text{CN})_5\text{Fe(II)(CN)Fe(III)(CN)}_5]^{6-}$ (24, 25)

Effective frequency, $\hbar\omega_0$	$460 \pm 50 \text{ cm}^{-1}$
Electron-vibrational coupling energy, χ	$7.8 \pm 1 \text{ kK}; 0.97 \pm 0.13 \text{ eV}$
$h\nu_{\text{max}}$	$7.8 \pm 1 \text{ kK}; 0.97 \pm 0.13 \text{ eV}$
E_0	$\cong 0$
$ c_{1p} ^2$	0.037
J	$1.5 \text{ kK}; 0.19 \text{ eV}$

In this complex, the energy gap $2J$ separating upper and lower potential surfaces is estimated to be $\sim 0.19 \text{ eV}$. This is evidently too large for the weak-interaction limit to hold. In other systems, J may, in fact, become so large that we have a single minimum, with a stationary delocalized electronic ground state.

The very simplest theoretical approach, with linear electron-phonon coupling, is in terms of a two-center (a,b) one-electron Hamiltonian (27), with just one harmonic mode, ω , associated with each center. This is (in second quantized notation, with $\hbar = 1$):

$$H = (n_a + n_b)E_{0a} + n_b\delta + J(c_b^\dagger c_a + c_a^\dagger c_b) + \frac{\omega_0}{4} \sum_{i=a,b} [\dot{Q}_i^2 + Q_i^2] + \sum_{i=a,b} g n_i Q_i \quad (4)$$

In eq 4, E_{oa} is the energy of an electron in ϕ_a , and δ is the difference $E_{ob} - E_{oa}$; δ is, of course, zero for a symmetrical complex. The electron occupation number for site i is n_i . The electronic coupling integral is J (assumed constant) and c_i^\dagger , c_i are electron creation and annihilation operators, respectively ($n_i = c_i^\dagger c_i$). The linear electron-phonon coupling constant is denoted by g , and Q_i is the dimensionless normal mode coordinate for mode ω_0 at site i . The Hamiltonian can be re-expressed in terms of coordinates

$$\begin{aligned} q_s &= \frac{1}{\sqrt{2}} (Q_1 + Q_2) - 2\sqrt{2} g/\omega \\ q_u &= \frac{1}{\sqrt{2}} (Q_1 - Q_2) \end{aligned} \quad (5)$$

In terms of the new coordinates, the Hamiltonian can be re-expressed as

$$\begin{aligned} \tilde{H} &= (n_a + n_b)E_{oa} + n_b\delta + J(c_b^\dagger c_a + c_a^\dagger c_b) - g^2/\omega_0 \\ &+ \frac{\omega_0}{4} [q_s^2 + q_s^2] + \frac{\omega_0}{4} [q_u^2 + q_u^2] \\ &+ \frac{g}{\sqrt{2}} (n_a - n_b)q_u \end{aligned} \quad (6)$$

Typical potential energies associated with such a Hamiltonian are shown in Figure 4 as a function of the parameter $\theta = \chi/2J$. The coordinate is the antisymmetric combination. The symmetric mode clearly adds a term to the total energy independent of coupling.

For a number of purposes, such a Hamiltonian and associated potential energy can be useful--for example, in discussing electron spin resonance (27, 28) and other properties where the over-all electron-phonon coupling energy is of most importance, and can be reasonably modelled in terms of a single 'effective' coupling mode. However, in real systems we will expect that many modes are operative--e.g., both from prediction and from the experimental results of Taube and of Meyer and their co-workers on the solvent dependence of frequency maxima of intervalence bonds, we know that phonon modes of the medium (as well as internal vibrational modes) are usually active in valence trapping. Thus, one would not expect the above Hamiltonian to be adequate for detailed discussion of the phonon structure of intervalence bands.

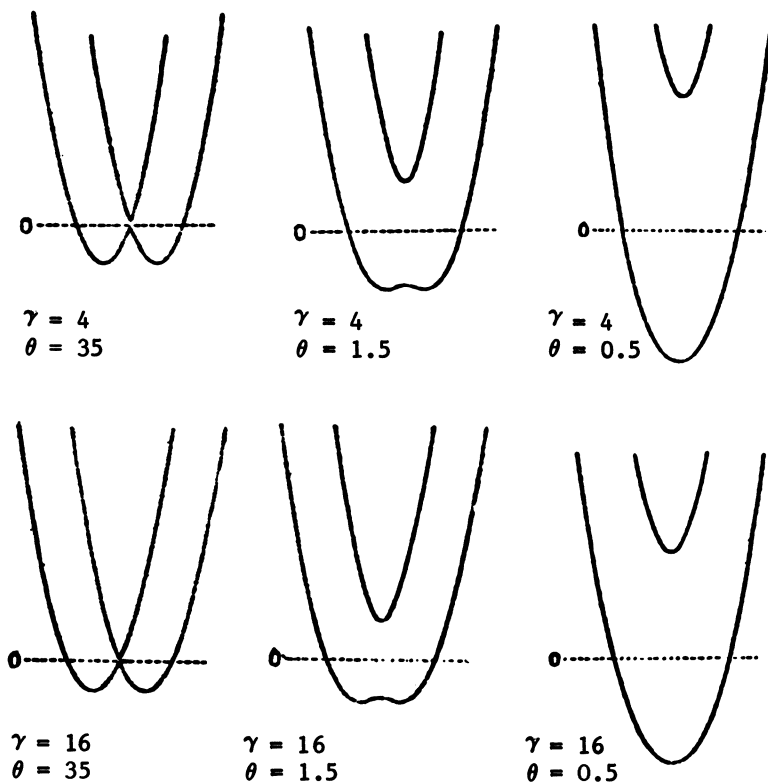


Figure 4. Potential energies for above Hamiltonian for different values of θ . The condition for appearance of a single minimum is $\theta (= \chi/2 J) < 1$.

The magnitude of the electronic interaction term, J , is also critical in determining the degree of electronic non-adiabaticity [such as Newton has been discussing] that may be present. The electronic transmission coefficient, κ , can be expressed as (21):

$$\kappa = (1 - e^{-\alpha}) , \quad \text{where } \alpha = \frac{J^2 \pi^{3/2}}{\hbar \bar{\omega}_1 [\chi k_B T]^{1/2}} \quad (7)$$

where $\bar{\omega}_1$ is an effective coupling frequency. Clearly, κ is very close to unity if J is large compared with $k_B T$. How is the approximate value of the electronic coupling energy, J , to be obtained?

There exist systems in which, in principle, J can be directly measured. An example is the μ -oxo silicon phthalocyanine dimer studied by Hush and Cheung (29). It is found directly from the valence ultraviolet photoelectron spectrum of the dimer that the energy gap, $2J$, in the radical dimer monocation is 0.32 eV, and that, in the gas phase, this is a delocalized system ($\chi/2J < 1$). Measurements of this kind are only easily made on initially uncharged systems.

It should be mentioned that one has to be careful in defining the 'localized' states whose interaction (in the single-particle approximation) results in the energy splitting. The Creutz-Taube ion [bis(pentaammine-ruthenium)pyrazine]⁵⁺ (30) provides an example of this. There is good reason to suppose (in spite of many earlier arguments to the contrary) that this is a fully delocalized mixed-valence system (27). In D_{2h} symmetry, the one-electron levels separated by energy gap $2J$ are calculated to have b_{2u} (bonding) and b_{3g} (antibonding) symmetry, respectively. These are shown in Figure 5. In the lower half of the figure, the sum and difference of these functions are shown. These are the 'localized' states. It is clear that neither is actually localized on one of the metal centers. They are both partially delocalized onto the pyrazine ring, and are approximately non-bonding in nature. Thus, if we are to attempt to calculate the electronic splitting factor for a given system, we may expect that it will usually be too severe an approximation to restrict this to an electronic wavefunction based on two nuclei only.

We have assumed here that J can be treated as a constant. In some types of calculation, the explicit distance-dependence of the electron coupling integral must be taken into account. Little is yet known of the appropriate form of such a dependence.

For mixed-valence systems which are not delocalized, but

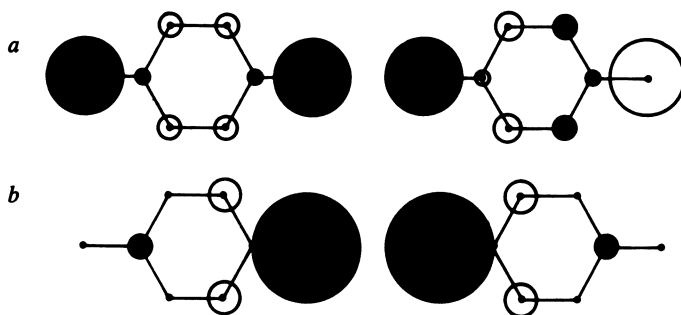


Figure 5. One-electron representation of $p\pi/d\pi$ orbitals involved in coupling in Creutz-Taube ion. Key: *a*, $2b_{2u}$ (doubly filled) and $2b_{3g}$ (half-filled); and *b*, localized orbitals $2^{-1/2}(2b_{2u} \pm 2b_{3g})$ (27).

which exhibit dynamic valence trapping, it is possible to estimate the value of J (assumed constant) from the oscillator strength of the intervalence absorption band. This is a very important source of such data. However, we must add a note of warning. If we were dealing with exact wavefunctions, then oscillator strength for an electric dipole-allowed transition could be expressed equivalently in a number of formalisms--dipole length, dipole velocity, dipole acceleration, etc. The relationship of the first two for transition $i \rightarrow j$ with transition energy ($E_j - E_i$) is:

$$\langle i | \vec{r} | j \rangle = \frac{-\hbar^2}{m(E_j - E_i)} \langle i | \vec{V} | j \rangle \quad (8)$$

length velocity

For approximate wavefunctions, however, the various formulations give rise to different theoretical predictions. This has been demonstrated in detail, for example, by Hush and Williams (31) for large aromatic systems. Thus, when we wish to obtain exact values of J , we must be very careful in deciding which formalism to use. A final point here is that the one-electron model does not take into account configuration interaction. Calculations for relatively simple systems would be useful here.

Nuclear Tunnelling

Electronic non-adiabaticity can give rise to a factor κ which is less than unity; the nuclear tunnelling factor, Γ , on the other hand, is always greater than or equal to unity.

Does Γ differ significantly from unity in typical electron transfer reactions? It is difficult to get direct evidence for nuclear tunnelling from rate measurements except at very low temperatures in certain systems. Nuclear tunnelling is a consequence of the quantum nature of oscillators involved in the process. For the corresponding optical transfer, it is easy to see this property when one measures the temperature dependence of the intervalence band profile in a dynamically-trapped mixed-valence system. The second moment μ_2 of the band, which is a measure of the bandwidth, ultimately becomes independent of temperature below the Debye temperatures for all the modes involved in electron-phonon interaction. Figure 6 shows a typical example of this behavior.

How important, though, is nuclear tunnelling for thermal outer-sphere reactions at ordinary temperature? If we work in the Golden Rule formalism, an approximate answer was given some time ago. In harmonic approximation, one obtains from consideration of the Laplace transform of the transition probability (neglecting maximization of pre-exponential terms) the following expressions for free energy (ΔG^*) and enthalpy (ΔH^*) of

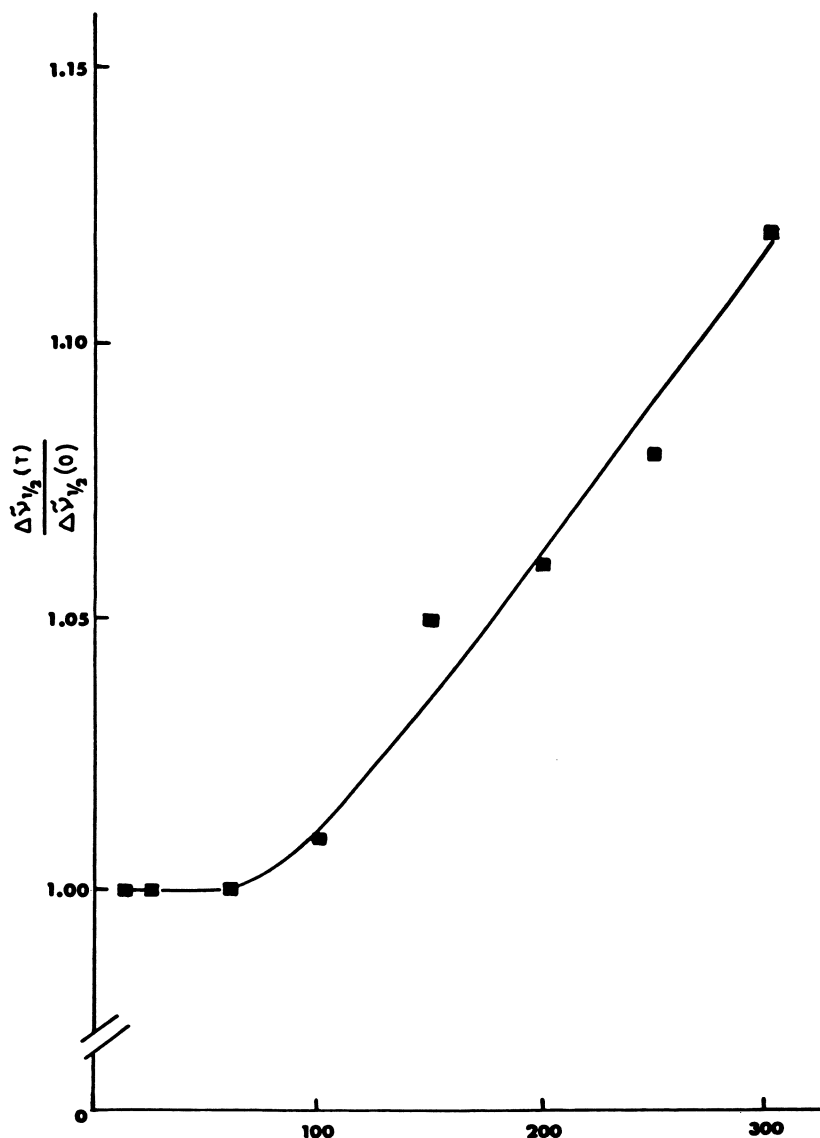


Figure 6. Temperature dependence of half-width of intervalence transfer absorption for $[(\text{NH}_3)_5\text{Ru}(4\text{-cyanopyridine})\text{Ru}(\text{NH}_3)_5]^{5+}$ mixed-valence (24, 25).

activation for a weak-interaction outer-sphere self-exchange (32):

$$\begin{aligned}\Delta G^* &= E' = \frac{kT}{2\hbar} \underline{\Delta\Omega} \tanh\left(\frac{\beta\hbar\Omega}{4}\right)\underline{\Delta} \\ \Delta H^* &= E' - T\left(\frac{\partial E'}{\partial T}\right) = \frac{1}{8}\underline{\Delta\Omega}^2 \operatorname{sech}^2\left(\frac{\beta\hbar\Omega}{4}\right)\underline{\Delta}\end{aligned}\quad (9)$$

In this expression $\underline{\Delta}$ and $\underline{\Omega}$ are distance dispersion resulting from electron-vibrational coupling, and frequency tensor (assumed identical in reactant and product states), respectively (work of formation of precursor and successor states is omitted). If we assume that the frequency tensor is diagonal, then we have simply a sum of independent terms for all inner and outer contributing modes. At sufficiently high temperature, the hyperbolic tangents become unity and we obtain the usual (in this approximation) high-temperature expression:

$$\Delta G^* = \Delta H^* = \frac{kT}{8\hbar} \underline{\Delta\Omega\Delta} = \chi/4$$

The value of χ can be also written as

$$\chi = \sum_{k=1}^N \chi_k = \sum_{k=1}^N \frac{1}{2}\omega_k^2 Q_k^2 = \sum_{k=1}^N S_k \hbar\omega_k \quad (10)$$

where the summation is over all active modes ω_k with normal coordinate Q_k . It is clear that the nuclear tunnelling factor, $\Gamma(T)$, is then a sum of the individual tunnelling factors $\Gamma_k(T)$ for each mode ω_k , i.e.,

$$\Gamma(T) = \sum_{k=1}^N \Gamma_k(T) \quad (11)$$

In order to estimate the Γ_k accurately (in the Golden Rule independent oscillator model), we need to take account also of the pre-exponential factor. Making use of the fact that we are considering, in effect, the zero-phonon line intensities, it is easy to show (26) that for $\hbar\omega_k \gtrsim 2k_B T$,

$$\Gamma_k(T) = \left[\frac{\hbar\omega_k}{2k_B T} \operatorname{csch}\left(\frac{\hbar\omega_k}{2k_B T}\right)\right]^{-\frac{1}{2}} \exp\left[S_k \left\{\frac{\hbar\omega_k}{4k_B T} - \tanh\left(\frac{\hbar\omega_k}{4k_B T}\right)\right\}\right] \quad (12)$$

Typical values of $\Gamma_k(T)$ so calculated (26) for frequencies in the range 100-400 cm^{-1} and number of quanta S_k involved in coupling to that mode are shown in Table IV.

Table IV
 Non-resonant Golden Rule Nuclear Tunnelling Factor Γ_k (298)
 for Self-exchange.
 (Value corresponds to factor for mode k
 with S_k quanta excited (32)).

ω_k (cm^{-1})	S_k : 2	5	10	15	20	25
100	1.006	1.008	1.011	1.014	1.017	1.020
200	1.028	1.042	1.066	1.090	1.115	1.141
300	1.075	1.123	1.210	1.303	1.403	1.510
400	1.152	1.275	1.509	1.786	2.114	2.502

It is interesting to calculate the tunnelling factor, using this analytical expression, for typical outer-sphere exchanges. We select the self-exchanges in water $\text{Fe(II)(H}_2\text{O)}_6/\text{Fe(III)(H}_2\text{O)}_6$ and $\text{Co(III)(NH}_3)_6/\text{Co(II)(NH}_3)_6$. The contributing modes are taken to be an average intramolecular metal-ligand breathing frequency, and two solvent modes (33, 36), of frequency 170 cm^{-1} and 1 cm^{-1} , respectively. The corresponding solvent dielectric constants (298K) are taken as $\epsilon_j = 78.3$, $\epsilon_{\text{ir}} = 5.0$, $\epsilon_{\text{op}} = 1.78$ [cf., refs (33, 36)]. With $\chi_2 = (\epsilon_{\text{ir}}^{-1} - \epsilon_{\text{op}}^{-1})(\chi_2 + \chi_3)^{-1}$ and $\chi_3 = (\epsilon_s^{-1} - \epsilon_{\text{ir}}^{-1})(\chi_2 + \chi_3)^{-1}$, we have (in cm^{-1}):

	$\text{Fe(II)(H}_2\text{O)}_6/\text{Fe(III)(H}_2\text{O)}_6$	$\text{Co(II)(NH}_3)_6/\text{Co(III)(NH}_3)_6$
χ_1	11720	16070
χ_2	5901	6452
χ_3	3053	3387

The average values of $\bar{\omega}_1$ are taken here to be 431 and 396 cm^{-1} for the iron and cobalt systems, respectively. From eq 12 we then obtain the nuclear tunnelling factors shown in Table V.

Table V
Non-resonant Nuclear Tunnelling Factor $\Gamma(298)$
for Self-exchange in Aqueous Solution

	Γ inner	Γ outer	Γ
$\text{Fe}^{\text{II}}(\text{H}_2\text{O})_6 - \text{Fe}^{\text{III}}(\text{H}_2\text{O})_6$	3.46	1.12	3.88
$\text{Co}^{\text{II}}(\text{NH}_3)_6 - \text{Co}^{\text{III}}(\text{NH}_3)_6$	4.19	1.13	4.73

These are essentially in agreement with values calculated by less direct methods (36). What is particularly interesting is the fact that, if the Golden Rule assumptions are indeed applicable, the nuclear tunnelling factor is less than an order of magnitude for these important systems. In particular, it is not expected to be important in determining the rate of a system which has traditionally been thought to be anomalous: the cobalt hexaammine exchange. It should be noted that work in progress in Professor Taube's laboratory (37) suggests that previous estimates of the rate of this exchange are probably considerably too low, so that the anomaly may be only an apparent one. The theoretical estimate of Jortner, et al. (38), appears to be definitely too low.

The Golden Rule approach has been used for many years by Levich, Dogonadze, and co-workers (39, 40), who have stressed the difference between the roles of "quantum" (high-frequency) and "classical" coupling modes in discussing the theory of electron transfer, and by a number of subsequent workers (16, 41).

For typical outer-sphere exchanges at ordinary temperatures, it seems probable that the original assumption of Hush and of Marcus that barrier penetration is a comparatively minor effect is correct. Moreover, it is, in a particular case, quite simple to calculate. The more general questions to which we do not yet have an answer are: how adequate is the Golden Rule approach in discussing tunnelling, and, in particular, what would be expected for systems strictly remaining on one surface (electronically adiabatic)? A number of fundamental issues involved here have been discussed in a recent series of papers (42-45).

Electron-Phonon Coupling Energies and Frequencies from Experimental Data

One experimental source of these essential data (for mixed-valence systems) is the intervalence transfer absorption band. The moments of the envelope (particularly the first and second moments) can be interpreted to yield values for χ and (from a study of temperature dependence) for an effective coupling frequency. The study of effects of solvent variation can also lead to separation of χ into intramolecular and environmental components.

Mention should be made here of recent attempts by Piepho, Schatz and Krausz (46) to give a general interpretation of intervalence bandshapes in terms of a Hamiltonian equivalent to that of eq 6. They use vibronic eigenfunctions (following the method of solution of Merrifield (47)) rather than adiabatic Born-Oppenheimer (ABO) functions. Thus, the aim is to interpret an observed spectrum in terms of one vibrational coupling mode, which is antisymmetric. Their analysis of the spectrum of the Creutz-Taube ion yields a value of θ of 1.215, i.e., a rather weakly localized ground state. Using their assumed unperturbed coupling vibration frequency (500 cm^{-1}), the resultant energy curves and vibrational eigenvalues for the Creutz-Taube ion are as shown in Figure 7.

The eigenvalues calculated either by the Merrifield or ABO method are nearly identical. As can be seen, this analysis leads to the prediction of a number of low-lying infrared absorption bands for this complex. In a discussion of the structure of the Creutz-Taube ion, I pointed out some time ago (27) that the evidence definitely favors a well-delocalized ground state ($\theta < 1$), and predicted that these infrared bands would, thus, not be observed. In a recent publication, Krausz, et al., report that a search for the bands indeed gave negative results, and withdraw their proposed interpretation of the spectrum (48).

The deficiencies of the Piepho-Krausz-Schatz modes are twofold. Firstly, only one coupling mode is assumed. This is unlikely to be realistic--the work by Meyer and coworkers on solvent effects on intervalence bands indicates very clearly the multimode nature of coupling. Secondly, however, the model makes no allowance for coupling to symmetric modes. This means that, in a delocalized complex, transition from a bonding to an antibonding electronic state cannot result in a change in molecular geometry, i.e., of bond lengths and angles. A simple molecular approach (27) shows that quite appreciable changes in bond order will be expected to accompany the intervalence transition; correlation of these with bond length/angle changes and transformation to symmetric mode normal coordinates could then yield the coupling constants for symmetric modes. This would appear quite naturally from an ab initio (all electron) calculation,

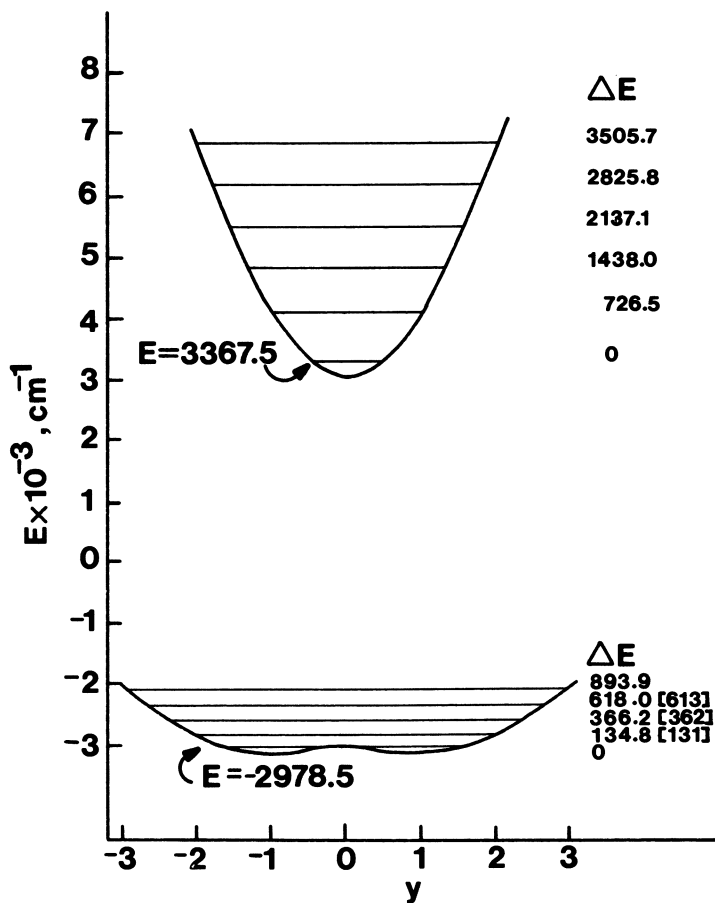


Figure 7. Potentials for lower and upper surfaces in Creutz-Taube ion calculated by method of Piepho, Krausz, and Schatz, as function of dimensionless coordinate, y , with $J = 0.4 \text{ eV}$, $\omega_0 = 500 \text{ cm}^{-1}$ and $\theta = 1.215$. Eigenvalues in brackets are vibrational levels given in Ref. 46.

in which ground and excited state geometries were separately optimized. Thus, for detailed analysis of phonon structure, the Hamiltonian eq 6 is quite inadequate. It can most simply be generalized, retaining the one-electron description, by including an additional term to allow for coupling to symmetric modes, with phenomenological coupling constants, perhaps calculated as suggested above from an approximate molecular orbital treatment. Coupling to symmetric modes, leading as it does to distance dispersion, has a much greater relative effect on bandwidth than coupling to antisymmetric modes, which leads only to frequency dispersion.

A striking effect of this kind is shown in Figure 8, where the intervalence spectrum of the Creutz-Taube ion, in which the bifunctional ligand is pyrazine, is compared with that of the corresponding ion in which a low-symmetry perturbation is introduced by substituting OMe for one hydrogen of the ring (24, 25). The much greater width of the band is calculated to be due mainly to distance dispersion induced by symmetric mode coupling.

Evaluation of Coupling Strengths

There are at least two ways in which detailed information about electron-vibrational coupling strengths can be obtained for mixed-valence complexes. Both are based on the fact that such coupling will be reflected in modifications of the vibrational spectrum. Thus, for example, coupling to antisymmetric modes in a symmetric ion will modify intensities and frequencies of the modes involved.

Figure 9 shows the result of a model calculation (using a mean-field approach) for a delocalized complex with $\theta = 0.60$, in which there is equal coupling to each of four modes ω_i ($\theta_i = 0.15$), with $\omega_i = 350, 500, 700$ and 1100 cm^{-1} , respectively (32). The frequency shifts are calculated to be $-66, -50, -54$ and -76 cm^{-1} , respectively, with relative induced intensities as shown. It is clear that a detailed investigation of the vibrational spectrum of mixed-valence systems should be rewarding.

The second source is resonance Raman spectra. The so-called A term of the polarizability tensor for one mode in such a spectrum is given in a usual notation by (49):

$$[\alpha_{\rho\rho}]_{gn,g0} = \frac{1}{hc} | [\mu_{\rho}]_{ge}^0 |^2 \sum \frac{\langle n_g | v_e \rangle \langle v_e | 0_g \rangle}{v \tilde{\nu}_{ev,g0} - \tilde{\nu}_0 + i\Gamma_{ev}} \quad (13)$$

where frequency differences of ground and excited states are

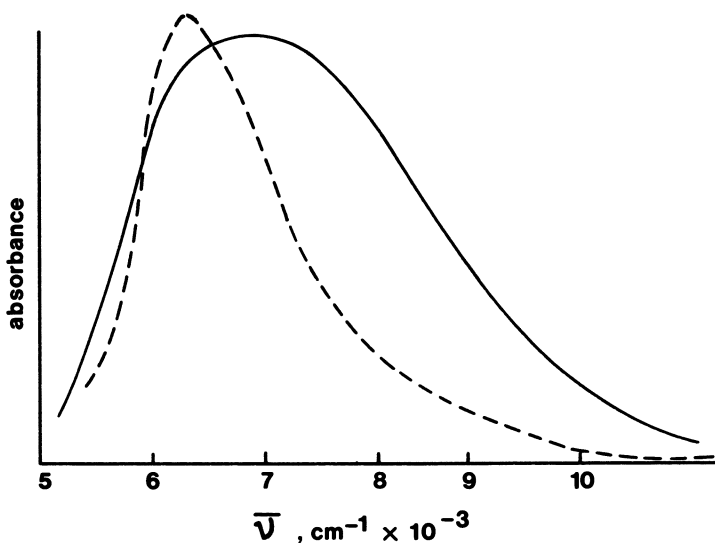


Figure 8. Intervalence spectrum of Creutz-Taube ion (---) and of the corresponding ion with 1-methoxypyrazine (—) instead of pyrazine (D_2O solution, 298 K). (24, 25).

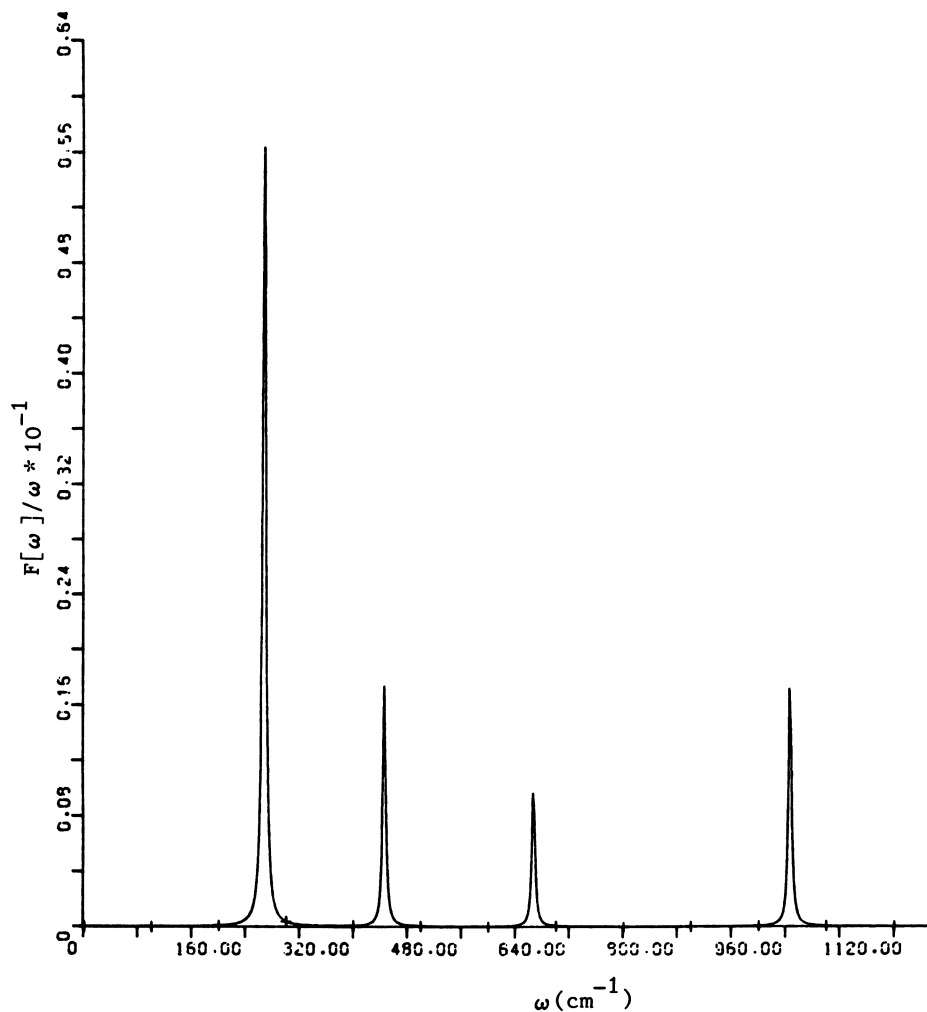


Figure 9. Electron-transfer-induced IR absorption with equal coupling to four modes (see text).

ignored. The vibrational overlap term is

$$\begin{aligned} \langle 0_g | 0_e \rangle &= \exp(-\Delta^2/2) \\ \langle 0_g | \nu_e + 1 \rangle &= - \frac{\Delta}{(\nu+1)^{\frac{1}{2}}} \langle 0_g | \nu_e \rangle \end{aligned} \quad (14)$$

where Δ is the displacement. This can be generalized to a multimode description. Already there is quite a sizable body of data accumulating on the resonance Raman spectroscopy of mixed-valence systems (49, 50). Some show the long overtone progression anticipated for very strong coupling (and hence large Δ) to a mode. Analysis of these will yield very useful detailed information about coupling strengths.

Methods discussed so far for determination of χ assume that two ions are present and that electron transfer can be observed --as, e.g., in a mixed-valence system. What can be obtained for systems (e.g., $\text{Fe(III)(H}_2\text{O)}_6/\text{Fe(II)(H}_2\text{O)}_6$) where this is not possible? In such cases, in particular, the study of photoemission from (single) ions or molecules in solution will become increasingly important. If, in the gas phase, one ionizes a molecule such as anthracene to form the radical cation in its ground state, the difference between adiabatic and vertical ionization potential is a measure of the coupling of the hole to the intramolecular vibrational system (χ_{inner}). If we ionize from the molecule in solution, the corresponding difference is $\chi_{\text{inner}} + \chi_{\text{outer}}$, as shown in Figure 10.

It will not always be possible to obtain both gas- and solution-phase values [e.g., for an ion such as $\text{Fe(II)(H}_2\text{O)}_6$]. However, the solution-phase value should still yield the overall value of χ . Thus, one can, in principle, find χ from a one-center spectrum, as distinct from the two-center intervalence spectrum. Interesting work in this area, which will lead to such determinations, has been pioneered by Delahay (51).

It is a somewhat surprising fact that information about vibrational frequencies and bond lengths in very common and important ions is very sparse. Clearly, many more such determinations are necessary. Only this year, for example, have data become available which enable metal-ligand displacements on electron removal for the aquo Fe(II)/Fe(III) and Co(II)/Co(III) systems to be obtained. In view of the importance of these partially unpublished data, I have reproduced them in Table VI. The values of Δ for the Fe and Co systems are 0.128-0.137, and 0.208 Å respectively. The variability of the Fe results points to the fact that caution must be exercised in using data obtained in crystal lattices for a solution environment. Spin-polarized neutron diffraction studies on the structure of solu-

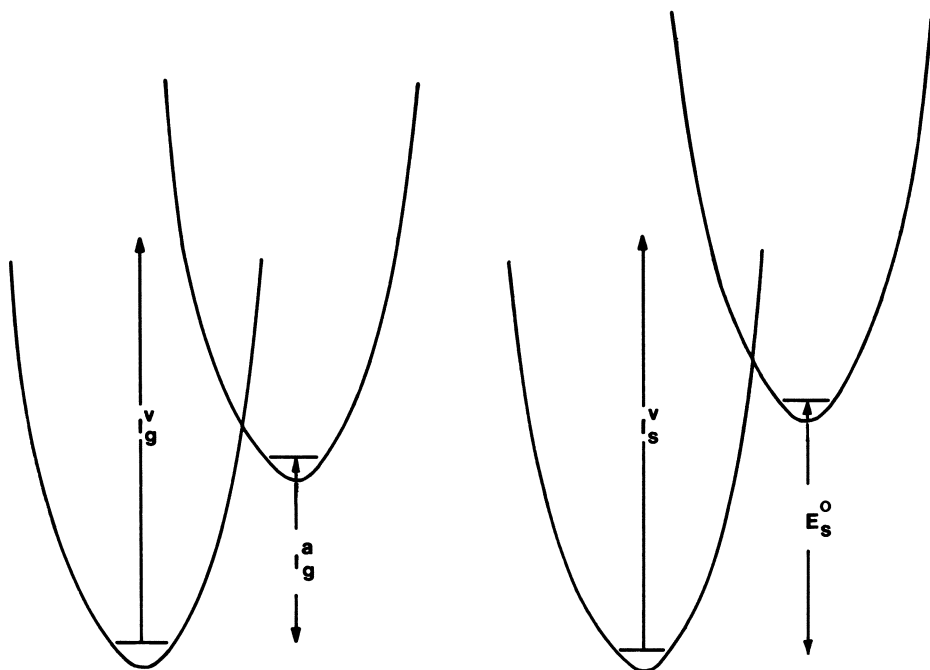


Figure 10. Comparison of photoionization $M \rightarrow M^+ + e^-$ from gas and solution phases. Key: left, gas phase $|g^v\rangle - |g^a\rangle = \chi_{inner}$, and right, solution phase, $|s^v\rangle - |s^o\rangle = \chi_{inner} + \chi_{outer}$.

tion shells of ions in solution may, in the near future, help to resolve this.

Finally, I refer back to the beginning of this paper, where the assumption of near-adiabaticity for electron transfers between ions of normal size in solution was mentioned. Almost all theoretical approaches which discuss the electron-phonon coupling in detail are, in fact, non-adiabatic, in which the perturbation Golden Rule approach to non-radiative transition is involved. What major differences will we expect from detailed calculations based on a truly adiabatic model--i.e., one in which only one potential surface is considered? [Such an approach is, for example, essential for inner-sphere processes.] In work in my laboratory we have, as I have mentioned above,

Table VI
Equilibrium Metal-Oxygen Distances
and (for Fe) Breathing Frequencies in Aquo Complexes.

$$\underline{\text{Fe}(\text{H}_2\text{O})_6^{3+}}: d(\text{Fe(III)-O}) = 1.986(7) \text{ \AA} \text{ in } \text{Fe}(\text{NO}_3)_3 \cdot 9\text{H}_2\text{O} \quad (52)$$

$$= 1.995(4) \text{ \AA} \text{ in } \text{CsFeSO}_4 \cdot 12\text{H}_2\text{O} \quad (53)$$

$$v_1(\text{Fe(III)-O}) = 524 \text{ cm}^{-1} \text{ in } \text{CsFeSO}_4 \cdot 12\text{H}_2\text{O} \quad (54)$$

$$\underline{\text{Fe}(\text{H}_2\text{O})_6^{2+}}: d(\text{Fe(II)-O}) = 2.123(6) \text{ \AA} \text{ in} \\ [\text{Fe}(\text{H}_2\text{O})_6][\text{Fe(II) citrate H}_2\text{O}] \cdot 2\text{H}_2\text{O} \quad (55)$$

$$v_1(\text{Fe(II)-O}) = 378 \text{ cm}^{-1} \text{ in} \\ [\text{Fe}(\text{H}_2\text{O})_6][\text{SiF}_6] \quad (56)$$

$$\underline{\text{Co}(\text{H}_2\text{O})_6^{3+}}: d(\text{Co(III)-O}) = 1.873(5) \text{ \AA} \text{ in } \text{CsCo}(\text{SO}_4) \cdot 12\text{H}_2\text{O} \quad (53)$$

$$\underline{\text{Co}(\text{H}_2\text{O})_6^{2+}}: d(\text{Co(II)-O}) = 2.081(1) \text{ \AA} \text{ in } \text{Co}(\text{SiF}_6) \cdot 6\text{H}_2\text{O} \quad (57)$$

begun to investigate these questions in a very general way; this has led, *inter alia*, to some criticism of the concepts employed by Wiener (58), to which Professor Schatz has referred. Continuation of theoretical work along these lines, together with the greatly increased possibilities for experimental determinations of quantities entering into rate expressions, will, one hopes, lead to greatly increased understanding both of electron and of atom transfer in the foreseeable future.

Literature Cited

1. Marcus, R. A. J. Chem. Phys. 1956, 24, 966.
2. Marcus, R. A. Can. J. Chem. 1959, 37, 155.
3. Marcus, R. A. Disc. Faraday Soc. 1960, 29, 21.
4. Marcus, R. A. Annu. Rev. Phys. Chem. 1964, 15, 155.
5. Hush, N. S. Proc. 4th Moscow Conf. of Electrochemistry [Eng. trans. Consultants Bureau, N. Y. 1961] 1956, 1, 99.
6. Hush, N. S. J. Chem. Phys. 1958, 28, 964.
7. Hush, N. S. Z. Elektrochem. 1957, 61, 734.
8. Hush, N. S. Trans. Faraday Soc. 1961, 57, 557.
9. Hush, N. S., Brookhaven Natl. Lab. Publ. No. 6561, 1963.
10. Hush, N. S. Disc. Faraday Soc. 1968, 45, 52.
11. Newton, M. D. Int. J. Quant. Chem. Quantum Chemistry Symp. 1980, 14, 363.
12. Taube, H. "Synthesis and Properties of Low-Dimensional Materials"; Epstein, A. J.; Miller, J. S., Eds.; New York Academy of Sciences; p 481; and references cited therein.
13. Meyer, T. J. Acc. Chem. Res., 1978, 11, 94; and references cited therein.
14. Sutin, N. Annu. Rev. Nucl. Sci. 1962, 12, 285.
15. Sutin, N. "Inorganic Reactions and Methods"; Zuckerman, J. J., Ed.; Springer-Verlag: West Berlin, in press; and references cited therein.
16. Efrima, S.; Bixon, M. Chem. Phys. 1976, 13, 447.
17. Hohenberg, P.; Kohn, W. Phys. Rev. 1964, 136, B864.
18. Kohn, W.; Shaw, L. J. Phys. Rev. 1965, 140, A1133.
19. Hush, N. S. Prog. Inorg. Chem. 1967, 8, 391.
20. Allen, G. C.; Hush, N. S. Prog. Inorg. Chem. 1967, 8, 357.
21. Hush, N. S. Electrochim. Acta, 1968, 13, 1004.
22. Berkooz, G.; Malamud, M.; Shtrikman, S. Solid State Commun. 1968, 6, 185.
23. Bransky, L.; Tallan, N. M.; Hed, A. Z. J. Applied Phys. 1970, 41, 1787.
24. Ellis, V. M., Ph. D. Thesis: University of Sydney, 1979.
25. Hush, N. S.; Ellis, V. M., to be published.
26. Glauser, A.; Hauser, U.; Herren, F.; Ludi, A.; Roder, P.; Schmidt, E.; Siegenthaler, H.; Wank, F. J. Am. Chem. Soc. 1973, 95, 8457.
27. Hush, N. S. "Mixed-Valence Compounds"; Brown, D. B., Ed.; D. Reidel: Dordrecht, Netherlands, 1980; 151.
28. Hush, N. S.; Edgar, A.; Beattie, J. K. Chem. Phys. Lett. 1980, 69, 128.
29. Hush, N. S. and Cheung, A. Chem. Phys. Lett. 1977, 47, 1.
30. Creutz, C.; Taube, H. J. Am. Chem. Soc. 1969, 91, 3988.
31. Hush, N. S.; Williams, M. L. Chem. Phys. Lett. 1971, 8, 179.
32. Hush, N. S., to be published.

33. "Water: A Comprehensive Treatise", Franks, F., Ed.; Plenum Press: New York, 1972.
34. Ovchinnikov, A. A.; Ovchinnikova, M. Ya Zh. Eksp. Teor. Fiz. 1969, 56, 1278.
35. Ovchinnikov, A. A.; Ovchinnikova, M. Ya Sov. Phys.-JETP (Engl. Transl.) 1969, 29, 688.
36. Marcus, R. A.; Siders, P. J. Am. Chem. Soc. 1981, 103, 748.
37. Taube, H. private communication, 1981.
38. Buhks, E.; Bixon, M.; Jortner, J.; Navon, G. Inorg. Chem. 1979, 18, 2014.
39. Dogonadze, R. R.; Kuznetsov, A. M.; Leivch, V. G. Electrochim. Acta 1968, 13, 1025.
40. Dogonadze, R. R. "Reactions of Molecules at Electrodes", Hush, N. S., Ed.; Wiley-Interscience: New York, 1971, 135.
41. Kestner, R. N.; Logan, J.; Jortner, J. J. Phys. Chem. 1974, 78, 2148.
42. Cribb, P. C.; Nordholm, S.; Hush, N. S. Chem. Phys. 1978, 29, 31.
43. Cribb, P. C.; Nordholm, S.; Hush, N. S. Chem. Phys. 1978, 29, 43.
44. Cribb, P. C.; Nordholm, S.; Hush, N. S. Chem. Phys. 1979, 44, 315.
45. Cribb, P. C.; Nordholm, S.; Hush, N. S. Chem. Phys., 1980, 47, 135.
46. Piepho, S. B.; Krausz, E. R.; Schatz, P. N. J. Am. Chem. Soc. 1979, 101, 2793.
47. Merrifield, R. E. Radiat. Res. 1963, 20, 154.
48. Krausz, E. R.; Burton, C.; Broomhead, J. Inorg. Chem. 1981, 20, 434.
49. Clark, R. J. H.; Dines, T. J. Mol. Phys. 1981, 42, 193.
50. Papavassiliou, G. C.; Layek, D. Z. Naturforsch 1980, 35b, 676.
51. von Burg, K.; Delahay, P. Chem. Phys. Lett. 1981, 78, 287.
52. Hair, N. J.; Beattie, J. K. Inorg. Chem. 1977, 16, 245.
53. Beattie, J. K.; Best, S. P.; Skelton, B. W.; White, A. H. J. Chem. Soc., Dalton Trans., in press.
54. Beattie, J. K., Best, S. P.; Armstrong, R. S., submitted for publication.
55. Strouse, J.; Layten, S. W.; Strouse, C. H. J. Am. Chem. Soc. 1977, 99, 562.
56. Lewis, J.; Jenkins, T. E. J. Raman Spec. 1979, 8, 111.
57. Ray, S.; Zalkin, A.; Templeton, D. H. Acta Cryst. 1973, B29, 2741.
58. Weiner, J. H., J. Chem. Phys. 1978, 68, 2492.

RECEIVED April 27, 1982.

General Discussion—Parameters of Electron-Transfer Kinetics

Leaders: S. Isied, P. P. Schmidt, and E. Buhks

DR. PAUL SCHATZ (University of Virginia): If one tries to get additional width, for example, in the Creutz-Taube ion intervalence band by putting in a symmetrical mode, and one works through the arithmetic, one finds that there is no intensity unless the force constants are different in the two oxidation states. And, furthermore, unless they are very different, the amount of intensity obtained will be very, very small. So I'm personally very skeptical of your calculation using the symmetrical modes to obtain additional width. I don't think it will work.

DR. HUSH: For an allowed electronic transition (such as the intervalence transition in a symmetrical delocalized mixed-valence complex), simultaneous excitation of quanta of all symmetrical vibrational modes is formally allowed. Such excitation will result in a displacement of the upper with respect to the lower potential surfaces for each mode. It is well-known that this is the most usual, major source of band broadening for allowed molecular electronic transitions, e.g., those of organic molecules or complex ions. This may or may not be accompanied by significant changes in force constants. For a model of the 2-site, one-electron system with linear electron-vibrational coupling to a set of doubly-degenerate harmonic oscillators, only the out-of-phase (antisymmetric) combination of modes contributes to the polaron-type binding energy [Hush, N. S.; in "Mixed-Valence Compounds," Brown, D. B., Ed.; D. Reidel Publishing Co.: Dordrecht, Netherlands, 1981; p 151]. When such a model is used to describe the intervalence absorption spectrum of a symmetrical delocalized mixed-valence complex, the only source of vibrational band broadening (i.e., contribution to the second moment of the absorption envelope) is, indeed, frequency dispersion, which is relatively inefficient. However, in a real delocalized complex, such a transition involves, in fact, excitation of an electron from a bonding to an antibonding molecular orbital. The distribution of these orbitals over the molecular framework determines the change of interatomic bond orders accompanying the electronic transition. These, in turn, can be correlated by standard techniques (or by direct geometry optimization) with changes in bond lengths - i.e., with excitation of quanta of symmetric vibrational modes, all of which are formally allowed. Thus, for example, we would expect the equilibrium Ru-N bond length to be different in ground and excited states, in reality. This would not be allowed for in the simplistic model that Dr. Schatz has for some time been using for these systems. The minimal requirement is to take account of the extended molecular nature of the electronic wavefunctions. A more detailed calculation would employ one of the standard ab initio methods for ground and excited state geometries of an

open-shell molecule. Once the calculated bond length changes accompanying the transition are calculated, one could then transform to normal coordinates to obtain the displacement of each symmetrical normal coordinate. Although a many-electron calculation should be employed, it is probable that extended-Hückel type calculations may give reasonable estimates of normal coordinate changes. This has been found, for example, by Peticolas [Peticolas, W.; Blazej, D. C. *Chem. Phys. Lett.* 1979, 63, 604] in his work on nucleic acid excited state geometries. I have suggested a tentative analysis of the intervalence absorption spectrum of the Creutz-Taube ion in terms of coupling to one dominant symmetric and one dominant antisymmetric mode. Only a very small coupling to a symmetric mode is required for this interpretation. This is in qualitative agreement with calculated bond order changes [Hush, N.S.; *op.cit.*].

I have predicted that the very unusual low-frequency IR behavior for the Creutz-Taube ion calculated by Piepho, Schatz and Krausz [Piepho, S. B.; Krausz, E. R.; Schatz, P. N. *J. Am. Chem. Soc.* 1978, 100, 2996] on the assumption of only antisymmetric mode involvement in electron-vibrational interaction would not be found, and that it was an artifact of the method. The failure of experiments designed to locate such IR bands has subsequently been reported by Krausz, et al.

DR. MICHAEL WEAVER (Michigan State University): There is a sense of self-satisfaction amongst some participants which is disturbing me. There are still many features of electron-transfer reactions, even for outer-sphere processes in solution and at electrodes, that the contemporary theories do not explain, or at least in which there is a marked discrepancy between theory and experiment. One of these is that the frequency factor for electron transfer is not well understood. One can obtain reasonable agreement between theory and experiment if you happen to select zero ionic strength, but the agreement is often much poorer at the high ionic strengths usually employed in experimental work. Secondly, as I pointed out earlier, I don't think the dependence of redox reactivity upon the thermodynamic driving force predicted by conventional theory is in satisfactory agreement with experiment for a number of reactions.

Although the theoretical framework put forward twenty years ago by Marcus and Hush has been developed extensively, it is perhaps unfortunate that the impression has become widespread that they are entirely successful. This, in turn, tends to bring about the misapprehension that electron-transfer kinetics, at least involving coordination compounds, is a "solved area". This has the effect of discouraging potential new investigators and, hence, inhibiting further progress. Research problems, such as understanding frequency factors for both intermolecular and intramolecular reactions, solvent effects, the influences of the electrode material upon heterogeneous electron transfer,

and the energetics of inner-sphere electron transfer, to name but a few topics at random, would seem to offer considerable challenges to both experimentalists and theoreticians in the next few years.

DR. HUSH: For myself, if I gave the impression of any feeling of self-satisfaction, it was certainly in the sense that I think we can say that there is a glimmer of light in the darkness. And in chemistry we must be grateful for the smallest spark. I have stressed also that our present theoretical approaches to rate calculations have been almost entirely confined to outer-sphere processes, and that the task of formulating reliable theories for inner-sphere transfers will be a formidable one.

DR. RODERICK CANNON (University of East Anglia): I'd like to hazard a guess that much of the progress in understanding electron transfer reactions will come in the future from studies on the solid state, on the one hand, and from gas phase studies on the other. And I have felt, having reviewed the literature fairly recently, that both of those areas have been most neglected.

I'd like to mention very briefly one piece of work done by a colleague of mine, David Rosseinsky, of Exeter University in England, where he has studied, in the solid state, thermal and optical electron transfer in the double salt of potassium manganate and the permanganate. I'm not sure how many people even realize that such an interesting compound exists. But he's been able to measure outer-sphere electron transfer between manganate and permanganate ion, which, of course, is the solid state analog of one of the very first electron transfer reactions ever studied in solution.

I think the very simplicity of the system, and the simplicity in the study of the crystal structure, suggests that people would do well to look very closely at the vibrational spectrum of the crystal and at the details of the electron transfer in that system.

On the other hand, if one looks at gas phase electron transfer we find that it's dominated by small molecules and non-methyl molecules and the system is quite remote from what we see in solution (H_2^+ ions, and so forth). And I do wonder whether people will turn their attention to using, for example, organometallic complexes, many of which are volatile and unstable in the gas phase.

Experiments with crossed molecular beams might entail a beam of ferrocene molecules against a beam of chloride ions in the close outer-sphere electron transfer in the gas phase. This should be a very similar process to what we have seen in solution. I'd just like to leave the thought that these are two possible directions in which future work will go.

Effect of Organized Assemblies on Chemical Reactions

J. K. THOMAS

University of Notre Dame, Chemistry Department, Notre Dame, IN 46506

The action of organized assemblies is discussed and the mode of interaction of organic and inorganic solutes with the assemblies indicated. The environments of the solutes in the assemblies are given, which immediately predict certain effects on reactions in the assemblies. Examples of several types of reactions, mostly photo-induced, are given and used to illustrate the earlier discussion.

The last decade has shown an increasing interest in the effects of organized assemblies on chemical reactions, in particular on photochemical reactions (1, 2, 3). Reactions may be promoted by 1000-fold or more or retarded by the same extent. Moreover, reactions that do not occur in simple homogeneous media often occur quite readily on, or in, an organized assembly. To date, most studies have concentrated on organic systems and, in particular, on systems of interest to solar energy storage. The number of assemblies used is quite large and it is now opportune to outline the nature of these systems in more detail.

Organized Assemblies

The organized assemblies used are usually organic in nature, although inorganic assemblies are receiving increased interest. Figure 1 shows, in a diagrammatical sense, several organic assemblies that can be constructed from a simple organic surfactant molecule such as sodium lauryl sulfate, NaLS, sodium diisooctyl sulfosuccinate, AOT, or cetyl trimethyl ammonium bromide, CTAB. Depending on the conditions of the system, these simple surfactants can be coaxed into forming small spherical entities called micelles, large rod micelles, bilayers, vesicles, microemulsions, and reversed micelles. The reader is referred to references 1 and 3 for a fuller description of these systems. However, for later discussion it is important to ex-

0097-6156/82/0198-0335\$06.00/0
© 1982 American Chemical Society

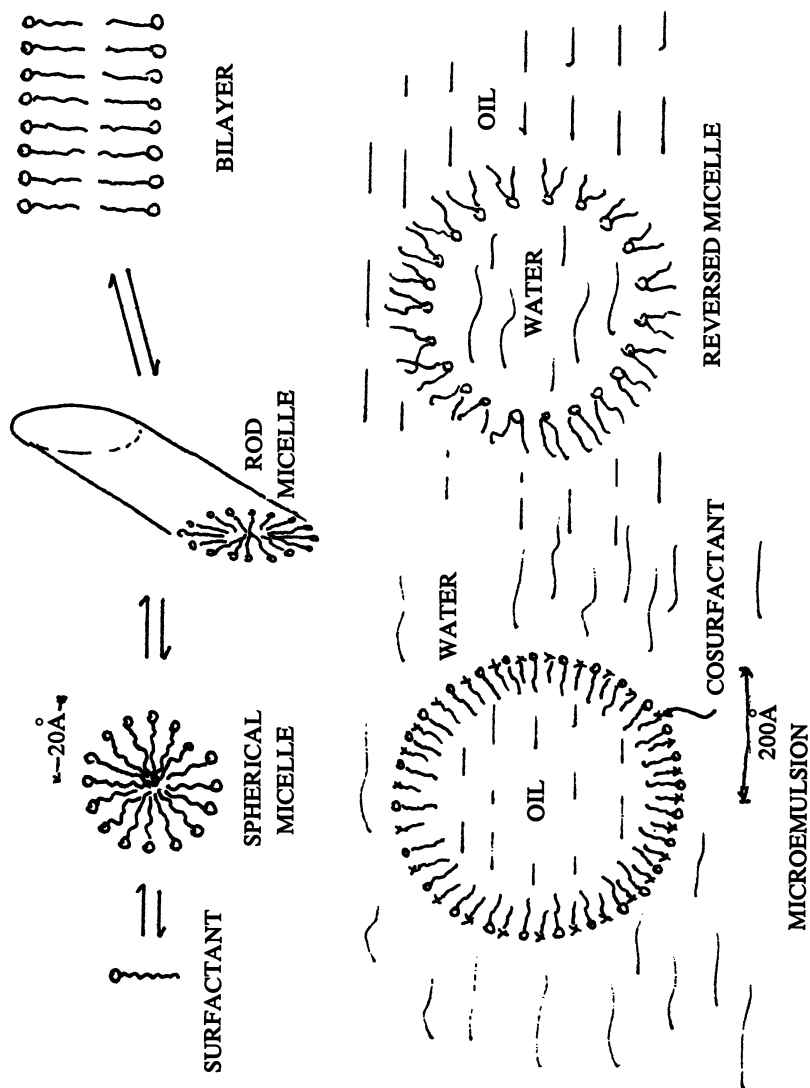


Figure 1. Various organized assemblies formed from a simple surfactant molecule in mixtures of water and oil.

amine the simple micelle in more detail and take it as a model for events on other systems.

The surfactant molecule consists of a hydrophobic hydrocarbon tail and a polar head group. Above a specific concentration in water, the surfactant molecules cluster to form discrete micelles. The hydrocarbon chains sequester together and are separated from the aqueous phase by a polar head group interface. The simple picture is of an oil drop in water. The dimensions are small, i.e., radius $\sim 20\text{\AA}$. If the head group is ionic, then a fraction of the aggregate ($N \sim 50$ to 100) will dissociate to give a large (20 to 30) positive or negative charge to the micelle surface. The micelle can be enlarged (200\AA or so) by reforming it around a large oil drop, thus forming a microemulsion. From here on, the term micelle will be used exclusively as a mode of describing reactions, the inference being that other structures behave similarly.

Other quite different assemblies can be formed, e.g., colloidal silica, metal oxides, colloidal metals, etc. They have many properties that are reminiscent of micelles, while also having specific features of their own. These systems will not be discussed.

Nature of Reactions

A micelle may solubilize two reactants, A and B, within a small fraction of the volume of the total system. The effective concentrations of A and B are increased and the reaction rates are correspondingly increased. Rate enhancements of 1000-fold are possible by means of this effect. The micelle may solubilize one reactant while the other is in the aqueous phase. If this reactant is charged, then the micellar charge controls the reaction rate. The micelle may organize A and B into a suitable configuration for optimum reaction and promote product separation. Finally, the highly charged micellar surface can influence the energetics of a reaction to a quite remarkable degree.

Interaction with Micelles

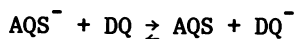
Organic molecules are solubilized by the organic constituents of a micelle. In small micelles the molecules lie close to the interface, while in large microemulsions considerable penetration into the core is observed (1). Inorganic materials are quite polar and have little interaction with the organic components of the micelle. However, the micelle counterions, Na^+ or Br^- , are inorganic and their ions may be exchanged for more interesting species, e.g., Tl^+ , Ag^+ , ruthenium(II), Cu^{++} , NO_3^- , I^- , etc.

In some instances, a long hydrocarbon chain can be attached to an organometallic compound, e.g., ruthenium trisbipyridyl or ferrocene, thus making a new surfactant which can be readily used to form micelles or can be incorporated into conventional micelles (4, 5). In other cases, a long chain crown ether can be constructed which will form micelles with a metal ion, M^{n+} , incorporated into the crown (6, 7). Most inorganic components enter into the micellar surface region. However, a hydrophobic metallo-organic component, such as ferrocene or zinc tetraphenyl porphyrin, could enter the oil region of a microemulsion.

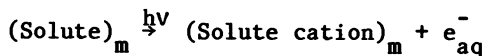
Environment of Reactants

It has been established by many studies (2) that the charge at the micelle-water interface, or Stern layer, is high, and that electric fields of 10^5 to 10^6 volts/cm exist in this region. The local micro-dielectric constant of the region is about 30 to 40, depending on the micelle (2, 8, 9), and this affects the physical properties (e.g., spectroscopic) of many molecules. The movement of molecules is restricted in this region due to the restrictive nature of the head group-counter ion interaction (10).

The high surface charge on a micelle (10^6 volts/a or 300mvolts/micelle) can strongly participate in redox exchange reactions (11). For example, the equilibrium between anthraquinone sulfonate (AQS^-) and duroquinone (DQ) and their reduced forms



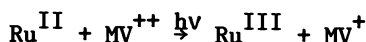
is strongly on the DQ^- side in water. In aqueous NaLS micelles, however, solubilization of DQ in the micelle pushes the equilibrium to the left and favors AQS^- . Electron transfer from a solute to water to give hydrated electrons, e_{aq}^- , occurs at much lower potentials ($\Delta E \sim 3-4$ eV) in micelles than in the gas phase.



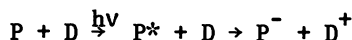
The physical restraints of the surface on a reaction are well illustrated by the reaction of Ag^{II} protoporphyrin and $IrCl_6^{2-}$ which occurs readily in homogeneous solution. The reaction is strongly inhibited in NaLS or CTAB micelles and is explained as being due to a shielding of the edge of the porphyrin ring by the micelle, such that e^- transfer is retarded (12).

Electron Transfer Reactions

One of the most popular photo-promoted electron transfer systems is the trisbipyridylruthenium(II)-methyl viologen (MV^{++}) system which, on excitation, produces Ru^{III} and reduced methyl viologen (MV^+):

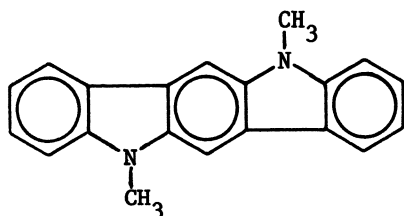


The back reaction of the products to give the original starting material severely reduces the quantum yield of the process. However, the introduction of a negatively charged assembly of NaLS promotes the reaction as both Ru^{II} and MV^{++} are bound, and the product Ru^{III} is maintained at the micelle while MV^+ regresses to the aqueous phase (12-15). The use of a Ru^{II} derivative with a long hydrocarbon chain also assists the reaction. If a negatively charged silica colloid is used in place of the anionic micelle, and MV^{++} is replaced with a diacid derivative such that the methyl viologen has no resultant charge ($MV^{++}R_2^{2-}$), then a greatly enhanced yield of $MV^+R_2^{2-}$ and Ru^{III} is produced (16). It is claimed that this is due to a higher negative charge on the SiO_2 colloid compared to an NaLS micelle. This may not be the full answer as the photoinduced electron exchange between pyrene, P, and dimethylaniline, D, on CTAB micelles and other CTAB structures, etc.,

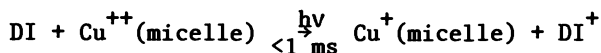


is markedly dependent on the nature of the assembly surface (17), the assembly promoting the e^- transfer to produce P^- and D^+ , while retarding the back neutralization so that D^+ can regress from the assembly. The lifetimes of the ions produced in this system are 10^4 greater than those in homogeneous media.

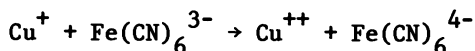
A good example of energy storage that is organized by an anionic micelle is given by the photoinduced e^- transfer from the dye 5,11-dimethyl-5,11-dihydroindolo(3,2-b)carbazole (DI)



to Cu^{++} on copper lauryl sulfate micelles (17). Excitation of DI rapidly leads to reduced Cu^{++} , i.e., Cu^+ .



The cuprous ion is rapidly lost from the micelle and is captured by $\text{Fe}(\text{CN})_6^{3-}$ in the water bulk,



This sequence of reactions is not possible in the absence of a micelle as the DI excited state is too short-lived to efficiently transfer to Cu^{++} . The micelle positions Cu^{++} and (DI)* in close proximity for efficient reaction, and, subsequently, separates the products and prevents back reaction. The crown ether type surfactants can be used to solubilize a cyanine dye in the organic portion while a metal ion, e.g., Ag^+ , is incorporated into the crown. Excitation of the dye leads to e^- transfer and the formation of Ag^0 which is stable over many days. The reaction is impossible without the aid of the micelle. Many similar examples appear in the literature and are summarized in references 1 and 3.

Energy Transfer

The organization of two reactants in close proximity by a micelle is of great utility in energy transfer studies. An organic molecule can be placed in a micelle and subsequently excited by light. Phosphorescence has been observed in my system by this technique (19-23). This is unique to micelles as efficient phosphorescence is only observed in a low temperature matrix where quenching is eliminated. Micelles protect the excited triplet state from such quenching, giving it a long lifetime and, hence, the possibility of efficient phosphorescence.

Inorganic ions, such as Tl^+ , Ag^+ , etc., can be incorporated as counterions on anion micelles containing the excited triplet. Spin orbit coupling ensues and enhanced phosphorescence is observed. The spin orbit coupling reaction is too inefficient to be observed in homogeneous media.

Energy transfer from excited triplets of naphthalene and biphenyl to Eu^{3+} and Tb^{3+} have been measured in NaLS micelles when part of the Na^+ counterions are replaced by Eu^{3+} or Tb^{3+} . The rate constants for these reactions are quite low even in

micelles ($k \sim 10^6$ to $10^5 \text{ M}^{-1} \text{ s}^{-1}$), and are too slow for observation in homogeneous media by our techniques.

Photo-induced electron transfer from ferrocene, Fe^{II} , to CCl_4 has been observed in micelle solution at low concentrations of CCl_4 ,



The extremely short lifetime of $\text{Fe}^{\text{II}*}$ ($< 10^{-10}$ s) is overcome by the close proximity of $\text{Fe}^{\text{II}*}$ and CCl_4 on the micelle (24).

Reversed Micelles

Figure 1 shows a reversed micelle where the bulk solvent is a hydrocarbon and the core is a water pool surrounded by surfactant. These systems possess unique features as the physical properties of the water pools only start to approach those of bulk water at high water content when the pool radii are $> 150 \text{ \AA}$; pools with radii as small as 15 \AA can be constructed (1, 25). These systems have been used to investigate the nature of several inorganic reactions by stopped flow methods (26, 27). They have also been used to produce so-called naked ions, i.e., ions that possess a minimum of aqueous solvation (28). The system strongly promotes many reactions, a fact attributed to the unusual nature of the water in this system.

Conclusion

Organized assemblies are useful to promote specialized features of a reaction, e.g., proximity effects, surface energy effects, or reactant organization. These features are useful in energy storage. As more is learned about these systems and their participation in reactions, it may be possible to obtain precise information on the effects of microscopic geometric arrangements of reactants on the subsequent course of reaction. Many assemblies are known; many others are available but have not been studied as yet.

Acknowledgement

This work was supported by the National Science Foundation (CHE 78-24867,02) and the Army Research Office (DAA G29-80-K-007).

Literature Cited

1. Thomas, J. K. Chem. Rev. 1980, **80**, 283.
2. Fendler, J. H.; Fendler, E. "Catalysis in Micellar and Macromolecular Systems"; Academic Press: N.Y., 1975.
3. Turro, N. J.; Grätzel, M.; Braun, A. M. Angew. Chemie 1980, **19**, 675.
4. Sprintschrick, G.; Sprintschrick, H. W.; Kirsch, P. P.; Whitten, D. G. J. Am. Chem. Soc. 1976, **98**, 2337.
5. Turro, N. J.; Kraeutler, B. J. Am. Chem. Soc. 1978, **100**, 7432.
6. Anguini, M.; Montanari, F.; Tundo, P. J. Chem. Soc., Chem. Commun. 1975, 393.
7. Nakamura, Y.; Imakura, Y.; Kato, T.; Morita, Y. J. Chem. Soc., Chem. Commun., 1977, 887.
8. Kalyana Sundaram, K.; Thomas, J. K. J. Phys. Chem. 1977, **81**, 2176.
9. Mukerjee, P. Adv. Colloid Interface Sci. 1967, **1**, 24.
10. Grätzel, M.; Thomas, J. K. in "Modern Fluorescence Spectroscopy"; Wehry, E., Ed.; Plenum: N.Y., 1976; p. 169.
11. Almgren, M.; Grieser, F.; Thomas, J. K. J. Phys. Chem. 1979, **83**, 3232.
12. Bricker, H.; Westerhausen, J.; Holzwarth, J. F.; Frehrhop, J. H. in "Techniques and Applications of Fast Reactions in Solution"; Jones, C. W., Ed.; London, 1979; p. 523.
13. Meyerstein, D.; Matheson, M. S.; Rabani, J. J. Am. Chem. Soc. 1978, **100**, 117.
14. Schneckl, R. H.; Whitten, D. G. J. Am. Chem. Soc. 1980, **102**, 1938.
15. Rodgers, M. A.; Foyt, D. C.; Zimek, Z. A. Rad. Res. 1976, **75**, 296.
16. Willner, I.; Otoos, J.; Calvin, M. J. Am. Chem. Soc. 1981, **103**, 3203.
17. Atik, S. S.; Thomas, J. K. J. Am. Chem. Soc. 1981, **103**, 3550.
18. Moroi, Y.; Brawn, A. M.; Gratzler, M. J. Am. Chem. Soc. 1979, **101**, 567.
19. Kalyanasundaran, K.; Grieser, F.; Thomas, J. K. Chem. Phys. Lett. 1977, **51**, 507.
20. Almgren, M.; Grieser, F.; Thomas, J. K. J. Am. Chem. Soc. 1979, **101**, 279.
21. Humphrey-Baker, R.; Moroi, Y.; Grätzel, M. Chem. Phys. Lett. 1978, **58**, 207.
22. Almgren, M.; Grieser, F.; Thomas, J. K. J. Am. Chem. Soc. 1979, **101**, 2021.
23. Turro, N. J.; Liu, K. C.; Chone, M. F.; Lee, P. Photochem. Photobiol. 1978, **27**, 523.
24. Papsun, D. M.; Thomas, J. K.; Labinger, J. A. J. Organometal. Chem. 1981, **208**, C36.
25. Menger, F. Acc. Chem. Res. 1979, **12**, 111.

26. Robinson, B.; James, A.; Steytler, D. C. "Protons Involved in Fast Dynamic Phenomena"; Elsevier: Amsterdam, 1978; p 287.
27. Robinson, B.; White, N. C. J. Chem. Soc., Faraday Trans. 1 1978, 74, 2625.
28. Sunamoto, J.; Hamada, T. Bull. Chem. Soc. Japan 1978, 51, 3130.

RECEIVED April 27, 1982.

General Discussion—Effect of Organized Assemblies on Chemical Reactions

Leader: Guillermo Ferraudi

DR. GUILLERMO FERRAUDI (University of Notre Dame): From your talk it appears that an important aspect of micelles is the modified reactivity imparted to excited states or chemical intermediates. If micelles are to be used to exploit this phenomenon, the structure of the micelle should be carefully defined. Can you tell us something more about the structural properties of micelles? For example, if triton X-100 is used to form micelles, a variation in conditions yields micelles with different shapes, different dimensions, etc.

DR. THOMAS: Of all the actual structures given, the micelle is the smallest entity and the least well-defined. The chains on the core are arranged randomly, and the units are much like drops of oil. However, Raman spectra tell us there is more order in the micelle chains than in a liquid hydrocarbon such as dodecane [Thomas, J. K.; Kalyansundaram, K. J. Phys. Chem. 1976, 80, 1462].

However, one can change the structure in a known fashion, micelle to rod, etc., with remarkable precision [Thomas, J. K. Chem. Rev. 1980, 80, 283]. In actual fact, a sodium lauryl sulfate micelle is a very precise entity containing 71 ± 1 units. A precise cooperative effect forms the micelle. If you change the conditions of the solution, such as the salt concentration, etc., then you can make other structures which are well identified.

I didn't use the triton X-100 example because it is a neutral entity. It is fine for an organic chemist, but inorganic entities can't interact with this micelle. However, a triton X-100 micelle is very well studied because biochemists are interested in using it as a model membrane since it makes big flat-disk micelles. Biochemists consider it as resembling a section of membrane, which can solubilize proteins. It is a good model for biological systems.

DR. FERRAUDI: You also reported a type of ejection of electrons from a micelle. It would appear that such a process could be significant for the storage of energy.

DR. THOMAS: Photoionization of a molecule in the micelle leads to the cation of the molecule, which is attached to the micelle [Dicuicio, P.; Thomas, J. K. Adv. Chem. Ser. 1980, No. 184, 97]. It is conventional to use a negatively charged micelle so that the cation is held to the electrostatically charged micelle. The electron is ejected into the water, and is observed as a hydrated electron. It is a very novel process, and works best in micelles. The major problem relative to storing energy is that you have two very high energy species, a cation and an electron, which are so reactive that they tear up

the system. Ideally, one would like to have a reversible system. Hence, it is better to donate the electron to an acceptor which could then give you enough time to move the e^- somewhere else where it could create useful chemistry, such as producing H_2 .

The reduction of the ionization potential in micelles results from solvation effects on the cation and on the electron, and also the surface energy. These are sufficient to drop the ionization potential by as much as 4 volts.

DR. KENNETH KUSTIN (Brandeis University): How can you distinguish experimentally between a reaction on the surface of the micelle and one in the interior of the micelle?

DR. THOMAS: That is a good question. First of all, one would attempt to make a derivative of one or both reactants which would favor their location either inside the micelle or on the surface. For example, if I wanted to work with pyrene, a simple organic molecule, I could readily locate it inside the micelle as it is a hydrophobic entity; with microemulsion I could put it right into the oil center. However, if I wanted to work on the surface I would use pyrene sulfonic acid or pyrene butyric acid, either of which would be located on the surface.

The second step is to work up the spectroscopy (e.g., NMR spectroscopy, fluorescence spectroscopy) of the system which should confirm the solute location.

DR. JOHN ENDICOTT (Wayne State University): How well-defined is the surface of the micelle?

DR. THOMAS: That really depends on the micelle, The solid micelles such as silica particles, etc., are very well-defined. But the fluid micelles which I spoke about, are kinetic entities. For example, we don't really know how well-defined the surface is, in the sense that it is in motion. It does not have a distinct boundary line, as I drew it. In actual fact, the monomer units are oscillating into and out of the micelle. However, the net effect is to leave a permanent entity. If you dilute a solution of micelles, they may all dissociate in about 0.1 seconds, whereas our reactions occur on time scales $<10^{-6}$ seconds.

It is thought that the micelle surface is undulating to some degree, so it is not a perfect entity. However, it is described well by double-layer theory, which requires some order. It is not easy to describe a micelle as nobody has ever seen one; it is something that is projected from all its properties. It is small (10^{-8} - 2×10^{-8} cm) and, of course, generally you can't isolate it.

Recently we have managed to isolate one by polymerizing it

(i.e., by utilizing a surfactant with a monomer group on it and then polymerizing the system). The product is too small to see in our electron microscope. Perhaps with a better electron microscope we could see it, as we can see a polymerized microemulsion $r \sim 100\text{\AA}$ [Atik, S. S.; Thomas, J. K. J. Am. Chem. Soc. 1981, 103, 4279].

DR. ENDICOTT: With regard to the kinetic nature of fluid micelles, how meaningful is the distinction between surface and interior?

DR. THOMAS: For a solute the meaningful thing is the degree of contact with the aqueous phase. In a small micelle the solute is close to or on the surface, and it is in contact with the water. In a larger microemulsion the molecule is in the oil, the other volume. However, depending on the solute, it may penetrate further into the micelle and you can then talk of the water or lipid side of the surface. We can control the location by use of a co-surfactant [Thomas, J. K. Chem. Rev., op. cit.].

DR. JOHN MALIN (National Science Foundation): I know that people have been worried about the dynamics of micelles and micelle formation and have studied these processes by NMR. I am wondering what the results of those studies have been. Without belaboring this point, do you know the residence time of a surfactant molecule in a given micelle before it transfers to a neighbor, or whether they fuse and come apart again?

DR. THOMAS: The kinetic parameters of micelles are very well known, having been determined by temperature-jump relaxation methods and various other techniques. There are several kinetic events which can be described. First of all, the fastest event is the exchange of the counter ion (e.g., the sodium counter ion, in sodium lauryl sulfate). These ions exchange with a mean lifetime of about 10^{-8} seconds. Thus, the counter ions are whipping back and forth into the water. Depending on the type of surfactant you use, the monomer units (including the entire hydrocarbon chain with the head group, etc.) move in and out of the micelle in times which are microseconds or longer. The slowest event is the collapse of the micelle by diluting it in a flow apparatus. This process requires long periods of time because the entire entity has to unravel.

For a while there was some confusion in the literature: the NMR studies indicated a rapid process was occurring while the flow studies indicated something slower. We now understand that they were looking at different events. Reversed micelles behave differently and fusion of the micelle is an important factor in solute exchange [Atik, S. S.; Thomas, J. K. J. Am. Chem. Soc. 1981, 103, 3543].

Generation of Reactive Intermediates via Photolysis of Transition-Metal Polyhydride Complexes

GREGORY L. GEOFFROY

Pennsylvania State University, Department of Chemistry, University Park, PA
16802

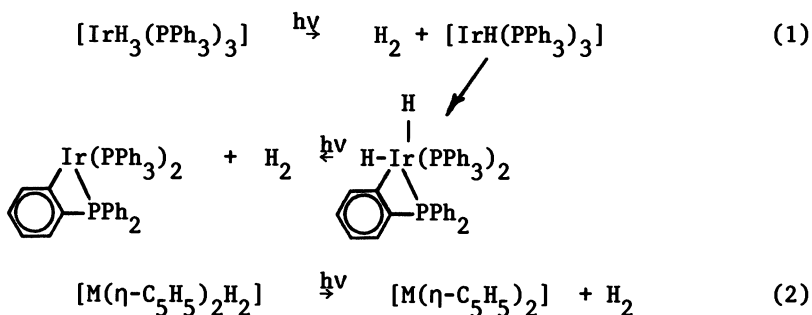
The photochemical properties of several transition metal polyhydride complexes are described. Irradiation of $[\text{MoH}_4(\text{dppe})_2]$ ($\text{dppe} = \text{Ph}_2\text{PCH}_2\text{CH}_2\text{PPh}_2$) and $[\text{MoH}_4(\text{PPh}_2\text{Me})_4]$ gives loss of H_2 . Under N_2 atmospheres the dinitrogen complexes $[\text{Mo}(\text{N}_2)_2(\text{dppe})_2]$ and $[\text{Mo}(\text{N}_2)_2(\text{PPh}_2\text{Me})_4]$ are formed in near quantitative yield. Irradiation of $[\text{ReH}_3(\text{dppe})_2]$ with UV light leads to elimination of H_2 with a 366-nm quantum yield of 0.07 ± 0.02 . The initial photoproduct is $[\text{ReH}(\text{dppe})_2]$ or a solvated derivative, but this species is highly reactive and rapidly adds N_2 , CO , C_2H_4 , C_2H_2 , and CO_2 to give adduct complexes. NMR evidence indicates that $[\text{ReH}(\text{dppe})_2]$ undergoes rapid but reversible ortho metalation and insertion into the C-H bonds of benzene. Irradiation of the complexes $[\text{ReH}_5\text{L}_3]$ ($\text{L} = \text{PMe}_2\text{Ph}$, PMePh_2 , PPh_3) and $[\text{ReH}_3(\text{PMe}_2\text{Ph})_4]$ gives efficient loss of phosphine in the primary photochemical reaction. The 366 nm quantum yields for the $[\text{ReH}_5\text{L}_3]$ complexes range from 0.13-0.18; the 366 nm quantum yield for PMe_2Ph loss from $[\text{ReH}_3(\text{PMe}_2\text{Ph})_4]$ is 0.4. Under an H_2 atmosphere, $[\text{ReH}_3(\text{PMe}_2\text{Ph})_4]$ is converted into $[\text{ReH}_5(\text{PMe}_2\text{Ph})_3]$ upon photolysis; the pentahydrides in turn lose another equivalent of phosphine to

American Chemical
0097-6156/82/0198-0347\$10.25/0
Society Library
© 1982 American Chemical Society
1155 16th St. N. W.

In Mechanistic and Organometallic Reaction, Corabacher, D., et al.;
ACS Symposium Series; American Chemical Society: Washington, DC, 1982.

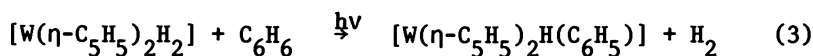
give the corresponding $[\text{ReH}_7\text{L}_2]$ complexes. The heptahydrides are themselves photosensitive and react to give a mixture of $[\text{Re}_2\text{H}_8\text{L}_4]$ and $[\text{Re}_2\text{H}_6\text{L}_5]$ dimers. The dinuclear compound $[\text{Pt}_2\text{H}_3(\text{dppm})_2]\text{PF}_6$, 4, ($\text{dppm} = \text{Ph}_2\text{PCH}_2\text{PPh}_2$) and $[\text{Pt}_2\text{H}_2\text{Cl}(\text{dppm})_2]\text{PF}_6$, 5, have been found to lose H_2 when irradiated in either the solid state or in solution with 366 nm quantum yields of 0.62 and 0.06, respectively. One mole of H_2 is rapidly evolved upon photolysis of 4 in CH_3CN solution and the photoproduct has been identified as $[\text{Pt}_2\text{H}(\text{CH}_3\text{CN})(\text{dppm})_2]\text{PF}_6$. ^1H NMR data indicate a structure for the latter having a direct Pt-Pt bond with a terminal hydride bound to one Pt and the CH_3CN ligand to the other. These experiments demonstrate the feasibility of H_2 loss upon photolysis of dinuclear di- and polyhydrides when at least one of the hydrides is bound in a terminal fashion.

A number of studies have demonstrated that photolysis of transition metal di- and polyhydride complexes can lead to the generation of very reactive intermediates, generally via photo-induced loss of H_2 (1,2). Two such examples are shown in eqs 1 (3) and 2 (4-8).



In the first example, photolysis of thermally stable $[\text{IrH}_3(\text{PPh}_3)_3]$ leads to loss of H_2 and formation of $[\text{IrH}(\text{PPh}_3)_3]$. This species is extremely reactive and does not persist as such but instead undergoes the ortho-metallation reaction shown in

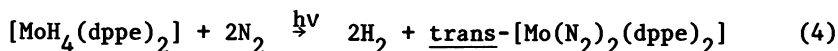
eq 1. This gives another dihydride complex which undergoes further photo-induced loss of H₂ to give [Ir(C₆H₄PPh₂)(PPh₃)₂] as the final product. Photolysis of the molybdenocene and tungstenocene dihydrides, eq 2, also leads to loss of H₂ and to the formation of the corresponding metallocenes. These are extremely reactive and either add substrate molecules or decay by insertion into C-H bonds of the coordinated C₅H₅ ligands. Green and coworkers (5-8) have shown in a series of studies that photogenerated tungstenocene behaves as an organometallic carbene and readily inserts into C-H bonds of a variety of solvent molecules, e.g., eq 3 (5).



Photoinduced reductive elimination of H₂ from polyhydride complexes, H_xML_n (x ≥ 3) can, in principle, lead to the generation of highly reactive compounds that should be capable of activating normally inert substrates such as N₂, CO₂, and perhaps hydrocarbons. Multiple H₂ loss can occur from polyhydride complexes having an even number of hydride ligands to give what may be called doubly coordinatively-unsaturated complexes and hence an extremely reactive species. Photolysis of complexes with an odd number of hydride ligands can give coordinatively-unsaturated complexes that still have hydride ligands and, hence, centers of reactivity. To test these notions we have undertaken a series of studies of the photochemical properties of polyhydride complexes and summarize our results herein.

Photoinduced Elimination of H₂ from MoH₄(dppe)₂ and MoH₄(PPh₂Me)₄

We initially irradiated the [MoH₄(dppe)₂] (dppe = Ph₂-PCH₂CH₂PPh₂) and [MoH₄(PPh₂Me)₄] complexes under an N₂ atmosphere (9), expecting to form the known bis(dinitrogen) complexes if photoinduced loss of all four hydride ligands were to occur. This expectation was realized, and high yields of trans-[Mo(N₂)₂(dppe)₂] and trans-[Mo(N₂)₂(PPh₂Me)₄] were obtained. For example, photolysis of a benzene solution of [MoH₄(dppe)₂] at 25°C for 12 h with 366-nm light under a continuous N₂ purge gave a 93% yield of trans-[Mo(N₂)₂(dppe)₂], eq 4. The nondescript



spectral changes which obtain upon photolysis and the necessity of the N_2 purge in order to drive the reactions have precluded accurate quantum yield measurements, although the time scale of the photolysis indicates that the quantum yields are low. The conversion shown in eq 4 has been observed to occur thermally (10) but at a rate much slower than that which obtains under photochemical conditions. We also found that photolysis of $[\text{MoH}_4(\text{dppe})_2]$ under a CO atmosphere gives a mixture of *cis*- and *trans*- $[\text{Mo}(\text{CO})_2(\text{dppe})_2]$. Irradiation under C_2H_4 , C_2H_2 , and CO_2 atmospheres leads to complex arrays of products which have proven difficult to separate and characterize.

An important question is what happens in the absence of a suitable substrate that can trap the photogenerated intermediate(s): Are reactive species such as $[\text{Mo}(\text{dppe})_2]$ and $[\text{Mo}(\text{PPh}_2\text{-Me})_4]$ photo-generated and do they persist in solution? Photolysis of rigorously degassed benzene solutions of $[\text{MoH}_4(\text{dppe})_2]$ with 366-nm light gives a color change from yellow to bright orange over a period of several hours. This color change is accompanied by a steady decrease in intensity of the 1714-cm^{-1} $\nu_{\text{Mo-H}}$ vibration and the $\delta = -3.6$ ppm hydride resonance characteristic of $[\text{MoH}_4(\text{dppe})_2]$. No new hydride resonances or metal hydride vibrations appear in either spectrum. The singlet at 83.5 ppm initially present in the ^{31}P NMR spectrum of $[\text{MoH}_4(\text{dppe})_2]$ in benzene- d_6 solution also decreases in intensity as the photolysis proceeds, and a new singlet at 80.2 ppm appears and grows in.

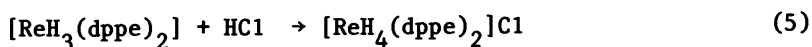
Mass spectral, gas chromatographic, and Toepler pump analyses of the gases above irradiated benzene solutions show the formation of H_2 with an average of 1.9 mole of H_2 released per mole of $[\text{MoH}_4(\text{dppe})_2]$ irradiated. Evaporation of solvent from these irradiated solutions gives an extremely air-sensitive orange solid which shows no metal hydride vibrations in its infrared spectrum and no hydride resonances in its ^1H NMR spectrum. The ^{31}P NMR spectrum of this compound is complex, showing 12 separate resonances, including an intense peak at 13.2 ppm attributable to free dppe. Repeated attempts at recrystallization and purification of this compound failed to give a pure product. Elemental analyses of compounds obtained from several different experiments did not agree well with each other nor with any obvious formulation.

The observation of loss of 1.9 mol of H₂ per mole of [MoH₄(dppe)₂] irradiated and the accompanying infrared, ¹H, and ³¹P NMR spectral changes are not inconsistent with the formation of [Mo(dppe)₂] upon irradiation of [MoH₄(dppe)₂] in degassed solution. However, the ³¹P NMR spectrum of the solid material isolated from these experiments clearly indicates that this species, if formed, is not sufficiently stable for isolation. We suspect that [Mo(dppe)₂], possibly solvated, may initially be photogenerated but that it subsequently decomposes or reacts with solvent when no other suitable substrate is available. Loss of H₂ from [Mo₄H₄(dppe)₂] presumably proceeds in a stepwise fashion via initial generation of [MoH₂(dppe)₂].

In regard to the question of whether or not [Mo(dppe)₂] is photogenerated from [MoH₄(dppe)₂], other workers (11,12) have concluded from a series of flash photolysis studies that irradiation of trans-[W(N₂)₂(dppe)₂] does give transient formation of the analogous [W(dppe)₂] complex, possibly as a solvated species. This latter complex subsequently reacts with N₂ to regenerate trans-[W(N₂)₂(dppe)₂] and with CO and H₂ to give [W(CO)₂(dppe)₂] and [WH₄(dppe)₂], respectively. The formation of [W(dppe)₂] in these reported studies clearly makes [Mo(dppe)₂] a reasonable intermediate in our experiments.

Photogeneration of Reactive [ReH(dppe)₂] via Photoinduced Loss of H₂ from [ReH₃(dppe)₂]

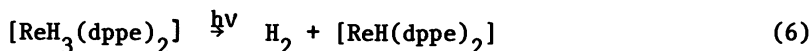
Although the chemistry of [ReH₃(dppe)₂] has not been extensively examined, the complex is known to be thermally quite stable [cf., (13)]. It shows no tendency to lose H₂ when heated to 180°C in an evacuated Carius tube (14) and it will not react to give the known [ReH(N₂)(dppe)₂] derivative when heated under 60 psi of N₂ (15). In contrast to most metal hydrides, treatment of [ReH₃(dppe)₂] with HCl gives simple protonation rather than loss of H₂, eq 5 (14).



Although [ReH₃(dppe)₂] does not undergo thermal loss of

H₂, it does readily occur upon photolysis to generate [ReH(dppe)₂] as a very reactive photoproduct (13). As detailed below, this species rapidly adds substrate molecules (N₂, CO, C₂H₂, C₂H₄, and CO₂) and inserts into C-H bonds of benzene solvent and the phenyl groups of the dppe ligands.

Photolysis of [ReH₃(dppe)₂] in Degassed Solution. Irradiation of degassed benzene solutions of the complex with 366-nm light gives a color change from yellow to gold with a corresponding intensification and shift in the absorption maximum from 320 to 310 nm. In the IR, as the irradiation proceeds, the ν_{M-H} (1860 cm⁻¹) and δ_{M-H} (850 cm⁻¹) bands of [ReH₃(dppe)₂] decrease in intensity and no new bands appear in the metal hydride region. The production of H₂ during photolysis was verified by mass spectral and gas chromatographic analyses of the gases above irradiated solutions. In three separate experiments, the gases above exhaustively photolyzed (6-10 days) solutions were periodically removed and quantitated by Toepler pump techniques, giving an average value of 0.94 ± 0.18 mol of H₂ released/mol of complex irradiated. These results clearly demonstrate the elimination of H₂ and suggest the stoichiometry shown in eq 6.



The 366-nm quantum yield of H₂ loss from [ReH₃(dppe)₂] is 0.07 ± 0.02.

Although the stoichiometry of the reaction (eq 6) and the reactivity experiments detailed below indicate that the primary photoproduct from [ReH₃(dppe)₂] is almost certainly [ReH(dppe)₂] or a solvated derivative, this species has proven difficult to detect and characterize directly because of its high reactivity. As shown by the following series of NMR and IR experiments, it undergoes reversible insertion into the C-H bonds of both benzene solvent and the phenyl groups of the dppe ligands. The ¹H NMR spectrum of a C₆D₆ solution of [ReH₃(dppe)₂] shows a steady decrease in intensity of the δ -7.35 [ReH₃(dppe)₂] resonance as the sample is irradiated, but no new resonances appear anywhere in the metal hydride region (δ 0 → -30). Exposure of such solutions to N₂ does not yield the

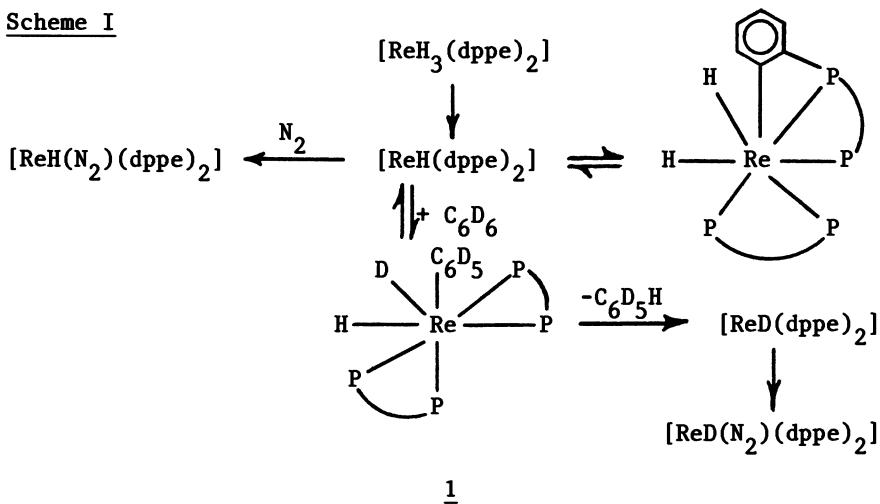
δ -9.5 resonance characteristic of the expected $[\text{ReH}(\text{N}_2)(\text{dppe})_2]$ product (see below); yet the IR spectrum of the solid material obtained after evaporation of solvent shows a strong $\nu_{\text{N}\equiv\text{N}}$ at 2006 cm^{-1} characteristic of this compound (16). The lack of a ^1H NMR resonance for the product thus indicates that the dinitrogen complex actually formed is the deuterated analogue, $[\text{ReD}(\text{N}_2)(\text{dppe})_2]$, and thus its solution precursor must be $[\text{ReD}(\text{dppe})_2]$. Further support for the $[\text{ReD}(\text{N}_2)(\text{dppe})_2]$ formulation comes from the presence of a weak band in its IR spectrum at 1330 cm^{-1} that is not present in the spectrum of $[\text{ReH}_3(\text{dppe})_2]$ and which may be attributed to a $\nu_{\text{Re-D}}$ vibration.

The other significant features of the IR spectrum of this material are the weak three-band pattern at 1542, 1557, and 1575 cm^{-1} characteristic of ortho-metalated arylphosphines (13, 17) and a weak broad band centered at 2260 cm^{-1} . The latter may be attributed to an aromatic C-D stretch (C_6D_6 , $\nu_{\text{C-D}} = 2277, 2267 \text{ cm}^{-1}$; $\text{P}(2,6\text{-C}_6\text{H}_3\text{D}_2)_3$, $\nu_{\text{C-D}} = 2254 \text{ cm}^{-1}$) which is presumed to arise from ortho-deuterated dppe ligands. Further evidence for the incorporation of deuterium into the dppe ligands comes from the ^1H NMR spectral changes in the δ 0-10 spectral region. $[\text{ReH}_3(\text{dppe})_2]$ shows a broad singlet at δ 7.5, a multiplet at δ 7.0, and a broad singlet at δ 2.1. The relative intensities of these resonances are in the ratio of 2:3:1, and they are logically attributed to the dppe ortho, meta/para, and methylene protons, respectively. Upon photolysis of $[\text{ReH}_3(\text{dppe})_2]$ in C_6D_6 solution, the δ 7.5 resonance completely disappears while the other resonances remain relatively unchanged. At the same time, the solvent $\text{C}_6\text{D}_5\text{H}$ resonance increases in intensity, thus indicating H/D exchange between solvent and coordinated dppe.

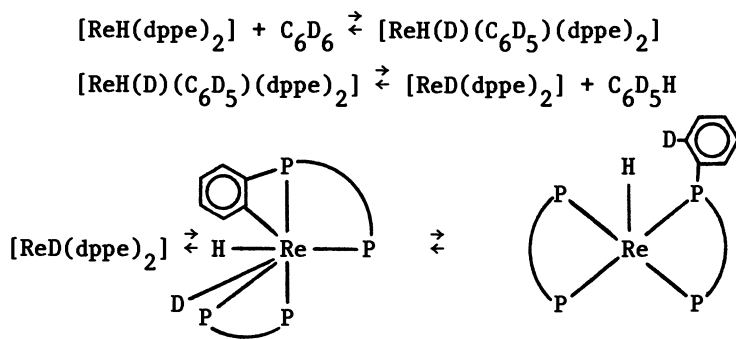
The results described above can be accounted for by the sequence of reactions outlined in Scheme I. Insertion into the C-D bonds of C_6D_6 presumably yields the seven-coordinate complex 1. This reaction must be readily reversible since the NMR and IR experiments detailed above indicate that it leads to H/D exchange to produce $[\text{ReD}(\text{dppe})_2]$ and $\text{C}_6\text{D}_5\text{H}$. The ready reversibility of this reaction presumably obtains because of severe steric crowding in 1 in which there are nine phenyl groups located around the central Re atom. $[\text{ReH}(\text{dppe})_2]$ also undergoes

reversible intramolecular insertion into the C-H bonds of the phenyl groups of the dppe ligands, i.e., ortho-metalation. If H/D exchange with solvent has previously occurred to yield $[\text{ReD}(\text{dppe})_2]$, this reaction leads to incorporation of deuterium into the dppe ligands via the sequence of reaction shown in Scheme II.

Scheme I



Scheme II



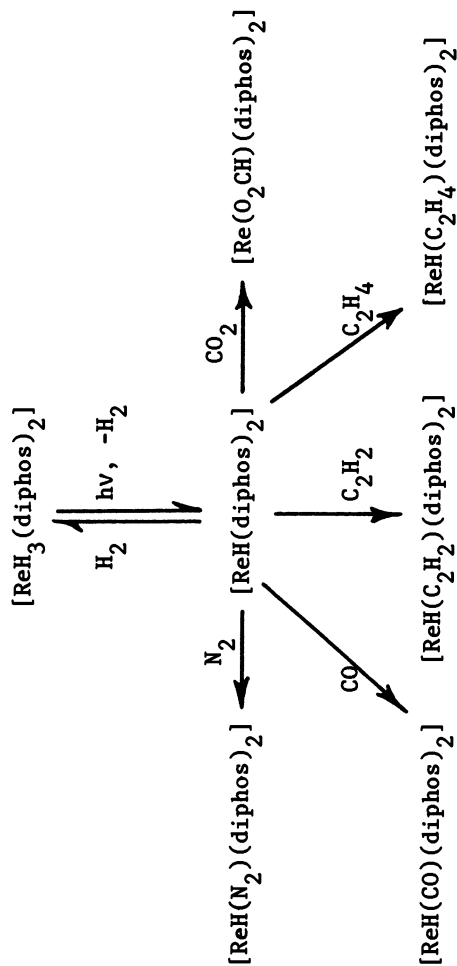
Photolysis of $[\text{ReH}_3(\text{dppe})_2]$ in the Presence of Reactant Gases

Irradiation of benzene solutions of $[\text{ReH}_3(\text{dppe})_2]$ under N_2 , CO, and C_2H_4 atmospheres leads to the respective adduct complexes $[\text{ReH}(\text{N}_2)(\text{dppe})_2]$, $[\text{ReH}(\text{CO})(\text{dppe})_2]$, and $[\text{ReH}(\text{D}_2\text{H}_4)(\text{dppe})_2]$ (Scheme III). These previously described compounds were identified primarily by comparison of their IR and ^1H NMR spectra to reported values (16).

Although the infrared spectra of the $[\text{ReH}(\text{L})(\text{dppe})_2]$ adduct complexes do not show the characteristic 1860- and 850- cm^{-1} bands of $[\text{ReH}_3(\text{dppe})_2]$, the ^1H NMR spectra of the photoproducts show a quintet at δ -7.35 ($J_{\text{P-H}} = 17.8$ Hz) indicative of residual trihydride. A comparison of the relative intensities of the hydride resonances of $[\text{ReH}_3(\text{dppe})_2]$ and $[\text{ReH}(\text{L})(\text{dppe})_2]$ indicates that approximately 50% conversion to the corresponding $[\text{ReH}(\text{L})(\text{dppe})_2]$ complexes occurs during 20-24 h irradiation. Increased conversion occurs with increased irradiation time, but it is difficult to drive these photoreactions entirely to completion. Adduct complexes prepared by this method are invariably contaminated with residual $[\text{ReH}_3(\text{dppe})_2]$.

The $[\text{ReH}(\text{dppe})_2]$ intermediate can also be trapped by acetylene. Irradiation of benzene solutions of $[\text{ReH}_3(\text{dppe})_2]$ under a C_2H_2 atmosphere gives a slow color change from yellow to light brown, and a brown solid can be isolated by solvent evaporation from the irradiated solutions. This material shows a weak band in its IR spectrum at 1690 cm^{-1} and a quintet at δ -4.35 ($J_{\text{P-H}} = 20$ Hz) in its ^1H NMR spectrum, in addition to a quintet at δ -7.35 due to residual $[\text{ReH}_3(\text{dppe})_2]$. The product is thermally unstable and solutions darken considerably upon standing under N_2 , eventually depositing an oily brown residue after several days. The IR band at 1690 cm^{-1} implies the presence of an alkyne ligand in the photoproduct, although $\nu_{\text{C}\equiv\text{C}}$ in alkyne complexes varies considerably with the nature of the complex and with the alkyne substituents (18, 19, 20). The upfield hydride resonance at δ -4.3 is in the range of the hydride resonances of the other adduct complexes (15) and thus formulation of the product as $[\text{ReH}(\text{C}_2\text{H}_2)(\text{dppe})_2]$ is indicated.

The photogenerated $[\text{ReH}(\text{dppe})_2]$ intermediate is also

Scheme III

readily scavenged by CO_2 . Irradiation of benzene solutions of $[\text{ReH}_3(\text{dppe})_2]$ in the presence of CO_2 gives a slow color change from yellow to orange, and a bright orange solid can be isolated by evaporation of solvent from the irradiated solutions. The IR spectrum of this material shows two new bands at 1554 and 1356 cm^{-1} which are not present in the spectrum of $[\text{ReH}_3(\text{dppe})_2]$. Substitution of $^{13}\text{CO}_2$ in the photolysis experiment gives an orange product with an infrared spectrum which shows bands at 1515 and 1334 cm^{-1} as expected for the $^{12}\text{C} \rightarrow ^{13}\text{C}$ substitution, and thus CO_2 has clearly been incorporated into the molecule. No $\nu_{\text{Re-H}}$ vibration is apparent in the metal hydride region of the IR spectrum. A group of bands is centered at 1960 cm^{-1} , but these appear to be due to the coordinated dppe ligands. The ^1H NMR spectrum of a benzene solution of the orange solid shows no new upfield resonances, although the ever present quintet at $\delta -7.35$ due to residual $[\text{ReH}_3(\text{dppe})_2]$ is evident. The $^{13}\text{C}\{^1\text{H}\}$ NMR spectrum of the $^{13}\text{CO}_2$ enriched product shows a single resonance at $\delta 171.9$ which splits into a doublet with $J_{\text{C-H}} = 202\text{ Hz}$ in the proton coupled spectrum.

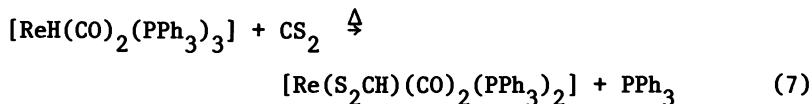
The product of the reaction with CO_2 is sensitive to thermal substitution of carbon dioxide. Storage of a benzene solution of the complex under an N_2 atmosphere results in a slow color change from orange to yellow. Removal of solvent from the yellow solution gives yellow crystals of $[\text{ReH}(\text{N}_2)(\text{dppe})_2]$, characterized by its strong $\nu_{\text{N=N}}$ at 2006 cm^{-1} . This reaction appears to be quantitative as evidenced by the complete disappearance of the 1554- and 1356-cm^{-1} IR bands. Similar treatment of the orange product with H_2 gives $[\text{ReH}_3(\text{dppe})_2]$. The orange product slowly decomposes when heated to $80\text{-}100^\circ\text{C}$, and mass spectral and gas chromatographic analyses of the gases above decomposed samples show the presence of CO_2 . Quantitative Toepler pump analysis of the evolved gases upon decomposition of the highest purity material that we have obtained gave a value of 0.97 mol of CO_2 given off/mol of complex.

The spectral properties of the product isolated from photolysis of $[\text{ReH}_3(\text{dppe})_2]$ in the presence of CO_2 are most consistent with its formulation as a formate derivative. Specifically, the IR bands at 1554 and 1356 cm^{-1} may be respectively

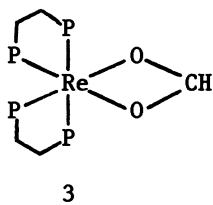
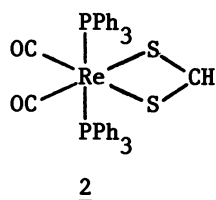
attributed to the $\nu(\text{CO}_2)_{\text{asym}}$ and $\nu(\text{CO}_2)_{\text{sym}}$ vibrations of a bidentate formate ligand. For comparison, $[\text{RuH}(\text{O}_2\text{CH})(\text{PPh}_3)_3]$, whose bidentate structure has been established by X-ray diffraction (21), shows bands at 1565 and 1340 cm^{-1} . Similarly, $[\text{IrClH}(\text{O}_2\text{CH})(\text{PPh}_3)_2]$ with a presumed bidentate structure has IR bands at 1550 and 1345 cm^{-1} (22). In contrast, complexes with unidentate formate ligands generally show the $\nu(\text{CO}_2)_{\text{asym}}$ above 1600 cm^{-1} (22, 23, 24). For example, addition of CO to the above-mentioned $[\text{IrClH}(\text{O}_2\text{CH})(\text{PPh}_3)_2]$ gives $[\text{IrClH}(\text{O}_2\text{CH})(\text{CO})(\text{PPh}_3)_2]$ with a unidentate formate ligand, and the corresponding IR bands are at 1687 and 1362 cm^{-1} (22). The IR spectrum of $[\text{Re}(\text{O}_2\text{CH})(\text{dppe})_2]$ shows no evidence for a $\nu_{\text{M-H}}$ vibration but does show a weak $\nu_{\text{C-H}}$ band at 2825 cm^{-1} that is not present in $[\text{ReH}_3(\text{dppe})_2]$ and which may be attributed to the formate C-H vibration.

The most definitive evidence for the formate formulation for $[\text{Re}(\text{O}_2\text{CH})(\text{dppe})_2]$ is the doublet at δ 171.9 ($J_{\text{C-H}} = 202$ Hz) in its ^{13}C NMR spectrum. Both the chemical shift and the coupling constant fall within the ranges established for organic formates (25). The chemical shifts of ethyl formate and formic acid, for example, are δ 160.7 and 166.7, respectively (25). The $^{13}\text{C-H}$ coupling constants for the formate carbon generally lie between 170 and 230 Hz with HCO_2^- showing a coupling constant of 194.8 Hz (25).

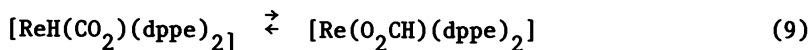
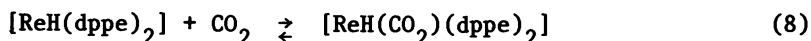
The rhenium dithioformate complex $[\text{Re}(\text{S}_2\text{CH})(\text{CO})_2(\text{PPh}_3)_2]$, prepared by Freni, et al. (26), via the reaction shown in eq 7,



has been characterized by X-ray diffraction and shown to have the structure 2 (27). This complex is isoelectronic with $[\text{Re}(\text{O}_2\text{CH})(\text{dppe})_2]$ and, thus, by analogy to $[\text{Re}(\text{S}_2\text{CH})(\text{CO})_2(\text{PPh}_3)_2]$, the most reasonable structure for $[\text{Re}(\text{O}_2\text{CH})(\text{dppe})_2]$ is that shown in 3.



The formation of $[\text{Re}(\text{O}_2\text{CH})(\text{dppe})_2]$ presumably proceeds via initial addition of CO_2 to photogenerated $[\text{ReH}(\text{dppe})_2]$ to give an adduct complex similar to those obtained with N_2 , CO , and C_2H_4 (eq 8). Hydride migration to CO_2 would then generate the observed formate derivative (eq 9). Both of these reac-



tions must be reversible, however, since CO_2 is readily displaced by N_2 and H_2 to yield $[\text{ReH}(\text{N}_2)(\text{dppe})_2]$ and $[\text{ReH}_3(\text{dppe})_2]$, respectively, and CO_2 is liberated upon thermal decomposition of $[\text{Re}(\text{O}_2\text{CH})(\text{dppe})_2]$.

Photodissociation of PR_3 Ligands from $[\text{ReH}_3(\text{PR}_3)_4]$ and $[\text{ReH}_5(\text{PR}_3)_3]$ Complexes

The above results led us to consider whether multiple hydrogen migration to a bound CO_2 or N_2 ligand might occur if the photogenerated intermediate possessed two or more hydrides. Photo-induced loss of H_2 from $[\text{ReH}_5(\text{PR}_3)_3]$, for example, would give $[\text{ReH}_3(\text{PR}_3)_3]$ with three hydrides which could potentially transfer. However, we have found that these pentahydrides do not undergo elimination of H_2 in the primary photochemical event but, instead, efficiently lose a PR_3 ligand. These compounds thus constitute the first class of monomeric di- and polyhydride complexes in which the dominant photoreaction has definitely been shown to be something other than H_2 loss. The trihydride complex $[\text{ReH}_3(\text{PMe}_2\text{PH})_4]$ has also been examined and found to undergo efficient PR_3 elimination. These latter results are discussed in view of those noted above for $[\text{ReH}_3(\text{dppe})_2]$ which loses H_2 .

Photo-induced Loss of PR_3 from $[\text{ReH}_5(\text{PR}_3)_3]$ Complexes.

$[\text{ReH}_5(\text{PMe}_2\text{Ph})_3]$ is thermally quite stable, showing no detectable reaction when heated in a degassed isooctane solution for 15 h at 80°C. However, 366 nm photolysis of an isooctane solution of the complex results in a rapid decrease in intensity of its electronic absorption band at 338 nm. However, as the photolysis proceeds, the spectral changes become more complex as secondary photochemical and/or thermal reactions occur. Irradiation of concentrated solutions of the complex gives an initial change from colorless to pale orange and the formation of an orange precipitate, identified as $[\text{Re}_2\text{H}_8(\text{PMe}_2\text{Ph})_4]$ as indicated by its ^1H NMR spectrum which shows a quintet at δ -6.31 ppm with $J_{\text{P-H}} = 9.52$ Hz. For comparison, $[\text{Re}_2\text{H}_8(\text{PEt}_2\text{Ph})_4]$ shows a quintet at δ -6.59 ppm with $J_{\text{P-H}} = 9.28$ Hz (28). Upon continued photolysis this precipitate redissolves to give a dark red solution. This coloration persists until one mole of H_2 per mole of initial $[\text{ReH}_5(\text{PMe}_2\text{Ph})_3]$ has been released. Exhaustive photolysis then results in a green coloration and eventually, after 1.5 equivalents of H_2 have been evolved, a white flocculent precipitate deposits. Evaporation of solvent at this point gives a green oil which has a strong odor of free PMe_2Ph .

The metal-hydride region ^1H NMR spectrum of a sample that had been irradiated up to the point of the red coloration is shown in Figure 1a. This spectrum shows the formation of $[\text{ReH}_7(\text{PMe}_2\text{Ph})_2]$ ($\delta_{\text{ReH}} -5.11$ t, $J_{\text{P-H}} = 20.2$ Hz), a trace amount of $[\text{ReH}_3(\text{PMe}_2\text{Ph})_4]$ ($\delta_{\text{ReH}} -6.74$ qt, $J_{\text{P-H}} = 20.2$ Hz), and a broad sextet at δ -8.23 ($J_{\text{P-H}} = 10.8$ Hz) which may be attributed to the $[\text{Re}_2\text{H}_6(\text{PMe}_2\text{Ph})_5]$ dimer which has been structurally characterized by Caulton, et al. (29). The $[\text{ReH}_7(\text{PMe}_2\text{Ph})_2]$ and $[\text{ReH}_3(\text{PMe}_2\text{Ph})_4]$ products were identified by comparison to spectra of authentic samples. A doublet at δ 1.05 ($J_{\text{P-H}} = 2.9$ Hz) due to uncoordinated PMe_2Ph is also present in the spectrum but not shown in Figure 1a.

The photoreaction is markedly inhibited by the presence of excess PMe_2Ph . For example, photolysis of $[\text{ReH}_5(\text{PMe}_2\text{Ph})_3]$ in the presence of a 100-fold excess of PMe_2Ph gave no detectable reaction after 8 h although a similarly prepared control sample without excess PMe_2Ph showed substantial reaction after 1 h irradiation.

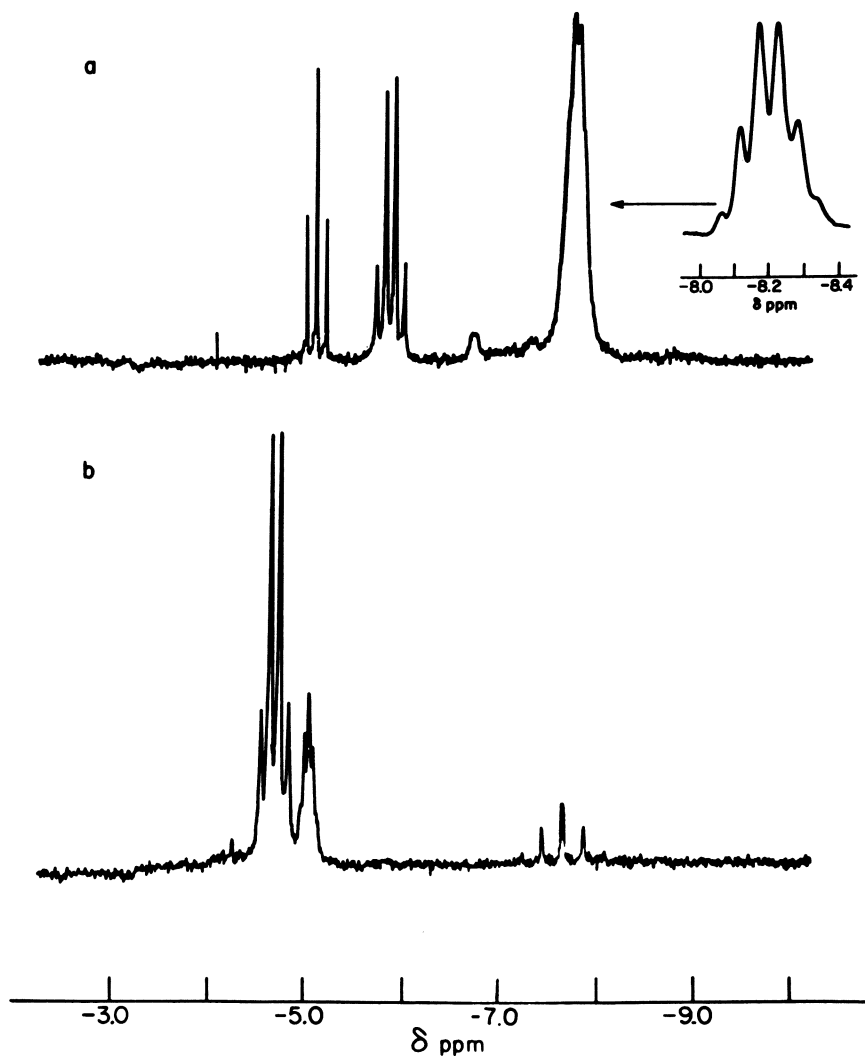
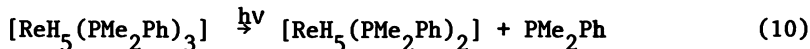


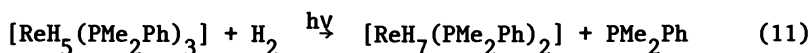
Figure 1. Comparison of the ^1H NMR spectra after 366-nm photolysis of $[\text{ReH}_5(\text{PMe}_2\text{Ph})_3]$ in cyclohexane- d_{12} solution (a), and $[\text{ReH}_5(\text{PPh}_3)_3]$ in benzene- d_6 solution (b).

The generation of free PMe_2Ph and the suppression of the photoreaction by excess PMe_2Ph both point to loss of PMe_2Ph from $[\text{ReH}_5(\text{PMe}_2\text{Ph})_3]$ in the primary photochemical event, eq 10.



However, the presumed $[\text{ReH}_5(\text{PMe}_2\text{Ph})_2]$ intermediate must undergo further reaction to give the mix of products described above.

The overall reaction is much cleaner when the irradiation is conducted in the presence of H_2 as evidenced by the UV-VIS spectral changes, Figure 2, which show a smooth, rapid decrease in the 338 nm absorption band as the irradiation proceeds. No suppression of the rate of reaction is observed under an H_2 atmosphere, in direct contrast to the situation found for those hydride complexes where the primary photoreaction is H_2 loss. The initial product of photolysis under an H_2 atmosphere is $[\text{ReH}_7(\text{PMe}_2\text{Ph})_2]$ (eq 11).



Consistent with the spectral changes shown in Figure 2, $[\text{ReH}_7(\text{PMe}_2\text{Ph})_2]$ shows no absorption maximum below 272 nm (Table I). ^1H NMR spectra from low conversion (~35%) photolysis experiments showed resonances attributable to $[\text{ReH}_5(\text{PMe}_2\text{Ph})_3]$, $[\text{ReH}_7(\text{PMe}_2\text{Ph})_2]$, a trace of $[\text{Re}_2\text{H}_6(\text{PMe}_2\text{Ph})_5]$, and free PMe_2Ph . Furthermore, irradiation of 0.5 g of $[\text{ReH}_5(\text{PMe}_2\text{Ph})_3]$ under an H_2 atmosphere, led to the isolation of a mixture of $[\text{ReH}_7(\text{PMe}_2\text{Ph})_2]$ and $[\text{Re}_2\text{H}_8(\text{PMe}_2\text{Ph})_4]$. The latter is a known thermal degradation product of $[\text{ReH}_7(\text{PMe}_2\text{Ph})_2]$ (30) and this $[\text{ReH}_7(\text{PMe}_2\text{Ph})_2] \rightarrow [\text{Re}_2\text{H}_8(\text{PMe}_2\text{Ph})_4]$ conversion has also been shown to be photoaccelerated (29). The quantum yield of PMe_2Ph loss from $[\text{ReH}_5(\text{PMe}_2\text{Ph})_3]$ under an H_2 atmosphere is 0.16 ± 0.02 .

As noted above, photolysis in degassed solutions does lead to evolution of H_2 and formation of $[\text{Re}_2\text{H}_8(\text{PMe}_2\text{Ph})_4]$ and $[\text{Re}_2\text{H}_6(\text{PMe}_2\text{Ph})_5]$. An attempt was made to determine the mechanism of this transformation by carrying out crossover experiments with $[\text{ReH}_5(\text{PMe}_2\text{Ph})_3]$ and $[\text{ReD}_5(\text{PMe}_2\text{Ph})_3]$. However, 10 min 366 nm photolysis of $[\text{ReD}_5(\text{PMe}_2\text{Ph})_3]$ in hexane solution gave a 1:4:8

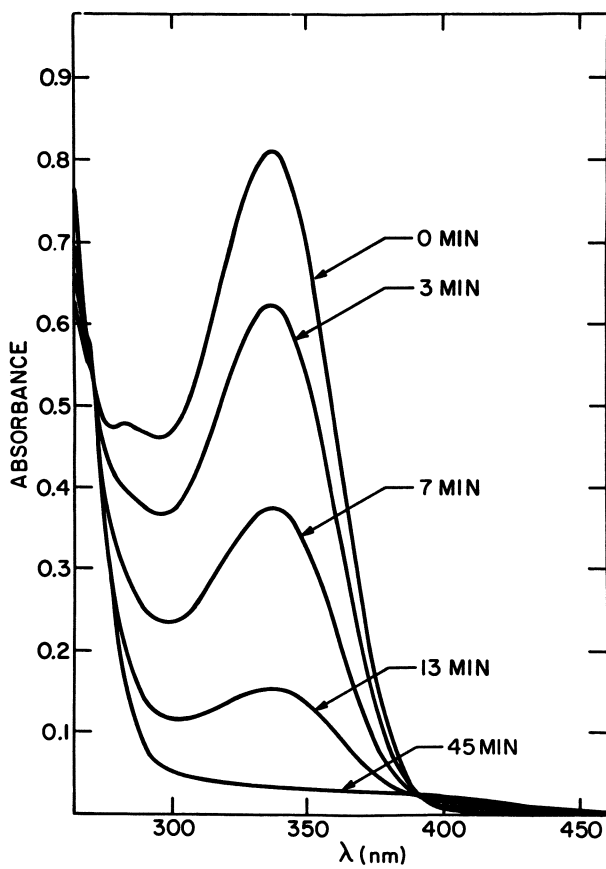


Figure 2. Electronic absorption spectral changes during 366-nm irradiation of an isoctane solution of $[ReH_5(PMe_2Ph)_5]$ under an H_2 atmosphere.

Table I. Spectral Data

Complex	¹ H NMR ^a		IR ^b		UV-VIS	
	δ _{Re-H} , ppm	J _{P-H} , Hz	ν _{Re-H} , cm ⁻¹	ν _{Re-H} , cm ⁻¹	λ _{max} , nm	(ε, M ⁻¹ cm ⁻¹)
[ReH ₃ (PMe ₂ Ph) ₄]	-6.74 (qt)	20.18	1952m, 1890m, 1784s, 1750m,sh	1952m, 1890m, 1784s, 1750m,sh	323 (4770), 380sh(1730)	---
[ReH ₃ (PPh ₃) ₄]	-7.56 (qt)	40.7	1983m,sh, 1962m	1983m,sh, 1962m	---	---
[ReH ₅ (PMe ₂ Ph) ₃]	-6.08 (q)	18.70	1949w,sh, 1931m, 1905m, 1852m	1949w,sh, 1931m, 1905m, 1852m	338 (4225)	---
[ReH ₅ (PMePh ₂) ₃]	-5.50 (q)	18.31	1935w,sh, 1953m,sh, 1982m, 1890m,sh, 1876m	1935w,sh, 1953m,sh, 1982m, 1890m,sh, 1876m	327 (5270)	---
[ReH ₅ (PPh ₃) ₃]	-4.66 (q)	18.37	1952s, 1891s	1952s, 1891s	332 (5900)	---
[ReD ₅ (PMe ₂ Ph) ₃]	---	---	1395w,sh, 1380m, 1371m, 1335m	1395w,sh, 1380m, 1371m, 1335m	---	---
[ReH ₇ (PMe ₂ Ph) ₂]	-5.11 (t)	20.43	1983w, 1965w,sh, 1893m,sh, 1862m, 1750vw,sh	1983w, 1965w,sh, 1893m,sh, 1862m, 1750vw,sh	---	---
[ReH ₇ (PMePh ₂) ₂]	-4.72 (t)	20.0	---	---	---	---
[ReH ₇ (PPh ₃) ₂]	-4.20 (t)	18.61	---	---	---	---
[Re ₂ H ₈ (PMe ₂ Ph) ₄]	-6.31 (qt)	9.52	---	---	---	---
[Re ₂ H ₈ (PMePh ₂) ₄]	-5.78 (qt)	8.85	---	---	---	---
[Re ₂ H ₈ (PPh ₃) ₄]	-5.01 (qt)	8.16	---	---	---	---

^aBenzene-d₆ solution; t = triplet; q = quartet; q = quartet; qt = quintet.

^bKBr pellet.

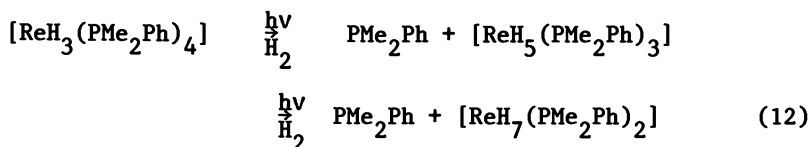
ratio of $D_2/HD/H_2$ as determined by mass spectral analysis of the gases above the irradiated solution. Photolysis of $[ReH_5(PMe_2Ph)_3]$ in cyclohexane- d_{12} gave <2% HD and no detectable D_2 . These two experiments indicate that extensive scrambling of hydrogen between the hydride and PMe_2Ph ligands occurs upon photolysis, and thus these crossover experiments would not be meaningful. 1H NMR spectra also demonstrated that photolysis of $[ReH_5(PMe_2Ph)_3]$ in benzene- d_6 leads to H/D exchange between solvent and ligand phenyl hydrogens. Surprisingly, the 1H NMR spectra showed that exchange occurs almost exclusively at the meta and para positions of the phenyl substituents. For example, 30 min 366 nm irradiation of a benzene- d_6 solution of $[ReH_5(PMe_2Ph)_3]$ showed nearly complete disappearance of the resonances in the δ 7.00-7.08 ppm chemical shift region due to the meta and para PMe_2Ph hydrogens whereas the δ 7.55 ppm multiplet due to the ortho hydrogens remained unchanged. These results are in direct contrast to those obtained with $[ReH_3(dppe)_2]$ which shows photoassisted H/D exchange with benzene- d_6 exclusively at the ortho positions of the dppe phenyl substituents (13). These results indicate an intermolecular exchange path for $[ReH_5(PMe_2Ph)_3]$ whereas exchange with $[ReH_3(dppe)_2]$ is intramolecular.

The photochemistry observed for $[ReH_5(PMePh_2)_3]$ is similar to that discussed above for $[ReH_5(PMe_2Ph)_3]$, except that all reactions were carried out in benzene solution to increase compound solubility. The UV-VIS spectral changes which occur upon 366 nm photolysis under an H_2 atmosphere show a smooth decrease in intensity of the 327 nm absorption band as the $[ReH_7(PMePh_2)_2]$ complex forms. A 1H NMR spectrum of a sample irradiated in degassed solution showed resonances attributable to $[ReH_7(PMePh_2)_2]$ (δ -4.72 t, $J_{P-H} = 20.0$ Hz), $[ReH_5(PMePh_2)_3]$ (δ -5.50 q, $J_{P-H} = 18.31$ Hz), and $[Re_2H_8(PMePh_2)_4]$ (δ -5.78 qt, $J_{P-H} = 8.85$ Hz). A broad resonance at δ -7.59 is also apparent and may be attributed to $[Re_2H_6(PMePh_2)_5]$ on the basis of its spectral similarities to $[Re_2H_6(PMe_2Ph)_5]$ (29). No resonances attributable to $[ReH_3(PMePh_2)_4]$ were observed in this spectrum. The 366 nm quantum yield for $PMePh_2$ loss from $[ReH_5(PMePh_2)_3]$ is 0.13 ± 0.02 .

As indicated in Figure 1b, the product mixture obtained upon photolysis of $[\text{ReH}_5(\text{PPh}_3)_3]$ in degassed solution is different from that observed for the PMe_2Ph derivative. Resonances due to $[\text{Re}_2\text{H}_8(\text{PPh}_3)_4]$ (δ -5.01 qt, $J_{\text{P-H}} = 8.16$ Hz) are observed but no upfield resonance which might be attributable to $[\text{Re}_2\text{H}_6(\text{PPh}_3)_5]$ is seen nor is there any evidence for $[\text{ReH}_7(\text{PPh}_3)_2]$. Instead, a quintet at -7.56 ppm ($J_{\text{P-H}} = 40.7$ Hz) is present. We attribute the latter to $[\text{ReH}_3(\text{PPh}_3)_4]$, although our ^1H NMR data for this compound differs from that previously reported in a review (31) of Re hydride complexes. However, following the recipe of Freni, et al. (32), for the preparation of this compound, we obtained a yellow microcrystalline product which shows a quintet at -7.56 ppm ($J_{\text{P-H}} = 40.7$ Hz) in its ^1H NMR spectrum and a corresponding quartet at 24.4 ($J_{\text{P-H}} = 40.7$ Hz) in its ^{31}P NMR spectrum in which the C_6H_5 hydrogens were decoupled. We are thus confident of the $[\text{ReH}_3(\text{PPh}_3)_4]$ formulation for this compound and suggest that the data in the review (31) is in error. Although difficult to resolve, the resonance patterns in the δ 6-8 ppm region of the ^1H NMR spectrum shown in Figure 1b indicate that little, if any, uncoordinated PPh_3 is present. This, of course, is consistent with the presence of $[\text{ReH}_3(\text{PPh}_3)_4]$. As with the other $[\text{ReH}_5(\text{PR}_3)_3]$ complexes, the rate of photoreaction is suppressed by the presence of excess PPh_3 and clean UV-VIS spectral changes occur upon photolysis under an H_2 atmosphere. Taken together, all these results point to PPh_3 elimination in the primary photoreaction, and the 366 nm quantum yield for this process is 0.18 ± 0.02 .

Photoinduced Dissociation of PMe_2Ph from $[\text{ReH}_3(\text{PMe}_2\text{Ph})_4]$.

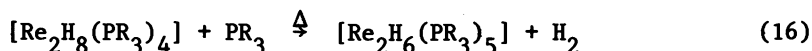
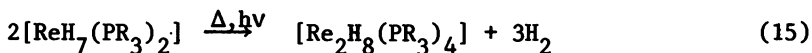
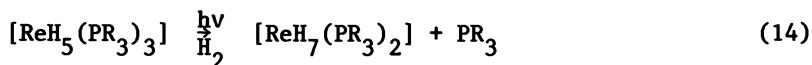
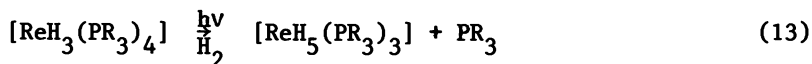
When irradiated in the presence of H_2 , $[\text{ReH}_3(\text{PMe}_2\text{Ph})_4]$ smoothly converts to the corresponding $[\text{ReH}_7(\text{PMe}_2\text{Ph})_2]$ complex via the intermediacy of $[\text{ReH}_5(\text{PMe}_2\text{Ph})_2]$, eq 12.



This is clearly illustrated by the UV-VIS spectral changes shown in Figure 3. As the irradiation proceeds, the 323 nm absorption maximum of $[\text{ReH}_3(\text{PMe}_2\text{Ph})_4]$ shifts to 338 nm, the maximum of $[\text{ReH}_5(\text{PMe}_2\text{Ph})_3]$. Continued photolysis then causes disappearance of all absorption bands below 270 nm as $[\text{ReH}_7(\text{PMe}_2\text{Ph})_2]$ forms. This sequence of reactions is also evidenced by the ^1H NMR changes observed for 366 nm photolysis of $[\text{ReH}_3(\text{PMe}_2\text{Ph})_4]$ under an H_2 atmosphere. These spectra show a progressive decrease in the δ -6.74 quintet due to $[\text{ReH}_7(\text{PMe}_2\text{Ph})_2]$ and the growth of the δ -6.08 ppm quartet due to $[\text{ReH}_5(\text{PMe}_2\text{Ph})_3]$. Free PMe_2Ph is also observed. The 366 nm quantum yield for PMe_2Ph loss from $[\text{ReH}_3(\text{PMe}_2\text{Ph})_4]$ is 0.40 ± 0.05 .

Discussion of the $[\text{ReH}_5(\text{PR}_3)_3]$ and $[\text{ReH}_3(\text{PR}_3)_4]$ Results.

The results described above clearly demonstrate that photolysis of the $[\text{ReH}_5(\text{PR}_3)_3]$ and $[\text{ReH}_3(\text{PR}_3)_4]$ complexes studied gives relatively efficient loss of a PR_3 ligand in the primary photo-reaction, but not H_2 elimination. In the presence of H_2 , the complexes are initially converted to $[\text{ReH}_7(\text{PR}_3)_2]$, although the latter is thermally and photochemically unstable with regard to conversion to $[\text{Re}_2\text{H}_8(\text{PR}_3)_4]$ (29, 30). The $[\text{Re}_2\text{H}_8(\text{PR}_3)_4]$ compounds in turn can react with the photoreleased PR_3 to give the corresponding $[\text{Re}_2\text{H}_6(\text{PR}_3)_5]$ complexes, an example of which has been characterized by Caulton, et al. (30). However, the extent of this latter transformation appears to be dependent upon the nature of PR_3 ; as shown in Figure 1b, no evidence for a $[\text{Re}_2\text{H}_6(\text{PPh}_3)_5]$ dimer was obtained upon photolysis of $[\text{ReH}_5(\text{PPh}_3)_3]$. The sequence of events which occur under an H_2 atmosphere is summarized in eqs 13-16.



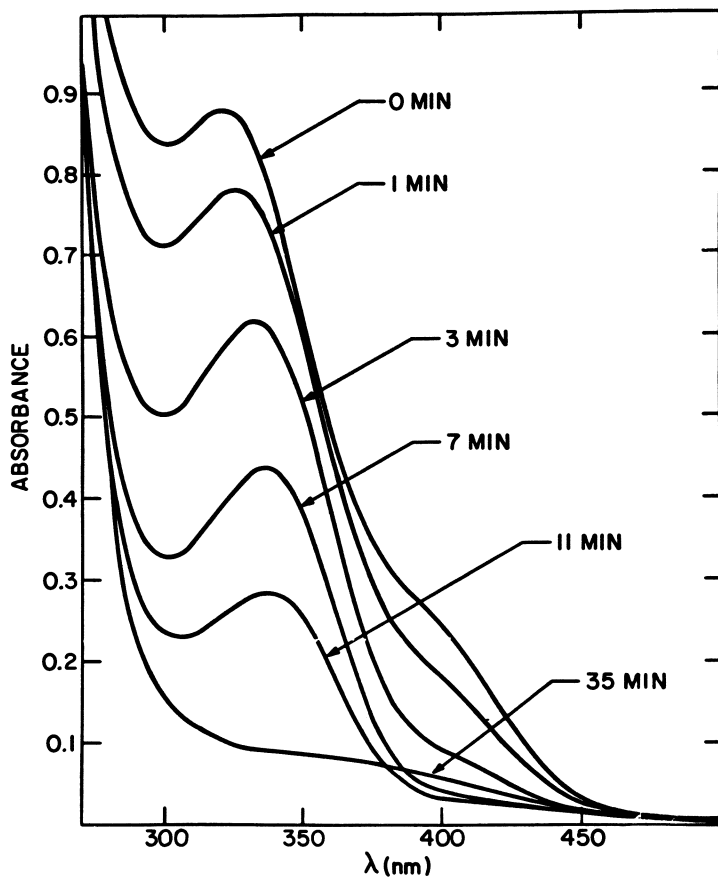
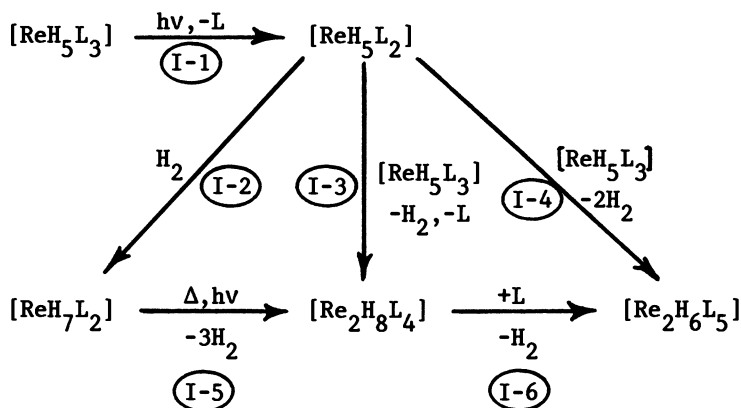


Figure 3. Electronic absorption spectral changes during 366-nm irradiation of an isoctane solution of $[\text{ReH}_3(\text{PMe}_2\text{Ph})_3]$ under an H_2 atmosphere.

The reactions are more complicated when the irradiation is conducted in the absence of H_2 . Here the products observed are $[ReH_3(PR_3)_4]$, $[ReH_7(PR_3)_2]$, $[Re_2H_8(PR_3)_4]$ and $[Re_2H_6(PR_3)_5]$ with the relative amount of each varying significantly with the nature of PR_3 . The experimental evidence again points to PR_3 loss in the primary photoreaction, although net H_2 loss does eventually obtain as the $[Re_2H_8(PR_3)_4]$ and $[Re_2H_6(PR_3)_5]$ dimers are produced. Scheme IV illustrates one possible route to $[ReH_7(PR_3)_2]$ and the dimeric products.

Scheme IV

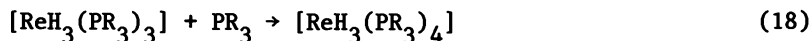


The photogenerated $[ReH_5(PR_3)_2]$ complex could undergo binuclear reactions with $[ReH_5(PR_3)_3]$, I-3 and I-4 in Scheme IV, to directly give the $[Re_2H_8(PR_3)_4]$ and $[Re_2H_6(PR_3)_5]$ dimers. Consistent with this proposal is the immediate observation of these dimers at the onset of photolysis and Norton's (38) studies of the dimerization of $H_2Os(CO)_4$ which proceeds by a similar bimolecular pathway. Reaction of the photogenerated $[ReH_5(PR_3)_2]$ with H_2 , released in the course of reactions I-3 and I-4, would yield $[ReH_7(PR_3)_2]$. $[ReH_7(PR_3)_2]$ thermally and photochemically decomposes to give the respective $[Re_2H_8(PR_3)_4]$ dimers which, in turn, are known to react with excess PR_3 to yield the $[Re_2H_6(PR_3)_5]$ dimers (29, 30). In our hands, this latter conversion occurs at room temperature immediately upon combining the reagents.

Another possible route to $[\text{ReH}_7(\text{PR}_3)_2]$ is via the disproportionation of photogenerated $[\text{ReH}_5(\text{PR}_3)_2]$ with $[\text{ReH}_5(\text{PR}_3)_3]$, eq 17.

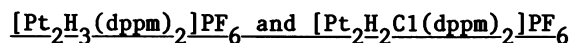


This reaction would also yield $[\text{ReH}_3(\text{PR}_3)_3]$ which could add the photoreleased phosphine to give $[\text{ReH}_3(\text{PR}_3)_4]$, a product observed in significant quantity for $\text{L} = \text{PPh}_3$, eq 18.



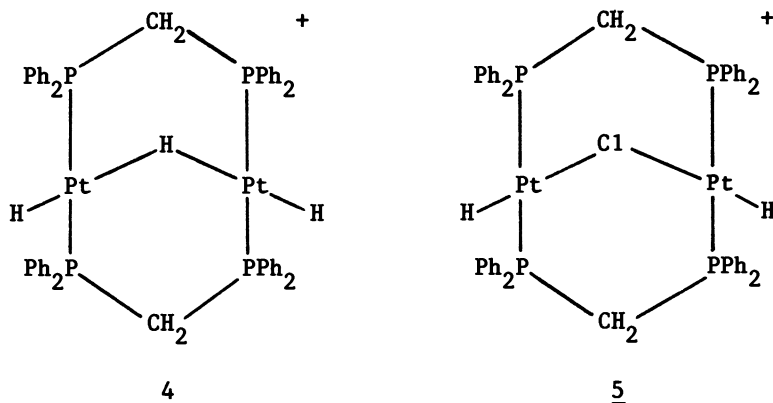
It is significant that $[\text{ReH}_3(\text{PMe}_2\text{Ph})_4]$ loses PMe_2Ph in its primary photoreaction, whereas for $[\text{ReH}_3(\text{dppe})_2]$ the observed reaction is clearly H_2 elimination (13). Note, however, that the quantum yields for these processes are vastly different. Elimination of H_2 from $[\text{ReH}_3(\text{dppe})_2]$ occurs with a quantum yield of 0.07 whereas loss of PMe_2Ph from $[\text{ReH}_3(\text{PMe}_2\text{Ph})_4]$ occurs with $\phi = 0.4$. We suspect that phosphine loss and H_2 elimination are competitive photoreactions in these rhenium hydride complexes, with phosphine loss the more efficient of the two. In the case of $[\text{ReH}_3(\text{dppe})_2]$, the chelating dppe ligands prevent net phosphine loss and the only observed reaction is H_2 loss.

Photoinduced Elimination of H_2 from the Dinuclear Complexes



Since photolysis of monomeric di- and polyhydride transition metal complexes often leads to elimination of H_2 as the dominant photoreaction, the question arises as to whether or not H_2 elimination will occur from di- and polynuclear hydride complexes in which the hydride ligands are bound to different metals or bridge two or more metal centers. Such dinuclear elimination reactions could be important in solar energy conversion schemes using soluble complexes for producing H_2 from H_2O (34, 35, 36). The few polynuclear hydridocarbonyl cluster complexes which have had their photochemistry examined do not show H_2 loss but instead either CO loss or metal-metal bond cleavage (37-40). In search of such H_2 elimination reactions

we have examined the dinuclear hydride complexes $[\text{Pt}_2\text{H}_3(\text{dppm})_2]\text{-PF}_6$, 4, ($\text{dppm} = \text{Ph}_2\text{PCH}_2\text{PPh}_2$) and $[\text{Pt}_2\text{H}_2\text{Cl}(\text{dppm})_2]\text{PF}_6$, 5, both of which have been well characterized by Brown, Puddephatt, and co-workers (41, 42, 43). The studies reported herein show that both of these complexes readily lose H_2 upon photolysis and demonstrate the feasibility of such reaction from di- and polynuclear hydride complexes.



Degassed acetonitrile solutions of 4 show little or no decomposition upon prolonged heating at 80°C , but photolysis ($\lambda \geq 300 \text{ nm}$) of thoroughly degassed CH_3CN solutions of $[\text{Pt}_2\text{H}_3(\text{dppm})_2]\text{PF}_6$ gives visible gas evolution and a rapid change from colorless to red. The UV-VIS spectral changes which occur are shown in Figure 4, and the maintenance of the isosbestic points at 337 nm and 372 nm indicates a clean conversion to products. The red color arises as a result of the weak visible absorption by the photoproduct ($\epsilon_{450} = 130 \text{ M}^{-1} \text{ cm}^{-1}$). One mole of H_2 per mole of complex irradiated is rapidly evolved ($\sim 30 \text{ min}$), although prolonged photolysis ($> 48 \text{ h}$) leads to secondary photochemical reactions and further slow evolution of H_2 . A total of 1.42 moles of H_2 were evolved in one 66 h experiment. Concentration and cooling of CH_3CN solutions irradiated to the point of evolution of 1 mole equivalent of H_2 gives a red solid which has been characterized as $[\text{Pt}_2\text{H}(\text{CH}_3\text{CN})(\text{dppm})_2]\text{PF}_6$. (Anal. Calcd. for $\text{C}_{52}\text{H}_{48}\text{F}_6\text{NP}_5\text{Pt}_2$: C, 46.39%; H, 3.57%. Found: C, 46.01%; H, 3.59%). The reaction shown in eq 19 is thus

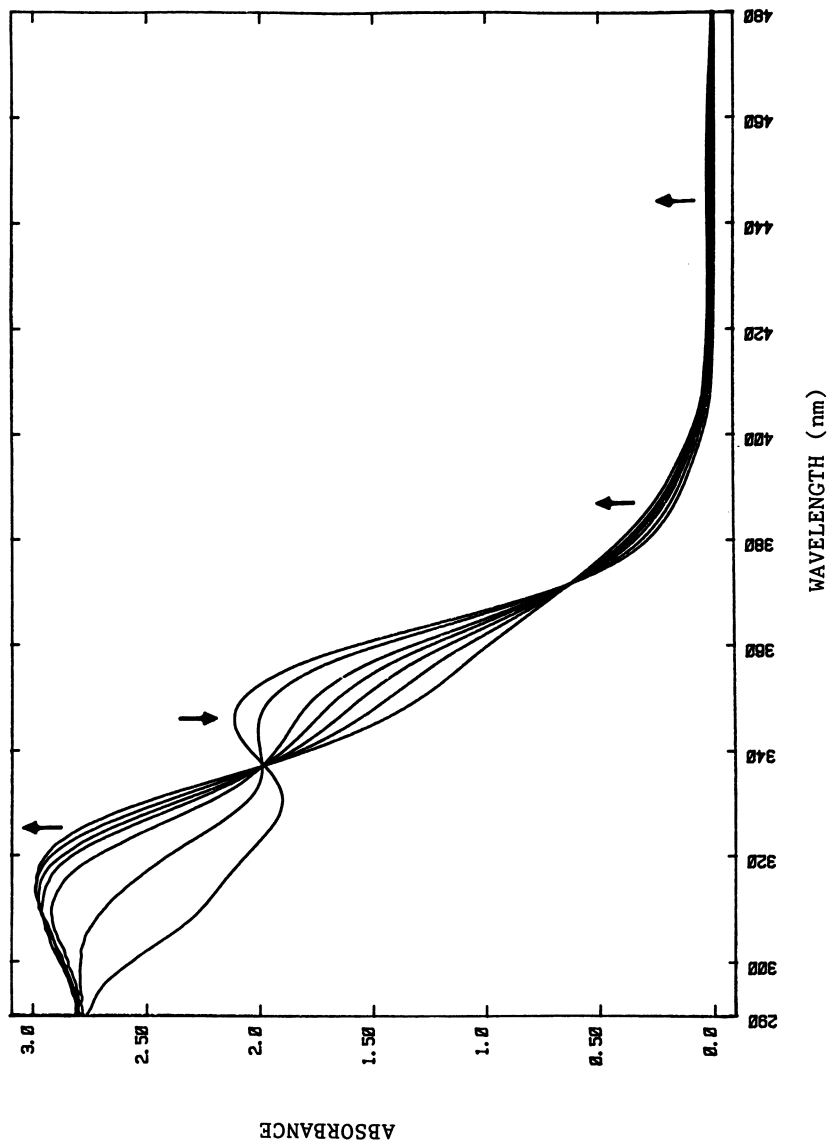
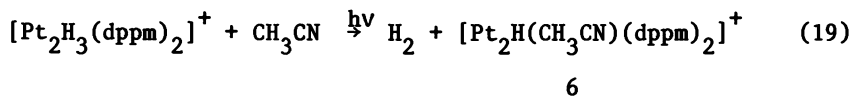
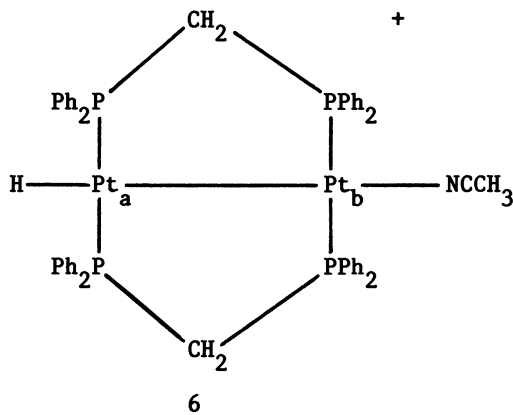


Figure 4. UV-visible spectral changes during 366-nm photolysis of a CH_3CN solution of $[\text{Pt}_4\text{H}_5(\text{dppm})_4]\text{PF}_6$. Arrows indicate the direction of the spectral changes after beginning photolysis; and the spectra were successively recorded after 0, 0.5, 1, 1.5, 2, 3, and 5 min total irradiation time.

indicated and spectroscopic data imply structure 6 for the photoproduct.



The IR spectrum of 6 shows a $\nu_{\text{Pt-H}}$ vibration at 2033 cm^{-1} , indicative of a terminal rather than bridging hydride, and a weak ν_{CN} stretch at 2258 cm^{-1} . The hydride resonance in the ^1H



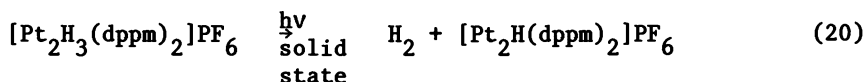
NMR spectrum of 6 in CD_3CN solution appears at $\delta -8.9$ as a pseudoquartet due to coupling to the four ^{31}P nuclei ($^2J_{\text{P-H}}$, $^3J_{\text{P-H}}$, = 9 Hz) with two sets of 1/4 intensity satellites from coupling to the two inequivalent ^{195}Pt atoms ($^1J_{\text{Pt}_a\text{-H}}$ = 975 Hz; $^2J_{\text{Pt}_b\text{-H}}$ = 73 Hz). As Puddephatt (44, 45, 46) has shown, this

satellite pattern is characteristic of a terminal hydride, whereas a 1:8:18:8:1 quintet pattern is expected for a bridging hydride. This ^1H NMR resonance pattern is similar to that observed for $[\text{Pt}_2\text{H}(\text{CO})(\text{dppm})_2]\text{PF}_6$ (45) and $[\text{Pt}_2\text{H}(\text{dppm})_3]\text{PF}_6$ (46) which have structures analogous to that proposed for 6. The ^1H NMR spectrum of 6 also shows a singlet at $\delta 1.95$ due to the methyl group of the CH_3CN ligand. The $[\text{Pt}_2\text{H}(\text{CH}_3\text{CN})(\text{dppm})_2]^+$ photoproduct reacts with CO and H_2 , both at 25°C and 1 atm pressure, to respectively yield $[\text{Pt}_2\text{H}(\text{CO})(\text{dppm})_2]$ (45) and

$[\text{Pt}_2\text{H}_3(\text{dppm})_2]^+$, providing further support for the proposed structure and also suggesting a rich derivative chemistry for this complex.

Photolysis of **4** in THF and acetone solutions gives similar results although the photoproducts, which are presumably analogous to **6**, are not as completely characterized. The spectral properties of the red solid isolated from photolysis of THF solutions of **4** are consistent with the formulation $[\text{Pt}_2\text{H}(\text{THF})(\text{dppm})_2]\text{PF}_6$. ^1H NMR monitoring of photolysis of **4** in CD_2Cl_2 solutions showed the formation of $[\text{Pt}_2\text{HCl}_2(\text{dppm})_2]^+$ (δ -12 m) and $[\text{Pt}_2\text{H}_2\text{Cl}(\text{dppm})_2]^+$ (δ -17 m) in an approximate 7:3 ratio.

H_2 loss also occurs when **4** is irradiated in the solid-state. White solid samples of **4** in vacuo or under N_2 rapidly turn red upon exposure to sunlight, fluorescent room light, or UV irradiation ($\lambda \geq 300$ nm). Mass spectral analysis of gases above irradiated solid samples showed the presence of H_2 ; quantitative measurements gave an average value of 0.90 moles of H_2 evolved per mole of complex irradiated. The red solid obtained from such solid-state photolysis shows a broad IR band at 2145 cm^{-1} (Nujol), indicative of a terminal hydride. Exposure of this material to CO rapidly gave the formation of $[\text{Pt}_2\text{H}(\text{CO})(\text{dppm})_2]\text{PF}_6$; reaction with H_2 slowly regenerated $[\text{Pt}_2\text{H}_3(\text{dppm})_2]\text{PF}_6$. These various results indicate the solid-state reaction shown in eq 20.



The exact nature of the $[\text{Pt}_2\text{H}(\text{dppm})_2]\text{PF}_6$ photoproduct is presently unclear although the 2145 cm^{-1} IR band implies a terminal, rather than bridging, hydride.

Similar results obtain for photolysis of solutions of **5** although the reactions occur much more slowly. Photolysis of **5** in THF gives a color change from colorless to yellow and evolution of H_2 . A yellow precipitate can be isolated from the photolyzed solution and this material rapidly reacts with CO in CH_2Cl_2 solution to give the known $[\text{Pt}_2\text{Cl}(\text{CO})(\text{dppm})_2]\text{PF}_6$ complex (**43**). A reaction analogous to that in eq 19 is thus indicated but with $[\text{Pt}_2\text{Cl}(\text{THF})(\text{dppm})_2]\text{PF}_6$ as the photoproduct.

tions or from dinuclear complexes where the hydrides are terminal, but no reasonable mechanism exists for simultaneously placing both hydrides on the same metal.

General Experimental Procedures

Irradiation Procedures. Samples were irradiated with a 450 w Hanovia medium pressure Hg arc lamp, a 100 w Blak-Ray B100A lamp equipped with a 366 nm filter, or on an optical bench equipped with a water cooled lamp housing (Photochemical Research Associates, Inc., Model ALH215), a 100 w high-pressure Hg arc lamp (Osram HBO 100 w/2), a monochromator (Photochemical Research Associates, Inc., Model B102), and a thermostated cell holder. Quantum yields were determined using the latter apparatus, and light intensities were measured using ferrioxalate actinometry (47). Samples were irradiated in 1-cm quartz UV-VIS spectrophotometer cells sealed to Kontes 4 mm quick-release teflon valves for attachment to a vacuum line. Samples were degassed by several freeze-pump-thaw cycles and then placed under 1 atm of H₂. After irradiation at 366 nm, samples were transferred to 0.1-cm quartz UV-VIS spectrophotometer cells, and the decrease in intensity of the absorption band maximum was measured. All determinations were performed in triplicate. Samples for NMR experiments were prepared either in standard NMR tubes sealed under vacuum or in a degassable NMR tube equipped with a stopcock and a 17/25 female F ground glass joint to allow solutions to be degassed and then placed under an H₂ atmosphere. Gases above irradiated solutions were quantitated by standard Toepler pump techniques and were analyzed by mass spectrometry.

Spectral Measurements. The following instruments were employed in this study: UV-VIS - Cary 17 or Hewlett-Packard HP 8450A; IR - Perkin-Elmer 580; Mass Spectra - AEI-MS-902; NMR - Varian A-60A, JEOL PS-100 FT, Bruker WH 200. ¹H NMR spectra were referenced externally to TMS or internally to the solvent, generally benzene. ³¹P NMR spectra were referenced to external 85% H₃PO₄ and downfield chemical shifts are reported as positive.

Acknowledgments

The research described herein was supported by the National Science Foundation (CHE-7728387). GLG gratefully acknowledges the Camille and Henry Dreyfus Foundation for a Teacher-Scholar Award (1978-1983), the Alfred P. Sloan Foundation for a Research Fellowship (1978-1981), and the many coworkers who contributed to the research described herein.

Literature Cited

1. Geoffroy, G. L.; Wrighton, M. S. "Organometallic Photochemistry"; Academic Press: New York, 1979.
2. Geoffroy, G. L. Prog. Inorg. Chem. 1980, 27, 123.
3. Geoffroy, G. L.; Pierantozzi, R. J. Am. Chem. Soc. 1976, 98, 8054.
4. Geoffroy, G. L.; Bradley, M. G. Inorg. Chem. 1978, 17, 2410.
5. Giannotti, C.; Green, M. L. H. J. Chem. Soc., Chem. Commun. 1972, 1114.
6. Elmitt, K.; Green, M. L. H.; Forder, R. A.; Jefferson, I.; Prout, K. J. Chem. Soc., Chem. Commun. 1974, 747.
7. Farrugia, L.; Green, M. L. H. J. Chem. Soc., Chem. Commun. 1975, 416.
8. Green, M. L. H.; Berry, M.; Couldwell, C.; Prout, F. Nouv. J. Chim. 1977, 1, 187.
9. Pierantozzi, R.; Geoffroy, G. L. Inorg. Chem. 1980, 19, 1821.
10. Archer, L. J.; George, T. A. Inorg. Chem. 1979, 18, 2079.
11. Thomas, R. J. W.; Lawrence, G. S.; Diamantis, A. N. Inorg. Chim. Acta 1978, 30, L353.
12. Caruona, A.; Kisch, H. Int. Conf. Organomet. Chem. 9th 1979, Abstract D10.
13. Bradley, M. G.; Roberts, D. A.; Geoffroy, G. L. J. Am. Chem. Soc. 1981, 103, 379.
14. Freni, M.; Demichelis, R.; Giusto, D. J. Inorg. Nucl. Chem. 1967, 29, 1433.
15. Ginsberg, A. P.; Tully, M. E. J. Am. Chem. Soc. 1973, 95, 4745.
16. Tully, M. E.; Ginsberg, A. P. J. Am. Chem. Soc. 1973, 95, 2042.
17. Bennett, M. A.; Milner, D. L. J. Am. Chem. Soc. 1969, 91, 6983.
18. Chisholm, M. H.; Clark, H. C. Inorg. Chem. 1971, 10, 2557.
19. Tang-Wong, K. L.; Thomas, J. L.; Brintzinger, H. H. J. Am. Chem. Soc. 1974, 96, 3694.
20. Nakamoto, K. "Infrared and Raman Spectra of Inorganic and Coordination Compounds"; 3rd Ed., Wiley: New York, 1978; p 387.
21. Kolomnikov, I. S.; Gusev, A. I.; Aleksandrov, G. G.; Lobeveva, T. S.; Struchkov, Y. T.; Vil'pin, M. E. J. Organomet. Chem. 1973, 59, 349.
22. Smith, S. A.; Blake, D. M.; Kubota, M. Inorg. Chem. 1972, 11, 660.
23. Johnson, B. F. G.; Johnston, R. D.; Lewis, J.; Williams, I. G. J. Chem. Soc., Dalton Trans. 1971, 689.

24. Nakamoto, K. "Infrared and Raman Spectra of Inorganic and Coordination Compounds"; 3rd Ed., Wiley: New York, 1978; pp 232-233.
25. Levy, G. C.; Nelson, G. L. "Carbon-13 Nuclear Magnetic Resonance for Organic Chemists"; Wiley: New York, 1972.
26. Freni, J.; Giusto, D.; Romiti, P. J. Inorg. Nucl. Chem. 1971, 33, 4093.
27. Albano, V. D.; Bellon, P. L.; Ciani, G. J. Organomet. Chem. 1971, 31, 75.
28. Bau, R.; Carroll, W. E.; Teller, R. G.; Koetzle, T. F. J. Am. Chem. Soc. 1977, 99, 3872.
29. Green, M. A.; Huffman, J. C.; Caulton, K. G., submitted for publication.
30. Chatt, J.; Coffey, R. S. J. Chem. Soc. A 1969, 1963.
31. Giusto, D. Inorg. Chim. Acta Rev. 1972, 6, 91.
32. Freni, M.; Valenti, V. Gass. Chim. Ital. 1961, 91, 1357.
33. Norton, J. R. Accts. Chem. Res. 1979, 12, 139.
34. Balzani, V.; Moggi, L.; Manfrin, M. F.; Bolletta, F.; Gleria, M. Science 1975, 189, 852.
35. Lewis, N. S.; Mann, K. R.; Gordon, J. G.; Gray, H. B. J. Am. Chem. Soc. 1976, 98, 7461.
36. Mann, K. R.; Lewis, N. S.; Miskowski, V. M.; Erwin, D. K.; Hammond, G. S.; Gray, H. B. J. Am. Chem. Soc. 1977, 99, 5525.
37. Epstein, R. A.; Gaffney, F. R.; Geoffroy, G. L.; Gladfelter, W. L.; Henderson, R. S. J. Am. Chem. Soc. 1979, 101, 3847.
38. Foley, H. C.; Epstein, R. A.; Geoffroy, G. L., submitted for publication.
39. Johnson, B. F. G.; Lewis, J.; Twigg, M. V. J. Organomet. Chem. 1974, 67, C75.
40. Graff, J. L.; Wrighton, M. S. J. Am. Chem. Soc. 1980, 102, 2123.
41. Brown, M. P.; Puddephatt, R. J.; Rashidi, M.; Seddon, K. R. J. Chem. Soc., Dalton Trans. 1978, 516.
42. Brown, M. P.; Puddephatt, R. J.; Rashidi, M.; Seddon, K. R. J. Chem. Soc., Dalton Trans. 1977, 951.
43. Brown, M. P.; Puddephatt, R. J.; Rashidi, M.; Seddon, K. R. J. Chem. Soc., Dalton Trans. 1978, 1540.
44. Puddephatt, R. J. ACS Symp. Ser. 1981, 155, 187.
45. Brown, M. P.; Fisher, J. R.; Mills, A. J.; Puddephatt, R. J.; Thompson, M. Inorg. Chim. Acta 1980, 44, L271.
46. Brown, M. P.; Fisher, J. R.; Muir, L. M.; Muir, K. W.; Puddephatt, R. J.; Thompson, M. A.; Seddon, K. R. J. Chem. Soc., Chem. Commun. 1979, 931.
47. Hatchard, C. G.; Parker, C. A. Proc. Soc. London Ser. A 1956, 235, 518.

RECEIVED April 27, 1982.

General Discussion—Generation of Reactive Intermediates via Photolysis of Transition-Metal Polyhydride Complexes

Leader: Guillermo Ferraudi

DR. GUILLERMO FERRAUDI (Notre Dame University): I was puzzled by your photo-ejection of hydrogen. I wonder if you have evidence or if you can speculate as to whether that process is a single step or whether you expect to find precursors for your reactive intermediate.

DR. GEOFFROY: In the few cases in which we have conducted mechanistic studies, using labeling techniques the results have shown fairly conclusively that the hydrogen comes off in a concerted fashion. The two hydride ligands simply come off coupled together as they leave the metal to produce hydrogen. We see no evidence for radicals or the production of ionic species.

DR. FERRAUDI: So one can think of the reaction as forming a three-atom arrangement at some point, with the rhenium and the two hydrogens forming a localized type bond?

DR. GEOFFROY: Right.

DR. JACK NORTON (Colorado State University): One interesting result that has just appeared is Ray Sweany's report of photochemical hydrogen loss from iron tetracarbonyl dihydride [Sweany, R. L. *J. Am. Chem. Soc.* 1981, 103, 2410]. This system is very close to the case in which I claimed some years ago that this process did not occur. First of all, do you have any possible explanations for the differing behavior? Why is Sweany's result different from the result of Tony Rest? Second, if hydrogen eliminates in a concerted process such as you have just described, why don't other species such as cis-methyl groups do likewise?

DR. GEOFFROY: Let me answer the last question first. I don't fully understand cis-methyl groups. When complexes containing those have been irradiated, one generally doesn't observe the formation of ethane. Instead, where the chemistry is well-defined, it looks as if solvolysis simply occurs to yield radicals. There are, however, some cases of diaryl complexes which, when irradiated, will couple two phenyl ligands to give biphenyl as a product.

Your first question is one which we have discussed previously. You know that the report by Rest is simply cited in a footnote somewhere. It has never been presented in detail. I think that what really counts is the stability of the organo-metallic product which is left behind. Certainly iron tetracarbonyl is an organo-metallic fragment which is produced in many reactions of iron carbonyls. But, as you know, osmium tetracarbonyl is apparently of such high energy that its forma-

tion is not favored, and the compound decomposes via other means.

I should also add that we do not understand why photolysis induces loss of hydrogen from these dihydride complexes. When you look at the list of compounds I showed, there were many different metals and many different ligand sets, with many different electronic configurations. Hydrogen loss was observed in all cases. Dr. Trogler has pointed out that there is strong coupling between the excited states and the vibrations which lead to hydrogen loss. But we don't understand the excited states, so I really can't answer your question properly.

DR. WILLIAM WOODRUFF (University of Texas): I would like to make a comment not so much on your paper as on mechanistic photochemistry in general. I think most of us would agree that if we are going to draw mechanistic conclusions, we really need to know what the structures of the reactants and products are. One of the problems in photochemistry is that we generally do not know the structure of the reactant, which is the excited state. There aren't very many structure-specific probes in solution, in fact, none below about the millisecond time scale where esr and NMR cease to be applicable. In our laboratory, we have been able to obtain the resonant spectra of excited states. In two of the three kinds of systems that we have observed so far, the structures of the excited states are not predictable in a straightforward way, either from the ground state structures or from calculations.

For example, transfer of the excited states of $\text{Ru}(\text{bpy})_3^{3+}$ to $\text{Ru}^{\text{III}}(\text{bpy})_2(\text{bpy}\cdot^-)$ cannot be predicted in a clear and straightforward way.

DR. DAVID McMILLIN (Purdue University): As you probably know, Wrighton has shown that in certain rhenium hydrides there is a large deuterium effect on the excited state lifetime [Graff, J. L.; Wrighton, M. S. *J. Am. Chem. Soc.* 1981, **103**, 2225]. So perhaps the hydrogen is specifically reactive because a lot of the energy gets channeled into these high-frequency modes.

DR. GEOFFROY: The compounds in which Wrighton saw the deuterium isotope effect were metal cluster compounds which do not lose hydrogen upon irradiation. Those are a special set of compounds. Some collaborative work with which we are currently involved includes a series of tungsten molybdenum tetrahydride complexes and tetra-deuterides which photo-eliminate hydrogen and also luminesce. However, we do not see any effect on the luminescence or the quantum yield of loss of hydrogen as we replace hydrogen with deuterium.

DR. McMILLIN: When you were talking about the dppe complex, you invoked the chelate effect. It seems to me that opening and closing the chelate ring would be a good channel for nonradiative decay. I don't see why that would help promote the production of hydrogen. I am wondering if there might be some other structural factors involving the transition state which could account for the observed behavior.

DR. GEOFFROY: We obviously don't know why the photochemistry changes. We know that it is reasonable that phosphine dissociation does not occur when we have a chelating diphosphine ligand. But we don't understand why we see hydrogen loss in this system when we don't see it in the other cases.

DR. MICHAEL BERGKAMP (Brookhaven National Lab): Do you have any direct evidence which indicates that when you irradiate these compounds the chelate ring actually opens up and closes?

DR. GEOFFROY: No. That is pure speculation.

DR. BERGKAMP: When you irradiate these compounds at 366 nm, do you know exactly what type of state you are irradiating?

DR. GEOFFROY: The 366 nm irradiations are clearly into the lowest absorption band. It is often a tail in these complexes. Unfortunately, the electronic structures of these compounds, as with most all organo-metallic systems, are not well-understood or well-defined. We could interpret the absorption spectrum in several different ways, and we could rationalize why we see hydrogen, depending on how we interpret the absorption spectrum. No matter what we do, we can rationalize hydrogen loss. But it is not very satisfying, because we do not know what the nature of the excited states is. That is an area which needs considerable study, to define the electronic structures of these kinds of compounds.

DR. ANTHONY POË (University of Toronto): As Dr. Geoffroy mentioned, there is a fair bit of work being done on dinuclear metal-metal bonded carbonyls but rather less on metal clusters [Geoffroy, G. L.; Wrighton, M. S., "Organometallic Photochemistry," Academic Press: New York, 1979]. We have been interested for some time in the thermal fragmentation of metal clusters, and have recently looked at some photochemical reactions as well. I would like to present some results here today which are very preliminary.

Previous results indicated that quantum yields for reactions of metal clusters are low [Graft, J. L.; Sanner, R. D.; Wrighton, M. S. *J. Am. Chem. Soc.* 1979, 101, 273; Tyler, D. R.; Altobelli, M.; Gray, H. B. *ibid.* 1980, 102, 3022]. That seemed to us a surprising observation. We also noticed when we looked

at the literature that almost none of the photochemical studies reported had investigated competing kinetic pathways and we decided to study the dependence of quantum yields on concentrations. It seems a fairly obvious thing to do, but it hadn't been done previously.

When we took ruthenium dodecacarbonyl and studied its photochemical reactions with triphenyl phosphine, we observed an increase in the quantum yield with increasing triphenyl phosphine concentration. The plot is curved and appears to be approaching a limiting value of ϕ . This implies that there is a reactive intermediate which can undergo competitive reaction, either in the forward direction (where the rate term is $k_f[L]$) or in the reverse direction (where the intermediate reverts back to the reactant with a rate constant k_r). Thus,

$$\phi = \frac{\phi(\text{lim})k_f[L]/k_r}{1 + k_f[L]/k_r}$$

The two kinetic parameters ($\phi(\text{lim})$ and k_f/k_r) can be resolved quite easily by means of a simple inverse plot. The limiting quantum yield for $L = \text{PPh}_3$ is quite substantial, having a value of about 0.15 ± 0.03 .

The limiting quantum yields for $L = \text{PPh}_3$ or P(OPh)_3 are not dependent on whether the solvent is cyclohexane or benzene. If that is generally true, then we find that the competition parameter is very dependent on solvent. That may not be surprising. It also appears that the limiting quantum yield may actually be dependent on the nature of the ligand. That is surprising. We must study more ligands to determine whether that conclusion is correct. There is clearly a wavelength dependence as well. Going from 436 nm to 313 nm, the quantum yield for $L = \text{CO}$ increases significantly.

For the reaction of $\text{Ru}_3(\text{CO})_9(\text{P-n-Bu}_3)_3$ with P-n-Bu_3 under argon, we observe a decrease in quantum yield with increasing $[\text{P-n-Bu}_3]$ with ϕ reaching a lower limiting value of approx. 0.01. Under carbon monoxide, we obtain a very low quantum yield indeed. Thus, in this system, the photochemical fragmentation is preceded either by dissociation of phosphine or by dissociation of CO, and not by some other process.

The whole question of what the intermediates are, how they react, how solvent-sensitive they are, and what determines the limiting quantum yields is unclear at this time and there is much systematic work yet to be done.

DR. WILLIAM TROGLER (Northwestern University): I wish to make a brief presentation of some results which relate to Dr. Geoffroy's talk. We have been employing a different approach to generate coordinatively unsaturated centers, utilizing a reduc-

tive elimination reaction. The system involves the oxalate ligand. It is well-known in the photochemistry of Werner complexes containing oxalate that one can photoreductively eliminate oxalate. The ferrioxalate actinometer is a classic example. The photochemical reaction involves a one-electron reduction of the metal with oxalate, generating oxalate anion radical as an intermediate, which can then transfer a second electron to another metal.

The trick is to use a metal that can undergo a two-electron reduction. This was actually first observed by Blake and Nyman [Blake, D. M.; Nyman, C. J. *J. Chem. Soc., Chem. Commun.* 1969, 483] about a decade ago, when they did some work on the $\text{Pt}(\text{P}\Phi_3)_2\text{C}_2\text{O}_4$ complex. It appeared that their results could be rationalized by formation of a $\text{Pt}(\text{P}\Phi_3)_2$ intermediate, which formally is a species that possesses two vacant coordination sites.

We went back and looked at that system, because we thought it had quite a bit of promise. It turns out that, with triphenyl phosphine, platinum(0) will attack the phosphorous phenyl bonds to produce red polymers which are phosphido-bridged platinum species. But we were more interested in the small alkyl phosphines, because we expect those to make the metal center even more reactive (being sterically unhindered and more basic).

These latter systems, in fact, work very well. For example, when $\text{Pt}(\text{PET}_3)_2(\text{C}_2\text{O}_4)$ is irradiated at 313 nm, we quantitatively extrude 2 moles of CO_2 and generate a reactive $\text{Pt}(\text{PET}_3)_2$ fragment. Thus far, we have studied about 15 different reactions in which this type of intermediate is generated. One of the simplest species which illustrates this point is the $\text{Pt}(\text{H}_2\text{C}=\text{CH}_2)(\text{PET}_3)_2$ complex where the intermediate has been quantitatively trapped as the zero valent ethylene complex.

In summary, it appears that we are able to initiate much interesting chemistry by using photoreductive elimination of coordinated oxalate to generate a metal center having two vacant coordination sites.

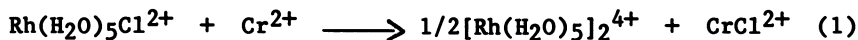
One-Electron Reduction Product of Tris(2,2'-bipyridine)rhodium(III)

CAROL CREUTZ, ANDREW D. KELLER, HAROLD A. SCHWARZ,
NORMAN SUTIN, and ARDEN P. ZIPP

Brookhaven National Laboratory, Chemistry Department, Upton, New York 11973

The physical and chemical properties of $\text{Rh}(\text{bpy})_3^{2+}$ generated via flash-photolytic and pulse-radiolytic methods in aqueous solutions are reported and discussed. The reduction potential (~ -0.86 V vs SHE) and electron-exchange rate ($\gg 10^9 \text{ M}^{-1} \text{ s}^{-1}$) for the $\text{Rh}(\text{bpy})_3^{3+}/\text{Rh}(\text{bpy})_3^{2+}$ couple suggest the formulation of $\text{Rh}(\text{bpy})_3^{2+}$ as the ligand-localized radical $[\text{Rh}^{\text{III}}(\text{bpy})_2(\text{bpy}^-)]^{2+}$. By contrast, the ultraviolet-visible absorption spectrum, disproportionation chemistry, and the substitution lability of the metal center require that $\text{Rh}(\text{bpy})_3^{2+}$ have substantial metal-centered radical ($4d^1$ Rh(II)) character.

The most common oxidation state of rhodium in aqueous solution is low-spin $4d^6$ rhodium(III). The lower oxidation state rhodium(I) has been extensively studied in organic solvents. By contrast, in aqueous solutions few studies of the lower oxidation states of rhodium have been made: Gray with Mann, Sigal and others has mapped the chemistry of polynuclear rhodium(I) and rhodium(II) complexes containing isonitrile ligands (1,2). Dimeric rhodium(II) complexes featuring rhodium-rhodium single bonds are known for a wide variety of bridging carboxylate derivatives. Mononuclear rhodium(II) species have, however, for the most part resisted characterization. This is a consequence of the fact that one-electron reduction of rhodium(III) results ultimately in either dismutation of rhodium(II) to rhodium(III) plus rhodium(I) or to dimerization, as illustrated by the work of Maspero and Taube (eq 1) (3).



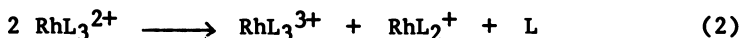
One of the few (perhaps the sole) successful efforts to characterize mononuclear rhodium(II) complexes in aqueous media

0097-6156/82/0198-0385\$06.00/0
© 1982 American Chemical Society

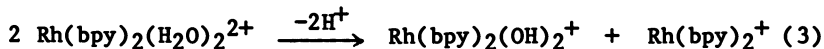
is that of Lilie, Simic, and Endicott who studied the products of one-electron reduction of rhodium(III) ammine complexes (4). Despite (and because of) the dearth of information concerning rhodium(II), the physical properties and reactivity of this (presumably) low-spin $4d^7$ metal center are of some interest. This paper describes the results of our experiments with the one-electron reduction products of tris(2,2'-bipyridine)rhodium(III) and related complexes. The work was originally motivated by the fact that the 2,2'-bipyridine complexes of rhodium(II) and (I) were implicated as intermediates in a complex system effecting the photoreduction of water (5,6,7). It has since evolved as a study of some fundamental interest in its own right.

Production and Decomposition of $\text{Rh}(\text{bpy})_3^{2+}$

Polypyridine rhodium(III) complexes (RhL_3^{3+}) may be reduced by one-electron reductants. The reductants which have been successfully employed include $^*\text{Ru}(\text{bpy})_3^{2+}$, the luminescent charge-transfer excited state of $\text{Ru}(\text{bpy})_3^{2+}$ (8,9) ($^*E_{3,2} = -0.84$ V, $k = 0.6 \times 10^9 \text{ M}^{-1} \text{ s}^{-1}$ at 25°C and $\mu = 0.5$ M), and e_{aq} (6,10) ($E^\circ \sim -2.8$ V, $k = 8 \times 10^{10} \text{ M}^{-1} \text{ s}^{-1}$). The product with $\text{L} = \text{bpy}$ has absorption maxima at ~ 350 nm ($\epsilon = 0.4 \times 10^4 \text{ M}^{-1} \text{ cm}^{-1}$) and at ~ 490 nm ($\epsilon \sim 0.1 \times 10^4 \text{ M}^{-1} \text{ cm}^{-1}$) (10,11). Before describing the properties of the one-electron reduction product of rhodium(III), we shall relate its ultimate fate because this restricts the experiments which may be carried out. The reduction product $\text{Rh}(\text{bpy})_3^{2+}$ disproportionates (6) to yield Rh(III) and Rh(I) (eq 2, $\text{L} = \text{bpy}$)

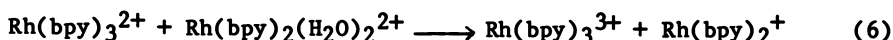
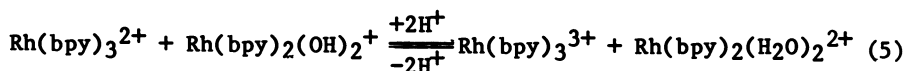
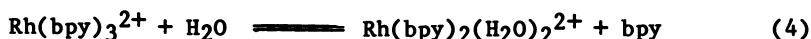


Analogous products are found (11) for the 4,4'-dimethyl-2,2'-bipyridine derivative (eq 2, $\text{L} = 4,4'-(\text{CH}_3)_2\text{bpy}$) and for $\text{Rh}(\text{bpy})_2(\text{H}_2\text{O})_2^{2+}$, the reduction product of $\text{Rh}(\text{bpy})_2(\text{OH})_2^+$ (eq 3).



With $\text{L} = \text{bpy}$, the Rh(I) product has been extensively characterized: its nature is a function of pH and total Rh(I) concentration (6,7). Four species, $\text{Rh}(\text{bpy})_2^+$, $[\text{Rh}(\text{bpy})_2]_2^{2+}$, $\text{Rh}(\text{bpy})_2(\text{H})(\text{H}_2\text{O})^{2+}$, and $[\text{Rh}(\text{bpy})_2]_2\text{H}^{3+}$, have been detected (12). However, at $\text{pH} > 8$ and very low $\text{Rh}(\text{bpy})_3^{2+}$ or $\text{Rh}(\text{bpy})_2(\text{H}_2\text{O})_2^{2+}$, the disproportionation product is purple $\text{Rh}(\text{bpy})_2^+$ and the disproportionation kinetics are readily followed through the growth of the absorption of this species ($\epsilon \sim 10^4 \text{ M}^{-1} \text{ cm}^{-1}$ at 505 nm). For $\text{Rh}(\text{bpy})_3^{2+}$ a surprising result is obtained (6,7,10,11). Disproportionation of $\text{Rh}(\text{bpy})_3^{2+}$ does not proceed via the direct second-order process eq 2 ($k_2 < 10^4 \text{ M}^{-1} \text{ s}^{-1}$).

Instead the formation of $\text{Rh}(\text{bpy})_2^+$ follows an exponential time profile with $k_{\text{obs}} = 1$ to 2 s^{-1} , regardless of the initial concentration of $\text{Rh}(\text{bpy})_3^{2+}$. Much more rapid $\text{Rh}(\text{bpy})_2^+$ production can, however, be obtained from mixtures of $\text{Rh}(\text{bpy})_3^{2+}$ and $\text{Rh}(\text{bpy})_2(\text{H}_2\text{O})_2^{2+}$; for such mixtures (which also contain $\text{Rh}(\text{bpy})_3^{3+}$ and $\text{Rh}(\text{bpy})_2(\text{OH})_2^+$ in large excess over the reduced species) the $\text{Rh}(\text{bpy})_2^+$ formation is no longer exponential. Rather plots of $(\Delta A_{505})^{-1}$ (the reciprocal of the absorbance change at 505 nm) versus time are linear. These observations have led to the mechanism given in eq 4-6 (6,7,11).



At 25°C , $k_4 = 1 \text{ s}^{-1}$, $k_5 > 10^6 \text{ M}^{-1} \text{ s}^{-1}$, $K_5 \sim 2$, and $k_6 = 0.3 \times 10^9 \text{ M}^{-1} \text{ s}^{-1}$ at pH 8.1 and $\mu = 0.5 \text{ M}$ and $k_4 = 0.6 \text{ s}^{-1}$, $k_{-4} = 0.2 \times 10^9 \text{ M}^{-1} \text{ s}^{-1}$, $k_6 = 0.3 \times 10^9 \text{ M}^{-1} \text{ s}^{-1}$ at pH 9 and $\mu = 0.01 \text{ M}$. As a consequence of this reaction pathway, the lifetime of $\text{Rh}(\text{bpy})_3^{2+}$ in the absence of $\text{Rh}(\text{bpy})_2(\text{OH})_2^+$ is about one second at room temperature. While this is a long lifetime by photochemical standards, it is sufficiently short to restrict the techniques applicable to the study of $\text{Rh}(\text{bpy})_3^{2+}$ to those with rather great time resolution. Thus we have extensively employed flash photolysis and pulse radiolysis methods, always in the presence of excess rhodium(III).

The above value of $k_4 = 1 \text{ s}^{-1}$ for bpy loss from $\text{Rh}(\text{bpy})_3^{2+}$ may be compared with $k_4 = 3 \text{ s}^{-1}$ for bpy loss from the formally related $\text{Co}(\text{bpy})_3^{2+}$ (13,14). Recently obtained results indicate that the rate constant for addition of bpy to $\text{Rh}(\text{bpy})_2(\text{H}_2\text{O})_2^{2+}$ ($k_{-4} = 0.2 \times 10^9 \text{ M}^{-1} \text{ s}^{-1}$) is greater than that for the comparable cobalt(II) reaction (13,14). The more-or-less comparable labilities of $\text{Rh}(\text{bpy})_3^{2+}$ and $\text{Co}(\text{bpy})_3^{2+}$ are not unexpected in light of data for rates of ammonia loss from the two metal centers which are also available: ammonia loss from rhodium(II) is quite rapid (10^6 s^{-1} to 10^2 s^{-1} with loss from $\text{Rh}(\text{NH}_3)_5 \text{H}_2\text{O}^{2+}$ being much faster than from $\text{Rh}(\text{NH}_3)_4^{2+}$, etc.) (4) but somewhat slower than the comparable process for cobalt(II) (15). Of course, here the relative affinities of the two metals for NH_3 are not known and so cannot be taken into account. A further reason these comparisons lack great validity is that, although these Co(II) complexes contain $3d^7$ metal centers, $\text{Co}(\text{bpy})_3^{2+}$ and $\text{Co}(\text{NH}_3)_n^{2+}$ are high-spin complexes i.e. the ground states are $(t_{2g})^3(e_g)^2$ whereas $4d^7$ species are expected to be low spin, $(t_{2g})^6(e_g)^1$. Furthermore, as will be seen shortly it is not clear that even "low spin $4d^7$ " is an adequate description of the

ground electronic state of $\text{Rh}(\text{bpy})_3^{2+}$. It is, however, apparent that these "Rh(II)" species are quite substitution labile.

Redox Properties of $\text{Rh}(\text{bpy})_3^{2+}$

Kew, DeArmond and Hanck have studied the $\text{Rh}(\text{bpy})_3^{3+}/\text{Rh}(\text{bpy})_3^{2+}$ couple by means of rapid sweep ($> 10 \text{ V s}^{-1}$) cyclic voltammetry on platinum electrodes in acetonitrile and found $E_{1/2}$ for this couple to be -0.83 V vs aqueous SCE in this solvent (16). In water (0.05 M sodium hydroxide, pyrolytic graphite electrode) $\text{Rh}(\text{bpy})_3^{3+}$ is reduced at a potential in the same range, but the process is irreversible (7) as is shown in Figure 1. No oxidation peak is observed - even at sweep rates as high as 100 V s^{-1} (7,17). We had originally thought the reduction to be a one-electron process which was rendered irreversible by a rapid ($k_f > 10^4 \text{ s}^{-1}$) succeeding chemical reaction (7). We recently reexamined this question. Having looked unsuccessfully in pulse-radiolysis experiments for a $\text{Rh}(\text{bpy})_3^{2+}$ reaction with a rate constant of 10^4 s^{-1} (11) or greater, we reinvestigated the magnitude of the current for the first reduction. Using $\text{Cr}(\text{bpy})_3^{3+}$ as a model for an $n = 1$ process (previously $\text{Ru}(\text{bpy})_3^{2+}$ was used instead) the $\text{Rh}(\text{bpy})_3^{3+}$ reduction in water was determined to correspond to $n = 1.9 \pm 0.1$ electrons. The chemical reaction introducing the irreversibility is now ascribed to a rapid reaction of $\text{Rh}(\text{bpy})_3^+$ (presumably bpy loss for which $k = 5 \times 10^4 \text{ s}^{-1}$ (11)); analogous behavior -- but at slower sweep rates -- has been reported in acetonitrile (16). Since the rapid Rh(I) reaction renders the $\text{Rh}(\text{bpy})_3^{3+}/\text{Rh}(\text{bpy})_3^{2+}$ couple effectively irreversible, the electrochemical results obtained in water cannot be used to extract information concerning the reduction potential for the one-electron process.

To estimate the potential for the $\text{Rh}(\text{bpy})_3^{3+}/\text{Rh}(\text{bpy})_3^{2+}$ and related couples in aqueous solution, an entirely different experimental approach has been used. As is well known, the rate constant for an electron-transfer reaction is a function of the driving force for the reaction (18,19,20). Under suitable conditions the magnitude of the rate constant can be used to estimate the driving force (and vice versa). A more reliable estimate can be obtained if a set of rate constants for a homologous series of reductants (or oxidants) can be obtained over a range of driving force. This is the heart of the Rehm-Weller method (21) for estimating the reduction potentials of excited molecules. As our homologous series of reductants, we have used the $\text{RuL}_3^{3+}/\text{RuL}_3^{2+}$ couples (22,23), where $^*\text{RuL}_3^{2+}$ is the luminescent excited state of RuL_3^{2+} . The electron exchange rate constants for these couples are very large ($k_{11} \gg 10^9 \text{ M}^{-1} \text{ s}^{-1}$) and the potentials span the range -0.77 to -1.10 V . Thus the reduction of $\text{Rh}(\text{bpy})_3^{3+}$ and related complexes by $^*\text{RuL}_3^{2+}$ is expected to be rapid if the $E_{1/2}$ for the $\text{Rh}(\text{bpy})_3^{3+}/\text{Rh}(\text{bpy})_3^{2+}$ couple lies in (or positive of) this range. We have determined the rate constants (k_q) for reduction

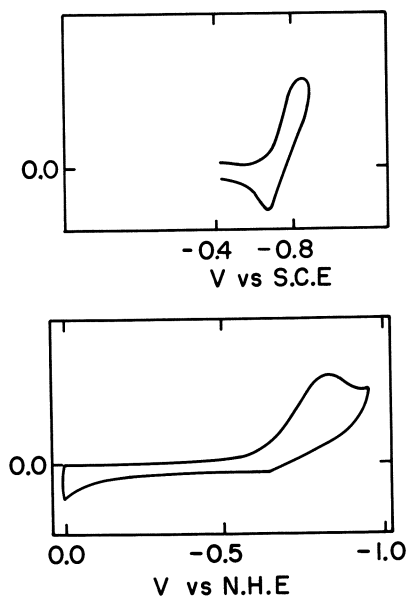
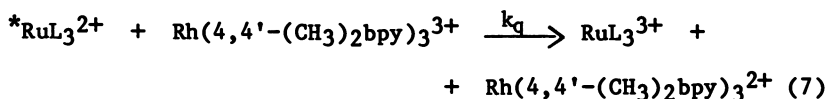
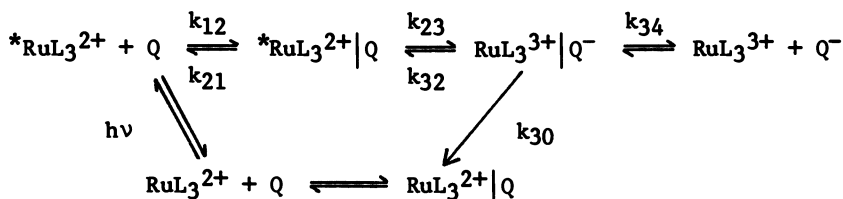


Figure 1. Cyclic voltammograms of $Rh(bpy)_3^{3+}$. Top: on Pt in acetonitrile, $\nu = 46$ V/s [adapted from Ref. 16]; and bottom, on pyrolytic graphite in aqueous 0.05 M sodium hydroxide $\nu = 50$ V/s (17).

of $\text{Rh}(\text{bpy})_3^{3+}$ and other polypyridinerhodium(III) complexes by several members of the $^*\text{RuL}_3^{2+}$ series. The most definitive results were obtained for the 4,4'-dimethyl-2,2'-bipyridine complex $\text{Rh}(4,4'-(\text{CH}_3)_2\text{bpy})_3^{3+}$ (24) for which the reaction studied is shown in eq 7.



The results obtained are shown in Figure 2, a plot of $\log k_{qc}$ (the logarithm of the diffusion corrected second-order rate constant for eq 7) versus $^*\text{E}_{3,2}$, the reduction potential of the $\text{RuL}_3^{3+}/^*\text{RuL}_3^{2+}$ couple. An unusual and significant feature of these data can be appreciated through comparison of these with results obtained (22) for oxidation of $^*\text{RuL}_3^{2+}$ by $\text{Eu}_{\text{aq}}^{3+}$. These are also shown in Figure 2. The slope of the line drawn through the $\text{Eu}_{\text{aq}}^{3+}$ points is 8.5 V^{-1} . This is the slope expected (albeit rarely observed) from the simple Marcus cross-relation; i.e., a plot of $\log k_q$ vs $\log K_q$ (where K_q is the equilibrium constant for electron transfer) is 0.50. For $\text{Rh}(4,4'-(\text{CH}_3)_2\text{bpy})_3^{3+}$, the local slope for $^*\text{E}_{3,2}$ between -0.77 and $\sim -0.9 \text{ V}$ is much greater than that found for $\text{Eu}_{\text{aq}}^{3+}$. Only at more negative $^*\text{E}_{3,2}$ values is curvature to the "usual" slope of $< 8.5 \text{ V}^{-1}$ seen. The extremely great sensitivity of k_{qc} to $^*\text{E}_{3,2}$ seen at the less negative $^*\text{E}_{3,2}$ values is due to endergonic electron transfer; the fact that net electron transfer from $^*\text{RuL}_3^{2+}$ to the rhodium(III) complex occurs in this region is due to the rapidity of the "back" electron transfer between RuL_3^{3+} and $\text{Rh}(4,4'-(\text{CH}_3)_2\text{bpy})_3^{2+}$ to form ground state RuL_3^{2+} and $\text{Rh}(4,4'-(\text{CH}_3)_2\text{bpy})_3^{3+}$. The detailed sequence required (21) to describe the observed behavior is shown below where $Q = \text{Rh}(4,4'-(\text{CH}_3)_2\text{bpy})_3^{3+}$ and the vertical lines indicate species within the solvent cage.



The separated reactants $^*\text{RuL}_3^{2+}$ and Q diffuse together (k_{12}) to form an ion pair ($^*\text{RuL}_3^{2+}|Q$) in which electron transfer from $^*\text{RuL}_3^{2+}$ to Q takes place with a first-order rate constant k_{23} . The products RuL_3^{3+} and Q^- are thus produced in close proximity (solvent cage, ion pair). They may then diffuse apart (k_{34}) or go back to reactants (k_{32}) or undergo "back" electron transfer

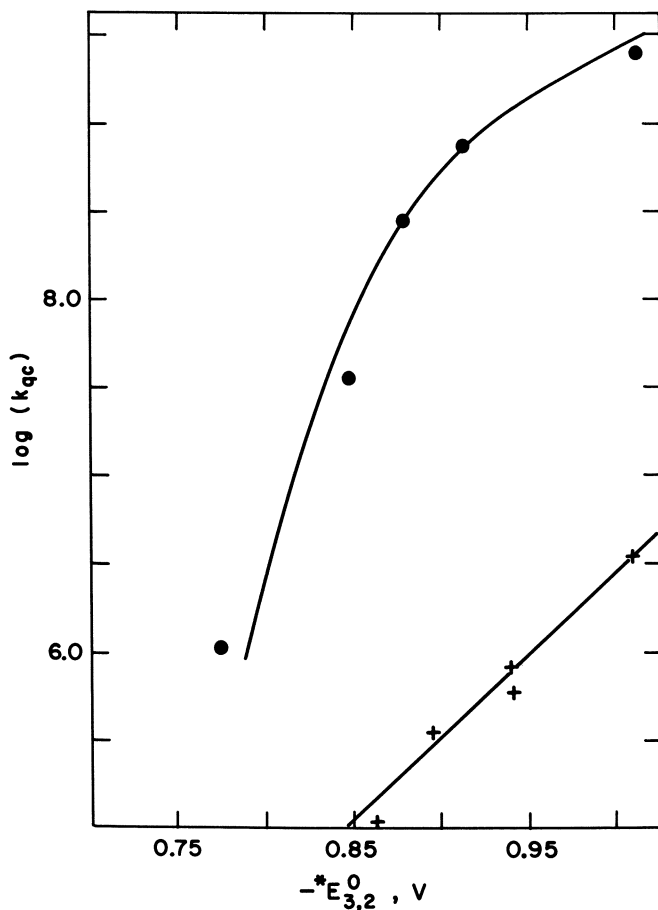


Figure 2. The logarithm of k_{qc} (the diffusion-corrected quenching rate constant) vs. $-E_{3,2}^0$ (the reduction potential for the $RuL_3^{3+}/^*RuL_3^{2+}$ couple) for quenching (left side, ●) by $Rh(4,4'-(CH_3)_2bpy)_3^{3+}$ (24) and (right side, +) by Eu_{aq}^{3+} (22). (Copyright 1982, American Chemical Society.)

(k_{30}) to form ground-state RuL_3^{2+} and Q. The latter reaction is thermodynamically very favorable and it is its rapidity which is responsible for the observation of net quenching $^*\text{RuL}_3^{2+}$ by Q ($k_{30} \gg k_{32}$).

The curve shown in Figure 2 for the $\text{Rh}(4,4'-(\text{CH}_3)_2\text{bpy})_3^{3+}$ data was calculated (24) on the basis of a steady-state treatment for $\text{RuL}_3^{3+}|\text{Q}^-$ and $^*\text{RuL}_3^{2+}|\text{Q}$ above, i.e. eq 8

$$k_{\text{qc}} = \frac{k_{12} k_{23} (k_{30} + k_{34})}{k_{21} (k_{32} + k_{30} + k_{34})} \quad (8)$$

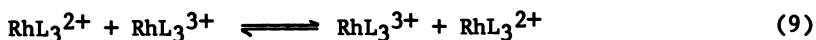
assuming the usual free energy dependence for k_{23} and appropriate values for k_{30} , k_{12} , k_{21} , and k_{34} (24,25). From this treatment, the estimate $E^{\circ} = -0.97 \text{ V}$ was obtained for the $\text{Rh}(4,4'-(\text{CH}_3)_2\text{bpy})_3^{3+}/\text{Rh}(4,4'-(\text{CH}_3)_2\text{bpy})_3^{2+}$ couple (24). Similarly, E° estimates were obtained from quenching data for other RhL_3^{3+} couples (24). In Table I these estimates ($E^{\circ}(\text{Q}/\text{Q}^-)$) are compared with $E_{1/2}$ values obtained via rapid sweep cyclic voltammetry in acetonitrile ($E_{1/2}(\text{CH}_3\text{CN})$).

Table I. Reduction Potentials of RhL_3^{3+} Complexes

<u>L</u>	<u>$E_{1/2}(\text{CH}_3\text{CN}), \text{V}$</u>	<u>$E^{\circ}(\text{Q}/\text{Q}^-, \text{H}_2\text{O}), \text{V}$</u>
4,4'-(CH ₃) ₂ bpy	-0.94 (24)	-0.97 (24)
bpy	-0.83 (16)	-0.86 (24)
phen	-0.75 (26)	-0.84 (24)

Notably, for L = bpy and L = 4,4'-(CH₃)₂bpy $E^{\circ}(\text{Q}/\text{Q}^-)$ vs SHE in water is 0.03 V more negative than $E_{1/2}$ measured vs aqueous SCE in acetonitrile. The same observation has been made for the reduction potentials of ruthenium couples: $\text{RuL}_3^{3+}/\text{RuL}_3^{2+}$ $E_{1/2}$ values measured in water relative to SHE are 0.03 V more negative than those measured in acetonitrile relative to aqueous SCE (22). From the relatively good agreement between $E^{\circ}(\text{Q}/\text{Q}^-)$ and $E_{1/2}(\text{CH}_3\text{CN})$ in Table I we conclude that the reversible acetonitrile electrochemistry can be used to estimate the reduction potentials of the RhL_3^{3+} complexes in water. The complexes examined so far have potentials in the -0.7 to -1 V range; thus RhL_3^{2+} is a rather strong reducing agent.

The reactivity of RhL_3^{2+} or RhL_3^{3+} toward outer-sphere oxidation or reduction is a function of the intrinsic reorganization barrier for the couple as well as the driving force for the electron transfer (18,19,27). The intrinsic electron-transfer barrier, determined by the need for reorganization of metal-ligand and intra-ligand bond lengths and of the solvent prior to electron transfer, is reflected in the magnitude of the electron-exchange rate constant i.e. eq 9.



The magnitude of this rate constant k_9 for $L = 4,4'-(\text{CH}_3)_2\text{bpy}$ comes from the treatment of the data in Figure 2; the data require $k_9 \geq 10^9 \text{ M}^{-1} \text{ s}^{-1}$. Similar exchange rate constants are also implicated for the other RhL_3^{3+} complexes we have studied — in both water and acetonitrile. The requirement that k_9 be large for the $4,4'-(\text{CH}_3)_2\text{bpy}$ complex can be appreciated qualitatively by inspection of Figure 2. Very large quenching rate constants (10^8 to $10^9 \text{ M}^{-1} \text{ s}^{-1}$) are observed even in the region where the slope of the plot indicates endergonic electron transfer — thus the intrinsic barrier to the electron transfer must be small indeed (as was mentioned earlier, the barriers for the $^*\text{RuL}_3^{2+}/\text{RuL}_3^{3+}$ couples are very small).

In magnitude, the self-exchange rates for the $\text{RhL}_3^{2+}/\text{RhL}_3^{3+}$ couples are of the same order as those for the $^*\text{RuL}_3^{2+}/\text{RuL}_3^{3+}$ couples. By contrast, the exchange rate constant for the formal first-transition series analogue, the $(t_{2g})^6(e_g^1)/(t_{2g})^6 \text{Co(terpy)}_2^{2+}/\text{Co(terpy)}_2^{3+}$ couple, is $\sim 10^4 \text{ M}^{-1} \text{ s}^{-1}$ (28). The $\text{Co(terpy)}_2^{2+}/\text{Co(terpy)}_2^{3+}$ value is much smaller than that for either the ground- or excited-state ruthenium polypyridine couples because substantial rearrangement of the metal inner-coordination spheres is required for electron transfer. Large distortions are generally expected for couples in which changes in the electron population of the e_g orbitals occur. In short, substantial inner-shell reorganization would also be expected for a $4d^7/4d^6$ rhodium(II)/rhodium(III) couple. By contrast the exchange rate constants implicated for the $\text{RhL}_3^{2+}/\text{RhL}_3^{3+}$ couples are of the order observed and calculated for systems in which metal-ligand and ligand-ligand distortions are negligible and only solvent reorganization is required (29). These considerations lead us to focus on the elementary question —

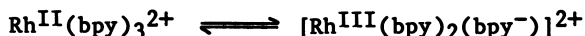
What is the nature of Rh(bpy)_3^{2+}

Is it a metal-centered or a ligand-centered radical? It is well known that polypyridine metal complexes may be reduced at either (or both) the metal center or the ligand center. For example, the sequential ligand reduction of M(bpy)_3^{2+} ($M = \text{Fe(II)}, \text{Ru(II)}, \text{Os(II)}$) to $[\text{M}^{\text{II}}(\text{bpy})_2(\text{bpy}^-)]^+$, $[\text{M}^{\text{II}}(\text{bpy})(\text{bpy}^-)_2]$, and $[\text{M}^{\text{II}}(\text{bpy}^-)_3]^-$ is observed (30,31) via cyclic voltammetry in nonaqueous solvents as three ~ 170 mV-separated peaks at -1.2 to -1.3 V vs SCE. The reducibility of the ligand depends on the metal charge and $E_{1/2}$ for the metal-bound bpy/bpy^- couple shifts to less negative potentials as the metal-center charge increases. Thus the first reduction of Ir(bpy)_3^{3+} , which occurs at -0.83 V vs SCE in acetonitrile, though ~ 400 mV positive of the $\text{M}^{\text{II}}(\text{bpy})_3^{2+}/[\text{M}^{\text{II}}(\text{bpy})_2(\text{bpy}^-)]^+$ potential, is ascribed to ligand, rather than metal, reduction (41). The

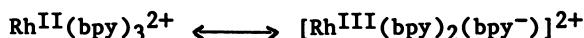
$\text{Ru}^{\text{III}}(\text{bpy})_3^{3+}/[\text{Ru}^{\text{III}}(\text{bpy})_2(\text{bpy}^-)]^{2+}$ potential, -0.81 V vs aqueous SCE in acetonitrile (25,33) is also consistent with this model. (The species $[\text{Ru}^{\text{III}}(\text{bpy})_2(\text{bpy}^-)]^{2+}$ is $^*\text{Ru}(\text{bpy})_3^{2+}$ which has recently been assigned as a localized bound bpy^- radical on the basis of its resonance Raman spectrum (34).) The fact that nearly identical $E_{1/2}$ values are found for the reduction of $\text{Ir}(\text{bpy})_3^{3+}$ and $\text{Rh}(\text{bpy})_3^{3+}$ suggests that both involve the same reduction site — the bound bpy . (By contrast, $E_{1/2}$ for metal-centered reduction of $\text{Co}(\text{bpy})_3^{3+}$ is $+0.30$ V (28).) Furthermore, as discussed above, the electron exchange rate for $\text{RhL}_3^{2+}/\text{RhL}_3^{3+}$, $\geq 10^9 \text{ M}^{-1} \text{ s}^{-1}$, being comparable to that for the $^*\text{RuL}_3^{2+}/\text{RuL}_3^{3+}$ couples, is of the order expected for $[\text{M}^{\text{III}}(\text{L})_2(\text{L}^-)]^{2+}/[\text{M}^{\text{III}}(\text{L})_3]^{3+}$ couples in which electron transfer between ligand— rather than metal—centers occurs.

The redox properties elicited for $\text{Rh}(\text{bpy})_3^{2+}$ and its congeners are thus entirely consistent with the description of these species as bound-ligand radicals. On the other hand, the disproportionation reactions eq 2-6 are not known to be characteristic of ligand-centered radicals, but are consistent with behavior expected for rhodium(II). Furthermore the substitution lability deduced for $\text{Rh}(\text{bpy})_3^{2+}$ and $\text{Rh}(\text{bpy})_2^{2+}$, while consistent with that expected for $\text{Rh}(\text{II})$, is orders of magnitude too great for $\text{Rh}(\text{III})$. Finally the spectrum observed for the intermediate $\text{Rh}(\text{bpy})_3^{2+}$ is not that expected for $[\text{Rh}^{\text{III}}(\text{bpy})_2(\text{bpy}^-)]^{2+}$. The spectrum measured has an absorption maximum at ~ 350 nm with $\epsilon = 4 \times 10^3 \text{ M}^{-1} \text{ cm}^{-1}$ and a broad maximum at ~ 500 nm with $\epsilon = 1 \times 10^3 \text{ M}^{-1} \text{ cm}^{-1}$. The spectra of free and bound bpy radical anions are quite distinctive (23,35-38): very intense absorption maxima ($\epsilon 1 \times 10^4$ to $4 \times 10^4 \text{ M}^{-1} \text{ cm}^{-1}$) are found at 350-390 nm and are accompanied by less intense maxima ($\epsilon \sim 5 \times 10^3 \text{ M}^{-1} \text{ cm}^{-1}$) at 400 to 600 nm. While the $\text{Rh}(\text{bpy})_3^{2+}$ absorption maxima are in the right regions for the bpy^- chromophore, the intensities observed for these bands are much less than has been observed in other systems.

In summary, some aspects of the behavior of $\text{Rh}(\text{bpy})_3^{2+}$ suggest its formulation as $[\text{Rh}^{\text{III}}(\text{bpy})_2(\text{bpy}^-)]^{2+}$ while others are more in accord with its description as a rhodium(II) complex. It may be that two electronic isomers in chemical equilibrium i.e.,



must be invoked. Alternatively, it could well be that the energies of the rhodium(II) e_g orbitals and the lowest $\text{bpy} \pi^*$ orbitals are very close so that $\text{Rh}(\text{bpy})_3^{2+}$ cannot properly be considered as either a ligand-centered or metal-centered radical. Rather a molecular orbital description taking into account both resonance structures



might then be required. This question cannot be answered by the approach we have used. Techniques such as EPR or resonance Raman spectroscopy may resolve this dilemma in the future.

Acknowledgments. This research was supported by the Division of Basic Energy Sciences of the U. S. Department of Energy. Andrew Keller was a participant in the Brookhaven National Laboratory Summer Student Program (1980). Arden P. Zipp was on sabbatical leave from SUNY, College at Cortland.

Literature Cited

1. Mann, K. R.; DiPierro, M. J.; Gill, T. P. J. Am. Chem. Soc. 1980, 102, 3965 and references cited therein.
2. Sigal, I. S.; Gray, H. B. J. Am. Chem. Soc. 1981, 103, 2220 and references cited therein.
3. Maspero, F.; Taube, H. J. Am. Chem. Soc. 1968, 90, 7361.
4. Lilie, J.; Simic, M. G.; Endicott, J. F. Inorg. Chem. 1975, 14, 2129.
5. Kirch, M.; Lehn, J. M.; Sauvage, J. P. Helv. Chim. Acta 1979, 62, 1345.
6. Brown, G. M.; Chan, S-F.; Creutz, C.; Schwarz, H. A.; Sutin, N. J. Am. Chem. Soc. 1979, 101, 7638.
7. Chan, S-F.; Chou, M.; Creutz, C.; Matsubara, T.; Sutin, N. J. Am. Chem. Soc. 1981, 103, 369.
8. Sutin, N.; Creutz, C. Pure Appl. Chem. 1980, 52, 2717 and references cited therein.
9. Balzani, V.; Bolletta, F.; Gandolfi, M. T.; Maestri, M. Top. Curr. Chem. 1978, 75, 1.
10. Mulazanni, Q. G.; Emmi, S.; Hoffmann, M. Z.; Venturi, M. J. Am. Chem. Soc. 1981, 103, 3362.
11. Unpublished observations.
12. Creutz, C.; Mahajan, D.; Sutin, N.; Zipp, A. P., manuscript in preparation.
13. Simic, M. G.; Hoffmann, M. Z.; Cheney, R. P.; Mulazanni, Q. G. J. Phys. Chem. 1979, 83, 439.
14. Davies, R.; Green, M.; Sykes, A. G. J. Chem. Soc., Dalton Trans. 1972, 1171.
15. Simic, M.G.; Endicott, J.F. J. Am. Chem. Soc. 1974, 96, 291.
16. Kew, G.; DeArmond, K.; Hanck, K. J. Phys. Chem. 1974, 78, 727.
17. Matsubara, T. unpublished observations.
18. Marcus, R. A. J. Chem. Phys. 1965, 43, 679.
19. Hush, N. S. Trans. Faraday Soc. 1961, 57, 557.
20. Chou, M.; Creutz, C.; Sutin, N. J. Am. Chem. Soc. 1979, 99, 5615.
21. Rehm, D.; Weller, A. Isr. J. Chem. 1970, 8, 259.

22. Lin, C-T.; Böttcher, W.; Chou, M.; Creutz, C.; Sutin, N. J. Am. Chem. Soc. 1976, 98, 6536.
23. Sutin, N.; Creutz, C. Adv. Chem. Ser. 1978, 168, 1.
24. Creutz, C.; Keller, A. D.; Sutin, N.; Zipp, A. P. submitted to J. Am. Chem. Soc.
25. Bock, C. R.; Connor, J.A.; Gutierrez, A. R.; Meyer, T. J.; Whitten, D. G.; Sullivan, B. P.; Nagle, J. K. J. Am. Chem. Soc. 1979, 101, 4815.
26. Kew, G.; Hanck, K.; DeArmond, K. J. Phys. Chem. 1975, 79, 1829.
27. Sutin, N.; Brunshwig, B. S. this volume.
28. Cummins, D.; Gray, H. B. J. Am. Chem. Soc. 1977, 99, 5158.
29. Brown, G. M.; Sutin, N. J. Am. Chem. Soc. 1979, 101, 883.
30. Tokel-Tokvaryan, N. E.; Hemingway, R. E.; Bard, A. J. J. Am. Chem. Soc. 1973, 95, 6582.
31. Saji, T.; Aoyagui, S. J. Electroanal. Chem. 1975, 63, 31.
32. Kahl, J. L.; Hanck, K. W.; DeArmond, K. J. Phys. Chem. 1978, 82, 540.
33. Navon, G.; Sutin, N. Inorg. Chem. 1974, 13, 2159.
34. Dallinger, R. F.; Woodruff, W. H. J. Am. Chem. Soc. 1979, 101, 4393.
35. Heath, G. A.; Yellowlees, L. J.; Braterman, P. S. J. Chem. Soc., Commun. 1981, 287.
36. Kaizu, Y.; Fujita, I.; Kobayashi, H. Z. Phys. Chem. (Frankfurt) 1972, 79, 298.
37. Mahon, C.; Reynolds, W. L. Inorg. Chem. 1967, 6, 1297.
38. König, E.; Kremer, S. Chem. Phys. Lett. 1970, 5, 87.

RECEIVED April 27, 1982.

General Discussion—One-Electron Reduction Product of Tris (2,2'-bipyridine)rhodium(III)

Leader: David Stanbury

DR. DAVID STANBURY (Rice University): Have you tried to get at Rh(II) production from the other direction -- by oxidizing rhodium(I)?

DR. CREUTZ: Not yet. I don't believe that can be done in quite the same way. You will notice that none of the reactions we used to reduce Rh(III) involved homogeneous reducing agents; that is because we have not found any which work. We anticipate difficulties with Rh(I) oxidation as well. Obviously, one would need conditions where oxidation of the Rh(I) to Rh(II) is more rapid than oxidation of the desired Rh(II). In pulse radiolysis experiments it might be possible to exploit oxidants such as $(\text{SCN})_2$ or Br_2 . But we haven't yet attempted such experiments.

DR. WILLIAM WOODRUFF (University of Texas): How about considering a little heresy in the case of $\text{Rh}(\text{bpy})_3^{2+}$? For $^*\text{Ru}(\text{bpy})_3^{2+}$, the metal-to-ligand charge-transfer excited state of $\text{Ru}(\text{bpy})_3^{2+}$, we have evidence that the bpy^- radical character is localized on one bpy, rather than delocalized over all three. There is a question as to the source of the driving force for the localization of the ligand radical on one ligand. One possibility would be that the d^5 core, which is degenerate, forces some degree of Jahn-Teller distortion which induces radical localization.

Perhaps for $\text{Rh}(\text{bpy})_3^{2+}$ there is also a ligand centered reduction, but delocalized in this case, since the metal ion is d^6 . I am simply suggesting that the ligand centered radical produced may be delocalized over all three ligands. That might result in the absorption spectrum which you observe, and also result in a self-exchange rate which is similar to the ruthenium case.

DR. CREUTZ: Either electronic structure (i.e., localized or delocalized bpy^-) will account for the exchange rate. But I don't believe there is any reason for any of the $\text{M}(\text{bpy})_2(\text{bpy}^-)$ species to be delocalized. I see no reason why the electron should not reside on one bipyridine.

DR. MORTON HOFFMAN (Boston University): I would like to present some of our results on the rhodium system. I would like to focus on the fate of the rhodium(I) species and, in particular, consider the path of the production of molecular hydrogen from water, which, of course, is the basis of so many of these studies of reduced metal species.

As Dr. Creutz has mentioned, the pulse-radiolysis technique can be used to reduce the rhodium(III) to rhodium(II) by the action of various reducing radicals such as the hydrated electron, CO_2 radical, or the 2-propanol radical. Such reactions are all very rapid with rate constants on the order of $10^9 - 10^{10} \text{ M}^{-1} \text{ s}^{-1}$. With sufficient excess of rhodium(III), one observes pseudo-first-order decay of the reactive radical, which is entirely consumed in a very short period of time.

We have found that the loss of the ligand from the rhodium(II) species that is produced is relatively slow ($k \sim 1 \text{ s}^{-1}$), followed by the very rapid disproportionation reaction (with $k \sim 10^8 \text{ M}^{-1} \text{ s}^{-1}$) producing the rhodium(I) species. As Dr. Creutz has pointed out, this species can exist in many different modifications including dimeric and hydride forms. The exact nature of these species is unknown.

We have examined the reduced species and have speculated upon the mechanistic pathways that can account for the generation of hydrogen and the reduction of water [Mulazzini, Q. G., Emmi, S.; Hoffman, M. Z.; Venturi, M. *J. Am. Chem. Soc.* 1981, 103, 3362; Mulazzini, Q. G.; Venturi, M.; Hoffman, M. Z. *J. Phys. Chem.*, in press]. From continuous radiolysis experiments, we have determined the yields of hydrogen and rhodium(I) as functions of pH, initial substrate concentration, and absorbed dose.

It must first be noted that there is a residual hydrogen yield formed by the radiolysis using 2-propanol radical as the reducing agent. The yield of extra hydrogen increases above this residual level at $\text{pH} < 7$ with maximum H_2 production occurring around $\text{pH} 4.2$. This is exactly the pH region where the rhodium(I) exists in its colorless form, which can be formally expressed as a rhodium(III)-hydride.

If one measures the yield of hydrogen as a function of the radiation dose, there is an induction period after which the G-value of H_2 is constant with time. The results indicate that some intermediate has to build up in concentration before hydrogen evolution commences. As the initial rhodium(III) concentration is increased, the hydrogen yield goes down and the rhodium(I) concentration goes up with the sum of the G values remaining constant. That suggests that rhodium(I) and hydrogen are related to each other in a direct stoichiometric manner.

As far as the uncatalyzed system is concerned, it doesn't appear that rhodium(I) in all its various forms, including the rhodium(III)-hydride or even the rhodium(II) species, is capable of generating hydrogen by itself. Rather, there must be subsequent reactions involving rhodium(I) and other species that ultimately produce the hydrogen.

We would like to suggest that the rhodium(III)-hydride

(rhodium(I) in acid solution) can engage in an electron transfer reaction with the non-labilized rhodium(II) species, which has a lifetime of about 1 second, to produce a reduced rhodium hydride species (as well as the rhodium(III) substrate), and it is this latter species that actually goes on to generate the hydrogen.

We estimate a rate constant of 10^6 - 10^7 $M^{-1} s^{-1}$ for the electron-transfer reaction and an E° for the rhodium-hydride couple that is similar to, or slightly less negative than, the E° value for the substrate. Our mechanism is summarized in Scheme I.

DR. JAMES ESPENSON (Iowa State University): At this conference we have heard presentations dealing with atom transfer reactions, with photogenerated reactive complexes, and with rhodium(II) chemistry. I want to present some results on a related study, involving a different ligand system, representing work done in collaboration with Dr. Ursula Tinner.

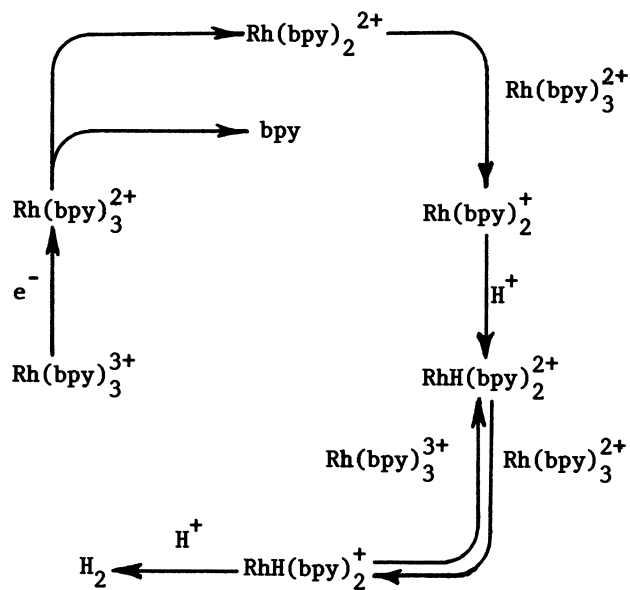
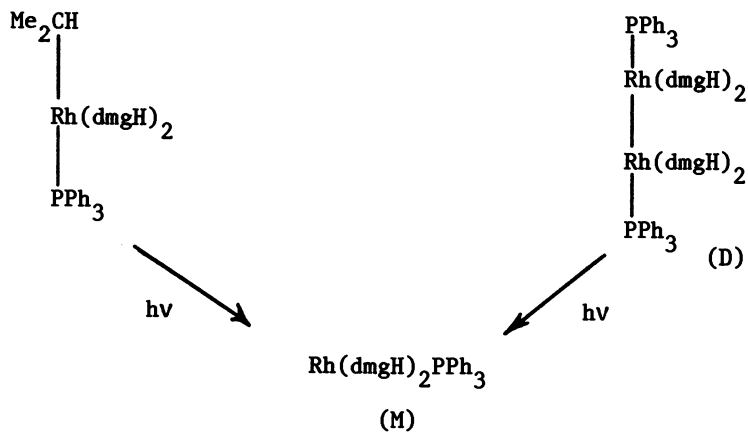
This system involves a mononuclear rhodium(II) d^7 complex derived from the bis(dimethylglyoximate) chelating ligand, the so-called rhodium(II) rhodoxime. That d^7 species can be made by two different photochemical routes flash-photolytically: either from the metal-metal bonded rhodium(II) dinuclear complex, whose structure is known [Caulton, K. G., Cotton, F. A. *J. Am. Chem. Soc.* 1971, **93**, 1914], or, equally suitably, from the organo-rhodium compound, such as the isopropyl complex [see Scheme II].

From both sources, the rhodium(II) mononuclear complex has a variety of options open to it. In the absence of other reagents, for example, it simply dimerizes and forms the metal-metal bonded species. However, it is quite a reactive species, and, among other things, it abstracts halogen atoms, for example, from organic halides [Scheme III].

One can set up to do this using the competition between dimerization and halogen atom abstraction from RX to form the rhodium(III) halide complex. As a function of [RX], the product ratio is quite easily evaluated. From that, one can get the rate constant ratio but, knowing independently the rate constant for dimerization, it is possible to extract from those data rate constants for reactions of the rhodium(II) complex with these organic halides. The rate constants obtained are listed in Table I.

If one takes out of this list the polyhalomethanes and tries to understand what the chemistry is about, certainly a simple-minded view is that this is simply a halogen atom abstraction reaction such as one finds in a gas phase reaction, like sodium atom with organic halides. There is a linear free energy correlation in that the logarithms of the rate constants bear a linear relation to one another.

Finally -- and this has to do with the nature of the bond strengths in such metal-metal bonded systems -- the dimer also thermally dissociates. With a very reactive halogen atom donor,

Scheme IScheme II

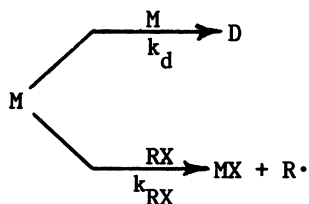
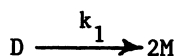
Scheme III

Table I.
Rate Constants for the Reaction of Rhodium(II)
Rhodoxime with Organic Halides

RX	$k_{\text{RX}}, \text{M}^{-1} \text{s}^{-1}$ (in EtOH at 25°C)
CHBr ₃	4×10^6
CCl ₄	2.5×10^5
PhCH ₂ Br	2.0×10^5
CH ₂ Br ₂	1.5×10^4
<i>i</i> -C ₃ H ₇ Br	5.0×10^3
CHCl ₃	1.5×10^3

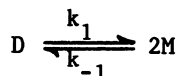
such as an oxidizing agent like ferric chloride or a number of other species, the rate limiting step is the monomer formation, and it is possible to evaluate the rate constant for that step [Scheme IV]. Therefore, the quotient of the thermal rate of monomer formation divided by the dimerization rate constant gives us $1.5 \times 10^{-10} \text{ M}$ as the equilibrium constant for the dimer-monomer equilibrium. Studies as a function of temperature also permit, therefore, the calculation of $\Delta H^\circ = 21 \text{ kcal mol}^{-1}$ for the latter reaction. Ignoring solvation differences, this value serves as an approximation of the metal-metal bond energy in a d^7-d^7 dimer such as this.

Scheme IV



$$-\frac{d[D]}{dt} = k_1[D]$$

$$k_1 = 5.4 \times 10^{-2} \text{ s}^{-1} \text{ (EtOH, } 25^\circ\text{)}$$



$$K_{\text{eq}} = k_1/k_{-1} = 1.5 \times 10^{-10} \text{ M}$$

$$\Delta H^0 (\cong D_{\text{Rh-Rh}}) = 21 \text{ kcal mol}^{-1}$$

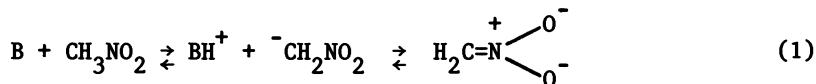
Proton-Transfer Reactions in Organometallic Chemistry

RICHARD F. JORDAN and JACK R. NORTON

Colorado State University, Department of Chemistry, Fort Collins, CO 80521

The Brønsted acid-base behavior of transition metal hydride complexes and their conjugate bases has been investigated. Deprotonation of transition metal hydrides often results in large changes of coordination geometry. This, in turn, results in large intrinsic activation barriers for deprotonation and correspondingly small rate constants for proton transfer. Degenerate proton exchange reaction rate constants between transition metal carbonyl hydrides and their conjugate bases are found to span a range of more than 10^6 , $\text{CpCr}(\text{CO})_3\text{H}$ exhibiting the largest "self-exchange" rate constant and hydrido-osmium tetracarbonyl complexes the smallest. There is a tendency for the rate of deprotonation to decrease with decreasing acidity of the hydrido complex.

Proton transfer reactions involving organic compounds have been the subject of extensive study (1-7), and there has also been some investigation of proton transfer reactions involving coordinated organic ligands (8). Proton transfers involving O-H bonds (e.g., from phenols to phenolate ions) are quite fast and frequently diffusion-controlled as are proton transfers involving N-H bonds. In comparison, proton transfers involving carbon acids, such as nitromethane, are generally quite slow in both the forward and reverse directions.



The contrast is explained by the extensive electronic and structural reorganizations that must take place when nitromethane and

0097-6156/82/0198-0403\$06.25/0
© 1982 American Chemical Society

other carbon acids are deprotonated or when the corresponding anions are protonated. Oxygen and nitrogen are relatively electronegative atoms and the lone pairs resulting from deprotonation of O-H and N-H bonds are correspondingly stable, whereas anions resulting from the deprotonation of carbon acids are stable only when there is extensive delocalization of the lone pair over more electronegative atoms as illustrated for nitromethane anion in reaction 1. This delocalization will, in general, be reflected in extensive structural differences between carbon acids and the corresponding anions.

If we consider proton transfer reactions involving transition metal-hydrogen bonds, it is apparent that they should have more in common with those of carbon acids than with those of oxygen or nitrogen acids. Transition-metal anions are generally stabilized by considerable charge delocalization onto π -acceptor ligands such as CO. The extent of the electronic rearrangement required as transition-metal hydrides such as HCo(CO)_4 and HMn(CO)_5 are deprotonated can be gauged from the fact that their carbonyl stretching frequencies typically change by over 100 cm^{-1} as a result, reflecting a substantial decrease in C-O bond order as π -backbonding increases.

Transition-metal hydrides also, like carbon acids, undergo considerable structural change upon deprotonation. Whereas a nitrogen or oxygen lone pair is stereochemically active, and the molecular geometry, therefore, changes little upon deprotonation, transition-metal "lone pairs" merely increase the formal d-electron configuration and are not stereochemically active. The deprotonation of a transition-metal hydride, therefore, produces considerable changes in coordination geometry (9). The contrast is illustrated by the recently reported (10) X-ray structure of $[\text{Me}_3\text{NH}][\text{Co(CO)}_4]$. The C-N-C angles average 109° , essentially equal to those of 110° found in Me_3N itself (11), whereas the C-Co-C angles average 106° , considerably larger than the C(axial)-Co-C(equatorial) angles of 99.7° found in the C_{3v} symmetry HCo(CO)_4 (12). The nitrogen is thus tetrahedrally coordinated in both Me_3NH^+ and Me_3N , whereas the coordination geometry of cobalt changes from a distorted trigonal bipyramid in HCo(CO)_4 to an approximately tetrahedral arrangement in $[\text{Co(CO)}_4]^-$.

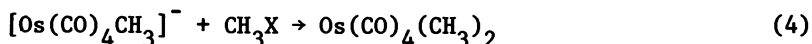
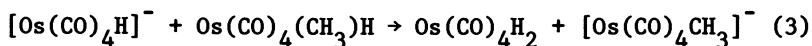
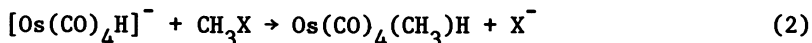
Information Pertinent to Proton Transfer

There is very little information on proton transfer rates involving M-H bonds against which to check the above prediction. Walker, Kresge, Ford, and Pearson (WKFP) have recently reported

(13) a stopped-flow study of the deprotonation of several hydrides by sodium methoxide in methanol in which they conclude that the rates "are remarkably small for a base as strong as methoxide ion" and "are quite comparable to rates of reaction of nitroparaffins with hydroxide ion". However, most of the hydrides studied were polynuclear.

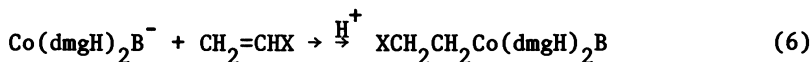
We believe that systematic information on the common mononuclear hydrides is needed and have begun such an investigation. We have chosen acetonitrile as a solvent for several reasons: 1) its high dielectric constant and strong solvation of alkali metal cations make it a good solvent for organometallic anions and minimize complications due to ion pairing in solution; 2) it dissolves most transition-metal hydrides without reacting with them; 3) its low self-ionization constant (14) permits the use of a wide range of acid and base strengths; 4) the existence of accurate pK_a data for a wide range of nitrogen bases (15, 16) allows straightforward determination of pK_a values for organometallic hydrides by IR spectroscopy. We have used acetonitrile distilled from P_2O_5 under nitrogen and handled by standard vacuum line techniques (21).

Both kinetic and thermodynamic data on organometallic hydrides should be very useful. The relative rates of proton transfer processes and other reactions determine a good deal of organometallic chemistry. For example, in our synthesis of *cis*-Os(CO)₄(CH₃)H, reactions 2-4, the comparative rates of methylation, reaction 2, and proton transfer, reaction 3, determine the yield of the desired monomethylated osmium complex versus that of unmethylated and dimethylated byproducts.



With methyl tosylate as CH_3X , the rates of reactions 2 and 3 are approximately equal, whereas with methyl fluorosulfonate as CH_3X , reaction 2 is much faster (17).

Thermodynamic data on the acidity of organometallic hydrides should help identify situations where apparent reactions of acidic transition-metal hydrides actually result from their conjugate bases. A case in which both species can react but give different products (as was pointed out by Prof. Espenson three years ago (18)) is the addition of hydridocobaloximes, $HCo(dmgh)_2B$, to olefins with electron-withdrawing substituents $CH_2=CHX$, reactions 5 and 6.



The direction of addition depends upon whether the hydridocobaloxime or its conjugate anion is the reactive species (19, 20). The fact that these reactions can both be observed suggests (but does not prove) that proton exchange between $\text{HCo}(\text{dmgH})_2\text{B}$ and $\text{Co}(\text{dmgH})_2\text{B}^-$ is slow.

Another way in which a transition-metal hydride may conceivably interact with a substrate is by rate-determining proton transfer to the substrate itself, reaction 7.



An understanding of kinetic acidity is necessary in order to distinguish such mechanisms from other ways in which hydrogen may become attached to a substrate, e.g., hydrogen atom transfer, reaction 8, and hydride transfer, reaction 9.



It should be both possible and profitable to divide all reactions of transition-metal hydrides into these three classes. Even concerted reactions, in which the metal interacts with the substrate at the same time as its hydrogen ligand does, can usefully be divided according to which of the above hydrogen transfer reactions they most resemble.

Proton Transfer in Osmium-Tetracarbonyl Complexes

All of our measurements of proton transfer rates in acetonitrile have been done by various NMR techniques. One of the simplest has been used to measure the rates of transfer from cis- $\text{Os}(\text{CO})_4\text{H}_2$ to Et_3N and back again (21). Whereas a mixture of cis- $\text{Os}(\text{CO})_4\text{H}_2$ and $\text{K}[\text{Os}(\text{CO})_4\text{H}]$ shows two sharp resonances in the hydride region of the ^1H NMR (Figure 1), the addition of Et_3N to $\text{Os}(\text{CO})_4\text{H}_2$ gives resonances at the same two positions which, however, are quite broad at some temperatures (Figure 2). The resonances correspond to unreacted $\text{Os}(\text{CO})_4\text{H}_2$ and to the $\text{Os}(\text{CO})_4\text{H}^-$ produced by its partial deprotonation by Et_3N . The line width is produced by the rapid operation of reaction 10 in both directions.

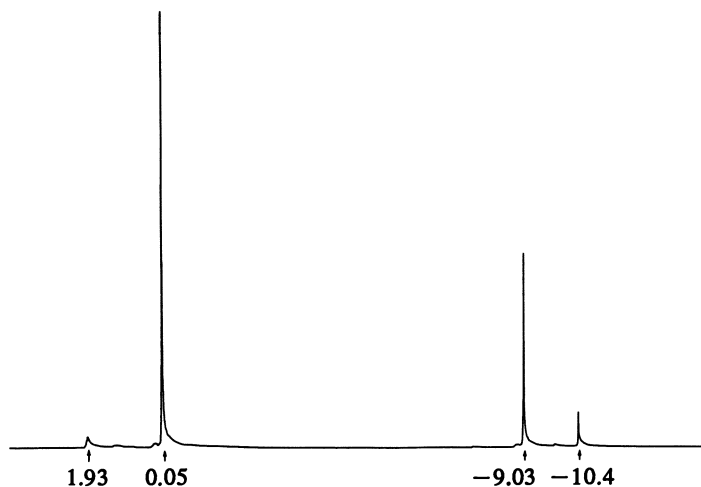


Figure 1. The 100-MHz ^1H NMR spectrum of $\text{cis-Os}(\text{CO})_4\text{H}_2$ (0.05 M), $\text{K}[\text{Os}(\text{CO})_4\text{H}]$ (0.08 M), and hexamethyldisiloxane (0.01 M) (used as an internal line width standard) in CD_3CN . Chemical shifts are illustrated in δ . The signal at δ 1.93 is due to residual solvent protons.

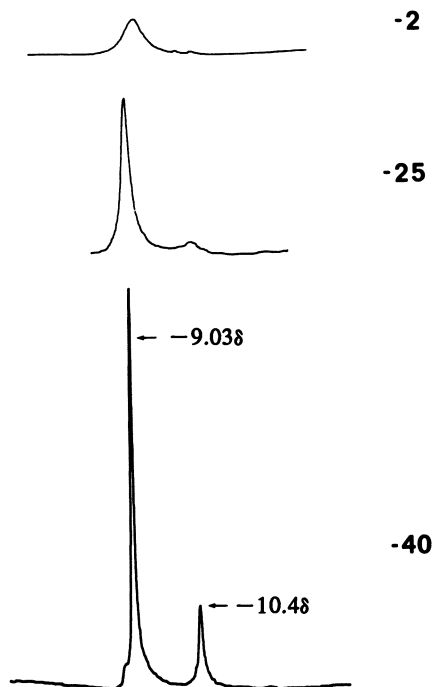
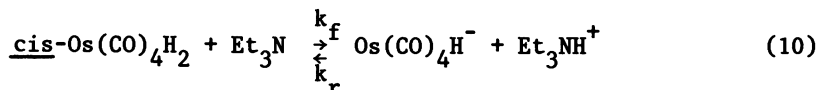


Figure 2. The 100-MHz ^1H NMR spectra (hydride region only) of a CD_3CN solution of 0.3 M $\text{cis-Os}(\text{CO})_4\text{H}_2$ and 1.5 M Et_3N as a function of temperature. Chemical shifts are illustrated in δ .



Division of the excess line width, $\Delta(\text{Os(CO)}_4\text{H}_2)$ (i.e., the increase in the $\text{Os(CO)}_4\text{H}_2$ line width due to reaction 10), by the concentration of Et_3N gives the forward rate constant k_f , and a similar procedure gives k_r .

$$k_f = \frac{\pi\Delta(\text{Os(CO)}_4\text{H}_2)}{[\text{Et}_3\text{N}]} \quad (11)$$

$$k_r = \frac{\pi\Delta(\text{Os(CO)}_4\text{H}^-)}{[\text{Et}_3\text{NH}^+]} \quad (12)$$

The $\text{Os(CO)}_4\text{H}^-$ peak is both smaller and, at a given temperature, broader, as equilibrium 10 lies far to the left.

The value of the equilibrium constant for reaction 10 can be calculated from k_f/k_r , from the ratio of the integrated intensities of the $\text{Os(CO)}_4\text{H}_2$ and $\text{Os(CO)}_4\text{H}^-$ peaks, and from spectrophotometric (carbonyl region IR) titration of $\text{Os(CO)}_4\text{H}_2$ with Et_3N . Fortunately, all three values agree quite well. The K_{eq} thus determined and the known pK_a of Et_3NH^+ in acetonitrile (15, 16) give the value for the pK_a of $\text{Os(CO)}_4\text{H}_2$ in acetonitrile as listed in Table I.

In principle, the NMR line widths also reflect $\text{Os(CO)}_4\text{H}_2/[\text{Os(CO)}_4\text{H}]^-$ proton exchange. ($\text{Et}_3\text{N}/\text{Et}_3\text{NH}^+$ proton exchange is extremely rapid and their NMR spectra are completely averaged under all conditions.) However, the sharp lines seen for the $\text{Os(CO)}_4\text{H}_2/K[\text{Os(CO)}_4\text{H}]$ mixture show that such exchange is extremely slow. (IR studies (21) confirm that there is little contact ion pair formation with organometallic ions in acetonitrile and suggest that a reaction which is slow for $K[\text{Os(CO)}_4\text{H}]$ will also be slow for $[\text{Et}_3\text{NH}][\text{Os(CO)}_4\text{H}]$.) It is, however, possible to measure the rate of this proton exchange by another technique, saturation transfer (22). As shown in Figure 3, irradiation of the $\text{Os(CO)}_4\text{H}^-$ resonance causes a decrease in the intensity of the $\text{Os(CO)}_4\text{H}_2$ resonance. From M_0 , the intensity

Table I. Thermodynamic and Kinetic Acidities of Metal Hydrides in Acetonitrile

Metal Hydride	Base Employed		pK _a of Metal Hydride (25C)	Base Employed for Kinetic Acidity Measurement	Second-order Rate Constant for H ⁺ Transfer 25C, M ⁻¹ s ⁻¹	ΔH [‡] , kcal/mol	ΔS [‡] , cal/deg/mol
	for Thermodynamic Acidity Measurement						
CpCr(CO) ₃ H	pyridine		13.3	CpCr(CO) ₃ ⁻	7.4 x 10 ⁴	8.8	-7
CpMo(CO) ₃ H	pyridine		13.9(OC)	CpMo(CO) ₃ ⁻	2.4 x 10 ³	6.8	-20
CpW(CO) ₃ H	morpholine		16.1	CpW(CO) ₃ ⁻ morpholine	640 1.0 x 10 ⁵	8.1 11.3	-19 2
Os(CO) ₄ H ₂	Et ₃ N		20.8	Os(CO) ₄ H ⁻ Et ₃ N	0.075 480	- 6.5	- -24
Os(CO) ₄ (CH ₃)H	tetramethyl-guanidine		23.0(OC)	Os(CO) ₄ CH ₃ ⁻	not measured, but presumably very slow	-	-
HOs(CO) ₄ Os(CO) ₄ H	Et ₃ N		20.4	Et ₃ N HOs(CO) ₄ Os(CO) ₄ ⁻ Et ₃ N	34 negligible 12	8.5	-23

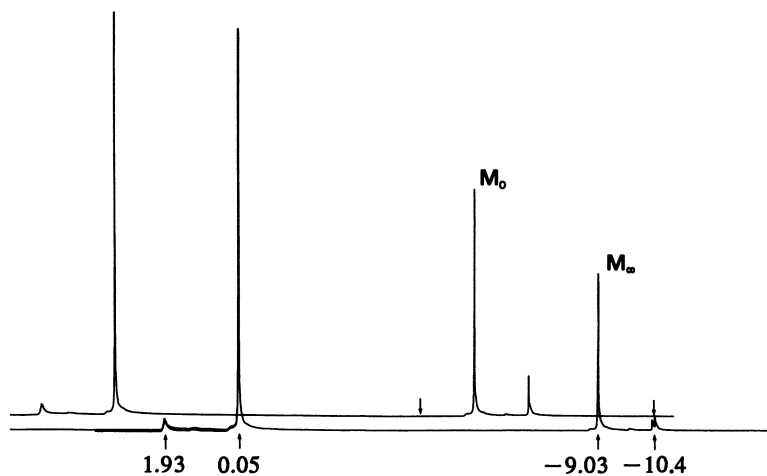


Figure 3. The 100-MHz ^1H NMR spectra at 40°C of a CD_3CN solution of $\text{cis-Os}(\text{CO})_4\text{H}_2$ (0.85 M) and $\text{K}[\text{Os}(\text{CO})_4\text{H}]$ (0.34 M), with (M_∞) and without (M_0) irradiation at the hydride resonance of $\text{K}[\text{Os}(\text{CO})_4\text{H}]$ (indicated by the arrow in lower spectrum). Ratio $M_\infty : M_0 = 0.7$. Chemical shifts are illustrated in δ . The signal at $\delta 1.93$ is due to residual solvent protons. Hexamethyldisiloxane (0.20 M), resonance $\delta 0.05$, is an internal intensity standard.

of the $\text{Os}(\text{CO})_4\text{H}_2$ signal without irradiation, M_∞ , its intensity after prolonged irradiation, and the spin-lattice relaxation time T_1 of $\text{Os}(\text{CO})_4\text{H}_2$, the rate constant for proton exchange $k^{\text{Os-Os}}$ can be obtained.

$$k^{\text{Os-Os}} = \frac{1}{[\text{Os}(\text{CO})_4\text{H}^-]} \times \frac{2}{T_1(\text{Os}(\text{CO})_4\text{H}_2)} \left[\frac{M_0(\text{Os}(\text{CO})_4\text{H}_2)}{M_\infty(\text{Os}(\text{CO})_4\text{H}_2)} - 1 \right] \quad (13)$$

The experiment can also be performed in the reverse direction and $k^{\text{Os-Os}}$ determined independently. However, as the time scale of this rate measurement technique is determined by T_1 , and as the T_1 of $\text{Os}(\text{CO})_4\text{H}^-$ is a great deal longer (240 seconds at 30C) than that of $\text{Os}(\text{CO})_4\text{H}_2$ (34.6 seconds) and is subject to considerable uncertainty, the value obtained from $\text{Os}(\text{CO})_4\text{H}^-$ irradiation is more reliable. From a single experiment, the two values agree reasonably well (for example, $0.058 \text{ M}^{-1}\text{s}^{-1}$ versus $0.037 \text{ M}^{-1}\text{s}^{-1}$ at 30C), but the measured rate constant varies somewhat from experiment to experiment. Considering the slowness of this proton transfer, the rate constant variation may reflect varying degrees of adventitious catalysis. As little as 10^{-6} M of an impurity with the kinetic basicity of Et_3N would explain the observed rate variation. The addition of a small amount of ethanol (which is not significantly deprotonated by $\text{Os}(\text{CO})_4\text{H}^-$) failed to affect the rate.

We have also looked at *cis*- $\text{Os}(\text{CO})_4(\text{CH}_3)\text{H}/\text{Et}_3\text{N}$ proton transfer by observing the collapse of the hydride quartet (Figure 4) (21). The observed and calculated spectra are quite similar to the 1957 ones - which have become standard textbook material - of Grunwald, Loewenstein, and Meiboom for the deprotonation of CH_3NH_3^+ (23).

Other Complexes

Finally, we have measured the rate constants of proton transfer reactions involving $(\eta^5\text{-C}_5\text{H}_5)\text{M}(\text{CO})_3\text{H}$ ($\text{M} = \text{Cr}, \text{Mo}, \text{W}$) by watching the coalescence of the cyclopentadienyl signals of the anion and of the neutral hydride (Figure 5) and by determining the excess line widths due to proton transfer in a mix-

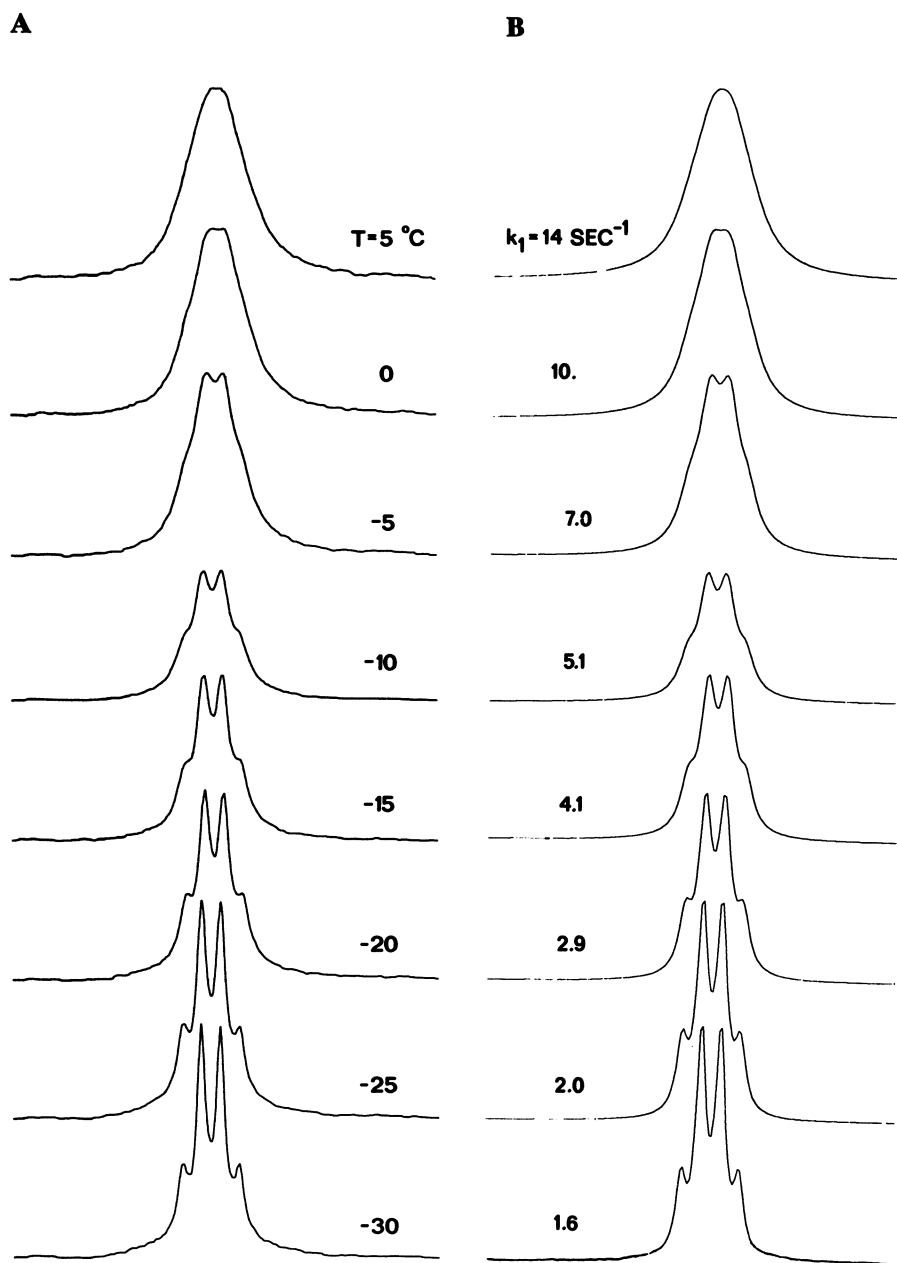


Figure 4. The hydride region 100-MHz ^1H NMR spectra observed for 0.31 M $\text{cis-Os}(\text{CO})_4(\text{CH}_3)\text{H}$ and 1.20 M Et_3N in CD_3CN as a function of temperature (5°C) where $k_1 = 14 \text{ s}^{-1}$ and calculated for the exchange rates (with respect to $\text{cis-Os}(\text{CO})_4(\text{CH}_3)\text{H}$) shown. Key: A, observed; and B, calculated.

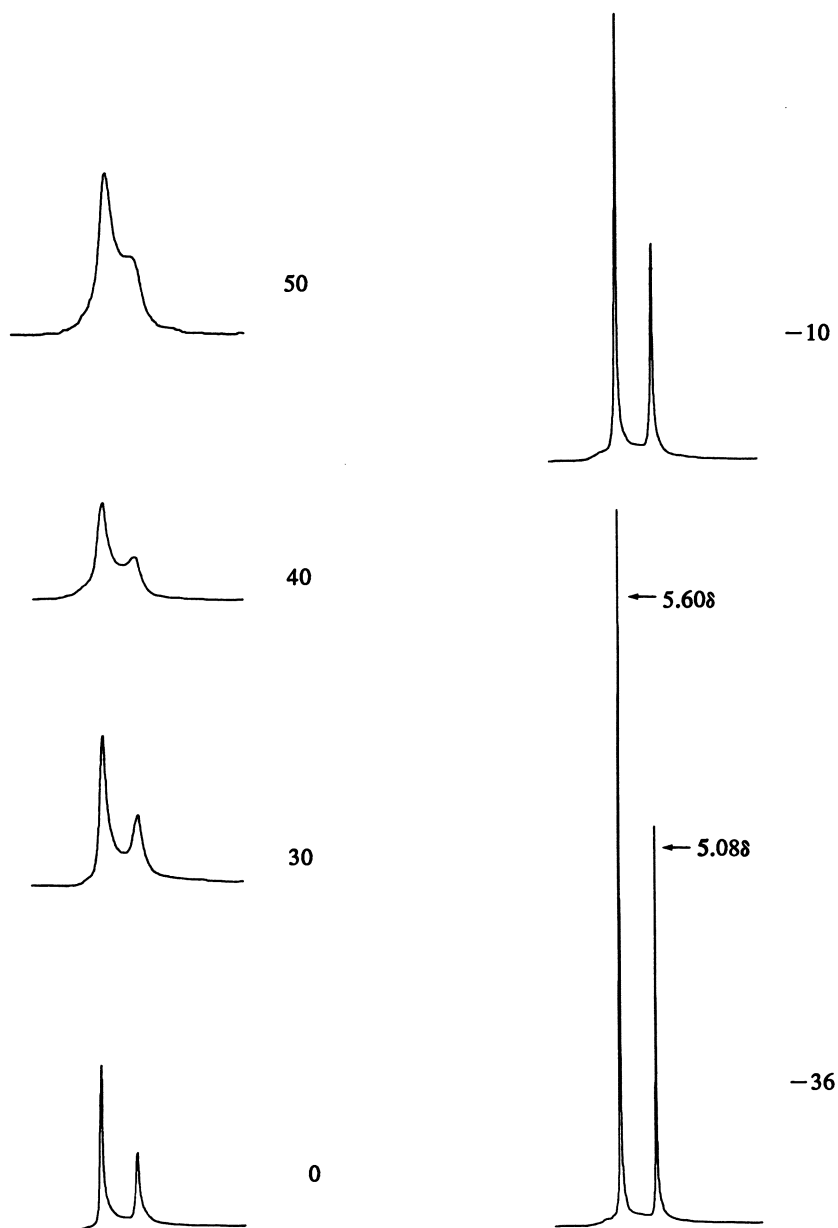


Figure 5. The 100-MHz ^1H NMR spectra of a CD_3CN solution of $(\eta^5\text{-C}_5\text{H}_5)\text{W}(\text{CO})_3\text{H}$ (0.092 M) and $[(\eta^5\text{-C}_5\text{H}_5)\text{W}(\text{CO})_3]^-$ (0.058 M) as a function of T . Only the region containing the cyclopentadienyl resonances is shown. Chemical shifts are illustrated in δ .

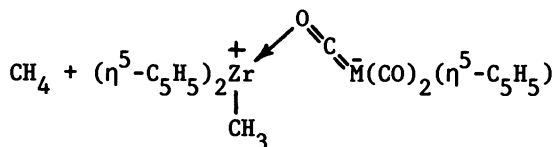
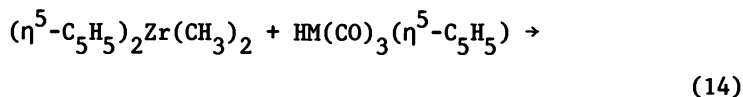
ture of $(\eta^5\text{-C}_5\text{H}_5)\text{W}(\text{CO})_3\text{H}$ and morpholine (21). All of these rate constants have been measured over a range of temperatures which give rates appropriate for the various methods of measurement. Activation parameters and values of the rate constants extrapolated to 25C are given in Table I, as are pK_a values arising from IR determination (checked by NMR when possible as above for $\text{Os}(\text{CO})_4\text{H}_2/\text{Et}_3\text{N}$) of equilibrium constants for the deprotonation of the hydride complexes by various nitrogen bases.

Conclusions

These results suggest a number of generalizations:

1) The equilibrium acidity decreases down a column in the periodic table ($\text{Cr} > \text{Mo} > \text{W}$). While this generalization has been offered before (24, 25), there has been no previous quantitative measurement of the acidity of all three members of such a series.

2) The kinetic acidity (rate constant for metal-to-metal proton exchange) also decreases down a column ($\text{Cr} > \text{Mo} > \text{W}$) in the periodic table. This parallels the order of rates we have observed for the dinuclear elimination of methane from $(\eta^5\text{-C}_5\text{H}_5)_2\text{Zr}(\text{CH}_3)_2$ and $\text{HM}(\text{CO})_3(\eta^5\text{-C}_5\text{H}_5)$ ($\text{M} = \text{Cr}, \text{Mo}, \text{W}$) and suggests that the latter reaction involves proton transfer.

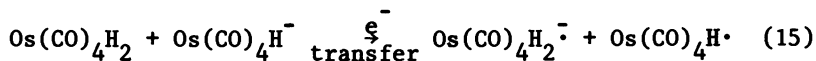


3) Replacement of a hydride ligand by a methyl substituent decreases both the thermodynamic and the kinetic acidity of the remaining hydrogen, while its replacement by an additional $\text{Os}(\text{CO})_4\text{H}$ unit increases the thermodynamic acidity but decreases the rate of deprotonation. The same additional delocalization that decreases the pK_a of $\text{Os}_2(\text{CO})_8\text{H}_2$ relative to that of $\text{Os}(\text{CO})_4\text{H}_2$ presumably increases the electronic rearrangement that must occur upon deprotonation and, therefore, decreases the rate of that process.

4) The transfer of protons from metal hydrides to metal

anions is much slower than transfer to nitrogen bases of comparable strength. For example, transfer from $(\eta^5\text{-C}_5\text{H}_5)\text{W}(\text{CO})_3\text{H}$ to $(\eta^5\text{-C}_5\text{H}_5)\text{W}(\text{CO})_3^-$ (pK_a of conjugate acid 16.1) is 156 times slower than to morpholine (pK_a of conjugate acid 16.6); transfer from $\text{Os}(\text{CO})_4\text{H}_2$ to $\text{Os}(\text{CO})_4\text{H}^-$ (pK_a of conjugate acid 20.8) is over 6,000 times slower than transfer to triethylamine (pK_a of conjugate acid 18.5). It appears that the prediction that proton transfer processes involving metals would be slower than comparable processes involving nitrogen is correct.

An Alternative Mechanism. Considering the facility of the electron transfer reactions to which a great deal of this symposium has been devoted, we have to worry whether our "proton transfer" reactions may not really be the result of electron transfer in the reverse direction followed by hydrogen transfer. As Bergman (26) has recently reported that another hydride anion may act as a one-electron reducing agent, and as we have evidence implicating $\text{Os}(\text{CO})_4\text{H}^\cdot$ as an intermediate in a number of other reactions, the mechanism of reactions 15 and 16 has to be considered as an alternative to direct $\text{Os}(\text{CO})_4\text{H}_2/\text{Os}(\text{CO})_4\text{H}^-$ proton exchange.

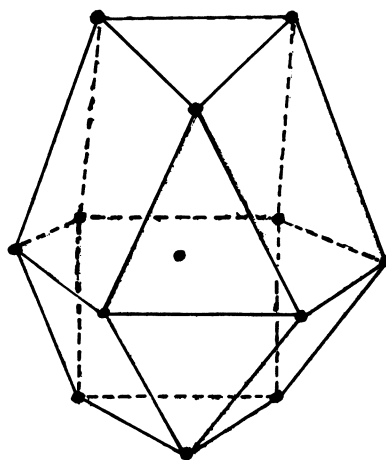


The operation of this alternative mechanism may explain why the rate of this reaction appeared to vary from experiment to experiment, although a more likely explanation is adventitious catalysis.

Directions for Future Work. The measurement of rates of proton transfer from a single acid to more bases differing only in thermodynamic base strength should allow the construction of Brønsted plots of kinetic versus thermodynamic acidity. The bases we have used at this early stage of development of the subject have involved different proton acceptor atoms and cannot be so used (although comparison of the Et_3N transfer rates of $\text{Os}(\text{CO})_4\text{H}_2$ and $\text{Os}(\text{CO})_4(\text{CH}_3)\text{H}$ suggests a Brønsted slope α of about 0.5). The slopes of such plots should give valuable knowledge of the details of proton transfer processes involving metals.

We intend to extend this work to include the comparison of hydrides of different types. In contrast to organic acids,

where the protons are bound to oxygen, nitrogen, or carbon in a few simple ways, acidic inorganic hydrides are known for virtually all the transition elements and display great structural variety. A particularly fascinating class, just now becoming widely recognized, is that of interstitial hydrides. An example is $[\text{Rh}_{13}(\text{CO})_{24}\text{H}_{5-n}]^{n-}$, where n ranges from two to four, one of many interesting structures for which we are indebted to the late Paolo Chini (27). The hexagonal-close-packed rhodium framework is illustrated in Figure 6. One, two, or three protons occupy semi-octahedral holes (28, 29). The rate of deprotonation of such systems is undoubtedly very slow and may reflect the rate at which interstitial hydrogens migrate to surface sites.



2 interstitial H

Figure 6. The hexagonal-close-packed rhodium framework of $[Rh_{13}(CO)_2H_{5-n}]^{n-}$.

Acknowledgments

This work was supported by NSF Grant No. CHE79-20373 and by the Colorado State University Regional NMR Center, funded by Grant No. CHE78-18581. The authors are grateful to Dr. Bruno Longato and Robin Eddidin for preliminary work on dinuclear elimination rates and to the Alfred P. Sloan Foundation for a fellowship to J. R. N.

Literature Cited

1. Bell, R. P. "The Proton in Chemistry"; Cornell U. Press: Ithaca, N. Y., 1973.
2. Reutov, O. A.; Beletskaya, I. P.; Butin, K. P. "CH-Acids"; Pergamon: New York, 1978.
3. Albery, W. J. Ann. Rev. Phys. Chem. 1980, **31**, 227.
4. Hibbert, F. In "Comprehensive Chemical Kinetics"; Bamford, C. H.; Tipper, C. F. H., Eds.; Elsevier: Amsterdam, 1977; Vol. 8, Chap. 2.
5. Crooks, J. E. ibid., Chap. 3.
6. Simmons, E. L. Progr. Reaction Kinetics 1977, **8**, 161.
7. Eyring, E. M.; Marshall, D. B.; Strobusch, F.; Süttinger, R., This Volume, Chap. 3.
8. Bannister, C. E.; Margerum, D. W.; Raycheba, J. M. T.; Wong, L. F. "Proton Transfer", Symposia Faraday Soc., Vol. 10; The Chemical Society: London, 1975; p 78.
9. Frenz, B. A.; Ibers, J. A. "Transition Metal Hydrides", Muetterties, E. L., Ed., Marcel Dekker: New York, 1971; Chap. 3.
10. Calderazzo, F.; Fachinetti, G.; Marchetti, F.; Zanazzi, P. F. J. Chem. Soc., Chem. Commun. 1981, 181.
11. Beagley, B.; Hewitt, T. G. Trans. Faraday Soc. 1968, **64**, 2561.
12. McNeil, E. A.; Scholer, F. R. J. Am. Chem. Soc. 1977, **99**, 6243.
13. Walker, H. W.; Kresge, C. T.; Ford, P. C.; Pearson, R. G. J. Am. Chem. Soc. 1979, **101**, 7428.
14. Coetzee, J. F. Prog. Phys. Org. Chem. 1967, **4**, 45.
15. Kolthoff, I. M.; Chantooni, M. K.; Bhowmik, S. J. Am. Chem. Soc. 1968, **90**, 23.
16. Coetzee, J. F.; Padmanabhan, G. R. J. Am. Chem. Soc. 1965, **87**, 5005.
17. Evans, J.; Okrasinski, S. J.; Pribula, A. J.; Norton, J. R. J. Am. Chem. Soc. 1976, **98**, 4000.
18. Chao, T.-H.; Espenson, J. H. J. Am. Chem. Soc. 1978, **100**, 129; and references therein.
19. Schrauzer, G. N.; Windgassen, R. J. J. Am. Chem. Soc. 1967, **89**, 1999.

20. Johnson, M. D.; Tobe, M. L.; Wong, L. Y. J. Chem. Soc. A. 1968, 929.
21. Jordan, R. F.; Norton, J. R. J. Am. Chem. Soc. 1982, 104, 1255.
22. Faller, J. W. "Determination of Organic Structures by Physical Methods", Nachod, F. C., Zuckerman, J. J., Eds.; Academic Press: New York, 1973; Vol. 5, Chap. 2.
23. Grunwald, E.; Loewenstein, A.; Meiboom, S. J. Chem. Phys. 1957, 27, 630.
24. Beck, W.; Hieber, W.; Braun, G. Z. Anorg. Allg. Chem. 1961, 308, 23.
25. Lokshin, B. V.; Pasinsky, A. A.; Kolobova, N. E.; Anisimov, D. N.; Makarov, Y. V. J. Organomet. Chem. 1973, 55, 315.
26. Jones, W. D.; Huggins, J. M.; Bergman, R. G. J. Am. Chem. Soc. 1981, 103, 4415.
27. Albano, V. G.; Ceriotti, A.; Chini, P.; Ciani, G.; Martinengo, S. J. Chem. Soc., Chem. Commun. 1975, 859.
28. Albano, V. G.; Ciani, G.; Martinengo, S.; Sironi, A. J. Chem. Soc., Dalton Trans. 1979, 978.
29. Ciani, G.; Sironi, A.; Martinengo, S. J. Chem. Soc., Dalton Trans. 1981, 519.

RECEIVED April 27, 1982.

General Discussion—Proton-Transfer Reactions in Organometallic Chemistry

Leader: Dennis Tuck

DR. GREGORY GEOFFROY (Pennsylvania State University): There was a recent paper [Vidal, J. L.; Walker, W. E. Inorg. Chem. 1981, 20, 249] which indicated that hydridorhodiumtetracarbonyl is much more acidic than hydridocobalttetracarbonyl. This goes against your general statement that acidity decreases with increasing atomic number within a group. Can you explain that?

DR. NORTON: I read that paper with some care. I am afraid I am not convinced by the result. The cobalt and iridium results are believable. They have been carefully measured and they agree with the general trend. The rhodium result is not well measured, and I am inclined, therefore, to be suspicious of the fact that it doesn't fit the general trend.

DR. GEOFFROY: Do you know anything about dihydridorutheniumtetracarbonyl compared to dihydridoironcarbonyl?

DR. NORTON: No.

DR. HENRY TAUBE (Stanford University): There is in the literature a description of bis-ethylenediaminedihydride osmium(IV) prepared by Malin [Malin, J.; Taube, H. Inorg. Chem. 1971, 10, 2403]. The interesting thing is that the compounds you describe, in which you have four carbon monoxides in place of the two ethylenediamines and where the formal oxidation state is lower, are actually much more acidic than Malin's dihydride, in which the oxidation state of Os is 4+. The comparison isn't exact, because Malin's work was done in aqueous solution, and bases are not as strong in aqueous solution as in nonprotic solvents, but, nevertheless, it testifies to the strong electron withdrawing power of something like carbon monoxide. Malin observed no diminution in the hydride nmr signal when his species, $\text{Os}(\text{en})_2\text{H}_2^{2+}$, was dissolved in 2M aqueous hydroxide.

DR. NORTON: It is also worth noting that the osmium dihydride is a rather weak acid if you compare it to these others.

DR. STEPHEN NEUMANN (Eastman Kodak Co.): In your observation of the proton transfer rates between the metal base and the amine base, do you have any feeling for whether the slower transfer is unique to the metal bases or whether it has to do more with the bulk of the overall base participating in the proton transfer? For instance, would a sterically hindered amine show rates similar to the metal bases.

DR. NORTON: That is a difficult question to answer at bottom. But I think the general trend is clear, namely that all

of the metal bases are slower than all of the comparable nitrogen bases. It is difficult to believe that this phenomenon is simply due to steric hindrance. I suppose that we should try putting a sterically hindered nitrogen base into the system. It is fair to say, however, that many of these metal anions are not exceptionally hindered. For example, hydridoosmiumtetracarbonyl anion is a trigonal bipyramidal species with minimal steric congestion.

DR. JOHN BRAUMAN (Stanford University): One of the points that is interesting in these proton transfer reactions is the observation that often hydrogen-bonded intermediates don't seem to be of much consequence as contrasted with oxygen or nitrogen lone pair bases. There is a very long, involved, and sometimes confusing literature about correlations of hydrogen bond strengths or hydrogen bonding with acidity, which invariably break down in peculiar situations. Is there any indication that you can see hydrogen bonding in these metal hydrides?

DR. NORTON: An excellent attempt to observe such hydrogen bonding was made recently by Fachinetti, et al. [Calderazzo, F.; Fachinetti, G.; Marchetti, F.; Zanazzi, P. F. *J. Chem. Soc., Chem. Commun.* 1981, 181]. They took hydridocobalttetracarbonyl and triethylamine, and crystallized out a species which one can only describe as the tetracarbonylcobaltate of protonated triethylamine. They proposed some type of interaction between the hydrogen and a face of the cobalt tetrahedral complex, but it was clear that the interaction was almost entirely with nitrogens. The conclusion I would draw is that the complex appears to proceed directly to full protonation of the amine without any observable evidence for a hydrogen bonded intermediate.

DR. BRAUMAN: But there are much weaker bases, such as ethers, which might show infrared changes in the metal hydride.

DR. NORTON: The metal-hydrogen stretches tend to be very broad. This would hamper such observations. I am aware of no reports of solvent dependence of metal-hydrogen stretches.

DR. DENNIS TUCK (University of Windsor): There are some stable dimetal carbonyl species in which the hydrogen bond actually holds the two anions together (i.e., HX_2^- species). Are these relevant to the kinetics you are looking at?

DR. NORTON: We are expecting to look at such systems but haven't yet done so. Clearly, the next step is to begin looking at cases where the hydrogen is bridging two metal systems.

DR. JAMES ESPENSON (Iowa State University): You have

talked about reactions in which the metal hydride acts as a proton donor toward a Lewis base. Are there cases in which the same metal complex can act as a hydride donor toward a Lewis acid?

DR. NORTON: I am not aware of any cases where the same complex has been shown to act in both ways. In general, one finds that metal hydrides tend to be fairly good at either one thing or the other.

DR. THOMAS MEYER (University of North Carolina): I feel that you have glossed over something that is actually very interesting, and that is the whole question of the Bronsted relationship. You have now observed a large number of systems, chromium, molybdenum, tungsten, which exhibit tricarbonyl anions. Have you looked at rate constants for all those species with the same hydride? You would then have three bases, all with identical structures.

DR. NORTON: The answer is, as yet, no. I think the experiment to do would be to take a weak base with all three of those hydrides as acids and look at the line broadening. By varying the concentration of the weak base over an enormous range, one should be able to obtain the proton transfer rate constants of all three of those hydrides to the same weak base. That is the next experiment on our list.

DR. DALE MARGERUM (Purdue University): You need to be careful because you may not obtain a true Bronsted plot from what you have just described. You don't want to make a plot where each system has a different rearrangement. You want to be certain to have a common type of acid or base with which you are reacting. The literature is full of inverse Bronsted relationships in which there has been a poor choice of reaction acid-base pairs. Much confusion has been generated as a result.

DR. NORTON: Unfortunately, all of these systems tend to be rather different sterically. That, as I understand it, makes the whole concept totally inapplicable. But in the case that Dr. Meyer has cited, one would be varying only the central metal with a common base. Simply by varying the central metal, I don't think one would be changing the geometry that much.

DR. MARGERUM: On the contrary, I think you are changing it very much. You could use one of your acids and react it with a series of different bases, all of which are similar amine bases.

DR. NORTON: That is, in fact, another set of experiments on our list. I would presume from what you are saying that the proper approach would be to take a constant hydride with a

single metal and a variety of closely related bases over a rather small pK_b range and measure the transfer rates.

DR. MARGERUM: Right. Otherwise, you will have different reorganizational terms or different work terms, all of which is going to confuse your Bronsted relationship.

DR. WILLIAM TROGLER (Northwestern University): You looked at exchange between the monohydride anion of osmium and the neutral dihydride. Have you ever studied the bimolecular self-exchange for a neutral dihydride? This could be followed by mixing one sample labelled with deuterium and one with hydrogen.

DR. NORTON: No. Bergman has seen one such case. I think this reaction can take place only when there is some type of base in the medium to catalyze that equilibration. I don't see it as a completely non-acid-base phenomenon.

Reactivity of Coordinated Dioxygen

JOHN F. ENDICOTT and KRISHAN KUMAR

Wayne State University, Department of Chemistry, Detroit, MI 48202

Contrasts between the reactivity of free and coordinated O_2 are considered with a special focus on the reactions of transient dioxygen adduct, $\underline{A} = \text{Co}([14]\text{aneN}_4)(\text{OH}_2)\text{O}_2^{2+}$, observed in aqueous mixtures of O_2 and $\text{Co}([14]\text{aneN}_4)(\text{OH}_2)_2^{2+}$. The greater reactivity of \underline{A} than O_2 towards outer-sphere electron transfer reagents is in part due to \underline{A} being the stronger oxidant. The preliminary observations also suggest a smaller intrinsic barrier for electron transfer to \underline{A} than to O_2 . Reactions of \underline{A} which result in formation of μ -peroxo adducts tend to be favored over outer-sphere electron transfer. The rate advantage of the pathways forming adducts appears to arise almost entirely from thermodynamic factors. The coordinated O_2 of \underline{A} is not a reactive radical with respect to hydrogen atom abstraction, addition to olefins, etc. The possibilities for oxygen atom transfer have only begun to be investigated. Some comparisons with the reactivity reported for μ -peroxo complexes are considered.

Oxidations dependent on molecular oxygen are of fundamental importance to many chemical and biochemical processes (1-6). A large number of these processes require the presence of some transition metal ion to "activate" the oxygen. The initial step in many of these reactions is the coordination of O_2 , and the nature of the coordinated dioxygen moiety has been of intense interest (1-12). Despite the extensive studies of the binding of O_2 to transition metal complexes, relatively little is known

0097-6156/82/0198-0425\$07.50/0
© 1982 American Chemical Society

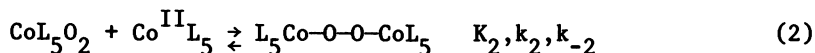
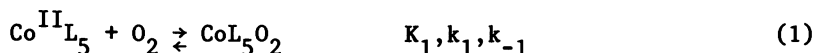
about the reactivity of coordinated O_2 . In fact there is an element of peculiarity to the "activation" of O_2 by coordination to metals, since the formation of even moderately stable complexes must reduce the net free energy available in the oxidation process (see Table I for pertinent thermochemical parameters of O_2). This paper will focus on the chemical reactivity of coordinated O_2 .

Table I
Summary of Dioxygen Thermochemistry ^a

$O_2 + 4H^+ + 4e^- \rightleftharpoons 2H_2O$	$E^0 = 1.23 \text{ V}$
$O_2 + e^- \rightleftharpoons O_2^-$	$E^0 = -0.15 \text{ V (pH 7)}$
$O_2^- + 2H^+ + e^- \rightleftharpoons H_2O_2$	$E^0 \cong 0.87 \text{ V (pH 7)}$
$HO_2 \rightleftharpoons O_2^- + H^+$	$pK_a = 4.88$
$O_2 \rightarrow 2O\cdot$	49 kJ mol^{-1}
$H_2O_2 \rightarrow 2OH\cdot$	146 kJ mol^{-1}

(a) Parameters from ref. (4); Latimer, W.M. "The Oxidation States of the Elements and their Potentials in Aqueous Solutions"; 2nd Ed., Prentice-Hall: Englewood Cliffs, NJ, 1952; Sawyer, D.T., Gibian, M.J. *Tetrahedron*, 1979, 35, 1471.

Many cobalt(II) complexes are very reactive towards dissolved oxygen. The reasonably complex kinetic behavior of these systems can usually be interpreted in terms of a simple two step mechanism (8, 10):



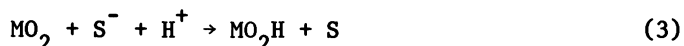
For a very large number of cobalt complexes it is possible to

isolate and purify the relatively stable 1:2 μ -peroxo dimers. It is often possible to manipulate reaction conditions, such as solvent or temperature, in order to detect, or sometimes even isolate, the more transient 1:1 adducts. Direct investigation of the chemistry of reactive 1:1 CoL_5O_2 adducts is generally hampered by their very short lifetimes and, consequently, small concentrations. We have found some macrocyclic tetraamine complexes of cobalt(II) to react rapidly with O_2 to form relatively intensely absorbing 1:1 adducts whose formation and decay may be monitored on a stopped-flow time scale. Thus for [14]ane $\text{N}_4 = 1,4,8,11$ -tetraazacyclotetradecane (cyclam), at 25C ($\mu = 0.1$), $K_1 = (8 \pm 2) \times 10^3 \text{ M}^{-1}$, $k_1 = (5.0 \pm 1.5) \times 10^5 \text{ M}^{-1}\text{s}^{-1}$, $K_2 = (8 \pm 3) \times 10^5 \text{ M}^{-1}$, and $k_2 = (4.9 \pm 0.4) \times 10^5 \text{ M}^{-1}\text{s}^{-1}$ (13). We have been using this system to explore the reactivity of the coordinated oxygen molecule. Enough information has been accumulated that we may make some preliminary comparisons between free O_2 , monomeric dioxygen complexes, and peroxo bridged binuclear complexes.

Possible Reactions of Coordinated Dioxygen

Five classes of reactions of coordinated O_2 may be usefully distinguished:

1. Outer-sphere electron transfer in which formation of a chemical bond between the reductant and O_2 is sterically difficult:



2. Formation of metastable μ -peroxo complexes (also adduct formation, nucleophilic substitution, radical coupling, etc.)



3. Hydrogen atom abstraction:



4. Oxygen atom transfer:



5. Heterolytic or homolytic displacement:



We have been seeking to illustrate each of these reactions clearly with a directly observed reaction of the $\text{Co}([\text{14}] \text{aneN}_4)(\text{OH}_2)\text{O}_2^{2+}$ complex.

Outer-Sphere Electron Transfer Reactions of O_2 Moieties

All known dioxygen moieties readily react with outer-sphere electron transfer reagents, provided the thermochemical requirements are met. A representative collection of data is presented in Table II. These outer sphere reactions can be used to make a comparison of the intrinsic reactivities of the dioxygen moieties. Thus, one may obtain free energy independent reactivities by correcting for the redox equilibrium constants, or one may correct for both the equilibrium constant and the counter reagent self-exchange rate constant (14) to obtain apparent self-exchange rate constants of the dioxygen moieties themselves (i.e., for $\text{O}_2 + {}^*\text{O}_2 \rightleftharpoons \text{O}_2 + {}^*\text{O}_2$, etc.). While the data in Table II are selective, they are, nevertheless, reasonably representative. Self-exchange parameters obtained from kinetic data reported in the literature are widely scattered (Table II) for both the O_2/O_2^- and μ -superoxo/ μ -peroxo couples. Despite various problems of detail, the intrinsic barriers to electron transfer are generally larger for the μ -superoxo/ μ -peroxo reactions than for the O_2/O_2^- reactions ($\sim 100 \pm 5 \text{ kJ mol}^{-1}$ compared to $\sim 45 \pm 5 \text{ kJ mol}^{-1}$). Much, but not all, of this difference in intrinsic barriers must arise from the differences in charge type of the reactions considered. The remaining contributions may originate in solvation effects since the changes in O-O bond length accompanying electron transfer make relatively small contributions ($< 5 \text{ kJ mol}^{-1}$; 13,15,16) to the activation barrier.

The reactions of the $\text{Co}([\text{14}] \text{aneN}_4)(\text{OH}_2)\text{O}_2^{2+}$ complex present us with some slightly different problems. First of all, the reactions are kinetically complex since reactions (3) occur in competition with (2). One must therefore perform relatively thorough kinetic studies, varying counter-reagent concentrations over a sufficient range that the rate becomes pseudo-first order in $[\text{S}^-]$, in order to sort out the reactions of interest. A characteristic collection of data is presented in Figure 1.

A matter of some concern has been the estimation of a re-

Table II
 Contrast in Outer-Sphere Electron-Transfer
 Reactivity of Dioxygen Complexes^a

M _n O ₂	Counter Reagent	Medium	k _{ab} M ⁻¹ s ⁻¹	E ^f (MO ₂)		E ^f (Counter reagent) V	k _{exch} (Counter reagent) M ⁻¹ s ⁻¹	k _{exch} (MO ₂) M ⁻¹ s ⁻¹
				V	V			
O ₂	Co(sep) ²⁺	0.2 M NaCl	45 ^b	-0.15 ^c	-0.3 ^b	5.1 ^b	1.3	
	Ru(NH ₃) ₆ ²⁺	1.0 M LiOAc	63 ^d	-0.15 ^c	-0.05 ^e	4x10 ^{3f}	9.9x10 ³	
	Ru(NH ₃) ₅ (isn) ²⁺	0.1 M HTFMS	0.108 ^d	-0.15 ^c	0.387 ^d	4.7x10 ^{5g}	1.0x10 ³	
	Ru(NH ₃) ₄ (phen) ²⁺	0.1 M HTFMS	7.7x10 ^{-3d}	-0.15 ^c	0.515 ^h	3.2x10 ^{6h}	1.7x10 ³	
	Ru(en) ₃ ²⁺	1.0 M LiOAc	36 ^d	-0.15 ^c	0.172 ^f	3.6x10 ⁴ⁱ	3.8x10 ⁴	
O ₂ ⁻	Ru(NH ₃) ₅ (isn) ³⁺	0.1 M NaHCO ₂	2.2x10 ^{8d}	0.15 ^c	0.387 ^d	4.7x10 ^{5g}	3.4x10 ³	
	Co(bpy) ₃ ²⁺	0.05 M KNO ₃	380 ^j	0.95 ^j	0.319 ^k	20 ^k	1.6x10 ⁻⁶	
	Co(phen) ₃ ²⁺	0.05 M KNO ₃	188 ^j	0.95 ^j	0.39 ^l	40 ^l	2x10 ⁻⁶	
	V ²⁺	1.0 M LiClO ₄	9.6x10 ^{4m}	0.95 ^j	-0.226 ⁿ	3x10 ^{-3o}	1x10 ⁻⁴	
[(NH ₃) ₅ Co]O ₂ ⁵⁺	Fe ²⁺	2.0 M LiClO ₄	2.8x10 ^{-2p}	0.95 ^j	0.74 ^k	4.0 ^q	7x10 ⁻⁸	
	Ru(NH ₃) ₆ ²⁺	0.1 M LiClO ₄	3.7x10 ^{6r}	0.95 ^j	0.05 ^e	4x10 ^{3f}	4.9x10 ⁻⁴	

(Continued on next page)

Table II (cont.)
 Contrast in Outer-Sphere Electron-Transfer
 Reactivity of Dioxygen Complexes⁻

M_nO_2	Counter Reagent	Medium	k_{ab} $M^{-1}s^{-1}$	E^f (MO_2) V	E^f (Counter reagent) V	k_{exch} (Counter reagent) $M^{-1}s^{-1}$	k_{exch} (MO_2) $M^{-1}s^{-1}$
{[(NH ₃) ₄ Co] ₂ (O ₂ ,NH ₂) ₄ ⁺ }	Co(bpy) ₃ ²⁺	0.05 M KNO ₃	90 ^j	0.75 ^j	0.319 ^k	20 ^k	6.7x10 ⁻⁵
	Co(phen) ₃ ²⁺	0.05 M KNO ₃	32 ^j	0.75 ^j	0.39 ⁿ	40 ⁿ	4.8x10 ⁻⁵
{[(NH ₃) ₄ Co] ₂ (O ₂ ,NH ₂) ₃ ⁺ }	Ru(bpy) ₂ ³⁺	1.0 M HCl	3.4x10 ⁵ ^s	0;75 ^j	1.26 ⁿ	2.0x10 ⁹ ^h	1.2x10 ⁻⁶
	Ru(NH ₃) ₆ ²⁺	0.1 M NaClO ₄ (pH 2)	2.4x10 ⁵ ^t	0.22 ^t	0.05 ^e	4x10 ³ ^f	4.9x10 ⁶
{Co([14]laneN ₄) (OH ₂) ₂ ²⁺ }	Co(sep) ²⁺	0.2 M NaClO ₄	4.7x10 ⁵ ^t	0.22 ^t	-0.3 ^b	5.1 ^b	1.9x10 ⁶
	V ²⁺	0.1 M HClO ₄	1.8x10 ⁵ ^t	0.22 ^t	-0.226 ⁿ	3x10 ⁻³ ^o	8x10 ⁵
{Co([14]laneN ₄) (OH ₂) ₂ ⁺ }	Ru(NH ₃) ₄ (phen) ³⁺	0.1 M LiClO ₄	~9x10 ⁸ ^t	0.22 ^t	0.515 ^h	3.2x10 ⁶ ^h	1.6x10 ⁶
	V ²⁺	0.1 M HClO ₄	~9x10 ⁸ ^t	0.22 ^t	0.515 ^h	3.2x10 ⁶ ^h	1.6x10 ⁶

Table II (cont.)
 Contrast in Outer-Sphere Electron-Transfer
 Reactivity of Dioxygen Complexes^a

M_nO_2	Counter Reagent	Medium	k_{ab} $M^{-1} s^{-1}$	E^f (MO_2) V	E^f (Counter reagent) V	k_{exch} (Counter reagent) $M^{-1} s^{-1}$	k_{exch} (MO_2) $M^{-1} s^{-1}$
{ $(NH_3)_4Co$ } ₂ { $(O_2, NH_2)_4$ } ₄	$Co(bpy)_3^{2+}$	0.05 M KNO_3	90^j	0.75^j	0.319^k	20^k	6.7×10^{-5}
	$Co(phen)_3^{2+}$	0.05 M KNO_3	32^j	0.75^j	0.39^n	40^n	4.8×10^{-5}
{ $(NH_3)_4Co$ } ₂ { $(O_2, NH_2)_3$ } ₃	$Ru(bpy)_2^{3+}$	1.0 M HCl	3.4×10^{5s}	0.75^j	1.26^n	2.0×10^{9h}	1.2×10^{-6}
	$Ru(NH_3)_6^{2+}$	0.1 M $NaClO_4$ (pH 2)	2.4×10^{5t}	0.22^t	0.05^e	4×10^{3f}	4.9×10^6
{ $Co([14]aneN_4)$ } ₂ { $(OH_2)_2O_2$ } ₂	$Co(sep)^{2+}$	0.2 M $NaClO_4$	4.7×10^{5t}	0.22^t	-0.3^b	5.1^b	1.9×10^6
	V^{2+}	0.1 M HClO ₄	1.8×10^{5t}	0.22^t	-0.226^n	3×10^{-3o}	8×10^5
{ $Co([14]aneN_4)$ } ₃ { $(OH_2)_2O_2$ } ₃	$Ru(NH_3)_4(phen)^{3+}$	0.1 M $LiClO_4$	$\sim 9 \times 10^{8t}$	0.22^t	0.515^h	3.2×10^{6h}	1.6×10^6

(Continued on next page)

Notes for Table II.

- a 25°
- b Creaser, I. I.; Harrowfield, J. McB.; Herlt, A. J.; Sargeson, A. M.; Springborg, J.; Geue, R. J.; Snow, M. R. J. Am. Chem. Soc. 1977, 99, 3181.
- c Ilan, Y. A.; Czapski, G.; Meisel, D. Biochim. Biophys. Acta 1976, 430, 209.
- d Stanbury, D. M.; Hass, O.; Taube, H. Inorg. Chem. 1980, 19, 518.
- e Lim, H. S.; Barclay, D. J.; Anson, F. Inorg. Chem. 1972, 11, 1460.
- f Meyer, T. J.; Taube, H. Inorg. Chem. 1968, 7, 2369.
- g Brown, G. M.; Krentzien, H. J.; Abe, M.; Taube, H. Inorg. Chem. 1979, 18, 3374.
- h Brown, G. M.; Sutin, N. J. Am. Chem. Soc. 1979, 101, 883.
- i Lavallee, C.; Lavallee, D. K.; Deutsch, E. A. Inorg. Chem. 1978, 17, 2217.
- j McLendon, G.; Mooney, W. F. Inorg. Chem. 1980, 19, 2.
- k Yee, E. L.; Cave, R. J.; Guyer, K. L.; Tyma, P.D.; Weaver, M.J. J. Am. Chem. Soc. 1979, 101, 1131.
- l Chou, M.; Creutz, C.; Sutin, N. J. Am. Chem. Soc. 1977, 99, 5615.
- m Hoffman, A. B.; Taube, H. Inorg. Chem. 1968, 7, 1971.
- n Latimer, W. M. "Oxidation Potentials": 2nd Ed., Prentice-Hall: Englewood Cliffs, N. J., 1952.
- o Krishnamurthy, K. C.; Wahl, A. C. J. Am. Chem. Soc. 1958, 80, 5921.
- p Davies, R.; Sykes, A. G. J. Chem. Soc. (A) 1968, 2831.
- q Silverman, J.; Dodson, R. W. J. Phys. Chem. 1952, 56, 846.
- r Hand, T. D.; Hyde, M. R.; Sykes, A. G. Inorg. Chem. 1975, 14, 1720.
- s Chandrasekaran, K.; Natarajan, P. J. Chem. Soc. Dalton Trans. 1981, 478.
- t Kumar, K.; Endicott, J. F., work in progress.

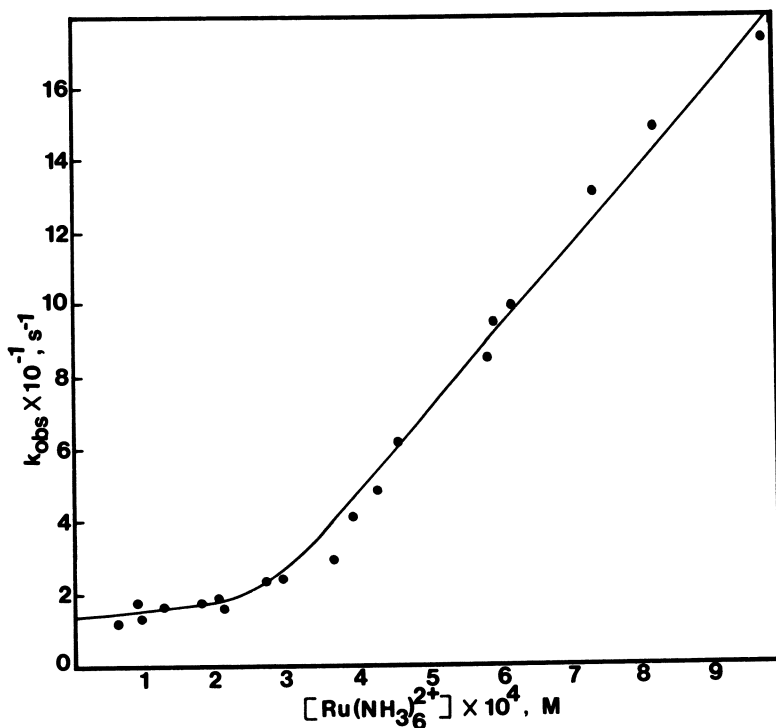
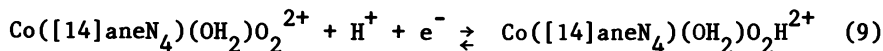
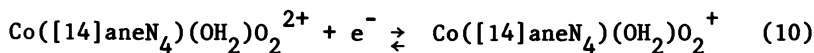


Figure 1. Competition kinetics for the $\text{Ru}(\text{NH}_3)_6^{2+}$ reduction of $\text{Co}([\text{14}]\text{aneN}_4)(\text{OH}_2)\text{O}_2^{2+}$. Reactions at 25°C , $\text{pH } 2$, and $\mu = 0.1(\text{NaClO}_3)$. Individual pseudo-first-order rate constants were determined from the exponential (to four half-lives) decay of $\text{Co}([\text{14}]\text{aneN}_4)(\text{OH}_2)\text{O}_2^{2+}$ absorbance at 360 nm . Reactions were performed by mixing a solution containing $\text{Ru}(\text{NH}_3)_6^{2+}$ and $\text{Co}([\text{14}]\text{aneN}_4)(\text{OH}_2)_2^{2+}$ ($1 \times 10^{-3} \text{ M}$) with a solution saturated in O_2 ($1.2 \times 10^{-3} \text{ M}$) in an Aminco stopped-flow system.

versible reduction potential for the $\text{Co}([\text{14}] \text{aneN}_4)(\text{OH}_2)\text{O}_2^{2+,+}$ couple. Geiger and Anson (17) have observed an irreversible oxidation of $\text{Co}([\text{14}] \text{aneN}_4)(\text{OH}_2)\text{O}_2\text{H}^{2+}$ at ~ 1 V and have argued that this is a reasonable potential for the half-reaction (9):



We have found the outer sphere reductions to be nearly pH independent, which argues that protonation occurs after electron transfer and that $\text{pK}_a < 1$ for $\text{Co}([\text{14}] \text{aneN}_4)(\text{OH}_2)\text{O}_2\text{H}^{3+}$. Consequently, we propose that the reversible couple is:



In order to estimate the potential for (10) we have combined kinetic data for several outer-sphere reductions of $\text{Co}([\text{14}] \text{aneN}_4)(\text{OH}_2)\text{O}_2^{2+}$ with data for the $\text{Ru}(\text{NH}_3)_4(\text{phen})^{3+}$ oxidation of $\text{Co}([\text{14}] \text{aneN}_4)(\text{OH}_2)\text{O}_2\text{H}^{2+}$. The cross-reaction rate constants, k_{ab} , are given in Table II. In the pH range 1-4.5, the predominant peroxo species has been found to be $\text{Co}([\text{14}] \text{aneN}_4)(\text{OH}_2)\text{O}_2\text{H}^{2+}$. The oxidation of this species decreased in rate with increasing $[\text{H}^+]$. From this acid dependence we infer $k_{ab} \sim 10^8 \text{ M}^{-1}\text{s}^{-1}$ for the $\text{Ru}(\text{NH}_3)_4(\text{phen})^{3+}/\text{Co}([\text{14}] \text{aneN}_4)(\text{OH}_2)\text{O}_2\text{H}^{2+}$ reaction, and we find $E^0 \sim 0.22\text{V}$, $k_{aa} \sim 10^5 \text{ M}^{-1}\text{s}^{-1}$ for the $\text{Co}([\text{14}] \text{aneN}_4)(\text{OH}_2)\text{O}_2^{2+,+}$ couple (18). Thus the $\text{Co}([\text{14}] \text{aneN}_4)$ -dioxxygen adduct has a smaller intrinsic barrier to electron transfer than the other dioxxygen species reported (see Table II). However, this adduct is a relatively weak oxidant.

Studies of the simple electron transfer properties of coordinated dioxxygen are in a preliminary stage. The definition of reactivity patterns is obscured by inconsistencies and the lack of key pieces of information, as indicated by the comments above. Nevertheless, there is hope that some general features will emerge:

- (i) All the dioxxygen species investigated exhibit appreciable intrinsic barriers to one electron transfer. The source of the intrinsic barriers is not totally clear, although a large solvation component is often implicated. This feature can contribute to a preference for adduct formation when this pathway is available (see below).

- (ii) Even in simple electron transfer reactions, we seem to find that there are two advantages of coordination by O_2 . First, there is a thermodynamic advantage of coupling adduct formation and electron transfer; this advantage appears to originate in the stability of M- O_2 bonding interactions. Second, the simple MO_2 adducts may have a relatively small intrinsic barrier for electron transfer to the coordinated O_2 moiety.

Adduct Formation

Most known reactions of dioxygen species involve inner-sphere pathways, or adduct formation. Our studies of the inner-sphere reactions of $Co([14]aneN_4)(OH_2)O_2^{2+}$ have so far employed as potential inner sphere reagents, $S \cdot = Co([14]aneN_4)-(OH_2)_2^{2+}$, $Co([15]aneN_4)(OH_2)_2^{2+}$, and Fe^{2+} (Table III).

The kinetics of the reaction of $Co(N_4)(OH_2)_2^{2+}$ with $Co([14]aneN_4)(OH_2)O_2^{2+}$ have been reported in detail (13) and involve formation of an isolable μ -peroxo complex (19). The $Fe^{2+}/Co([14]aneN_4)(OH_2)O_2^{2+}$ reaction also results in formation of a new intermediate species, apparently the mixed metal μ -peroxo complex, $((H_2O)_5Fe-O-O-Co([14]aneN_4)(OH_2))^{4+}$. This new species has about a 1 s lifetime (aqueous solution, 25C, excess Fe^{2+}) and a unique absorption spectrum (Figure 2). The ultimate products of this reaction are $Co([14]aneN_4)(OH_2)_2^{3+}$ and Fe^{3+} (20). A few minutes after mixing the reactants, the product mixture contains a substantial amount (> 60%) of $Co([14]aneN_4)(OH_2)-O_2H^{2+}$ and some $[H_2OCo([14]aneN_4)]_2O_2^{4+}$.

The kinetic advantage to the inner-sphere pathway is nicely illustrated in Figure 3 in which the kinetic data are treated as one would treat outer-sphere electron transfer reactions. Thus, for reactants designated with a and b subscripts,

$$k_{ab} = 10^{11} \exp(-\Delta G_{ab}^\ddagger / RT)$$

$$\Delta G_{ab}^\ddagger = \frac{1}{2}(\Delta G_{aa}^\ddagger + \Delta G_{bb}^\ddagger) + \frac{1}{2}\Delta G_{ab}^\circ + (\Delta G_{ab}^\circ)^2 / 8(\Delta G_{aa}^\ddagger + \Delta G_{bb}^\ddagger)$$

The use of outer-sphere parameters predicts a much larger activation barrier (or smaller rate constant) than is actually observed. It appears that much of this kinetic advantage derives from differences in the equilibrium constants for outer-

Table III.
 Summary of Rate Constants for Adduct Formation:
 $\text{Co}([\text{14}]\text{aneN}_4)(\text{OH}_2)_2^{2+} + \text{S} \rightarrow [(\text{H}_2\text{O})([\text{14}]\text{aneN}_4)\text{Co} - \text{O}_2 - \text{S}]$

S	Medium	k_4 $\text{M}^{-1}\text{s}^{-1}$	$E^f(\text{s}')$ V(NHE)	$k_{\text{exch}}(\text{s}'/\text{s}^+)$ $\text{M}^{-1}\text{s}^{-1}$
Fe^{2+}	0.2 M NaClO_4 + 0.1 M HClO_4	1.1×10^3 a	0.74 b	5 c
$\text{Co}([\text{14}]\text{aneN}_4)(\text{OH}_2)_2^{2+}$	0.2 M HClO_4	4.9×10^5 d	0.42 d	8×10^{-4} e
$\text{Co}([\text{15}]\text{aneN}_4)(\text{OH}_2)_2^{2+}$	0.1 M HClO_4	3.7×10^4 a	0.65 a	6×10^{-3} a

a Kumar, K.; Endicott, J. F., work in progress.

b Latimer, W. M. "Oxidation Potentials"; 2nd ed.; Prentice-Hall: Englewood Cliffs, N. J., 1952.

c Silverman, J.; Dodson, R. W. *J. Phys. Chem.* 1952, 56, 846.

d Ref. 13.

e Endicott, J. F.; Durham, B.; Glick, M. D.; Anderson, T. J.; Kuszaj, J. M.; Schmonsees, W. G.; Balakrishnan, K. P., *J. Am. Chem. Soc.* 1981, 103, 1431.

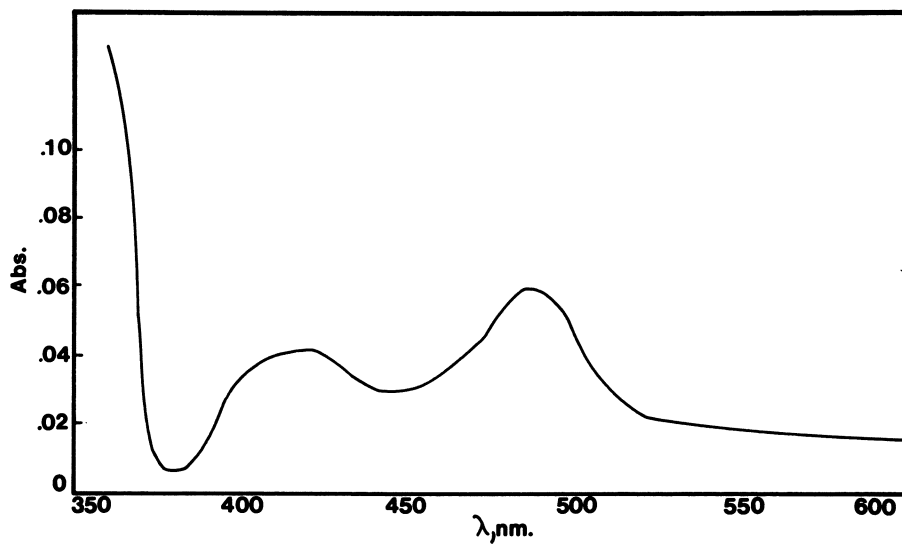


Figure 2. Absorption spectrum of $[H_2O([14]aneN_4)Co-O-O-Fe]^{4+}$. Determined point-by-point in 0.1 M $HClO_4$ and 0.2 M $NaClO_4$ at ~ 100 ms after mixing. Solutions initially contained 6×10^{-4} M $Co([14]aneN_4)(OH_2)_2^{2+}$, 6.3×10^{-4} M O_2 , and 0.26 M Fe^{2+} .

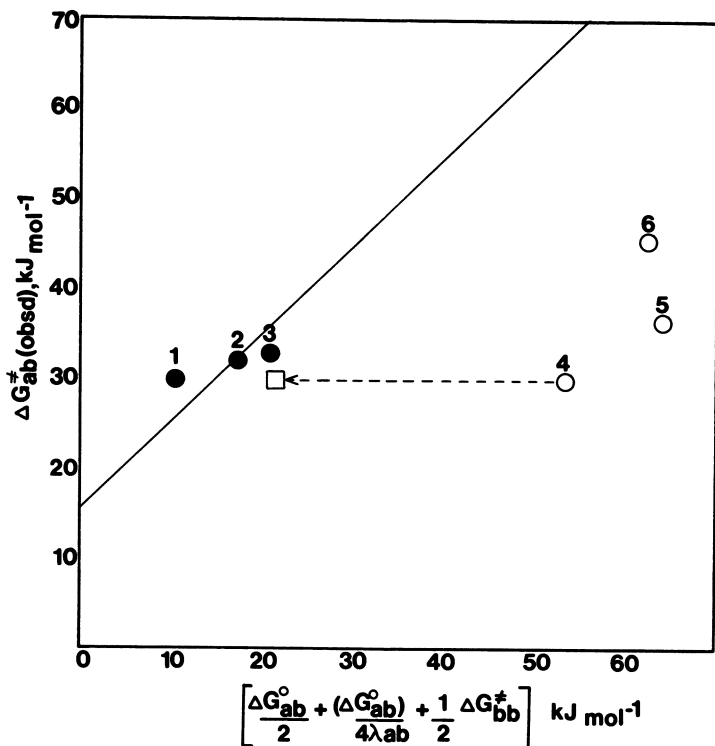


Figure 3. Outer-sphere correlation of the rates of various reductions of $\text{Co}([\text{14}] \text{aneN}_4)(\text{OH}_2)_2^{2+}$. Outer-sphere reductants (●) are: $\text{Co}(\text{sep})^{2+}$, 1; $\text{Ru}(\text{NH}_3)_6^{2+}$, 2; and V^{2+} , 3. Potentially inner-sphere reductants (○) are: $\text{Co}([\text{14}] \text{aneN}_4)(\text{OH}_2)_2^{2+}$, 4; $\text{Co}([\text{15}] \text{aneN}_4)(\text{OH}_2)_2^{2+}$, 5; and Fe^{2+} , 6. Values of $\Delta G_{\text{ab}}^\circ$ and $\Delta G_{\text{bb}}^{\ddagger}$ appropriate for outer-sphere electron transfer have been used for both open and solid circles. The open square corresponds to use of the measured K_{ab} for the reaction of $\text{Co}([\text{14}] \text{aneN}_4)(\text{OH}_2)_2^{2+}$ with $\text{Co}([\text{14}] \text{aneN}_4)(\text{OH}_2)_2^{2+}$. The solid line has been drawn with unit slope through the solid circles.

sphere electron transfer and for adduct formation. For example, use of the measured equilibrium constant for the $\text{Co}([\text{14}] \text{aneN}_4)(\text{OH}_2)_2^{2+} / \text{Co}([\text{14}] \text{aneN}_4)(\text{OH}_2)_2^{2+}$ reaction does reduce the magnitude of the deviation from the outer-sphere correlation (see Figure 3). In addition, parameters used in the present analysis suggest that the net intrinsic barrier to adduct formation is smaller than the barrier to simple electron transfer.

Hydrogen Atom Abstraction

We have made a few preliminary attempts to observe reaction (5). As yet we have found no evidence for such a typically radical reaction of $\text{Co}([\text{14}] \text{aneN}_4)(\text{OH}_2)_2^{2+}$. For example, we found no reaction with 2-propanol ($k_5 < 20 \text{ M}^{-1} \text{ s}^{-1}$), ascorbic acid, or allyl alcohol. Since the $\text{Co}([\text{14}] \text{aneN}_4)(\text{OH}_2)_2^{2+}$ adduct is reasonably stable, one would expect to observe reaction (5) only when exceptionally stable radicals ($\text{S}\cdot$) are formed. We do have some preliminary indications that reactive radicals are formed in the decomposition of $\text{Co}([\text{14}] \text{aneN}_4)(\text{OH}_2)_2\text{H}^{2+}$.

Oxygen Atom Transfer

Our studies of reaction (6) are only just commencing. Some of the very obvious and simple reagents have proved unreactive; e.g., $\text{P}\phi_3$ ($k_6 < 10^4 \text{ M}^{-1} \text{ s}^{-1}$) and SO_2 ($k_6 \leq 20 \text{ M}^{-1} \text{ s}^{-1}$). Consideration of reaction (6) suggests that these reactions fail, despite the stability of the $\text{O-P}\phi_3$ and SO_3 products, because the primary product cobalt species is an unstable cobalt(III)-radical complex, $\text{Co}(\text{O}\cdot^-)$. This, in turn, suggests that oxygen atom transfer could succeed if accompanied by electron transfer. We have found a facile reaction with $\text{S}_2\text{O}_4^{2-}$, presumably a reaction of $\text{SO}_2\cdot^-$; however this is most likely an outer sphere electron transfer reaction.

An attempt to combine electron transfer with atom transfer, employing a $\text{Cu}(\text{C}_2\text{H}_4)^+$ reductant, has resulted only in formation of $\text{Co}([\text{14}] \text{aneN}_4)(\text{OH}_2)_2\text{H}^{2+}$, presumably by means of a pathway involving a μ -peroxo, mixed metal binuclear intermediate as described above (21).

An additional constraint, mitigating against oxygen atom transfer in Co-O_2 adducts, may be the requirement of proton transfer to stabilize the $\text{Co}^{\text{III}}(\text{O}^{2-})$ product. This constraint

would be eliminated if the reaction produced a M=O product. Such a pathway may be a possibility with the oxygen adducts of chromium(II). Thus, the rapid $\text{Cr}^{2+}/\text{O}_2$ reaction (22) produces a product which persists for relatively long time periods (23) and which is strongly oxidizing towards simple electron transfer agents (18, 23). At the present time the chromium systems are not well characterized.

Heterolytic or Homolytic Displacement

Metal ion catalyzed substitutions for the halide (or methyl) ligands of cobalt(III) complexes are well documented (24, 25). Mercury(II) is particularly effective in catalyzing such simple hydrolytic substitutions on Co(III). However, Hg^{2+} does not affect the decay of $\text{Co}([\text{14}] \text{aneN}_4)(\text{OH}_2)\text{O}_2^{2+}$ during its short lifetime ($k < 10^3 \text{ M}^{-1} \text{ s}^{-1}$).

The homolytic transfer of coordinated O_2 , formally as O_2^{2-} , seems likely to be a more easily observed process provided the substrate can function as a two-electron donor.

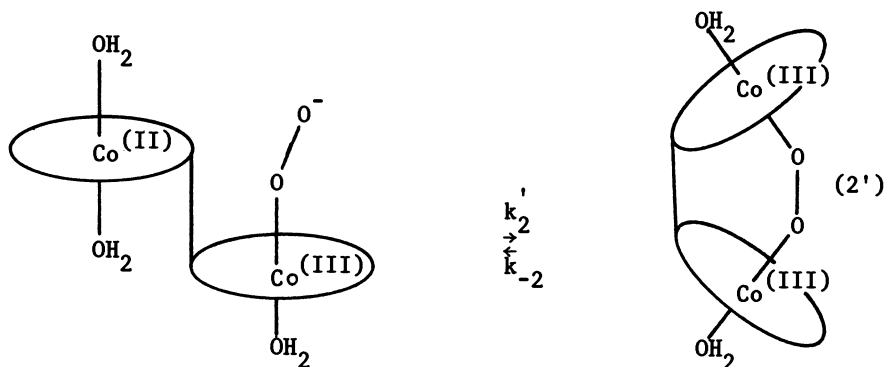
Summary Comments

A large range of intrinsic reactivities has been identified for O_2/O_2^- , $\text{M}(\text{O}_2^-)/\text{M}(\text{O}_2^{2-})$, and $\text{M}(\text{O}_2^-)\text{-M}/\text{M}(\text{O}_2^{2-})\text{-M}$ couples. The factors contributing to the large intrinsic barriers to electron transfer, or to their variation, are not yet understood. The $\text{Co}([\text{14}] \text{aneN}_4)(\text{OH}_2)\text{O}_2^{2+,+}$ couple appears to have the smallest intrinsic barrier to electron transfer yet found among such dioxygen systems. Largely for thermochemical reasons, the inner-sphere pathway tends to be favored over the outer-sphere pathway in reactions of $\text{Co}([\text{14}] \text{aneN}_4)(\text{OH}_2)\text{O}_2^{2+}$.

Perhaps the most interesting of the inner-sphere pathways are those which result in the net transfer of an oxygen atom. The factors governing the viability of this pathway are still speculative. For cobalt- O_2 adducts, thermochemical considerations suggest that oxygen atom transfer should be accompanied by electron transfer in the reverse direction. Similarly, this pathway should be enhanced for MO_2 complexes in which the metal M can formally transfer an electron to the remaining O-atom (e.g., $\text{M}^{\text{II}}\text{-O}^- \rightarrow \text{M}^{\text{III}}\text{=O}$).

In contrast to the relative ease of reduction of $\text{Co}([\text{14}] \text{aneN}_4)(\text{OH}_2)\text{O}_2^{2+}$, the μ -peroxo complex $[\text{H}_2\text{OCo}([\text{14}] \text{aneN}_4)]_2\text{O}_2^{4+}$ is

very difficult to reduce. One possible route to enhancing the reactivity of μ -peroxo complexes might be to labilize the Co-(O₂Co) bond (k_{-2}) to facilitate formation of a reactive superoxo intermediate. One means of accomplishing this labilization is steric, as in a binuclear complex in which the Co-O-O-Co bond angles are somewhat distorted. Thus if reaction (2) is unimolecular, as in (2'),



the percentage of oxygen bound can be quite large even if $k'_2 \sim k_{-2}$. We have initiated studies of a singly coupled bis-macro-cyclic-dicobalt complex (26) in which $k'_2 \sim 6 \text{ s}^{-1} > k_{-2}$. In complexes such as cofacial porphyrins (27), where k_{-2} need not be accompanied by large conformational changes or water substitution, both k'_2 and k_{-2} could be large, and k_{-2} could provide an efficient kinetic pathway for dioxygen reduction via a superoxo intermediate.

There are an amazing number of complex mechanistic issues connected with the reactivity of dioxygen complexes of transition metals. It is to be hoped that future studies of well defined systems will resolve some of these issues.

Abbreviations

[14]aneN₄ = 1,4,8,11-tetraazacyclotetradecane

[15]aneN₄ = 1,4,8,12-tetraazacyclopentadecane

sep = sepulchrate =

(S)-1,3,6,8,10,13,16,19-octaazabicyclo[6.6.6] eicosane

Acknowledgment

We are grateful to the National Institutes of Health for partial support of the research reported here from our laboratories.

Literature Cited

1. Taube, H. J. Gen. Physiol. 1965, 49, 29.
2. Schultz, J.; Cameron, B. F., Eds. "The Molecular Basis for Electron Transport"; Academic Press: New York, N.Y., 1972.
3. Bennett, L. E. Progr. Inorg. Chem. 1973, 18, 1.
4. Fallab, S. Angew Chem., Int. Ed. Engl. 1967, 6, 496.
5. Hayaishi, O., Ed. "Molecular Mechanisms of Oxygen Activation"; Academic Press: New York, N.Y., 1974.
6. Spiro, T. G., Ed. "Metal Ion Activation of Dioxygen"; Wiley: New York, 1980.
7. Basolo, F.; Hoffman, B. M.; Ibers, J. A. Acc. Chem. Research 1976, 9, 175.
8. McLendon, G.; Martell, A. E. Cood. Chem. Rev. 1976, 18, 125.
9. Sykes, A. G.; Weil, J. A. Progr. Inorg. Chem. 1970, 13, 1.
10. Wilkins, R. G. Adv. in Chem. Ser. 1971, 100, 111.
11. Collman, J. P. Acc. Chem. Res. 1977, 10, 265.
12. Drago, R. S.; Corden, B. B.; Zombeck, A. Comments on Inorg. Chem. 1981, 1, 53.
13. Wong, C.-L.; Switzer, J. A.; Balakrishnan, K. P.; Endicott, J. F. J. Am. Chem. Soc. 1980, 102, 5511.
14. Marcus, R. A. Annu. Rev. Phys. Chem. 1964, 15, 155.
15. Stanbury, D. M.; Haas, O.; Taube, H. Inorg. Chem. 1980, 19, 518.
16. Switzer, J. A., Ph. D. Dissertation: Wayne State University, 1979.
17. Geiger, T.; Anson, F. J. Am. Chem. Soc. 1981, 103, 7489.
18. Kumar, K.; Endicott, J. F., work in progress.
19. Bosnich, B.; Poon, C. K.; Tobe, M. L. Inorg. Chem. 1966, 5, 1514.
20. Wong, C.-L.; Endicott, J. F. Inorg. Chem. 1981, 20, 2233.
21. Munakata, M.; Endicott, J. F., work in progress.
22. Sellers, R. M.; Simic, M. G. J. Chem. Soc., Chem. Commun. 1975, 4.
23. Ramasami, T., private communication.
24. Olson, A. R.; Simonson, T. R. J. Chem. Phys. 1949, 49, 1167.
25. Ridley, W. P.; Dizikes, L. J.; Wood, J. M. Science 1977, 197, 329.
26. Mares, I.; Switzer, J. A.; Endicott, J. F., work in progress.
27. Collman, J. P.; Denisevich, P.; Konai, Y.; Marrocco, M.; Koval, C.; Anson, F. C. J. Am. Chem. Soc., 1980, 102, 6027.

RECEIVED April 27, 1982.

General Discussion—Reactivity of Coordinated Dioxgen

Leader: David Stanbury

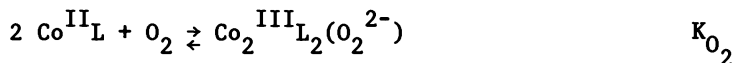
DR. ANTHONY POE (University of Toronto): A somewhat related feature is shown by the reaction of $\text{Re}_2(\text{CO})_{10}$ with triphenylphosphine under oxygen. This is a slow reaction that goes very cleanly at 160-170C to form the substituted product $\text{Re}_2(\text{CO})_8(\text{P}\Phi_3)_2$. When one runs the reaction under oxygen, one still obtains virtually 100% yield of the product, but copious quantities of triphenylphosphine oxide are formed at the same time. This means that the reactive intermediate, which is present at steady-state concentrations, is highly reactive towards oxidizing triphenylphosphine. We think it is an $\cdot\text{Re}(\text{CO})_5\text{O}_2$ intermediate radical species, which is somewhat similar electronically to the system you were discussing.

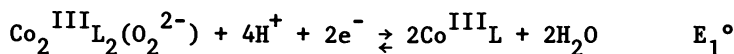
DR. ENDICOTT: In fact, the cobalt-cyclam-oxygen adduct can have a very short lifetime depending on the competition reactions. If the cobalt dioxgen adduct is generated in the presence of greater concentrations of $\text{Co}^{\text{II}}([\text{14}] \text{aneN}_4)$, the intermediate lifetime is clearly shortened. The classical studies made by Ralph Wilkins, for instance, were carried out under conditions in which intermediates only achieved small stationary state concentrations.

We have attempted to find conditions which will allow us to watch the species build up, to isolate it kinetically, and to observe its reactions directly. That does not imply that the intermediate is unreactive. The remarkable feature of the intermediate in your rhenium system is the apparently facile oxygen atom transfer.

DR. THOMAS MEYER (University of North Carolina): Does anyone have any further comments to make about Collman's [Collman, J. P.; Denisevich, P.; Konai, Y.; Marrocco, M.; Koval, C.; Anson, F. C. *J. Am. Chem. Soc.* 1980, 102, 6027] observation of the rapid catalytic reduction of O_2 in cofacial porphyrins?

DR. DAVID STANBURY (Rice University): With regard to the problem of the electrocatalytic reduction of oxygen, I have attempted to formalize some ideas regarding the constraints of thermodynamics in order to elucidate the probable character of cobalt complexes which may catalyze the oxygen electrode via binuclear peroxo-bridged intermediates. The following gross mechanism is presupposed:





The net reaction is then



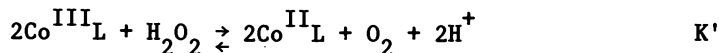
and, therefore,

$$E_3^\circ = 1.23 \text{ V} = \frac{1}{2}(E_1^\circ + E_2^\circ) + 6.42 \times 10^{-3} \ln K_{\text{O}_2}$$

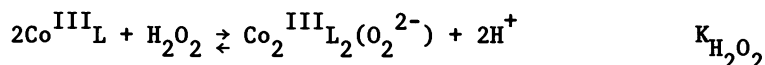
where the conventions are 25C, aqueous solution, one atmosphere O_2 , and the normal hydrogen electrode. Note that for the ideal electrode

$$E_3^\circ = E_2^\circ = E_1^\circ \text{ and } K_{\text{O}_2} = 1 \text{ atm}^{-1}\text{M}^{-1}$$

With an eye towards useful and interesting catalysts rather than ideal catalysts, we ask: what are the constraints imposed by a half-cell operating at voltages greater than 0.69 V, the approximate E° value for $\text{O}_2/\text{H}_2\text{O}$? There seem to be two well-defined constraints. One is that E_2° must not be much less than 0.69 V; if it were otherwise, then only a small fraction of the catalyst would be in the reduced state and available for oxygenation. This constraint is indicated by the vertical line in Figure 1. The second constraint is that the peroxo-bridged intermediate must be more stable than free hydrogen peroxide. This is formulated by first defining K'



such that $K' = \exp(38.93(2)(E_2^\circ - 0.69))$ and then defining $K_{\text{H}_2\text{O}_2}$ as in



such that $K_{\text{H}_2\text{O}_2} = K'K_{\text{O}_2}$. Note that $K_{\text{H}_2\text{O}_2}$ is a dimensionless quantity and is thus an absolute measure of the ability of the catalyst to stabilize peroxide. Therefore, $K_{\text{H}_2\text{O}_2}$ must exceed

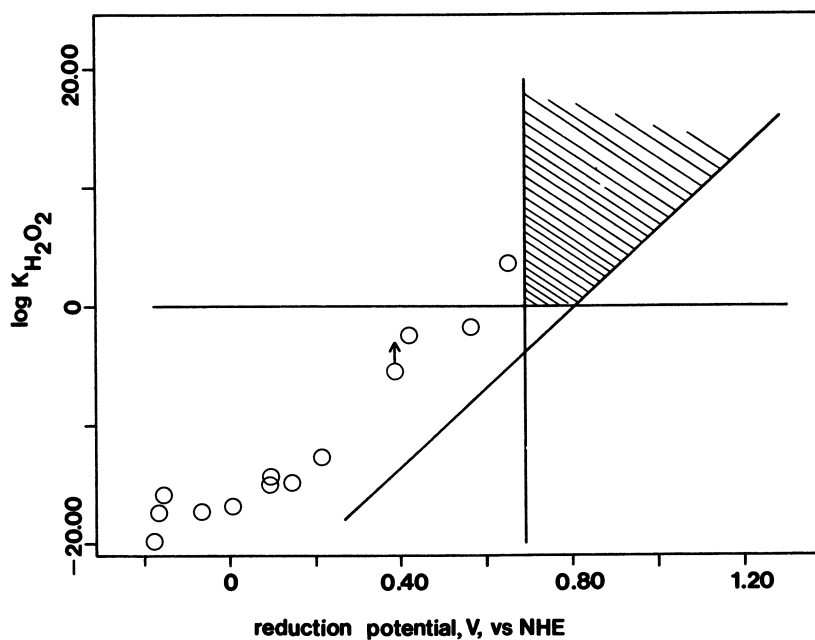


Figure 1. Thermochemical constraints on potential catalysts of the O_2/H_2O couple. Ideal catalysts should fall into the shaded region, based on their abilities to stabilize peroxide (see text).

unity for a useful catalyst. This constraint is indicated in Figure 1 by the horizontal line.

A third constraint, which is not quite as well defined, arises from a consideration of rates of oxygenation. A reasonable estimate is that a good rate will impose an upper limit of 5 kcal on K_{O_2} . This constraint results in the diagonal line in Figure 1.

These three constraints define the shaded area in Figure 1. This area is the place to look for interesting catalyst candidates.

The recent data of Martell [Harris, W. R.; McLendon, G. L.; Martell, A. E.; Bess, R. C.; Mason, M. *Inorg. Chem.* 1980, **19**, 21] and of Endicott [Wong, C.-L.; Switzer, J. A.; Balakrishnan, K. P.; Endicott, J. F. *J. Am. Chem. Soc.* 1980, **102**, 5511] provide hope that such candidates can be designed. Their data for a variety of $Co^{II}L$ complexes are presented in Table I and are also plotted in Figure 1. The plot shows an encouraging trend--of increasing $K_{H_2O_2}$ with increasing E_f . Extrapolation leads

directly into the area of interest. Incidentally, this trend is consistent with the notion of peroxide as a donor ligand.

Although these data are encouraging, they should be viewed with some caution. In the case of Martell's work, there is considerable uncertainty as to the nature of the coordination environments to which E_2° refers. In the case of Endicott's data, various laboratories have reported different E_2° values.

An unanswered question is: what additional constraints will be imposed when a detailed analysis of E_1° is performed? Step E_1° includes the transfer of 2 electrons and 4 protons and the cleavage of the O-O bond. The considerable mechanistic complexity here is an area for future investigation.

There is one further caveat. The above arguments have been developed in terms of a mononuclear catalyst. At the very least some entropy corrections will be needed for comparison with binuclear catalysts. [Note: These considerations were developed during postdoctoral work at Stanford University with Professor Henry Taube.]

Table I
Thermodynamic Properties of Cobalt Complexes
Reacting with Oxygen

Ligand	E_f, V	$\log K_{O_2}$	$\log K'$	$\log K_{H_2O_2}$
TEP	-0.156	12.83	-28.65	-15.82
4-imDIEN	-0.176	9.57	-29.33	-19.76
EPYDEN	-0.166	11.56	-28.99	-17.33
PYDIEN	-0.066	8.36	-25.61	-17.25
PYDPT	+0.114	4.7	-19.52	-14.82
IMDPT	+0.004	6.44	-23.24	-16.80
2-IMDPT	+0.094	5.28	-20.20	-14.92
(hys) ₂	+0.214	3.5	-16.14	-12.64
(Pap) ₂	+0.094	5.9	-20.20	-14.30
[15]aneN ₄	+0.65	5±1	- 1.35	> + 3.65
[14]aneN ₄	+0.42	6.8	- 9.17	- 2.37
Me ₂ [14]1,11- dieneN ₄	+0.384	> 5	-10.39	> - 5.39
Me ₆ [14]4,11- dieneN ₄	+0.564	2.6	- 4.30	- 1.70

Collman may well have entered the "region of interest" with his face-to-face porphyrin; it seems to be in a region where the peroxide is in a considerably different stability regime from anything that has been looked at so far. So it is quite conceivable he does have something special going on.

DR. HENRY TAUBE (Stanford University): Another interesting point about Collman's complex should be noted. Let us presume that a peroxide intermediate is generated in his case. In all of Dr. Endicott's examples, the remarkable observation is that it is very difficult to reduce the O-O bond kinetically in the binuclear μ -peroxo complexes. In Collman's case, this reduction

American Chemical
Society Library
1155 16th St. N. W.

occurs at potentials as positive as +0.7 V. That is a purely kinetic phenomenon which we would like to understand. I think that this difference in behavior between Collman's system and the systems studied by Endicott and by Martell is quite remarkable.

DR. ALBERT HAIM (State University of New York at Stony Brook): Dr. Endicott has discussed the reactions of bound oxygen. I would like to comment on the outer-sphere reactions of free oxygen.

In approaching this problem I thought I would do something useful with the reaction between excited state $\text{Ru}(\text{bpy})_3^{2+}$ and paraquat (PQ^{2+}). If you leave a little oxygen in the system, the paraquat radical formed in the quenching step reacts with oxygen and produces O_2^- . This is a very nice way of generating O_2^- radical. The PQ^+/O_2 reaction (rate constant of about $10^9 \text{ M}^{-1}\text{s}^{-1}$) competes effectively with the $\text{PQ}^+/\text{Ru}(\text{bpy})_3^{3+}$ reaction. Consequently, following the efficient quenching of $^*\text{Ru}(\text{bpy})_3^{2+}$ by PQ^{2+} and the PQ^+-O_2 reaction, one may observe directly the recombination of O_2^- and ruthenium(III) at 450 nm. The reaction rate may be studied as a function of pH to produce a kinetic titration curve. The limiting reaction at high pH involves $\text{Ru}(\text{bpy})_3^{3+}$ and O_2 . The reaction rate slows in proportion to the extent of protonation of O_2^- . Using Bielski's [Bielski, B. H. J., *Photochem. Photobiol.* 1978, 28, 645] value for the pK_a of HO_2^- , we infer that the O_2^- reaction is diffusion controlled and the HO_2^- species is essentially unreactive. Thus, even in acid solution, the little bit of O_2^- in equilibrium with HO_2^- carries the reaction. The potentials of the oxygen and ruthenium couples are sufficient to make singlet oxygen, so one must actually determine whether singlet or triplet oxygen is produced.

Let us reconsider the original $^*\text{Ru}$ quenching reaction. Why is paraquat required as a mediator in order to bring about the electron transfer from $^*\text{Ru}$ to oxygen to produce O_2^- which is then followed by the reaction of O_2^- with ruthenium(III)? Why can't this reaction take place directly?

The explanation for this is found in the 1973 report by Demas [Demas, J. N.; Diementi, D.; Harris, E. W. *J. Am. Chem. Soc.* 1973, 95, 6865.] in which he noted that the reaction of $^*\text{Ru}$

with oxygen does not produce O_2 . Rather oxygen quenches $*Ru$ with a rate constant (in aqueous solution) of $3.3 \times 10^9 M^{-1}s^{-1}$. But there is no net reaction, only energy transfer. Demas demonstrated that by putting traps in methanol, not in water. He obtained singlet oxygen in high yields. The resulting interpretation is that the reaction of $*Ru$ with oxygen produces a singlet oxygen directly.

In 1976 Dr. Sutin [Lin, C.-T.; Sutin, N. *J. Phys. Chem.* 1976, 80, 77] placed a footnote in one of his articles suggesting the possibility that $*Ru$ reacts with O_2 to make O_2^- , which then turns around and back reacts with ruthenium(III) to produce singlet oxygen.

Drs. Stanbury and Taube [Stanbury, D. M.; Mulac, W. A.; Sullivan, J. D.; Taube, H. *Inorg. Chem.* 1980, 19, 3735] have also commented on the Demas study. They have used a rate constant for the self-exchange involving $O_2-O_2^-$ to calculate the rate constant for the $*Ru$ oxygen reaction. They obtained a value of $\sim 2 \times 10^9 M^{-1}s^{-1}$, which is very close to the value of $3.3 \times 10^9 M^{-1}s^{-1}$ which Demas measured. They have noted that these results suggest that Demas' arguments may not be very conclusive. I would like to suggest that it is not possible to distinguish between the energy transfer and the electron transfer mechanism for the reaction of $*Ru(bpy)_3^{2+}$ with O_2 without doing a complete kinetic analysis of the systems with and without paraquat.

The pertinent experiment is to take the system where we know that we are making O_2 from the paraquat system and determine what kind of oxygen we are obtaining from the recombination reactions. We can then repeat Demas' experiment in aqueous solution and compare the results. Unfortunately, it is very difficult to find soluble traps for singlet oxygen in aqueous solution. So one has to utilize one of these "soups". The soup which I have used contains O_2 , DPBF, D_2O , paraquat, and a detergent. This composition was selected on the basis of a paper in 1979 by Lindig and Rodgers [Lindig, D. A.; Rodgers, M. A. *J. Phys. Chem.* 1979, 83, 1683] in which they studied the lifetime of the singlet oxygen state in aqueous solution by solubilizing this trap by means of an aqueous micellar dispersion.

The rate constant for the reaction of the trap with singlet oxygen is very high. In D_2O the lifetime of the singlet oxygen is relatively long, 53 microseconds. Thus, the critical experiment consists of placing excited state ruthenium(II), paraquat, oxygen, and the trap in D_2O , and observing whether the trap disappears at the rate which Lindig and Rodgers reported or, alter-

natively, whether there is no consumption. Then the experiment is repeated in the absence of paraquat.

Fortunately, we obtained four measurements, two for each one of these systems. So I believe they are good results.

In the case of the system containing paraquat, we are certain that there is O_2^- . The reaction of O_2^- and ruthenium(III) consumes the singlet trap. Therefore, we conclude that the reaction produces singlet oxygen. Repeating Demas' experiment, but now in aqueous solution, the trap disappears at the rate which Lindig and Rodgers reported and in the amount required for high yields of singlet oxygen in this reaction.

So we conclude that the excited state ruthenium(II)-oxygen reaction produces singlet oxygen, as does the one involving ruthenium(III) and O_2^- .

DR. KENNETH KUSTIN (Brandeis University): I would like to bring to your attention a developing field which I believe should be getting more notice from mechanistic inorganic chemists, namely, the field of oscillating reactions. Up until recently, the only oscillators that had been discovered were discovered by serendipity. But now we are involved in a specific program of trying to design new oscillating systems based on chemical principles rather than relying on accidental discoveries. And we appear to be having considerable success.

Our progress in this field depends on two techniques that have not been mentioned previously at this conference. First of all, those of us who learned something about relaxation will appreciate the fact that one can use conventional equipment for carrying out relaxation experiments. When one has a complicated waveform, as is the case in oscillating reactions, there is still no reason why that waveform cannot be perturbed by, for example, injecting into the system a pulse of some reactant and then observing the change (that is, the relaxation) that ensues. This perturbation and the ensuing relaxation can then be analyzed in the typical fashion. Thus, one can still use a concentration jump experiment in an operating system.

The other technique which has proved valuable in this area is computer simulation. When the kinetic data become very complicated, as with oscillating reactions involving two elementary steps, it is still possible to obtain rate constants from the data by doing computer simulation. That is actually not as outlandish as it might appear. It is really in the same category as the Fourier transform approach. I think this is an area that will make a considerable impact upon inorganic kinetic studies in the future.

Inorganic Reaction Mechanisms—Past, Present and Future

RALPH G. WILKINS

New Mexico State University, Department of Chemistry, Las Cruces, NM 88003

Studies of inorganic reaction kinetics continue to develop in sophistication and scope. A number of important issues and areas of study which have not been emphasized in previous papers in this volume are singled out for discussion. Of particular importance is the application of techniques for the generation and detection of short-lived transient species of mechanistic interest. A variety of combinations of laser flash photolysis or pulse radiolysis with resonance Raman, epr, rapid scan spectrophotometry, etc., give hope for the characterization of reactive intermediates of chemical significance. The further study of some slower substitution reactions has continued to reveal new reaction pathways and has demonstrated some weaknesses in established mechanistic dogmas. Studies of complexes containing ligands designed to play a specific role are bound to reveal new and interesting mechanistic problems. Other classes of reactions continue to be elucidated. It remains surprising how little we understand about the reactivity of so simple a molecule as O_2 .

Even a cursory examination of the last few issues of a journal such as "Inorganic Chemistry" will convince the reader of the exciting 'state of the art' of inorganic reaction kinetics, both in the sophistication of the systems being examined and of the methods being used to measure rates. In this account, some areas of current and future interest will be singled out, emphasizing those which have not been covered at the Conference.

A substantial number of reactions and processes involving inorganic and bioinorganic molecules are rapid or extremely

0097-6156/82/0198-0453\$06.00/0
© 1982 American Chemical Society

rapid at room temperature and require specialized techniques for their measurement (1). Some that are currently available and the reaction time range of their utility are shown in Figure 1. It can be seen that we are now down to picosecond observation times, which is generally the limit of interest to the chemist. An equally important development, I feel, is the increasing variety of monitoring methods which can now be linked to the versatile flow and (simple) relaxation techniques. It is inappropriate to list here all the recent developments, but important developments have involved the linking of flow methods to fluorescent and CD monitoring, to calorimetry, to NMR (2; successive replacement of $\text{Al}(\text{DMSO})_6^{3+}$ by the three donor nitrogens of terpyridine, can be unambiguously viewed, from the release of coordinated DMSO, using stopped-flow F.T. H NMR) and of pulse radiolysis combined with EPR, Resonance Raman (3) or rapid scan spectrophotometry (4); the streak camera recordings of transient spectra in 200 μs intervals demonstrated two distinct transients in a pulse radiolytic study of the OH radical reaction with $\text{Cr}(\text{en})_2(\text{SCH}_2\text{COO})^+$). Important information on the structure and properties of transients can now be obtained, and this approach is likely to be exploited for some time to come. There is also the possibility of using lowered temperatures to study reactions, with the advantages of slower rates and easier characterization of intermediates. These were recognized early by a coordination chemist (5,6) but exploited more recently by biochemists (7,8).

Rapid Substitution Processes

As we have seen, an area of major importance and of considerable interest is that of substitution reactions of metal complexes in aqueous, nonaqueous and organized assemblies (particularly micellar systems). The accumulation of a great deal of data on substitution in nickel(II) and cobalt(II) in solution (9) has failed to shake the dissociative mechanism for substitution and for these the statement "The mechanisms of formation reactions of solvated metal cations have also been settled, the majority taking place by the Eigen-Wilkins interchange mechanism or by understandable variants of it" (10) seems appropriate. Required, however, are more data for substitution in the other labile bivalent metal ions. For example, ΔV^\ddagger values for water exchange of $\text{Mn}_{\text{aq}}^{2+}$ and $\text{Fe}_{\text{aq}}^{2+}$ suggest a degree of associative character, which may show up as variable rate constants for ligation (11,12). The practical difficulties in measuring these rates may be circumvented by producing the bivalent complexes extremely rapidly in situ by the reduction of the corresponding ter-

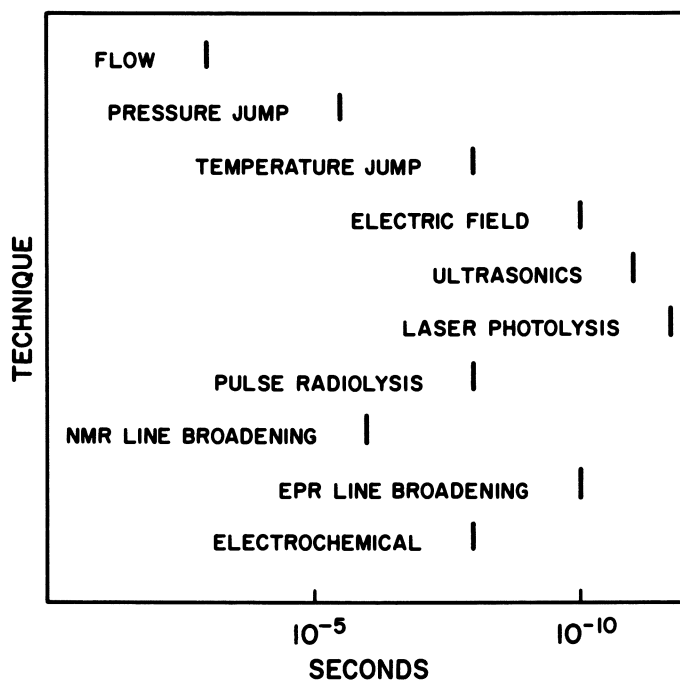
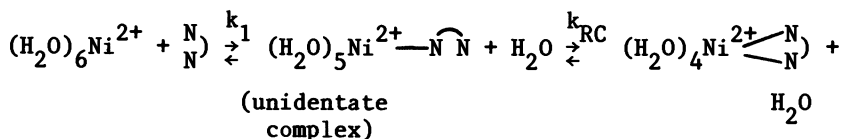


Figure 1. Upper limit of measurable relaxation times for various techniques.

valent complexes, using pulse radiolysis (13) or laser photolysis (14) methods. The subsequent dissociation of the bivalent complex (in the μs to ms region) can be monitored by conductivity methods. Combination of the dissociation rate constants with stability constants will give the desired formation rate constants.

Transient Methods. The method of rapid generation of transients (even possible in picoseconds), and subsequent *in situ* examination of some property of the transient, or of utilizing its reactivity, has been a continuing theme in this Conference. It will continue to be exploited as facilities for, and utility of, the approach becomes even more recognized. For example, a wide variety of metal ions in unusual oxidation states have been generated by pulse radiolysis methods, and the rates of their subsequent reactions (disproportionation, reaction with added substrate, etc.) determined (15,16). An interesting example of this is in the use of the dye pyridine-2-azo-p-dimethylaniline (PAD) to study metal complexing. The binding of this dye to proteins, mediated by metal ions, had been examined in the early 50's (17). The value of PAD to examine the rates of reaction with a number of metal ions was recognized in some of the earliest temperature-jump experiments (18). Most recently, the photochemical perturbation of the Ni^{2+} -PAD system has been studied (19). One of the relaxation times observed, following photochemical perturbation of the system, can be assigned to the ring closure step (k_{RC}) of the unidentate complex ($\text{N-N} = \text{PAD}$):



The value of k_{RC} indicates, as had been assumed, that formation of the chelate is mainly controlled by the k_1 step. Information on k_{RC} cannot be easily obtained from temperature-jump measurements, since at equilibrium the concentration of the unidentate complex is quite small. These approaches cannot help but give insight into the details of chelation.

Substitution in Inert Complexes

Simple methods can, and need to, still be employed, however. The effects of added ions on the rates of complex ion reactions, discussed by Wahl at this meeting, need to be further explored. In the substitution area, the observations of ion pair formation concomitant with the substitution reactions of $\text{M}(\text{NH}_3)_5\text{OH}_2^{3+}$ ($\text{M} = \text{Co}, \text{Rh}$ and Cr) have been challenged (20).

Even that most sacred of mechanisms, the S_N1CB for base hydrolysis, established after a long and fruitful rivalry (21), is under some attack, at least as a universal mechanism (22-24). A concerted E2 mechanism is suggested for the base hydrolysis of $cis\text{-Co}(\text{cyclen})\text{Cl}_2^+$. Proton transfer from a coordinated N-H and cleavage of a Co-Cl bond are considered to occur synchronously (24). Is there a 5-coordinated intermediate $\text{Co}(\text{NH}_3)_5^{3+}$ in induced reactions of $\text{Co}(\text{NH}_3)_5\text{X}^{2+}$, and if so what form does it take in order to explain puzzling competition results (25,26)? Clearly more experiments are needed with a wider range and type of reactants. These may be difficult to conceive, carry out and interpret. One subject with potential ramifications in the metalloprotein area is that related to the remarkable enhancement of the lability of the M-OH₂ bond by M-coordinated ligands. Coordinated H₂O in Fe(III) porphyrin complexes is some 10^4 - 10^5 times more labile than that in the aquated ion (27). Very surprising, and needing more study, is the effect of coordinated EDTA on the enhanced rates of substitution of $\text{M}(\text{EDTA})\text{H}_2\text{O}^-$ compared with $\text{M}(\text{NH}_3)_5\text{H}_2\text{O}^{3+}$ for M = Cr(III), Ru(II) and Os(III) but not Co(III) nor Rh(III)! (28-30). Sometimes there are unexpected rewards for carrying out apparently routine studies. The acid hydrolysis of $\text{Ru}(\text{NH}_3)_5\text{NH}_2\text{CH}_2\text{COOC}_2\text{H}_5^{3+}$ behaves quite differently from that of the Co(III) analog, in that an unusual linkage isomerism is observed (31). This is a lesson that we should take to heart, for it tells us that we are far away from a complete understanding of many "simple" inorganic processes.

Metallo-Enzyme Models

There have been some beautiful ligand syntheses, designed to form complexes with a specific purpose, often to simulate naturally occurring systems. Straight to mind, of course, comes the iron complexes which model the behavior of the oxygen-carrying globins (32) and the iron-sulfur proteins (33). Two binuclear copper(II) complexes have been described, one with (34), and one without (35) bridging between the coppers. These are reversibly reduced to the corresponding binuclear copper(I) complexes by two mono-electronic steps which are simultaneous. It is certain that these types of studies will continue and that investigations of the dynamic aspects of these model complexes are likely to follow those of the synthetic and thermodynamic. This is the usual sequence, but too often there is a considerable time gap between the thermodynamic and kinetics studies.

Rapid Conformational Changes and Electronic Spin Relaxation

One cannot help but be impressed by the explorations in the past decade of the rates of rapid changes in conformation and in coordination number of metal complexes (36-42). For example, equilibria between inclusive (metal ion completely enclosed) and exclusive (metal ion only partly surrounded by organic ligand) complexes of Cs^+ with the cryptand 2:2:2 have been examined by Cs-133 NMR (42). Some of these processes are shown in Table I. The rates of intersystem-crossing processes in certain Co(II), Fe(II) and Fe(III) complexes have also been measured (43-46) (Table II). Recently, the first high spin \rightleftharpoons low spin equilibria in a Co(III) and in a Mn(III) complex have been characterized (47,48) and rate measurements on these may be anticipated. These rapid processes require the specialized techniques referred to in Figure 1. A start has been made by theoretical chemists on the description and calculation of the rates in Table II (49). It is a fair guess that the examination of such fundamental processes, important in biological systems (46,49,50), will be continued. What is the spin-equilibrium function (if any) in the iron proteins?

Electron Transfer Reactions

Electron transfer reactions and theory have been highlighted in this Conference. It is apparent that detailed characterization of the electron transfer process both in the ground and excited states will be continued. The empirical and theoretical correlations of redox rate parameters with known properties of the donor and acceptor centers, the intersite distance for electron travel, and the nature of the medium (51) will continue to be amassed. Such results have been, and promise to be, important ingredients for success with bioinorganic systems (52-55).

Photochemistry

Some future directions in inorganic photochemistry have been outlined by Adamson (56). A pessimistic picture of the practical uses of solar energy conversion systems is painted, but a rosy view of the academic future of the subject is held. It is anticipated that there will be further examination of thermally equilibrated excited (thexi) states--their lifetimes, and spectroscopic and structural properties--and an extension of present efforts to organometallics and metalloproteins is also envisaged (56). The interpretation of spectroscopic data from excited states will continue to be controversial and require future experimentation (57).

Table I. Rate Constants for Some Rapid Stereochemical Changes in Metal Complexes.

System	k_f, s^{-1}	k_r, s^{-1}	Conditions	Technique	Ref.
<u>Planar</u> \rightleftharpoons <u>tetrahedral</u>					
Cl_2Ni $P\phi_2$	4.5×10^5	6×10^5	$23^\circ, CH_3CN$	Photochemical perturbation	<u>36</u>
<u>Square pyramidal</u> \rightleftharpoons <u>planar</u>					
$Ni(L)H_2O \rightleftharpoons Ni(L) + H_2O$ L = 2,2,4-trimethyl-10,11-benzo-1,5-diaza-8,13-dithia-cyclopentadeca-1,10-diene	1.5×10^7	4.5×10^6	$20^\circ, H_2O$	Nanosecond laser photolysis	<u>38</u>
<u>Octahedral</u> \rightleftharpoons <u>Planar</u>					
$Ni(L)(H_2O)_2 \rightleftharpoons Ni(L)H_2O \rightleftharpoons NiL + H_2O$ L = [12]aneN ₄	-	3.2×10^5	$25^\circ, H_2O$	NMR and T-jump	<u>40</u>
L = $\alpha, \beta, \gamma, \delta$ -tetra(4-N-Mepyridyl)porphine	-	2.5×10^5	$25^\circ, H_2O$	Laser Raman T-jump	<u>39</u>
<u>5</u> \rightleftharpoons <u>6</u> <u>coordinated</u>					
<u>EDTA</u>					
$Co(EDTA)^{2-} + H_2O \rightleftharpoons Co(EDTA)H_2O^{2-}$	3×10^6	9×10^6	$25^\circ, H_2O$	Ultrasonic absorption	<u>41</u>

Table II. Rate Constants for Intersystem-Crossing Processes in Co(II), Fe(II) and Fe(III) Complexes.

System	k_f, s^{-1}	k_r, s^{-1}	Conditions	Technique	Ref.
$^2E(1s)Co(II) \rightleftharpoons$ $^4T(1s)Co(II)$					
$\begin{array}{c} CH=N \cdot NHCH_3 \\ N \quad Co_{1/2} \\ CH=N \cdot NHCH_3 \end{array}$	3.2×10^6	9.1×10^6	$25^\circ, CH_3CN/$ CH_3OH	Laser Raman T- Jump	<u>43</u>
$^1A(1s)Fe(II) \rightleftharpoons$ $^5A(1s)Fe(II)$					
$Fe(6-Mepy)(py)_2^-$ $tren^{2+}$	4×10^5	8×10^6	$20^\circ, H_2O$	Laser Raman T- jump	<u>44</u>
$^2T(1s)Fe(III) \rightleftharpoons$ $^6A(1s)Fe(III)$					
$Fe \text{ acac}_2 \text{ trien}^+$	1.6×10^8	3.2×10^8	$25^\circ, H_2O$	Ultrasonic absorption and Laser Raman T-jump	<u>45</u>
metmyoglobin hydroxide	3.9×10^7	2.8×10^7	$1^\circ, H_2O$	Laser Raman T-jump	<u>46</u>

Oxyions

The measurement of the lability of oxyions from ^{18}O exchange studies has not been particularly popular, both because of the complexity of the systems (see, for example, the complexity of isotopic oxygen exchange between H_2O and $\text{V}_{10}\text{O}_{28}^{6-}$ and the pH effect (58) and the tediousness of the techniques (the rapid exchange ($t_{1/2}$, msec-secs) of ^{18}O between H_2O and IO_3^- needs to be studied by multi-mixer, chemical quenching techniques (59)). The burden of measuring the extent of exchange may be relieved in certain instances by *in situ* examination of NMR spectra, using isotope shifts (60)). However, these are fundamentally important reactions and steady progress in rate measurements can be anticipated. Also likely to occur is increased attention to other aspects of the heteropolyanion field, such as large anion interconversions (61), complexing of metal ions by oxyanions, e.g., $\text{As}_4\text{W}_{40}\text{O}_{140}^{28-}$ leading, in this case, to allosteric behavior (62) and reduction of heteropolyanions with production of both firmly trapped and even distribution of the added electrons (63,64). The mechanistic aspects of these cluster molecules have been neglected, but they occur in large varieties and their behavior is relevant to that of solid-state lattices. Work on these might represent the major increased interest of the 80's.

Volumes of Activation and Other Areas

The values of the volumes of activation of inorganic processes are becoming increasingly useful in assignment of mechanism as more and more data accumulate (65,66). However, ambiguities in interpretation still exist (67-69), particularly in estimating the contribution of solvation effects ($\Delta V_{\text{solv}}^\ddagger$) as distinct from mechanistic effects ($\Delta V_{\text{intr}}^\ddagger$) (70). Other current controversies are also likely to lead to future studies. Included in these are the mechanisms of geometrical isomerism of planar complexes (71,72) (a number of distinct types have been promoted by various investigators; 73), the importance of covalent hydration in certain reactions of complex ions of the bipyridyl types (74,75), the intrinsic reactivity of the zwitterion ligand in complex formation (76-78), and the nature of the intermediate in induced reactions of cobalt(III) complexes (22,23,25,26).

Oxygen Chemistry

Lest we become too complacent in our assessment of the marked progress that has been made in understanding inorganic reaction mechanisms, we should consider the simple and very important redox systems:



The thermodynamics are fairly well characterized (79,80) but, as so often happens in chemistry, the rate aspects are much less well understood. Only estimates from the application of Marcus theory for the O_2 , O_2^- electron transfer are available (81).

Although the feasibility of reaction 1 (an important component of the Haber-Weiss mechanism for Fe(II)-mediated decomposition of H_2O_2)



has been questioned (79,80,82), the rate constant has been determined and its low value has eliminated reaction 1 as a potential OH radical source in biological systems (83).

Given the ingenuity of the inorganic kineticist and the array of measuring equipment now available, answers to these and other problems will surely emerge during the remainder of the century.

Literature Cited

1. "Investigation of Rates and Mechanisms of Reactions, Part II. Investigation of Elementary Reaction Steps in Solution and Very Fast Reactions," Hammes, G. G., Ed., in "Techniques of Chemistry" Vol VI, 3rd Edition, 1974, Wiley.
2. Brown, A. J.; Howarth, O. W.; Moore, P.; Parr, W. J. E. J. Chem. Soc. Dalton 1978, 1776.
3. Dallinger, R. F.; Guanci, J. J., Jr.; Woodruff, W. H.; Rodgers, M. A. J. J. Am. Chem. Soc. 1979, 101, 1355.
4. Sullivan, J. C.; Deutsch, E.; Adams, G. E.; Gordon, S.; Mulac, W. A.; Schmidt, K. H. Inorg. Chem. 1976, 15, 2864.
5. Bjerrum, J.; Poulsen, K. G. Nature 1952, 169, 463.
6. Bjerrum, J.; Poulsen, K. G.; Poulsen, I. Proc. Symp. Coord. Chem. (Denmark), 1954, 51.
7. Douzou, P. "Cryobiochemistry," Academic Press, New York, 1977.
8. Fink, A. L. Accts. Chem. Res. 1977, 10, 233.

9. Margerum, D. W.; Cayley, G. R.; Weatherburn, D. C.; Pagenkopf, G. K., in "Coordination Chemistry," Martell, A. E., Ed., Am. Chem. Soc., 1978, p. 1.
10. Burgess, J. "Metal Ions in Solution," Ellis Horwood Ltd., Chichester, 1978, p. 469.
11. Ducommun, B. Y.; Newman, K. E.; Merbach, A. E. Inorg. Chem. 1980, 19, 3696.
12. Swaddle, T. W. Coordn. Chem. Revs. 1974, 14, 217.
13. Shinohara, N.; Lilie, J.; Simic, M. G. Inorg. Chem. 1977, 16, 2809.
14. Lilie, J. J. Am. Chem. Soc. 1979, 101, 4417.
15. Buxton, G. V. and Sellers, R. M., National Bureau of Standards, NSRDS-NBS 62, 1978.
16. Meyerstein, D. Accts. Chem. Res. 1978, 11, 43.
17. Klotz, I. M.; Loh Ming, W. C. J. Am. Chem. Soc. 1954, 76 805.
18. Wilkins, R. G. Inorg. Chem. 1964, 3, 520.
19. Robinson, B. H.; White, N. C. J. Chem. Soc. Faraday I, 1978, 2625.
20. van Eldik, R.; Palmer, D. A.; Kelm, H. Inorg. Chem. 1979, 18, 1521.
21. Pearson, R. G. J. Chem. Educ. 1978, 55, 720.
22. Buckingham, D. A.; Edwards, J. D.; Lewis, T. W.; McLaughlin, G. M. Chem. Commun. 1978, 892.
23. Reynolds, W. L.; Hafezi, S. Inorg. Chem. 1978, 17, 1819.
24. Hay, R. W.; Norman, P. R., Chem. Commun. 1980, 734.
25. Reynolds, W. L.; Alton, E. R. Inorg. Chem. 1978, 17, 3355.
26. Jackson, W. G.; Lawrance, G. A.; Sargeson, A. M. Inorg. Chem. 1980, 19, 1001.
27. Ostrich, I. J.; Liu, G.; Dodgen, H. W.; Hunt, J. P. Inorg. Chem. 1980, 19, 619.
28. Ogino, H.; Watanabe, T.; Tanaka, N. Inorg. Chem. 1975, 14, 2093.
29. Sulfab, Y.; Taylor, R. S.; Sykes, A. G. Inorg. Chem. 1976, 15, 2388.
30. Matsubara, T.; Creutz, C. Inorg. Chem. 1979, 18, 1956.
31. Yeh, A.; Taube, H. J. Am. Chem. Soc. 1980, 102, 4725.
32. Traylor, T. G. Accts. Chem. Res. 1981, 14, 102.
33. Holm, R. H., in "Biological Aspects of Inorganic Chemistry;" Addison, A. W.; Cullen, W. R.; Dolphin, D.; James, B. R., Eds., John Wiley, New York, N. Y., 1977, p. 71.
34. Fenton, D. E.; Schroeder, R. R.; Lintvedt, R. L. J. Am. Chem. Soc. 1978, 100, 1931.
35. Gisselbrecht, J. P.; Gross, M.; Alberts, A. H.; Lehn, J. M. Inorg. Chem. 1980, 19, 1386.
36. McGarvey, J. J.; Wilson, J. J. Am. Chem. Soc., 1975, 97, 2531.
37. Campbell, L.; McGarvey, J. J. Chem. Commun. 1976, 749.
38. Campbell, L.; McGarvey, J. J.; Samman, N. G. Inorg. Chem. 1978, 17, 3378.

39. Pasternack, R. F.; Sutin, N.; Turner, D. H. J. Am. Chem. Soc. 1976, 98, 1908.
40. Coates, J. H.; Hadi, D. A.; Lincoln, S. F.; Dodgen, H. W.; Hunt, J. P. Inorg. Chem. 1981, 20, 707.
41. Harada, S.; Funaki, Y.; Yasunaga, T. J. Am. Chem. Soc. 1980, 102, 136.
42. Popov, A. I. Pure and Appl. Chem. 1979, 51, 101.
43. Simmons, M. G.; Wilson, L. J. Inorg. Chem. 1977, 16, 126.
44. Hoselton, M. A.; Drago, R. S.; Wilson, L. J.; Sutin, N. J. Am. Chem. Soc. 1976, 98, 6967.
45. Binstead, R. A.; Beattie, J. K.; Dewey, T. G.; Turner, D. H. J. Am. Chem. Soc. 1980, 102, 6442.
46. Dose, E. V.; Tweedle, M. F.; Wilson, L. J.; Sutin, N. J. Am. Chem. Soc. 1977, 99, 3886.
47. Gutlich, P.; McGarvey, B. R.; Kläui, W. Inorg. Chem. 1980, 19, 3704.
48. Sim, P. G.; Sinn, E. J. Am. Chem. Soc. 1981, 103, 241.
49. Buhks, E.; Navon, G.; Bixon, M.; Jortner, J. J. Am. Chem. Soc. 1980, 102, 2918.
50. Perutz, M. F.; Sanders, J. K. M.; Chenery, D. H.; Noble, R. W.; Pennelly, R. R.; Fung, L. W. M.; Ho, C.; Giannini, I.; Pörschke, D.; Winkler, H. Biochemistry 1978, 17, 3640.
51. Cannon, R. D. "Electron Transfer Reactions," Butterworths, London, 1980.
52. "Tunneling in Biological Systems," Chance, B.; deVault, D. C.; Frauenfelder, H.; Marcus, R. A.; Schieffer, J. R.; Sutin, N., Eds., Academic Press, New York, 1979.
53. Armstrong, F. A.; Henderson, R. A.; Sykes, A. G. J. Am. Chem. Soc. 1980, 102, 6545.
54. Scott, R. A.; Gray, H. B.; J. Am. Chem. Soc. 1980, 102, 3219.
55. Mauk, A. G.; Scott, R. A.; Gray, H. B. J. Am. Chem. Soc. 1980, 102, 4360.
56. Adamson, A. W. Pure Appl. Chem. 1979, 51, 313.
57. Shipley, N. S.; Linck, R. G. J. Phys. Chem. 1980, 84, 2490.
58. Murmann, R. K.; Giese, K. C. Inorg. Chem. 1978, 17, 1160.
59. von Felten, H.; Gamsjäger, H.; Baertschi, P. J. Chem. Soc., Dalton 1976, 1683.
60. Risley, J. M.; Van Etten, R. L. J. Am. Chem. Soc. 1979, 101, 252.
61. Masters, A. F.; Gheller, S. F.; Brownlee, R. T. C.; O'Connor, M. J.; Wedd, A. G. Inorg. Chem. 1980, 19, 3866.
62. Robert, F.; Leyrie, M.; Hervé, G.; Tézé, A.; Jeannin, Y. Inorg. Chem. 1980, 19, 1746.
63. Kazansky, L. P.; Fedotov, M. A. Chem. Commun. 1980, 644.
64. Prados, R.; Pope, M. T. Inorg. Chem. 1976, 15, 2547.
65. Lawrance, G. A.; Stranks, D. R. Accts. Chem. Res. 1979, 12, 403.
66. Palmer, D. A.; Kelm, H. Coordn. Chem. Revs. 1981, 36, 89.

67. Langford, C. H. Inorg. Chem. 1979, 18, 3288.
68. Newman, K. E.; Merbach, A. E. Inorg. Chem. 1980, 19, 2481.
69. Swaddle, T. W. Inorg. Chem. 1980, 19, 3203.
70. Burgess, J.; Duffield, A. J.; Sherry, R. Chem. Commun. 1980, 350.
71. Romeo, R.; Minniti, D.; Lanza, S. Inorg. Chem. 1979, 18, 2362.
72. van Eldik, R.; Palmer, D. A.; Kelm, H.; Louw, W. J. Inorg. Chem. 1980, 19, 3551.
73. Anderson, G. K.; Cross, R. J. Chem. Soc. Rev. 1980, 9, 185.
74. Farvar, O.; Monsted, O.; Nord, G.; J. Am. Chem. Soc. 1979, 101, 6119.
75. Al-Obaidi, K. H.; Gillard, R. D.; Kane-Maguire, L. A. P.; Williams, D. A. Trans. Met. Chem. 1977, 2, 64.
76. Cassatt, J. C.; Wilkins, R. G. J. Am. Chem. Soc. 1968, 90, 6045.
77. Letter, J. E., Jr.; Jordan, R. B. J. Am. Chem. Soc. 1975, 97, 2381.
78. Kustin, K.; McClean, J. L. J. Phys. Chem. 1978, 82, 2549.
79. Fee, J. A.; Valentine, J. S. in "Superoxide and Superoxide Dismutases," Michelson, B. M.; McCord, J. M.; Fridovich, L., Eds., Academic Press, New York, N. Y., 1977, p. 19.
80. Wilshire, J.; Sawyer, D. T. Accts. Chem. Res. 1979, 12, 105.
81. Stanbury, D. M.; Haas, O.; Taube, H. Inorg. Chem. 1980, 19, 518.
82. Gibian, M. J.; Ungerman, T. J. Am. Chem. Soc. 1979, 101, 1291.
83. Weinstein, J.; Bielski, B. H. J. J. Am. Chem. Soc. 1977, 101, 58.

RECEIVED March 8, 1982.

INDEX

- A**
- Absorption spectrum, mixed metal μ -peroxo complex 437*f*
- Acetonitrile
 proton transfers in 71–73
 solvent for transition-metal hydrides 405
- Acid interaction with nickel(II)
 ethylenediamine 19*f*
- Acid-catalyzed dechelation of poly-amine complex, mechanism 16–18
- Acidity
 metal hydrides in acetonitrile 409*t*
 hydridorhodiumtetracarbonyl 420
- Actinide redox couples 161*t*, 162*t*
- Activated complex and solvent
 configuration 110, 113*f*
- Activation energy 85, 216
 definition 264, 265
 electron transfer process as function of electronic energy gap of reaction 252*f*
 thermal 308, 309*f*
- Activation free energy 186
 definition 271
 exoergic electrochemical and homogeneous reactions 198*f*, 204*f*, 205
 and overall free energy relationship 306, 307*f*
 vs. thermodynamic driving force 188*f*
- Activation parameters 271
 calculated based on TST, SCT, and WMT 276*t*
- Co(III)-Ru(II) complexes separated by amino acids 226*t*
 decomposition based on SCT
 rate constant 277*t*
 electrochemical 184
 intramolecular electron transfer 223
 NMR data 58
- Activation volumes 461
 pressure dependence 40–45
 for solvent exchange 51*t*
 for water exchange 4, 5*t*, 47–50
- Activationless electron transfer processes 218
- Adduct formation, dioxygen species 435–439
- Adiabatic density functional approach 306, 307*f*
- Adiabatic electron transfer 108, 117
- Adiabatic potential surface 293
- Adiabatic states, splitting 273*f*
- Adiabatic surfaces at diabatic crossing point, splitting 267
- Adiabaticity factor 119*t*
 cobalt hexaamine exchange 126
- Alkoxide
 and halide exchange,
 intrinsic barriers 91
 leaving group ability 92, 93
- Alkyl substituents, steric effects 67*t*
- Amine base-metal base proton transfer 420
- Amino acid linkage influence on intramolecular electron transfer rates 225–227
- Aminoisobutyric acid 25, 27*t*
- Ammine complexes
 deuterium isotope effect for electron transfer between 253*f*
 electrochemical reorganization parameters 190, 196
 and water exchange 46*f*
- Ammineruthenium species 167
- Amplitudes, reaction path states .. 304, 305*t*
- Anodic transfer coefficient 187, 197
- Anthraquinone sulfonate and duroquinone, equilibrium 338
- Antisymmetric combination of inner-sphere breathing model 262–264
- Aqua—*See* Water
- Aqueous exchange—*See* Water exchange
- Aqueous reactions of Cr(III) and Co(III) amines 46*f*, 47
- Aquo cations, oxidation 200, 201*f*
- Aquo compounds of transition metal ions 128
- Aquo ligands, hydrogen bonding 205
- Aquo redox couples, reorganization parameters 192*t*
- Aquo-iron complexes
 Fe(II)/Fe(III) self-exchange,
 kinetic parameters 302*t*
 rate constants 111*t*, 120
- Aquo-uranium complex and aquovanadium complex oxidation .. 164–165
- Arylphosphines o-metalation mechanistic scheme and IR spectrum analysis 353–354
- Associative interchange in substitution reactions 48, 49
- Atom transfer reactions 151–179
- Atomic orbitals, electron transfer between t_{2g} - $3d$ 257, 260, 261*f*

Autoionizing solvents	74f, 75	Bronsted plots of kinetic vs. thermodynamic acidity	415
Axial substitution rate constants for Ni(III)cyclam(H ₂ O) ₂ ³⁺	11t	Bronsted plots for proton-transfer reactions of Cu-triglycine and -tetraglycine complexes	20, 21f
B			
Backbonding, π	404	Bronsted relationships	422, 423
Bacteriopheophytin-quinone electron transfer and bacterium photosynthesis	215	C	
Band broadening, molecular electronic transitions	330, 331	Cage formation from solvent molecules	18
Band energy vs. total reorganization energy	291, 292f	Carbanion protonation rates	68
Base protonation, rate constants	66t	Carbon dioxide incorporation into [ReH ₃ (dppe) ₂]	357, 358
Benzonitrile, proton transfer	7-73	Carbonyl derivative of [MoH ₄ (dppe) ₂]	350
Bidentate formate ligand, vibrations ..	358	Carboxylate radical anion and ClO ₄	174
Bimolecular rate constant	258	Carboxylic acid oxygen coordination to nickel	19f
Binuclear complexes, electron transfer	222, 223	Catalysts of O ₂ /H ₂ O couple, thermochemical constraints	444-446
Biological systems, quantum-mechanical theory of diffusion-independent electron transfer	214-218	Cathodic transfer coefficients	187, 197
2,2'-Bipyridine		Cetyl trimethyl ammonium bromide (CTAB) micelles, simple surfactants	338
dimers, intervalence transfer bands	139	Changes in coordination spheres	153
ligands	138	Charge localized vs. delocalized wave functions	270, 271
Rh(II) complexes	385-402	Charge transfer— <i>See also</i> Electron transfer	
ring, electron transfer through π^* -orbitals	118, 119t	bands, intensities	118
Bipyridine-metal charge-transfer excited states	249	excited state of Ru(bpy) ₃ ²⁺	397
Bipyridyl ligands	239	transitions, donor-acceptor complexes	145
Bipyridyl and Ni(phen)(H ₂ O) ₄ ²⁺ substitution	13, 14f	transitions, optical	137-150
Bis(dimethylglyoximate) chelating ligand	399	vs. wavelength spectrum	236
Bis(ethylenediamine) dihydride osmium(IV)	420	Chelates	
[Bis(pentaammine-Ru)pyrazine] ⁵⁺ — <i>See</i> Creutz-Taube ion		factors affecting formation rate constants	11-28
Bis(triglycine) complex	33	ring opening of Ni(en)(H ₂ O) ₄ ²⁺ , acid-catalyzed	13, 16-20
Bond dissociation enthalpy, heterolytic	93	ring opening reaction of polyamine complex	16-18
Bond distances		stereochemical change in complexes	42
aquo complexes	327t	substitution reactions	3-28
outer sphere mechanisms	129	Chelation-controlled substitution	12
Bond energy, metal-metal, d ⁷ -d ⁷ dimer	402	Chemical reactions, effect of organized assemblies	335-346
Bond length changes, electronic transitions of mixed-valence complex	330, 331	Chemical shifts of ethyl formate and formic acid	358
Born-Oppenheimer approximation	112	Chloride ions as bridges	153
Breathing frequencies, aquo complexes	327t	Chlorite reaction with S ⁴⁺	151, 152
Bridging chloride from Pt(IV) to Pt(II)	153	Chromium ion, reducing agent for ClO ₄ ⁻	167
Bridging ligand and charge transfer	137	Chromium-aquox complex, electrochemical free energy of activation	198f
Bromate reduction	160	Chromium-carbon bond cleavage reaction	60, 61
Bromide ion ligation of Cr(DMF) ₆ ³⁺ ..	42		

- Chromium-DMF complex, Br⁻ ligation 42
- Chromium(II), reduction of MnO₂ in presence of ClO₄⁻ 175
- Chromium(III) amines and water exchange 46f
- Classical formalism for electron-transfer model 107-110
- Cobalt complexes
- dioxygen adducts
- oxygen-atom transfer 440
- thermodynamic properties 447t
- ethylenediamine complex
- reorganization parameters 192-196
- hexaammine
- exchange 318, 319
- rate constants 126
- slow electron 250
- reorganization parameters 196
- hexaquo, metal-O distances and breathing frequencies 327t
- nitrogen distances in hexa-ammines 126, 127
- pentaamine sulfate, equation 47
- peroxo, reactivity enhancement 441
- Rubidium amino acid complexes 223-226
- sepulchiate, self-exchange rate constants 126
- trisethylenediamine, self-exchange rate constants 126
- water bond lengths 129
- Cobalt(II) complexes
- rate constants for intersystem-crossing processes 460t
- reactivity with O₂ 426
- Cobalt(III) amines and water exchange 46f
- Cobalt(III) quenching 227-230
- Colloidal media, use 37
- Colloidal suspensions, measurement ion transfer kinetics 69
- Colloidal systems involving titanium 78
- Compressibility data for ionic solids .. 45
- Computer simulation and oscillating reactions 450
- Conductivity, frequency dependent ... 309f
- Configuration changes of species during electron transfer 105, 106, 216
- Conformational changes 458
- Contact distance 255
- Coordinated dioxygen, reactivity ... 425-450
- Coordinating acids and dechelation of polyamine complex 18, 19f
- Coordination
- Cu(II)/Cu(I) redox couples 211
- transition metal hydride
- deprotonation 404
- Coordination—(Continued)
- tripeptide Cu(II) complexes 23, 24f
- Copper lauryl sulfate micelles 340
- Copper polypeptide complexes 31, 32
- Copper triglycine, EDTA reaction ... 33
- Copper(II) complexes
- peptide 6, 7f, 20, 21f
- polythioether ligands 34
- pyridine, cis/trans effects 36
- tripeptide, nucleophilic substitution reactions 23-28
- Copper(II)/Copper(I) self-exchange rate constant 211, 212
- Copper(III) substitution reactions ... 6-13
- Corrosion of steel 78
- Coulombic repulsion of reactants, ion-atmosphere-shielded 240
- Coupling 272
- energies, electron-phonon 320-322
- integral, electronic 311, 313, 315
- strength, evaluation 322, 324-327
- Creutz-Taube ion 331
- intervalence band 286-292
- intervalence spectrum 323f
- ppi/dpi orbitals involved in coupling 313, 314f
- tunnel-type transitions 299
- vibrational eigenvalues 320
- Cross-reaction
- energetics of activation 303
- intrinsic barrier for, definition 96
- [ReH₅(PMe₂Ph)₃] and [ReD₅(PMe₂Ph)₃] 362, 365
- Crossing energy 273f
- Crown ether and micelle formation 338, 340
- Cyclam 427
- Cyclam-Ni(III) complex, axial substitution rate constant 11t
- Cyclic voltammograms of Rh(bpy)₃³⁺ 389f
- Cytochrome c oxidation rate 214
- D**
- Debye-Hyckel treatment for electron transfer 106
- Degrees of freedom, nuclear 215
- Delocalization of metal T_{2g} electron density 118
- Density functional approach 306, 307f
- Deprotonation of transition-metal hydride 404
- Deuterium exchange
- [ReH₅(PMe₂Ph)₃] 362, 365
- tungsten-molybdenum tetrahydride complexes 380
- Deuterium incorporation into dppe ligands 353, 354

Deuterium isotope effects on electron-exchange reactions	251, 253f	Dissociation rate of nickel(II) ethylenediamine	16, 17f
DI—See 5,11-Dimethyl-5,11-dihydroindolo(3,2- <i>b</i>)carbazole		Dissociation reactions of nickel(II)-peptides	8
Diabatic functions	266	Dissociative interchange in substitution reactions	48, 49
Diabatic states, energy profiles	273f	Distance dependence of electron transfer rates	213–233
Dielectric constants	264	Donor-acceptor complexes, optical transmission energy	145
Dielectric continuum theory	262, 264	Donor-acceptor interactions in biomolecular reactions, probes of electronic component	227
Dielectric interaction energy	209	Donor-acceptor separation	218
Diffusion-corrected quenching rate constant vs. reduction potential for ruthenium and rhodium complexes	390–391	Dye, photoinduced electron transfer	339, 340
Diffusion-limited rate constant	240	Dynamics	
Diffusion-reaction equation for pair distribution function of reactants	236	electron transfer across	
Diffusion in electrochemical processes	212	polypeptides	221–227
5,11-Dimethyl-5,11-dihydroindolo-(3,2- <i>b</i>)carbazole	339, 340	micelles	346
Dimethylaniline/pyrene electron exchange	339		
Dimethylphenylphosphine dissociation from $[\text{ReH}_3(\text{PMe}_2\text{Ph})_4]$	366, 367	E	
Dinitrogen complex $[\text{ReD}(\text{N}_2)(\text{dppe})_2]$ formation	353, 354	E_2 mechanism for base hydrolysis of <i>cis</i> -Co(cyclen) Cl_2^+	457
Dinuclear hydride complexes, photoinduced elimination of H_2	370–376	Edwards equation	154, 155
Dioxygen	425–450	Efficiency for exothermic reactions	83, 85
adducts		EFTA reaction with copper	
formation		triglycine	33
rate constants	436t	Eigen's mechanism for proton-transfer reactions between acids and bases	63–65
reactions	435	Eigen-type Bronsted plot	20, 21f
heterolytic or homolytic displacement reactions	440	Eigen-Wilkins mechanism	4, 31
hydrogen-atom abstraction reactions	439	Eigenfunctions	285
oxygen-atom transfer		Eigenvalues	
reactions	439, 440	Creutz-Taube ion	320, 321f
advantage of coordination	435	Schrodinger equation	266
bound, reactivity	425–450	Electric field jump (E-jump)	
complexes		relaxation technique	69, 71
outer-sphere electron transfer reactivity	429t–432t	Electric field jump study of proton transfer between <i>p</i> -nitrophenol and triethylamine and between picric acid and methyl red	72
moieties electron transfer reactions	427–435	Electrocatalytic reduction of oxygen	443, 444
reactions, intrinsic barriers to electron transfer	428, 434	Electrochemical activation parameters	184
reduction		Electrochemical exchange reactions, reorganization parameters	192t, 193t
cofacial porphyrins	441, 443	Electrochemical free energy of activation for chromium complex	198f
superoxo intermediate, kinetic pathway	441	Electrochemical and homogeneous reaction energetics, relationship between	186–189
thermochemistry, summary	426t	Electrochemical kinetic data for aquo cations oxidation	204f
Dipicrylamine structure and proton transfer	72	Electrochemical rate formulations	182–185
Dipole-allowed transition, oscillator strength for electric	315	Electrochemical transfer coefficient	183
Disproportionation reaction		Electrode kinetics	182
rhodium(I) species	398	Electrode potential	186, 196
thallium(II) rate constant	134		

- Electron charge, unit 143
- Electron coupling matrix element 109f
- Electron density
delocalization of metal 118
and solvent exchange 51
- Electron donor and acceptor sites,
non-overlapping 143
- Electron exchange—*See also*
Electron transfer 189–196
- Electron exchange kinetics using
electronic structure techniques 255–279
- Electron exchange mechanism
for Fe^{2+} – Fe^{3+} 274
- Electron exchange rate constant 392, 393
- Electron exchange, pyrene/dimethyl-
aniline 339
- Electron occupation number 310
- Electron spin resonance (ESR) for
nickel(III) complex 10f
- Electron transfer—*See also* Charge
transfer, Donor-acceptor inter-
actions, and Electron exchange
- binuclear complexes 222, 223
- bipyridine ring through
 π^* -orbitals 118, 119t
- diffusion-independent, quantum-
mechanical theory 214–218
- enhancement 230, 231
- ferrocene 341
- frequencies 110t
- future research areas and
developments 235–253, 331–332
- hemerythrin, intramolecular 218–221
- and hydride transfer 415
- IR absorption 322, 324f
- kinetics, parameters 331, 332
- kinetics, parameters 301–332
- and micelles 339–340
- $\text{MnO}_3^-/\text{MnO}_4^-$ 332
- model, semiclassical and classical
formalism 107–122
- nuclear tunneling factor 114, 116f
- optical vs. thermal 141
- oxygen moieties 427–435
- polypeptides, dynamics 221–227
- process, frequency-dependent
conductivity 309f
- rate 291
- amino acid linkages
influences 225–227
- calculation progress 302, 303
- distance dependence 213–233
- intramolecular 223
- rate constants 105–106
- rate constants, semiclassical
formalism 112
- reactions 458
- ruthenium to rhodium complex 390
- weak overlap and inversion
effect 235, 236
- Electron transfer—(*Continued*)
weakly interacting systems 105–135
- Electron transmission factor 265
- Electron tunneling spectroscopy 299
- Electron-hopping rate constant 258
- Electron-phonon coupling 215, 216
constant 311
energies from experimental data 320–322
- Electronegative atoms, proton transfer 64
- Electronic absorption spectral changes
during irradiation of
[$\text{ReH}_5(\text{PMe}_2\text{Ph})_3$] and
[$\text{ReH}_5(\text{PMe}_2\text{Ph})_4$] 363f, 367, 368f
- Electronic component of donor-
acceptor interactions in bio-
molecular reactions 227
- Electronic coupling
integral 311, 313, 315
matrix elements 117–120
phonon 215–216
coupling constant 311
coupling energies 320–322
transfer rate 294f
- Electronic energy transfer,
Co(III) quenching 227–230
- Electronic Hamiltonian operators 282
- Electronic interaction term 310–315
- Electronic matrix elements for
nonorthogonal functions 256
- Electronic nonadiabaticity 129, 315
- Electronic spin relaxation 458
- Electronic state of $\text{Rh}(\text{bpy})_3^{2+}$ 387
- Electronic structure of bipyridine 397
- Electronic structure techniques,
electron-exchange kinetics
using 255–279
- Electronic transitions of mixed-
valence complex, bond length
changes 330
- Electronic transmission
coefficient 112, 117–122
- Electronic transmission factor for
Fe-Fe separations 273f
- Electronic wave function
determination 269, 270
transferring electron 304
- Elimination
 H_2 from [$\text{Pt}_2\text{H}_2\text{Cl}(\text{dppm})_2$] $^+$ 375
methane from ($\text{eta}_5\text{-C}_5\text{H}_5$) $_2\text{Zr}(\text{CH}_3)_2$
and $\text{HM}(\text{CO})_3(\text{eta}_5\text{-C}_5\text{H}_5)$ 414
- Energetics of activation
cross-reaction 303–307
- Energetics of electrochemical and
homogeneous electron-transfer
reactions 181–212
- Energies, vibronic 284
- Energy
activation 141
barrier 85–88
environmental change 205

Energy—(Continued)	
gap	
electronic states for electron transfer processes	215
ground and excited state	144
law	216
transition state and reactants	98
mean band vs. reorganizational	291–292
metal-metal bond in d^7 - d^7 dimer	402
profiles of diabatic states	273f
weak-interaction electron transfer	308, 309f
Energy storage and micelles	344
Energy transfer	
electronic, Co(III) quenching of *Cr(III)	227–230
and micelles	340, 341
rates in solution	306, 307f
Enthalpy	
activation	
definition	271
weak-interaction outer-sphere self-exchange	317
heterolytic bond dissociation	93
Entropies of activation	129
definition	271
weak-interaction outer-sphere self-exchange	317
Environment of reactants in micelles	338
Environmental energy, change	205
Equilibrium acidity	414
Equilibrium constant for	
dimer-monomer equilibrium	402
Equilibrium constant for precursor complex formation	107
Equilibrium constant, K , equation	40
Equilibrium radial distribution function	106
Ethanes	
homolytic cleavage	62, 62f
Ethylamine-Ni(II) complex and Ethylenediamine-Ni(II) complex, rate constant	12
Europium	
redox reaction	164, 390, 391f
redox reaction rate	210, 211
Europium(II)/Eu(III) exchange	308
Exchange reaction	
comparison of semiclassical and classical calculations of rate constants for	121t
experimental reorganization parameters for	192t, 193t
first-order rate constant	114
potential energy surface	113f
rate constants	110, 111t, 120
rate constants and thermodynamic parameters	191t, 290t
	F
Fermi rule—See also Golden rule	215, 293
Ferrocene/ferrocenium ion exchange	132
Ferrocene, electron transfer	341
Ferrous-ferric—See also Iron entries	
Ferrous-ferric outer-sphere symmetrical exchange	302
First-order rate constant for an exchange reaction	114
Flow methods	454
Fluid micelles, kinetic nature	346
Fluorescence—See also Quenching	
Fluorescent probe	79, 80
Fluorine-19-NMR studies of association of PF_6^- with $Cr(phen)_3^{3+}$ complex	131, 132
Force constant for charge states	264
Forces between ions and neutral molecules	83
Formate and derivative formation of $[ReH_3(dppe)_2]$ and $[Re(O_2CH)(dppe)_2]$	357, 359
Formation rate constants of chelates, factors affecting	11–28
Formation rate constants for ligands reacting with $Ni(phen)(H_2O)_4^{2+}$	15f
Formation of $[Re(O_2CH)(dppe)_2]$	358, 359
Formation of yl ions	164–165
Forster quenching	228
Franck-Condon factor	114, 216
contribution of polar solvent	238
matrix elements	268
principle	107
Free energy	
activation	
chromium complex	197–199
homogeneous and heterogeneous processes, correlation	209
homolytic cleavage of substituted ethanes	62, 63f
intrinsic	183–184
transfers at metallic electrodes	209
barrier	
exchange reaction	108
outer-sphere cross-reaction	200–205
thermodynamics	184
electron-transfer step	182, 183
halogen reaction with oxygen	156
quadratic dependence on	
overall	306, 307f
vs. nuclear tunneling factor	114, 116f
vs. predicted reaction rates	303–308
vs. rate constants for ruthenium complex reaction	241, 242f, 245f
Frequencies	
aquo complexes breathing	327t
effective nuclear	114, 117

Frequencies—(Continued)

- electron transfer110*t*, 309*f*, 331
 exchange reaction 108
 experimental data 320–322
 intramolecular vibrations 143
 Fulvic acid fluorescence, quenching ..37, 38*f*

G

- Gas phase, S_N2 reactions 2
 Gas-phase electron transfer 332
 Generation of reactive intermediates
 via photolysis of transition
 metal polyhydride complexes 347–383
 Golden Rule
 expression for rate constant 267
 nuclear tunneling factor for
 self-exchange317–319
 Gouy-Chapman theory 184

H

- Halide and alkoxide exchange,
 intrinsic barriers 91
 Halide-oxygen bond strength 156
 Halides, quenching rate constant 230
 Halogen atoms abstraction
 from RX399, 402
 Halogen and oxygen bond strength
 vs. oxidation state 156*t*
 Hamiltonian
 2-center310, 311
 1-*e*⁻310, 311
 potential energies associated
 with 311, 312*f*
 Hamiltonian matrix elements 268
 Hamiltonian operators, electronic 282
 Harmonic oscillator functions 284
 Harmonic oscillator model for
 oxidation of aquo cations203, 205
 Hemerythrin, intramolecular electron
 transfer reactions218–221
 Heterolytic bond dissociation enthalpy 93
 Hexagonal-close-packed Rh frame-
 work of complex 417*f*
 Hexahydrate complexes, contact
 limit 260
 Homogeneous and electrochemical
 reaction energetics186–189
 Homogeneous exchange reactions,
 reorganization parameters ..192*t*, 193*t*
 Homogeneous reactions, intrinsic
 barriers202, 205
 Homogeneous self-exchange reactions,
 rate constants and thermo-
 dynamic parameters190*t*, 191*t*
 Homolytic bond cleavage 54
 Homolytic cleavage of substituted
 ethanes62, 63*f*

- Homolytic displacement with
 bound O₂428, 440
 Homolytic dissociation, rate constant 60, 61
 Huckel-type calculations 330
 Hush approach 304
 Hydride ligands347–383
 Hydride migration to CO₂ 359
 Hydride resonances 350
 Hydride transfer vs. hydrogen
 atom transfer 406
 Hydridocarbonyl cluster complexes .. 370
 Hydridocobaloximes addition to
 olefins405, 406
 Hydridoosmiumtetracarbonyl anion .. 420
 Hydridorhodiumtetracarbonyl acidity 420
 Hydrofluoric acid, IR spectrum 74*f*
 Hydrogen atom transfer vs.
 hydride transfer 406
 Hydrogen bonding
 with aquo ligands 205
 between H₂O and electron pair
 on amine nitrogen 12
 in metal hydrides 421
 and metal ion substitution 12
 Hydrogen fluoride as autoionizing
 solvent74*f*, 75
 Hydrogen generation from Rh
 hydride species 400
 Hydrogen ion dependence of rate of
 exchange of water on Fe(III) 43*f*
 Hydrogen molecule, photoinduced
 loss from polyhydride
 complexes348–354
 Hydrogen peroxide
 reaction with nucleophiles154, 155
 reaction with Rh complexes175–178
 Hydrogen photoinduced elimination
 from dinuclear complexes370–376
 Hydrogen-atom abstraction by
 bound O₂427, 439
 Hydrogen-bond breaking reactions ...64, 65
 Hydrogen-deuterium exchange
 reaction353, 354
 Hydrophobic bonding and stacking
 interactions 13
 Hydrophobic substances, effect on
 proton exchange rates 64, 68
 Hydrophobicity of ligands 221
 Hydroxyisopropyl chromium cation ..60, 61
 Hydroxyl radical formation 177

I

- ICB12, 57
 Ice studies 69
 ICR 82
 Inert anions, effect on complex
 formation kinetics 34
 Inner- and outer-shell distortions 110, 113*f*

Inner-shell ligands	273f	Intrinsic nucleophilicity	88t
Inner-sphere		vs. leaving group ability	92, 93
contact distance	257, 260, 261f	Inversion effect with electron	
contribution to E^*	264	transfer	235, 236
and medium energy contributions ..	305	Iodochromium(III) ion substitution	
modes, nuclear tunneling factors ...	112	reaction	59-61
Inorganic reaction mechanisms ...	453-465	Ion cyclotron resonance (ICR)	
Insertion into C-D bonds of C_6D_6 ...	353, 354	spectroscopy	82
Insertion into C-H bonds	352	Ion pair, sterically favorable	
Intensities of charge-transfer bands ...	118	configuration	257, 261f
Interaction term, electronic	310-315	Ion recombination rate constant	73
Intermolecular electron transfer		Ion solvation changes	71
in proteins	222	Ion-atmosphere-shielded Coulombic	
Internal conjugate base (ICB)		repulsion of reactants	240
mechanism	12, 57	Ion-molecule reactions, single-mini-	
Internuclear separation	143, 144	mum potential surface	84f
Interpenetration of reactants	260-262	Ion-pair formation	131
Intersystem-crossing processes in		Ionic charge influences on	
Co(II), Fe(II), and Fe(III)		protonation reactions	66t
complexes	460t	Ionic strength	259
Intervalence absorption spectrum of		Ionization potential in micelles,	
mixed-valence complex	330, 331	reduction	345
Intervalence band		IR behavior for Creutz-Taube ion ...	331
and calculated contour for		IR laser-excited solvents, proton	
Creutz-Taube ion ...	229f, 288, 292f	transfer	73
of Creutz-Taube ion	286-288	IR spectra	
position, solvent effect	291	hydrofluoric acid	74f
width and symmetric mode		platinum polyhydride complex	373
contribution	288, 290	rhenium polyhydride complex ...	352-358
Intervalence spectrum of [bis(penta-		Iridium polyhydride complexes	348
amine-Ru)1-methoxy-pyraz-		Iron cor. plexes, rate constants for	
zine] $^{5+}$	323f	intersystem-crossing processes ..	460t
Intervalence spectrum of		Iron redox couple electron-exchange	
Creutz-Taube ion	323f	mechanism	274
Intervalence transfer	308-316	Iron redox reactions in	
Intervalence transfer absorption band	320	hemerythrin	218, 220, 221
Intervalence transfer bands	138	Iron tetracarbonyl dihydride,	
Intramolecular disproportionation		photochemical H_2 loss	379
path for hemerythrin	220	Iron-aquo complex at inner-sphere	
Intramolecular electron transfer		contact distance	257, 260, 261f
rates	223-227	Iron-aquo complex, H ⁺ AB for	272
reactions in hemerythrin	218-222	Iron-hexaaquo complexes metal-O	
Intramolecular H-bond breaking		distances and breathing	
reactions	65, 67t, 68	frequencies	327t
Intramolecular hydride migration	375	Iron-hexaaquo exchange	318, 319
Intrinsic barrier for cross-reaction,		Iron-phenanthroline complex	241
definition	96	Iron-water complexes, rate	
Intrinsic barrier vs. methyl cation		constants	111t, 120
affinity for nucleophiles	90f, 93	Iron- μ -peroxo complex formation ...	435
Intrinsic barriers	85-92	Iron(III), study of water exchange ...	49, 50
to electron transfer for μ -superoxo/		Iron(III)tetra(4-N-methylpyridyl)-	
μ -peroxo and O_2/O_2^-	428-431	porphyrin	59
for halide and alkoxide exchanges ..	91	Irradiation procedures	376
for homogeneous reactions	202, 205	Isonicotinate bridging ligand	225
rate constants and efficiencies	89t	Isotope labeling studies	380
structure effects	93	IT—See Intervalence transfer	
Intrinsic free energy of			
activation	183, 184	J	
Intrinsic free energy barriers	187	Jahn-Teller distortion	397

K	M
Kinetic acidity	Macrocyclic ligands
metal hydrides in acetonitrile	Macrocyclic tetrapeptide complex
Kinetic activation parameters for oxida-	Malin's dihydride
tion of Ru(II) complexes	Malonic acids substituent effect on
Kinetic data	H-bonding
for aquo cations oxidation	Manganate/MnO ₄ ⁻ outer-sphere
for <i>cis</i> -Os(CO) ₄ H ₂ proton transfer	electron transfer
reactions	Manganese substitution behavior
Kinetic measurements	Manganese(II) solvent-exchange
for Os(II)-Fe(III) reaction	rate constant
for T1 ion reduction	Manganese(III) tetra(4- <i>N</i> -methyl-
Kinetic parameters	pyridyl)porphyrin
for electron transfer	Marcus cross-relationship, breakdowns
for Fe ³⁺ /Fe ²⁺ self-exchange	in applicability
in water	Marcus equation quantities,
of micelles	relationship between
for photochemical reactions with	Marcus equations
PPh ₃	Marcus model
for plutonyl/Pu exchange	Marcus relationship plot for
Kinetic pathway for dioxygen reduction	cross-reactions
via superoxo intermediate ..	Marcus theory
Kinetic study of rhodium complex ..	application to electron transfer ..
Kinetics	proton transfer
of electron transfer between small	use with respect to transfer of
molecule redox reagents and	large groups
proteins	Matrix elements
of inorganic electrode reactions ..	Mechanism
of ion recombination in water	of acid-catalyzed dechelation of
of proton transfer to colloidal	polyamine complex
particles	for acid decomposition of Cu(III)
of protonating carbanions	tetraglycine
of reactions in polar solvents be-	for acid dissociation of
tween transition-metal	Ni(II)(H-3G4a)
complexes	for proton-transfer reactions of
in relation to thermodynamics	metal-peptide complexes
Kosower <i>Z</i> -value	of substitution reactions of metal
	complexes
	Mechanistic photochemistry
	Mercaptide ions
	Metal complexes
	acidities in acetonitrile
	hydrogen bonding
	mechanisms of substitution
	reactions
	outer-sphere electron-transfer
	reactions
	rate constants for rapid stereo-
	chemical changes
	Metal ions
	chemistry in aquo or ammonio
	systems
	reaction with terpyridine
	reduction of ClO ₄ ⁻
	Metal orbitals, exchanged electron ..
	Metal-bipyridine charge-transfer
	excited states
	Metal-ligand charge transfer
	in mixed solvents
	transitions

- Nucleophilic substitution 81-102
 reactions of trien with Cu(II)-
 tripeptide complexes 23
 and redox changes 154, 155
 Nucleophilicities, intrinsic 88f
 Nucleophilicity vs. leaving
 group ability 92, 93
- O**
- Olefins, hydridocobaloximes,
 addition to 405, 406
 One-electron reduction product of
 tris(2,2'-bipyridine)Rh(III) 385-402
 Optical charge-transfer transitions 137-150
 Optical and thermal electron transfer 141
 Optical transfer—*See also*
 Intervalence transfer
 Optical transfer and nuclear
 tunneling 315
 Optical-thermal transfer probabilities
 relationship 308, 309f
d-Orbital energies 166
d-Orbital occupancy and δV^* for
 solvent exchange 51
 π -Orbital overlap 118, 119t
 Orbital symmetry and ClO^+
 reduction 172
 Orbitals, exchanged electrons in
 ligand and metal 274t
 Orbitals, Gaussian type 272
 Organic halides, rate constants for
 Rh(II) rhodoxime reaction 401t
 Organic molecules, interaction with
 micelles 337
 Organic organized assemblies 335, 336f
 Organic radical-trapping reagents 177
 Organized assemblies
 effect on chemical reactions 335-346
 formed from organic surfactant
 molecules 336f
 Organochromium cations 62f
 Organometallic chemistry, proton-
 transfer reactions 403-423
 Organometallic photochemistry,
 generation of reactive
 intermediates 347-383
 Oscillating reactions 450
 Oscillator strength for electric
 dipole-allowed transition 315
 Oscillator strength of intervalence
 band 310
 Osmium salts as reducing agent
 for ClO^+ 168
 Osmium tetracarbonyl 379, 380
 Osmium-bipyridyl complexes,
 oxidation 130, 131
 Osmium-bis(ethylenediamine
 dihydride) complex 420
- cis*-Osmium-tetracarbonyl complex,
 methylation 405
 Osmium-tetracarbonyl complexes,
 proton transfer 406-411
 Osmium(II)-Fe(III) reaction 131
 Outer-sphere association constant 11-13
 Outer-sphere complex formation in
 substitution reactions 56
 Outer-sphere correlation of rates of
 reductions of cobalt complexes .. 438f
 Outer-sphere electron transfer
 between $\text{MnO}^{3-}/\text{MnO}^{4-}$ 332
 bound O_2 427-435
 classical model 195
 metal complexes 120
 Outer-sphere processes 130
 Outer-sphere reactions
 of free oxygen 448
 thermal, and nuclear tunneling .315, 317
 Oxidation of aquo cations 200, 201f
 Oxidation of Pt(II) by Pt(IV) 153
 Oxidation of Rh(I) to Rh(II) 397
 Oxidation of tris(4,7-dimethylbi-
 pyridyl)Os(II) 130, 131
 Oxo-Ru complex, reaction with NO^{2-} 173
 μ -Oxo silicon phthalocyanine dimer .. 313
 Oxyanions, redox chemistry 151, 152
 Oxygen
See also Dioxygen
 bound molecular, reactivity 425-450
 chemistry 462
 electrocatalytic reduction 443, 444
 removal from ClO^+ 151
 thermodynamic properties of Co
 complexes reacting with 447t
 Oxygen atom transfer to V(II) 174
 Oxygen-atom transfer 151-179
 with bound O_2 427, 439, 440
 Oxygen-exchange between H_2O_2
 and H_2O 155
 Oxyions 461
- P**
- ^{31}P NMR spectrum of
 $[\text{MoH}_4(\text{dppe})_2]$ 350, 351
 Pair distribution function of reactants 236
 Partial molal volumes of aqueous ions
 and δV^* for water exchange 52
 Peptide-metal complexes
 proton-transfer reactions 18, 19f
 substitution reactions 6, 7f
 Perbromate ion as oxidizing agent ... 159
 Perchlorate concentration, effect on
 rate constant 34
 Perchlorate ion
 reducibility 152, 153
 reduction 155-160
 reduction by metal ion 160-170

Perchlorate ion—(Continued)	
substitution rate	152
Perchlorate reaction	
with carboxylate radical anion	174
with V(II)	163, 174
Perchlorate reduction, effect of elec- tronic structures of reductants ..	169
Permanganate/MnO ³⁺ outer-sphere electron transfer	332
Peroxide as donor ligand	446
Perturbation theory expression for nonadiabatic rate constant	238
Perturbation theory formalism	267–269
pH effect on dissociation rate constant for Nien ²⁺	16, 17f
Phenol–amine complexes	65
Pheophytin–quinone electron exchange	218
Phonon	
electron coupling constant	311
electron coupling energies from experimental data	320–322
modes of medium	311
occupation number	215, 216
structure, analysis	322
Phosphido-bridged platinum species ..	383
Phosphine loss in Re hydride complexes	369, 370
Phosphines, elimination of PR ₃ from rhenium hydride complexes	359–370
Photochemical H ₂ loss from Fe tetracarbonyl dihydride	379
Photochemical reactions, organized assemblies effects	335
Photochemistry	458
Photodissociation of PR ₃ ligands from [ReH ₃ (PR ₃) ₄] and [ReH ₅ (PR ₃) ₃] complexes	359–370
Photoejection of H ₂	379
Photoemission, study	325
Photogeneration of reactive [ReH(dppe) ₂]	351–354
Photoinduced dissociation of PMe ₂ PH from [ReH ₃ (PMe ₂ Ph) ₄]	366, 367
Photoinduced electron exchange between pyrene P and dimethylaniline	339
Photoinduced electron transfer	
from dye	339, 340
from ferrocene to CCl ₄	341
Photoinduced elimination of H ₂ from dinuclear hydride complexes	370–376
from molybdenum complexes	349–351
Photoinduced loss of H ₂ from [ReH ₃ (dppe) ₂]	351–354
Photoinduced loss of PR ₃ from [ReH ₅ (PR ₃) ₃]	360–366
Photoionization from gas and solu- tion phases, comparison	325, 326f
Photolysis	
of molybdenocene and tungsteno- cene dihydrides	348, 349
of [ReH ₃ (dppe) ₂] in degassed solution	352–354
of [ReH(dppe) ₂] in presence of reactant gases	355–359
of [ReH ₅ (PR ₃) ₃] and [ReH ₃ (PR ₃) ₄]	367, 370
of transition metal polyhydride complexes	347–383
Photon energy	291
Picric acid	
anion protonation	71, 72
structure	72
Platinum bis(triphenylphosphine) intermediate	383
Platinum dinuclear hydride com- plexes, elimination reactions	371–376
Platinum(II) oxidation to Pt(IV)	153
Plutonyl/Pu exchange, kinetic parameters	303f
Polarizability of O ²⁻	165, 166
Polarization effects and stacking interactions	13
Polyhydride complexes, transition metal, generation of reactive intermediates via	347–383
Polypeptide complexes, substitution reactions	31, 32
Polypeptides, dynamics of electron transfer across	221–227
Polypyridine–metal complexes	385–402
Porphyrins	
cofacial, O ₂ reduction in	441, 443
water-soluble, and pressure effects ..	59
Potential energies associated with Hamiltonian	311, 312f
Potential energy	
reactants and products as function of nuclear configuration	109f
surfaces	83–85, 262–264
diagrams for symmetrical electron	139–141
for exchange reaction	113f
vs. normal mode coordinate for symmetrical electron transfer ..	140f
vibrational	283
Potential surface	
adiabatic	293
for gas-phase nucleophilic dis- placement reactions	84f
for ion-molecule reactions, single-minimum	84f
Potential-energy contours for complete active space	263f
Potentials for surfaces in Creutz–Taube ion	321f
Pressure data analysis in terms of solvational change	45–47

- Pressure dependence
of components of rate coefficient
for water exchange on Fe(III) 44*f*
of δV^* for reactions involving
charge development40, 41*f*
of volumes of activation40–45
Pressure effect58, 59
Pressure effects and substitution
mechanisms39–54
Pressure-accelerated water exchange
reactions and associative
interchange 49*t*
Pressure–coordination rule 48
Pressure-decelerated water-exchange
reactions and dissociative
interchange 48*t*
Pressure-jump method 69
Probability density for transferring
electron 305
Probability of electron transfer 269
Prosthetic groups 221
Protein electron transfer reactions 221, 222
Proton exchange rates effect of
hydrophobic substances 64, 68
Proton NMR spectra
osmium tetracarbonyl hydride
complexes407*f*, 410*f*, 412*f*
platinum polyhydride complexes .. 373
rhenium polyhydride complexes352,
353, 355, 360, 361*f*
Proton transfer
to dipicrylamine 72
in IR laser-excited solvents 73
to and from a membrane 79
in mixture of tungsten complex
and morpholine 414
in osmium tetracarbonyl
complexes406–411
Proton transfer kinetics, future
research 70*t*
in methanol, acetonitrile, and
benzonitrile71–73
pertinent information404–406
solvent properties and rate-limiting
steps 74*t*
Proton transfer rates between metal
base and amine base 420
Proton-transfer kinetic studies,
future trends69–71
Proton-transfer reactions
between acids and bases63–65
with deprotonated metal–peptide
complexes 23*t*
generalization63–68
of metal–peptide complexes,
mechanism 21*f*
of metal–peptides20–23
in organometallic chemistry403–423
rates and mechanisms63–80
Protonation
of ethylenediamine nitrogens 16
of pyridine 72
rates for carbanions 68
reactions, ionic charge influences .. 66*t*
Pyrene/dimethylaniline electron
exchange 339
Pyridine, protonation 72
- Q
- Quadratic dependence on overall
free-energy306, 307*f*
Quantum mechanical theory
(QMT)267–271, 276*t*
Quantum yield, [(PPh)₃] effect 382
Quantum-mechanical theory of dif-
fusion-dependent electron trans-
fer in biological systems214–218
Quantum-mechanical vs. classical
approach 251
Quenching
of *Cr(III) by Co(III)227–230
of fulvic acid fluorescence37, 38*f*
rate constant for halides 230
rate constant vs. reduction potential
for RuL₃³⁺/*RuL₃²⁺
couple 391*f*
of *Ru(bpy)₃²⁺ by paraquat 448
Quinone–chlorophyll electron transfer 215
- R
- Radial distribution function at
equilibrium 106
Radial distribution of reactants259–262
Radial flux density236, 237
Radial pair distribution function 258
Radical-trapping reagents, organic 177
Radical-trapping studies 179*t*
Rate coefficient for water exchange
on Fe(III) 44*f*
Rate constant
for acid dissociation of
nickel(III) complex8, 9*f*, 11
for acid pathway in dissociation
of Nien²⁺ 20*t*
for base protonation 66*t*
bimolecular 258
for bipyridine loss from Rh(bpy)₃³⁺ 387
calculated base on TST, SCT,
and QMT 276*t*
for Co(III)–Ru(II) complexes
separated by amino acids 226*t*
for conversion of precursor to
successor complex 108
for Cu(III) tetraglycine acid
decomposition 6, 7*f*

Rate constant—(Continued)	
dependence on separation	
distance	237, 238
for dioxygen adduct formation	436 <i>t</i>
for dissociation of Nien(H ₂ O) ₄ ²⁺	
as function of pH	17 <i>f</i>
and efficiencies used to extract	
intrinsic barriers	89 <i>t</i>
for electrochemical exchange and	
homogeneous self-exchange	
reactions	190 <i>t</i> , 191 <i>t</i>
for electron transfer reactions	105, 106
within precursor complex	107
within semiclassical formalism	112
for exchange reactions	110, 111 <i>t</i> , 120, 121 <i>t</i>
for Fe ²⁺ /Fe ³⁺ electron exchange	
reaction	255
for formation of aquonickel(II) ion	
with amines	6 <i>t</i>
for homolytic dissociation	60, 61
for intersystem-crossing processes	
in Co(II), Fe(II) and Fe(III)	
complexes	460 <i>t</i>
<i>k_{el}</i>	258, 262–267
ligand–ligand vs. metal–metal	
coupling effect	272
for metal–metal proton exchange	414
of Ni(II) with ethylenediamine	12
for rapid stereochemical changes	
in metal complexes	459 <i>t</i>
for reaction of Rh(II) rhodoxime	
with RX	401 <i>t</i>
for reactions of trien with	
Cu(II) tripeptides	27 <i>t</i>
for Rh(III) reduction to Rh(II)	398
for ruthenium complex reaction	
vs. δ-Go	241, 242 <i>f</i> , 245 <i>f</i>
for solvent and protonation path-	
ways in complex dissociation	16 <i>t</i>
at δ-Go	235, 240, 244, 246
Rate constant–overpotential plot	198 <i>f</i>
Rate of electron transfer, amino acid	
linkages influences	225–227
Rate formulations, electrochemical	182–185
Rate law	
for BrO ⁴⁻ reduction	159
for Ti ³⁺ reduction of ClO ⁴⁻	160, 163
for V ²⁺ oxidation	163
Rate measurement of gas phase,	
ion–molecule reactions	82, 83
Rate theory, unimolecular	83
Rate, intramolecular electron	
transfer	223
Rates of electron transfer,	
distance dependence	213–233
Rates and mechanisms for	
proton-transfer reactions	63–80
Rates of reaction of ClO ⁴⁻ with	
nucleophilic reducing agents	159
Rates of transfer from	
<i>cis</i> -Os(CO) ₄ H ₂ to Et ₃ N	406, 408
Reactant separation	259
Reactants, interpenetration	260–262
Reactants, radial distribution	259–262
Reaction entropy for redox couple	185
Reaction rates, contrasts in predicted	
free-energy dependence	303–308
Reactions of coordinated	
dioxygen	427, 428
Reactions involving solvational	
change	42
Reactions in micelles	337
Reactivity of coordinated	
dioxygen	425–450
Reciprocity	271
Recombination in water, kinetics	73, 75
Redox changes and nucleophilic	
substitution	154, 155
Redox chemistry of oxyanions	151, 152
Redox couple	
electrochemical, kinetic, and	
thermodynamic parameters	189–193
energetics of electron transfer	185
reaction entropy	185
transition metal ion	160–162
Redox properties of Rh(bpy) ₃ ²⁺	388–393
Redox reactions and 2e ⁻ changes	153
Reducing agents, nucleophilic,	
rates of reaction of ClO ⁴⁻	159
Reduction of ClO ⁴⁻	
general	155–160
metal ions	160–170
Reduction of ionization potential	
in micelles	345
Reduction potential for cobalt	
complex	434
Reduction potentials of rhodium	
complexes	392 <i>t</i>
Reduction product of tris(2,2'-	
bipyridine)Rh(III)	385–402
Reduction of Rh(III) to Rh(II)	398
Rehm–Weller method for estimating	
reduction potentials of excited	
molecules	388
Relaxation experiments and	
oscillating reactions	450
Relaxation techniques	
electric field jump	71–73
pressure-jump method	69
Relaxation times for various	
techniques	455 <i>f</i>
Reorganization energy	216, 252 <i>f</i> , 288
for Co and Fe systems	318, 319
definition	317
Resonance exchange reactions	229

- Resonance structures contribution to
 S_N2 transition state 93
- Respiratory protein, intramolecular
 electron transfer reactions 218–221
- Reversed micelles 341
- Rhenium dithioformate complex 358, 359
- Rhenium formate complex structure.. 359
- Rhenium heptahydride bis(trialkyl-
 phosphine) complexes 369, 370
- Rhenium pentacarbonyl dimer
 reaction with PPh_3 443
- Rhenium pentahydride trialkyl-
 phosphine complexes 367–370
- Rhenium trihydride complexes
 photoinduced loss of H_2 from 351–354
 photolysis in presence of reactant
 gases 355–359
- Rhodium framework of
 $[Rh_{13}(CO)_{24}H_{5-n}]n$ 417f
- Rhodium hydride species and H_2
 generation 398, 399
- Rhodium tris(bipyridine) ion
 characterization 393–395
 charge-transfer excited state 397
 production and decomposition 386, 387
 redox potentials 388–393
- Rhodium, oxidation state 385
- Rhodium(II) rhodoxime formation 399, 400
- Rhodium(II) rhodoxime reaction
 with RX, rate constants 401t
- Rhodium(III) halide complex
 formation 399, 402
- Rhodium(III) one-electron reduction 385
- Rhodium(III) reduction to Rh(II) 398
- Rhodium(4,4'-dimethyl-2,2'-
 bipyridine) complex 390–393
- Ru–Oxo complex reaction with NO^2- 173
- Ruthenium dodecacarbonyl,
 photochemical reactions with
 triphenylphosphine 382
- Ruthenium spin-orbit coupling 297
- Ruthenium tris(bipyridine) activated
 complex 448, 449
- Ruthenium trisbipyridyl 338
- Ruthenium–bipyridine complexes
 exchange reaction 118
 rate constants 111t, 120
- Ruthenium–Co amino acid
 complexes 223–226
 rate constants 111t, 120
- Ruthenium–hexaammine complex
 reaction with ClO_4^- 178
 reaction with H_2O_2 178
- Ruthenium–polypyridyl complexes 145
- Ruthenium(II) complexes
 reaction with ClO_4^- 167, 168
 reaction with H_2O_2 175–178
- Ruthenium(II)–bipyridyl complex 239, 240
- Ruthenium(III) excited state
 formation 245f
- S**
- Saddle-point method 112, 306
- Schrödinger equation 282
 eigenvalues 266
 Hamiltonian 268, 269
 vibronic 285
- Second-order rate constants for
 reactions of triene with Cu(II)
 tripeptides 23, 27t
- Self-exchange rate constant for
 Cu(II)/Cu(I) 211, 212
- Self-exchange rates for Rh couples 393
- Self-exchange reactions
 nuclear tunneling factor 318t, 319t
 rate constant and thermo-
 dynamic parameters 190t, 191t
- Semiclassical formalism for electron
 transfer model 110–122
- Semiclassical theory (SCT) 265, 266
 rate constants 276t, 277t
- Semicontinuum model 297
- Semimethemerythrin dispropor-
 tionation system 220
- Separation distance 237
- Silica colloid 339
- Silver(II) protoporphyrin reaction
 with $IrCl_6^{3-}$ 338
- Singlet oxygen, lifetime 449, 450
- Singlet vs. triplet oxygen
 generation 448, 449
- Sipunculids 218
- S_N1 reactions 82, 92, 102
- S_N2 nucleophilic attack on ClO_3^- 152
- S_N2 potential energy surfaces 96
- S_N2 transition state 93
- Sodium lauryl sulfate micelles 338, 339
- Solar energy conversion and
 dinuclear elimination 370
- Solubilization of reactants by
 micelle 337
- Solvation effect for S_N2 exchange 91, 92
- Solvation thermodynamics 297
- Solvational change between initial
 and transition states 42
- Solvational change, pressure
 data analysis 45–47
- Solvent combination to E^* 264
- Solvent composition, effect on
 divalent metal ions 35, 36
- Solvent configuration for activated
 complex 113f
- Solvent dependence of CT
 transitions 145
- Solvent effect on intervalence
 band position 291
- Solvent effects in vibronic coupling
 model for mixed-valence
 compounds 281–299
- Solvent exchange reactions and molal
 volumes of transition states 52

Solvent polarization mode	262-264	Substitution reactions—(Continued)	
Solvent properties and rate-limiting steps for proton transfer	74t	polypeptide complexes	31, 32
Solvent-exchange rate constant for Mn(II)	56	Sulfosalicylic acid reaction with Fe complex	37
reactions—See also Water exchange reactions, nonaqueous	50-52	Sulfur nucleophiles	100
Spatial separation between donor and acceptor centers	215, 218	Superoxo intermediate, kinetic pathway for dioxygen reduction	441
Spectral data for Rh(bpy) ₃ ²⁺	394	Surface of micelle	345, 346
Spectral data, photolysis of ReHx(PR ₃) _x complexes	357, 364t	Surfactant molecule	335, 336
Spherical contact distance	261, 262	Symmetric probability distribution	270
Spin multiplicity changes in donor-acceptor reactions	227	Symmetric vibrational modes	330
Spin relaxation, electronic	458	Symmetrical electron transfer, potential energy vs. normal mode coordinate	140f
Spin-orbit coupling	126		
low-symmetry splitting	297	T	
Splitting of adiabatic states	273f	Tait equation	45
Splitting of adiabatic surfaces at diabatic crossing point	267	Temperature dependence of cytochrome oxidation rate in chromatium	216, 217f
Stability constants of Cu(II)-tripeptide complexes	25, 27t	Temperature dependence of rate for activated and activationless processes	218, 219f
Stabilization of electrochemical transition state	194	Temperature effect on nuclear tunneling	114, 115f
Stacking interaction in reaction between bipy and Ni(phen)(H ₂ O) ₄ ²⁺	13, 14f	Temperature-dependent activation energy	271
Stacking interactions	13	Temperature-jump study of hydroxide ion reaction with H-bond malonic acid monoanions	65, 67t
Static dielectric constant of bulk water	259	Terpyridine, reaction with metal ions	32
Static problem	282-284	1,4,8,11-Tetraazacyclotetradecane	427
Steel corrosion	78	Tetraglycinamide complex	8
Stereochemical change in chelate complexes	42	Tetraglycine triply deprotonated complex	6-8
in metal complexes	459t	Thallic ion reduction by Fe ²⁺	133
Steric effect in substitution	33	Thallium(II) disproportionation reaction rate constant	134
Steric factor	262	Thermal activation energy	308, 309f
Steric hindrance and H-bond strength in ligand-ligand displacement reaction	65, 67t	Thermal outer-sphere reactions and nuclear tunneling	315, 317
Storage of energy	344	Thermochemical constraints on potential catalysts of O ₂ /H ₂ O couple	444-446
Structural properties of micelles	344	Thermochemical parameters of O ₂	426t
Substitution chemistry, instrumentation requirements	36, 37	Thermodynamic acidities of metal hydrides in acetonitrile	409t
Substitution mechanisms and pressure effect	39-54	Thermodynamic driving force influence	196-206
Substitution rate constants for aquonickel(II) ion with amines ..	5, 6t	vs. activation free energy plot	188f
Substitution reactions associative interchange	49t	Thermodynamic free-energy barrier ..	184
of chelates	3-38	Thermodynamic parameters for electrochemical exchange and homogeneous self-exchange reactions	190t, 191t
dissociative interchange	48t	Thermodynamic properties of Co complexes reacting with O ₂	447t
dissociative vs. associative mechanisms	4-6	Thermodynamics, kinetics in relation to	40
factors affecting (kf)	12t		
homolytic vs. heterolytic bond cleavage	60-62		
outer-sphere complex formation	56		

- Thiolates 100
- Time-dependent calculations of
 k_{obs} vs. δ -Go 244, 245f
- Tin(II), reducing agent for ClO^+ 172
- Titanium, colloidal systems involving 78
- Titanium(III) reduction of ClO^+ 160, 163
- Titration of fulvic acid with Cu(II) ion 38f
- Toepler pump analysis of evolved
gases 357
- Total reorganization energy vs.
band energy 291, 292f
- Transfer coefficient 196
- Transfer rate vs. absolute t as
function of electronic coupling .. 294f
- Transfer, intervalence 308–315
- Transition metal anions and charge
delocalization 404
- Transition metal complexes, kinetics
of reactions in polar solvents 257
- Transition metal hydride,
deprotonation 404
- Transition metal ions
aquo compounds 128
redox couples 106–162
reduction of ClO^+ 160–170
- Transition metal polyhydride
complexes 347–383
- Transition metal redox couples,
electrochemical kinetic and
thermodynamic parameters 189–193
- Transition metals—*See also* Metals
*and entries under specific
elements*
- Transition probability, Laplace
transform 315
- Transition state characterization 83, 85
- Transition state and reactants,
energy difference between 98
- Transition state for $\text{S}_{\text{N}}2$ exchange 91
- Transition state stabilization, homo-
geneous vs. electrochemical 194
- Transition state theory (TST) 265, 266
rate constants and activation
parameters for Fe^{2+} - Fe^{3+}
reaction 276f
- Transition state of water exchange 54
- Triethylamine and *p*-nitrophenol
proton transfer 72
- Triethylenetetramine nucleophilic
substitution reactions 23, 27f
- Tripeptide–polyamine ternary
complexes 23, 24f
- Triphenylphosphine, photochemical
reactions with ruthenium
dodecacarbonyl 382
- Tris[bipyridylruthenium(II)]–methyl
viologen system 339
- Triton X-100 micelle 344
- Trivalent metal complexes, substi-
tution characteristics 6, 7f
- Tungsten–molybdenum tetrahydride
complexes 380
- Tungstenocene dihydrides
photolysis 348, 349
- Tunnel-type transitions for
Creutz-Taube ion 299
- Tunneling in connection with
proton transfer 79
- Tunneling transitions 286, 287f
- U**
- Unimolecular rate theory 83
- Uranium as reducing agent for ClO^+ 163
- Uranium–aquo complex oxidation 164, 165
- UV–VIS spectral changes
on acid addition to
Ni(III)(H-3G4a) 8, 10f
during irradiation of rhenium
complexes 362, 363f, 367, 368f
during photolysis of platinum
complexes 371, 372f
- V**
- Vanadium–aquo complex oxidation .. 164
- Vanadium(II)
reaction with ClO^+ 172
as reducing agent for ClO^+ 163, 174
- Vanadyl ion formation 164, 165
- Van der Waals contact 255
- Vibrational coupling limit 249
- Vibrational eigenvalues for
Creutz-Taube ion 320
- Vibrational energy exchange 268
- Vibrational force constants 205
- Vibrational modes in electron transfer 216
- Vibrational potential energy 283
- Vibrational trapping 139
- Vibrational wave function overlap 143
- Vibrational wave functions 269
- Vibrations of a bidentate formate
ligand 358
- Vibronic coupling model for
mixed-valence compounds 281–299
- Vibronic energies 284
- Vibronic matrix elements 268
- Vibronic Schrödinger equation 285
- Vibronic wave function 269, 284
- Vidicon rapid scan UV–VIS spectral
changes on acid addition to
Ni(III)(H-3G4a) 10f
- W**
- Water—*See also* Aqua
- Water exchange, limits to δ -V* 47–50

Water-exchange rate constant	11	Work-corrected rate constant	183, 184
for Ni(terpy)(H ₂ O) ₃ ²⁺	13		
Water-exchange reactions			
and associative interchange	49 <i>t</i>		Y
and dissociative interchange	48 <i>t</i>	Y1 bond, formation	165-167
Wave functions		Ytterbium ion redox reactions	164
charge localized vs. delocalized	270, 271		
determination	269, 270		Z
and nonadiabatic character	266, 267	Zinc tetraphenylporphyrin	338
overlap	143		

Jacket design by Joan Wolbier

Production by Kathy Mintel and Karen Gray

Elements typeset by Service Composition Co., Baltimore, Md

Printed and bound by Maple Press Co., York, Pa.